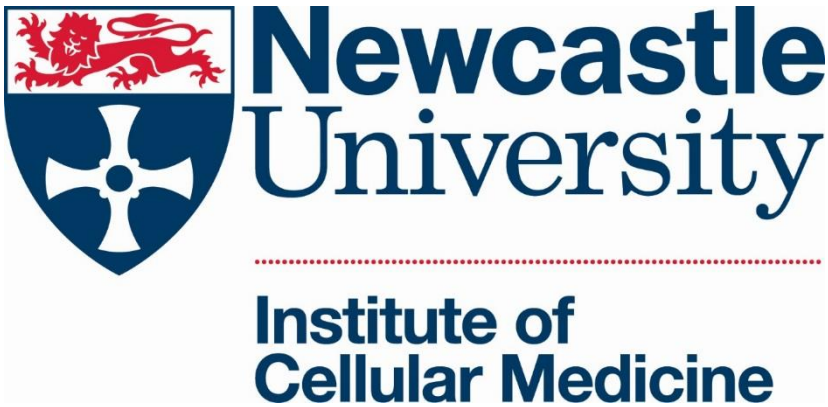

THE ROLE OF CXCR4, CXCR7 AND CCR7 IN BREAST CANCER METASTASIS

Irene del Molino del Barrio

A thesis submitted in partial fulfilment of the requirements for the degree of Doctor of Philosophy

Institute of Cellular Medicine

Newcastle University

March 2017

Abstract

Breast cancer (BrCa) metastasis is a process mediated by the expression of chemokine receptors by BrCa cells, which migrate towards their chemokine ligands presented by glycosaminoglycans (GAGs) in distant organs. Although this metastatic spread is the cause of most BrCa deaths, there are no effective strategies to target this process. This study was designed to investigate whether BrCa cell migration can be controlled by cross-desensitisation of chemokine receptors or by use of non-GAG binding chemokines.

Initial experiments showed that the chemokine receptors CXCR4, CXCR7 and CCR7 were upregulated in primary BrCa and that CXCR4 and CXCR7 could form heterodimers in transfected CHO cells. This co-expression modified CXCR4's potential to activate Akt but did not affect ERK phosphorylation. To assess this signalling disparity, receptor internalisation was assessed. It was found that CXCR7 was recycled to the surface whilst CXCR4 was degraded, a process that could be partially inhibited with a proteasome inhibitor. Internalisation was also assessed using the CXCR7 agonist VUF11207, which caused both CXCR4 and CXCR7 to be degraded after internalization, highlighting its potential as a dual targeting drug. It was also found that only CXCR4 played a role in metastasis by promoting calcium flux, and CXCR7 co-expression did not significantly reduce CXCR4-mediated cellular migration.

The role of GAGs in CCR7-mediated lymph node metastasis was investigated by creating a non-GAG binding CCL21 (mutCCL21). *In vitro*, mutCCL21 bound CCR7 and triggered diffusion gradient chemotaxis, but failed to induce transendothelial cell migration. This was recapitulated in a murine model of BrCa, where daily injections of mutCCL21 significantly reduced lymph node metastases, highlighting the therapy potential of disrupting GAG-chemokine interactions

In summary, these findings suggest that each chemokine receptor has a different but vital role in BrCa metastasis, and should be considered as targets for future therapies.

294/300 words

DECLARATION

I declare that no portion of the work compiled in this thesis has been submitted in support of any other degree or qualification at Newcastle University or any other university or institute of learning. The work has been carried out by myself unless otherwise stated. All sources of information have been acknowledged accordingly by means of reference.

ACKNOWLEDGEMENTS

The work described in this thesis was carried out in the Applied Immunobiology Group in the School of Surgical and Reproductive Sciences, University of Newcastle. The project was generously funded by the Woman's Cancer Detection Society and the NHS Trust from the Queen Elizabeth hospital in Gateshead without whose support, my studies would not have been possible.

I would like to thank my supervisors Prof John Kirby, Prof Simi Ali, Dr Annette Meeson and Mr David Browell for supporting and helping me throughout my PhD, particularly on the first year when I had no clue what I was doing! I have learned so much during these three years and I could not imagine better supervisors. I would also like to thank Dr Andy Filby for answering my million questions about flow cytometry and going above and beyond his duties in helping me out. I'll miss our (almost) weekly chats. A massive THANK YOU to Dr Ben Miller and Katie Cook for their help with all the mouse work that I was too squeamish and un-licensed to do myself, without you guys it will have literally not been possible. The work in this thesis also benefited from the wisdom and knowledge of Barbara Innes, resident staining queen and primary tissue *connoisseur*. And of course thanks to all the members of the lab past and present (I miss you Cat!) & office mates who have either helped me or simply made this experience all the more enjoyable through their presence and banter. You set the bar high for future colleagues. In particular, I'd like to thank Shameem Ladak for being there from the beginning (we're almost there!), Rachel Etherington for all her cake and beer sampling (outside office hours, of course), Sarah Thompson for letting me steal all of her reagents and only scowling at me, and Helen for answering all my thesis questions due to the dubious honour of being the last person to graduate. At last, I'd also like to extend my thanks to the Tyson-Capper and Marchbank lab – I guess you guys are alright too. (I also want to thank my Dolce Gusto machine for providing me with coffee and preventing me from spending a small fortune in Costa coffee whilst writing my thesis).

If there is something I want to convey for future generations of breast cancer scientists to come is this – MDA-MB-231 is a lousy breast cancer cell line despite what literature may tell you. And do not be discouraged if your thesis writing looks more like this:

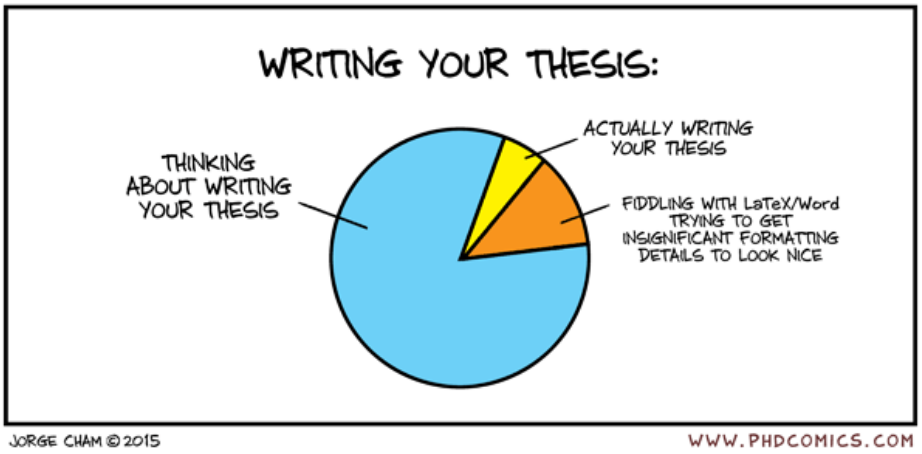

Many thanks also go to those outside of the lab, particularly the people I met during my masters years that also have carried the (joy) of doing a PhD. I can't believe how quickly time has gone by. Thanks to my family for their encouragement during my studies, and for spoiling me whenever I went back home.

TABLE OF CONTENTS

LIST OF FIGURES

LIST OF TABLES

LIST OF ABBREVIATIONS

ABC	Antigen binding capacity
ACKR	Atypical chemokine receptor
ADP	Adenosine diphosphate
Akt (PKB)	AK thymoma (Protein kinase B)
ANOVA	Analysis of variance
AP	Alkaline phosphatase
APC	Allophycocyanin
APS	Ammonium persulfate
ATCC	American Type Culture Collection
ATP	Adenosine triphosphate
BCA	Bicinchoninic acid
Bcl-2	B-cell Lymphoma 2
(k)bp	(kilo) base pairs
BR	Bloom-Richardson
BSA	Bovine serum albumin
CAFs	Cancer associated fibroblasts
cAMP	Cyclic adenosine monophosphate
CBE	Clinical Breast Examination
CBR2	Cannabinoid Receptor 2
CD	Cluster of differentiation
cDNA	Complementary DNA
CHIP	Chromatin immunoprecipitation
CHO	Chinese hamster ovary
CMV	Cytomegalovirus
COSHH	Control of substances hazardous to health
Ct	Crossing threshold
CT	Computerized Tomography
CTL	Cytotoxic T lymphocytes
CTLA-4	Cytotoxic T-lymphocyte associated protein 4
(k)Da	(Kilo) Daltons
DAB	3, 3’ diaminobenzidine
DAG	Diacylglycerol
DAPI	4',6-diamidino-2-phenylindole
DC	Dendritic cells

DCIS	Ductal carcinoma in situ
DEPC	Diethyl pyrocarbonate
DMEM	Dulbecco's Modified Eagle's medium
DMSO	Dimethyl sulphoxide
dNTP	Di-Nucleotide Triphosphate
dsRNA	Double stranded RNA
(c)DNA	(Complemtary) Deoxyribonucleic acid
DPX	Dibutylphthalate Xylene
ELC	EBI1-Ligand Chemokine
E.coli	*Escherichia coli*
ECL	Enhanced chemoluminescence
ECM	Extracellular Matrix
EDTA	Ethylenediaminetetraacetic acid
EGFR	Epidermal growth factor receptor
EMT	Epithelial-to-mesenchymal transition
ELISA	Enzyme-linked immunosorbent assay
ELR	Glutamic acid-leucine-arginine
ER	Oestrogen receptors
ERK	Extracellular signal regulated kinases
FACS	Fluorescent activated cell sorting
FAM	6-carboxyfluorescein
FBS	Foetal bovine serum
FGF-2	Fibroblast growth factor-2
FITC	Fluorescein isothiocyanate
FKH	Forkhead
FNAC	Fine needle aspiration
FOXP3	Forkhead box P3
FRET	Fluorescence Resonance Energy
FSC	Forward scatter
GAG	Glycosaminoglycan
GAPDH	Glyceraldehyde 3-phosphate dehydrogenase
GDP	Guanosine diphosphate
GFP	Green fluorescent protein
GPCR	G protein coupled receptor
GRK	G protein coupled receptor kinase
GTP	Guanosine triphosphate

H&E	Haematoxylin and Eosin
HEK	Human embryonic kidney cells
HER2	Human epidermal growth factor receptor 2
HEVs	High endothelial venules
HGF	Hepatocyte growth factor
HIF-1α	Hypoxia inducible factor-1 alpha
HIV	Human immunodeficiency virus
HMEpC	Human mammary epithelial primary cells
HMEC-1	Human Microvascular Endothelial Cell line-1
HPF	High power field
HRP	Horse radish peroxidase
HPRT1	Hypoxanthine-guanine phosphoribosyltransferase
HRT	Hormone replacement therapy
HS	Heparan Sulphate
HTA	Human tissue act
H_2O_2	Hydrogen peroxide
ICAM	Intercellular adhesion molecule
IDC	Invasive ductal carcinoma
IF	Immunofluorescence
IFNγ	Interferon gamma
IHC	Immunohistochemistry
IL	Interleukin
ILC	Invasive lobular carcinoma
IP_3	Inositol trisphosphate
IPEX	Immunodysregulation polyendocrinopathy enteropathy X-linked
i.p.	intraperitoneal
i.v.	intravenous
JAK	Janus kinase
JNK	c-jun N-terminal kinase
KO	Knock out
LB	Lysogeny broth
LCIS	Lobular carcinoma in situ
LFA-1	Lymphocyte Function-Associated Antigen-1
LMWHs	Low-molecular-weight heparins
LPS	Lipopolysaccharide
mAb	Monoclonal antibodies

MAPK	Mitogen activated protein kinase
MCS	Multiple cloning site
MFI	Median fluorescence intensity
MMP	Matrix metalloproteinase
MTA	Material Transfer Agreement
mTOR	Mammalian target of rapamycin
NF-κB	Nuclear factor-κB
NK cell	Natural Killer cell
NHSBSP	National Health Service Breast Screening Programme
NPA	No primary antibody control
NPI	Nottingham prognostic index
NSCLC	Non-Small Cell Lung Cancer
OC	Oral contraceptives
OCT	Optimal cutting temperature
PAGE	Polyacyralymide gel electrophoresis
PAMPs	Pathogen-associated molecular patterns
PBMC	Peripheral blood monocytes
PBS	Phosphate buffered saline
PCA	Protein complementation assay
(q)PCR	(quantitative) Polymerase chain reaction
PD-1	Programmed cell death protein 1
PDGR	Platelet-derived growth factor receptor
PE	Phycoerythrin
PEN	Polyethylene naphthalate
PFA	Paraformaldehyde
pH	Power of hydrogen
PI3K	Phosphotidylinositol-3-OH kinase
PIP_2	Phosphatidylinositol (3,4,5)-bisphosphate
PKA	Protein kinase A
PKC	Protein kinase C
PLC	Phospholipase C
PMT	Photomultiplier tubes
PNAd	Peripheral-node addressins
PR	Progesterone receptors
PVDF	Polyvinylidene fluoride
QE	Queen Elizabeth

qPCR	Real-time quantitative polymerase chain reaction
Rb	Retinoblastoma
RDC-1	Receptor Dog cDNA 1
RIN	RNA Integrity Number
RISC	RNA-induced silencing complex
ROI	Region of interest
RPMI	Roswell Park Memorial Institute medium 1640
RU	Resonance units
S1PR	Sphingosine 1-phosphate receptor
SDF-1	Stromal cell-derived factor-1
SDS	Sodium dodecyl sulphate
SEM	Standard Error of the Mean
siRNA	Small interfering RNA
SKP2	S-phase kinase protein 2
SLC	Secondary lymphoid tissue chemokine
shRNA	Small hairpin RNA
SPR	Surface plasmon resonance
SSC	Side scatter
STAT	Signal transducer and activator of transcription
STR	Short tandem repeats
TAE	Tris-acetic acid-EDTA buffer
TAMRA	Tetramethylrodamine
TBS	Tris-buffered saline
TEM	Trans -endothelial migration
TEMED	Tetramethylethylenediamine
TGFβ	Transforming growth factor beta
TNFα	Tumour necrosis factor alpha
TNM	Tumour Node Metastasis staging system
TP53	Tumour protein 53
TReg	Regulatory T cells
TSP-1	Thrombospondin-1
UV	Ultraviolet
VCAM	Vascular cell adhesion molecule
VEGF	Vascular endothelial growth factor
VHL	Von-Hippel Lindau
VIP	Vasoactive intestinal peptide

WB	Western blot
ZO-1	Zonula occludens

1. INTRODUCTION

1.1. BREAST CANCER

Breast cancer is the most prevalent cancer in the United Kingdom despite being predominantly a female disease, with 53,696 new cases in 2013. It is also the third most common cause of cancer death after lung and bowel cancers, with 11,433 deaths in 2014. However, despite having an increasing incidence (4% in the last decade), the mortality rate from mid-1980s has decreased by 40%. This success is due to both the implementation of the National Health Service Breast Screening Programme (NHSBSP) in 1986 and an expanding knowledge about the disease and its mechanisms (Cancer Research UK, 2010).

Although breast cancer incidence has increased due to longer life expectancy and better diagnostic tools, it is far from a recent disease. The first recorded evidence of breast cancer dates back to 3,000-2,500 BC in Egypt, where Imhotep describes the disease in the Edwin Smith Surgical Papyrus (Breasted, 1930). More evidence can be found in Greek medical documents, with references to carcinomas (*karkinoma*) and the first hypothesis as to their cause (Papavramidou et al., 2010). More extensive descriptions of surgical removal of breast tumours can be found during the 1st and 2nd century AD with documents from Galen and Leonides of Alexandria (Lewison, 1953). No more progress was achieved until the 18th century, where the first references to the lymph (Sappey, 1874) and lack of sex (Mustacchi, 1961) being the cause of breast cancer can be found. The first breakthrough, however, was in 1757, where French physician Henri Le Dran suggested that the removal of both the tumour and the surrounding armpit lymph nodes could cure the disease (Le Dran, 1768), leading to the first cases of total mastectomy. During the following centuries, surgery was the first line of treatment for breast cancer, a process which was constantly improved with the introduction of anaesthetic and a precise protocol for the removal of the affected organs (Vaidya et al., 2004). The first link between hormones and breast cancer was in the late 19th century, when the Scottish surgeon George Beatson discovered that removal of the ovaries helped his patients' prognostic (Beatson, 1901). This was further expanded half a century later, when it was found that oestrogen could also be produced from the adrenal and pituitary glands (Huggins and Yang, 1962). Soon after, more conservative approaches started emerging for the treatment of breast cancer, such as radiation or chemotherapy (Fisher et al., 1976).

Nowadays, 74% of breast cancer patients still undergo major surgical resection (Cancer Research UK, 2010).

1.1.1. Structure of the breast

The breast is a gland situated in the frontal upper part of the chest and is composed by adipose and connective tissue (stroma) and glandular tissue, which in turn is divided into lobules and ducts (as represented in Figure 1-1). Adult females usually have between 15-20 lobes, which in turn are divided into 20-40 lobules (Osborne, 2000). As an apocrine gland, its main function is the production of milk in the lobules (specifically, in the terminal duct lobular units), which will be transported to the nipple through the ducts. After menopause the number and size of the lobules shrinks, increasing the proportion of fatty tissue in the breast and thus decreasing breast density (Fuller et al., 2015).

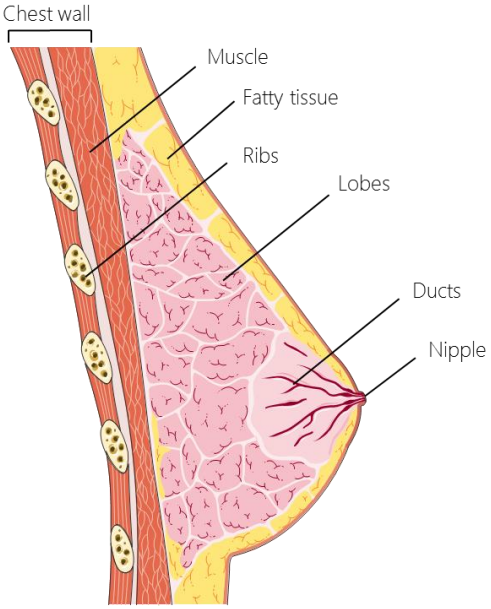

Figure 1-1. Representation of the female breast.
Milk is produced in the lobules' bulbs, which in turn form the lobes. The lobes are linked by ducts, which are small tubes surrounded by fat that transport the milk to the nipple. The breast is supported by the pectoralis major muscle, and usually extends from the second to the sixth ribs. The lymphatic vessels drain the lymph from the breast to the lymph nodes present around the armpit. Image created using Servier image bank (http://www.servier.fr/smart/banque-dimages-powerpoint).

The breast also contains numerous blood vessels, which supply blood through the internal thoracic, axillary, and intercostal arteries, which in turn drain to the subclavian artery. There are also lymph vessels present which extend towards the axilla, where 20 to 30 lymph nodes are present. Thus, the lymph vessels mostly drain to the axillary nodes (75%), but also to the parasternal nodes (20%) and posterior intercostal nodes (5%), which are located in the sternum and the ribs respectively (Krag et al., 1993).

These lymph vessels contain a fluid called lymph, which is normally composed of lymphocytes, tissue fluid and waste products, but which can also contain cancer cells that have left the primary tumour. This facilitates the entry of cancer cells to the bloodstream, increasing the chances of the cancer metastasizing to other organs.

1.1.2. Breast cancer identification

Breast cancer can be asymptomatic or present several manifestations - nevertheless, none of these symptoms are exclusive to breast cancer alone and may be caused by another condition. Some of the changes that can indicate breast cancer are:

- A lump around the breast and armpit area. This is the most common symptom, albeit it is usually benign (cysts, etc.).
- A change in size or shape of the breast.
- A change in the shape of the nipple, especially if it turns inwards ("inverted nipple").
- Irritation, dimpling or puckering in the skin of the breast.
- Discharge of blood or other non-milk fluid.
- Change in the colour or texture of the breast's skin or nipple, such as scaliness, redness, or swelling (Paget's disease).
- Breast and nipple pain.

During the NHS breast screening programme, a doctor will check for the presence of lumps in the breast in a procedure called Clinical Breast Examination (CBE). If positive, a mammogram (essentially an X-ray of the breast) or an ultrasound will be carried out to show if the lump is solid or filled with fluid (which is known as a cyst). If the tests are inconclusive, a fine needle aspiration (FNAC) can be carried out – in it, fluid from the lump is taken out to ascertain whether it is clear or bloody, the latter being a possible indicator or cancer. In that case, the collected cells are usually stained and undergo a cytology exam.

In cysts, the liquid will be completely removed using a needle, whilst in solid lumps a biopsy may be required in order to look at the tissue under the microscope. This can mean removal of the entire lump (excisional biopsy) or only of a part (incisional biopsy).

If results are positive, further tests will be carried out to characterize the cancer and decide the optimal treatment. This includes measuring the amount of oestrogen and

progesterone receptors in the cancerous tissue and the quantification of the human epidermal growth factor type 2 receptor (HER2/neu) together with its gene expression. Patients that overexpress HER2 usually present a more aggressive cancer, higher recurrence rates and worse prognosis (Slamon, Clark et al. 1987).

CT (Computerized Tomography) scans and chest X-rays may also be performed to detect whether the cancer has spread to neighbouring organs. Excisional biopsy of the first lymph node that receives the waste from the tumour (what is known as "sentinel lymph node") is also a common procedure in order to look for cancer cells (Veronesi et al., 1997).

1.1.3. Causes

1 in 8 women and 1 in 870 men will be diagnosed with breast cancer at some point in their lives. With such high incidence, it is not surprising that the causes for breast cancer are diverse. 73% of the breast cancers are caused by unavoidable factors, with age being the predominant one - indeed, 46% of the cases occur in females over 65 years of age. Another important factor is high levels of endogenous hormones such as oestrogen, progesterone and testosterone. These correlate with a younger menarche (first menstrual period) and an older age at menopause, with each increasing the risk around 3% (Collaborative Group on Hormonal Factors in Breast Cancer, 2012). This is due to being exposed to oestrogen for a longer time period.

Interestingly first childbirth increases the risk short term, but has a protective effect after 10 years. This is likely due to the high cell proliferation that takes place during pregnancy, which could lead to a quick expansion of cancer cells. As having aberrant cells becomes more likely with age, when having children after age 35 the protective effect is off-balanced with the higher risk (Rosner et al., 1994). Overall, there is a 40% higher risk when having children after 35 versus before 20, and an overall 30% reduction in risk versus having no children (Ewertz et al., 1990). However, after the first birth every following birth reduces the risk, especially if they are close together (Barnard et al., 2015). Breastfeeding also contributes to this protective effect.

Family history of breast cancer also plays a role, which includes abnormalities in the hereditary *BRCA1* and *BRCA2* genes – carriers of mutations in *BRCA1* will develop cancer 55-65% of the time, whilst carriers of the *BRCA2* mutation will develop cancer 45% of the time by age 70 (Antoniou et al., 2003). These mutations are uncommon (0.1-

0.12% of the general population) but there are some ethnic groups with a higher carrier number. For instance, Ashkenazi Jews have a 10-fold higher number of mutations in BRCA1/2 compared to the general population (Egan et al., 1996). Other rarer gene mutations such as p53, CHEK2, ATM or PALB2 also increase breast cancer risk.

However, the remaining 27% are related to lifestyle choices, including excessive weight (9%), high alcohol consumption (6%), a sedentary life (3%) (Kelsey, 1993), hormone replacement therapy (HRT) to help manage menopausal symptoms (3%) and use of oral contraceptives (OC, 1%) (Parkin, 2011). In particular, it is estimated that OC users have a 1.24 to 1.33 higher breast cancer risk than those who never took them (Collaborative Group on Hormonal Factors in Breast Cancer, 1996, Hunter et al., 2010), although other studies report no increased risk (Marchbanks et al., 2002). Increased risk for oestrogen-progesterone HRT users has also been extensively reported, with Colditz et al. (1995) describing a 1.2 to 2 times higher risk than those who had never taken HRT, and Collaborative Group on Hormonal Factors in Breast Cancer (1997) reporting a 1.53 increased risk for combined therapy. For UK women, this risk may increase to 2.21 if used for more than 5 years (Million Women Study Collaborators, 2003). In all these studies, oestrogen therapy alone significantly reduced the risk as compared to oestrogen-progesterone therapy. In both OC and HRT users, this risk disappears 5 years after stopping its use (Key et al., 2001).

1.1.4. Types of breast cancer

If the biopsy from a lump comes back positive, it is classed as a carcinoma. Most carcinomas of the breast are adenocarcinomas, which indicates the tumour originated from glandular tissue. In turn, breast cancer can develop in the lobes or in the ducts, which gives name to the two main types of cancer: invasive ductal breast cancer and invasive lobular breast cancer (Ellis et al., 1992).

Patients can also present with abnormal non-invasive cells inside the breast structures that can become cancerous over time. Depending on whether these cells are contained inside the breast ducts or lobules this condition is called ductal carcinoma in situ (DCIS) or lobular carcinoma in situ (LCIS). Whilst LCIS very rarely develops into breast cancer and only yearly follow ups are required, DCIS has a greater possibility of spreading to the surrounding tissue. DCIS patients usually undergo surgery to remove the affected

area and may also undergo radiotherapy or tamoxifen treatment depending on the carcinoma's characteristics (Pinder, 2010).

Other times, however, the cancer may have spread outside the lobes or the ducts. The cancer may have spread to the surrounding tissue (fat and muscle), nearby lymph nodes, distal lymph nodes or secondary organs – in all cases, it is classified as invasive breast cancer. Much like with in situ carcinomas, several types exist. In women, the most common is invasive ductal carcinoma (IDC, also known as invasive carcinoma of no special type) and accounts for 50-75% of all invasive cases. The second most common is the invasive lobular carcinoma (ILC), which includes 5-15% of all invasive cases (Borst and Ingold, 1993). In men, high testosterone and low oestrogen stops the development of breast tissue during puberty and thus lobules are often absent and only rudimentary ducts are present. That's why infiltrating ductal carcinoma is the most common type of male breast cancer and lobular cancer is very rare.

Other rarer types of cancer include tubular breast cancer (characterised by cells looking like a tube), mucinous breast cancer (characterised by the cells looking as if they were in mucous), medullary breast cancer (characterised by a clear division between cancer and surrounding tissue) and papillary breast cancer (characterised by cells looking like a fern) among others. There are also some special forms of breast cancer which include inflammatory breast cancer, Paget's disease and metaplastic breast cancer. Inflammatory breast cancer is an aggressive form of local cancer characterized by the blockage of the lymph vessels which causes inflammation of the tissue. It has a higher proportion of positive lymph nodes and metastasis compared to IDC. Paget disease is a cancer that affects the skin of, or surrounding, the nipple and presents very similarly to eczema or psoriasis. Usually, but not always, there are breast cancer cells (in situ or invasive) growing underneath the nipple or aureole. Metaplastic breast cancer is a characterised by the presence of two different types of cell due to adenocarcinoma undergoing epithelial to mesenchymal transition. It is usually poorly differentiated (Shah et al., 2012).

Several staging strategies exist, but one of the more commonly used is the "number staging". The pathology report will classify the tumour in 5 stages depending on the lymph node status, the tumour size, and the presence of metastasis. The classification is as follows:

Stage		***Description***
Stage 0 (carcinoma in situ)		DCIS.
		LCIS.
		Paget´s disease in the nipple.
Stage 1	*1A*	Tumour has a diameter or 2 cm or less. No presence in the lymph nodes.
	1B	Tumour has a diameter or 2 cm or less; or there is no breast tumour. One or more lymph nodes have isolated cancer cells clusters with a diameter between 0.2mm and 2 mm.
Stage 2	*2A*	Tumour has a diameter or 2 cm or less; or there is no breast tumour. 1-3 lymph nodes in the armpit or near the breastbone have cancer tumours (more than 2mm in diameter).
		Tumour diameter is between 2 and 5 cm. No presence in the lymph nodes.
	2B	Tumour diameter is between 2 and 5 cm. One or more lymph nodes have isolated cancer cells clusters with a diameter between 0.2mm and 2 mm; or 1-3 lymph nodes from the armpit or near the breastbone have cancer tumours.
		Tumour diameter is more than 5 cm. No presence in the lymph nodes.
Stage 3	*3A*	Tumour can be not present or of any size. 4-9 lymph nodes from the armpit or near the breastbone have cancer tumours.
		Tumour diameter is more than 5 cm. One or more lymph nodes have isolated cancer cells clusters with a diameter between 0.2mm and 2 mm; or 1-3 lymph nodes in the armpit or near the breastbone have cancer tumours.
	3B	Tumour can be not present or of any size. It presents with swelling or an ulcer due to having spread to the breast's skin and/or the chest wall. Cancer may also have spread to up to 9 lymph nodes in the armpit or near the breastbone.
	3C	Tumour can be not present or of any size. It presents with swelling or an ulcer due to having spread to the breast's skin and/or the chest wall. Cancer has also spread to 10 or more lymph nodes in the armpit; or below or above the collarbone; or lymph nodes in the armpit and near the breastbone.
Stage 4		Cancer has spread to another organ (brain, lung, liver, bones, etc.).

Table 1-1. Classification of the different number stages in breast cancer.

The 5-year relative survival rate has greatly improved throughout the years, with values ranging from 100% (non-invasive) to 72% (stage III). Thus, death due to breast cancer usually occurs when the cancerous cells metastasize and target vital organs – at this stage, the survival rate drops to 22%. (American Cancer Society, 2013).

When biopsies come back positive for breast cancer, several tests are usually carried out in order to determine the prognosis and the best course of treatment. Pathology reports look at:

- Hormone receptor status: presence of oestrogen (ER) and progesterone receptors (PR) that tumour cells use to grow.
- HER2 status: presence of HER2 on the cancer cell's surface.
- Proliferation rate: some tumours grow more quickly than others, which puts them in higher risk to metastasise to other organs. Ki-67 is usually used as a marker for proliferation – tumours that are over 10% positive are considered to be aggressive (Fasching et al., 2011)

1.1.5. Treatment

Thanks to early prevention, breast cancer deaths have fallen by 20% in the last ten years in the UK even though incidence rates have increased by 4%. Indeed, there were 570,000 female breast cancer survivors in the UK in 2010.

Surgery is usually the first treatment option in order to remove the cancer from a local area, although sometimes it is preceded by chemotherapy and/or radiotherapy in order to shrink the tumour (Early Breast Cancer Trialists' Collaborative Group, 2006). Depending on the size, position, type and stage of the tumour, surgery can encompass removal of only the tumour and surrounding tissue ("lumpectomy"), removal of a part of the breast ("partial mastectomy"), removal of the whole breast ("total mastectomy") or removal of the whole breast together with many of the underarm lymph nodes and even some chest muscle ("modified radical mastectomy"). Whenever a partial mastectomy is carried out, it is often followed by radiotherapy treatment, which involves the use of high levels of radiation from X-rays to either kill or stall the growth of cancer cells around the breast area (Fisher et al., 1995).

Chemotherapy uses drugs to either kill or stop the division of cells that are actively multiplying. It is used both to diminish the chance of recurrence after surgery and to diminish the size of the tumour before the operation ("adjuvant therapy") (Azim et al.,

2011). There are 6 drugs that are commonly given to treat breast cancer, either alone or (more often) in combination: Cyclophosphamide, Docetaxel, Doxorubicin, Epirubicin, Methotrexate and Paclitaxel. Other drugs are also given when the cancer has metastasized – these include, but are not limited to, Capecitabine, Carboplatin and Cisplatin. Chemotherapy drugs are usually given orally or intravenously in cycles for up to 3-6 months.

The receptor status in the cancer cell is also key in determining treatment. ER and PR positive cancer cells require oestrogen and progesterone to grow and thrive and thus these receptors can be used as a target. If that is the case and the woman is not postmenopausal, tamoxifen is given in order to prevent the binding of oestrogen to its receptor (Early Breast Cancer Trialists' Collaborative Group, 2011). Ovarian ablation is also another possible treatment, in which patients are given drugs such as leuprolide or goserelin to prevent oestrogen production from the ovaries. More rarely, the ovaries are surgically removed to avoid all hormone production. In postmenopausal woman, aromatase inhibitors are usually prescribed in order to block the small amount of oestrogen produced by lipid cells. Drugs such as anastrazole, exemestane or letrozole prevent the aromatase enzymes from converting other hormones into oestrogen (Early Breast Cancer Trialists' Collaborative Group, 2015).

Biological therapies are the most selective as they target specific antigens present in the cell. Monoclonal antibodies (mAb) are the most common type of biological therapy. For instance, 20% of the breast cancers express HER2/neu (Mitri et al., 2012) and thus patients can benefit from the mAb trastuzumab (commercialized as Herceptin). Similarly to hormone therapy, trastuzumab prevents the binding of growth factors to the receptor by targeting the subdomain IV of HER2, blocking the multiplication of cancer cells. If patients are not responsive or the cancer has metastasized, other options such as pertuzumab, sorafenib or lapatinib exist which target different points in the signalling pathway (Citri and Yarden, 2006). Pertuzumab works by blocking the formation of HER2 dimers, thus effectively blocking the signalling pathway (Harbeck et al., 2013). Both sorafenib and lapatinib target protein kinases in the signalling pathways, but whilst sorafenib has several targets such as C-RAF, B-RAF, VEGFR (vascular endothelial growth factor receptor) and PDGFR (platelet-derived growth factor receptor) (Liu et al., 2006), lapatinib only binds to the ATP-binding domain in EGFR (Epidermal growth factor receptor) and HER2 (Scaltriti et al., 2009).

1.1.6. Tumour development

Cancer is an incredibly heterogeneous disease – in fact, it was originally described as a compendium of diseases that share **six common hallmarks** (Hanahan and Weinberg, 2000).. Normal cells slowly acquire these six traits that will allow them to gain their tumorigenic potential and ability to disseminate, whilst still displaying enormous intra-heterogeneity thanks to their constant interaction with the microenvironment.

First, tumour cells have increased proliferative signalling. Normal cells respond to growth signals in a progressive manner so that tissue structure remains unchanged and functional. However, tumour cells have acquired the ability to over-stimulate themselves in a variety of ways (Perona, 2006, Witsch et al., 2010). Some cancer cells can synthesise their own growth factors for autocrine stimulation, whilst others stimulate the neighbouring, non-cancer cells in order for them to produce these signals (Cheng et al., 2008, Bhowmick et al., 2004). Cancer cells can also over-express receptors, so they become extra-sensitive to the growth factors present, or just permanently activate the signalling pathways as to become independent to the presence of growth factors in the environment. This is due to mutations in key signalling enzymes which constitutively activate them (Davies and Samuels, 2010, Yuan and Cantley, 2008) or deactivating mutations in molecules which would stop the signalling (Amit et al., 2007)

Second, tumour cells can evade growth-suppressor signals. Non-cancerous cells need to pass several checkpoints before being allowed to grow and proliferate – if they fail, the processes are halted and apoptosis can be triggered. However, cancer cells present mutations in two of the main tumour suppressor genes, RB (retinoblastoma-associated) and TP53 (tumour protein 53, which encodes p53). RB regulates growth by gathering some intracellular but mostly extracellular signals, such as contact inhibition (which controls density and allows cells to grow in a monolayer) or TGF-β (Transforming growth factor β) (Burkhart and Sage, 2008). TP53, on the other hand, reacts to intracellular signals, such as oxygen deprivation, lack of nutrients or DNA damage (Sherr and McCormick, 2002). Interestingly, none of these genes are essential as mouse knock-out (KO) demonstrated redundancy of the pathway (Ghebranious and Donehower, 1998).

Third, they are resistant to cell death. In healthy cells, both intracellular and extracellular stress signals will converge in the activation of members of the Bcl-2 (B-cell lymphoma 2) family, which will then determine whether to trigger the activation of a caspase cascade. This family is composed of anti-apoptotic factors, such as Bcl-2, and pro-apoptotic ones, such as Bax and Bak. The latter are attached to the mitochondrial membrane, where the anti-apoptotic family members usually keep them in a latent state. When activated, they cause the release of cytochrome c, which in turn will cause the caspase activation. In cancer cells, these pro-apoptotic molecules may be downregulated whilst the anti-apoptotic members are upregulated, among other pathways. A similar strategy is seen in the inhibition of autophagy, a process in which the cell digests its own organelles in order to obtain energy, usually in response to starvation.

Fourth, they can acquire unlimited replicative potential. Healthy cells can only undergo a certain number of divisions before entering senescence and eventually crisis. Some cells, however can recover from crisis and gain limitless replicative capability, a trait called "immortalisation". In healthy cells, cell replication causes the shortening of the telomeres protecting the chromosomal ends and the loss of these telomeres causes genetic instability that eventually leads the cell to enter senescence. These telomeres can be extended through the enzyme telomerase, a DNA polymerase, but it is present at very low levels in noncancerous cells. Many cancers, however, present multiple copies, which allows them to avoid triggering senescence (Kim et al., 1994); others survive this senescence thanks to the lack of TP53 (Artandi and DePinho, 2000).

Fifth, cancer cells can induce angiogenesis in order to obtain nutrients and oxygen that will sustain their progressive growth. These new aberrant vessels will also help in removing the waste and carbon dioxide generated by the tumour (Hanahan and Folkman, 1996). In order to achieve this, tumour cells activate VEGF-A in a myriad of ways, such as through *Ras*, *Myc* (Dews et al., 2006) or even immune cells (Zumsteg and Christofori, 2009); or downregulate the antiangiogenic thrombospondin-1 (TSP-1) through p53 (Grant et al., 1997, Dameron et al., 1994). Furthermore, cancer cells have altered their metabolism to transform glucose into pyruvic acid even in the presence of oxygen ("aerobic glycolysis") (Hsu and Sabatini, 2008). This process is less efficient, and thus the cancer cell compensates by upregulating GLUT1 (a glucose transporter) through Hypoxia-inducible factor 1 (HIF-1) (Semenza, 2010).

Last, they can activate metastasis and invasion which is the last phase in tumour progression – a multistep process described in more detail in section 1.1.7. However, it is important to note that tumour cell dissemination does not always correlate with a successful colonization. Indeed, in the primary tumour neoplastic growth is supported by epithelial-to-mesenchymal transition (EMT) signals from the neoplastic stroma; and it has been observed that albeit some tumours disseminate early, the lack of stimulation from the new microenvironment can cause these micrometastases to remain dormant for years (Klein, 2009, Aguirre-Ghiso, 2007).

However, as our knowledge of cancer increases new complexities arise, and further elements had to be added to the original roster (Hanahan and Weinberg, 2011). In particular, the acquisition of the six hallmarks described above is only possible due to two underlying "**enabling characteristics**". First, genomic instability allows for a higher number of mutations due to either external mutagenic agents, or alteration and loss of the DNA-maintenance machinery which usually detects and repairs damaged DNA (Negrini et al., 2010). When these mutations accumulate, tumorigenic traits start to emerge and tumour cells with a favourable genotype are clonally selected to proliferate further.

Second, it is becoming increasingly apparent that tumours show an inflammatory state. Indeed, most tumours show immune cell infiltration, particularly of macrophages and T-cells (Mahmoud et al., 2011). Although it was originally believed that this was the immune system's response to eradicate the tumour, it is becoming increasingly apparent that the consequent inflammation is pro-tumorigenic as it supplies the tumour with growth, proangiogenic and survival factors, matrix metalloproteinases (MMPs) and mutagenic agents such as reactive oxygen species (Colotta et al., 2009, Qian and Pollard, 2010, Grivennikov et al., 2010).

Furthermore, there are two "**emerging hallmarks**" to add to the original 6. First, in order to support the cancer cell's uncontrolled growth and division, there must be changes in the energy metabolism. In particular, even in the presence of oxygen there is a shift to favour glycolysis instead of mitochondrial oxidative phosphorylation. Even though this process is less efficient, it is balanced by an increase in glucose transporters and other enzymes of the pathway (Jones and Thompson, 2009). The reasons for this switch have not been extensively explored, but some studies suggest it is the intermediates that the cancer cell uses to divide (Vander Heiden et al., 2009).

Second, the cancer cells must evade the immune system to escape elimination. There is the widespread theory that most cancers are detected and destroyed by the immune system (a process known as "immunoediting"), and only those that manage to evade it can find a niche and thrive. Indeed, cancers grow more in immunocompromised individuals (Vajdic and van Leeuwen, 2009) and mice (Kim et al., 2007), which supports the hypothesis that only weakly immunogenic cancer cells can avoid detection. Indeed, when cancers that had grown in immunodeficient hosts were transplanted to immunocompetent mice, they failed to thrive (Kim et al., 2007).

This school of thought has sparked interest in checkpoint inhibitors such as programmed cell *d*eath protein 1 or PD-1 and *c*ytotoxic *T*-*l*ymphocyte-*a*ssociated protein 4 or CTLA-4. In health, these receptors are key in regulating autoimmunity and setting a low-activation threshold to avoid immune response against self-antigens (Francisco et al., 2010). In particular, CTLA-4 is upregulated by naive T-cells when auto-reactive antigens displayed by APCs are recognised in the lymph nodes, whilst PD-1 edits activated T-cells in the peripheric tissue cells after exhaustion by constant cell activation in chronic infections or cancer (Fife and Bluestone, 2008). Cancer cells express these receptors or their ligands on their surface and downregulate the immune response by binding to their counterparts present in T-cells. Thus, inhibition of these targets using antibodies results in an increased T-cell activation, allowing the immune system to detect cancer cells that would have used self-tolerance as a mechanism to evade deletion; and to reactivate anti-tumour cells that had become quiescent (Fife and Bluestone, 2008).

Currently, there are several FDA-approved antibodies for melanoma and non-small cell lung cancer that target these checkpoint proteins, including Nivolumab (Opdivo) and Pembrolizumab (Keytruda) against PD-1, Atezolizumab (Tecentriq) against its ligand PD-L1 and Ipilimumab (Yervoy) against CTLA-4 (Raedler, 2015a, Raedler, 2015b, Tarapchak, 2016, Sondak et al., 2011) with more in clinical trials for other types of cancers. Although combination of both blocking antibodies would be desirable, it is important to note that autoimmune side effects would be exacerbated (Postow, 2015).

In breast cancer, the involvement of CTLA-4 overexpression is still unknown although there have been reports of upregulation in patient's PBMCs (Jaberipour et al., 2010); and PD-L1 upregulation has also been described in both the tumour and infiltrating lymphocytes in triple negative patients (Ghebeh et al., 2008). Unfortunately, these

checkpoint inhibitors have not been approved for breast cancer as they appear to be only effective in combination and/or in certain subtypes such as triple negative patients (Emens et al., 2015, Nanda et al., 2015, Adams et al., 2015). However, there is still promise given their lesser side effects and clinical trials of anti-PD-L1 antibodies in combination are currently taking place (Segal et al., 2014, Emens et al., 2015)

1.1.7. Metastasis

Metastasis is a non-random process with several steps that need to be completed for the cells to successfully invade a secondary organ (Fidler, 2003). In the beginning, metastatic cells separate from the breast tumour to its surrounding support tissue. These tumour-associated stromal cells are mainly fibroblasts (Micke and Östman, 2005) and promote the migration of the cancerous cells by producing growth factors and cytokines. The key players in this invasion process are proteins from the cadherin family - downregulation of E-cadherin causes a weakening of the cell-to-cell junction in epithelial breast cells, which facilitates the invasion of cancer cells (Wendt et al., 2011). Furthermore, the substitution of E-cadherin with N-cadherin enhances the EMT (Bonnomet et al., 2010), a process that supports the adhesion of cancer cells to the stroma and the degradation of the extracellular matrix (ECM) by inducing MMPs (Cavallaro and Christofori, 2004). The breaking down of the ECM further allows the invasion of cancer cells, which adhere to the tissue using the transmembrane receptors integrins (which include collagen, fibronectin, etc.) (Felding-Habermann et al., 2001). Several integrins also participate by upregulating the expression of MMPs, further enhancing the tissue invasion (Stetler-Stevenson, 1999). Oestrogen has also been shown to contribute in the ECM degradation by inducing the expression of heparanases (Elkin et al., 2003), which break down the proteoglycan heparan sulphate. This process not only weakens the integrity of the ECM, but also causes the release of growth and angiogenic factors that were bound to heparan sulphate, potentiating the tumour growth (Bashkin et al., 1989).

The second step is the intravasation to the blood and lymphatic vessels, from where the cells will migrate towards their target organs (Wyckoff et al., 2000). Although both systems are similar in that their routes will determine the final destination of the circulating cancer cells, they are structurally different. Although both are lined by a single layer of endothelial cells, the hematopoietic endothelium presents tight cell-to-cell junctions, whilst in the lymph vessels there are gaps between cells (Pepper, 2001).

Thus, in the haematopoietic system, thin-walled venules are the most common target, as they present an easier entry into the circulation. On the other hand, cancer cells can penetrate the surrounding lymph vessels with ease due to their leakiness and then drain to the neighbouring lymph nodes (Shayan et al., 2006). Indeed, it has been proposed that this occurs at the earliest stages of metastasis (Fidler, 2003) and thus "sentinel lymph node biopsies" are used to assess whether spread has occurred as they are the first lymph nodes to receive natural drainage (Morton et al., 1992, Park et al., 2005). Interestingly, although lymphatic spread is widely regarded as a passive phenomenon (Pepper, 2001), more recent studies have suggested that specific interactions between the cancer cell and the endothelium may also be taking place (Qian et al., 2001).

Once the tumour cells reach the capillaries´ lumen, they usually aggregate during the passage to survive the journey. To migrate to distant lymph nodes and organs, they will follow chemokine gradients and adhere to the vessel walls of distant organs (Nathanson, 2003). The tumour cells will then extravasate using several mechanisms very similar to the ones observed during invasion (Langley and Fidler, 2011). This metastatic process is summarised in Figure 1-2.

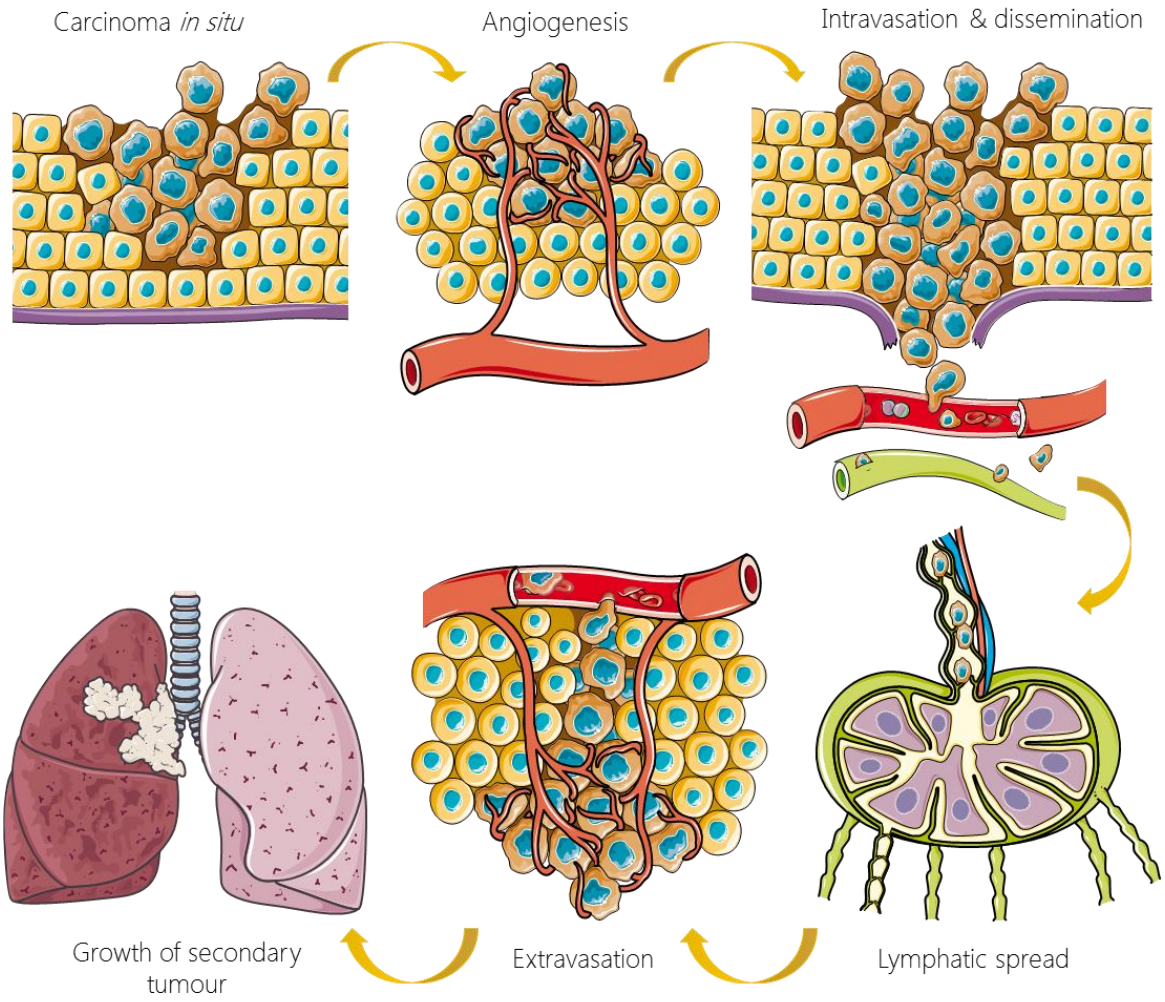

Figure 1-2. Schematic representation of the steps in metastasis.
As cancer cells acquire their metastatic potential, they will display the 6 hallmarks of cancer, including the sprouting of new vessels (angiogenesis). Cells will then intravasate the lymph vessels and colonise the lymph nodes, from where they will travel to distant parts of the body. Cells will then extravasate to the new niche and form a micrometastasis. Image created using Servier image bank (http://www.servier.fr/smart/banque-dimages-powerpoint).

Nevertheless, physical dissemination is not enough for a successful metastases. Once the cancer cells arrive to the new organ, they must then survive by promoting angiogenesis (Folkman, 1986) and evading the host's immune system. These micrometastasis, however, may remain dormant until there is a change in the environment (such as an increased supply of nutrients or oxygen) as most of them lack the ability to induce angiogenesis (Naumov et al., 2008). Other times the primary tumour may induce this dormant state, and thus micrometastasis will only start to grow when it is excised (Demicheli et al., 2008), with cells often migrating back to the site of the primary tumour (Kim et al., 2009).

Furthermore, this complex colonisation process cannot be completed without the microenvironment promoting the tumour's growth and proliferation (Fidler, 2002), which is known as the "seed and soil" hypothesis (Fidler, 2003). The microenvironment

is composed by many different cell types, including fibroblasts, epithelial cells, endothelial cells and leukocytes among others. Stromal fibroblasts, for instance, produce TGF-β which enhances cancer cell motility (due to loss of cell junction), impairs leukocyte action and increases angiogenesis (Bhowmick et al., 2004). Another example are tissue-associated macrophages, which by associating with breast cancer cells promote metastasis and avoid detection from the immune system (Bhowmick et al., 2004). Organ-specific cells also play an important role: in the bone, osteoblasts and osteoclasts not only promote the formation of normal bone tissue but also support the growth of metastatic cancer cells (Langley and Fidler, 2011). Thus, the expression of some cells in the pre-metastatic niche (such as marrow-derived haematopoietic cells that express VEGFR1; and activated perivascular fibroblasts) can determine whether the colonisation will be successful (Kaplan et al., 2005). It is thus implicit that many micrometastasis never become macrometastasis.

1.2. CHEMOKINES AND CHEMOKINE RECEPTORS

1.2.1. Chemokines in cancer

Since their discovery over 30 years ago, numerous chemokines have been identified, with new roles emerging past the homing of leukocytes (Baggiolini, 1998). Chemokines, or *chemo*tactic cyto*kines* are small (8-14 kDa) proteins that bind to G-protein-coupled chemokine receptors (GPCR) composed of seven transmembrane domains in order to induce chemotaxis (Baggiolini 1998). Chemokines can activate multiple signalling pathways and the expression of several genes, but it was their role in promoting the migration of leukocytes to the site of inflammation that allowed for the finding of the link between chemokines and cancer metastasis (Müller et al., 2001). Previous to 2001, it was believed that metastasis was regulated through factors such as the size of the vessels or the difference in pressure between the blood and organs (Morris et al., 1993). The discovery that cancer cells overexpress CXCR4 and CCR7, which directs them to organs that express their ligands CXCL12, and CCL19 and CCL21, respectively, lead to an increase in reports confirming that chemokine receptors were present in a non-random manner in many other cancers. A summary compiling some of these data can be found in Table 1-2. A positive correlation between chemokine receptor expression and worse prognosis has been found in most, but not all, cancers.

As discussed above, chemokines also contribute to the immunological milieu, attracting leukocytes to the tumour and controlling the inflammation by polarizing T-cells (Coussens and Werb, 2002). For instance, the expression of CXCL9 and CXCL10 by Natural Killer (NK) cells, CD4 Th1 cells and CD8 cytotoxic T lymphocytes (CTL) creates a feedback loop that promotes polarisation to a Th1 phenotype in the cancer milieu (Groom et al., 2012, Wendel et al., 2008, Hensbergen et al., 2005). Similarly, a Th2 polarisation can be induced through CCL5 expression by M2 macrophages (González-Martín et al., 2011). This leukocyte recruitment usually leads to a pro-inflammatory microenvironment, which as previously described alters the tumour stroma to favour the cancer cells. For example, several chemokines can induce the production of MMPs, which facilitates the invasion and extravasation of tumour cells (Cavallaro and Christofori, 2004), or act as growth (Lázár-Molnár et al., 2000) or angiogenic factors (Belperio et al., 2000) which promote tumour development.

Cancer	***Receptor***	***Reference***
Bladder	CXCR4, CXCR7	(Eisenhardt et al., 2005, Hao et al., 2012)
Breast	CXCR4, CXCR7, CCR7, CCR9, CXCR3	(Müller et al., 2001, Li et al., 2004, Miao et al., 2007, Luker et al., 2012, Johnson-Holiday et al., 2011, Ma et al., 2009)
Colorectal	CXCR4, CXCR7, CXCR5, CXCR3, CCR7	(Kim et al., 2005, Günther et al., 2005, Schimanski et al., 2005, Xu et al., 2011a, Qi et al., 2014, Kawada et al., 2007)
Cervical	CXCR4, CXCR7, CCR7	(Kodama et al., 2007, Schrevel et al., 2012)
Oesophageal	CXCR4, CXCR7	(Kaifi et al., 2005, Ding et al., 2003, Tachezy et al., 2013)
Endometrial	CXCR4, CXCR7, CCR7	(Kodama et al., 2006, Walentowicz-Sadlecka et al., 2014)
Gallbladder	CXCR4, CXCR7	(Yao et al., 2011)
Gastric	CCR7, CXCR4	(Mashino et al., 2002, Arigami et al., 2009)
Head and Neck	CXCR4, CXCR5, CCR7	(Muller et al., 2006, Katayama et al., 2005)
Leukaemia (Acute lymphoblastic)	CXCR4, CXCR3, CXCR7	(Corcione et al., 2006, Melo et al., 2014)
Leukaemia (Chronic myelogenous)	CXCR4, CXCR5, CXCR3	(Burger and Kipps, 2002, Trentin et al., 2004)
Lung (Non-Small Cell Lung Cancer)	CXCR4, CCR7, CXCR7	(Phillips et al., 2003, Takanami, 2003, Miao et al., 2007, Iwakiri et al., 2009)
Melanoma	CXCR4, CCR10, CCR7, CCR9, CXCR3	(Müller et al., 2001, Letsch et al., 2003, Scala et al., 2005, Kawada et al., 2004)
Neuroblastoma	CXCR4, CXCR7	(Russell et al., 2004, Liberman et al., 2012)
Osteosarcoma	CXCR4, CXCR7	(Laverdiere et al., 2005, Goguet-Surmenian et al., 2013)
Ovarian	CXCR4, CXCR7, CCR9	(Milliken et al., 2002, Yu et al., 2014, Singh et al., 2011)
Pancreas	CXCR4, CXCR7	(Marchesi et al., 2004, Marechal et al., 2009)
Prostate	CXCR4, CXCR7, CXCR5, CCR9	(Darash-Yahana et al., 2004, Wang et al., 2008b, Singh et al., 2009, Singh et al., 2004b)

Renal	CXCR4, CXCR7	(D'Alterio et al., 2010, Schrader et al., 2002, Pan et al., 2006)

Table 1-2. Expression of several chemokine receptors.
Chemokine receptors are overexpressed by almost all cancers. A compilation of these studies was adapted from (Zlotnik, 2006) and is shown in this table.

1.2.2. Chemokines

The chemokine family encompasses over 50 members, which can be either homeostatic or pro-inflammatory. The former are constitutively expressed in certain tissues and have roles in tissue development (such as angiogenesis or neovascularization) or basal leukocyte migration; whilst the latter are released due to a pathology or foreign insult. Briefly, an infection or other pro-inflammatory stimuli will cause the induction of chemokines that will direct the recruitment of leukocytes towards the site of injury (Zlotnik et al., 2011). Depending on the type of inflammation, a different immune cell subset will recruited to the site (Griffith et al., 2014). However, it is important to note that although this categorisation can be useful, it is not always accurate – for instance, some homeostatic chemokines (such as CCL19, CCL21 and CXCL13) have also been found to be induced in inflammation (Marsland et al., 2005, Carlsen et al., 2004).

Structurally, chemokines are divided into four groups depending on the position of the first two *N*-terminal (N-ter) cysteine residues: CXC, CC, CX_3C and C, where C represents the cysteine and X is any amino acid (see Figure 1-3). Chemokines have a total of four cysteines: the first two cysteines are located near the N-ter, whilst the third occupies a central position and the fourth is located towards the C-terminus (C-ter). The bonds between these cysteines determine the tertiary structure of the chemokine - typically, the first cysteine forms a disulphide bond with the third one and the second with the fourth one (Baggiolini et al., 1997). Nevertheless, despite all chemokines having very similar tertiary structures, their sequence homology can be as low as 20% (Allen et al., 2007). CXC and CC are the two most common chemokine groups and their members are secreted to the environment (Schall and Bacon, 1994, Wells et al., 1996), whilst there is only one member of the CX_3C family, which can be either secreted or bound to the membrane (Bazan et al., 1997). Lastly, C chemokines have only two of the typical four cysteines, lacking the two central ones (Zlotnik and Yoshie, 2000).

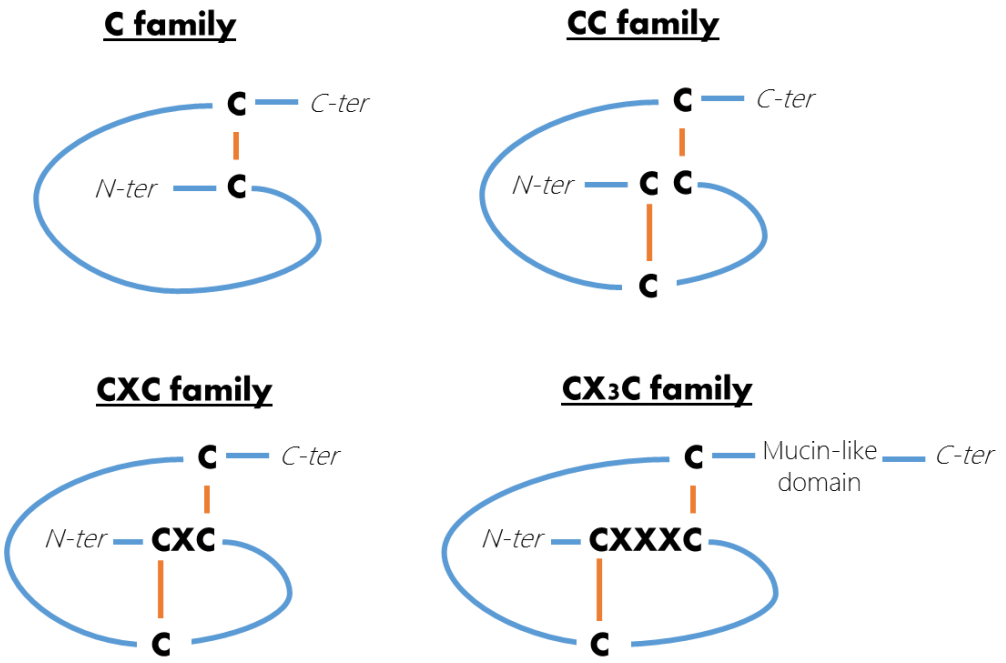

Figure 1-3. Representation of the four chemokine families.
Depending on the position of the cysteine residue (C) in relation to any amino acid (X), chemokines can be in the C, CC, CXC or CX_3C families. Blue lines represent the peptide chain, whilst orange lines represent the disulphide bond between chemokines.

In mammals, the 17 described CXC chemokines are further divided in two groups depending on whether they present the motif glutamate–leucine–arginine (E–L–R) before the first cysteine. The presence or absence of this motif gives the chemokine angiogenic or angiostatic properties, respectively (Strieter et al., 1995). CXCL12 is the only exception to this rule, which is an angiogenic chemokine lacking this motif. Interestingly, this disparity translates to the genetic level, with ELR+ and ELR- present in different sub-clusters in chromosome 4 (O'Donovan et al., 1999).

During the 20th century, cytokines were named by the groups that discovered them without any kind of consensus – thus, some were named depending on their function or which cell they bound or which cell produced them, among others. To solve this issue, in 2000 the International Union of Pharmacology created a systematic nomenclature based on the chemokine structure (Murphy et al., 2000). This classification uses the chemokine family, followed by the letter L or R (depending on whether it is a ligand or a receptor) and a number that indicates the order of discovery. A comprehensive list can be found in Table 1-3 below.

Family	***Current name***	***Previous names***
C family	XCL1	Lymphotactin, SCM-1α (Single Cistein Motif 1α)
	XCL2	SCM-1β
CC family	CCL1	I-309
	CCL2	MCP-1 (Monocyte chemoattractant protein-1)
	CCL3	MIP-1α (macrophage inflammatory protein-1α)
	CCL4	MIP-1β
	CCL5	RANTES (regulated on activation, normal T-cell expressed and secreted)
	CCL7	MCP-3
	CCL8	MCP-2
	CCL11	Eotaxin
	CCL13	MCP-4
	CCL14	HCC-1 (Hemofiltrate CC chemokine-1)
	CCL15	HCC-2
	CCL16	HCC-4, LEC (Liver-expressed chemokine)
	CCL17	TARC (Thymus and activation-regulated chemokine)
	CCL18	PARC (pulmonary and activation-regulated chemokine), DC-CK1(dendritic-cell chemokine-1)
	CCL19	ELC (EBV-induced molecule 1 ligand chemokine), Exodus-3, MIP-3β
	CCL20	LARC (Liver and activation-regulated chemokine), Exodus-1, MIP-3α
	CCL21	SLC (Secondary lymphoid-tissue chemokine), 6Ckine, exodus-6
	CCL22	MDC (macrophage derived chemokine)
	CCL23	MPIF-1 (myeloid progenitor inhibitory factor-1), Ckβ8
	CCL24	Eotaxin-2, MPIF-2, Ckβ6
	CCL25	TECK (thymus-expressed chemokine)
	CCL26	Eotaxin-3, MIP-4α
	CCL27	CTACK (cutaneous T-cell-attracting chemokine), ILC (interleukin-11 receptor α-locus chemokine)
	CCL28	MEC (mucosal epithelial chemokine)

CXC family	CXCL1	Gro-α (growth-related oncogene-α)
	CXCL2	Gro-β, MIP-2α
	CXCL3	Gro-γ, MIP-2β
	CXCL4	PF-4 (platelet factor-4)
	CXCL5	ENA-78 (epithelial neutrophil activating peptide 78)
	CXCL6	GCP-2 (granulocyte chemotactic protein-2)
	CXCL7	NAP-2 (neutrophil-activating peptide-2)
	CXCL8	IL-8 (interleukin-8), NAP-1
	CXCL9	MIG (Monokine induced by interferon)
	CXCL10	IP-10 (interferon -inducible protein-10)
	CXCL11	I-TAC (interferon-inducible T-cell α-chemoattractant)
	CXCL12	SDF-1 (stromal cell– derived factor-1)
	CXCL13	BCA-1 (B cell-attracting chemokine 1)
	CXCL14	BRAK (breast and kidney–expressed chemokine), bolekine
	CXCL16	SRPSOX (Scavenger receptor for phosphatidylserine and oxidized lipoprotein)
	CXCL17	DMC (dendritic cell and monocyte chemokine-like protein), VCC-1 (VEGF-correlated chemokine 1)
CX_3C family	CX3CL1	Fractalkine, Neurotactin

Table 1-3. Nomenclature for human chemokine families.
Chemokine were given a new nomenclature in 2000 – their old name(s) are shown in the third column. Table adapted from (Bacon et al., 2003).

Depending on how chemokines are presented, they can elicit different types of cell movement involving adhesion, migration or both. With soluble chemokines, cells can *migrate* in a random pattern (chemokinesis) or directionally in response to a soluble chemokine gradient (chemotaxis) (Lämmermann et al., 2008), however they cannot trigger lymphocyte arrest (Shamri et al., 2005). In order for cells to extravasate from the bloodstream and *adhere* to the endothelium, chemokines need to be bound to the glycosaminoglycans (GAGs) present in the ECM (Rot and von Andrian, 2004, Ley et al., 2007). This is an electrostatic interaction: often, the chemokine C-terminal region is positively charged due to the presence of basic amino acids such as lysine and arginine; whilst GAGs are highly negatively charged due to the presence of carboxylate and sulphate residues (Kuschert et al., 1999). The binding immobilises the chemokines, allowing for their presentation to chemokine receptor-expressing cells and creating a

concentration gradient (Proudfoot et al., 2003). This adhesive migration following immobilised gradients is referred to as haptotaxis, whilst when the movement is random it is known as haptokinesis (Friedl et al., 2001). In mature dendritic cells, for instance, immobilised CCL21 causes haptotaxis and integrin activation whilst soluble CCL21 or CCL19 induces chemotaxis, and both can occur in combination (Schumann et al., 2010).

1.2.3. Chemokine receptors

Currently 22 chemokine receptors have been identified in humans, with four of them being "atypical" receptors. Chemokine receptors are seven-transmembrane receptors, with seven helical transmembrane domains (connected by three intracellular and three extracellular loops), a short extracellular N-ter that will bind to the ligand and an intracellular C-ter which is coupled to the G proteins that will initiate the signalling (Müller et al., 2001). All chemokine receptors have a molecular weight of approximately 40 kDa. As with chemokines, chemokine receptors are divided in the same four families, with the name indicating the family they bind. Thus, CXC receptors bind CXC chemokines and so on. Unlike chemokines, structurally chemokine receptors are quite similar even among different families (Kufareva et al., 2015).

Most chemokines bind several receptors and a single receptor can often bind several chemokines, forming an intertwined web in which a sole role can be played by several elements. KO in mice seem to indicate this overlapping is due to redundancy (Power, 2003) but we may be missing a more precise fine-tuning *in vivo* (Devalaraja and Richmond, 1999, O'boyle, 2012). Indeed, more recent studies indicate that chemokines have a role in the chemotaxis of very specific T cell (Heydtmann and Adams, 2002) or monocyte (Geissmann et al., 2003) subsets that had not been identified 20 years ago.

It has also been suggested that this apparent redundancy is a result of chemokines evolving to neutralise pathogens that have learned to avoid detection by the immune system (Mahalingam and Karupiah, 1999), particularly viruses (Alcami, 2003). For instance, poxvirus can present GPCR-like (Cao et al., 1995) or chemokine-like (Krathwohl et al., 1997) molecules called viroreceptors and virokines that can act as agonists or antagonists, thus driving the need for new chemokines that will not be recognised but still maintain the same function. In addition to these homologs, viruses can also secrete unique viral products able to bind and neutralise chemokines by

preventing their binding to their receptor or GAGs (Liston and McColl, 2003). Some of these viral molecules have a broad spectrum of action, such as Kaposi's sarcoma-associated herpesvirus' macrophage inflammatory protein 2 (vMIP2), which can bind and displace CCL2, CCL3 and CXCL12 (Kledal et al., 1997); whilst others are specific, such as the human herpesvirus 6's U51, which only binds CCL5 (Milne et al., 2000).

A depiction of this "promiscuity" can be found in Figure 1-4.

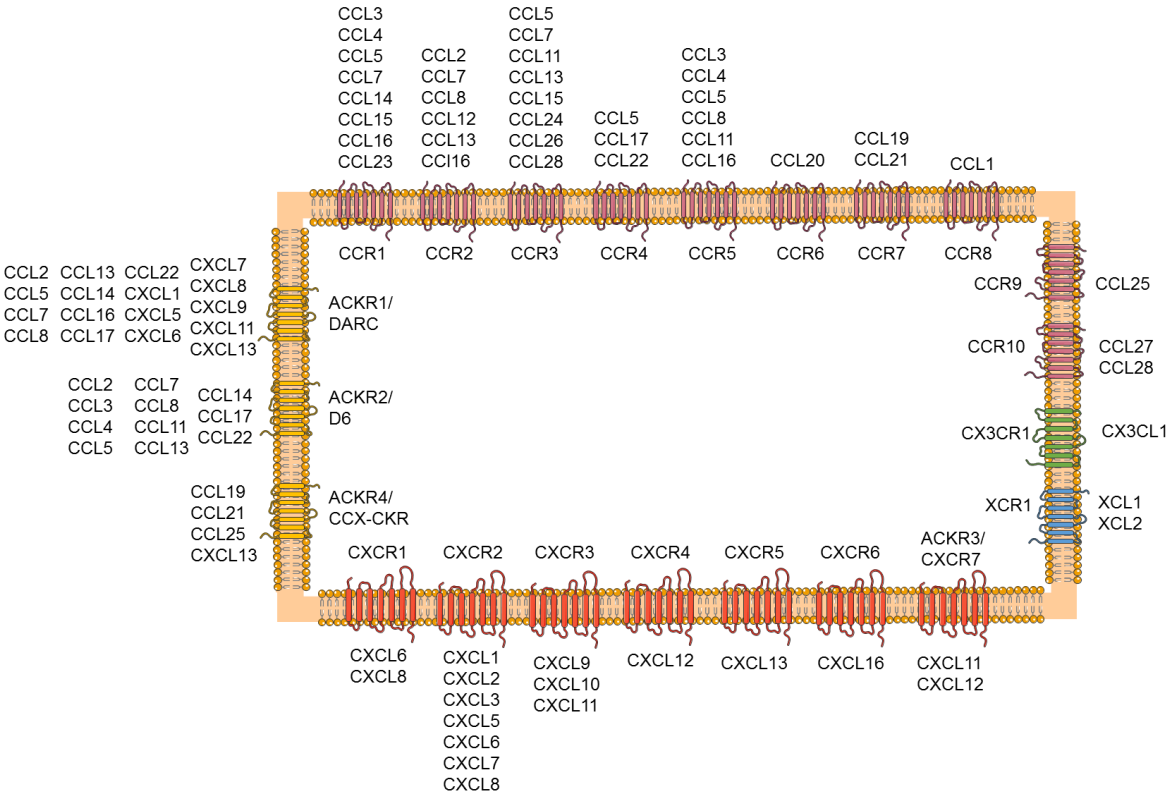

Figure 1-4. Representation of the four chemokine families and their canonical and atypical receptors.
The C family is depicted in blue, the CC family is depicted in pink, the CXC family is depicted in red, the CX_3C family is depicted in green and the atypical receptors (with the exception of ACKR3) are depicted in yellow. Image adapted from Lazennec and Richmond (2010), Bachelerie et al. (2014) and Rot and von Andrian (2004) using Servier image bank.

Most chemokine receptors bind heterodimeric G proteins in their intracellular domain, earning them the name GPCRs. In literature we can also find four "atypical" receptors that bind chemokines with high affinity but that present either no signalling or signalling which is not mediated by G proteins. This group of receptors, which has also been named "decoy" or "scavenger" receptors due to their role in mopping up chemokines (Hansell et al., 2006), has been recently renamed to "ACKR", the acronym of *a*typical *c*hemo*k*ine *r*eceptor (Bachelerie et al., 2014). A brief overview can be found in Table 1-4.

New nomenclature	***Previous names***	***Function***
ACKR1	DARC, Duffy antigen, Fy antigen, CD234	Neutralise inflammatory chemokines, regulate chemokine concentrations.
ACKR2	D6, CCR9, CCR10, CCBP2, CMKBR9	Ligand scavenging.
ACKR3	CXCR7, RDC1, CMKOR1	Ligand scavenging, chemokine gradient formation.
ACKR4	CCRL1, CCX-CKR, CCR11	Ligand scavenging.

Table 1-4 New and previous nomenclature for atypical chemokine receptors and their functions.

Interestingly, ACKR2, ACKR3 and ACKR4 have been described for their ability to quickly bind, internalise and degrade chemokines (Comerford et al., 2006, Weber et al., 2004), whilst ACKR1 keeps chemokines intact after internalisation and can present them at a later time (Nibbs and Graham, 2013). More details about ACKR3 can be found in section 1.3.2.

1.2.3.1. *Receptor signalling*

As their name indicates, "canonical" GPCRs (including CXCR4) can interact with G-proteins through the second intracellular loop where the conserved DRYLAIV (Asp-Arg-Tyr-Leu-Ala-Ile-Val) motif is present (Murphy, 1994). This motif, however, is absent or modified in the ACKRs: ACKR1 has no DRYLAIV motif, ACKR2 presents a DKYLEIV motif, ACKR3 has a DRYLSIT motif and ACKR4 has a DRYVAVT motif (Nibbs and Graham, 2013, Ulvmar et al., 2011). The binding of a chemokine to its receptor causes the conformational change of the attached G protein, activating it, which in turn leads to the exchange of a GDP for a GTP. This process causes the splitting of the Gα subunit from the Gβγ subunit and the receptor.

The Gα subunit can be subdivided in four families: $G_{\alpha s}$, $G_{\alpha i}$, $G_{\alpha q}$ and $G_{\alpha 12}$, with each one activating different effectors. The $G_{\alpha s}$ and $G_{\alpha i}$ subunits both regulate the cAMP (cyclic-adenosine monophosphate)-dependent pathway by modulating the adenylate cyclase activity – the $G_{\alpha s}$ subunit will stimulate it, whilst the $G_{\alpha i}$ subunit will inhibit the enzyme. If activated, the adenylate cyclase will synthesize cAMP from ATP, which in turn will activate the protein kinase A (PKA). This enzyme has many roles, including the regulation of gene expression via the phosphorylation of several transcription factors (Neves et al., 2002, Dorsam and Gutkind, 2007). The $G_{\alpha q}$

subunit activates the phospholipase C-β (PLCβ), which cleaves PIP_2 (phosphatidylinositol 4,5-biphosphate) into inositol trisphosphate (IP_3) and diacylglycerol (DAG). IP_3 works by regulating intracellular calcium release, which helps DAG activate the protein kinase C (PKC). Much like the PKA, PKC has a wide range of substrates which elicit diverse actions. Lastly, the $G_{\alpha q}$ and $G_{\alpha 12}$ subunits can also modulate members of the Ras, Rho and mitogen-activated protein kinase (MAPK) families. Particularly, the GTPase Rho controls the activation of various proteins that regulate cytoskeleton remodelling, which has an impact in migration (Busillo and Benovic, 2007). The MAPK family also includes the kinases ERK (extracellular signal-regulated kinase), JNK (c-jun N-terminal kinase) and p38, which play a key role in cell growth through the phosphorylation of several transcription factors (Marinissen and Gutkind, 2001).

The Gβγ subunits have a more limiting signalling role, which mainly comprises the regulation of several ion channels (such as G protein-coupled inwardly-rectifying potassium channels) and some phosphoinositide-3-kinase (PI3K) isoforms such as PI3Kγ. Furthermore, they can also contribute to the activation of PLCβ (Dorsam and Gutkind, 2007). This is of special importance as most chemokine receptors are $G_{\alpha i}$-coupled and not $G_{\alpha q}$-coupled, which raises the question of how the calcium flux is mobilised. Interestingly, in those GPRCs the release is mediated through the Gβγ subunits and PLC, which catalyses the cleavage of PIP_2 (Teicher and Fricker, 2010, Mellado et al., 2001a).

1.3. CHEMOKINE-DRIVEN BREAST CANCER METASTASIS

1.3.1. CXCR4 and CXCL12

The chemokine receptor CXCR4 is highly upregulated in breast cancer cells (Li et al., 2004). CXCL12 is the only known ligand for CXCR4, although CXCL12 can also bind to the atypical receptor CXCR7. CXCL12 is expressed constitutively throughout the body, but its expression is particularly high in the brain, bones and lungs, which are the most common metastatic organs in breast cancer patients (Müller et al., 2001). Despite chemokines being rapidly evolving molecules, it is interesting to note that CXCL12 and CXCR4 have a high grade of homology with its murine counterparts (99% and 94%, respectively) (O'Brien et al., 1999).

Previously named stromal cell-derived factor-1 (SDF-1), CXCL12 not only promotes cell motility, invasion and metastasis of cancer cells, but also plays an important role in the mobilisation of hematopoietic stem and progenitor cells (Hattori et al., 2001). When expressed in the target tissues, CXCL12 also supports the growth and survival of cancer cells *in vitro* (Scotton et al., 2002), together with promoting angiogenesis (Petit et al., 2007). In health, CXCL12 production is usually triggered by pro-inflammatory molecules such as tumour necrosis factor α (TNFα) or lipopolysaccharides. A mouse KO also revealed a role in cardiac and neuronal development (Ma et al., 1998) - a similar effect can be seen when its receptor CXCR4 is knocked out *in vivo* (Zou et al., 1998).

CXCL12 was initially described as having 2 isoforms, CXCL12α and CXCL12β, both of which have a role in leukocyte migration. The former is the most common isoform, whilst the latter has 4 extra amino acids in the C-ter end, increasing the chemokine size from 89 to 93 amino acids. This extra length confers it an extra resistance to proteolysis in blood, making it more common in highly vascularized organs (liver, spleen and kidneys) (Janowski, 2009). However, recently four other isoforms have been identified, all with different C-ter due to alternative splicing - CXCL12γ, CXCL12δ, CXCL12ε and CXCL12φ (Liekens et al., 2010). CXCL12γ presents four BBXB motifs (B stands for basic, and can represent either arginine or lysine, whilst X is a non-consensus amino acid) which confers the chemokine a higher affinity for heparan sulphate. This enforces its interaction with GAGs from the cell surface, potentiating chemotaxis (Ali et al., 2002). CXCL12δ, CXCL12ε and CXCL12φ do not present any extra BBXB motifs, though they have different potencies in their biological activity in comparison to the main isoform.

CXCL12δ presents a longer, hydrophobic C-ter; CXCL12ε has an asparagine and cysteine residues instead of the lysine in the C-ter; and CXCL12φ's C-ter consists of 11 hydrophobic amino acids instead of the lysine (Altenburg, 2008).

Still much remains unknown about chemokine binding, but some *in vitro* studies suggest that CXCL12 is monomeric and dimers would only occur at high concentrations (over 5 mM) (Baryshnikova and Sykes, 2006). These dimers have been shown to actually inhibit chemotaxis in a murine model of colon cancer (Drury et al., 2011) and melanoma (Takekoshi et al., 2012) due to their lack of induction of chemotaxis and actin remodelling.

CXCR4 is a 352 amino acid rhodopsin-like GPCR and has been found to be overexpressed in more than 23 cancers (Balkwill, 2004). In normal tissue it is expressed by many lymphocytes (including monocytes and macrophages (Lapham et al., 1999), dendritic cells (DCs) and T and B cells (Lee et al., 1999)), hematopoietic progenitor and stem cells (Liles et al., 2003), endothelial cells (Tachibana et al., 1998), microglia, neurons and astrocytes (Zou et al., 1998) among others. *Cxcr4* gene knockout caused a lethal phenotype in mice, indicating its vital role in vascularisation, hematopoiesis and organogenesis (Ma et al., 1998). Due to its role in the HIV pathogenesis, much research on CXCR4 has taken place in the last twenty years. In particular, the binding of the HIV-1 gp120 protein to the CXCR4 receptor in CD4+ T-cells, and consequent virus entry was the main focus of many studies. This allowed the development of many CXCR4 blockers (including antibodies and antagonists) which have been of great use in cancer (Donzella et al., 1998). Indeed, CXCR4/CXCL12 interaction-inhibiting approaches using anti-CXCR4 (Müller et al., 2001) or anti-CXCL12 antibodies (Orimo et al., 2005) and CXCR4-targeted small interfering RNA, siRNA (Lapteva et al., 2005) have been able to reduce the number of metastasis and cancer growth in murine models, proving the vital role they play in breast cancer. A more extensive review of these therapeutic approaches can be found in section 1.7.

The binding of CXCL12 to CXCR4 occurs in two steps. The initial interaction causes a conformational change in CXCR4 that exposes its binding pocket, allowing further interaction (Huang et al., 2003). This interaction causes the dimerization of CXCR4 and triggers a cascade of signalling pathways and molecules which promotes metastasis, but also other events which support invasion (Vila-Coro et al., 1999), a process summarised in Figure 1-5.

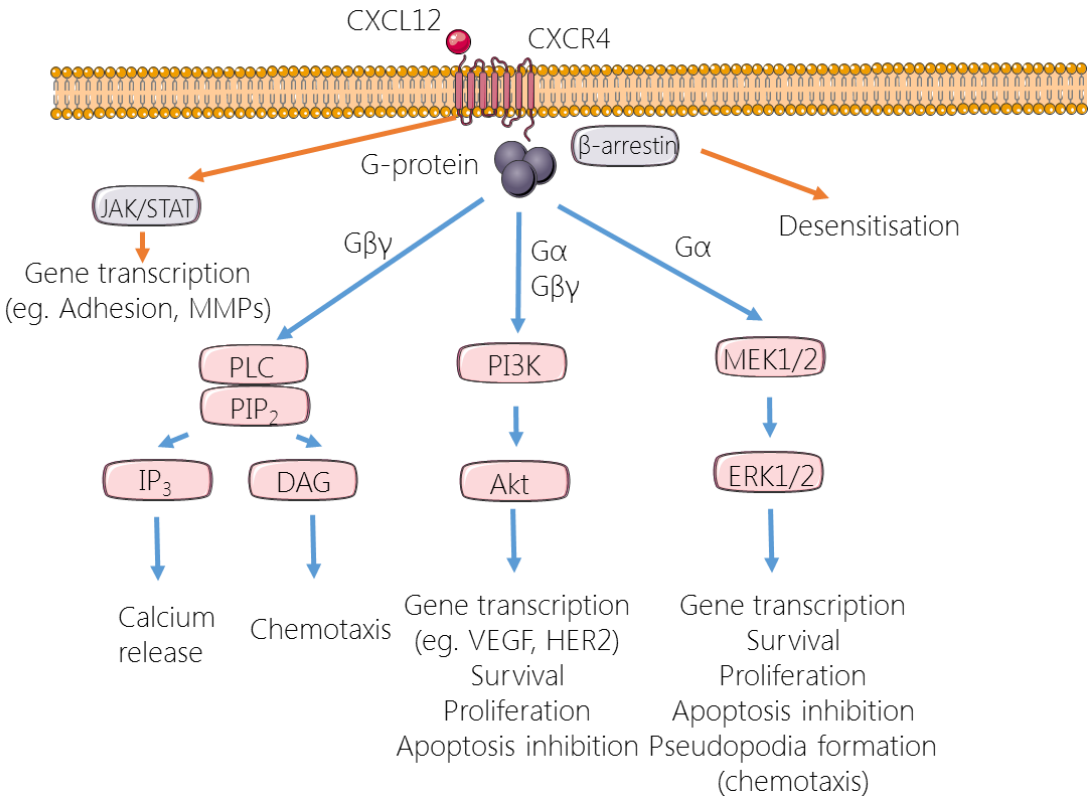

Figure 1-5. Schematic of the signalling pathways activated through CXCR4/CXCL12 and their functional consequences.
Image created using Servier image bank (http://www.servier.fr/smart/banque-dimages-powerpoint).

This includes the polymerisation of actin and formation of pseudopodia; promoting cell motility via the JAK/STAT pathway (Burger et al., 1999); the upregulation of integrins and other adhesion components (Cardones et al., 2003) and the degradation of the ECM by secreted MMPs (Kang et al., 2005). Cell survival, promotion of proliferation and inhibition of apoptosis are also promoted through the PI3K/Akt and MAPK/Erk pathways (Teicher and Fricker, 2010, Suzuki et al., 2001). Indeed, there are several reports linking CXCL12 to proliferation and survival in ovarian (Scotton et al., 2002), glioma (Zhou et al., 2002b), kidney (Schrader et al., 2002), glioblastoma (Barbero et al., 2003) and small cell lung carcinoma (Kijima et al., 2002) among others. Although still poorly understood, these levels of CXCL12 are enough to create an immunosuppressed environment where cancer cells are stimulated to grow and divide, but without hampering their migration to secondary organs. Similarly, angiogenesis has been reported to be caused by the production of VEGF through the PI3K/Akt pathway (Kijowski et al., 2001), a process which has also been reported in cancer (Luker and Luker, 2006). Furthermore, phosphorylation by the Src kinase can also enhance HER2 expression (Cabioglu et al., 2005a).

After the signalling pathway has been activated, CXCR4 becomes desensitised and degraded. More details can be found in section 1.6.

1.3.1.1. *CXCR4 upregulation inducers*

The causes for the upregulation of CXCR4 are still poorly understood, but several factors play a role. A summary diagram can be found in Figure 1-6.

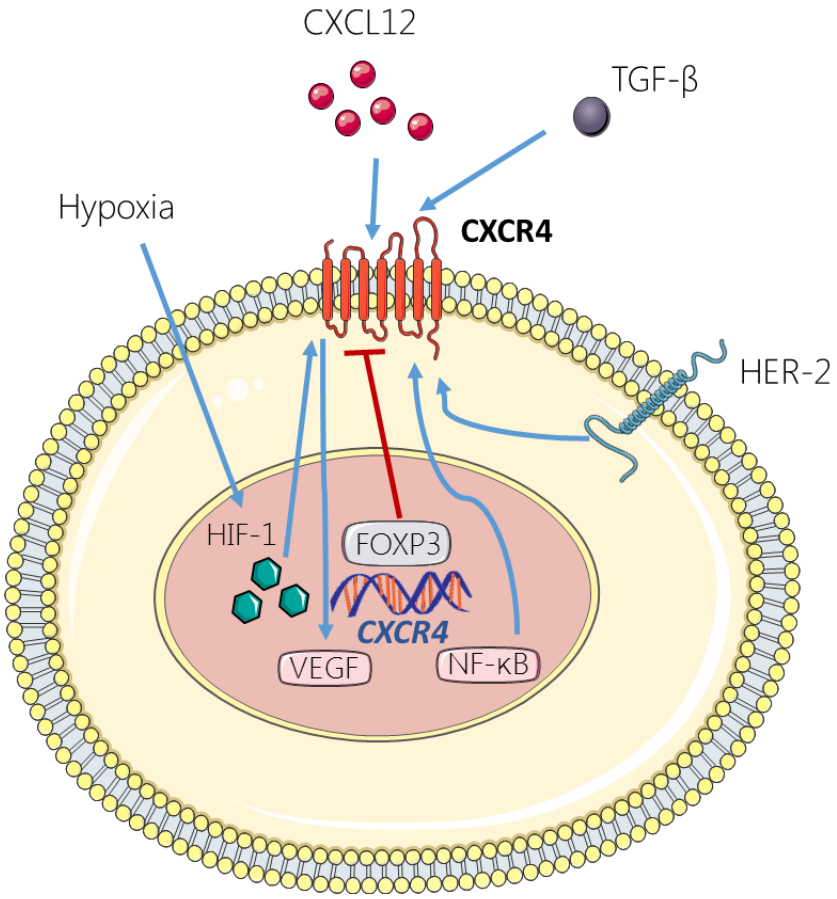

Figure 1-6. Schematic of the factors contributing to CXCR4 expression in breast cancer.
Image created using Servier image bank (http://www.servier.fr/smart/banque-dimages-powerpoint).

1.3.1.1.1. Hypoxia

Ischaemia during hypoxia and reperfusion are part of a finely regulated system where CXCL12 induction plays a key role. In many diseases such as diabetes, hypertension or stroke, the supply of oxygen to a tissue can be reduced, making them ischemic. To repair this damage, CXCL12 is upregulated in order to enhance the recruitment of resident stem cells into the injury site (Ceradini et al., 2004). In cancer a similar situation occurs, where the tumour growth is so rapid that the existing vasculature is not enough to transport sufficient nutrients and oxygen to the centre of the tumour. Indeed, the median oxygen pressure in normal breast

are between 65-67 mm Hg (mercury), whilst it more than halves in breast cancer tumours (Vaupel et al., 1991).

In conjunction to this CXCL12 upregulation, low concentrations of oxygen promote the expression of HIF-1. Briefly, HIF-1 is a transcription factor that consists of an α and a β subunits – the former is upregulated when there is a lack of oxygen, whilst the latter is constitutively expressed (Semenza, 2001). In hypoxia, HIF-1 binds the regulatory region of the *CXCR4* gene and increases its expression (Schioppa et al., 2003). This HIF-1 upregulation is exacerbated by the inactivation of the von Hippel-Lindau (*VHL*) tumour suppressor gene during hypoxic conditions (Zagzag et al., 2005). In normoxia, pVHL ubiquinates the HIF-1α subunit, marking it for degradation (Staller et al., 2003) and thus reducing the HIF-1 available to bind to *CXCR4*.

In combination, this overexpression of CXCR4 and CXCL12 creates an autocrine loop that enhances breast cancer cells' migration to new niches in search of a higher oxygen supply, thus increasing their metastatic potential (Cronin et al., 2010).

1.3.1.1.2. HER2

The proto-oncogene HER2 is another key factor in CXCR4-mediated metastasis, as it inhibits CXCR4 degradation after CXCL12 stimulation (Li et al., 2004). Thus, CXCR4 expression can be modulated by anti-HER2 antibodies such as Herceptin (Trastuzumab). Interestingly, a feedback loop is also present, and HER2 levels also can be supressed using anti-CXCR4 antibodies.

1.3.1.1.3. FOXP3

FOXP3 (forkhead box P3) is a forkhead transcription factor with a dual role – in regulatory T-cells (Treg) it participates in the inactivation of auto-reacting T-cells; whilst in epithelial cells it represses several oncogenes (Martin et al., 2010). Thus, FOXP3 downregulation in cancerous cells promotes the expression of HER2, SKP2 (S-phase kinase-associated protein 2) and cMYC, with recent studies also showing a correlation with an increase in CXCR4 (Overbeck-Zubrzycka, 2012, Douglass et al., 2012). Indeed, it has been shown that following FOXP3 knockout, this increase in CXCR4 correlates with higher cell motility (Douglass et al., 2014). Furthermore, similar to what has been observed with oncogenes such

as HER2, SKP2 and c-Myc, a poorer prognosis is correlated with the incorrect location of FOXP3 in the cytoplasm instead of the nucleus (Merlo et al., 2009, Ladoire et al., 2011).

The *FOXP3* gene is located in the p arm of the X chromosome (in position Xp11.23) and is formed by 11 coding exons. It encodes a 431 amino acid protein with four main domains: a repressor domain, a zinc finger, a leucine zipper motif, and the DNA-binding forkhead (FKH) domain (Douglass et al., 2012). This FKH domain is characteristic of the FOX protein family, and acts as the transcriptional activator and repressor of approximately 700 genes. Nevertheless, it is important to note that as long as the repressor domain (a region between residues 67 and 132) is intact, the absence of the FKH domain does not significantly diminish gene transcription repression (Lopes et al., 2006). Furthermore, human *FOXP3* presents two isoforms in equal proportion – the full length, and a splicing variant lacking exon 3. Apart from not being able to generate Th17 cells, no other differences in function have been reported between the two (Allan et al., 2005).

The FOXP3 protein presents a high percentage of homology with other mammals (from 97% in rhesus monkey to 86% in mice) and has a short half-life of about 21 minutes before being degraded (Lee et al., 2008). Its mode of action involves binding near the transcriptional start of the target gene and modulating the histone modifications. Briefly, acetylation of H3 and H4 and tri-methylation of H3K4 cause the chromatin to de-condense and thus be open for transcription (Lee and Workman, 2007). FOXP3 recruits MOF (a histone acetyltransferase) which acetylates the histone H4K16, the first event that regulates chromatin de-condensation; and displaces the demethylase PLU-1.

Chromatin-immunoprecipitation (ChIP) studies have identified several FOXP3-binding sites in breast cancer cells, including the *CXCR4* gene (Katoh et al., 2011). In particular, the binding site for CXCR4 is found in the negative strand of chromosome 2,770 bp from the transcription start site. mRNA expression was shown to decrease 4.29 times after FOXP3 was induced, supporting the link between the two (Katoh et al., 2011).

1.3.1.1.4. Others

There are many other pathways that upregulate CXCR4 expression, making targeting the upstream effectors a hard task. *In vitro*, TGF- β1 has been shown to upregulate CXCR4 (Zhao et al., 2010), enhancing tumour cells' metastatic potential. VEGF also increases CXCR4 expression but in an autocrine manner (Bachelder et al., 2002). Briefly, CXCL12 binding to CXCR4 enhances VEGF promoter activity through the Akt pathway (Liang et al., 2007b) - VEGF will in turn bind to the receptor Neuropilin, regulating CXCR4 expression. Similarly, the transcription factor NF-κB can also be abnormally constitutively activated, which upregulates CXCR4 – this potentially activates the PI3K/Akt pathway, which would in its turn induce NF-κB (Helbig et al., 2003).

Post-transcriptional and post-translational changes in CXCR4 can also enhance its expression. Oestrogens upregulate the expression of CXCR4 (and CXCL12) by binding to their promoters (Boudot et al., 2011, Sengupta et al., 2009), whilst the hepatocyte growth factor (HGF) upregulates CXCR4 through the atypical PKCζ – however, the mechanisms behind this are still unclear (Huang et al., 2012).

1.3.2. CXCR7 and CXCL12

CXCR7 is a chemokine receptor which has been found to be upregulated in many cancers, including breast (Zlotnik and Yoshie, 2000, Miao et al., 2007), and seems to correlate with malignancy. It is also vital for correct embryogenesis to occur, due to its role in neuronal (Infantino et al., 2006, Wang and Zhou, 2011), cardiac (Sierro et al., 2007, Gerrits et al., 2008, Klein et al., 2014) and lymphatic vascular development (Klein et al., 2014), primordial germ cell migration (Boldajipour et al., 2008, Doitsidou et al., 2002) and B-cell localisation (Thelen and Thelen, 2008).

Unlike other chemokine receptors, CXCR7 has not been shown to activate G-proteins, most likely due to a change in the alanine and valine in the DRYLAIV motif that may affect the potential coupling (Thelen and Thelen, 2008). This means that upon the binding of its ligands CXCL11 and CXCL12 it does not activate G-proteins, and thus there is no calcium flux or integrin activation *in vitro* (Rajagopal et al., 2010). Instead, when CXCR7 is upregulated in the cell it mediates the capture and degradation of its ligands, and for many years it was known as a scavenging receptor. Indeed, CXCR7 has a tenfold higher affinity for CXCL12 than CXCR4, thus is able to reduce CXCL12's

availability and promote its internalization and degradation via β-arrestin *in vitro* (Luker et al., 2010). However, it has also been pointed out that in situations where CXCL12 is released continuously, scavenging may not be enough to regulate its signalling (Uto-Konomi et al., 2013).

CXCR7 (previously known as RDC-1, *R*eceptor *D*og *c*DNA 1) was first de-orphanized in 2005, where Balabanian and colleagues (Balabanian et al., 2005) first described it as a CXC chemokine receptor which bound CXCL12 with high affinity, but without triggering the signalling pathway. Previously, CXCR7's ligand was unknown for many years – first it was thought to be a vasoactive intestinal peptide (VIP) receptor (Cook et al., 1992, Libert et al., 1991) and then a receptor for adrenomedullin (Autelitano, 1998). Sequencing (Heesen et al., 1998) and phylogenetic studies (Heesen et al., 1998), together with its observed role in HIV-1 pathogenesis (Shimizu et al., 2000), finally put scientists on the right track to classify it as a chemokine receptor that can bind CXCL11, CXCL12 and small peptide ligands such as proenkaphalin A (Ikeda et al., 2013) and adrenomedullin. In particular, it is the latter than mediates cardiac and lymphatic vascular development, being able to rescue the cardiac hyperplasia and lymphatic hyperproliferation in *Cxcr7*$^{-/-}$ mice (Klein et al., 2014).

In the absence of ligand, CXCR7 gets internalised into endosomal compartments and comes back to the surface in a cyclic manner. A similar pattern can be seen in the presence of CXCL12, with CXCR7 degrading CXCL12 even at saturating concentrations (Naumann et al., 2010) through β-arrestin and clathrin coated pits (Kalatskaya et al., 2009). As previously mentioned, CXCR7 was shown to not be coupled to G-protein (Burns et al., 2006), but reports on its signalling cascade and its functional consequences are often contradictory. There are currently three proposed mechanisms of action through which CXCR7 can mediate. First, as a non-signalling entity, it has been suggested that CXCL12 scavenging allows for a formation of a steeper chemokine gradient, enhancing the migration of CXCR4-expressing cells in zebrafish (Dambly-Chaudière et al., 2007, Boldajipour et al., 2008). A second theory is that the signalling is mediated by the formation of CXCR4 and CXCR7 heterodimers, which can modify the G-protein signalling pathways (Levoye et al., 2009). Indeed, several studies showed a clear link between CXCR4 and CXCR7 expression (Infantino et al., 2006). A third, and most recent hypothesis, is that CXCR7 not only mediates CXCL12 degradation through β-arrestin, but can also signal through this non-G-protein

mediated pathway (Rajagopal et al., 2010). In the canonical pathways, the GPCR gets phosphorylated after ligand activation and recruits β-arrestin, which in turn mediates the binding of clathrin and the AP-2 complex. The receptor then can get internalised to the endosomes, from where it can be degraded or recycled (Pierce and Lefkowitz, 2001). However, it has recently been proposed that β-arrestin can serve as a scaffold to which several kinases can bind and become activated (Luttrell et al., 2001)– this includes ERK1/2 and its cascade elements Raf and MEK (Tohgo et al., 2002, Luttrell et al., 2001) and JNK3 with the kinases ASK1 and MKK4 (Pierce and Lefkowitz, 2001, McDonald et al., 2000). Indeed, there are also studies proposing β-arrestin can regulate NF-κB (Gao et al., 2004, Witherow et al., 2004) and p53 (Wang et al., 2003) through IκBα and MDM2, respectively.

Furthermore, recently CXCR7 was shown to be overexpressed in many cancers, including lung cancer (Goldmann et al., 2008, Iwakiri et al., 2009), prostate cancer (Wang et al., 2008b), glioma (Hattermann et al., 2010), liver cancer (Zheng et al., 2010), pancreatic cancer (Marechal et al., 2009) and melanoma (Schutyser et al., 2007). However, reports between cancers are contradictory on whether CXCR7 expression is pro- or anti-tumorigenic.

In prostate cancer, studies have shown that CXCR7 enhanced tumour growth (Wang et al., 2008b), adhesion and invasion, probably through CD44 and cadherin 11 activation. CXCR7 also increased angiogenesis through the upregulation of IL-8 or VEGF via Akt (Wang et al., 2008b). Indeed, due to its role during embryo development, CXCR7 expression has repeatedly been associated with proangiogenic factors such as VEGF (Wang et al., 2008b, Zheng et al., 2010, Hernandez et al., 2011). Similarly, an increased adhesion to fibronectin and invasion potential was also observed in hepatocarcinoma cells, in addition to increased VEGF secretion (Zheng et al., 2010). In lung, blocking CXCR7 through siRNA (Miao et al., 2007) or an antagonist (Burns et al., 2006) results in smaller tumours in *in vivo* mouse models.

Similarly, studies in breast cancer have shown that CXCR7 causes increased tumour growth (Burns et al., 2006) and metastases through the MAPK pathway (Miao et al., 2007). CXCR7 has also been linked to increased tumour cell survival by preventing apoptosis in prostate (Wang et al., 2008b) and breast cancer (Burns et al., 2006) in cell lines *in vitro* and *in vivo*. Other studies also suggest that CXCR7 enhances pancreatic cancer cells' migration and invasion, but this time through the mTOR signalling

pathway (Guo et al., 2016). Furthermore, in rhabdomyosarcoma cell linesCXCR7 has also been linked to MMPs expression and enhanced metastatic potential (Grymula et al., 2010). Further to CXCR7's metastatic involvement, other studies suggest that CXCL12 scavenging establishes the formation of chemokine gradients, allowing directional migration of cancer cells instead of random movement that would occur in constant levels of CXCL12 (Luker et al., 2012, Torisawa et al., 2010). Indeed, studies with primary T-cells (Balabanian et al., 2005) and rhabdomyosarcoma cell lines (Grymula et al., 2010) have reported CXCR7 plays a role in chemotaxis towards CXCL12 *in vitro* and *in vivo*. Relatedly, $CXCR4^{+}$ lymphocytes of β-arrestin-deficient mice failed to show chemotaxis to CXCL12 (Fong et al., 2002), a phenomena also seen *in vitro* in HEK-293 cells (Sun et al., 2002), hinting at the importance of β-arrestin mediated signalling.

On the other hand, different studies affirm CXCR7 plays no role in chemotaxis at all. In opposition to Balbanian and colleagues, another study shows that CXCR7 does not mediate T-cell chemotaxis *in vitro* (Hartmann et al., 2008), whilst another reports that it may play a role in trans-endothelial migration, but not in bare filter chemotaxis *in vitro* (Zabel et al., 2009). Indeed, there are several reports linking CXCR7 to an enhanced adhesion to HUVEC (Burns et al., 2006) and HBMEC cells (Wang et al., 2008b) to fibronectin (Zheng et al., 2010, Grymula et al., 2010). Studies by Hernandez and colleagues (Hernandez et al., 2011) also show that CXCR7 does not have an effect on the chemotaxis of mammary adenocarcinoma cells *in vitro*. In contrast to other studies, it has also been reported that CXCR7 plays no role in cell proliferation or survival in rhabdomyosarcoma cell lines (Grymula et al., 2010). Inhibition of CXCR7 also did not impact on migration or development of metastases in non-small cell lung cancer cell lines (Choi et al., 2014). Furthermore, in mammary adenocarcinoma CXCR7 expression *in vivo* actually reduces invasion, intravasation and metastasis, probably through its scavenging function and a lack of MMP12 induction (Hernandez et al., 2011). Similarly, other studies have shown than in neuroblastoma cell lines, CXCR7 expression actually reduces both *in vitro* and *in vivo* growth, and can even reduce metastasis (Liberman et al., 2012). Furthermore, unlike CXCR4, CXCR7 expression is not correlated with a poorer prognosis in oesophageal (Tachezy et al., 2013) or rectal cancer (D'Alterio et al., 2014).

In summary, even though it has been reported that CXCR7 plays an important role in cancer, it is still not clear which specific functions it is involved in. So far, there are four hypothesis: (1) CXCR7 mediates as a scavenger, (2) CXCR4 and CXCR7 activate similar signalling pathways but through G-proteins and β-arrestin, respectively, (3) CXCR4 and CXCR7 mediate different functions, for instance migration vs adhesion and (4) CXCR4 and CXCR7 form heterodimers and potentiate certain pathways in favour of others. This latter possibility will be further explored in section 1.5.

Taken together, this literature suggests that CXCR7's role may vary in different cancers and may be dependent on ligand concentration. One proposed hypothesis is that at lower concentrations, the predominant effect of CXCR7 is preventing the binding of CXCL12 to CXCR4, thus supressing chemotaxis (Levoye et al., 2009); whilst at higher concentrations it may help the formation of a steep CXCL12 gradient (Hernandez et al., 2011). A second important point is that some of these studies did not consider the possibility of CXCR4/CXCR7 heterodimers, which may require a reinterpretation of the results. Lastly, it is important to note that some of the CXCR7 antibodies used in the studies are not specific (Berahovich et al., 2010a), and thus the results should be taken with caution.

1.3.3. CCR7 and CCL21

In cancer, a similar scenario to CXCR4 can be observed with CCR7 and its main ligands CCL19 and CCL21, which are overexpressed in the lymph nodes (Müller et al., 2001). Indeed, CCR7 has been shown to play a role in the metastasis of melanoma (Takeuchi et al., 2004, Shields et al., 2007a), breast (Cabioglu et al., 2005b, Liu et al., 2010, Müller et al., 2001), hepatocellular (Schimanski et al., 2006), prostate (Heresi et al., 2005), thyroid (Sancho et al., 2006), colorectal (Günther et al., 2005), cervical (Kodama et al., 2007), oesophageal (Ding et al., 2003), head and neck (Wang et al., 2008a) and non-small cell lung cancer (Koizumi et al., 2007). In the majority of these cancers, a poorer survival rate was associated with CCR7 expression, and in some cancers a relation with larger tumour size and deeper invasion was also found (Takeuchi et al., 2004, Günther et al., 2005, Ishigami et al., 2007).

In health, CCL21 and CCL19 are constitutively expressed at the beginning of the lymphatic vessels, and in lymphoid organs they are present on the high endothelial venules (HEVs) and on several stromal cells. CCR7, a GPCR, is commonly expressed by

mature DCs (Ohl et al., 2004), thymic T-cells (Misslitz et al., 2004) and the T-cell subset central memory cells (Sallusto et al., 1999), B cells (Reif et al., 2002) and other rarer cell subsets such as CD4+ CD25+ splenocytes (Szanya et al., 2002).

CCL21 was first identified in 1997 (Nagira et al., 1997) due to its ability to mobilise lymphocytes to the various lymphoid tissues where it was expressed, giving it the name, *s*econdary *l*ymphoid tissue *c*hemokine (SLC). As CCL21 presents two additional cysteines, it was also known as 6Ckine (Fernandez and Lolis, 2002, Hedrick and Zlotnik, 1997). On the same year, CCL19 was also identified and found to bind the then-orphan receptor EBI1, and was aptly named *E*BI1-*L*igand *C*hemokine (ELC). Soon after, EBI1 was renamed CCR7 due to its newly discovered role in the migration of activated B and T lymphocytes. One year later, CCL21 was also identified as a ligand for CCR7 (Yoshida et al., 1998). These two chemokines can also bind and be scavenged through the atypical chemokine receptor CCX-CKR (Comerford et al., 2006, Gosling et al., 2000).

Interestingly, even though both CCL19 and CCL21 can activate CCR7's G proteins with similar affinity and induce the ERK1/2 signalling pathway and calcium flux, redundancy is unlikely. First, only CCL19 causes receptor desensitisation, a process where CCR7 is phosphorylated, internalised, and recycled back to the surface after a chemokine wash (Bardi et al., 2001), implying that CCL19 effects may be more transient than with CCL21. CCR7 desensitisation and its ERK activation is mediated through β-arrestin, which may explain why the phosphorylation is four times stronger than with CCL21 (Kohout et al., 2004).

Second, their structures differ. Unlike CCL19, CCL21 presents a 32 amino acids long, basic C-ter, which allows CCL21 binding to GAGs and its immobilisation in the surface of endothelial cells (Yoshida et al., 1998). This means that only CCL21 is required for the intravasation into afferent lymphatic vessels (Britschgi et al., 2010, Weber et al., 2013) – indeed, *in vivo* C-ter truncation prevents lymphocyte adhesion and extravasation to the HEVs (Stein et al., 2000). Interestingly, in DCs immobilised CCL21 causes haptokinesis (random movement) and integrin-mediated adhesion, whilst soluble CCL19 causes chemotaxis (directed migration). When both chemokines were present (or had both soluble and immobilised CCL21), DCs migrated through a combined directional haptokinesis (Schumann et al., 2010). This model allows for cells to migrate even against turbulences, whilst still maintaining the directionality that DCs show in lymphatic organs.

CCR7 has been widely reported to mediate naive T-cell homing to the lymph nodes through the HEVs (Förster et al., 1999), a process that requires interaction with the lymphatic vessel's endothelium as depicted in figure 1-7. Once on the lymph node, they will remain in the paracortex thanks to the fibroblastic reticular cell network (Bajénoff et al., 2006) which expresses CCL21 and CCL19, eliciting non-directional migration with no firm integrin adhesion (Worbs et al., 2007). Moving T-cells may become activated in the lymph nodes, where DCs continuously migrate and present antigens. DCs in their naïve state reside in the skin and mucosa and only migrate to the towards the afferent lymph vessels at low frequencies (Banchereau and Steinman, 1998); but when there is an infection they become activated by pathogen-associated molecular patterns (PAMPs) or inflammatory cytokines and mature. DC maturation causes the upregulation of MHC class II and CCR7 among other co-stimulatory molecules, allowing the presentation of antigens (Sozzani et al., 1998, Yanagihara et al., 1998). It is still not well characterised how mature DCs traffic to the lymph nodes via the afferent lymphatics, although studies show that CCR7 overexpression is key (Dieu et al., 1998, Clatworthy et al., 2014, Saeki et al., 1999). Furthermore, it has been proposed that when DCs reach the lymph nodes they are guided from the subcapsular sinus to the T-cell rich areas by CCL21 and CCL19, where DCs will prime the T-cells.

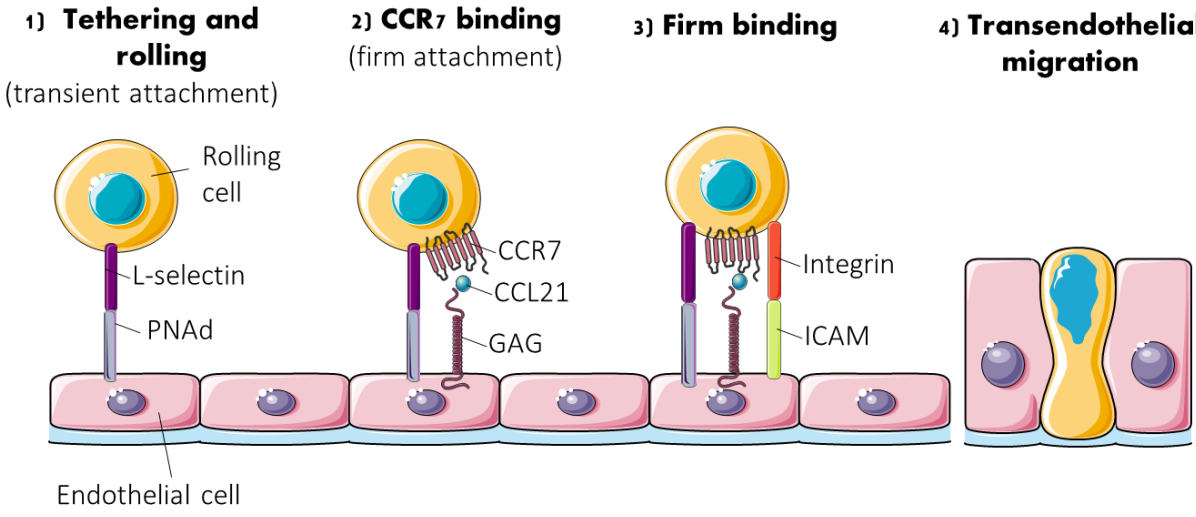

Figure 1-7. CCR7 role in transendothelial chemotaxis.
Cancer cells mediate metastasis in a very similar manner than naïve T-cells migrate to the peripheral lymph nodes. Briefly, the l-selectin expressed by the migratory cell binds to peripheral-node addressins (PNAd) expressed by the endothelial cells lining the blood vessels. This provides a transient attachment before the blood whisks the cell away, which will then bind to the next PNAd in the venule in a "rolling" motion. At this point, the CCR7 expressed on the migratory cell can be activated by the CCL21 presented by the GAGs in the endothelium. The CCR7 signalling will mediate a conformational change in the αLβ7 integrin (also known as lymphocyte function associated antigen 1, LFA-1) which will increase its affinity for its ligands, the intercellular adhesion molecule 1 (ICAM1 or CD54) and ICAM2 (CD102). This allows a firm binding of the cell to the endothelium and its migration towards the lymph node. Image adapted from (Förster et al., 2008) and created using Servier image bank (http://www.servier.fr/smart/banque-dimages-powerpoint).

Other roles for CCR7 have also been suggested, including the migration of "double negative" thymocytes through the cortex and medulla compartments of the thymus , and the retention of "single positive" cells in the medulla (Misslitz et al., 2004). However, more studies are required to pinpoint the exact functions of this chemokine pair and their receptor.

Initial reports suggested that CCL21 and CCL19 were anti-tumorigenic, as they could attract lymphocytes that would attack the tumour (Kim et al., 1999, Vicari et al., 2000, Braun et al., 2000). However, it has now been described that in CCL21-expressing tumours the chemokines create a tolerogenic environment where lymphocytes behave similarly to the lymph node stroma (Shields et al., 2010). Cancers may also impair DC migration to the draining lymph nodes (Triozzi et al., 2000), perhaps by affecting the availability of some molecules necessary for the optimal migration of DC in addition to CCR7 (Randolph, 2001). Another possibility is that immature DCs may attach to the cancer cells, a phenomena seen in breast cancer patient samples (Bell et al., 1999) and melanoma cells *in vitro* (Remmel et al., 2001), effectively sequestering them and preventing them from activating T-cells.

There is also a lack of consensus regarding the consequences of ligand overexpression in the lymph nodes. One study observed that CCL19 and CCL21 levels are higher in lymph nodes with a metastatic spread (Wilson et al., 2006), whilst another described that in melanoma patients, CCL21 levels are higher in metastasis-negative lymph nodes (Takeuchi et al., 2004). Interestingly, another study suggests we should be looking at generation of the chemokines by the tumour cells themselves instead of the lymphatic vessels (Shields et al., 2007b). This autocrine secretion uses the interstitial flow to generate a gradient towards the lymphatics, and this migration can be boosted by the homeostatic chemokine secreted by the lymphatic cells.

Apart from its role in cancer cell recruitment to the lymph nodes, CCR7 has also been shown to induce actin polymerisation and pseudopodia formation in breast cancer cells *in vitro* in response to ligand binding, which confers the cell its chemotactic and invasive properties (Müller et al., 2001). Similarly, CCR7 overexpression increases *in vitro* adhesion and trans-endothelial migration of primary cancer cells in leukaemia (Hasegawa et al., 2000, Till et al., 2002) and lung cancer through the overexpression of α4β1-integrin and the adhesion to VCAM-1 (Koizumi et al., 2007). Increased adhesion has also been described *in vitro* in thyroid cancer but, interestingly, this also correlated

with increased MMP-2 and MMP-9 secretion (Sancho et al., 2006), an overexpression also observed in leukaemia primary cells (Redondo-Muñoz et al., 2008) and colon cancer cell lines (Li et al., 2011a). CCL21 has also been linked to MMP-2 and MMP-9 secretion and apoptosis inhibition in bladder cancer (Mo et al., 2015). Similarly, other studies in non-small cell lung cancer have also linked CCR7 to the promotion of proliferation through cyclin upregulation (Xu et al., 2011b) and the prevention of apoptosis through bcl-2 and caspase-3 (Xu et al., 2012) via the ERK pathway *in vitro*.

CCR7 has also been linked to the creation of new blood and lymphatic vessels in pancreatic cancer (Zhao et al., 2011) and breast cancer (Tutunea-Fatan et al., 2015) patient samples, though the mechanism is still not well understood. The current hypothesis is that this lymphangiogenesis is mediated through VEGF-C and its receptors VEGFR-2 and VEGFR-3 (Guo et al., 2013, Tutunea-Fatan et al., 2015). Indeed, overexpression of this growth factor has been well documented to increase lymph node metastasis (Skobe et al., 2001, Mandriota et al., 2001, He et al., 2005). Interestingly, there are also studies suggesting that whenever tumour cells express CCL21 it has an anti-tumorigenic effect through the inhibition of angiogenesis (Vicari et al., 2000) and increase of leukocyte recruitment, in particular of $CD8^+$ T-cells and DCs (Vicari et al., 2000, Nomura et al., 2001). However, on its own this immune response is suboptimal – as stated previously, this could be due to the lack of maturation of the DCs.

Despite all the evidence linking CCR7 expression to a poorer prognosis, still much remains unknown about the mechanisms behind its upregulation. In breast cancer, hypoxia has been shown to increase CCR7 expression through the HIF-1 mediated activation of endothelin receptor A (Wilson et al., 2006). Indeed, other studies have reported the overexpression of endothelins in breast tissues (Alanen et al., 2000). Epigenetic factors could also play a role in CCR7 upregulation, with histone deacetylation and DNA methylation playing a role in gene activation (Mori et al., 2005).

1.3.4. CXCR4 and CXCR7 in the microenvironment

As mentioned previously, the microenvironment is key in supporting and promoting the growth and survival of the tumour. Part of this process is mediated through CXCR4 and CXCL12, which are expressed by cancer associated fibroblasts (CAFs). The CXCL12 secreted by these cells can directly stimulate CXCR4-expressing cancer cells (paracrine stimulation) or recruit endothelial progenitor cells which will enhance angiogenesis (endocrine stimulation) (Orimo et al., 2005).

In prostate cancer, stromal cells can also upregulate CXCR4 expression by secreting TGF-β. This causes epithelial cells to become responsive to CXCL12 and trigger the Akt pathway, which induces tumorigenesis in these cells (Ao et al., 2007). In turn, cells become refractory to TGF-β which would halt their aberrant growth. A similar situation occurs in neuroblastoma, where IL-5 and IFN-γ can modulate CXCR4 expression (Zhang et al., 2007).

Interestingly, CXCR7 has been found to also be upregulated in the surrounding microenvironment, in particular tumour associated vasculature in breast, lung (Miao et al., 2007), brain (Madden et al., 2004), liver (Monnier et al., 2012) and colorectal cancer (Guillemot et al., 2012). These studies propose that it is CXCR7 expression in the tumour vessels, instead of the tumour cells, which is upregulated in all cancers. Other studies also found upregulation of CXCR7 in the endothelium of breast cancer, however they proposed endothelial CXCR7 has a protecting effect, limiting tumour growth, survival and intravasation (Stacer et al., 2015). Supporting this, deletion of CXCR7 from the vascular endothelium in breast cancer caused increased CXCL12 levels in plasma, which in turn internalised CXCR4 and impaired chemotaxis.

1.4. GLYCOSAMINOGLYCAN (GAG) BINDING

The ECM and surfaces of most mammalian cells are coated with GAGs, a type of polysaccharide formed by the repeat of a disaccharide unit. Depending on the nature of these two sugars and the length of the chain (their weight can vary from 10 to 100 kDa), they can be classified in several families. A first classification can divide GAGs into (1) non-sulphated, which includes hyaluronic acid/hyaluronan and (2) sulphated, which includes chondroitin sulphate, dermatan sulphate (previously known as chondroitin sulphate B), keratan sulphate and heparan sulphate (HS)/ heparin (Gandhi and Mancera, 2008). These latter four families have different disaccharide units and posttranslational modifications – a summary can be found in the table 1-5 below.

Name	***Hexosamine***	***Hexuronic acid***	***Sulphation***	***Synthesis***	***Glycosi-lation***
Chondroitin sulphate	Galactosamine	α-L-iduronic acid or β-D-glucuronic acid	X-sulphated	Golgi	O-linked
Dermatan sulphate	Galactosamine	α-L-iduronic acid or β-D-glucuronic acid	X-sulphated	Golgi	O-linked
Heparan sulphate/ heparin	Glucosamine	α-L-iduronic acid or β-D-glucuronic acid	X-sulphated Y-sulphated /acetylated	Golgi	O-linked
Hyaluronic acid	Glucosamine	β-D-glucuronic acid	None	Integral plasma membrane synthase	
Keratan sulphate	Glucosamine	β-D-galactose	X-sulphated	Golgi	O-linked or N-linked

Table 1-5. Compilation of the five glycosaminoglycan families and their main characteristics.

Except heparin and hyaluronan, which are secreted to the extracellular space, these GAG are membrane-bound. Each GAG can be sulphated in both the amino acid and the sugar chain, but whilst the former can only be sulphated in a few residues, the latter can have over a million different sulphations. At physiological pH, all these sulphate groups

(together with the carboxyl groups) are protonated, making GAGs a highly negatively charged entity (Capila and Linhardt, 2002).

This highly variable structure and location allows them to have a vast range of substrates, including growth factors (e.g. fibroblast growth factor-2 (FGF-2)), proteases (e.g. MMPs), cell matrix proteins (e.g. fibronectins), angiogenic factors (e.g. VEGF) and chemokines, among others. Thus, GAGs are involved in many cell signalling activities, including during morphogenesis (Toole, 2001) and angiogenesis (Iozzo and San Antonio, 2001, Vlodavsky et al., 2002) but also in cancer (Sanderson et al., 2005, Sasisekharan et al., 2002, Liu et al., 2002) and microbial pathogenesis (Shukla et al., 1999, Rostand and Esko, 1997). However, GAGs are probably best known for their anticoagulating properties (Damus et al., 1973) and role in wound healing. Indeed, heparin is still used to prevent deep vein thrombosis and pulmonary embolism (among other conditions) given its inhibitory action against thrombin. Nowadays, the use of low-molecular-weight heparins (LMWHs) is more widespread given their lesser side effects and comparable efficacy. It was thanks to these clinical trials that it was observed that patients treated with LMWHs had a prolonged cancer survival (Smorenburg and Van Noorden, 2001, Zacharski et al., 2000), an effect not seen with other anticoagulants like warfarin. Indeed, studies in our group have shown that heparin can inhibit *in vitro* migration and metastasis in a murine *in vivo* model (Mellor et al., 2007, Harvey et al., 2007). However, still much remains unknown about the exact mechanism through which they mediate this effect.

Recently there has been an increased interest in GAGs' role in forming chemokine gradients given their importance during metastasis. Although generally chemokines are small monomeric proteins, in order to bind GAGs some form dimers or other oligomers (Proudfoot et al., 2003). Interestingly though, only monomers can bind chemokine receptors which means chemokines need to dissociate before binding their receptor (Kufareva et al., 2015). Furthermore, *in vitro* studies have shown that binding to HS is observed in the majority of chemokines (Lortat-Jacob et al., 2002), a binding that can be very specific. Indeed, the variations in the GAGs' sulphation patterns promote the binding of specific chemokines, and thus some chemokines will have a higher affinity for some GAGs than others (Witt and Lander, 1994). This, together with the variations seen between different chemokines' GAG-binding residues, hints at GAGs being able to differentiate between chemokines (Johnson et al., 2005, Lau et al., 2004). This interaction is further complicated by the presence of sulphotransferases in the intracellular space,

which may increase chemokine binding through a higher GAG sulphation (Carter et al., 2003). At last, GAGs have also been reported to promote chemokine oligomerisation (Hoogewerf et al., 1997), a process that is vital for *in vivo* (but not *in vitro*) functionality (Proudfoot et al., 2003).

Given this complexity, it is not surprising that the interaction between chemokines, chemokine receptors and GAGs is still a point of study. To complicate the matter further, this interaction may also be altered by external components. For instance, it has been described that plasmin activity can shed immobilised IL-8 that is bound to the HS syndecan-1 so gradients are disrupted (Marshall et al., 2003). Conversely, matrilysin can also cleave the syndecan-1 sequestering CXCL1, which can then form a soluble gradient (Li et al., 2002). A similar effect can also be seen in heparanase-mediated release of growth factors. Finally, soluble GAGs can also bind chemokines and prevent binding to its receptor (Kuschert et al., 1999), a phenomena observed with CCL5 and chondroitin sulphate (Mack et al., 2002).

In most cases, chemokine presentation through GAGs does not induce any signalling pathway. There is however one exception, in which GAG-coated CD44 can serve as a functioning receptor for high concentrations of CCL5 (Roscic-Mrkic et al., 2003, Chang et al., 2002). This lack of signalling, together with GAGs moderate affinity for chemokines, mean that soluble heparin and LMWHs can to some extent compete with chemokines receptors for its ligands. Previous studies have shown that heparinoids can inhibit adhesion and migration in T-cells (Hecht et al., 2004) and migration in breast cancer cell lines (Harvey et al., 2007) when competing with CXCR4 for CXCL12. However, their anticoagulating properties prevent their continuous administration in therapy.

The high variability in GAGs, combined with their difficulty to be synthesised, makes certain GAGs more commonly investigated than others. For instance, HS is one of the best studied GAGs - it is formed by the repetition of uronic acid and glucosamine, which can be modified at the 2-O of the former or the 6-O and 3-O of the latter (Bishop et al., 2007, Conrad, 1997). This makes HS a highly sulphated GAG, making it an ideal model to investigate protein binding (Whitelock and Iozzo, 2005) as these heavy anionic sulphated sequences are the ones binding the cationic amino acid domains in the proteins. *In vivo*, HS is often found binding to several proteins (forming proteoglycans) and thus can be further divided into three different types: syndecans and glypicans, which are membrane-bound, and perlecans, which are secreted to the extracellular matrix.

GAGs play an important role in tumour growth and angiogenesis, with some GAG fragments being pro-tumorigenic and others being anti-tumorigenic depending on whether they are anchored to a cell surface or not (Liu et al., 2002). Indeed, a markedly different GAG sequence, structure and abundance between normal and cancerous tissues has been described (Sasisekharan et al., 2002, Sanderson, 2001). As previously described, their more well-known role in cancer is the migration of the tumour cells through the binding of chemokines such as CXCL12, CCL21 and CCL10 (Johnson et al., 2005), but they can also promote tumour growth by binding growth factors. GAGs also bind anti-angiogenic factors such as endostatin, but this time sequestering them to prevent their action (Blackhall et al., 2003). Furthermore, GAGs present on the cancer cell surface mediate cell adhesion to the blood vessels via both P-selectin and integrins, facilitating extravasation (Sasisekharan et al., 2002, Varki and Varki, 2002). GAGs on the endothelial cells' surface also contribute to the tumour growth by promoting angiogenesis through the binding of VEGF and FGF2 (Nillesen et al., 2007).

At the same time, GAGs also mediate important anti-metastatic effects as the LMWH trials showed. First, as part of the ECM GAGs provide a barrier for cancer cells to surpass in order to migrate to distant organs. Cancer cells have also been described to secrete heparanases together with MMPs to degrade HS GAGs (Blackhall et al., 2003) and even linked with a higher metastatic rate in breast cancer (Kelly et al., 2005) and myeloma patients (Kelly et al., 2003, Yang et al., 2005). To counter this, mimics of heparan sulphate have been proved successful in blocking the heparanase activity (Parish et al., 1999), also preventing the release of FGF2. The anticoagulant properties of heparin could also counteract the thrombin produced by cancer cells, breaking down the fibrin barrier that envelops and hides tumours from the immune system (Godlee et al., 1999). Heparin also plays a role by blocking the P-selectin expressed by platelets, preventing their binding to circulating cancer cells and thus hampering their chances at successfully metastasising (Varki and Varki, 2002).

However, much of GAGs still remains unknown given the difficulty to obtain a homogenous sample. Indeed, heparin is the only one widely available, and as a soluble GAG it has many shortcomings in the investigation of chemokine presentation through GAGs.

1.5. RECEPTOR HETERODIMERIZATION

Although it was initially believed that GPCR existed as monomers, studies over the last 20 years have established that GPCR can not only oligomerise, but that it is a necessary step for their correct function (George et al., 2002). Indeed, it has been shown that if dimerization is blocked no signalling occurs (Wang et al., 2006). Although most studies to date have focused in dimerization, the most common and least complex oligomer, it is important to note that GPCR tetramers (Nimchinsky et al., 1997, Lee et al., 2000) and even octamers have been described (Chidiac et al., 1997) .

When this dimerization occurs, however, is still a point of debate. The generally accepted theory is that dimers are formed in the endoplasmic reticulum (ER), where extensive quality control will be carried out before the receptor is sent to the cell surface. This co-localisation has been observed in CCR5 (Issafras et al., 2002), C5a receptor (Floyd et al., 2003), serotonin 5-HT2C receptor (Herrick-Davis et al., 2006) and oxytocin and vasopressin V1a and V2 receptors (Terrillon et al., 2003). However, this does not mean that ligands could not play a role in receptor dimerization – most likely, this varies on a case by case basis. On one hand, studies reporting that ligand binding brings the two receptors closer together has been described in CCR2 and CCL2 (Rodríguez-Frade et al., 1999), CXCR4 and CXCL12 (Toth et al., 2004), β2-adrenergic receptor and isoproterenol (Angers et al., 2000), somatostatin and somatostatin receptor, dopamine and dopamine receptor (Wurch et al., 2001, Rocheville et al., 2000, Patel et al., 2002) and thyrotropin-releasing hormone and its hormone (Kroeger et al., 2001, Zhu et al., 2002), among others. On the other hand, there is also literature describing that ligand binding has no effect in CCR5 (Issafras et al., 2002), CXCR4 (Babcock et al., 2003), CXCR2 (Trettel et al., 2003), melatonin receptors (Ayoub et al., 2002), adenosine A2A and dopamine D2 receptors (Canals et al., 2003) and neuropeptide y receptors (Dinger et al., 2003). Another source of disagreement has been how the dimer pairs interact, the most prominent hypotheses being disulphide bonds (Cvejic and Devi, 1997, Zeng and Wess, 1999) and transmembrane domain interactions (Lemmon et al., 1992). However, this discrepancies should not come as a surprise as the GPCR family encompasses almost 900 receptors which share little homology among themselves.

Heterodimerisation, or dimerization of two different receptors, was first observed in δ- and κ-opioid receptors (Jordan and Devi, 1999) and since then is has been described in many other GPCR (Mellado et al., 2001b, Rodríguez-Frade et al., 2001) but is still poorly

understood. There is compelling evidence, however, that these complexes can have distinct effects from their corresponding homodimers (Mellado et al., 2001b), possibly through differential recruitment. For instance, it has been described that CCR5 and CCR2 heterodimers can associate with a different G-protein family than their corresponding homodimers, and require lower chemokine concentrations to trigger calcium flux (Mellado et al., 2001b). Differential interaction between β-arrestin and the receptor could also play a role, as β-arrestin can assume different conformations depending on the partner it binds (Gurevich and Gurevich, 2004). It would not be far-fetched to speculate that these different conformations could be adopted depending on the receptor's phosphorylation sites, which could vary between hetero- and homodimers. Indeed, when agonists directly interact with β-arrestin for signalling, it has been seen that the binding site varies depending on β-arrestin's conformation (Azzi et al., 2003). This could be another source of the variation seen in signalling, as different kinases could bind β-arrestin with varying affinities.

As previously discussed, CXCR7 can affect chemotaxis by sequestering CXCL12, but also through the formation of heterodimers with CXCR4. In fact, it has been previously described that CXCR7 can form heterodimers with CXCR4 as efficiently as homodimers (Luker et al., 2009b, Sierro et al., 2007, Levoye et al., 2009), and thus heterodimer formation is dependent on the receptors' relative concentration. Whether these heterodimers are constitutively expressed or are formed after CXCL12 binding is still not well documented. Indeed, there are even conflicting reports about CXCR4 homodimers, with some studies proposing that CXCL12 binding is necessary (Vila-Coro et al., 1999), others reporting that dimerization is ligand-independent (Babcock et al., 2003) and others suggesting that ligand binding can enhance CXCR4 dimerization but it is not vital for its formation (Toth et al., 2004). This was further explored by studies demonstrating that CXCL12 stimulation does not cause the formation of new dimers or increased affinity between them, but changed the dimer conformation (Percherancier et al., 2005).

Furthermore, the functional consequences of CXCR4/CXCR7 heterodimers are still contradictory. A study proposes that the formation of this heterodimer causes conformational changes that affect the CXCR4/$G_{\alpha i}$ interaction, which is reflected in changes in the signalling response (Levoye et al., 2009). This was further explored by Décaillot and colleagues, who suggested that heterodimerisation caused the abrogation of G-protein in favour of β-arrestin signalling, causing a shift from the transient and early

ERK activation seen in CXCR4 homodimers to a late but prolonged ERK activation (Décaillot et al., 2011). This is consistent with other studies also reporting a late ERK activation when both receptors were co-expressed (Sierro et al., 2007), and has been observed too in μ-δ opioid receptor heterodimers (Rozenfeld and Devi, 2007). In pancreatic cancer cell lines, studies also report that in dual expressing cells, CXCR7 mediates ERK phosphorylation through β-arrestin, but not K-Ras activation (Heinrich et al., 2012). However, studies in CXCR4-CXCR7-expressing primary astrocytes and glioma cells showed that CXCR7 activation of Akt, ERK and calcium release are mediated not by β-arrestin, but $G_{i/o}$ proteins (Ödemis et al., 2012), hinting that different mechanisms may take place in different cell types.

Functionally, co-expression of CXCR4 and CXCR7 increases chemotaxis *in vitro* in mammary adenocarcinoma cell lines, but reduces invasion and metastasis compared to CXCR4 alone, probably due to CXCR7's reduced ability to induce MMP expression and thus degrade the ECM (Hernandez et al., 2011). Another study also shows that co-expression enhances chemotaxis of breast cancer (Décaillot et al., 2011) and neuroblastoma cell lines to the bone marrow (Mühlethaler-Mottet et al., 2015). However, Hartmann and colleagues describe that when there is co-expression of CXCR4 and CXCR7, blocking of CXCR7 has no effect in chemotaxis or Akt activation, but blocks the activation of integrins (Hartmann et al., 2008). Conversely, blocking CXCR4 only in dual expressing Jurkat T-cells prevented calcium flux release, but did not block ERK-mediated chemotaxis *in vitro* (Kumar et al., 2012).

Paradoxically, it has also been proposed that the anti-cancer activity of several compounds is not due to its antagonist CXCR4 activity, but due to CXCR7 agonistic activity. By mechanisms not yet completely elucidated, studies have reported that co-expression alters the trafficking of the receptors after stimulation. Terrillon and colleagues described that when the heterodimer is stimulated by a ligand (CXCL12 or an agonist), it induces the degradation of CXCR4, but the recycling of CXCR7 (Terrillon et al., 2004). When CXCR7 is back in the surface it can further modulate the response, negatively regulating angiogenesis (Uto-Konomi et al., 2013). However, in the absence of ligand CXCR7 expression has a minimal effect on CXCR4's levels on the cell surface.

Heterodimerisation, thus, adds a new layer of complexity to receptor-ligand interactions, but also opens exciting possibilities for a more precise targeting strategy.

1.6. RECEPTOR DESENSITISATION

Receptor desensitisation is a process by which the GPCR becomes refractory after repeated stimulation with its agonist (Kelly, Bailey et al. 2008) in a process mediated by the phosphorylation of the receptor by G-protein receptor kinases (GRKs). The phosphorylated receptor is then recognised by members of the β-arrestin family, which uncouple the GPCR from the Gα subunit and halt signal transduction (Hüttenrauch, Pollok-Kopp et al. 2005). β-arrestin can then interact with several endocytic proteins such as the adaptor protein AP2, which will in turn allow for the formation of clathrin-coated pits. The β-arrestin/GPCR complexes will undergo endocytosis and be either degraded in the lysosomes or recycled back to the surface. This process is common to not only GPCR but to all 7-transmembrane receptors (Kohout and Lefkowitz, 2003) and involves seven GRKs and four arrestins (Lefkowitz and Shenoy, 2005).

In CXCR4's case this phosphorylation occurs in serine 339 present in the intracellular C-ter (Woerner et al., 2005, Orsini et al., 1999). Indeed, C-ter truncations of CXCR4 have been linked with the autoimmune disease WHIM (warts, hypogammaglobulinemia, infections, and myelokathexis) syndrome, where CXCL12 overstimulates CXCR4, preventing neutrophils from leaving the CXCL12-expressing bone marrow (Hernandez et al., 2003). In functional CXCR4, the receptor becomes degraded after internalisation in a process mediated by the E3 ubiquitin ligase AIP4 (Marchese et al., 2003).

This desensitization can be homologous or heterologous ("cross-desensitisation"), depending on whether the receptors form homo- or hetero- dimers (Kelly et al., 2008). Indeed, heterodimerisation has been reported to affect receptor internalisation, with stimulation of only one of the receptors being enough to promote co-internalisation. This has been reported in many receptors including δ-opioid/β2 adrenergic receptor dimers (Gomes et al., 2001), with chemokines being able to desensitise opioid receptors (Szabo et al., 2002). However, heterologous desensitisation between chemokine receptors has not been as studied, with the first reports describing the chemokine receptors CCR5 and CXCR4 becoming desensitised to CCL5 and CXCL12 respectively after IL-8 stimulation (Richardson et al., 2003) or after CXCL12, CCL4 or CCL5 stimulation (Hecht et al., 2003, Honczarenko et al., 2002). Several studies in our group have further investigated heterologous desensitisation as a mechanism to prevent exacerbated inflammation – for instance, we have found that a CXCR3 agonist can desensitise not only CXCR3 but also CXCR4 and CCR5 (O'Boyle et al., 2012). Furthermore, we have also shown that non-GAG

binding variants of CCL7 (Ali et al., 2007, Lapteva et al., 2005) and CXCL12 (O'Boyle et al., 2009) can impair leukocyte migration to other chemokines. These data suggests that heterologous desensitisation is a yet unexplored avenue to target the chemotaxis of cancer cells (Menten et al., 2002, Rubin, 2009).

1.7. CHEMOKINE RECEPTORS AS A THERAPEUTIC TARGET

7-transmembrane receptors are the most common drug target (Lefkowitz and Shenoy, 2005), with around 50% of the total drugs in the market modulating GPCRs (Howard et al., 2001). However, despite chemokine's roles in diseases such as asthma, rheumatoid arthritis, multiple sclerosis, HIV or cancer, drugs targeting chemokine receptors remain elusive, with dozens of drugs failing at Phase II trials. So far, only Maraviroc (Celsentri®), a CCR5 antagonist against HIV, and AMD3100 (Perixaflor®), a CXCR4 antagonist for hematopoietic stem cell mobilisation, have been approved by the FDA (Horuk, 2009); with Mogamulizumab (Poteligeo®), a anti-CCR4 antibody, having been approved in Japan for lymphoma (Subramaniam et al., 2012). CCR4 is expressed by adult T-cell leukemia–lymphoma tumour cells and some subtypes of peripheral T-cell lymphoma and cutaneous T-cell lymphoma (Ishida et al., 2004), which allows Mogamulizumab binding. Natural killer cells, monocytes and macrophages can then recognise the Fc region of the antibody and attack the cancer cell (Duvic et al., 2016).

Indeed, some of the most common drug discovery problems are exacerbated when targeting chemokine receptors. First, the drug needs to compete with the chemokines present in the body, some of which present K_d as low as 1nM (Liang et al., 2000). If micromolar levels need to be administered for the drug to be efficacious, it risks having potential cross-reaction with other GPCRs (Hesselgesser et al., 1998). Albeit this may not be necessarily an unwanted effect, it is very hard to assess which benefits come from the intended target and which are off-target effects. Furthermore, chemokine receptors usually work in cooperation and targeting one may not have the desired effect due to redundancy of the receptors and the chemokines themselves (Tak, 2006). For these diseases combination therapies would be necessary, which makes them considerably less feasible. Another option is the synthesis of a "promiscuous" antagonist that would bind two chemokine receptors with an affinity in the low nanomolar level. Indeed, some studies have already tried this approach – for instance, the small molecule antagonist UCB35625 can inhibit both CCR1 and CCR3 (Sabroe et al., 2000, Naya et al., 2003), TAK-

779 can inhibit CCR5 and, to a lesser extent, CCR2b (Baba et al., 1999) and repaxirin is an antagonist for both CXCR1 and CXCR2 (Allegretti et al., 2005, Kim et al., 2011), as is SCH-527123 (Dwyer et al., 2006, Gonsiorek et al., 2007).

With all these hardships, it is not surprising that most CXCR4-targeted drugs never gained approval for use in humans. Most of the CXCR4 modulators currently available were originally developed to prevent HIV-1 infection by inhibiting the binding of the virus to CXCR4. For instance, AMD3100 was in clinical trials as an anti-HIV drug (Donzella et al., 1998) when leukocytosis was observed (Liles et al., 2003). Indeed, CXCR4's recently discovered role in metastasis has given drug companies a push to try to repurpose old HIV drugs. The rationale behind CXCR4 antagonists is not only their role in preventing chemotactic migration, but in stopping the adhesion of tumour cells to the stroma via β-integrins. This interaction confers the tumour cells a greater resistance to chemotherapy, as they receive survival and drug resistance signals from the stroma (Sethi et al., 1999). Thus, these CXCR4-targeted approaches would not be applied as stand-alone therapies, but in conjunction with the currently available treatments. However, CXCR4's multiple homeostatic functions are feared to cause important side effects if an antagonist is administered for a prolonged time.

Furthermore, the recently discovered CXCR7 also opens the possibility of using cross-desensitisation to prevent metastasis. Indeed, as heterodimers may present different functions to the corresponding homodimers, it may be interesting to develop drugs that enhance or diminish their action. For instance, by blocking the dimerisation interface with bivalent antibodies or small peptides linked with chemical spacers.

Briefly, six main approaches can be distinguished in regard to CXCR4 targeting:

1. Small peptide CXCR4 antagonists

   Examples: T22, T140 and analogues TN14003 and TE14012, CTCE-9908, POL6326, BKT140 and FC131 and analogues. Most of these antagonists are chemically modified peptides from anti-HIV natural compounds which can either target the binding pocket of CXCR4 or bind elsewhere and inhibit downstream processes.

   T22 is a peptide of only 18 amino acids which was isolated from the American horseshoe crab (Murakami et al., 1997) and has been shown to reduce pulmonary

metastasis of melanoma cells in a murine model, but has no effect in primary tissue growth (Murakami et al., 2002).

Similarly, T140 and its analogues inhibited migration of breast cancer cells *in vitro* and reduced the number of lung metastases in a mouse model (Tamamura et al., 2003). This was confirmed for the analogue TN14003, which significantly reduced the number of lung metastases in murine models of breast cancer (Liang et al., 2004) and a squamous cell carcinoma of the head and neck (Yoon et al., 2007). However, it is important to note that some of these analogues have a poor oral availability which complicates their distribution.

CTCE-9908 showed promise *in vitro* and reduced in half the number of metastasis to the lung in a mice model of osteosarcoma (Kim et al., 2008). Similarly, a reduction in tumour burden and in metastatic burden was seen in a breast cancer model (Huang et al., 2009). However, in a different study CTCE-9908 failed to prevent metastases, although it diminished their size (Richert et al., 2009). And conversely, reductions in the metastatic burden were seen in a prostate model, albeit it had no effect in the primary tumour growth (Wong et al., 2014), an effect which has been linked to a suppression of VEGF (Porvasnik et al., 2009) .

2. Small non-peptide CXCR4 antagonists

Example: AMD-070 (AMD11070), MSX-122, GSK812397 and KRH-3955.

MSX-122 is a partial CXCR4 antagonist that unlike AMD3100 does not cause the mobilisation of stem cells. Although it does not prevent CXCL12 binding, it is able to inhibit select signal transductions and presented good toxicity tolerance in monkeys and a good oral bioavailability (Natchus et al., 2008). It was also shown to diminish the amount of lung metastasis in a breast cancer model (Liang et al., 2012) and have antitumour properties in a lung cancer murine model (Zhang et al., 2008).

AMD070 is a CXCR4 inhibitor with good oral bioavailability and little side effects (Schols et al., 2003, Mosi et al., 2012, Moyle et al., 2009). Its effect in cancer has been tested in melanoma cell lines, where it had no effect in cell viability but was able to impair cell migration *in vitro* to similar or higher levels than AMD3100 (O'Boyle et al., 2013). It also inhibited the invasion of pancreatic cancer cell lines through Matrigel (Morimoto et al., 2016) and the *in vitro* migration of acute lymphoblastic

leukemia cells, increasing mouse survival *in vivo* (Parameswaran et al., 2011). GSK812397 (Jenkinson et al., 2010) and KRH-3955 (Murakami et al., 2009b) antagonistic potential have only been tested as an HIV antiviral but not for anticancer properties.

3. CXCR4 antagonists with CXCR7 agonistic activity

Example: AMD3100 and TC 14012.

AMD3100 is a bicyclam, that is, a small molecule formed by two cyclam rings that are connected by a phenylene linker, and which binds acid residues in CXCR4. In particular, one ring binds Asp171 in the transmembrane region 4 of CXCR4 and the other is inserted between the transmembrane regions 6 and 7 and binds the residues Asp262 and Glu288 (Hunter et al., 2005, Rosenkilde et al., 2004). The residues Asp182 and Asp193 also intervene but are not key for the binding (Hatse et al., 2001). This hydrophobic interaction is possible due to the protonation of the cyclams' nitrogen at physiological pH, which can then bind the aspartic acid's carboxylate groups in CXCR4 and thus inhibit CXCL12 binding (Fricker et al., 2006).

Unlike its predecessor, the polyoxometalates, the simplicity of AMD3100's structure allowed for a well-tolerated dosage and good pharmacokinetics (Hendrix et al., 2000). As previously described, despite its lack of antiviral effect (Hendrix et al., 2004), it was approved for the mobilization of hematopoietic stem cells soon after (Liles et al., 2003, Pusic and DiPersio, 2010). It is thus not surprising that AMD3100 has been extensively tried *in vitro* in the prevention of CXCR4-mediated metastasis. *In vivo* studies also showed that AMD3100 inhibited lung and lymph node metastasis in an oral squamous cell carcinoma model (Uchida et al., 2007, Uchida et al., 2011), liver metastasis in a colon cancer model (Matsusue et al., 2009) and lung and liver metastasis in a prostate model (Saur et al., 2005).

Furthermore, its potential in combination with other compounds has also been assessed, in particular synergizing with checkpoint inhibitors as described in section 1.1.6. One study used AMD3100 to accumulate T-cells within a murine pancreatic tumour, and then administered PD-L1 to elicit cytotoxic T-cell mediated destruction of cancer cells (Feig et al., 2013). A similar T-cell re-distribution by AMD3100 was also reported by Chen et al. (2015b), who also described anti-tumour

activity in a murine model of hepatocellular carcinoma when used in combination with an anti-PD-1 antibody and sorafenib, a tyrosine kinase inhibitor.

4. CXCR4 agonists

Examples: CTCE-0214 (peptide analogue of CXCL12), CTCE-0021 and ATI-2341.

Both CTCE-0214 and CTCE-0021 have been used in the mobilisation of hematopoietic stem cells (Pelus et al., 2005, Perez et al., 2004) but its use in preventing metastasis has not been assessed. The pepducin ATI-2341 also showed mobilisation of stem cells from the bone marrow (Tchernychev et al., 2010) but interestingly it induced a different phosphorylation pattern of the receptor, which prevents β-arrestin from binding and promotes G-signalling pathways instead (Quoyer et al., 2013).

5. CXCR4 antibodies

Example: MDX-1338 and ALX-0651.

Small molecules have been the most popularly researched antagonists given their size – indeed, bigger molecules such as antibodies may have trouble reaching the target sites and even then may fail to bind their target sequence when conformational changes occur. Commercially available antibodies have decreased the tumour burden and bone metastasis in a murine prostate model (Sun et al., 2005) but fully human antibodies are needed for therapy. One of the main concerns is antibody displacement by CXCL12 from the binding pocket if their affinity is not strong enough (Zhou et al., 2002a). To this end, most antibodies target the sulfotyrosine residues present in the N-ter, as in particular sulfotyrosine 21 is key for CXCL12 binding to CXCR4 (Veldkamp et al., 2010). So far, MDX-1338 (Ulocuplumab®) has shown promising antitumoural activity and is currently in clinical trials (Kashyap et al., 2016, Kuhne et al., 2013). However ALX-0651, the first synthesised GPCR nanobody, did not show sufficient activity and development was stopped after the Phase I clinical trials (Ramsey and McAlpine, 2013). Nanobodies, or single-domain antibodies, are antibody fragments that consist of the heavy chain only and thus are much smaller than normal antibodies, but are equally as specific and robust (Muyldermans et al., 2009).

6. CXCR4 siRNA

Albeit a popular option *in vitro*, delivery of siRNA has been proved difficult *in vivo* (Li et al., 2008). However, CXCR4 silencing has successfully decreased CXCR4's mRNA level in two murine models of breast cancer. Direct intravenous (i.v.) injection of two naked siRNA showed a decrease in lung metastases (Liang et al., 2005), and in mice injected with breast cancer cells that had been silenced with siRNA, mice remained tumour-free until culled at 45 days (Lapteva et al., 2005).

CXCR7 targeting is still scarce, with only three antagonists being available: CCX733, CCX771, or the inactive form CCX704. Interestingly only CCX771 but not CCX733 can be formulated for injection in *in vivo* studies. In glioblastoma, one study showed that CCX733 and CCX771, but not CCX704, could block cell growth and migration (Liu et al., 2013). Conversely, another study showed that these two compounds had no effect in glioblastoma cell growth (Rao et al., 2012). CCX733 and CCX771 were however successful in inhibiting CXCL12-mediated migration of renal cancer cells (Consales et al., 2010). Furthermore, in a breast cancer mouse model CCX771 diminished primary tumour growth, but had no effect in metastasis to the lymph nodes (Luker et al., 2012). Thus, so far no clinical relevance has been shown for these antagonists albeit they have been paramount in the study of CXCR7's function and signalling.

1.8. HYPOTHESES AND AIMS

Although progress has been made in the identification of breast cancer at an early stage through an extensive screening program, prognosis for metastatic breast cancer remains poor. Indeed, only 15% of patients who were diagnosed with stage IV metastatic cancer survive five years post-diagnosis in contrast to 99% at stage I. This metastatic spread is strongly linked with expression of the chemokine receptor CXCR4, which is not present in normal breast epithelial cells. These CXCR4-expressing breast cancer cells can then migrate to organs expressing CXCL12, such as the lungs, bone marrow and bone. A similar process can be seen with CCR7, which is also expressed by breast cancer cells and mediates the spread to the lymph nodes where CCL21 is present. Furthermore, it has been recently discovered that breast cancer cells also express the atypical chemokine receptor CXCR7, which was originally thought to be a non-signalling receptor that scavenged CXCL12 to stop its signalling. However, several studies have suggested that CXCR7 can signal through β-arrestin, which may have an impact on the chemotaxis of breast cancer cells.

This study was designed to address the following questions:

i. **Are CXCR4, CXCR7 and CCR7 expressed in both the tumour and the surrounding stroma of patient samples? Is this expression higher in patients with lymph node involvement?**

   The microenvironment and in particular CAFs have been reported to promote carcinogenesis through CXCL12. However, the expression of these receptors in the microenvironment has been very little, if at all, studied. We aim to assess the presence of CXCR4, CXCR7 and CCR7 in patient samples and determine the expression levels of CXCR4 and CXCR7 in the tumour and the surrounding stroma of patient samples with or without lymph node involvement.

ii. **Does the loss of FOXP3 directly upregulate CXCR4 expression?**

   CXCR4 can be upregulated through several mechanisms such as HIF-1 and HER2. In its turn, HER2 can be upregulated by the downregulation of the forkhead transcription factor FOXP3, which in health represses this oncogene. We aim to explore the nature of the relationship between FOXP3 downregulation and CXCR4 upregulation.

iii. **How does co-expression of CXCR7 and CXCR4 affect ERK and Akt signalling through time? If there are changes, are they mediated by different internalisation pathways being triggered after ligand stimulation? Do those differences affect wound healing and calcium flux? Can we change these by cross-desensitising CXCR4 with the CXCR7 agonist VUF11207?**

In order to assess this, CHO cells will be transfected with one or both of these receptors. First, the cell's ability to phosphorylate ERK and Akt will be assessed using Western Blot and cell based ELISA. Next, we will assess whether this activation correlates with receptor internalisation and subsequent degradation and recycling, and whether this can be altered when using a CXCR7 agonist instead of CXCL12. Finally, we will assess the functional consequences of the receptor activation by measuring calcium mobilisation (an indicator of chemotaxis) using flow cytometry and its effects in wound healing assays.

iv. **Can we reduce *in vivo* metastasis to the lymph nodes using a non-glycosaminoglycan (GAG) binding CCL21 in a murine model of breast cancer?**

Chemokine presentation by endothelial cells' GAGs is a vital step in directional chemotaxis as it allows cancer cells to attach to the surface of blood and lymph vessels to extravasate. Previous studies in our group showed that a non-GAG binding CCL21 could still bind CCR7 and induce calcium flux and bare-filter chemotaxis, but *in vitro* transendothelial chemotaxis was hampered. In this study, we aim to assess whether our mutated CCL21 can reduce the metastatic spread to the lymph nodes in a murine model of breast cancer.

2. GENERAL MATERIALS AND METHODS

2.1. CELL LINES AND CULTURE MEDIA

Breast cancer is a very diverse disease, and thus different cell lines can only emulate some aspects of the patient's illness (Holliday and Speirs, 2011).

2.1.1. MDA-MB-231

MDA-MB-231 is an immortalized human breast adenocarcinoma derived from the pleural effusion of the metastatic site of a 51 year old female Caucasian in 1973 (Cailleau et al., 1974). These cells have a quick doubling time of 23 hours and present an invasive phenotype, forming tumours in nude mice and metastasizing. These cells are triple negative (and thus do not express ER, PR or HER2) but express CXCR4, which allows them to migrate towards CXCL12 in chemotaxis assays (Müller et al., 2001).

These adherent cells were cultured in Dulbecco's Modified Eagle Media (DMEM) without phenol red (Sigma-Aldrich) supplemented with 10% FBS, 100U/ml penicillin, 100µg/ml streptomycin, and 0.146g/l L-gluCtamine (Sigma-Aldrich).

This cell line was STR fingerprinted on the 10/4/2013 when it was at passage 20.

2.1.1.1. *MDA-MB-231-CXCR4 and MDA-MB-231-CXCR7*

MDA-MB-231 cells were transfected by Dr. Luker (Center for Molecular Imaging, Department of Radiology, University of Michigan, Ann Arbor, MI, USA) using Clontech's lentiviral vector pLVX Ef1α IRES. Single transfectants (MDA-CXCR7 and MDA-CXCR4) were transfected with both (a) a vector containing CXCR7 or CXCR4 and mTagBFP as transduction marker and (b) a vector with β-arrestin and mCherry as transduction marker. Further to these fluorescent markers, the cells present CBGreen-based (*C*lick *B*eetle *Green* luciferase) complementation which allows us to assess binding of the receptor to β-arrestin. Briefly, after being activated the receptor recruits β-arrestin, allowing for CBGreen complementation and the restoring of the luciferase activity. When its substrate *(d-luciferin)* is added, luminescence can be measured using a luminometer or a plate reader, indicating β-arrestin and CXCR4 or CXCR7 are in close proximity (Villalobos et al., 2010). A diagram of this complementation can be seen in Figure 2-1.

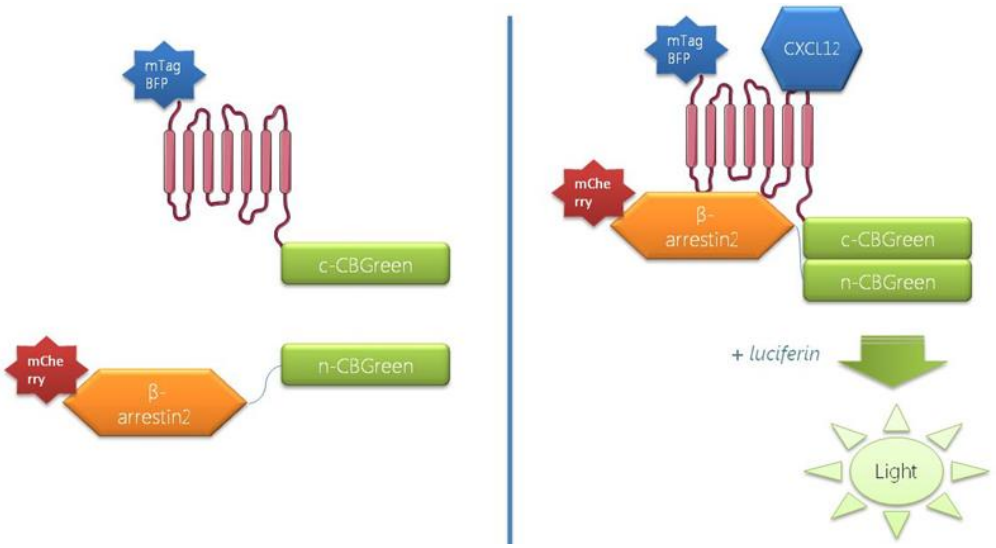

Figure 2-1. Schematics of the single transfected MDA-MB-231 cells.
Diagram showing the CBGreen protein complementation assay (PCA) when β-arrestin is recruited to CXCR4 (in MDA-MB-231-CXCR4) or CXCR7 (in MDA-MB-231-CXCR7).

2.1.1.2. *MDA-MB-231-CXCR4-CXCR7*

The double transfectant MDA-MB-231 cell line was cloned by Dr. Luker using the lentiviral vector FUW. This vector does not have any fluorescent markers, but the cells still present protein complementation with β-arrestin. In particular, CXCR7 and β-arrestin interaction is mediated by CBRed whilst CXCR4 and β-arrestin interaction can be detected thanks to CBGreen using bioluminescence as above. A diagram of this complementation can be seen in Figure 2-2.

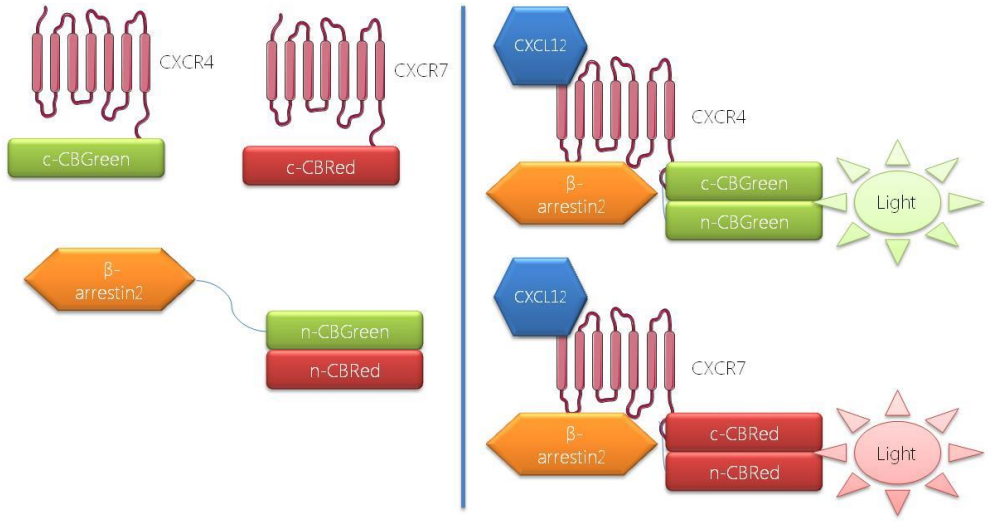

Figure 2-2. Schematics of doubly transfected MDA-MB-231 cells.
Diagram showing the CBGreen protein complementation assay (PCA) when β-arrestin is recruited to CXCR4 or CXCR7. When β-arrestin2 is recruited to the receptor, the n-ter and c-ter of the luciferase get in close proximity, restoring its activity. If substrate is added, green bioluminescence can be detected if β-arrestin is binding CXCR4 or red bioluminescence if it is binding CXCR7.

2.1.2. MCF-10A

This cell line was kindly provided by Anita Wittner from the Northern Institute for Cancer Research (Paul O'Gorman Building, Framlington Pl, Newcastle upon Tyne NE2 4AD). MCF-10A is an immortalized non-transformed mammary epithelial cell line derived from breast tissue with fibrocystic disease of a 36 year old female Caucasian (Soule et al., 1990). These cells lack tumorigenicity and need constant stimulation from growth factors and hormones to survive. They also lack ER expression but do express common epithelial markers such as cytokeratins, and have the typical cobblestone morphology seen in breast epithelial cells.

These adherent cells were cultured in DMEM/F12 (Invitrogen) supplemented with 10% horse serum (Invitrogen), 20 ng/ml epithelial growth factor (EGF) (Peprotech), 0.5 µg/ml hydrocortisone (Sigma-Aldrich), 100 ng/ml cholera toxin (Sigma-Aldrich), 10 µg/ml insulin (Sigma-Aldrich), 100U/ml penicillin and 100µg/ml streptomycin (Sigma-Aldrich).

2.1.3. MCF-7

MCF-7 is an immortalized human breast adenocarcinoma derived from a pleural effusion of the metastatic site of a 69 year old female Caucasian in 1970 (Soule et al., 1973). These cells express both ER and PR but not HER2, making them a good model for hormone therapy. Thus, in order to reach their full tumorigenic potential *in vivo* it is necessary to supplement them with oestrogen in murine models (Aonuma et al., 1999, Holliday and Speirs, 2011).

These adherent cells were cultured in DMEM without phenol red (Sigma-Aldrich) supplemented with 10% FBS, 100U/ml penicillin, 100µg/ml streptomycin, and 0.292g/l L-glutamine (Sigma-Aldrich).

2.1.4. T47D

T47D is an immortalized human breast ductal carcinoma derived from the pleural effusion of the metastatic site of a 54 year old female (Keydar et al., 1979). Like MCF-7, these cells express both ER and PR but not HER2, making them a good model for hormone therapy. However, even with oestrogen supplementation these cells have a poor tumorigenic potential in nude mice (Holliday and Speirs, 2011, Fogh et al., 1977).

These adherent cells were cultured in DMEM without phenol red (Sigma-Aldrich) supplemented with 10% FBS, 100U/ml penicillin, 100µg/ml streptomycin, and 0.146g/l L-glutamine (Sigma-Aldrich).

2.1.5. SKBR3

SKBR3 is an immortalized human breast adenocarcinoma derived from a pleural effusion of the metastatic site of a 43 year old female Caucasian in 1970 (Trempe, 1976). These cells do not express ER or PR but do express HER2, making them responsive to trastuzumab. However, these cells have a low tumorigenic potential and will only form poorly differentiated adenocarcinomas in nude mice (Holliday and Speirs, 2011, Fogh et al., 1977).

These adherent cells were cultured in McCoy's 5A (Sigma-Aldrich) supplemented with 10% FBS, 100U/ml penicillin, 100µg/ml streptomycin, and 0.146g/l L-glutamine (Sigma-Aldrich).

2.1.6. Primary human mammary epithelial cells (pHMEC)

Human mammary epithelial cells (pHMEC) were purchased from Gibco (Life technologies) and kept in liquid nitrogen until use. pHMEC are non-immortalized, adherent, mammary epithelial cells isolated from reduction mammoplasty tissue. Cells were tested by Gibco for the presence of HIV-1, mycoplasma, hepatitis C, hepatitis B, bacteria and fungi before shipment. Furthermore, cells from the same lot have also been tested via immunofluorescence to confirm the presence of cytokeratins 5, 6, 8 and 18 and E-cadherin.

2.1.7. THP1

THP1 is a non-adherent human monocytic cell line derived from the peripheral blood of a 1 year old male infant with acute monocytic leukaemia (Auwerx, 1991). These cells have a doubling time of 35 to 50 hours and need to be kept at densities below $1x10^6$ cells/ml in order to avoid clumping. As they are leukocytes, they express high levels of CXCR4 making them an excellent positive control.

THP1 cells were cultured in RPMI-1640 media (Roswell Park Memorial Institute medium 1640) (Sigma-Aldrich) supplemented with 10% FBS, 100U/ml penicillin, 100µg/ml streptomycin, and 0.146g/l L-glutamine (Sigma-Aldrich) (Moore et al., 1967). These cells grow in suspension and thus a modified protocol to the one described in the General Materials and Methods needs to be followed for culturing.

Briefly, cells are grown in vertical T-75 flasks in a maximum volume of 50 ml. When cells reach maximum confluency, four fifths of the volume containing cells is discarded and substituted with fresh media.

2.1.8. CHO-K1

The CHO-K1 cell line was created from the parental CHO (Chinese hamster ovary) cell line derived from the ovary of an adult Chinese hamster in 1957 (Tjio and Puck, 1958). From here onwards, the terminology "CHO" will be used to refer to CHO-K1 cells. This adherent cell line presents an epithelial-like morphology and a doubling time of 25 hours on average, requiring a 1:8 splitting rate.

These cells were cultured in Ham's F-12 media (Sigma-Aldrich) supplemented with 10% FBS, 100U/ml penicillin, 100µg/ml streptomycin, and 0.146g/l L-glutamine (Sigma-Aldrich).

CHO-CXCR4 cells were previously created by Dr. James Harvey in the department and require the addition of zeocin to the media to maintain antibiotic selection. CHO-CXCR7 cells were created in this study and require the addition of G418 to the media. More details can be found in section 5.2.3.1 in this chapter.

2.1.9. 4T1 and 4T1-Luc

4T1 is an adherent murine stage IV breast carcinoma cell line derived from BALB/cfC3H mice (Dexter et al., 1978) which exhibits resistance to the chemotherapeutic drug 6-thioguanine (Dexter et al., 1978). This cell line presents an epithelial morphology and has been described to form spontaneous metastasis in the lymph nodes, liver, lung, brain and bone even after surgical removal of the primary tumour (Aslakson and Miller, 1992, Lelekakis et al., 1999).

Cells were cultured in DMEM's media (Sigma-Aldrich) supplemented with 10% FBS, 5 ml of MEM Non-Essential Amino Acids Solution (100X), 100U/ml penicillin, 100µg/ml streptomycin, and 0.146g/l L-glutamine (Sigma-Aldrich). Cells should not be allowed to reach complete confluency and thus were split 1:4 when they reached 80% confluency (approximately twice a week).

4T1-Luc cells were a generous gift from Prof. G. Lazennec (Centre national de la recherche scientifique (CNRS) Sys2Diag, Cap delta, 1682 rue de la Valsière, CS 61003, 34184 Montpellier Cedex 4, France). Briefly, 4T1 cells were stably transfected with a plasmid containing the firefly luciferase gene, allowing for the visualisation of the

tumour cells *in vivo* after the addition of its substrate, luciferin (Tao et al., 2008). Selection was carried out with G418 to ensure the maintenance of high luciferase expression.

2.1.10. HMEC-1

HMEC-1 is an immortalised, non-transformed dermal endothelial cell line created from the transfection of human dermal microvascular endothelial cells (HMECs) with a plasmid containing the simian virus 40 (SV40) large T antigen (Ades et al., 1992). These cells present a cobblestone-like endothelial morphology and express endothelial markers such as CD31, CD36, CD44, many integrins, e-selectin, VCAM-1 and ICAM-1 (Xu et al., 1994).

These cells were grown in MCDB131 media (Gibco), supplemented with 10% FBS, 10ng/mL epidermal growth factor (EGF), 1 µg/mL hydrocortisone, 100U/ml penicillin, 100µg/ml streptomycin, and 0.146g/l L-glutamine (Sigma-Aldrich). Cells were split 1:4 after reaching complete confluency, but due to their tight adherence to the flask, longer (10-15 min) digestions with trypsin were often required.

2.2. CELL CULTURE METHODS

All laboratory work was carried out in a containment level II laboratory in accordance to the University Health and Safety policy. Furthermore, all the relevant COSHH and bioCOSHH forms for risk assessment were read and signed before starting the work.

2.2.1. Subculturing of immortalised cell lines

Cell culture procedures were performed in class II laminar flow cabinets. Cells were conventionally grown in 75cm^2 (T-75) tissue culture flasks (Greiner Bio-One) in 10-15 ml of their respective media in a humidified incubator (37°C, 5% CO_2) until 90%-100% confluent. Adherent cells were grown in horizontal position to maximize space in which to grow, whilst non-adherent cells were grown in vertical flask to allow for more suspension volume.

Briefly, when adherent cells were confluent media was aspired and cells were washed with phosphate buffer saline (PBS) (Sigma-Aldrich) in order to remove excess protein. 5 ml of 1mM Trypsin-EDTA solution (Sigma-Aldrich) was then added and the flasks were incubated for approximately 5 minutes at 37°C until all cells were detached. 5 ml of protein-containing complete media was added in order to neutralize the trypsin and cells were pelleted by centrifugation (5 minutes at 300xg) in a universal tube. The supernatant was then discarded and cells were resuspended in the appropriate volume of culture medium to be split in a ratio from 1:3 to 1:6 in T-75 flasks.

For MCF-10A, the following changes were made to the protocol: only 2 ml of trypsin-EDTA solution were added, and 2 ml of media were needed to inactivate it together with an extra 1 ml to rinse the flask. As these cells are very adherent, detachment took approximately 20 minutes. Furthermore, cells were spun down at 150xg for 5 minutes to prevent stress.

2.2.2. Cryopreservation of cell lines

In order to maintain a cell stock, cells were cryopreserved in liquid nitrogen at an early passage number. Cells were resuspended in 0.5 ml of culture medium after being pelleted and then 0.5ml of freezing medium (20% dimethyl sulphoxide (DMSO, Sigma-Aldrich) in FBS) was added to make a final volume of 1 ml. The suspension was transferred to a cryovial, placed in a "Mr.Frosty" (ThermoFisher scientific) and stored at -80°C. Mr.Frosty is a freezing container filled with isopropyl alcohol which allows a

temperature reduction of 1 degree per minute, preventing loss of cell viability due to temperature shock. Cryovials were transferred to liquid nitrogen the following day.

To recover cells, vials were quickly thawed by placing the cryovial in the water bath at 37°C. Cells were transferred to a universal tube with 4 ml of the appropriate media, pelleted, and resuspended. The cells were then cultured in a T-75 as previously described.

2.2.3. Mycoplasma testing

Mycoplasma infection is one of the major causes of contamination in cell culture. Unlike fungi, its small size (approximately 0.15-0.3 μm) prevents it from being seen by the naked eye or on the microscope. Furthermore, due to not having a cell wall, these bacteria are resistant to the penicillin and streptomycin present in the media. The presence of mycoplasma can only be suggested by slower growth or abnormal cell morphology, as they alter cell metabolism and proliferation and cause chromosome aberration among other cellular changes.

The MycoAlert™ mycoplasma testing kit (Lonza) was used following the manufacturers' instructions in order to detect possible contamination. Briefly, 2 ml of a 48h culture was aliquoted and centrifuged at 500xg for cells to pellet. 100 µl of the cell culture supernatant was incubated for 5 minutes with 50µl of the mycoAlert™ reagent and baseline luminescence was measured (TD-20/20 turner design luminometer, Promega). The reagent will lyse any mycoplasma present, causing the release of enzymes which are found in most mycoplasma species. 50 µl of mycoAlert™ substrate was then added to the mixture and incubated for 10 minutes. The substrate contains D-luciferin, luciferase and ADP (adenosine diphosphate), which in the presence of the mycoplasma enzymes will be converted to ATP (adenosine triphosphate). This ATP, together with D-luciferin, will be catalysed by the enzyme luciferase to produce light and other co-products. After the incubation, a second luminescence reading was taken and a ratio between the first and second reading was calculated. A negative control was also performed at the same time, using fresh media instead of the culture supernatant.

Ratios of 1 and lower are classed as negative, whilst ratios between 1 and 1.2 are borderline and ratios higher than 1.2 are positive. All cell lines used in this project tested negative for mycoplasma infection.

2.2.4. Cell counting

For experiments that required a precise number of cells, cells were counted using an improved Neubauer chamber haemocytometer. Briefly, 10 µl of the resuspended cells were mixed with 10 µl of 0.4% trypan blue (Sigma-Aldrich) in an Eppendorf tube (Eppendorf). Trypan blue is a carcinogenic vital dye, which cannot penetrate viable cells with an intact membrane. When the cell is necrotic or apoptotic, trypan blue can enter and stain the cytoplasm blue.

10 µl of the mix were injected in each chamber, which was covered with a coverslip. Viable cells located in the centre square (which is subdivided in twenty-five 0.04 mm^3 squares) were counted– for accurate results the number should be between 20 to 300 cells. Blue cells were not counted, and only cells that overlapped the edge on the top and right side were included. As seen in Figure 2-3, each large square large square equals a volume of 10^{-4} mL (1 mm (length) × 1 mm (width) × 0.1 mm (depth) = 0,1 mm^3 = 10^{-4} cm^3 = 10^{-4} mL), so in order to calculate the number of cells per ml the cell count was multiplied by the dilution factor (½ due to the trypan blue) and 10^4. In order to calculate the total number of cells, this number was multiplied by the volume the cells were resuspended in.

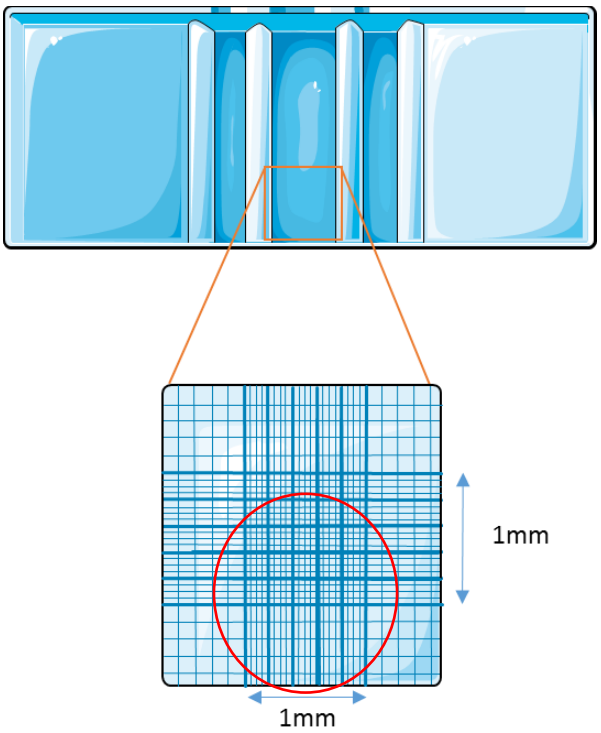

Figure 2-3. Diagram showing the layout of a haemocytometer.
In an improved Neubauer, the counting area is divided into 9 squares, which in turn are divided into 25 squares. The central square is further divided so each of the 25 squares has 16 internal squares. Each large square is 1 mm long and 1 mm wide. Diagrams were created using the Servier's image bank, http://www.servier.fr/smart/banque-dimages-powerpoint.

2.3. MOLECULAR METHODS

2.3.1. RNA isolation

In order to prevent any contamination of the sample, all reagents used were RNase free and designed for molecular biology. Special care was taken to ensure that the surfaces and pipettes were decontaminated, the latter by UV light exposure for 30 minutes. Only sterile filter tips and autoclaved Eppendorf tubes were used during the whole procedure.

RNA samples were stored short-term at -20°C and long-term at -80°C.

2.3.1.1. *RNA isolation using Trizol*

TRI reagent (Sigma-Aldrich) was used to isolate the total RNA when a high amount of cells ($5x10^6$) was available. Cells were detached and pelleted as described in section 2.2.1. 1ml of TRI reagent was added to the pellet in the universal tube and homogenised. The mixture was transferred to an Eppendorf tube and left for 5 minutes to ensure the dissociation of nucleoprotein complexes. TRI reagent contains a mixture of guanidinium isothiocyanate and phenol, which works by denaturing proteins (including the ribosomes attached to the rRNA) and dissolving the proteins and lipids present, respectively. 200 µl of chloroform (Sigma-Aldrich) was then added to the mixture, shaken and incubated for 5 minutes at room temperature before centrifuging for 15 minutes at 12,000xg and 4°C. The addition of chloroform allows for the formation of an aqueous phase where the RNA remains, whilst the DNA is present in a white interphase and the proteins and lipids stay in the pink organic layer together with the phenol and chloroform.

The clear, aqueous phase was carefully removed and transferred to a new Eppendorf tube. 500 µl of cold isopropanol were added and the mixture was incubated on ice for 10 minutes whilst the RNA precipitated. The sample was centrifuged for 10 minutes at 12,000xg and 4°C and the supernatant was removed leaving only the pellet. In order to wash the pellet, 1 ml of 70% (v/v) ethanol was added, left on ice for 10 minutes, and then centrifuged for 5 minutes at 7,500xg and 4°C. The wash was carefully discarded and the remaining ethanol was left to air-dry. Finally, the pellet was resuspended in 30-50 µl of diethyl pyrocarbonate (DEPC) treated water.

2.3.1.2. *RNA isolation using the RNeasy® Plus Mini kit*

When small cell numbers caused a barely visible RNA pellet, the RNeasy® Plus Mini kit (Qiagen) was used according to the manufacturers' instructions.

Briefly, cells were detached and pelleted as described in section 2.2.1. 350µl of RLT Plus buffer (with 10µl of β-mercaptoethanol per 1 ml RLT Plus buffer) were added to the pellet to lyse the cells and the mixture was vortexed for 30 seconds. The lysate was then transferred to a gDNA eliminator spin column and centrifuged for 30s at 8,000xg. The column was discarded and 350 µl of 70% ethanol was added to the flow-through. The mixture was then transferred to an RNeasy spin column and centrifuged for 15s at 8,000xg in order to bind total RNA. The flow-through was discarded and 3 washes were performed by adding 700 µl of Buffer RW1 (centrifuge for 15s at 8,000xg), 500 µl of Buffer RPE (centrifuge for 15s at 8,000xg) and 500 µl of Buffer RPE (centrifuge for 2minutes at 8,000xg). After discarding the last flow-through, a last centrifugation was carried out for 1 minute at full speed in order to eliminate any possible ethanol and buffer carryover. Finally, the RNeasy spin column was placed in a new Eppendorf tube and 30-50 µl of DEPC water were added directly to the spin column membrane. The tube was then centrifuged for 1 minute at 8000xg in order to elute the RNA.

If RNA had to be extracted from frozen or RNA*later*-stored tissue, it was homogenised beforehand using the Qiagen Tissue lyser II (see Figure 2-4). Briefly, tissue was placed in rounded Eppendorf tubes containing a metallic bead and 350 µl of the lysis buffer from the RNAeasy kit. Samples were then placed in a -20°C holder, clamped into the machine and homogenised mechanically twice. Foamy lysates were transferred to a new Eppendorf tube and centrifuged for 3 minutes at full speed to pellet debris. RNA from the supernatant was then extracted following the procedure described above.

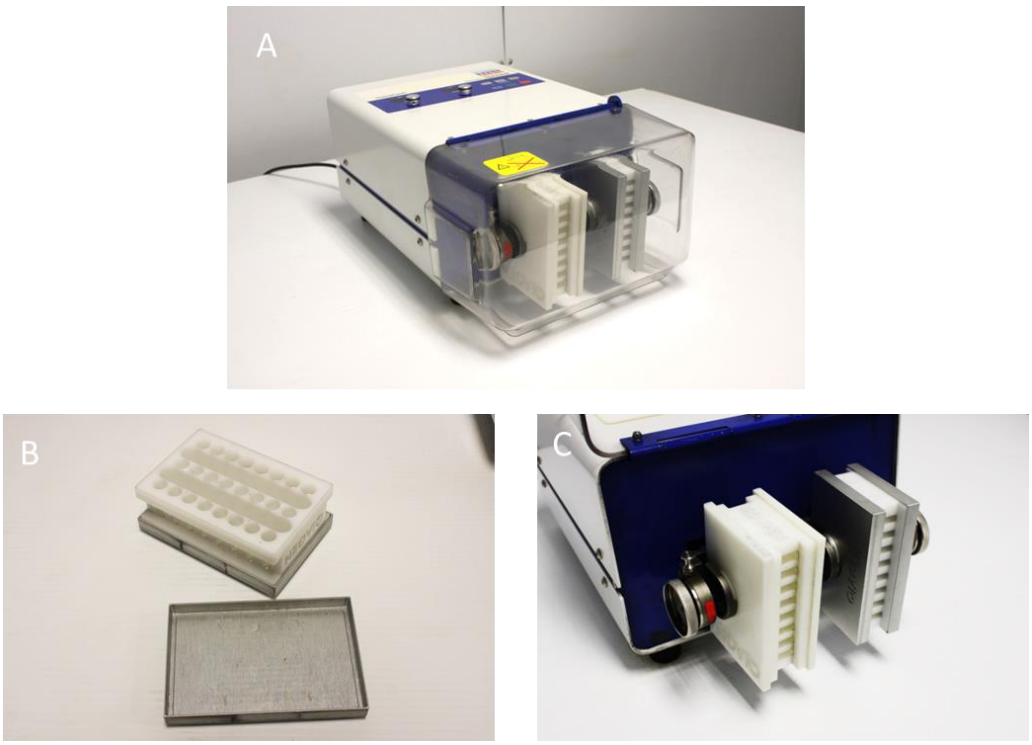

Figure 2-4. Mouse tissue was homogenised using the Qiagen Tissue lyser II.
(A) Image of the Qiagen Tissue lyser II. **(B)** Samples were placed in Eppendorf tubes containing 350 µl of lysis buffer and inserted into a frozen holder. Lid was placed on top of the holder and **(C)** the sandwich was clamped into the Qiagen Tissue lyser. Samples were homogenised for 20s at 15 Herts twice, changing the orientation of the plate for the second round.

2.3.1.3. *Laser capture and RNA isolation from frozen patient samples*

In order to separate tumour cells from the surrounding tissue, laser micro-dissection was performed using a Leica AS LMD7 microscope system by Mrs Barbara Innes, Miss Katie Cooke or Miss Rachel Etherington in the Centre for life. Briefly, 4µm cryosections were placed on PEN (polyethylene naphthalate) membrane glass slides (Leica) and stained using H&E in order to observe the tissue structures for cutting. The slides were visualised using the Leica microscope at 20x and the regions of interest were drawn using the Leica Laser Microdissection software (see Figure 2-5A). The UV laser (4 nanosecond pulse) was then used to dissect the area of interest from above and place it in a 0.5 ml Eppendorf lid for RNA extraction (see Figure 2-5B). Thus, in order to correctly separate tumour cells from microenvironment the sample needed to present a clear morphology. Unfortunately, most samples had not been snap frozen in isopentane before being placed in liquid nitrogen, causing the cell membranes to burst and preventing successful assessment of which cells corresponded to the tumour and which to the stroma. An example of a properly and improperly processed sample can be seen in Figure 2-5C and Figure 2-5D, respectively.

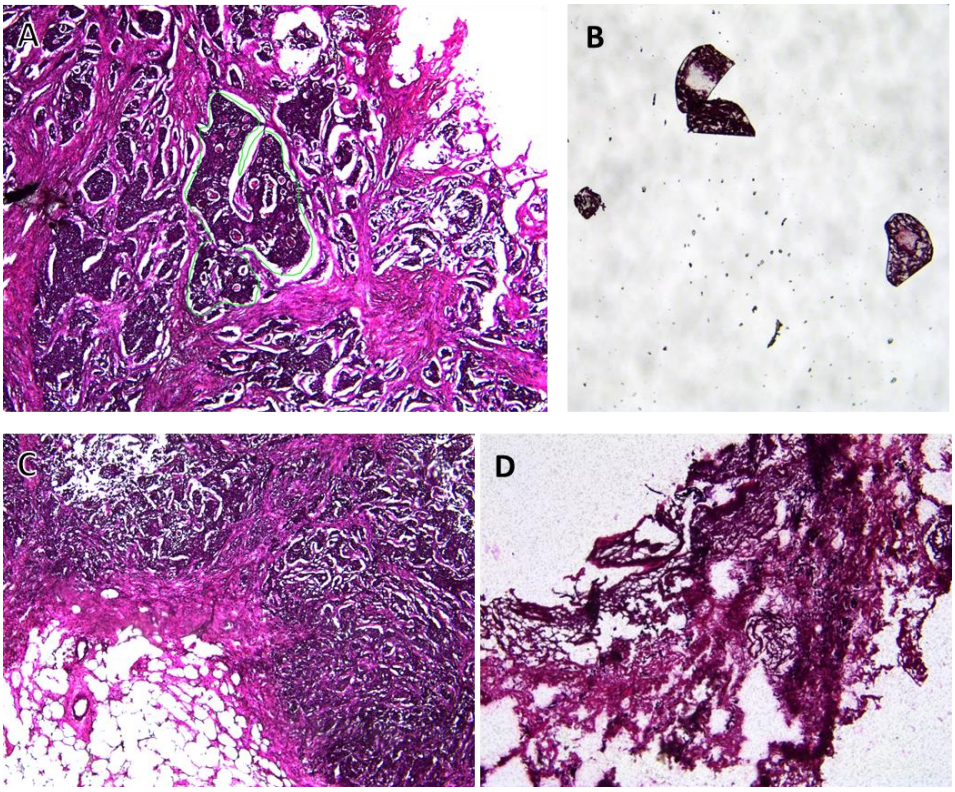

Figure 2-5. Microdissection images captured using the Leica AS LMD microscope system.
(A) The tumour cells were traced from the surrounding tissue (see green line), dissected using a UV laser, and **(B)** it was ensured that the correct piece of tissue had been successfully cut out into the Eppendorf lid. **(C and D)** Examples of well and badly frozen breast tumour tissue samples after H&E staining. As seen in the image, the tissue structure in **(D)** has been lost due to poor freezing technique or sample preservation, making it very difficult to discriminate between cancer and surrounding tissue.

In order to obtain enough tissue quantity for RNA extraction, 4 to 5 slides from sister sections were cut from each sample - for reference, sister sections refer to successive sections cut from the same frozen or paraffin-embedded block (Ertault-Daneshpouy et al., 2009). In order to extract RNA from a small number of cells, the Arcturus PicoPure RNA isolation Kit (ThermoFisher) was used according to manufacturer's instructions. Briefly, fresh tissue was placed in 50 µl of extraction buffer, quickly centrifuged and incubated for 30 minutes in a heat block at 42°C to extract the RNA. Concurrently, 250 µl of conditioning buffer were pipetted onto the RNA purification column's filter membrane and incubated for 5 minutes at room temperature. The column was then centrifuged at 16,000xg for one minute to remove the buffer. Next, 50 µL of 70% Ethanol were mixed with the RNA extract and the mixture was pipetted into the pre-conditioned purification column. To bind RNA to the column, the mixture was centrifuged for 2 minutes at 100xg, immediately followed by a centrifugation at 16,000xg for 30 seconds to remove the flow-through. 100 µL Wash Buffer were pipetted into the purification column and centrifuged for one minute at 8,000xg, followed by two further centrifugation cycles with 100 µL

Wash Buffer 2 for one minute at 8,000xg and for two minutes at 16,000xg. To remove the wash residue in the columns, another spin at 16,000xg for one minute was carried out before transferring the purification column to a new 0.5 mL microcentrifuge tube. Finally, 13 µl of Elution Buffer were pipetted directly onto the membrane of the purification column, incubated for one minute at room temperature and centrifuged for one minute at 1,000xg to distribute the buffer in the column, followed for one minute at 16,000xg to elute RNA.

Sample was then stored at – 80°C or immediately used to synthesise cDNA as described in section 2.3.4. of the General materials and methods.

2.3.2. Determination of RNA concentration and purity

2.3.2.1. *Assessment using the Nanodrop ND-1000*

RNA concentration and purity were quantified using a Nanodrop spectrophotometer (Nanodrop ND-1000 spectrophotometer, Thermo Scientific). This machine measures the absorbance at 230nm (for organic solvents), 260nm (for nucleic acids) and 280nm (for protein content) and then calculates two ratios to assess RNA purity - 260/280 and 260/230.

In order to operate the machine, 1 µl of the sample was placed in the Nanodrop after blanking with DEPC water. The machine then displayed the sample concentration in ng/µl and the two ratios. Ratios between 1.8 and 2.2 were considered as pure RNA, free from organic solvent or protein contamination and were used for cDNA synthesis. An example of a pure RNA sample can be seen in Figure 2-6.

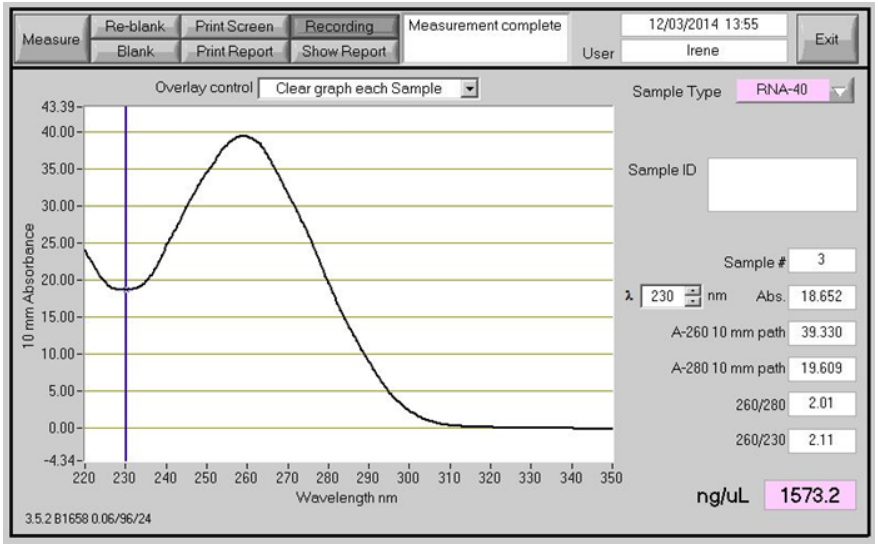

Figure 2-6. Representative image of a MDA-MB-231 RNA measurement using a Nanodrop spectrophotometer. RNA quality and concentration was analysed by placing 1 µl of the sample in the Nanodrop pedestal. 260/280 ratio indicates protein contamination, whilst the 260/230 ratio determines organic solvents contamination.

2.3.2.2. *Assessment using the Agilent 2100 Bioanalyzer*

To confirm the quality of the samples, RNA was analysed using the Agilent 2100 Bioanalyzer system. Briefly, 1 µl RNA was diluted to less than 500ng/µl before mixing it with 5 µl of fluorescent marker and loading 6 µl into the RNA chip. This was carried out for 12 samples and a ladder before starting the electrophoresis gel run, in which the sample components are separated by size as they move through microchannels. The RNA was then detected through the intercalated fluorescent dye and the RNA Integrity Number (RIN) was calculated, where 10 stands for the highest RNA quality and 1 for a completely degraded RNA. RNA concentration was also calculated by determining the area under the electropherogram (see Figure 2-7). Samples with RIN above 7 were used.

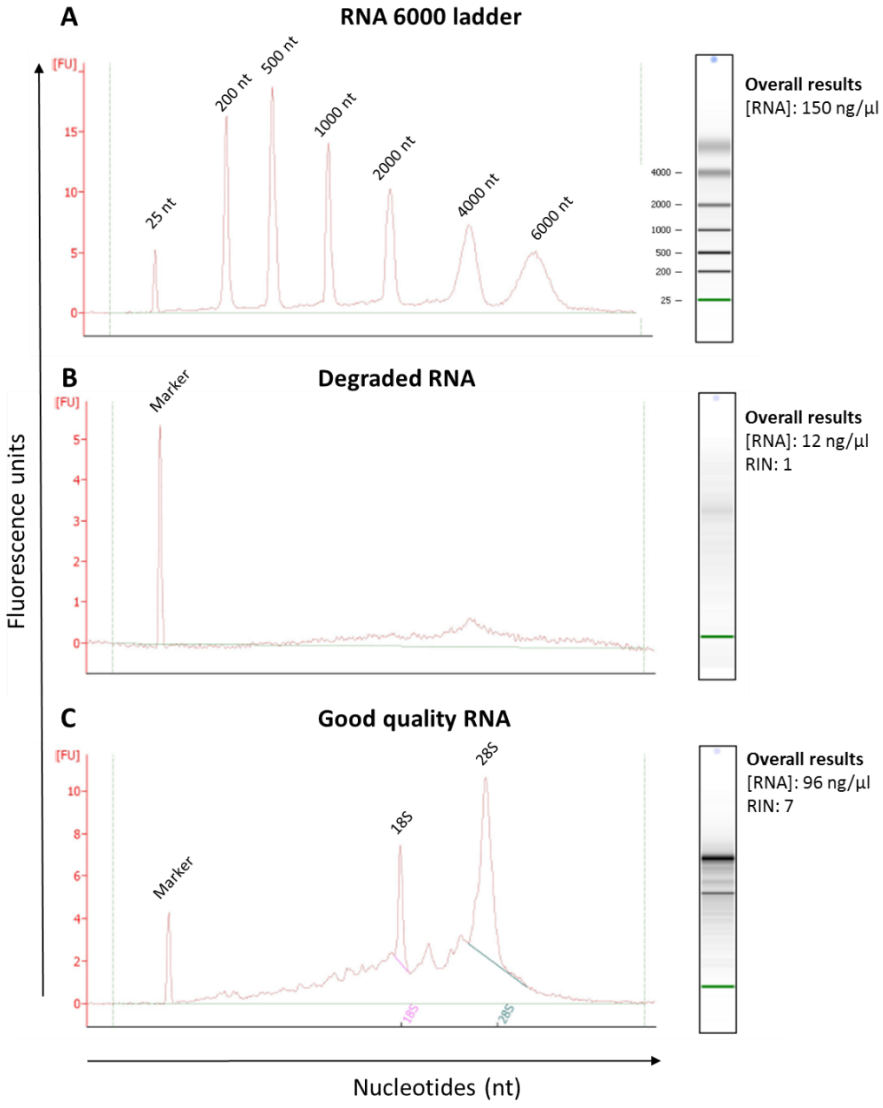

Figure 2-7. Sample electropherograms from (A) the RNA 6000 ladder (ThermoFisher) and (B) bad and (C) good quality lymph node samples.
Pictured on the right is an image of the sample run in an electrophoresis gel, where the 18S and the 28S bands should be present.

2.3.2.3. *Assessment using agarose gel electrophoresis*

In order to either separate DNA fragments of different size or ensure RNA integrity, an agarose gel is needed. By using electrophoresis, smaller linear molecules will migrate faster through the gel pores, whist bigger and less compact molecules will be slower.

10x TAE buffer was first prepared by dissolving 48g of tris base, 11.4 mL of glacial acetic acid and 20 mL 0.5M EDTA at pH 8.0 (Sigma-Aldrich) in 1 litre of distilled water. This stock solution was diluted 1:10 in order to make a 1x working solution with final concentration of 40 mM Tris, 20 mM acetic acid and 1 mM EDTA.

To make a 1% agarose gel of small size, 0.5 grams of agarose were added to 50 ml of 1xTAE buffer and dissolved by gentle heating in a microwave oven for 1 minute. The solution was then cooled under running cold water and 3µl of ethidium bromide were added to the mixture for a final concentration of 0.5 µg/ml. Ethidium bromide is a DNA intercalating agent which emits an orange fluorescence when exposed to ultraviolet light, allowing us to see the RNA or DNA bands. The gel was allowed to set for 15 minutes before removing the comb and being assembled in an electrophoresis tank filled with 1x TAE buffer.

Running samples were prepared by mixing 10 µl of Orange G loading dye with 3 µl of the sample. The loading dye has a dual role: it increases the density of the sample, allowing it to sink into the well, and permits the observation of the samples' position during electrophoresis as a consequence of its orange colouration. 4 µl of the GeneRuler 1kb DNA ladder (Fermentas) were also loaded alongside the samples in order to determine their size. The gel was run at 90V for about 45 min, or until the orange band from the dye had migrated through three quarters of the gel. Gels were then visualized using an Alpha Imager® Instrument (Alpha Innotech Corporation, San Leandro, CA, USA) to observe the two bands corresponding to the 18S and 28S ribosomal subunits as seen in Figure 2-8.

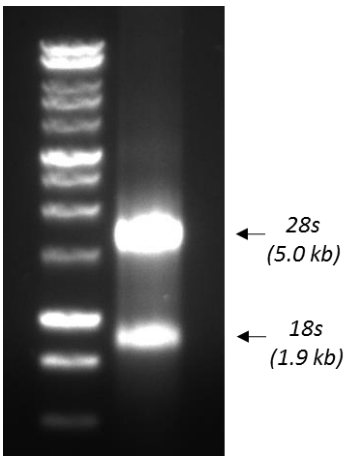

Figure 2-8. Confirmation of RNA integrity.
Following RNA isolation and quantification using Nanodrop, RNA was run on a 1% agarose gel. As the sample is most abundant in rRNA, the 18S and 28S ribosomal subunits can be clearly observed in the gel, indicating there is no RNA degradation.

2.3.3. Elimination of gDNA contamination in RNA samples

Despite using the gDNA eliminator columns, qPCR showed DNA contamination in most of the lymph node samples. To eliminate DNA from RNA that had already been extracted, RQ1 RNase-Free DNase (Promega) was used as per manufacturer's instructions. Briefly, in a PCR Eppendorf tube (a) 1 µl RQ1 RNase-Free DNase 10X Reaction Buffer, (b) 1 µl RQ1 RNase-Free DNase per every 1 µg RNA and (c) 1-8 µl RNA were mixed and incubated at 37°C for 30 minutes. To stop the DNase activity, 1 µl RQ1 DNase Stop Solution was added and incubated for a further 10 minutes at 65°C. New concentrations were then re-assessed using the nanodrop and samples were stored at -20°C until used for cDNA synthesis (see section 2.3.4. of the General Materials and Methods) and luciferase expression assessment using qPCR.

2.3.4. cDNA synthesis

The complementary DNA (cDNA) was reverse transcribed from the RNA using the Tetro cDNA Synthesis Kit (Bioline) according to manufacturer's protocol. Briefly, between 1-2µg of total RNA were mixed with 1 µl of Oligo $(dT)_{18}$ Primer Mix, 1µl of 10mM dNTP (**d**eoxy**n**ucleotide **t**ri**p**hosphate) mix, 4µl of 5xReverse transcriptase) buffer, 1µl of (10u/µl) Ribosafe RNase inhibitor, 1µl of (200u/µl) of Tetro Reverse Transcriptase and DEPC water up to 20µl. It is important that all samples are synthesised with the same amount of RNA so they can be compared.

The mixture was then placed in a thermocycler (T100™ Thermal Cycler, Bio-RadHercules) and incubated at 45°C for 30 minutes, 5 minutes at 85°C (to terminate the reaction) and then chilled on ice. The cDNA was stored long term at -20°C.

2.4. REAL-TIME POLYMERASE CHAIN REACTION

The polymerase chain reaction (PCR) is a technique used to amplify particular genes from a cDNA template using specific primers that mark the beginning and the end of the sequence. The polymerase will then extend the primers by incorporating the complimentary bases, obtaining more copies of the sequence in an exponential manner. Thus, more copies will be obtained for abundant genes, as the starting template will be higher. In conventional PCR, the amplified product can only be measured at the end of the reaction, whilst in real-time PCR or quantitative PCR (qPCR), the quantification takes place at the same time as the amplification. This allows for a more precise comparison of the expression of a gene between different samples, by assessing the relative gene expression in comparison to a "housekeeping gene" that serves as endogenous control. These genes should be constitutively expressed at the same level between the samples (Schmittgen and Zakrajsek, 2000, Sun et al., 2012). Some of the most used genes are ACTB (β-actin), GAPDH (Glyceraldehyde 3-phosphate dehydrogenase) and HPRT1 (Hypoxanthine-guanine phosphoribosyltransferase) among others.

2.4.1. Taqman assays

In real-time PCR, the amplified product detection is carried out by fluorescent dyes. In this project, Taqman primer probes were used to both amplify and detect the product. Taqman probes are specific oligonucleotide sequences that contain a fluorescent reporter at the 5' end and a fluorescence quencher at the 3' end. The close proximity between the two causes the quencher to absorb the fluorescence emitted by the reporter using fluorescence resonance energy transfer (FRET). The Taqman probe will bind in a DNA region that will be flanked by the forward and the reverse PCR primers. During the amplification process, the *Taq* polymerase will start synthesising the new complementary strand from the forward primer. When it reaches the Taqman probe, its exonuclease activity will cleave it. This will cause the reporter and the quencher to separate from each other, allowing the fluorescence to be detected by the instrument. A schematic of this process can be seen in figure 2-9.

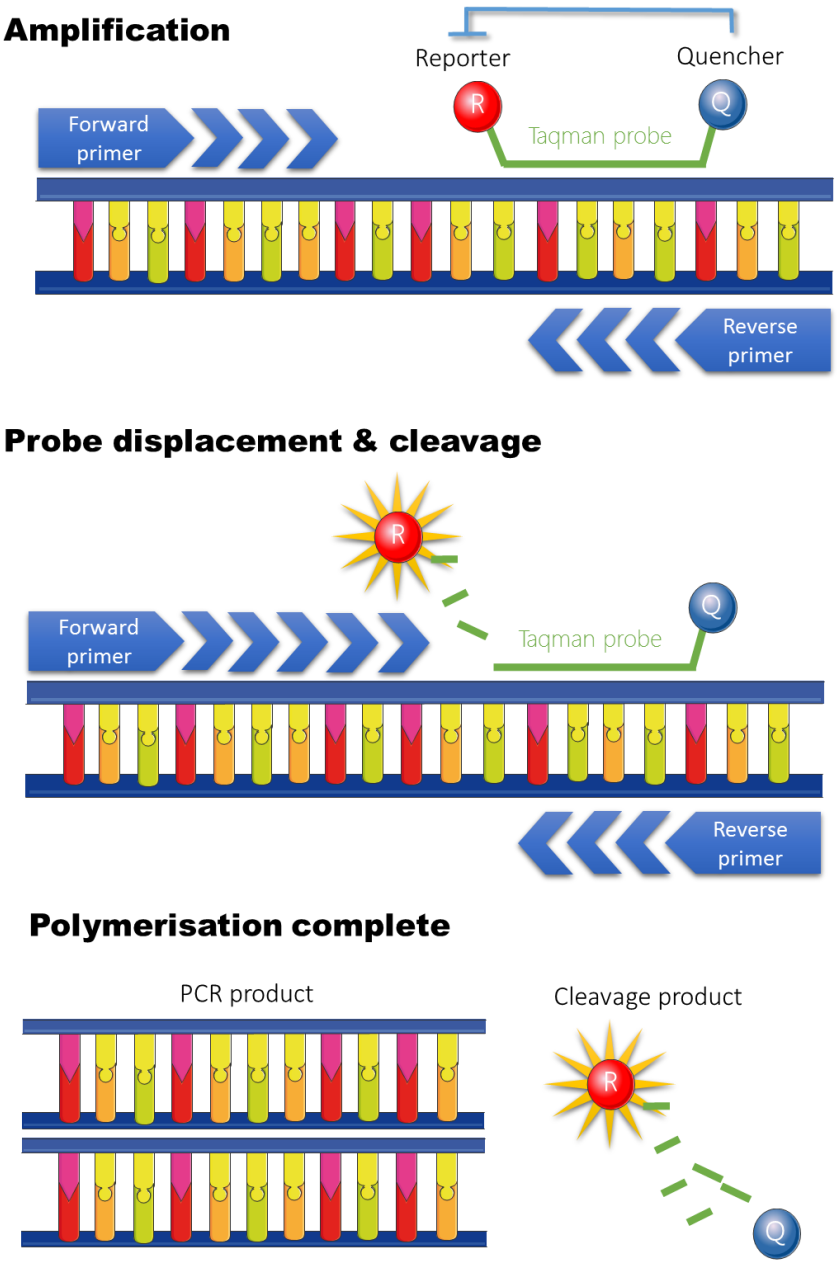

Figure 2-9. Amplification of the cDNA template using Taqman probes in real-time PCR.
In the initial step, both the forward and reverse Taqman primers and the Taqman probe anneal to their complementary DNA sequence. The Taqman probe is flanked by a fluorescent reporter (usually FAM) and a fluorescence quencher (usually TAMRA) that quells any fluorescence. Following denaturation of the cDNA, the DNA polymerase starts extending the template until it reaches the Taqman probe, where it activates its exonuclease activity and degrades it. When the probe is cleaved, it allows for the separation of the reporter and quencher and the release of fluorescence. Thus, the fluorescence detected is proportional to the amount of template in the sample. Diagrams were created using the Servier's image bank, http://www.servier.fr/smart/banque-dimages-powerpoint

In order to measure the gene expression, for each well 2 µl of the cDNA template were mixed with 1 µl of the Taqman primer-probe (Applied Biosystems), 10 µl of the SensiFast Probe Hi-ROX Mix (Bioline) and 7 µl of DEPC water. Each sample was done in triplicate and 20 µl of the mixture were loaded into the well of a 96-well Thermal Cycling plate. The plate was then placed in the StepOnePlus™ PCR machine (Applied Biosystems) and the correct program was run in the instrument.

In the first cycle, the mixture was heated to 95°C for 5 minutes in order to activate the *Taq* polymerase enzyme. In the second cycle, the temperature was maintained at 95°C for 10 seconds to allow the template to denature and then lowered to 60°C for 20 seconds. At this temperature the two primers and the Taqman probe can anneal to their complementary sequence in the DNA. The binding of the probe can span an exon junction (probe is labelled with the suffix *_m* or *_g,* the second may detect genomic DNA) or bind in a single exon together with the primers (suffix *_s).* After that, the *Taq* polymerase will synthesize the new complimentary strand by extending the primers from 5' to 3' with dNTPs, cleaving the Taqman probe in the process. This second cycle will be repeated 40 times, with the product doubling exponentially after each cycle.

Once the reaction ends, the amplification curve displayed should present three phases: exponential (components are in excess), linear (components decrease and product does not double in each cycle anymore) and plateau (components are over and no more product is synthesized). From the real-time PCR amplification plot, a baseline can be drawn to determine background fluorescence, together with a threshold halfway through the exponential phase. The intersection between the threshold line and the amplification curve for a specific gene will determine its C_t (threshold cycle). A low Ct, thus, indicates a higher amount of template as it requires a smaller number of cycles to enter the exponential phase.

A list with all the Taqman probes used can be found in the "Specific Materials and Methods" in each results chapter.

2.4.2. Primer efficiency

If there are no PCR inhibitors, the PCR products should double in every cycle and the PCR efficiency should be 100%. In order to calculate the primers' efficiency, a serial dilution of a cDNA sample was carried out and the Cts measured. The Ct value was plotted on the y axis against the logarithm of the dilution (for instance, 1:4 = log(0.25) = -0.6) on the x axis and the slope was determined. Efficiency was calculated using the following equation:

$$Efficiency\ (\%) = \left(10^{-1/slope} - 1\right)x\ 100$$

Thus, to have 100% efficiency the gradient should be -3.32. Slopes between -3.60 (90%) and -3.10 (110%) are acceptable, values higher and lower may mean poor cDNA quality or pipetting errors. An example of the real-time PCR amplification plot and efficiency curves of some Taqman probes can be seen in figure 2-10.

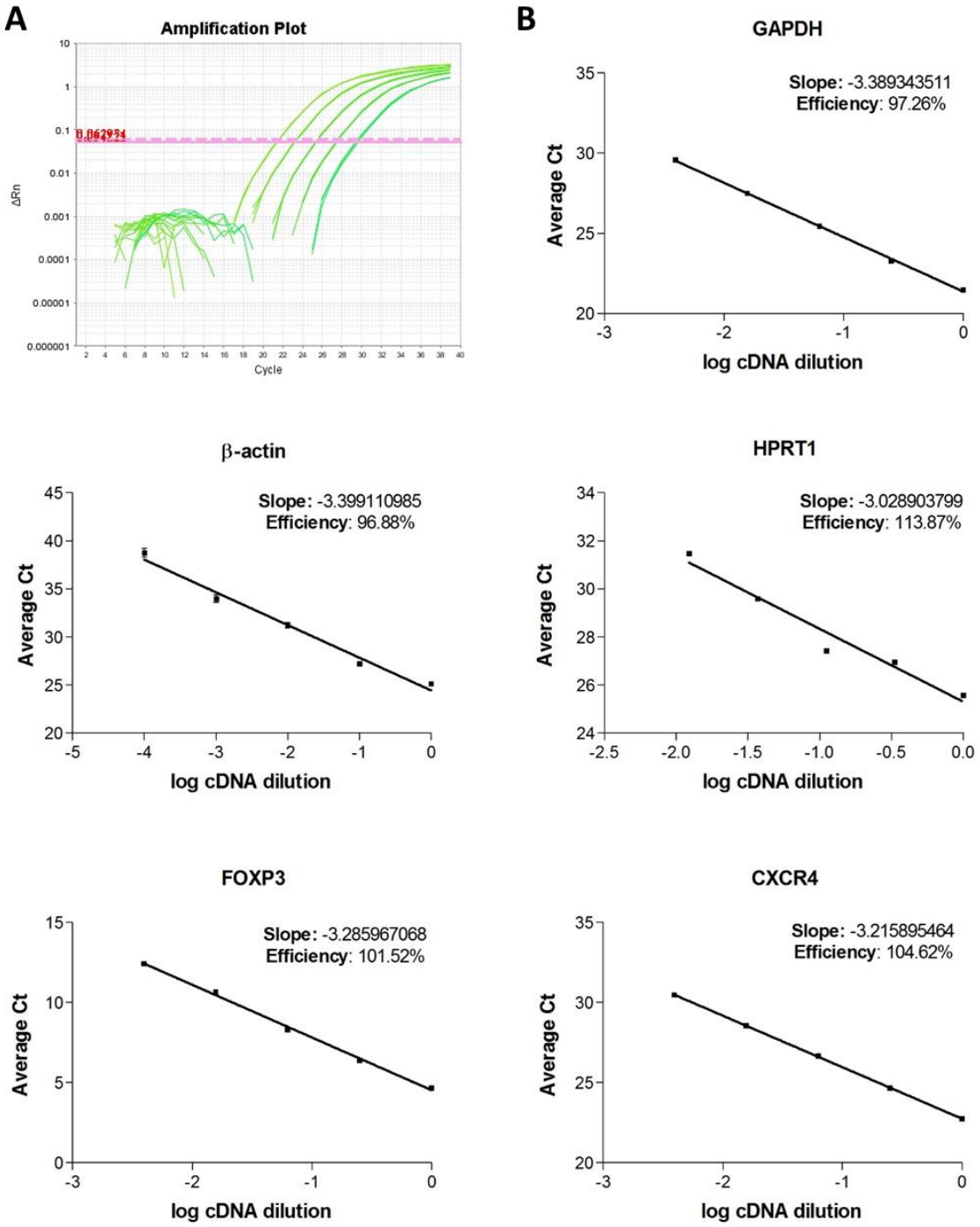

Figure 2-10. Efficiency of several Taqman probes for real-time PCR.
(A) In order to assess the primer's efficiency, cDNA was serially diluted (1:3 for HPRT1, 1:4 for GAPDH, FOXP3 and CXCR4, and 1:10 for β-actin) and the Ct measured after running for 40 cycles. **(B)**The Ct values obtained were plotted against the logarithm of the dilution in order to obtain the slope of the linear regression. The efficiency was then calculated using the following equation: efficiency (%) = $(10^{(-1/slope)} - 1) \times 100$. Graphs show the mean Ct ± SEM.

2.4.3. Relative quantification of gene expression

In order to assess the change in gene expression between a treated and a control group, expression of both the target gene(s) and a housekeeping gene needs to be measured through their Ct. The final compared expression level will then be converted to the fold change in the following manner:

1) $\Delta CT_{treated}$= CT target gene (treated) - CT housekeeping gene (treated).
   This step was repeated for as many treatments or time points there were.

   $\Delta CT_{control}$= CT target gene (control) - CT housekeeping gene (control)

2) $\Delta\Delta CT = \Delta CT_{treated} - \Delta CT_{control}$

3) Fold change= $2^{-\Delta\Delta Ct}$

2.4.4. List of Taqman probes used

For this study five genes, three of which are housekeeping genes, were assessed – their Assay IDs can be found in table 2-1. All these probes had 6-carboxyfluorescein (FAM) as a fluorophore and tetramethylrhodamine (TAMRA) as the quencher.

Sequence	*Assay ID*	*Manufacturer*
FOXP3	Hs01085834_m1	Applied Biosystems
CXCR4	Hs00607978_s1	Applied Biosystems
	Hs00237052_m1	Applied Biosystems
CXCR7	Hs00664172_s1	Applied Biosystems
CCR7	Hs01013469_m1	Applied Biosystems
Luciferase	Mr03987587_mr	Applied Biosystems
GAPDH	Hs02758991_g1	Applied Biosystems
β-actin	Hs01060665_g1	Applied Biosystems
HRTP1	Hs02800695_m1	Applied Biosystems

Table 2-1. List of the Taqman probes used in RT-PCR.
Hs indicates the primers were designed to be used with human samples (Homo sapiens), whilst the suffix indicates whether the probe spans an exon junction (_m1 or _g1) or binds in a single exon together with the primers (suffix _s1). _g1 nevertheless may still detect genomic DNA.

2.5. CELL TRANSFORMATION AND TRANSFECTION

2.5.1. Transient transfection using siRNA

siRNA, or small interfering RNA, are small double stranded RNA (dsRNA) sequences of 20-24 bp in length that can interfere with the expression a specific gene. In endogenous processes, siRNA are created by the cleavage of longer dsRNA or small hairpin RNA (shRNA) by the Dicer enzyme. Exogenous siRNA can enter the cell via liposomes, where one of its strands will bind and activate the *R*NA-*i*nduced *s*ilencing *c*omplex (RISC). The complex will then bind to its complementary mRNA sequences and induce the Argonaute enzyme, which will cleave the target mRNA. This sequence-specific silencing is transient, and is maintained for 3-5 cell divisions until more mRNA is synthesized.

This process can be emulated by transfecting predesigned sequences using several approaches. In this project, siPORT™NeoFX™ (Ambion), a lipid-based transfection reagent was used. The desired siRNA is encapsulated in a closed lipid bilayer which facilitates the release of the siRNA inside the cell whilst protecting it in the intracellular space. Transfections were carried out following the manufacturer's protocol for reverse transfection in which cells are transfected after being detached, minimising transfection time and increasing transfection efficiency.

Briefly, *Silencer Select* siRNA stock was diluted from 100 µM to a 1 µM working solution. For a six-well plate, cells were detached as described in General Materials and Methods, resuspended in Opti-MEM media (Invitrogen) at a density of 2.3 x 10^5 cells/ml and kept at 37°C. For each well, 10 µl of siPORT™ NeoFX™ Transfection Agent were added to 125µl of Opti-MEM and incubated for 10 minutes at room temperature. In the meantime, 15 µl of 1µM *Silencer Select* siRNA were diluted in 125 µl of Opti-MEM, whilst for *Silencer* siRNA, 9 µl of 10µM *Silencer* siRNA were diluted in 125 µl. After 10 minutes, the diluted siPORT™ NeoFX™ Transfection Agent and the diluted RNA were combined and the mixture was incubated for a further 10 minutes to allow transfection complexes to form. 250 µl of the complexes were then dispensed in each well of a 6-well plate together with 2.25ml of the resuspended cells for a final siRNA concentration of 5nM (for the *Silencer Select* siRNA*)* and 30nM (for the *Silencer* siRNA). The cells were then incubated at 37°C and the knockdown effect was assessed.

Transfection was also performed with Negative control siRNA, which sequence has been computer-generated to not match any mRNA in the genome. This allows us to see if any downregulation is due to off-target effects.

2.5.2. Transformation of competent *E.coli*

In order to create CHO-CXCR7 and CHO-CXCR4-CXCR7 transfectants, a vector that contained a different eukaryotic selection marker to the CHO-CXCR4 cells (Zeocin) was needed. From the vectors available in the department, pcDNA3 was chosen as it had been extensively used in literature and it possessed a Neo/Kan resistance to several antibiotics such as G418. G418, also known as geneticin, is an antibiotic which causes cell death by inhibiting the binding of the next tRNA to the eukaryotic ribosome, halting the elongation step in protein biosynthesis. G418 resistance is conferred by the *Neo* gene, which encodes the neomycin phosphotransferase. This enzyme phosphorylates several aminoglycoside antibiotics (such as kanamycin, neomycin and G418), inactivating them (Yenofsky et al., 1990). Zeocin, on the other hand, works by intercalating into DNA and causing double strand cleavage by mechanisms that are still not known. Zeocin resistance is acquired through the *Sh ble* gene, whose protein binds to the zeocin and prevents its action (Trastoy et al., 2005).

Either ampicillin or kanamycin can be used to select the transformed *E.coli*, as the vector also possesses an ampicillin resistance (*ampR*) gene. Ampicillin is a β-lactam antibiotic that inhibits the bacterial enzyme necessary for the synthesis of their cell wall, which leads to cell lysis. Ampicillin resistance is conferred by the *ampR* gene which encodes the β-lactamase enzyme, causing the hydrolysis of ampicillin's antibacterial β-lactam ring.

E.coli containing the pcDNA3 vector were generously donated by Dr. Jeremy Palmer and Dr. Andrew Knight.

2.5.2.1. *Extraction of plasmid DNA from E.coli*

A pCMV-XL5/CXCR7 plasmid was previously purchased from Origene and transformed into *E.Coli*. pCMV-XL5 is a 4.7kb vector with ampicillin as a bacterial selection marker but no mammalian cell resistance, and thus the CXCR7 insert had to be cloned into a new vector. Frozen CXCR7-*E.coli* were thawed from the -80°C freezer, 10 µl spread onto an LB plate with 100µg/ml of ampicillin and grown overnight in an incubator at 37°C. The next day, a colony was picked from the plate

and grown in 5ml of LB broth (Sigma) with 100µg/ml ampicillin in a universal tube on the shaker (150 rpm, 37°C) overnight.

LB, or Lysogeny Broth (Sigma-Aldrich) is a nutritionally rich medium composed by 10g/L bacto-tryptone, 5g/L bacto-yeast extract, and 10g/L NaCl (at pH7). In order to make the media, 10 g/l of the LB powder was added to distilled water and autoclaved (121°C for 15 minutes) in order to sterilise the broth. To make LB agar plates, 10 g/l of agar were added to 10g/l of LB broth before being autoclaved. Once cooled to about 50°C, the liquid was poured on Petri dishes and allowed to solidify. Any necessary antibiotic (mainly 100 µg/ml ampicillin; Sigma-Aldrich) was also added at this stage.

The plasmid was then isolated using a QIAprep Spin miniprep kit (Qiagen) according to the manufacturers' instructions. Briefly, the bacterial culture was centrifuged at 4,600xg for 5 minutes at room temperature and the pellet resuspended in 250µl of buffer to lyse the cells and eliminate the RNA. 250µl of buffer P2 was added and the solution was incubated for a maximum of 5 minutes to allow the cell lysis to occur. 350 µl of buffer N3 were then added and the solution mixed by inversion in order to stop the reaction, turning the solution from blue to colourless. The lysate was centrifuged at 18,000xg for 10 minutes to pellet cell debris, protein, chromosomal DNA and lipids. The supernatant was transferred to a QIAprep spin column and centrifuged for 1 minute at 18,000xg in order for the plasmid to bind to the silica. The column was then washed twice by centrifuging 1 minute at 18,000xg with 500 µl of buffer PB and then 700 µl of buffer PE, the flow through discarded. An extra 1 minute spin was carried out at 18,000xg to remove residual wash buffer before eluting the plasmid in 50µl of buffer EB into a new Eppendorf tube.

This was carried out for the pCMV-XL5/CXCR7 *E.coli*, the pcDNA3 *E.coli* and the pmaxGFP *E.coli*. The latter plasmid can be used to assess transfection efficiency as successfully transfected cells will present green fluorescence.

2.5.2.2. *Digestion of plasmid DNA with restriction enzymes*

In order to cut the CXCR7 insert from the previous vector and clone it into the new one, restriction enzymes are needed. This group of bacterial enzymes can recognize and hydrolyse specific short, symmetrical base pairs sequence called "restriction site". In bacteria, this serves as a defence mechanism against virus as the enzyme

cleaves the foreign DNA whilst the bacterial DNA, which is methylated, is not recognised. This restriction can produce either "blunt" or "sticky" (overhanging) 3'-OH and 5'-OH ends. Blunt ends can bind to other blunt ends in a non-specific manner; but sticky ends can only bind with other sequences with the same overhanging sequence to restore the original restriction site. In figure 2-11 we can see the restriction sites present in the multiple cloning site (MCS) of both vectors. Originally, CXCR7 had been inserted in the pCMV-XL5 vector using the NotI restriction sites and thus those sites in between were believed to be lost. In order to confirm this, the plasmid was sent for sequencing to Source BioScience (Nottingham, UK), which revealed the presence of more restriction sites. Thus, the enzymes EcoR I (Promega) and Not I (Promega) were chosen in order to allow directional cloning. The optimal buffer for the double digest was selected using the Promega Restriction enzyme tool.

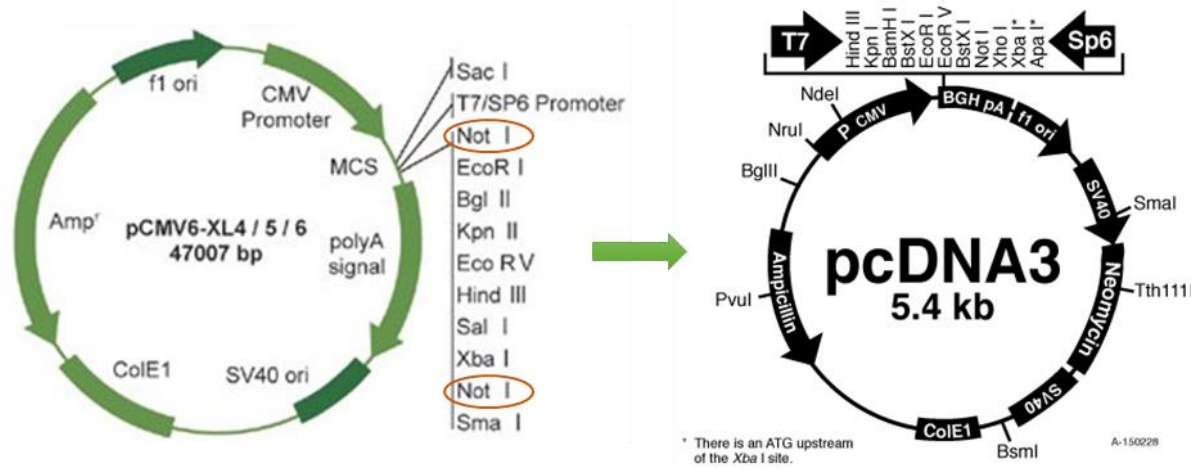

Figure 2-11. Enzyme maps from the origin vector (pCMV6-XL5) and the destination vector (pcDNA3).
CXCR7 had previously been cloned into the pCMV6-XL5 vector which lacks a mammalian selection gene. As the *CXCR4* gene had already been cloned in a vector with Zeocin resistance, a different antibiotic was required. Thus the vector pcDNA3, with Neomycin (G418) resistance, was chosen. The pCMV6-XL5 vector map is from http://www.origene.com/cdna/trueclone/vectors.mspx, and the pcDNA3 vector map from https://www.addgene.org/12965/.

Briefly, for plasmid digestion the enzyme activity is defined in units, where one unit is the amount of enzyme needed to digest 1 µg of DNA in 1 hour at 37°C. Nevertheless, in restriction reactions usually a two- to tenfold excess of enzyme is used to ensure a complete digestion. For this digestion, 2µl of restriction enzyme buffer (Buffer H, 10X), 0.2µl of acetylated BSA (10 µg/µl), 1 µl of DNA (optimally 1 µg/µl, up to 2.5 µg/µl), 0.5µl EcoRI (10u/µl) and 0.5µl NotI (10u/µl) were mixed with DEPC water for a final volume of 20 µl. The components were gently mixed and incubated at 37°C for 2-3 hours.

This reaction was carried out for both the pCMV-XL5/CXCR7 plasmid and the pcDNA3 vector.

2.5.2.3. *DNA extraction from agarose gel*

3 µl of each digest was loaded in an agarose gel as described in section 2.3.3. After confirming the correct digestion by looking at the bands' size, the remaining digest was loaded into another agarose gel and electrophoresis was carried out. The bands were then visualized under the UV light, and the CXCR7 insert and the pcDNA3 vector cut out carefully using a sterile scalpel blade, weighted and placed in an Eppendorf tube.

In order to elute the insert and vector from the gels, the QIAquick Gel Extraction Kit (Qiagen, Manchester, UK) was followed according to the manufacturer's instructions. Briefly, 3 volumes of buffer QG were added to each volume of gel (e.g. 300 µl to 100 mg of gel) and incubated at 50°C for 10 minutes. After the gel slice had completely dissolved, 1 gel volume of isopropanol was added and mixed well to precipitate the DNA. The sample was then transferred to a QIAquick column and centrifuged at maximum speed for 1 minute to bind the DNA to the silica whilst the impurities (enzymes, salt, agarose, etc.) flowed through. The DNA was then washed twice with 0.5 ml of buffer QG and 0.75 ml of buffer PE by centrifuging for 1 minute at 18,000xg and discarding the flow-through. An extra 1 minute spin was carried out at 18,000xg to remove residual wash buffer before eluting the plasmid in 30 µl of buffer EB into a new Eppendorf tube.

3 µl of each sample was then was loaded in another agarose gel as described in in section 2.3.3 to confirm the correct extraction of the DNA and assess the relative quantities of the vector and the insert.

2.5.2.4. *Ligation into pcDNA3 vector*

In order to bind the insert and the vector together, DNA ligase is required. This enzyme works by creating a phosphodiester bond between the 3'-OH overhanging end of the vector with the 5'-P of the insert using ATP as the adenylating agent. In a usual ligation, three reactions are prepared with the following vector to insert proportions – 1:1, 1:3 and 1:9. These quantities can be measured using a Nanodrop or approximated from the band´s intensity.

Briefly, 10 µl of Ligase 2X buffer and 1 µl of ligase (Quick Ligation™ Kit, New England Biolabs) were added to the vector and insert together with DEPC water up to 20 µl. The ligation mixture can then be incubated from 10 minutes at room temperature up to overnight at 4°C. The same reaction was also carried out without the insert to serve as a control for correct vector digestion. If not completely digested, the vector can re-circularize and confer ampicillin resistance to non-insert containing *E.coli* when transfected.

2.5.2.5. *Bacterial transformation*

In order to clone the CXCR7 plasmid, Subcloning Efficiency™ DH5α™ Competent Cells were purchased from Invitrogen (Life technologies). DH5α are chemically competent *E.coli*, which indicates they have been treated with calcium chloride to facilitate plasmid entry.

For transformation, manufacturer's protocol was followed. Briefly, cells were thawed on ice and 50 µl were aliquoted in an Eppendorf tube. Then, 4 µl of the ligation product was added to the cells and incubated on ice for 30 minutes to allow the attachment of the plasmid to the cell membrane. Cells were heat shocked by placing them in a water bath at 42°C for 30 seconds, opening pores in the cells' membranes and allowing the plasmid to enter. Afterwards, cells were put back on ice for 2 minutes to close the pores. 950 µl of pre-warmed LB broth was added to the cells and the tubes were incubated in the shaker (37°C, 150 rpm) for 1 to 2 hours. Finally, 100 µl of the cells were spread in a LB plate with 100 µg/ml ampicillin and incubated at 37°C overnight. A control with no cells was also incubated to ensure there was no contamination.

2.5.2.6. *Culture and preservation of bacterial cells*

Positive colonies were picked with a sterile loop and grown in 10 ml of liquid LB overnight at 37°C on the shaker and then spread in LB agar plates and grown at 37°C on the incubator overnight. New cultures were then expanded from the plate as needed. In order to conserve the transformed cell line, 500 µl of the overnight bacterial culture were mixed with 500 µl of sterile 50% glycerol and stored at -80°C.

2.5.3. Transfection of CHO-K1 cells

2.5.3.1. *Killing curve*

As previously discussed, the CHO-CXCR4 cell line was created by transfecting CHO cells with the pcDNA3.1+Zeo vector, conferring them resistance against Zeocin; whilst the CHO-CXCR7 cells were transfected with the pcDNA3 vector, giving them G418 resistance. Each wild type cell line has a different sensibility to a certain antibiotic, so it is important to determine the smallest dose that will cause the untransfected cells' death.

In order to assess this, $4x10^4$ wild type CHO cells were seeded in two 6-well plates and incubated overnight until ~30% confluent. Cells were then treated with scaling concentrations of Zeocin ranging from 0-400 μg/ml or G418 with concentrations ranging from 0 to 1200 μg/ml. Fresh media with new antibiotic was changed every three days and viability was assessed for a period of 9 days through confluency.

2.5.3.2. *CHO cell stable transfection and cloning strategy*

Two strategies were carried out to optimise CHO cell transfection with the pmaxGFP plasmid. A control with no plasmid was also carried out to assess treatment toxicity.

First, cells were transfected by electroporation using an Amaxa Nucleofector™ Device (Lonza). Briefly, for each transfection confluent cells were trypsinised and $1x10^6$ CHO cells were resuspended at in 100 μl of warm electroporation media. As we had no Amaxa™ Nucleofector™ solution V available, cells were resuspended in PBS or basal media. 1 μg of pmaxGFP was added to the cells and transferred to the electroporation cuvette. Samples were then electroporated with program U-027 or U-023 and immediately 500 μl of culture media was added to the cells - dead cells were visible as a white pellet. Cells were then transferred to a 6-well plate containing 1 ml of media and left to grow.

Second, cells were transfected through lipid-base reagents using Effectene (Qiagen) and the manufacturer's protocol was followed. Briefly, cells were seeded in two 6-well plates at a concentration of $1x10^5$ and $2.5x10^5$, respectively, and left to grow overnight. The following day, for each well 0.4 μg of plasmid were mixed with 3.2 μl of enhancer and volume was made up to 100 μl. Sample was vortexed for 1 second and left to stand for 5 minutes at room temperature. In order to optimise the transfection, the sample was divided into three Eppendorf tubes and three different

Effectene volumes (4, 10 and 20 µl) were added. Samples were vortexed for 10 seconds and left to incubate for 10 minutes at room temperature to allow the formation of transfection complexes. In the meantime, cells were washed with PBS and 1.6 ml of new media were added to the cells. Finally, 600 µl of media was added to the transfection complexes and added drop by drop to the cells. The media was swirled to ensure a uniform distribution and the cells were left to incubate overnight. Fluorescence was assessed the next day.

For the transfection of CHO and CHO-CXCR4 cells, Effectene was chosen given its lesser cell death, with a seeding concentration of $2x10^5$ cells and 10 µl of Effectene. The day after transfection, media was replaced with media with an optimised concentration of antibiotic and replaced every three days until colonies reached the desired size (two to three weeks), as pictured in Figure 2-12A. Roughly, colonies should be visible to the naked eye when looked from underneath against the light. Ideally colonies should be big enough to fill the field of vision at 20x in the microscope, but not too close to each other.

Once appropriate-sized colonies were observed, they were isolated using cloning rings. The day before, silicone grease (Fisher scientific) in a glass petri dish, forceps and cloning rings (Sigma) were autoclaved. On the day, colonies were first circled using a permanent marker by looking against the light and presence was confirmed using a microscope. Media was then removed from the well and the plate rinsed with PBS to remove any floating cells. Using sterile forceps, a cloning cylinder was picked up and lightly coated in vacuum grease before placing it over a marked colony and gently pressed down with the forceps, taking care to not slide the cylinder over the cells and form a silicone seal. Then, 200 µl of warm trypsin were added to the cloning cylinders as pictured in Figure 2-12B and placed in the incubator for 2 to 5 minutes. In the meantime, 24-well plates were prepared with 1 ml of media with the selection antibiotic. Cell detachment was confirmed by looking at cells under the microscope – floating cells appear round and glowing albeit no movement can be observed. Trypsin was then pipetted up and down four times before adding it to one of the prepared plate wells and the cylinder was rinsed with 200 µl of media to transfer any remaining cells. This process was repeated for up to 30 colonies and then plates were placed in the incubator and allowed to grow until completely confluent (one to two weeks) before transferring colonies to 6-well plates and expanded.

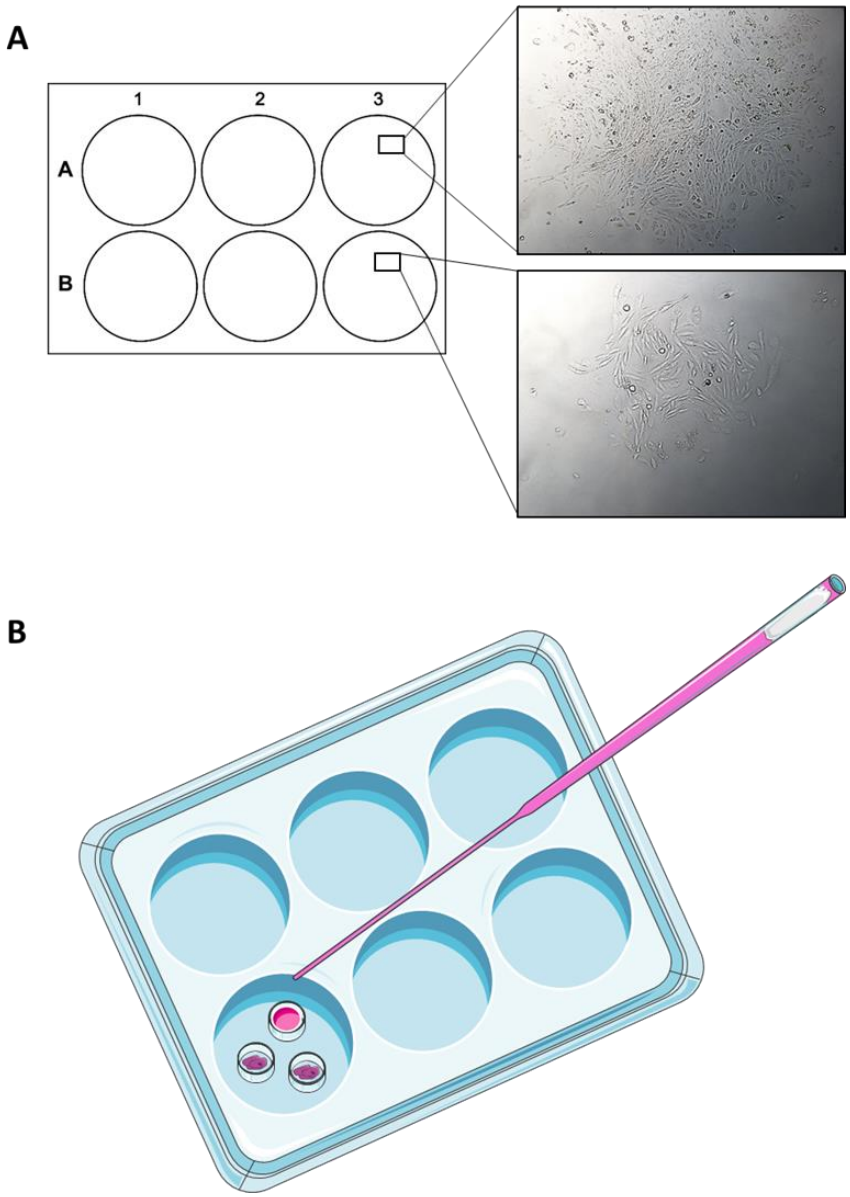

Figure 2-12. Cloning strategy for CHO-CXCR7 and CHO-CXCR4-CXCR7 cells.
(A) Transfected CHO cells were grown in 6-well plates until medium-sized colonies could be seen. **(B)** Cloning cylinders were lightly coated in autoclaved vacuum grease and placed surrounding colonies. Cylinders were then filled with trypsin and incubated at 37°C for 5 minutes before pippeting up and down to ensure detachment. Detached colonies were placed in 24 well plates and expanded. Diagrams were created using the Servier's image bank, http://www.servier.fr/smart/banque-dimages-powerpoint

2.5.3.3. *Single cell dilution*

Despite taking care to select only single colonies, some presented two populations with different expression levels of CXCR4 and CXCR7. To remedy this, single cell dilution of the highest-expressing colonies was carried out. Briefly, for each colony 20 cells were placed on the first row of a 96-well plate and serially diluted 1:2 with media containing antibiotic to a final volume of 200 µl. A schematic of the process can be found in Figure 2-13. Cells were then incubated for 10 days, marking wells where a single colony was present. Those wells were then expanded and expression assessed using flow cytometry.

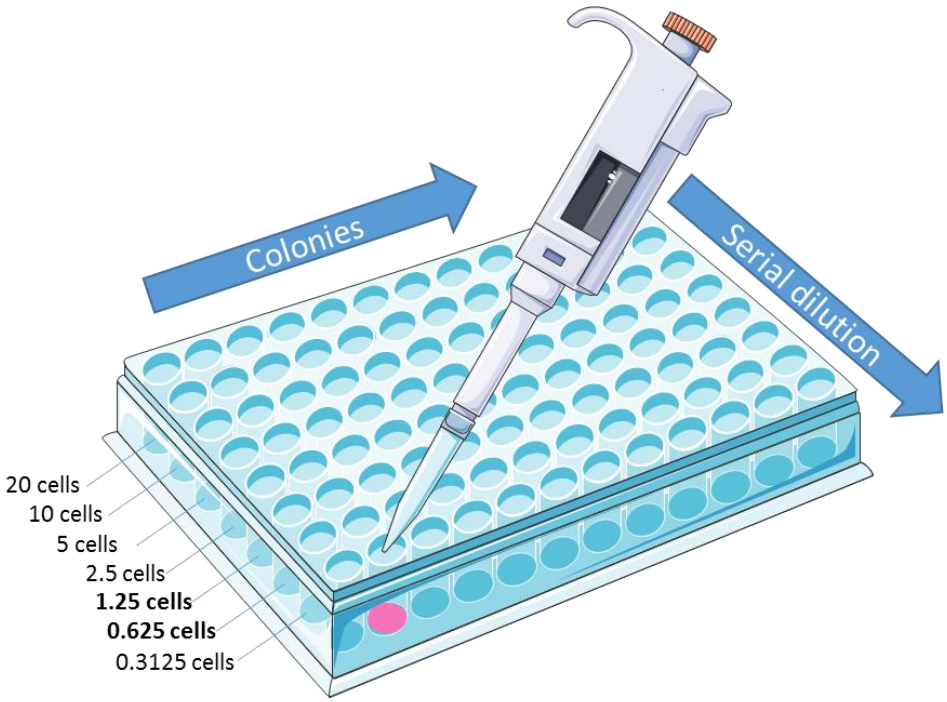

Figure 2-13. Single cell dilution.
20 cells of selected colonies were seeded in the different columns of a 96 well plate and a serial dilution (1:2) was performed throughout the rows until a single cell was present per well (see bolded rows). Cells were allowed to grow and wells with single colonies were expanded. Diagrams were created using the Servier's image bank, http://www.servier.fr/smart/banque-dimages-powerpoint

2.5.3.4. *CHO cell transient transfection optimisation*

Unfortunately, double transfected cells did not maintain a stable expression through passages and thus it was decided to create transient transfected cells. For this, the transfection protocol was optimised in a 60 mm petri dish according to manufacturer's instructions. Briefly, three different DNA quantities (0.5, 1.0 and 2.0 µg) and three different DNA to Effectene ratios (1:10, 1:25 and 1:50) were trialled. A summary of the different transfection treatments can be found in Table 2-2.

	DNA	***Enhancer***	***Effectene***
Treatment A	0.5 µg	4 µl	5 µl
Treatment B	0.5 µg	4 µl	12.5 µl
Treatment C	0.5 µg	4 µl	25 µl
Treatment D	1 µg	8 µl	5 µl
Treatment E	1 µg	8 µl	12.5 µl
Treatment F	1 µg	8 µl	25 µl
Treatment G	2 µg	16 µl	5 µl
Treatment H	2 µg	16 µl	12.5 µl
Treatment I	2 µg	16 µl	25 µl

Table 2-2. Quantities of DNA, Enhancer and Effectene needed for the optimisation of CHO-CXCR4 cell transfection in 60 mm petri dishes.

2.6. IMMUNOHISTOCHEMISTRY

Paraffin blocks containing tumour samples were cut using a microtome into 4μM thick sections and mounted on positively charged slides. This charged surface helps with binding tissues to the slide, which is necessary for fatty tissues as the section can lift off on normal slides. Samples were deparaffinised in xylene for 5 minutes, hydrated through alcohols (99% → 95% → 70%) and washed in distilled water. Endogenous peroxidase was blocked by immersing the samples in 0.3% hydrogen peroxide for 10 minutes. This is important as antigen detection is carried out using horseradish peroxidase (HRP) and the endogenous peroxidase could cause non-specific background staining.

Antigen retrieval was then optimised by heating the samples in a pressure cooker for 2 minutes with 1.5l of citrate buffer (10 mM Sodium citrate, 0.05% Tween 20, pH 6.0) or EDTA buffer (10 mM Tris base, 1 mM EDTA solution, 0.05% Tween 20, pH 9.0), or by digesting in trypsin for 5 minutes. Briefly, trypsin solution was prepared by adding 5 ml of trypsin and 5 ml of citrate to 90 ml of distilled water (pH7.8) and warming it up to 37°C. Slides were then placed for 5 minutes in distilled water at 37°C, followed by the trypsin for 10 minutes at 37°C. After all treatments slides were washed under running cold water and transferred to PBS. This step is crucial to unmask any antigens that may have been crosslinked as a result of the formalin fixation.

Samples were then stained using the Vectastain ABC kit (Vector) as per the manufacturer's instructions (depicted in Figure 2-14). Briefly, samples were incubated with blocking buffer for 10 minutes, followed by the primary antibody for the optimised time and dilution. The antibodies used are in Table 2-3 as follows:

Antigen	***Origin (Species)***	***Reactive species***	***Manufacturer***	***Catalogue number***
CXCR4	Mouse monoclonal	Human, feline	R&D Systems	MAB172
CXCR7	Rabbit polyclonal	Human, mouse	Abcam	ab38089
CCR7	Mouse monoclonal	Human	R&D Systems	MAB197
Luciferase	Goat polyclonal	Firefly (*Photinus pyralis*)	Promega	G7451

Table 2-3. Primary antibodies used in immunohistochemistry.

Next, the biotinylated secondary antibody was added for 30 minutes and the tertiary solution for another 30 minutes at room temperature. It is important to note that a

different kit was used depending on the species the primary antibody had been raised against.

DAB (3,3'-Diaminobenzidine) substrate was then prepared using the DAB Peroxidase (HRP) Substrate Kit (Vector) following the manufacturer's instructions. DAB substrate was dispensed on top of the samples and incubated for 2 minutes before washing under running tap water. Samples were counterstained with haematoxylin for 1 minute 20 seconds and "blued" under running tap water. Slides were then placed in Scott's water for a minute and dehydrated through ascending alcohol concentrations (70% → 95% → 99%) before placing them in xylene. Finally, the slides were mounted using DPX (Sigma-Aldrich) and allowed to dry.

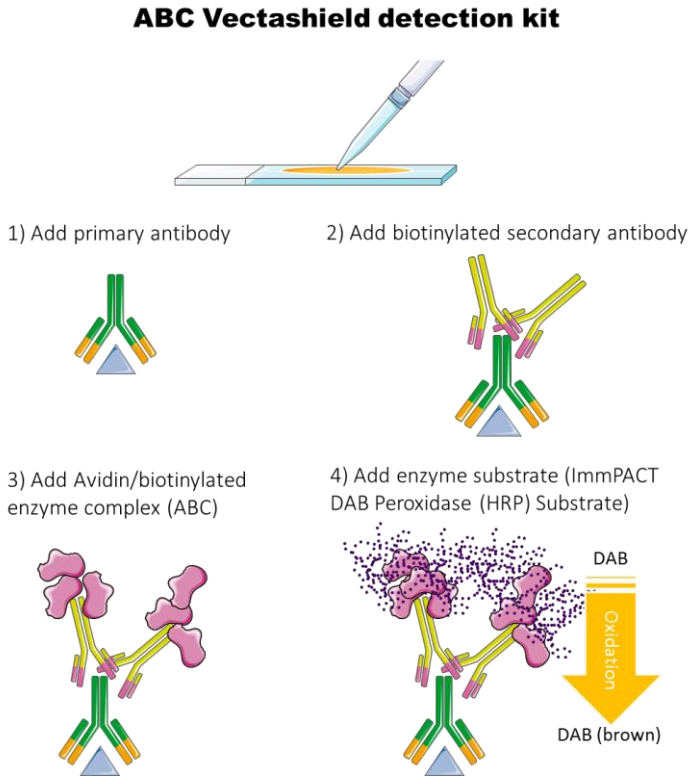

Figure 2-14. Schematic of the ABC Vectashield detection kit.
4µm tissue sections are deparaffinised, rehydrated and antigen retrieval carried out before using the ABC kit. Firstly, samples are blocked using the kit's blocking serum - this is usually the same species as the secondary antibody. Then, the primary antibody is added as per the manufacturer's instructions before washing with TBS and adding the secondary biotinylated antibody for thirty minutes. Next, the VECTASTAIN ABC Reagent is added for 30 minutes – this is a mixture of avidin and its paired biotinylated enzyme (peroxidase). For each biotin present in the secondary antibody, four avidins will bind with very high affinity, amplifying the signal. Finally, the enzyme's substrate, DAB, is added. The DAB will be oxidised by the peroxidase, giving a visible dark brown product. Diagrams were created using the Servier's image bank.

If frozen samples had to be cut for immunohistochemistry, samples were embedded beforehand in OCT (Optimal cutting temperature) compound and cut using the cryostat in 7µm sections – this was carried out by Miss Barbara Innes or Miss Katie Cook. Staining was then carried out as described above but without the antigen retrieval process.

2.7. IMMUNOFLUORESCENCE

In order to validate the cell line used, immunofluorescence (IF) experiments were carried out. Cells were grown in 8-chamber slides at a density of $5x10^4$ cells/chamber and cultured with 250µl of media until confluent (usually after 1-2 days). The media was then removed and cells were washed with PBS and fixed with 250 µl 4% paraformaldehyde for 30 minutes or ice-cold methanol for 10 minutes and left to air-dry. Cells were washed and permeabilised by adding 100µl of 0.1% Triton X-100 detergent (Sigma-Aldrich) for 15 minutes to allow the antibodies to reach intracellular antigens. In order to prevent non-specific binding, the chambers were blocked by adding 100 µl 5% BSA/PBS. When non-specific staining could still be observed, chambers were blocked instead with 200µl 20% goat's serum. After 30 minutes, the solution was removed and 100µl of the primary antibody (diluted in 1% BSA) were added and incubated at 4°C overnight in a humid chamber. A control well with no primary antibody was also carried out to assess non-specific binding. A list with the antibodies used can be found in each results chapter.

The next day, slides were washed 3 times in PBS for 5 minutes and incubated with 100 µl of a fluorochrome-conjugated secondary antibody (diluted in 1% BSA) for 2 hours at room temperature or overnight at 4°C. The slides were washed three times and mounted using 2-3 drops of Vectashield mounting media containing 4',6-**d**i**a**midino-2-**p**heny**l**indole (DAPI, DAKO). DAPI is a dye that, when excited at 358nm, emits its peak fluorescence at 461nm (blue) when bound to double-stranded DNA, but emits no fluorescence when unbound. This allows for the observation of the cells' nuclei. A coverslip was then placed on top, any bubbles removed and the mounting media was left to dry for 30 minutes before sealing the edges of the coverslip with nail polish. Slides were viewed using the Zeiss Axio Imager II microscope (Filter number Zeiss 49, with excitation at 335-385nm and emission at 420-470nm for DAPI).

2.7.1. List of antibodies used for IF

For immunofluorescence, the following antibodies in table 2-4 were used:

Antigen	*Origin (Species)*	*Reactive species*	*Manufacturer*	*Dilution*	*Catalogue number*
α-tubulin	Mouse monoclonal	Human	Sigma-Aldrich	1:500	T6074
CCR7	Rat monoclonal	Mouse	R&D Systems	1:20	MAB3477
	Mouse monoclonal	Human	R&D Systems	1:20	MAB197
CXCR4	Mouse monoclonal	Human	R&D systems	1:100	MAB172
CXCR4 (p- S339)	Rabbit monoclonal	Human	Abcam	1:500	Ab74012
CXCR7	Mouse monoclonal	Human	R&D systems	1:100	MAB4227
Cytokeratin 19	Mouse monoclonal	Human	Biolegend	1:100	628502
E-Cadherin	Mouse monoclonal	Human	Biolegend	1:50	324101
E-cadherin	Mouse polyclonal	Human, Rat, Dog, Mouse	BD Biosciences	1:100	610181
FOXP3	Mouse monoclonal	Human	Abcam	1:100	ab20034
Integrin αV	Mouse monoclonal	Human	R&D systems	1:50	MAB12191
Ki-67	Rabbit monoclonal	Human	Abcam	1:100	Ab15580
S100-A4	Mouse monoclonal	Human	Abnova	1:100	H00006275-M01
Vimentin	Rabbit polyclonal	Mouse, Rat, Human	Santa Cruz Biotechnology	1:100	SC-7557-R
ZO-1	Rabbit polyclonal	Chicken, Dog, Human, Pig, Mouse	Abcam	1:20	Ab59720-50

Table 2-4. Primary antibodies used in immunofluorescence.

As a secondary antibody, the following antibodies in table 2-5 were used:

Reactive species	***Origin (Species)***	***Fluorochrome***	***Manufacturer***	***Dilution***	***Catalogue number***
Rabbit	Goat	AlexaFluor 488	Life technologies	1:100	A11008
Rabbit	Goat	FITC	Sigma-Aldrich	1:100	F0382
Mouse	Goat	AlexaFluor 488	Life technologies	1:100	A11001
Mouse	Goat	FITC	Sigma-Aldrich	1:100	F0257
Rat	Goat	DyLight-488	Immuno Reagents	1:100	GtxRt-003-E488NHSX

Table 2-5. Secondary antibodies used in immunofluorescence.

2.8. FLOW CYTOMETRY

2.8.1. Principle

Flow cytometry is a technique that allows the characterization of cells through their physical characteristics. In it, individual cells are suspended in liquid and passed through a laser in a single cell stream. This is possible thanks to a phenomenon called hydrodynamic focusing, which consists in surrounding a stream of cells by a second, cell-free faster liquid stream called the sheath stream, which forces the cells to align in a single row. Once the cells are intercepted by the laser, light is scattered in two angles. The forward light scatter (FSC) is gathered by detectors positioned at less than 10° from the cell beam and measures the cell size; whilst the side light scatter (SSC) is collected at 90° and reflects cell granularity and their internal structures. The combination of these two parameters can help identify different cell types present in one sample.

Furthermore, the cells' antigens can be labelled with different fluorescent dyes which can be excited by the laser light at a specific wavelength. After being stimulated, the fluorochrome will return to its unexcited state and emit light at lower energy (hence a higher wavelength). This emitted fluorescence will be reflected by dichroic mirrors, selected by optical filters and fed into photomultiplier tubes (PMT). These detectors will transform the light (number of protons) into an electric current that will be interpreted by the computer as fluorescence intensity. Thus, the fluorescence intensity correlates with the amount of antigen present in the cell. This schematic is depicted in Figure 2-15.

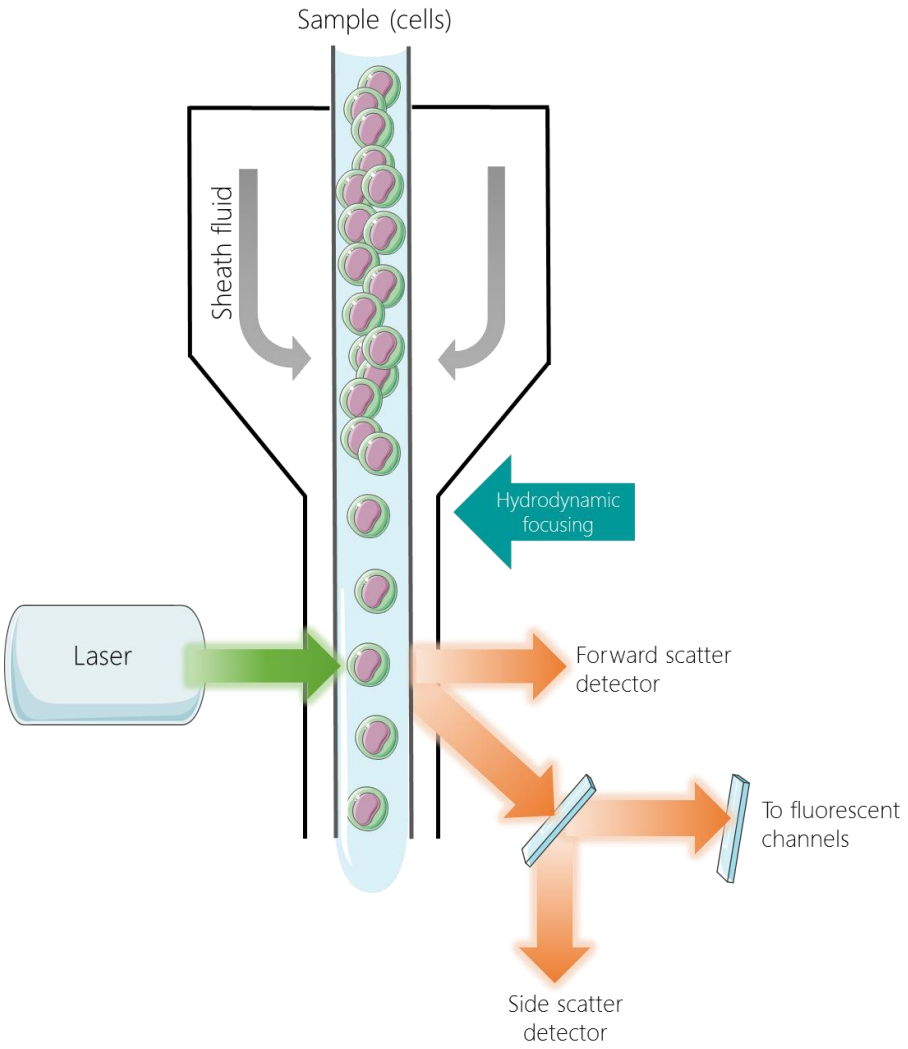

Figure 2-15. Schematic of fluorochrome excitation and detection in a flow cytometer.
The sample is injected into the machine and drawn into a single file thanks to the sheath fluid running on both sides, a phenomenon called hydrodynamic focusing. Thus, cells go through the laser one at a time, which excites the cell-bound fluorochromes and causes the disruption of light. Forward light is collected by the forward scatter detector (FSC) and gives a measurement of the cell size, whilst the side scatter (SSC) and fluorescent light bounces off in a 90° angle and are collected by a series of lenses. The SSC gives a measurement of the cell granularity, whilst the fluorescent light is further transferred through a fluorescence collection lens to filters that transmit specific wavelengths of light and photodetectors. The detected light is then converted to electronic signals and processed for analysis. Diagrams were created using the Servier's image bank, http://www.servier.fr/smart/banque-dimages-powerpoint.

When choosing the fluorescent dyes to use, it is important to know that some fluorochromes will contribute a signal to several detectors. When one dye produces fluorescence that spills over to a second filter, it may cause a "spectral overlap" with a second dye, with the second filter picking up the fluorescence emission from both dyes. For instance, FITC and PE are both excited with the 488 nm laser. FITC is usually detected using the 530/30 filter (meaning it has a pass-band centred at 530 nm, and thus will only let through wavelengths between 515-545nm), which captures 47.4% of its emission. However, 12.5% of that emission can also be detected by the 585/42 filter. When used alone, this has no effect into the analysis. However, if the 488 nm laser is

also exciting PE, the 585/42 filter will detect 70.4% of the PE emission together with the 12.5% emission of FITC, making the PE signal appear stronger than it truly is. This can be visualised in Figure 2-16. Because of this, electronic "compensation" must be carried out in order to subtract the contribution of the undesired fluorochrome to the detector.

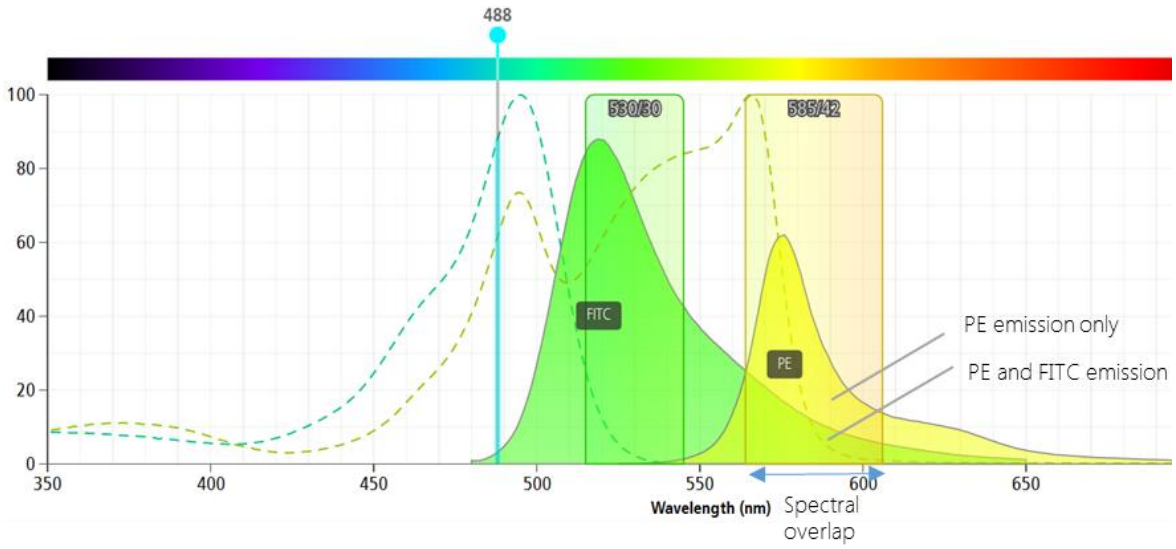

Figure 2-16. Excitation and emission spectra for FITC and PE.
Both FITC and PE are excited sub-optimally at 488 nm (green and yellow dotted lines, respectively) and their fluorescence is detected using 530/30 and 585/42 filters, respectively. However, the 585/42 filter also detects part of the FITC emission. In order to correct that, compensation is applied in order to subtract the unwanted fluorescence (green) from the fluorochrome of interest (yellow). Spectral adapted from http://www.bdbiosciences.com/eu/s/spectrumviewer

Although compensation is sometimes unavoidable, it is recommended to try to purchase fluorochromes that are excited by different lasers in order to minimise overcomplicating the acquisition of data. For instance, if measuring three antigens with a FACSCanto II, Phycoerythrin (PE, 488nm blue laser, 585/42 filter), Allophycocyanin (APC, 633nm red laser, 660/20 filter) and Brilliant Violet 421 (405nm violet laser, 450/50 filter) require no compensation.

2.8.2. Cell viability determination

Dead cells are present in virtually all cell preparations and thus it is important to gate them out when analysing our data. This is key because (a) dead and dying cells will unspecifically bind antibodies, giving a false positive result; and (b), dead cells have increased autofluorescence due to changes in internal components like flavoproteins and porphyrins, which will appear in the green channels such as FITC.

As we are using non-fixed cells, "classic" DNA dyes such as DAPI, propidium iodide (PI) and 7-amino-actinomycin D (7-AAD) can be used. Briefly, DAPI was added to the cells

at 20% of the cell volume (e.g. 20 µl for a 100 µl cell suspension) and left for a couple of minutes before collecting the events in the flow cytometer. Cells with a non-intact membrane, such as dying cells, will take up the dye and be positive in either the violet laser (405 450/50) in the Canto II or in the ultraviolet laser (355 450/50) in the Fortessa X-20.

2.8.3. Surface staining

The work in this project was carried out using either a Becton Dickinson FACS Canto II or a Fortessa X20 flow cytometer (Becton Dickinson, Franklin Lakes NJ, USA).

In order to prepare the samples for analysis, cells were detached using 4 ml of Accutase (Biolegend) for 5 minutes at 37°C and spun at 300xg for 5 minutes to pellet the cells. The use of trypsin is not recommended as this can cause degradation of the cell surface antigens. Cells were then resuspended in FACS buffer (2% FBS in PBS), counted, and $2x10^5$ cells were placed in each FACS tube. If the cells were in a volume larger than 100µl, tubes were spun down and supernatant was decanted before being resuspended in 50µl of FACS buffer. The presence of low quantities of FBS in the FACS buffer helps prevent non-specific staining whilst keeping the cells viable and preventing them from sticking to each other.

Prior to any experiment, antibody saturation curves were carried out in order to define the antibody concentration to stain with. A saturating concentration was defined as the concentration above which there is less than a 10% increase in fluorescence. Cells were then incubated with the optimised antibody volume and time at 4°C in the dark and washed twice with 1 ml of FACS buffer before being resuspended in 200 µl of FACS buffer. Incubating on ice is vital for surface receptor staining as it immobilises the cell membrane, preventing the receptor from internalising. Tubes were kept at 4°C in the dark until analysis.

Cells were also stained with matching primary isotype control antibodies. This allows for the measurement of the non-specific fluorescent background, as antibodies can bind non-specifically to Fc receptors or other cellular antigens. An Fc block (BD biosciences) can be used for 20 minutes previous to antibody staining if the isotype shows high unspecific binding.

All data were analysed using FlowJo software version 7 (Becton Dickinson) and GraphPad prism software version 5.

2.8.3.1. *Antibodies used for FC*

For flow cytometry, the following antibodies in table 2-6 were used:

Antigen	*Reactive species*	*Origin (Species)*	*Fluoro-chrome*	*Manufacturer*	*Catalogue number*
MHC Class I	Human, Mouse, Rat, Hamster, Pig, Bovine, Guinea Pig, Hamster, Sheep	Mouse monoclonal	APC	Novus Biologicals	NB100-65938APC
CCR7	Human	Mouse monoclonal	PE	R&D systems	FAB197P
CCR7	Mouse	Rat monoclonal	PE	R&D systems	FAB3477P
CXCR7	Human, Mouse	Mouse monoclonal	APC	R&D systems	FAB4227 A
CXCR4	Human	Mouse monoclonal	PE	R&D systems	FAB170P

Table 2-6. Antibodies used in flow cytometry

2.8.4. Cytometric bead assay for antibody binding capacity

In order to compare receptor numbers across different fluorochromes, antigen binding capacity (ABC) was assessed using Quantum Simply Cellular anti-mouse IgG (Bangs Laboratories). The manufacturer's protocol was followed – briefly, three tubes were prepared in addition to the transfected cells: (A) one drop (≃50 µl) of uncoated blank beads in 50 µl of FACS buffer, (B) one drop of coated beads #1, #2, #3 and #4 and 20 µl of CXCR4-PE antibody in 50 µl FACS buffer and (C) one drop of coated beads #1, #2, #3 and #4 and 20 µl of CXCR7-APC antibody in 50 µl FACS buffer. Cells were also stained separately and incubated in the dark at 4°C for 90 minutes. Then, tubes were washed twice with 1 ml FACS buffer by centrifuging at 2500g for 5 minutes and resuspended in 500 µl FACS buffer. Beads and cells were run on low (100-200 events/second) until 1,000 events per bead were collected and data analysed using the excel sheet provided in the Bangs Laboratories website.

2.8.5. FRET

Fluorescence Resonance Energy Transfer (FRET) is a phenomena that occurs when the energy of one chromophore (in our case, a fluorochrome) is transferred to another fluorochrome in close proximity, in particular within 5-10 nm of each other (Förster, 1965). This can be carried out with any pair of fluorochromes where the *emission* spectrum of the donor overlaps with the *excitation* spectrum of the acceptor, but the

emission and excitation pairs' spectra are far apart (Kumar et al., 2009). In this study PE and APC were used by exciting PE at 488 nm, a wavelength where APC is barely excited. PE emission falls inside the APC excitation range, overlapping roughly between 530nm and 690nm and allowing for the detection of energy transfer between 650-670 nm with the 660/20 filter. Indeed, between those wavelengths there is barely any PE emission but contains the APC emission peak. All this can be seen in Figure 2-17 below.

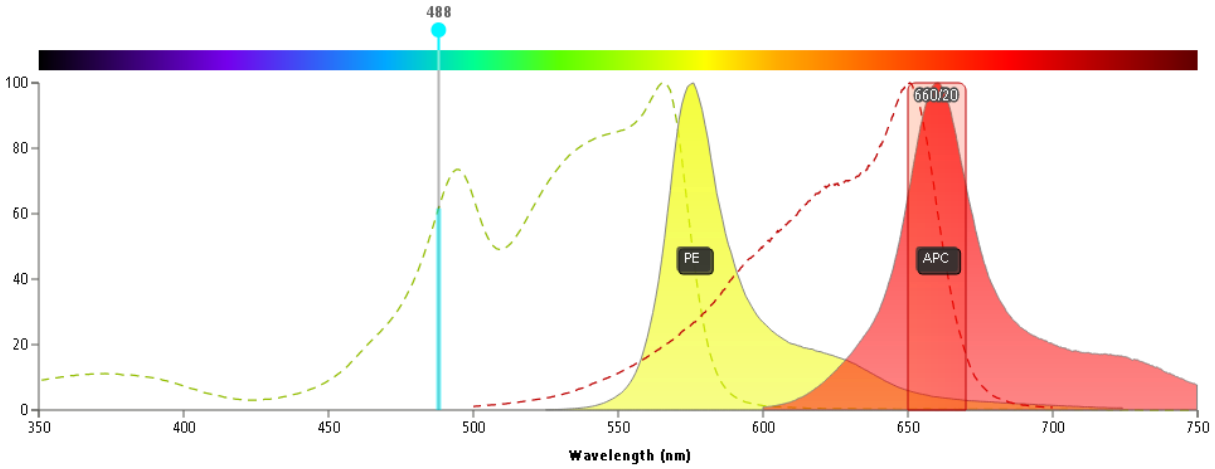

Figure 2-17. Diagram of the laser excitation, emission and absorbance spectra of PE and APC and filter required to detect FRET.
PE (in yellow) is excited with the 488nm laser and the energy transfer to APC (in red) is detected with the 660/20 laser. Excitation spectra is shown as a dotted line, whilst emission spectra is colour filled. In this diagram, the emission spectra has not been normalised to laser excitation. Diagram was created using BD fluorescence spectrum viewer.

With this assay we aimed to assess whether CXCR4 and CXCR7 were forming heterodimers by measuring the FRET between the two. In order to carry this out, 500,000 cells were stained as described in section 2.7.2. for both receptors individually and in combination. Furthermore, half of the doubly stained cells were also treated with CXCL12 for 20 minutes at 37°C to see the effect of ligand binding in receptor proximity. A negative FRET control with CXCR4 and MHC I was also carried out.

Before running the cells in the FACS Canto II, the 670LP filter was changed for another 660/20 filter. Thus, for each sample the following parameters were measured and compensated: PE (excitation laser at 488, emission filter at 585/42), APC (excitation laser at 635, emission filter at 660/20) and FRET (excitation laser at 488, emission filter at 660/20).

2.8.6. ImageStream

The Amnis ImageStreamX MkII is an imaging flow cytometer which combines the single cell analysis of fluorescent markers of flow cytometry with the visual imaging of microscopy. A similar staining process as the one described in section 2.7.2. was followed but with higher numbers. Briefly, 2 million cells were stained with 20 µl of antibody and resuspended in 60 µl FACS buffer – this is due to the cytometer needing cell concentrations of at least $2x10^7$ cells/ml.

2.8.7. Calcium flux

Calcium flux can be quantified using Indo-1 AM dye (BD Bioscience, 2017) as a consequence of its dual emission peak. Briefly, in the absence of calcium Indo-1 AM emits radiation at ~410-420 nm when excited with a UV laser, but this emission shifts to ~485-510 nm in the presence of calcium, which is released as part of the G-protein activation cascade.

Briefly, $5x10^6$ cells were resuspended in 1ml of FACS buffer and stained with 4 µl of 1mg/ml Indo-1 AM for a final 4 µM concentration. Cells were then incubated at 37°C for 30 minutes before centrifuging at 400xg, discarding the supernatant, and washing in FACS buffer. At this point, any staining was carried out if needed as described in section 2.7.2. Finally, cells were resuspended in 1 ml of basal media with 0.5% BSA – unlike FACS buffer, media contains calcium which helps visualising the shift. In particular, DMEM/F-12 contains 1.05 mM calcium whilst RPMI-1640 contains 0.42 mM of calcium (Sigma-Aldrich, 2017), with 1mM calcium being recommended for this assay. Cells were then incubated in a water bath at 37°C for 15-30 min before being run in the Fortessa X-20.

Before running the cells, the 730/45 filter was changed for a 530/30 filter in order to capture the shift in emission. Thus, for each sample the following parameters were measured: free Indo-1 AM (excitation laser at 355nm, emission filter at 450/50) and calcium-bound Indo-1 AM (excitation laser at 355nm, emission filter at 530/30). Cells were then run in the Fortessa X-20 for one minute to establish the baseline before adding 1µl of CXCL12 (10 nM final concentration) and run for 5 minutes. Then, 5 µl of 1mg/ml ionomycin (1 µM final concentration) were added before running for 4 more minutes. Ionomycin is an antibiotic which can bind to calcium with high affinity (Liu and Hermann, 1978) and thus can stimulate the release of calcium from the internal

stores (Morgan and Jacob, 1994), serving as an excellent positive control. After running each sample, a 30 second clean with FACSclean and water was carried out to eliminate any traces of ionomycin that might stimulate the following batch of cells.

Finally, the ratio between the two wavelengths $\left(\frac{355\ 450/50}{355\ 530/30}\right)$ was calculated and plotted against time in order to calculate the peaks of calcium release. To calculate the intracellular calcium concentration, the following formula was used:

$$[Calcium\ (nM)] = Kd\ x\ \frac{CXCL12\ peak - baseline\ peak}{Ionomycin\ peak - CXCL12\ peak}$$

Where Kd is 844 nM, the dissociation constant of calcium and Indo-1 (Mason, 1999, Bassani et al., 1995).

2.9. WESTERN BLOT

Western blot or immunoblot is a common assay employed to detect a specific protein from a cell or tissue lysate. The proteins in the sample are first denaturated and separated by size in an electrophoresis gel before being transferred to a membrane where the primary antibody can bind. A labelled secondary antibody will then be added, enabling the protein's detection through a chemiluminescent reaction after the addition of substrate.

2.9.1. Cell lysate preparation

Lysis buffer was prepared by mixing 10 ml of CelLytic M Cell Lysis Reagent (Sigma), 1 tablet of cOmplete™ Mini Protease Inhibitor Cocktail (Roche) and 1 tablet of PhosSTOP™ Phosphatase Inhibitor Cocktail (Roche); which was then aliquoted and kept at -20°C. To prepare the cell lysate, cells were serum starved and treated as required before adding 50 µl of lysis buffer, vortexing and incubating on ice for 10 minutes. Samples were then spun at 15,000xg for 10 minutes at 4°C to pellet DNA and cell debris; and supernatant was transferred to a fresh Eppendorf tube. Samples were either quantified immediately or stored at -20°C for later use.

2.9.2. Protein quantification

In order to determine the lysate protein concentration, Pierce™ BCA Protein Assay Kit (ThermoFisher) was used following the manufacturer's instructions. Briefly, the unknown protein concentration is determined through a bovine serum albumin (BSA) standard curve; where the stock BSA is serially diluted 1:2 from 2000 ng/ml to 125 ng/ml whilst the unknown sample is diluted 1:10 in triplicate. 10 µl of the standard or sample was then added to a 96-well plate and mixed with 200 µl of the working reagent, which is a 1:50 mixture of Reagent A and Reagent B. Reagent A is a mixture of bicinchoninic acid (BCA) in an alkaline solution (pH 11.25) whilst reagent B contains 4% Copper (II) sulphate (also known as cupric sulphate) – in the presence of protein, the alkaline environment causes the formation of light-blue coloured chelate complexes with the cupric ions. This reduction of Cu^{2+} to Cu^{1+} by the peptide bonds is commonly known as the biuret reaction and is dependent on the amount of protein in the sample. Next, two molecules of bicinchoninic acid will chelate with one Cu^{1+}, forming a new purple-coloured BCA/copper complex. The plate was then incubated for 30 minutes at 37°C to allow for this reaction to develop, and read at 492 nm. Increasing

the temperature or the time will speed up the colour development, decreasing the minimum detection level and the overall detection range. The water-soluble BCA/copper complex has a strong absorbance at 562 nm that correlates with protein concentration, allowing for the determination of the unknown sample using the standard curve. An example can be seen in figure 2-18.

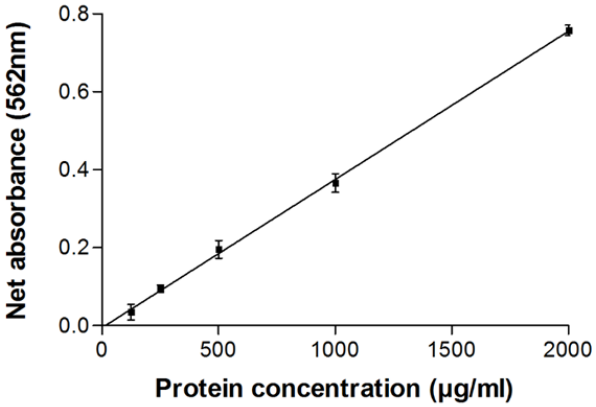

Figure 2-18. Representative BSA (bovine serum albumin) protein standard curve carried out to quantify protein lysate.
In order to determine a lysate's protein concentration, a standard curve was prepared using Pierce® BCA protein assay kit. BSA was serially diluted from 2000µg/ml to 0µg/ml and kit's protocol was followed. After 30 minutes incubation at 37°C, absorbance was measured at 562 nm and the relationship between concentration and absorbance was determined using a linear regression. Error bars are representative of mean ± SEM (n=3).

2.9.3. SDS-PAGE electrophoresis

In order to run proteins in their denatured state, *s*odium *d*odecyl *s*ulfate (SDS) *P*oly*a*crylamide *g*el *e*lectrophoresis (PAGE) is necessary. As a detergent, SDS can break the non-covalent bonds in proteins, and due to its anionic nature it can impart an even distribution of negative charge along the linearized protein.

To prepare the PAGE, a stacking gel needs to be assembled on top of the resolving or running gel – its components can be found in Table 2-7, and the ingredients in Table 2-8. APS (Ammonium persulphate) is used as a source of radicals, which are catalysed by Tetramethyl-ethylenediamine (TEMED) to start acrylamide's polymerisation and gel formation. In this process, bisacrylamide will form crosslinks between acrylamide molecules and thus its percentage will determine the gel's pore size and how fast proteins will run. In general, lower percentages are used for bigger proteins (e.g. 8% for 200 kDa) and vice-versa. The bigger pore in the stacking gel allows for all the proteins to form a migrating edge so they can enter the running gel at the same time.

10 % Running gel	*5% Stacking gel*
• 4 ml Water • 3.3 ml 30% Acrylamide • 2.5 ml 1.5M Tris-HCl pH 8.8 • 100 µl 10% SDS • 100 µl 10% APS • 4 µl TEMED	• 4.1 ml Water • 1 ml 30% Acrylamide • 750 µl 0.5M Tris-HCl pH6.8 • 60 µl 10% SDS • 60 µl 10% APS • 6 µl TEMED

Table 2-7. Components of a 10% running and a 5% stacking gel for SDS-PAGE electrophoresis.

1.5 M Tris-HCl	• 45.48g Tris base • Water up to 250 ml Adjust pH to 8.8 with HCl
0.5 M Tris-HCl	• 6.055g Tris base • Water up to 100 ml Adjust pH to 6.8 with HCl.
10% SDS	• 10 g SDS • Water up to 100 ml
10% APS	• 0.2g Ammonium persulphate • 2ml water Lasts 3 months in the fridge

Table 2-8. Ingredients necessary to assemble a 10% running and a 5% stacking gel for SDS-PAGE electrophoresis.

Briefly, gels were hand casted using a 1.5mm spacer plate and a short plate from the Mini-PROTEAN® Tetra handcast systems (Bio-Rad) according to manufacturer's instructions. 10 ml of resolving gel were prepared in a Falcon tube, added to the assembly and topped with methanol to remove any bubbles and achieve a straight surface. The gel was allowed to polymerise for 20-30 minutes before pouring off the methanol, adding 5 ml of stacking gel and placing a comb to form the wells. After 15 minutes, the comb was removed and the cast gel was placed in a tank containing 1x electrophoresis buffer.

To prepare the samples, 40 µg lysates were mixed with the same volume of 2x loading buffer. Samples were then heated for 10 minutes at 100°C to allow β-mercaptoethanol to break down the tertiary structure of the proteins. The components of the electrophoresis and loading buffer can be found in Table 2-9.

5x Electrophoresis buffer	*2x loading buffer (Laemmli Buffer)*
• 15.1g Tris base • 72g glycine • 50 ml 10% SDS (or 5 g SDS) • Water up to 1000 ml Adjust pH to 8.3 with HCl. Dilute 1:10 with dH_20 before use.	• 0.605 g Tris base • 4g SDS • 10 ml glycerol • 4 mg Bromophenol blue • Water up to 50 ml Adjust pH to 6.8. Before use, add 100 µl β-mercaptoethanol per 1 ml 2x loading mix

Table 2-9. Components of 5x electrophoresis buffer and 2xLoading buffer in Western Blot.

Up to 40 µl of the prepared samples and 10 µl PageRuler™ Prestained Protein Ladder (ThermoFisher) were loaded into the gel and run at 120V for around 1 h. Proteins were then separated according to their mass and molecular weight was determined thanks to the ladder.

2.9.4. Membrane transfer

After the electrophoresis gel, proteins were transferred to a nitrocellulose membrane using the Trans-Blot® Turbo™ Transfer System. Briefly, a gel-sized membrane was cut and activated by placing it in methanol for 20 seconds and washed in distilled water for 5 minutes. Then, the membrane and 8 gel-sized pieces of Whatman filter paper (Sigma) were wetted in working transfer buffer for 5 minutes and the blotting sandwich was assembled in the cassette by placing four filter papers, the activated membrane, the gel and four more filter papers. Air was removed using a roller before closing the cassette and starting the transfer by selecting the STANDARD SD protocol. The recipe for the transfer buffer can be found in Table 2-10. After transfer, membrane was washed for 5 minutes with PBS/0.1% Tween to remove residual transfer buffer.

5x Transfer buffer	• 15.15 g Tris base • 72g glycine • Water up to 1000 ml For the working buffer, mix 160 ml 5x buffer, 200 ml methanol and water up to 1000 ml.

Table 2-10. Components of 5x transfer buffer.

2.9.5. Ponceau staining

If issues have occurred during transfer, correct protein transfer can be assessed using Ponceau S – composition can be found in table 2-11. The membrane was placed in a

tray containing Ponceau S working solution and incubated for 10 minutes until protein bands were visible. Membrane was then washed twice for 1 minute in water to remove excess Ponceau S and observe clear bands. To remove the remaining Ponceau, membrane was washed twice for 5 minutes in water; and washed for 5 more minutes in PBS/0.1% Tween.

Ponceau S (stock)	• 2g of Ponceau S • 30g of Trichloroacetic acid • 30g of Sulfosalicylic acid • Water up to 100 ml To make working solution mix 1 part Ponceau S with 9 parts water.

Table 2-11. Components of Ponceau S solution.

2.9.6. Immunoblotting

Membrane was blocked with 5% milk powder or 5% BSA (for phospho-proteins) in PBS/0.1% Tween for 1 h at room temperature to avoid unspecific binding. Primary antibody was then diluted in blocking buffer according to manufacturer's instructions and membrane was placed with 4 ml of the diluted antibody in a 50 ml falcon and left to incubate in the roller at 4°C overnight. The next day, membrane was washed three times for 5 minutes in PBS/0.1% Tween before incubating for 1 hour at room temperature with the secondary HRP-conjugated antibody at the recommended dilution. A list of the antibodies used can be found in Table 2-12:

Antigen	***Origin (Species)***	***Reactive species***	***Manufacturer***	***Catalogue number***
p-ERK	Rabbit	Human, Mouse, Rat, Hamster, Monkey, Mink, D. melanogaster, Zebrafish, Bovine, Dog, Pig, S. cerevisiae	Cell signaling	4370
p-Akt	Rabbit	Human, Mouse, Rat, Hamster, Monkey, D. melanogaster, Zebrafish, Bovine	Cell signaling	4060
Pan-ERK	Rabbit	Human, Mouse, Rat, Hamster, Monkey, Mink, D. melanogaster, Zebrafish, Bovine, Dog, Pig, C.elegans	Cell signaling	4695
Pan-Akt	Rabbit	Human, Mouse, Rat, Monkey, D. melanogaster	Cell signaling	4691
GAPDH	Mouse	Human, mouse, rat	Santa Cruz	sc-365062

Table 2-12. Primary antibodies used in Western blot.

Membrane was washed thrice again for 5 minutes in PBS/0.1% Tween before adding SuperSignal™ West Pico Chemiluminescent Substrate (ThermoFisher) according to manufacturer's instructions. Briefly, 1 ml of Detection reagent 1 (luminol) was mixed with 1 ml of Detection reagent 2 (peroxide) and poured on top of the membrane for 1 minute. In the presence peroxide, the peroxidase will oxidise the luminol, producing chemiluminiscence. Excess working solution was then removed and membrane was placed in plastic wrap before being exposed to CL-XPosure X-ray film (ThermoScientific) for an optimised time period (generally, 1-5 min). Film was then developed by being placed for one minute in developer, water, fixer and water again.

In order to assess the presence of another protein, including a loading control such as GAPDH, membranes were first stripped by incubating for 20 minutes with stripping buffer – recipe can be found in table 2-13. Membranes were then washed three times for 5 minutes in PBS/0.1% Tween before blocking the membranes again and re-probing with a different antibody.

Stripping buffer	• 15 g glycine • 1g SDS (or 10 ml 10% SDS) • 10 ml (1%) Tween 20 • Up to 1000 ml of water Adjust pH to 2.2

Table 2-13. Components of stripping buffer.

2.10. CELL-BASED ELISA

Relative protein phosphorylation of adherent cells can also be determined using a cell-based ELISA. Cell-based ELISAs measure the levels of two proteins simultaneously through fluorescence, allowing for their immediate normalisation. Unlike Western blot, cell lysis is not required and it provides a more quantitative result.

For this purpose, Human/Mouse/Rat Phospho-ERK1 (T202/Y204) / ERK2 (T185/Y187) cell-based ELISA (R&D systems) was carried out. Briefly, reagents were prepared according to manufacturer's instructions and 100 µl of $2x10^4$ cells were grown in a 96-well plate. The next day, cells were treated in triplicate with 10 nM CXCL12 at the desired timepoints and fixed with 4% formaldehyde for 20 minutes at room temperature. Formaldehyde was removed and wells washed thrice with 200 µl of wash buffer for 5 minutes before adding 100 µl of quenching buffer to remove the endogenous peroxidase activity. After incubating for 20 minutes at room temperature, quenching buffer was removed and plate was washed thrice with 200 µl of wash buffer for 5 minutes and 100 µl of blocking buffer were added to prevent unspecific binding. Blocking buffer was incubated for 1 hour at room temperature before washing thrice with 200 µl of wash buffer for 5 minutes and adding 100 µl of the primary antibody mixture which detects the phosphorylation sites T202/Y204 on ERK1 and T185/Y187 on ERK2. Three wells were filled with blocking buffer instead to serve as a no primary antibody control, and plate was incubated overnight at 4°C.

The next day, the plate was washed three times with 200 µl of Wash buffer per well for 5 minutes and 100 µl of the secondary mixture containing antibodies labelled with either HRP or alkaline phosphatase (AP) were added for 2 hours at room temperature. Cells were then washed twice with 200 µl of Wash buffer for 5 minutes and twice with 200 µl of PBS before adding 75 µl of Substrate F1 to each well - this contains fluorogenic substrate for HRP. After 40 minutes at room temperature in the dark, 75 µl of Substrate F2 (containing the fluorogenic substrate for AP) were added to Substrate F1 and incubated for a further 30 minutes. Fluorescence was then measured at excitation 540nm and emission at 600nm (for phospho-ERK) and at excitation 360nm and emission at 450nm (for total ERK). Phospho-ERK fluorescence was then normalised to total ERK fluorescence and plotted.

2.11. WOUND HEALING USING IBIDI INSERTS

In order to assess cell migration through time, a wound healing assay was carried out with images being captured every hour using the NIKON Biostation. Unlike Boyden-based chemotaxis assays where cells are in suspension, this assay assesses the movement of a cell front thanks to cell-to-cell interactions remaining intact – this is known as "sheet migration". In traditional wound healing assays, cells are grown in a confluent monolayer before creating a scratch with a sharp object (such as a pipette tip) and migration into the cell-free gap is monitored. However, it is difficult to create a uniform width throughout the gap that is also reproducible between different experiments; furthermore cell damage may cause the release of growth factors that could mask the result. Thus, in order to standardize the assay a physical exclusion method using 2-well silicone inserts (Ibidi) was chosen instead. In this method, cells are grown on both sides of a plastic barrier so when the insert is removed, cells can migrate to the cell-free area.

Briefly, the insert was placed into a 12-well plate with sterile tweezers and gently pushed in place. 70 µl of $4x10^5$ cells/ml were added into each side of the insert and left to grow overnight. It is important not to overgrow cells to avoid attachment to the sides of the insert, causing cells to be pulled out when it is removed and creating a jagged edge. Inserts can be used for up to three times before adherence to the plate is compromised. The next day, the insert was gently removed with tweezers and cells were washed with PBS before adding 1 ml of serum-reduced media. The percentage of BSA added was optimised for our cell type beforehand in order to minimise cell proliferation but avoid apoptosis. This process was repeated for each wells individually to avoid cells drying out.

Treatment was then added and cells were brought to the Nikon BioStation CT, a cell incubator and monitoring system. The system was programmed to take an image of the gap every hour for 48 hours at 5x and 10x magnification and data were acquired automatically – an example can be seen in Figure 2-19. By using the Biostation we can avoid having to remove the plate from the incubator to take a picture, thus attaining constant temperature and CO_2 levels. Wound closure was then analysed using the wound healing application from the NIS-Elements AR software and the gap area was obtained.

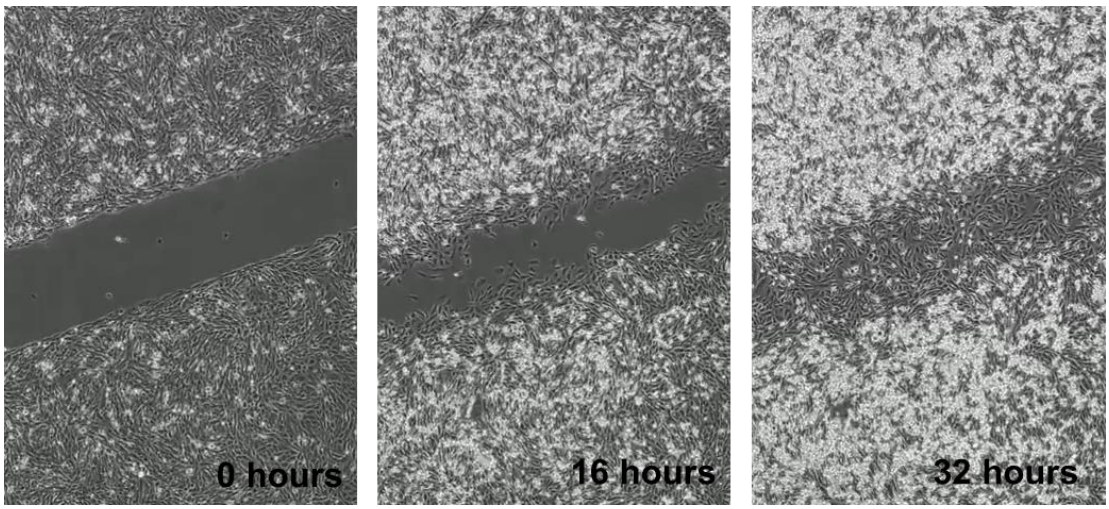

Figure 2-19 Example of images captured during a "wound healing" or "scratch" assay.
Cells were seeded into Ibidi inserts and grown overnight until confluent. Inserts were then removed, creating a "wound" and wells were filled with 1% FBS media with or without 10 nM CXCL12. Wound closure was monitored hourly for 48h using a Nikon Biostation – images of CHO-CXCR4 at 0, 16 and 32 hours can be seen.

Finally, cell front velocity was calculated as follows. First, the total area of the picture was calculated in μm^2 – in our case, that was 2,000*2,000 = 4,000,000 μm^2. Second, the total area was multiplied by the difference in gap area between the beginning and the end of the experiment (area at 0h minus area at 48h). The resulting number was then divided by the total time (48 hours) and the height of the picture (2,000 μm) to obtain the cell front velocity in μm/hour.

2.12. CHEMOTAXIS ASSAYS

Chemotaxis assays are used to assess the migration of cells towards a chemoattractant, and thus are key to evaluate the response of chemokine receptor-expressing cells towards their ligand. Given their simplicity and quickness of use, two-chamber techniques are the most commonly used to assess chemotaxis, in particular commercial polycarbonate versions of a Boyden chamber (Boyden, 1962). The simplest modality is known as "transfilter" chemotaxis. Briefly, two chambers are separated by a filter of known pore size through which a chemokine diffusion gradient can be formed. The pore size will depend on the cell size – a 8-μm pore was used for mammalian epithelial cells such as CHO or 4T1, but smaller pore sizes are necessary for PBMC (for instance, a 5-μm pore size for lymphocytes and monocytes and a 3-μm pore size for neutrophils). As these pores are slightly smaller than the cells, it ensures that only directional chemotaxis is taking place as cells need to undergo morphological and cytoskeletal changes to fit through. This assay, however, solely relies on the strength of the chemokine-receptor interaction and cell-to-cell interaction impact in migration is disregarded.

To emulate the cell barrier in blood and lymph vessels, the filter can be coated in advance with endothelial cells such as HMEC-1. This assay, called "trans-endothelial" chemotaxis, offers a more physiological approach to migration as it takes into account adhesion and extravasation. More details on this process can be found in section 6.2.4.

2.12.1. Transfilter chemotaxis

Chemotaxis assays were carried out using cell culture inserts and 24-well companion plates (BD Falcon) in a setup similar to the one depicted in Figure 2-20. Cells were serum starved for a minimum of one hour, whilst companion plates were blocked with 1ml of 1% BSA/DMEM for 1 hour to prevent chemokine depletion due to its binding to the plate. Whenever measuring the migration of adherent cells, the filters of the cell culture inserts were upturned and coated with 150μl 4 μg/ml fibronectin. Inserts were incubated with fibronectin for 30 minutes at room temperature, then excess fibronectin was removed and filters allowed to dry for a further 30 minutes at room temperature before use. This helps the adhesion of migratory cells to the apical side of the filter.

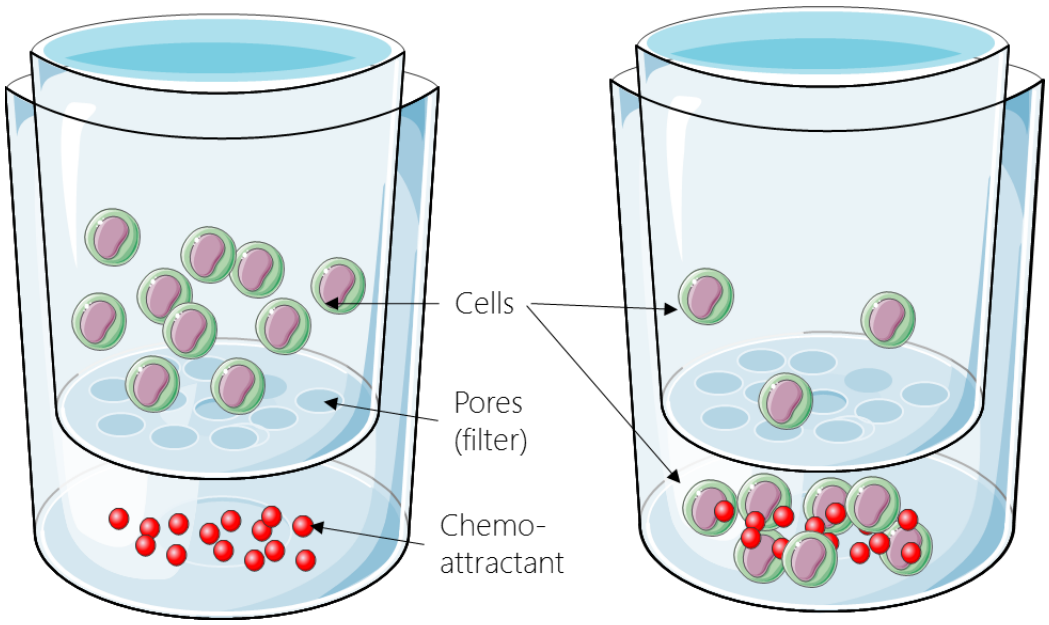

Figure 2-20. Layout of a Boden-chamber based transfilter chemotaxis assay.
Cells were serum starved and placed on top of a filter above the chemoattractant-containing well. Cells are then incubated at 37°C for the optimised period of time and migrated cells counted. Epithelial cells can be counted by staining the lower side of the filter, whilst PBMC that have migrated to the lower well can be counted by flow cytometry using counting beads.

After cells have been serum starved, they were harvested using Accutase as described in section 2.2.1. Cells were resuspended in 0.2% BSA/DMEM to a final concentration of $4x10^5$ cells/ml, and 500 µl of the cell solution was added to the cell culture insert. The absence of serum is vital as it contains cytokines and growth factors that will mask the effect of the chemokine added, preventing the formation of a steep chemokine gradient.

Next, 1% BSA/DMEM was removed from the companion plate and replaced with 800 µl 0.1% BSA/DMEM containing the optimal chemokine concentration. Inserts were then carefully lowered into plate wells, allowing for the creation of a chemotactic gradient. Chemotaxis assays were incubated at 37°C and 5% CO_2 overnight for adherent cells.

After incubation, media was removed and the inside of the filters was gently wiped with a cotton bud to remove non-migrated cells. Filters were then fixed in methanol at -20°C for 1 hour and washed with tap water. Hematoxylin was added for 30 minutes to each well to stain migrated cells, followed by Scotts' tap water to blue the stain for 10 minutes. Filters were then dehydrated by placing them through ascending alcohol concentrations (50% → 70% → 90% → 100%) and left to air dry for one hour. Finally, filters were carefully cut from the insert using a scalpel and mounted in slides using DPX (Sigma), placing three filters per slide. Migrated cells were then counted (5 high power fields per filter).

2.12.2. Transendothelial chemotaxis

As described in section 2.8. of the General Materials and Methods, Boyden-chamber based chemotaxis assays are the gold standard to assess migration. However, in order to emulate *in vivo* conditions, endothelial cells can be added to coat the filter. Briefly, 72 hours prior to the assay 200,000 HMEC-1 cells were added to the inserts in 500 µl of complete media and placed in an empty plate – this is important as media on the bottom well could encourage the HMEC-1 cells to migrate across the filter and grow on the lower surface. The day prior to the assay, when HMEC-1 cells are approximately 80% confluent, 100U/ml IFNγ and 100ng/ml TNFα were added to the media to activate the cells and induce expression of adhesion molecules. The next day, the HMEC-1 monolayer should be completely confluent to avoid migratory cells from passing through the gaps between cells during the assay. Following this, the protocol described in section 2.8.1 should be followed starting with the starvation and addition of the migrant cells.

In order to assess the quality of the HMEC-1 monolayer, two approaches were taken. First, an extra filter was coated with HMEC-1 to which no 4T1 cells were added – this filter was not wiped with the q-tip and thus the intact monolayer could be observed. Second, the migratory 4T1 cells were stained with a cell-tracker fluorescent probe – these dyes can easily pass through the membrane, but once inside the cell they will react with the thiol (SH) groups present in proteins, converting them to impermeable dyes. Their fluorescence is then stable for up to three days inside the cell. In order to stain cells with orange CMRA (Life Technologies), the manufacturer's protocol was followed. Briefly, the reconstituted dye was diluted from 10 mM to 10 µM (MW= 550.4) in 10 ml of serum free media and warmed to 37°C. Media was then removed from a T-75 flask containing 4T1 cells, replaced by the diluted dye solution and incubated for a further 30 minutes at 37°C. Solution was then removed and cells were harvested, resuspended in 0.1% BSA/DMEM and added on top of the insert.

If the 4T1 cells appeared "clumpy" when counting even after having extensively pipetted the cells up and down, cells were disaggregated by very gently passing them through an insulin syringe (31G). This process, however, will cause the lysis of around 20% of the cells and thus it is important to use trypan blue to assess cell death when calculating the seeding cell number.

PBMC were also used as a positive control to ensure the correct reconstitution of new batches of chemokines. These cells were kindly provided by Mr. Jonathan Scott and come from healthy blood donors; it was thus assumed that around 70-90% of the total cells were lymphocytes and around 10% were monocytes. When migrating, monocytes will adhere to the underside of the filter whilst lymphocytes will migrate through the monolayer and into the bottom well. As only a small percentage of monocytes express CCR7 (Gordon and Taylor, 2005), only the migrated lymphocytes were assessed using counting beads and thus no staining of the filter was necessary.

Further to this, some adjustments to the protocol from section 2.8.1 were carried out when PBMCs were used. First, given their lesser size, a smaller pore size and a higher cell number are necessary, and thus a 3-μm pore and a cell concentration of $1x10^6$ cells/ml are required for the assay. Second, chemotaxis is quicker so incubation time was reduced to 90 minutes before assessing migration. Last, as cells migrate to the bottom well they were counted using CountBright™ Absolute Counting Beads in a flow cytometer as epr manufacturer's instructions. Briefly, 8 μl of beads were added to the migrated cells in a FACS tube to have the known number of 8,000 beads. When running the cells in the cytometer, a gate was drawn around the beads and the acquisition was set to stop when 1,000 bead events were acquired. Then, the number of migrated cells was calculated with the following formula:

$$\text{Labelled cells} = \frac{\text{No. of labelled cell events (P1)}}{\text{No. of bead events (P2)}} \text{x No. of beads added}$$

$$\text{Labelled cells} = \frac{\text{P1}}{1{,}000} \text{x } 8{,}000 = \text{ P1 x } 8$$

2.13. LUMINESCENCE ASSAYS

In order to ensure that luciferase was being expressed at detectable levels, two different assays were carried out. Briefly, in the presence of ATP, magnesium and oxygen, the enzyme luciferase oxidises its substrate, the beetle luciferin, into oxyluciferin and light (De Wet et al., 1987), which can then be detected.

2.13.1. Dual-Luciferase® Reporter Assay System

The Dual-Luciferase® Reporter Assay System (Promega) allows for the quick detection of the firefly and *Renilla* luciferases using a luminometer or plate reader. The *Renilla* is used as a negative control to normalise any variance. This kit is designed for the detection of luciferase in mammalian cells from culture, but was also successfully adapted for the detection of luciferase in tissue.

For luciferase detection from cultured 4T1-Luc cells, manufacturer's instructions were followed. Briefly, the following reagents were prepared and brought to room temperature before the assay (see Table 2-15). For each well of a 96-well plate:

1xPassive Lysis Buffer (PLB)	• 50 µl 5xPLB • 200 µl of distilled water Keep at 4°C for 1 month
Luciferase Assay Reagent II (LAR II)	• Lyophilized Luciferase Assay Substrate • 10ml Luciferase Assay Buffer II Reagent can then be aliquoted and kept at -20°C
Stop & Glo reagent	• 2 µl of 50x Dual-Glo® Stop & Glo® Substrate • 98 µl of Dual-Glo® Stop & Glo® buffer Keep at -20°C for 15 days.

Table 2-14. Reagent preparation for the Dual-Glo® Luciferase Assay System.
These reagents should be prepared immediately before the beginning of the assay.

In order to determine whether luminescence was cell number dependent, cells were detached, counted and pelleted before adding 250 µl of 1xPLB and gently rocked for 15 minutes at RT. The lysate was then transferred to an Eppendorf tube and stored at -20°C if necessary. In a new Eppendorf tube, 20 µl of the lysate were mixed with 100 µl of LAR II, and firefly luciferase was measured in a luminometer with a 2-second premeasurement delay followed by a 10 second measurement period. This immediate reading is possible due to the presence of the coenzyme A (CoA) in the LAR II mixture,

which helps the reaction kinetics (Stanley and Kricka, 1991). 100 µl of the Stop & Glo reagent were then added and the mixture vortexed to quench the luminescence from the firefly luciferase and provide the substrate for the *Renilla* luciferase. Sample was then measured for *Renilla* luciferase activity – these readings should be carried out immediately to avoid loss of signal (approximately 50% in 10 and 3 minutes respectively for each luciferase). A sample with just lysis buffer instead of cell lysate was also carried out to stablish background luminescence.

In order to measure tissue luminescence, a 2 mm x 2 mm piece of tissue was immersed in liquid nitrogen and ground into a fine powder using a pestle and mortar. 250 µl of 1xPLB were then added to the tissue powder and the mixture was transferred to an Eppendorf tube to incubate for 15 minutes at room temperature. Samples were then centrifuged at 12,000xg for 2 minutes at 4°C to pellet the debris and the rest of the procedure was followed as above using the supernatant. If the value was out of range, tissue lysate was diluted 1:10 before performing the assay again.

2.13.2. Luminescence assay with d-luciferin

In order to ensure that the d-luciferin (Intrace medical) worked correctly as substrate, 4T1-Luc cells were detached, counted and plated in a 96-well plate with 100 µl of complete media. 1 µl of 15mg/ml d-luciferin was added into each well and incubated in the dark for 5 minutes at 37°C before reading the luminescence using a plate reader. After 15 minutes, the plate was read again to assess loss of luminescence with time. A blank well with only media was prepared as a negative control.

Next, the same protocol was repeated but luminescence was assessed at 10 minutes in the IVIS spectrum CT to confirm the presence of signal.

2.14. STATISTICAL ANALYSIS

Statistical analysis was carried out using GraphPad prism software version 5 (GraphPad Software, San Diego, USA). The error bars on the graph bars represent the standard error of the mean (SEM) of the mean plotted.

Comparison between several groups was assessed by performing a one way analysis of variance (ANOVA) followed by a Tukey test as a post hoc test to compare the different samples between each other. The significance was set at $P<0.05$ (marked as *), whilst $p<0.01$ and $p<0.001$ were marked as ** and *** respectively.

Comparison between two groups was assessed by performing a Student´s t-test. The significance value was also set at $P < 0.05$.

3. *IN VIVO* LEVELS OF CXCR4, CXCR7 AND CCR7 EXPRESSION IN PRIMARY BREAST CANCER

3.1. INTRODUCTION

Several studies have reported overexpression of the chemokine receptors CXCR4 (Liang et al., 2004, Salvucci et al., 2006) and CCR7 (Cassier et al., 2011, Pan et al., 2008, Mashino et al., 2002) in breast cancer patients, but there is still some ambiguity in regards to CXCR7 expression in cancer. For instance, Wu et al. (2015) reported that CXCR7 is overexpressed in breast cancer in relation to the surrounding tissue, whilst McConnell et al. (2016) described that CXCR7 is absent in primary melanoma but overexpressed in the surrounding tissue, and Miao et al. (2007) reported that CXCR7 is highly expressed in both tumour and surrounding tissue in breast cancer and other cancers. Furthermore, the expression of CXCR4 and CXCR7 has mostly been assessed individually or in correlation to other markers (Liu et al., 2010, Andre et al., 2006, Cabioglu et al., 2005b), but rarely together.

It is also increasingly apparent that the microenvironment can play a key role in tumour progression by increasing chemokine receptor expression in the tumour cells (see section 1.3.4. of the Introduction) – for instance, CXCR4 upregulation in cancer cells though CXCL12 production by the stroma has been widely reported (Helbig et al., 2003, Burger and Kipps, 2006, Burger and Peled, 2009, Orimo et al., 2005). However, there are conflicting reports about overexpression of chemokine receptors in the microenvironment cells. On one hand, CXCR7 upregulation in the vasculature and endothelium surrounding tumours has been reported in breast cancer (Miao et al., 2007, Stacer et al., 2015) but also in lung, bone, brain, liver and colon cancer (Miao et al., 2007, Monnier et al., 2012, Guillemot et al., 2012, Goguet-Surmenian et al., 2013, Madden et al., 2004). Meanwhile, CXCR4 expression by the microenvironment is still not clear - for instance, Allinen et al. (2004) reported no expression in myoepithelial cells and myofibroblasts, whilst Papatheodorou et al. (2014) found high expression in intratumoural fibroblasts, highlighting the importance of cell type identification.

3.1.1. Breast cancer classification

"Number staging" is the most common strategy for tumour classification, where tumours are categorised in in 5 stages depending on the lymph node status, the tumour size, and the presence of metastasis (more details in section 1.1.4. of the Introduction). However, pathologists also define the cancer by the Bloom-Richardson grade (Bloom and Richardson, 1957) to determine aggressiveness, and the Nottingham Prognostic index (Galea et al., 1992, Haybittle et al., 1982) to assess patient predicted survival. Depending on these scores, different courses of treatment will be recommended for the patient.

3.1.1.1. *Bloom-Richardson grade*

Whilst staging looks at the location and size of the tumours, grading takes into consideration the morphology of the cells in comparison to normal tissue. There are many cancer grading systems, but in breast cancer the Bloom-Richardson grading system (or BR grading) is the one currently used by the NHS in the UK. This system has been modified since its introduction in 1957 to increase reproducibility (Elston and Ellis, 1991, Scarff and Torloni, 1968) and is also referred to as the Bloom-Richardson-Elston Grading system (or BRE system), the Scarff-Bloom-Richardson Grading (or SBR grading) or the Nottingham system (not to be confused with the Nottingham Prognostic index) among others. However, they all look at three morphological features of the cancerous cells to determine their aggressiveness: tubule formation, number of mitoses and nuclear pleomorphism (Bansal et al., 2012, Rakha et al., 2010).

Tubularity gives an approximation of how differentiated the cells are by assessing their ability to form normal glands, with cells grouped around a central space or tube. As cells become less differentiated, their ability to form cell to cell junctions decrease and tissue structures break down. Briefly, 1 point is given if over 75% of the area forms glandular structures, 2 points if it is 75% to 10% of the area, and 3 points if it is less than 10%.

Mitotic activity gives an estimate of cell proliferation by assessing the number of hyperchromatic or mitotic figures in 10 high power fields at 40x. Briefly, after finding the area with the most dividing cells, mitotic figures (cells in metaphase, anaphase or telophase with no nuclear membrane) are consecutively counted. For a

0.27 mm^2 field area, 1 point is given if there are 9 or less mitoses, 2 points if there are 10 to 19 mitoses, and 3 points if there are 20 or more mitoses. As described previously, cancer cells have overridden division checkpoints so they can divide aberrantly and thus present a higher number of mitoses.

Nuclear pleomorphism indicates how abnormal cells look and correlates with gene dysregulation as nuclei become more irregular. Briefly, 1 point is given if the cells are of similar size to normal cells and nuclei are relatively small, with clear margins and uniform chromatin; 2 points if cells are slightly bigger, with pleomorphic nuclei (variable size and shape) and visible nucleoli; and 3 points if nuclei are large and very pleomorphic, with prominent or multiple nucleoli.

Points are then added up and graded according to Table 3-1. Higher grade cells divide more quickly, increasing the size of the tumour and risk of metastases and thus have worse prognosis (Hatteville et al., 2002).

Score	***Grade***
3-5 points	Grade 1 / BR low grade / Well-differentiated
6-7 points	Grade 2 / BR intermediate grade / Moderately differentiated
8-9 points	Grade 3 / BR high grade / Poorly differentiated

Table 3-1. Bloom-Richardson scoring system.
Breast cancer tumours are scored given their tubularity, mitotic activity and nuclear pleomorphism and the points added to assess their grade.

3.1.1.2. *Nottingham prognostic index*

The Nottingham prognostic index (NPI) was first described in 1982 (Haybittle et al., 1982) and is used to predict patient prognosis depending on the size of the tumour, number of involved lymph nodes, and the grade of the tumour according to the Bloom-Richardson system. It is calculated with the following formula (Galea et al., 1992):

$$NPI = (0.2\ x\ S) + N + G$$

Where S is the tumour diameter in cm, N is the lymph node stage (1 if there is no involvement, 2 if there are 1-4 positive lymph nodes and 3 if there are 5 or more) and G is the tumour grade. Patients are then classified into four groups as depicted in Table 3-2 below, and 5 and 10-year survival can then be calculated for different populations (Kollias et al., 1999, Blamey et al., 2007, Fong et al., 2012).

NPI score	***Prognosis***
Less than 2.4	Excellent
2.4-3.4	Good
3.5-5.4	Moderate
More than 5.5	Poor

Table 3-2. Nottingham prognostic index scoring system.
NPI is calculated depending on tumour size, lymph node involvement and tumour grade to predict 5-year survival.

3.1.2. Specific aims

Although the expression of chemokine receptors such as CXCR4, CXCR7 and CCR7 by the tumour cells has been widely reported, their expression in the microenvironment has not been well characterised. We aim to assess the presence of CXCR4, CXCR7 and CCR7 in patient samples with or without lymph node involvement, and determine the expression levels of CXCR4 and CXCR7 in the tumour and the surrounding stroma.

- To characterise the expression of CXCR4, CXCR7 and CCR7 in paraffin-embedded breast cancer samples using immunohistochemistry.
- To perform transcript analysis of differences in CXCR4 and CXCR7 expression between cancer and surrounding tissues.

3.2. SPECIFIC MATERIALS AND METHODS

3.2.1. Ethics approval

Ethical approval for the use of paraffin-embedded and frozen human sections was submitted through the Integrated Research Application System (IRAS) to the NHS Research Ethics Committee. The application was then proportionately reviewed by the Yorkshire & The Humber - Leeds East Research Ethics Committee and approved in March 2016 under the REC reference 16/YH/0117 for the study "Role of metastatic markers in breast cancer". For the use of samples isolated prior to the Human Tissue Authority (HTA) act for immunohistochemistry, approval had already been granted under the REC reference 06/Q0906/12 for the study "Role of chemokine/GAG interactions in breast cancer metastasis".

Furthermore, for the transport of frozen samples from the Queen Elizabeth Hospital to Newcastle University, a Material Transfer Agreement (MTA) was drafted and signed by the corresponding authorities in August 2016. Samples were transported on dry ice.

3.2.2. Paraffin-embedded patient samples

8 primary breast cancers were surgically removed at the Royal Victoria Infirmary (Newcastle upon Tyne) during 2005 and consented for use in research. The samples were anonymised as patients 1 to 8 – their details, including lymph node status and BR grading, can be found in Table 3-3.

Patient	*Location*	*Cancer type*	*BR grading*	*Lymph node involvement*
1	Breast tumour	Invasive ductal carcinoma	1	6 LN
2	Breast tumour	Invasive lobular carcinoma	2	No
3	Breast tumour	Invasive ductal carcinoma 3a: DCIS region 3b: invasive region	2	No
4	Breast tumour	Invasive lobular carcinoma (contiguous to tumour)	2	No
5	Breast tumour	Invasive ductal carcinoma (multifocal)	2	2 LN
6	Lymph node	Invasive ductal carcinoma	2	No
7	Breast tumour	Invasive ductal carcinoma	2	No
8	Breast tumour	Invasive ductal carcinoma 8a: upper margin 8b: lower margin	3	No

Table 3-3. Patient details from paraffin-embedded tumour samples.

3.2.3. Frozen patient samples

33 breast cancer tumours were surgically removed at the Queen Elizabeth Hospital (Gateshead) during the years 2005-2007 and consented for their use in research under the study "The establishment of a database of prognostic markers in patients with breast cancer". Frozen samples were kept in the hospital at -80°C until their transport to Newcastle University, where they were stored in an HTA-compliant -80°C freezer.

The original research strategy was to select 10 patients with lymph node involvement and 10 patients without lymph node involvement from a total of 37 patients and separate the tumour cells from the surrounding tissue using laser capture. RNA would then be extracted and CXCR4 and CXCR7 levels would be assessed using qPCR. However, given the poor quality of the samples (further discussed in the previous section), only 7 samples in total could be used. To anonymise the samples, they were referred as patients A to G – their details, including lymph node status, BR grading, NPI and receptor status can be found in Table 3-4.

Patient	*Type*	*Tumour dimensions*	*Lymph node involvement*	*BR grading*	*NPI*	*Receptor status*		
						ER	**PR**	**HER2**
A	Lobular	23 mm	No (0/9)	2	3.5	Pos	Neg	N/A
B	Ductal	24 mm	No (0/9)	3	2.48	Pos	Neg	N/A
C	Ductal	12 mm	No (0/7)	2	3.24	Pos	Pos	N/A
D	Ductal	16 mm	No (0/8)	3	4.32	Neg	Neg	Neg
E	Ductal	35 mm	Yes (3/9)	2	4.7	Pos	Pos	Neg
F	Ductal	40 mm	Yes (2/12)	3	5.8	Pos	Pos	Neg
G	Ductal	70 mm	Yes (3/4)	3	6.4	Pos	Neg	Neg

Table 3-4. Patient details from frozen tumour samples.
Pos = positive, Neg = negative

3.3. RESULTS

3.3.1. Optimisation of CXCR4, CXCR7 and CCR7 staining

Several studies have reported the overexpression of the chemokine receptor CXCR4 in cancer, but whether it is mainly expressed in the cell surface, in the cytoplasm or even the nuclei is still poorly understood (Yasuoka et al., 2008, Cabioglu et al., 2005b, Woo et al., 2008, Salvucci et al., 2006, Zhang et al., 2014, Kato et al., 2003, Schmid et al., 2004) and may vary among cancers (Wang et al., 2005).

First, we optimised the detection of CXCR4 using immunohistochemistry in placenta tissue as positive control, as other studies report high CXCR4 expression in the trophoblasts in the placental villi (Kumar et al., 2004, ISHII et al., 2000). As seen in Figure 3-1, two different concentrations of antibody (1:20 and 1:50) and three different antigen retrieval pre-treatments (Citrate buffer, EDTA buffer or Trypsin) were tried, and no pre-treatment was found to give the most intense staining of the lining trophoblast cells, with the least background. Staining was located in the cytoplasm and membrane of the trophoblasts as reported in literature (Wu et al., 2004). A second optimisation was carried out with several antibody dilutions and 1:40 was chosen for further staining (not shown).

Although CXCR7 has been described as being upregulated in breast cancer cell lines and breast tumours, especially in the tumour vasculature (Miao et al., 2007, Luker et al., 2012, Wang et al., 2008b), very little research has focused on CXCR7 location in the tumour cell. In order to assess this, CXCR7 staining was first optimised using term placenta by trying out 3 different pre-treatments for antigen retrieval and three different antibody dilutions (1:50, 1:100 and 1:200). Similarly to CXCR4, CXCR7 expression was determined to be high in the trophoblast cells, particularly in term placenta, with similar cytoplasmic and membrane staining (Berahovich et al., 2014). As seen in Figure 3-2, Citrate buffer pre-treatment gave the clearest staining of trophoblasts and 1:150 was chosen for intensity.

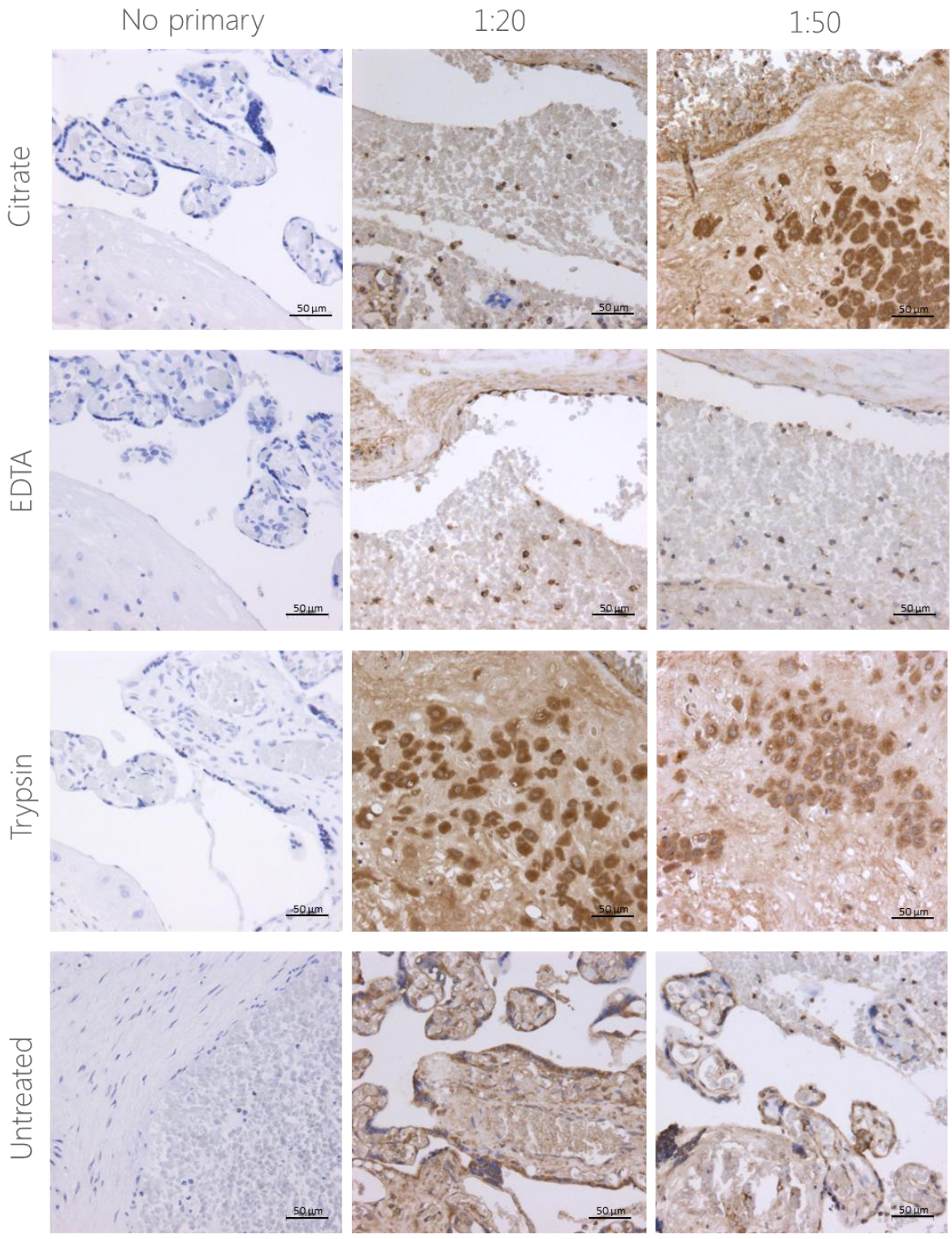

Figure 3-1. Optimisation of CXCR4 staining using IHC in placenta tissue.
4µm sections from human placenta were stained for CXCR4 using immunohistochemistry following three different antigen retrieval pre-treatments (Citrate buffer, EDTA buffer or Trypsin) or no pre-treatment. Two different antibody concentrations, 1:20 and 1:50, were used. Briefly, protocol from the VECTASTAIN ABC HRP kit was followed, signal was developed using DAB (brown stain) and counterstained with haematoxylin (blue). No primary antibody was used as a control.

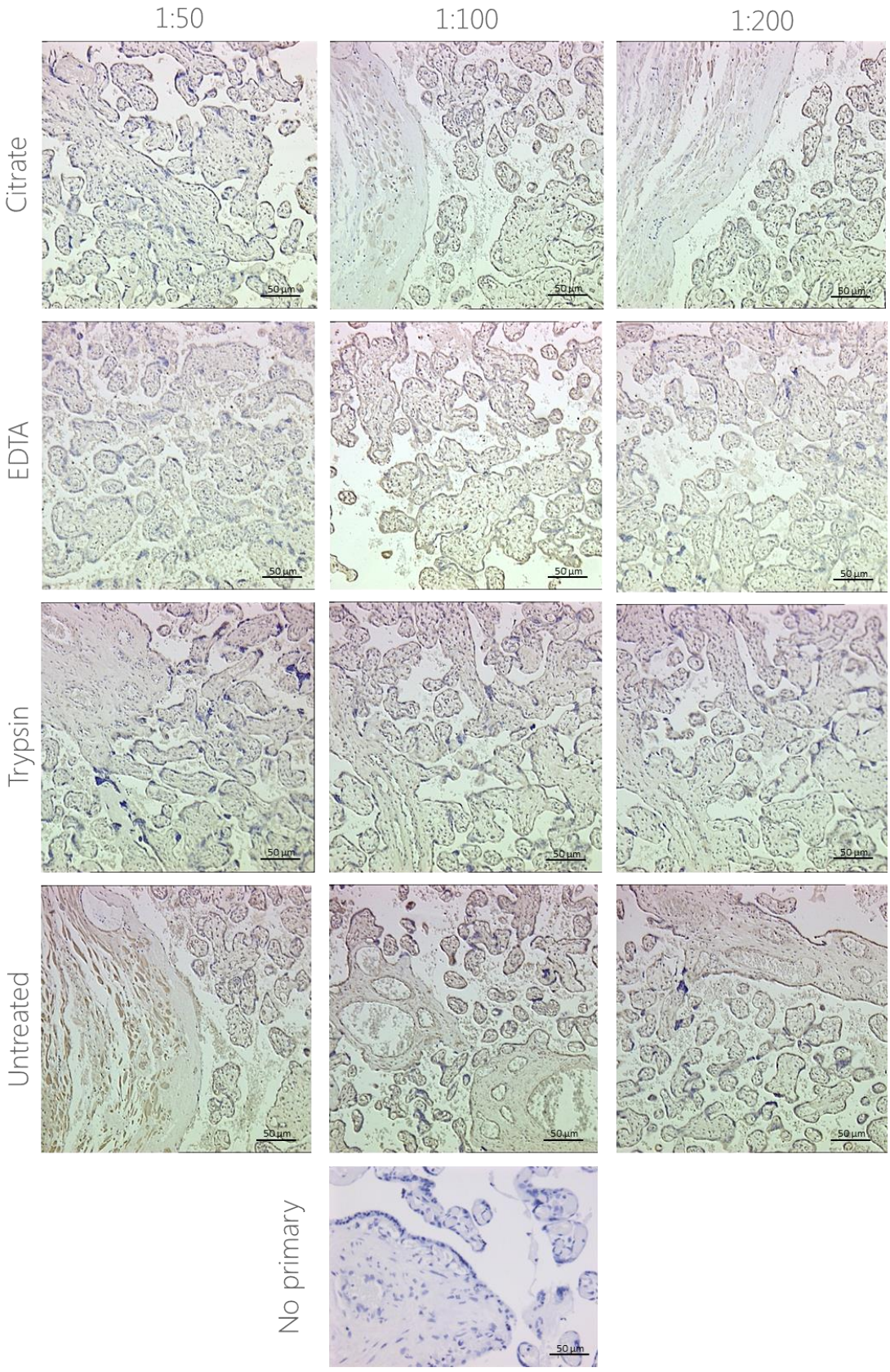

Figure 3-2. Optimisation of CXCR7 staining using IHC in placenta tissue.
4µm sections from human placenta were stained for CXCR7 using immunohistochemistry following three different antigen retrieval pre-treatments (Citrate buffer, EDTA buffer or Trypsin) or no pre-treatment. Three different antibody concentrations, 1:50, 1:100 and 1:200, were used. Briefly, protocol from the VECTASTAIN ABC HRP kit was followed, signal was developed using DAB (brown stain) and counterstained with haematoxylin (blue). No primary antibody was used as a control.

In vivo *levels of CXCR4, CXCR7 and CCR7 expression in primary breast cancer*

Similarly to CXCR4, CCR7 has also been described to be upregulated in breast cancer tissue and to mediate metastasis to the lymph nodes, however its location has not been extensively assessed (Cabioglu et al., 2005b, Cabioglu et al., 2007). In order to determine CCR7 expression, staining was first optimised in tonsil in collaboration with undergraduate student Pan Ching Yeong who worked under my guidance. As described in the introduction, CCR7 is responsible for the homing of lymphocytes to secondary lymphoid organs, and thus staining of T cells within the tonsil was expected (Campbell et al., 2001). As seen in Figure 3-3, staining was carried out first with three antigen retrieval pre-treatments, and no antigen retrieval was chosen to proceed further given its lesser unspecific staining of the squamous epithelium, which has been reported as CCR7-negative (The human protein atlas, 2017). For the second optimisation, three antibody concentrations were carried out (1:20, 1:50 and 1:100) and 1:50 was chosen (see Figure 3-4). Although specific cytoplasmic and some membrane staining could be observed in both optimisations, important background staining was still present in some samples. Indeed, a higher degree of background staining is expected in tonsil given the high number of cell types (e.g. monocytes, B-cells) that express endogenous Fc receptors to which antibodies can bind non-specifically (Buchwalow et al., 2011).

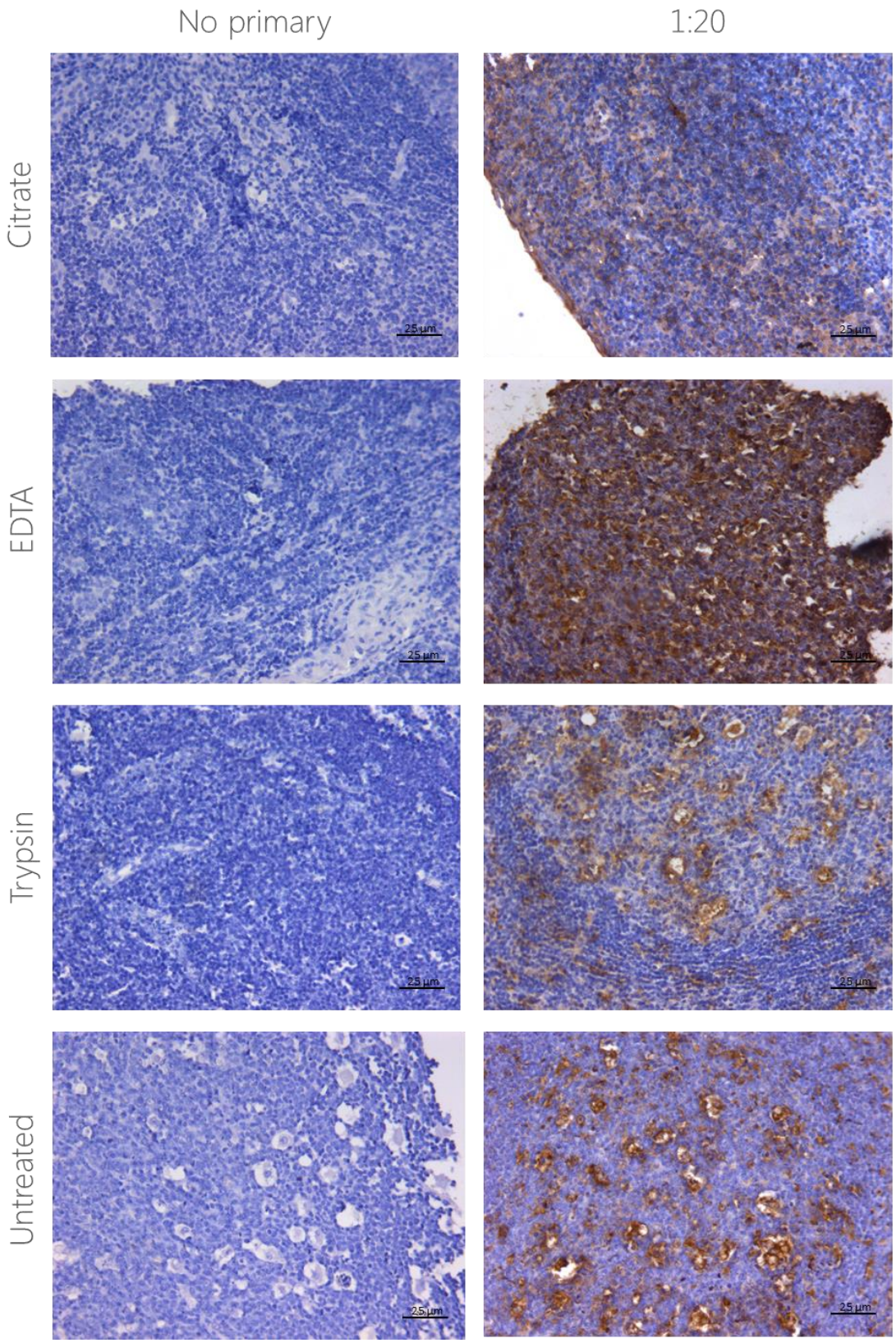

Figure 3-3. Optimisation of CCR7 pre-treatment using IHC in tonsil tissue.
4µm sections from human tonsil were stained for CCR7 using immunohistochemistry following three different antigen retrieval pre-treatments (Citrate buffer, EDTA buffer or Trypsin) or no pre-treatment. Briefly, the protocol from the VECTASTAIN ABC HRP kit was followed with 1:20 dilution of the CCR7 antibody; signal was developed using DAB (brown stain) and counterstained with haematoxylin (blue). No primary antibody was used as a control.

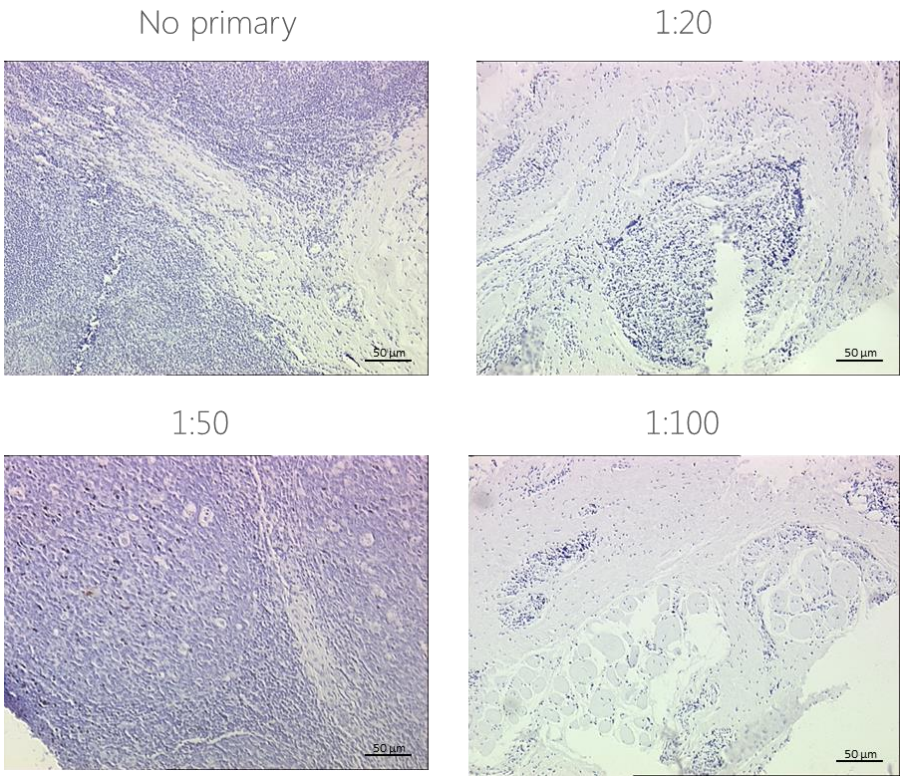

Figure 3-4. Antibody concentration optimisation for CCR7 staining using IHC in tonsil tissue.
4µm sections from human tonsil were stained for CCR7 using immunohistochemistry following or no antigen retrieval pre-treatment. Briefly, the protocol from the VECTASTAIN ABC HRP kit was followed with 1:20, 1:50 or 1:100 dilution of the CCR7 antibody; signal was developed using DAB (brown stain) and counterstained with haematoxylin (blue). No primary antibody was used as a control.

In order to further reduce CCR7 background staining, the ImmPRESS™ Polymer Detection Systems kit (Vector) was used instead of the Vectastain ABC kit. Unlike the Vectastain kit, where secondary and tertiary antibodies need to be added before the substrate, the ImmPRESS kit provides a micropolymer of peroxidase enzymes attached to the secondary antibody, facilitating its binding to the primary antibody due to the lack of steric hindrances. As seen in Figure 3-5, background staining was diminished thanks to the reduced cross-reactivity of the micropolymer, and thus it was chosen to be used in breast cancer tissue samples.

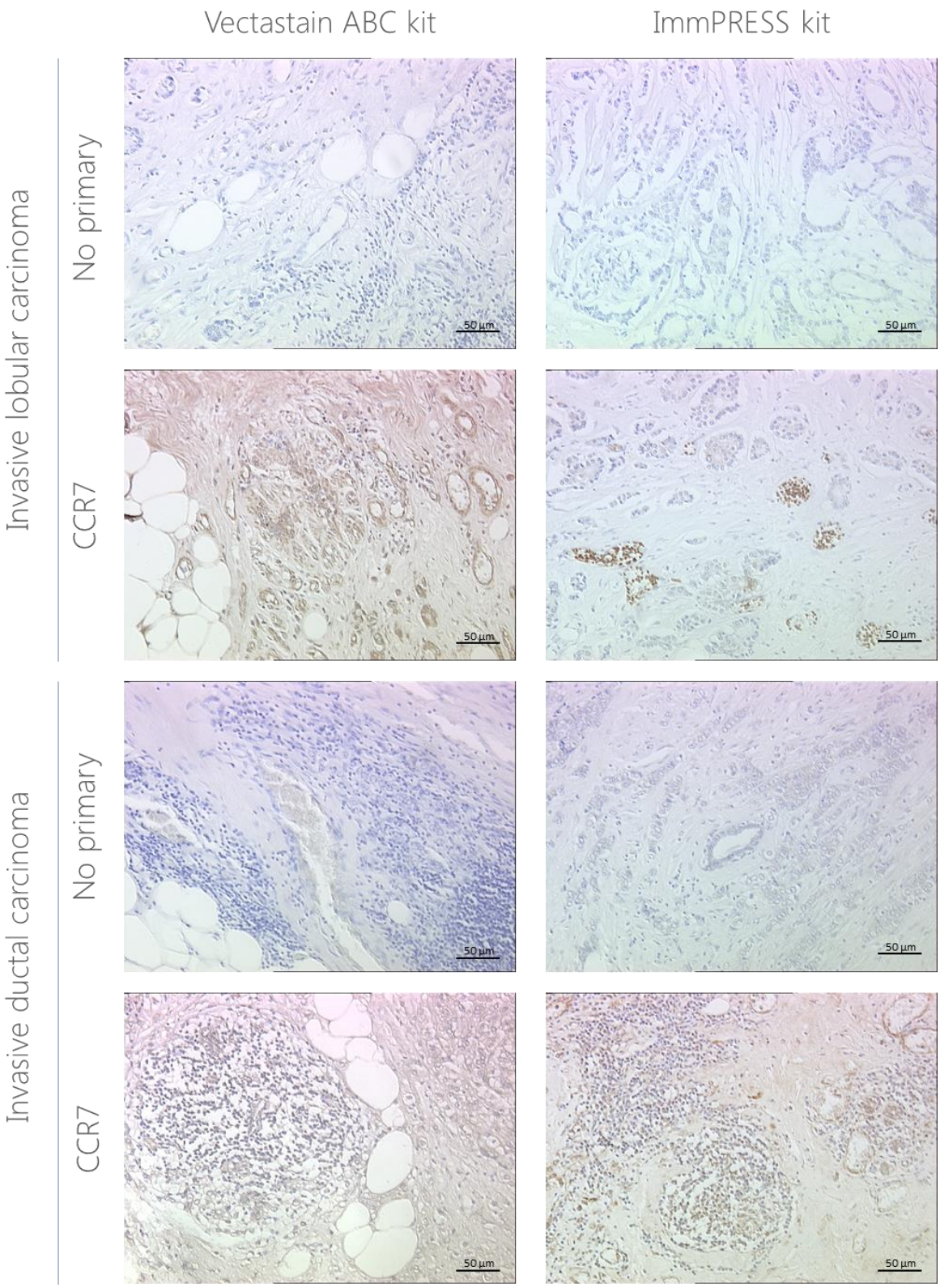

Figure 3-5. Staining kit optimisation for CCR7 staining using IHC in breast cancer tissue.
4µm sections from human breast cancer were stained with 1:50 CCR7 using two different IHC kits: the VECTASTAIN ABC HRP kit and the ImmPRESS polymer detection kit. Signal was developed using DAB (brown stain) and counterstained with haematoxylin (blue). No primary antibody was used as a control.

3.3.2. CXCR4, CXCR7 and CCR7 expression in paraffin-embedded breast cancer samples

As seen in Figure 3-6, both CXCR4 and CXCR7 were highly expressed in ductal and lobular carcinoma samples. In particular, CXCR4 staining in ductal carcinoma was mainly present in the cytoplasm and in the cell surface of some cells, particularly around the ducts. Some artefacts were also noted on the secretions (eosinophilic material) inside the ducts. Meanwhile, CXCR4 staining in lobular carcinoma was also widely present in the cytoplasm, usually with stronger staining than in ductal carcinoma, and in the nucleus of infiltrating cells in some areas, albeit never in the ducts. Some background staining was also present in the most fibrotic areas.

Interestingly, CXCR7 staining followed the same pattern as CXCR4 – unfortunately, the slides were not sister sections and thus direct area comparison is not possible. In ductal carcinoma CXCR7 was exclusively present in the cytoplasm, whilst in lobular carcinoma it was mostly expressed in the cytoplasm but around 20% of cells also presented nuclei staining. Unlike CXCR4, in both patients staining was also particularly strong in the walls of blood vessels.

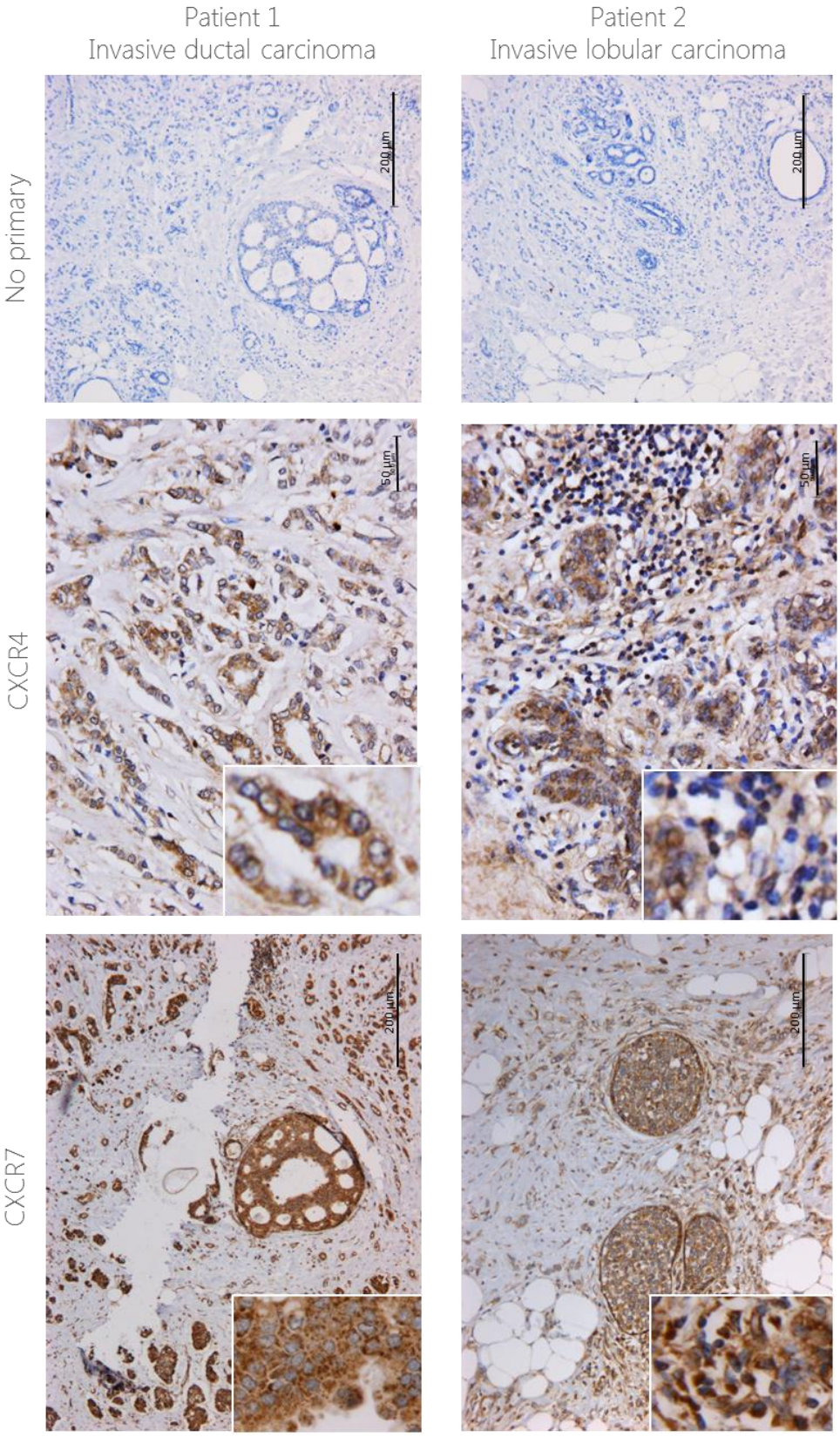

Figure 3-6 CXCR4 and CXCR7 staining using IHC in breast cancer tissue.
4µm sections from human breast cancer were stained for CXCR4 (1:40) and CXCR7 (1:150) using immunohistochemistry following no pre-treatment or Citrate antigen retrieval pre-treatment, respectively. Briefly, protocol from the VECTASTAIN ABC HRP kit was followed, signal was developed using DAB (brown stain) and counterstained with haematoxylin (blue). No primary antibody was used as a control. The differences in staining pattern and localisation can be seen in the 40x magnification insert in the bottom right corner.

As seen in Figure 3-7, staining for CCR7 was in general more variable between the different types of breast carcinomas than CXCR4 and CXCR7, and slightly fainter. Both patient 2 and 4 presented with invasive lobular carcinoma and no lymph node involvement, and were positive for CCR7. In particular, patient 2 showed very strong CCR7 staining in both the cytoplasm and the nucleus, with higher nuclear staining in the cells infiltrating the ducts. Patient 4 also showed intense staining, particularly nuclear and surrounding the abnormally-shaped ducts and vessels.

Patients 3, 6, 7 and 8 presented with invasive ductal carcinoma without lymph node involvement, and different CCR7 localisation could be observed. In patient 3, only very faint cytoplasmic staining was observed in the DCIS area of the tumour (sample a), however CCR7-positive cells could be detected in the ductal infiltrate of the invasive area (sample b), with most of the staining being cytoplasmic. Similarly, most of the staining in the CCR7-positive cells of patient 7 was cytoplasmic, although there was also some nuclear staining which was localised in or around the ducts. The samples from patient 8 corresponded to the two edges of the tumour, which increased the background staining due to tissue fibrosis. However, we could still observe cytoplasmic staining (sample a), and cytoplasmic and nuclear staining (sample b) in the cells infiltrating the ducts. Lastly, the sample collected from patient 6 corresponded to the lymph node and surprisingly, no specific CCR7 staining was seen. However, location of CCR7-positive T-cells and dendritic cells is very zone-specific and thus this lack of expression could be due to the section corresponding to a CCR7-negative area such as the germinal centre.

Patients 1 and 5 presented with invasive ductal carcinoma with positive lymph nodes. Interestingly, no staining could be seen in patient 1 with the exception of artefacts in the dysplastic ducts (marked with arrow). In patient 5, a few cytoplasmic CCR7-positive cells could be observed, but the high unspecific background staining made assessment difficult

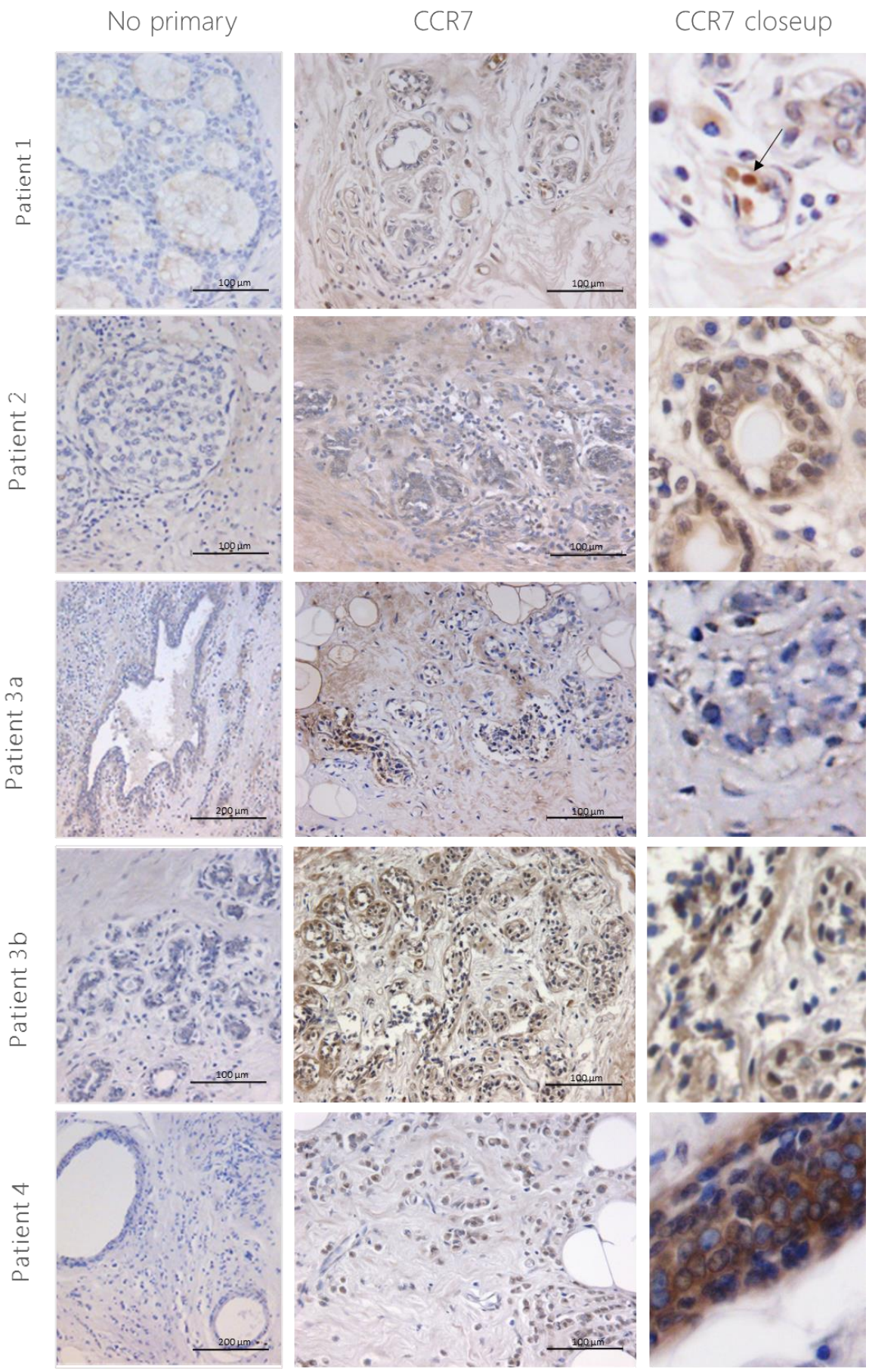
No primary
CCR7
CCR7 closeup
Patient 1
Patient 2
Patient 3a
Patient 3b
Patient 4
100 µm
200 µm

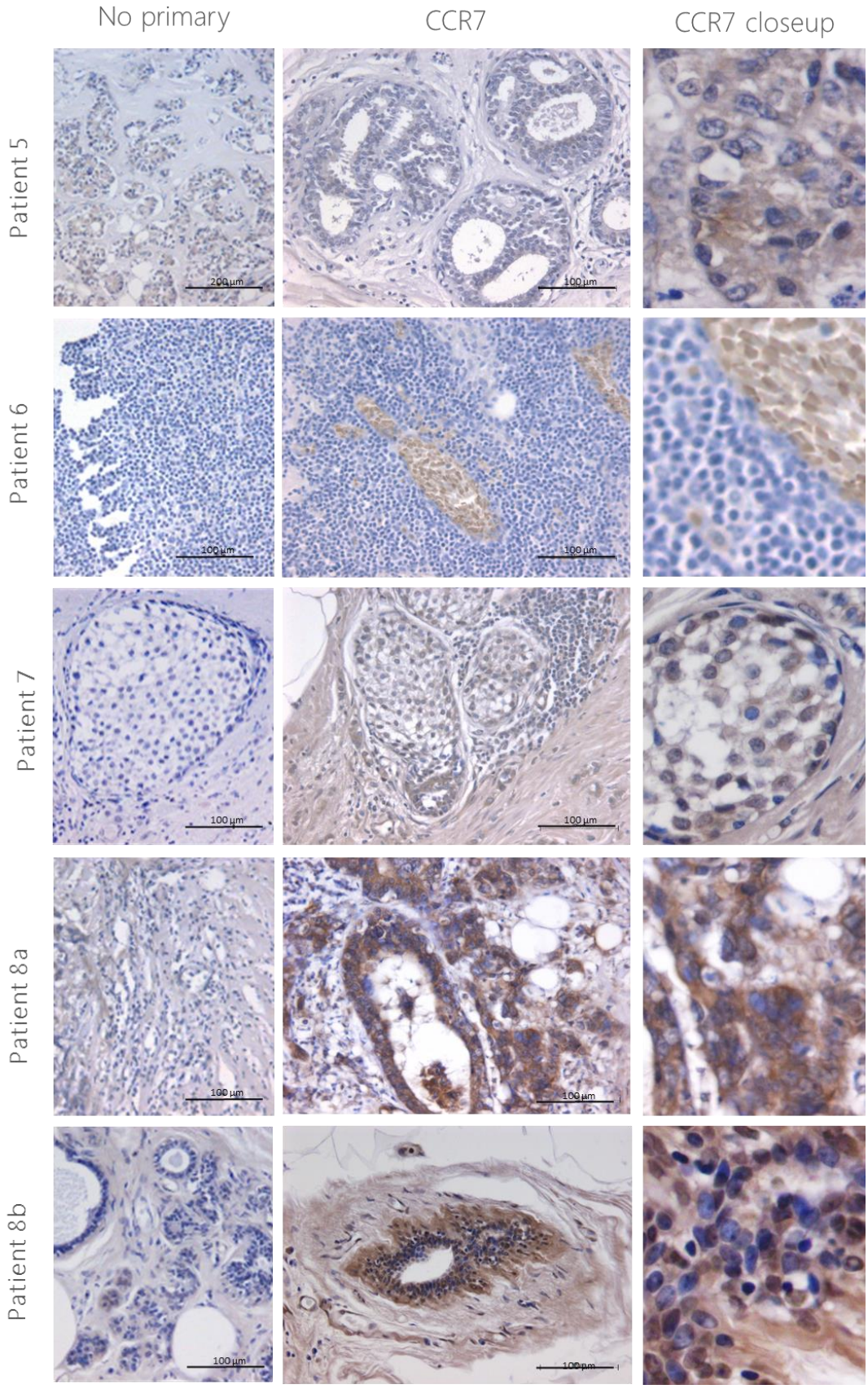

Figure 3-7. CCR7 staining using IHC in breast cancer tissue.
4µm sections from human breast cancer were stained for CCR7 (1:50) using immunohistochemistry following no pre-treatment, demonstrating the variability of staining intensities between tumours. Briefly, protocol from the ImmPRESS polymer detection kit was followed, signal was developed using DAB (brown stain) and counterstained with haematoxylin (blue). Microscopy images were taken at 20x magnification. No primary antibody was used as a control, depicted in the upper left corner of the stained samples at 10x magnification.

3.3.3. CXCR4 and CXCR7 RNA expression in frozen breast cancer samples

Tumour and microenvironment from frozen samples were separated using laser capture and RNA was extracted and retro-transcribed to measure CXCR4 and CXCR7 expression. As seen in Figure 3-8 (top), no significant difference in CXCR4 expression was seen between lymph node positive and lymph node negative patients in either the tumour or the stroma. Furthermore, expression between paired tumour and stroma was not significantly different (see Figure 3-9, left). Similarly, CXCR7 expression did not follow any recognisable pattern, although expression in the tumour was more variable than in the microenvironment (see Figure 3-8 (bottom)). Briefly, from the patients with no lymph node involvement, two of them had lower CXCR7 expression in the tissue surrounding the tumour than the tumour itself and two had higher expression. From the patients with lymph node involvement, two had higher CXCR7 expression in the stroma and one had lower expression in the surrounding tissue (see Figure 3-9, right), however no difference was statistically significant.

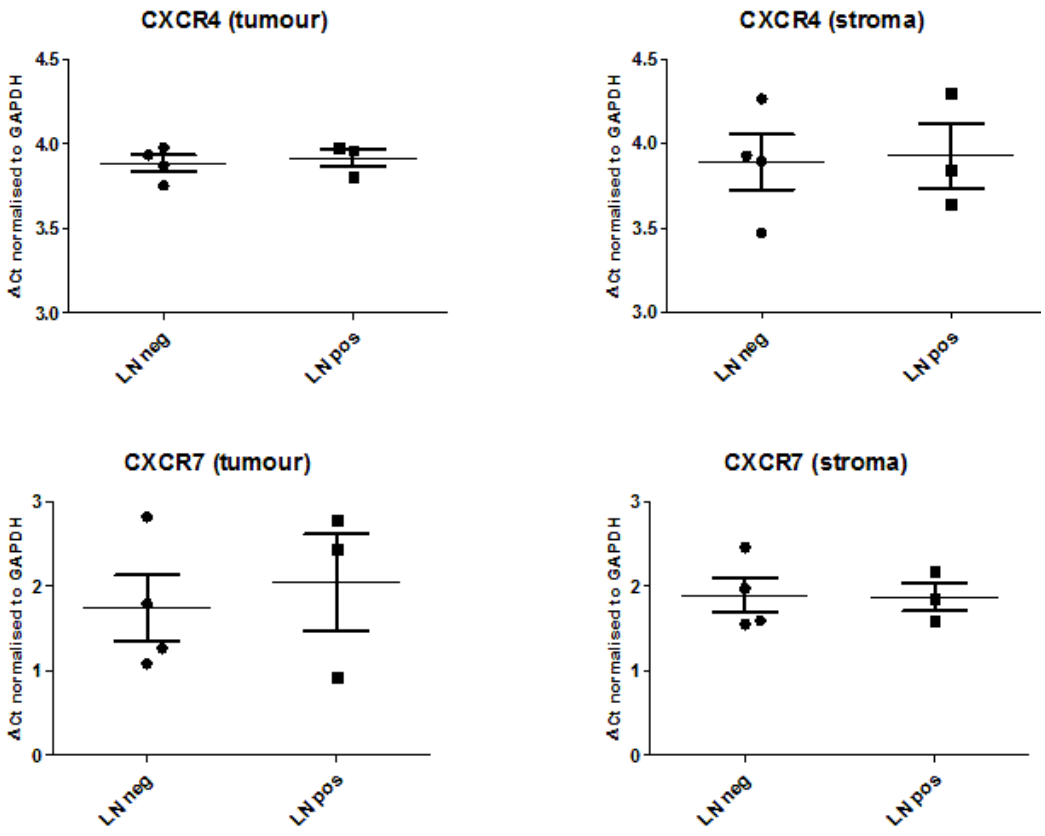

Figure 3-8. CXCR4 and CXCR7 expression in lymph node positive and lymph node negative patient samples. Tumour was separated from microenvironment using laser capture and RNA was extracted using the Arcturus PicoPure RNA isolation Kit. RNA was retro-transcribed and RT-PCR was carried out for CXCR4 and CXCR7. The mean relative expression levels from each sample were grouped into their lymph node status and compared using an unpaired t-test (not significant, $p>0.6$).

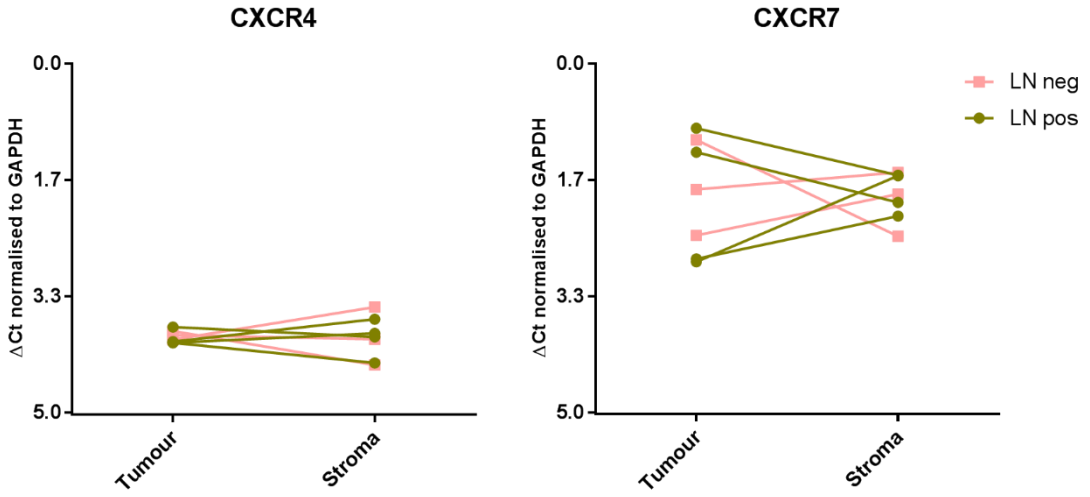

Figure 3-9. Individual CXCR4 and CXCR7 expression in patient samples.
Tumour was separated from microenvironment using laser capture and RNA was extracted using the Arcturus PicoPure RNA isolation Kit. RNA was retro-transcribed and RT-PCR was carried out for CXCR4 and CXCR7 and normalised for GAPDH. Each patient tumour and stroma pair are linked, with patients with lymph node involvement depicted in green and those withour in pink. Data were plotted as ΔCt normalised to GAPDH and difference between tumour and stroma was compared using an unpaired t-test (not significant).

For both CXCR4 and CXCR7, no relationship was seen between their ΔCt and the tumour dimensions, percentage of positive lymph nodes, NPI or BR grading, with the exception of CXCR7 in the stroma which correlated with BR grading (see Appendix 1, Figure 0-1 and Figure 0-2).

3.4. DISCUSSION

Since the discovery that many chemokine receptors are upregulated in breast cancer (Müller et al., 2001), CXCR4 and CCR7 have been widely explored not only as possible drug targets, but also as biomarkers for disease prognosis. Furthermore, location of the chemokine receptors could also prove key in predicting the aggressiveness of the tumour and risk of metastasis, a direction that few studies have taken. From our study, although no conclusive results can be drawn given the small sample size, some clear trends can be seen.

CXCR4

There are opposing reports in the literature regarding the localization of CXCR4 within the tumour cell and whether its expression correlates with other prognostic factors such as tumour size, lymph node involvement or hormonal receptors. In our study, CXCR4 expression was strongly present in both lobular and ductal carcinoma with or without lymph node involvement, correlating to previous studies in the department (Douglass et al., 2014, Douglass, 2014). However, nuclear expression was only observed in the patient with lobular carcinoma and no lymph node involvement. Furthermore, cells were not homogenously stained, but rather had positive cells near cells that expressed no CXCR4, a pattern that Kato et al. (2003) described as “focal”.

Consistent with our findings, many studies found that staining could be both cytoplasmic or nuclear, with membrane staining being more rare (Salvucci et al., 2006, Papatheodorou et al., 2014, Hao et al., 2007, Kato et al., 2003, Aravindan et al., 2015, Sun et al., 2014); although some studies reported only cytoplasmic staining (Andre et al., 2006, Tsoli et al., 2007). In particular, similar to our study, Salvucci et al. (2006) reported that staining did not vary significantly between ductal and lobular carcinomas, and that there was no difference in CXCR4 positivity between tumours with or without lymph node involvement (Kato et al., 2003, Salvucci et al., 2006). Furthermore, he also observed that cytoplasmic expression was associated with higher lymph node status, whilst nuclear staining was not associated with lymph node positivity. This correlation between cytoplasmic CXCR4 staining in positive lymph node tumours, and nuclear CXCR4 with lymph node negative tumours has also been reported by Liu et al. (2009a), Su et al. (2006), Woo et al. (2008), Tsoli et al. (2007) and Cabioglu et al. (2005b), albeit this tendency was not always significant. Indeed, in our hands nuclear staining was only observed in the patient with no lymph node

metastasis. However, the function of CXCR4 in the nuclei has yet to be elucidated, although it has been speculated that this location may prevent CXCL12 binding and thus inhibit signalling, hampering tumour metastasis (Spano et al., 2004).

The relevance of cytoplasmic CXCR4 is still not clear either, but some studies suggest that cytoplasmic staining may be a more relevant marker than membrane staining, as activated CXCR4 will be internalised (Salvucci et al., 2006). However, Blot et al. (2008) reported the opposite, with membrane but not cytoplasmic staining being a significant prognostic factor for lymph node metastasis. Indeed, different studies have also reported that cytoplasmic CXCR4 staining has no correlation with the presence of metastasis (Andre et al., 2006) or grade (Schmid et al., 2004). However, we must also bear in mind that receptor expression does not necessarily correlate with functional activity and thus all extrapolations should be taken with caution.

Conflicting studies also exist regarding overall CXCR4 expression, with Holm et al. (2007) reporting no relation between CXCR4 overexpression and axillary lymph node status, and Sun et al. (2014), Wu et al. (2015) and Hao et al. (2007) describing an association between CXCR4 staining and lymph node metastasis. However, a recurring theme is that high CXCR4 expression reduces the survival rate, even when no correlation with metastasis is observed, suggesting that CXCR4 may regulate other markers which worsen prognosis.

A similar dichotomy has been also described in other cancers – for instance, CXCR4 staining in melanoma has been described both as mainly cytoplasmic (Scala et al., 2005) and cytoplasmic and nuclear (McConnell et al., 2016), although no correlation with location and clinical outcome has been drawn. Meanwhile, CXCR4 staining in nasopharyngeal carcinoma is mainly nuclear (Wang et al., 2005) and does not correlate with clinical outcome. In opposition to most breast cancer studies, staining in hepatocellular carcinoma (Shibuta et al., 2002) and pancreatic cancer (Koshiba et al., 2000) has been described as cytoplasmic and with no correlation to lymph node involvement. However, similarly to our studies and others in breast cancer, in non-small cell lung carcinoma nuclear staining has been correlated with better survival (Spano et al., 2004), although less patients present nuclear staining than cytoplasmic. Furthermore, similar CXCR4 profiles have also been described in both oesophageal squamous cell and adenocarcinoma, where comparable levels of staining were present in both histological types (Gockel et al., 2006).

Overall, these differences in results can be due to a several reasons apart from discrepancies between cancer types – for instance, racially different cohorts (eg. Asian vs Caucasian),

different CXCR4 antibodies used, and differences in the assessment of positivity in staining. However, despite our small sample number limiting the conclusions, our study suggests that cytoplasmic, but not nuclear CXCR4, favours metastasis to the lymph nodes.

Furthermore, at RNA level we observed no difference in CXCR4 expression between the tumour and the surrounding stroma. Indeed, Cabioglu et al. (2005b) described CXCR4 staining in "normal" tissue surrounding the tumour in cells such as adipocytes and stromal cells. Supporting this, CXCR4 has been described to be present not only in DCIS but also in premalignant lesions such as atypical duct dysplasia (Schmid et al., 2004) and several reports exist describing resting endothelial cells expressing CXCR4 (Feil and Augustin, 1998, Volin et al., 1998). Furthermore, Mirisola et al. (2009) also reported a similar CXCR4 staining pattern and levels between the tumour and the endothelium. However, contrary to our findings most studies report higher expression in the tumour than the surrounding tissue, both at mRNA level (Wu et al., 2015) and in IHC (Papatheodorou et al., 2014, Hao et al., 2007). However, this difference could be due to the location of the microenvironment in relation to the tumour – indeed, we chose tissue immediately contiguous to the tumour, whilst other studies could have selected areas further away. Furthermore, in other cancers CXCR4 was present in both malignant and non-malignant tissue, particularly in endothelial cells of vessels surrounding the tumour in hepatocellular carcinoma (Shibuta et al., 2002) and pancreatic cancer (Koshiba et al., 2000). Indeed, it has been reported that hypoxia drives CXCR4 expression, which in turn promotes VEGF-mediated angiogenesis, creating a feedback loop with CXCR4 in the newly formed blood vessels (Liang et al., 2007b, Hao et al., 2007, Wu et al., 2010b).

CXCR7

In our study, CXCR7 staining was observed mainly in the cytoplasm of ductal and lobular carcinoma cells, albeit nuclear staining was also present in some cells in the latter disease. Similarly to our findings, Miao et al. (2007) also described CXCR7 staining in both invasive and lobular carcinomas, and cytoplasmic CXCR7 staining was described in several breast cancer cell lines; however nuclear staining was only present in prostate cells (Salazar et al., 2014). Importantly, unlike CXCR4, nuclear CXCR7 could still function as β-arrestin can move between the nucleus and the cytoplasm to mediate its action (Torossian et al., 2014).

However, CXCR7 presence and location can vary between cancers as demonstrated by several studies. For instance, in non-small cell lung carcinoma CXCR7 is more highly

expressed in squamous cell carcinoma than adenocarcinoma (Iwakiri et al., 2009), whilst we found similar levels between the two types of breast cancer. Location varies too - CXCR7 was only expressed in the cytoplasm in gallbladder cancer (Yao et al., 2011), oesophageal squamous cell carcinoma (Goto et al., 2015) and normal neurons (Shimizu et al., 2011); however, in hepatocellular carcinoma CXCR7 was widely expressed in both cytoplasm and cell membrane (but not nucleus) (Zheng et al., 2010), a pattern that was also seen in brain metastasis from different non-central nervous system tumours (Salmaggi et al., 2009). There are also conflicting reports within pancreatic cancer, with adenocarcinoma presenting cytoplasmic CXCR7 staining with some cell surface expression (Gebauer et al., 2011), whilst Marechal et al. (2009) describes exclusively cytoplasmic staining. Interestingly Gebauer et al. (2011) also noted that all specimens positive for CXCR7 were also positive for CXCR4, a pattern we have also observed. Slightly different CXCR7 staining were also described in renal cancer - Wang et al. (2005) describes CXCR7 expression mainly in cytoplasm, with membrane and nuclear in less than 10% of the samples each; whilst D'Alterio et al. (2010) describes cytoplasmic and membrane staining but not nuclear.

Interestingly, there was no CXCR7 expression in primary melanoma but it was present in the microenvironment, particularly lining blood vessels (McConnell et al., 2016). Indeed, this is a recurring theme that we also observed in our samples, where staining was particularly strong in the walls of blood vessels, which is consistent with CXCR7´s relationship with VEGF (Lazennec and Richmond, 2010, Murphy et al., 2000). Miao et al. (2007) described that CXCR7 was highly expressed in the vascular endothelium surrounding breast tumours, but not on normal blood vessels; similarly CXCR7 was also expressed in the endothelium of blood vessels surrounding pancreatic carcinoma (Gebauer et al., 2011, Marechal et al., 2009). Furthermore, CXCR7 staining was also reported in the associated endothelial cells of brain metastasis from different non-central nervous system tumours, including the brain parenchyma (Salmaggi et al., 2009). However, CXCR7 expression in the surrounding tissue was generally lower than in the tumour, as reported by Wu et al. (2015) in breast cancer and Wang et al. (2012a) in renal cancer. In our case, we observed two cases where expression was significantly higher in the tissue surrounding the tumour, three cases where it was lower and two in which there was no statistical difference. Given the literature, we could hypothesise that this difference is due to some stroma samples being from highly vascularised areas and thus

presenting a high density of blood vessels, which as mentioned previously express high CXCR7 levels. Furthermore, reflecting our results, no study showed a correlation between CXCR7 and lymph node involvement or other clinical data except survival (Wu et al., 2015, Gebauer et al., 2011, Wang et al., 2012a).

Overall, this indicates that CXCR7 expression is present in many cancers including breast cancer, but nuclear staining seems less common than we observed. However, tumour-associated vasculature extensively expresses CXCR7 regardless of the tumour type, hinting that this may be the mechanism through which CXCR7 supports tumour growth.

CCR7

CCR7 is upregulated in breast cancer in comparison to normal tissue (Pan et al., 2008), but interestingly the pattern we observed in our CCR7 samples was the opposite of what was described in literature, with samples from patients with ductal carcinoma and no lymph node involvement presenting higher expression than the samples with positive lymph nodes. Indeed, most studies have found a correlation between CCR7 and increased lymph node metastasis (Cabioglu et al., 2005b, Liu et al., 2010, Mashino et al., 2002, Takanami, 2003, Sellappan et al., 2004, Shang et al., 2009, Arigami et al., 2009, Kodama et al., 2007) or metastasis to other organs (Cabioglu et al., 2009, Andre et al., 2006), albeit it has not always been determined as an independent prognostic factor for metastatic spread. Indeed, contrary to our findings, van den Bosch et al. (2013) reports that uveal melanoma presents strong staining only in cancers with metastasis, whilst staining is less intense in non-metastatic samples. However, this difference could be due to variable CCR7 expression between cancers.

We also assessed the location of the staining, and found it was mostly nuclear in lobular carcinoma and mostly cytoplasmic in ductal carcinoma, with cytoplasmic staining being more common overall. Indeed, Cabioglu reported staining was mostly cytoplasmic, but also observed nuclear staining, albeit rarely without cytoplasmic staining too (Cabioglu et al., 2005b, Cabioglu et al., 2009, Cabioglu et al., 2007). However, he also reported that lymph node positive tumours showed more cytoplasmic CCR7 and that nuclear staining was exclusive to lymph node negative tumours, whilst we saw no difference in metastatic spread between the two. Also in opposition to what we observed, another study reported only cytoplasmic or cell membrane CCR7 staining in breast cancer (Liu et al., 2010). Most interestingly, a third study reported that CCR7 was not expressed by breast cancer cells

but myofibroblasts in the stroma (Cassier et al., 2011). Although the reasons for these discrepancies are not clear, they could be due to different antibodies used or incubation times, different antigen retrieval pre-treatments and blocking agents, or different assessments of positivity.

Other cancers display a similar pattern – indeed, CCR7 staining is present in cell membrane and cytoplasm in gastric carcinoma (Mashino et al., 2002, Sellappan et al., 2004, Ishigami et al., 2007, Arigami et al., 2009), non-small cell lung carcinoma (Takanami, 2003) and pancreatic cancer (Guo et al., 2013), and only in cytoplasm in primary central nervous system lymphoma (Jahnke et al., 2005), uveal melanoma (van den Bosch et al., 2013) and oral squamous cell carcinoma (Shang et al., 2009, Tsuzuki et al., 2006). Interestingly, nuclear staining in 14% of the samples is described in cervical cancer, and unlike cytoplasmic expression it does not correlate with lymph nodes metastasis (Kodama et al., 2007) – indeed, we only observed nuclear staining in patients with negative lymph nodes. Furthermore, Kodama et al. (2007) also described differential staining between squamous cell carcinoma and adenocarcinomas (with the former having higher expression), a difference we also observed between lobular and ductal cancer. CCR7 staining of the vessels surrounding the tumour and adjacent tissue was also observed in NSCLC (Takanami, 2003), but we did not observe this pattern in our samples.

Conclusions

Overall, we characterised the expression of CXCR4, CXCR7 and CCR7 in paraffin-embedded breast cancer samples using immunohistochemistry. We observed positive staining for CXCR4, CXCR7 and CCR7 in breast cancer patients, albeit not always in all samples. This staining was mostly cytoplasmic but we also observed some nuclear staining which correlated with samples with no lymph node involvement.

We also carried out RNA analysis of CXCR4 and CXCR7 expression in the tumour and surrounding tissues, although with a smaller sample size due to poor tissue quality. We observed no difference in CXCR4 expression between the tumour and the stroma, whilst CXCR7 expression was variable and showed no discernible trends, although this variation may be due to differences in the stroma's angiogenesis.

Importantly, whilst IHC results seemed to indicate a higher expression of CXCR4 and CXCR7 in the tumour than in the stroma, qPCR did not support these results, showing a similar expression between the two. One possible explanation is data being skewed due

to the small sample size for both experiments, with only one patient for IHC and three (with lymph node involvement) or four (with no lymph node involvement) for qPCR. A second possibility is that the stroma area analysed is different – whilst for IHC the whole area was examined and representative pictures were taken, in qPCR only the area surrounding the tumour cells was cut for RNA extraction of the stroma. It is thus possible that the area analysed for qPCR was more vascularised and thus had a higher proportion of chemokine receptors. At last, RNA and protein levels do not always correlate (Li et al., 2011b, Schwanhäusser et al., 2011, Taniguchi et al., 2010, Vogel and Marcotte, 2012), with some genes in breast cancer only showing moderate correlation between IHC and qPCR (Sinn et al., 2017). Thus, we can also hypothesise that CXCR4 and CXCR7 expression can be influenced by transcriptional and post-translational modifications, which would alter the protein levels regardless of transcript abundance.

In summary, we observed high expression of CXCR4, CXCR7 and CCR7 in tumours from breast cancer patients. However, the multiple mechanisms regulating this overexpression are still not clearly defined. As CXCR4 is the main regulator of chemokine-mediated metastasis to secondary organs, we next aimed to assess one of the potential causes for its upregulation.

4. THE ROLE OF FOXP3 IN REGULATING CXCR4 EXPRESSION

4.1. INTRODUCTION

As described in section 1.3.1.1, FOXP3 is a forkhead transcription factor with a dual role – in Tregs it participates in the inactivation of auto-reacting T-cells; whilst in epithelial cells it represses several oncogenes including HER2. Thus, FOXP3 downregulation in cancerous cells promotes the expression of HER2, which has been shown to increase CXCR4 expression. In turn, CXCL12-CXCR4 signalling enhances HER2 expression, creating a feedback loop (Li et al., 2004).

Previous studies in our group (Douglass et al., 2012) demonstrated the potential of FOXP3 to regulate oncogenes such as SKP2 or c-Myc but also CXCR4. However, whether the latter's regulation is mediated by direct binding or indirectly through HER2 is not yet confirmed. In order to assess this, *FOXP3* silencing in primary human mammary epithelial cells (pHMEC) was carried out using siRNA and CXCR4 expression was then assessed.

4.1.1. Specific aims

- To characterise the cell lines MDA-MB-231 and MCF-10A.
- To determine the timeline in which CXCR4 is induced after *FOXP3* silencing.

4.2. RESULTS

4.2.1. Characterisation of MDA-MB-231 cell line

MDA-MB-231 cells have been extensively used in breast cancer and have been reported to overexpress CXCR4 (Sun et al., 2014) and recent studies in our group described a low expression of FOXP3 (Douglass et al., 2014). MDA-MB-231 cells present a spindle-shaped morphology as observed in Figure 4-1, with a higher number presenting protrusions at the leading edge when cultured at lower confluency.

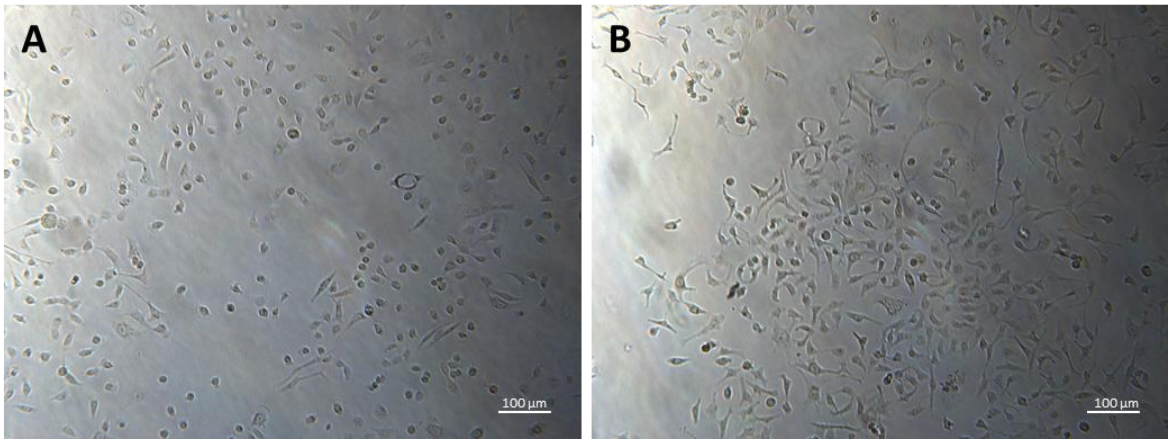

Figure 4-1. Morphology of MDA-MB-231 cells.
MDA-MB-231 cells were grown in a T-75 flask and imaged with a microscope at 10x magnification when they were at 40% (A) and 80% (B) confluency.

In order to validate the cell lines used, immunofluorescence experiments were carried out to assess the expression of several proteins. The MDA-MB-231 cell line was stained for cytokeratin 19, E-cadherin and S100A4 for characterisation and FOXP3, CXCR4, CXCR7 to assess their expression. As shown in Figure 4-2, the cells expressed low levels of CXCR4, high levels of S1004 and cytokeratin 19 and no expression of E-cadherin, FOXP3 and CXCR7.

In order to further confirm the cell quality, passage 20 MDA-MB-231 cells were tested by STR Fingerprinting in the MD Anderson Cancer Centre. Short tandem repeat, or STR fingerprinting, measures the number of repeats in areas in the genome where a small (2 to 13 nucleotides) sequences are repeated for hundreds of times. The exact number of repeats is unique for each sample or cell line and very rarely does this sequence mutate, making it ideal for identity verification (Reid et al., 2013). As seen in Figure 4-3, the cells used in the current study were a match for the MDA-MB-231 sequence in the database.

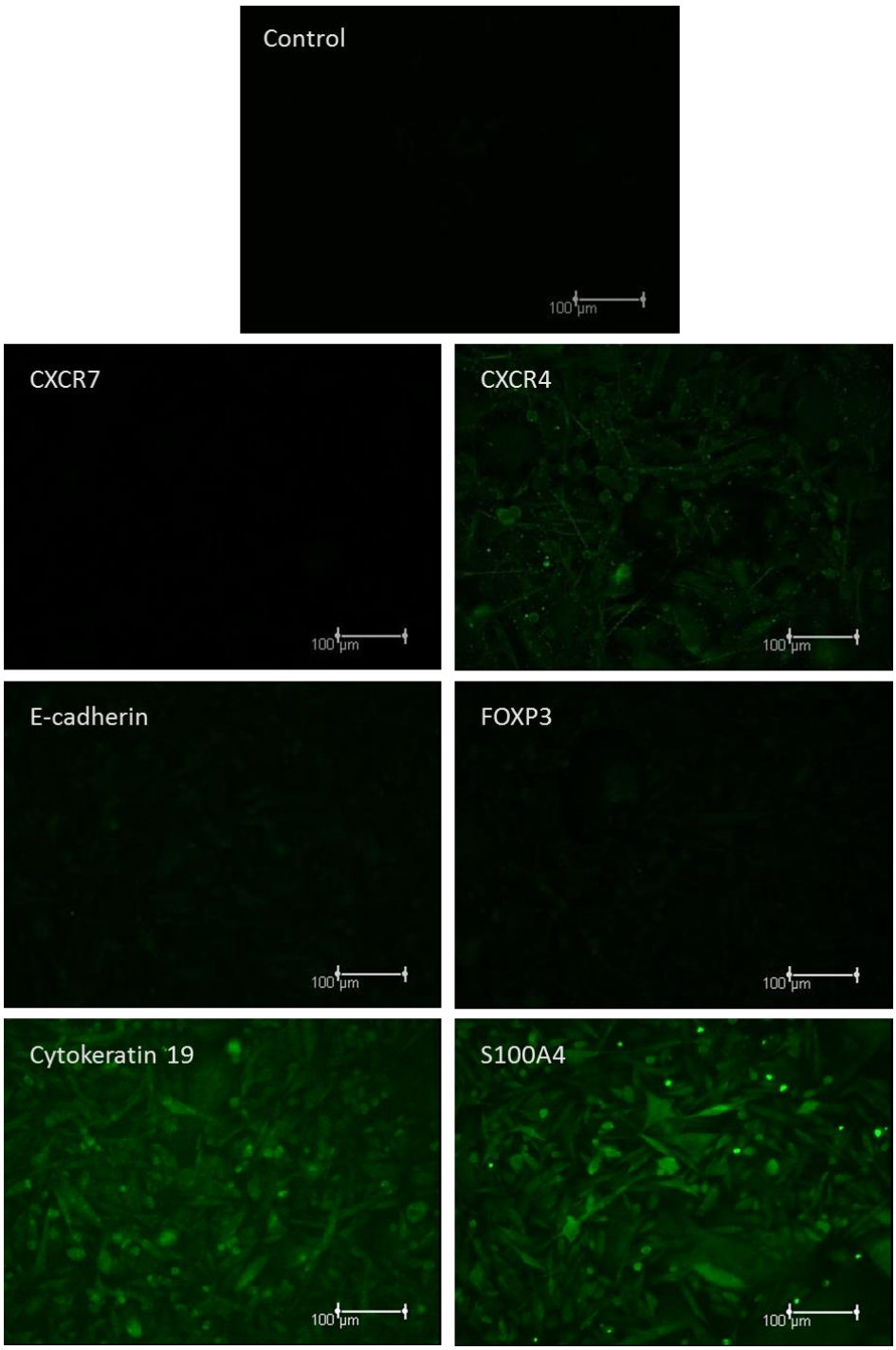

Figure 4-2. Immunofluorescence staining of several markers in MDA-MB-231 cells.
MDA-MB-231 cells were seeded in a 8-well chamber and grown until confluent. Cells were then fixed with 4-paraformaldehyde and permeabilised with triton X-100 before being incubated overnight with antibodies for CXCR7, CXCR4, e-cadherin, FOXP3, cytokeratin 19 and S100A4. The next day cells were incubated with a FITC-conjugated secondary antibody and counterstained with DAPI before visualization. No primary antibody (NPA) was included as a control.

Sample_Name	AMEL	CSF1PO	D13S317	D16S539	D18S51	D21S11	D3S1358	D5S818	D7S820	D8S1179	FGA	TH01	TPOX	vWA	Comments
MDA-MB-231	X	12,13	13	12	16	30,33.2	16	12	8	13	22,23	7,9.3	8,9	15	
MDA-MB-231	X	12,13	13	12	11,16	30,33.2	16	12	8,9	13	22,23	7,9.3	8,9	15,18	MATCH

Figure 4-3. Fingerprinting results.
Top row corresponds to the MDA-MB-231 cell line sent whilst the bottom row shows the values present in the National Cancer Institute public database.

qPCR was also carried out to determine the level of mRNA expression of FOXP3 and CXCR4. Before all else, expression levels of GAPDH, HPRT1 and β-actin were assessed at three different passages in order to decide the housekeeping gene to use as internal control. A comparison between the three can be seen in Figure 4-4 – both GAPDH and HPRT1 were chosen as control genes given their higher expression levels and lower variability, respectively. As described in section 2.4.1., Cts or cycle threshold indicate the amount of cycles necessary for the amplification curve to pass the threshold – thus higher Cts and ΔCts indicate little template and thus less abundant genes.

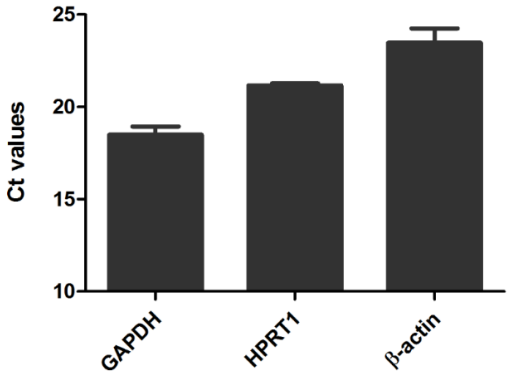

Figure 4-4. Average threshold cycles (Ct) of the housekeeping genes GAPDH, HPRT1 and β-actin was carried out to assess gene expression variability between different MDA-MB-231 passages.
RNA of MDA-MB-231 cells was isolated and retrotranscribed to cDNA using the same amount of RNA in order to assess the expression levels of GAPDH, β-actin and HPRT1. The lower the Ct, the more abundant the gene is. Error bars (SEM) show the fold change in gene expression between three different passages of MDA-MB-231 cells.

Both CXCR4 and FOXP3 levels were low, with averages Cts of 30.56 and 31.74 respectively – their ΔCt values normalised to GAPDH can be seen in figure 4-5. These CXCR4 levels were lower than expected from the literature, which consistently report MDA-MB-231 as a cell line that overexpresses CXCR4 (Akekawatchai et al., 2005, Müller et al., 2001, Liang et al., 2004).

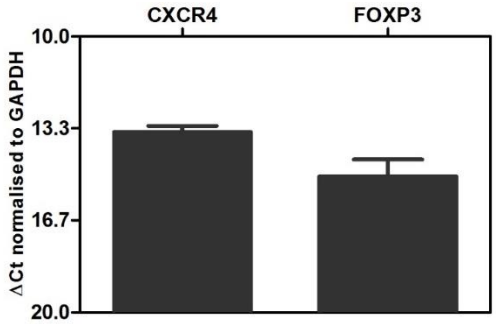

Figure 4-5. Gene expression of CXCR4 and FOXP3 in MDA-MB-231 cells.
RNA of MDA-MB-231 cells was isolated and retrotranscribed to cDNA in order to assess the expression levels of CXCR4 and FOXP3 using Taqman probes and the StepOnePlusTM PCR machine. ΔCt of CXCR4 and FOXP3 relative to the housekeeping gene GAPDH was carried out, where a higher ΔCt corresponds with lesser gene abundance. Error bars (SEM) show the fold change in the expression of the genes.

In order to increase the CXCR4 levels, MDA-MB-231 cells were treated with 400µM of cobalt chloride ($CoCl_2$) to establish hypoxia-mimetic conditions. Indeed, hypoxia has been widely reported to increase CXCR4 expression (Oh et al., 2012, Staller et al., 2003), as discussed in section 1.3.1.1.1. of the introduction. The $CoCl_2$ treatment, however, affected the expression of GAPDH between the treated and untreated samples, and thus HPRT1 was used as endogenous control. An example the housekeeping gene's variation can be seen in Figure 4-6 (A). As shown in Figure 4-6 (B), CXCR4 expression increased by almost a five-fold after a 24 hour treatment with $CoCl_2$, demonstrating that MDA-MB-231 cells are capable of expressing higher levels of CXCR4.

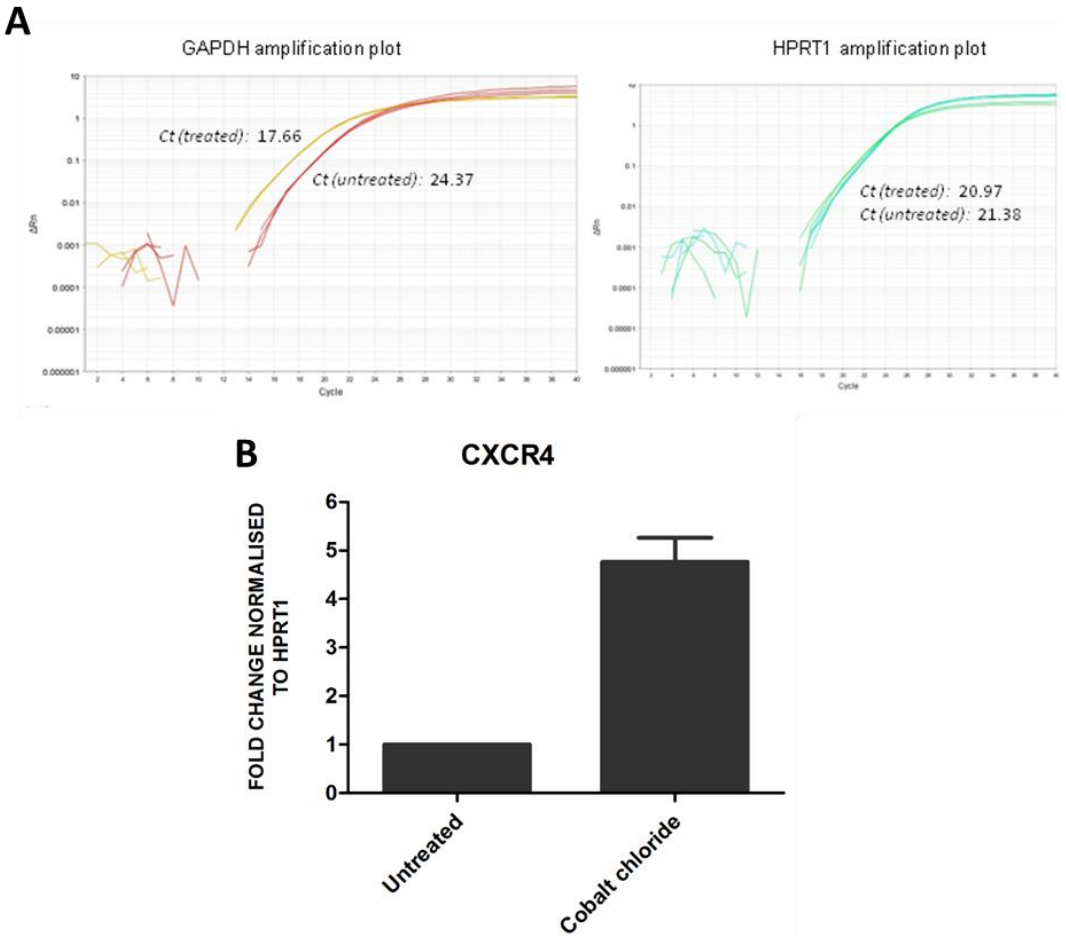

Figure 4-6. CXCR4 expression increase in MDA-MB-231 cells after treatment with cobalt chloride.
MDA-MB-231 cells were grown in a T-75 flask and stimulated with 400 µM $CoCl_2$ for 24 hours to induce hypoxia. Cells were then harvested and RNA isolated and retrotranscribed to cDNA and CXCR4 expression was analysed using Taqman qPCR. **(A)** GAPDH was shown to be very variable after $CoCl_2$ treatment (as seen on the left amplification plot), whilst HPRT1 remained stable (right). **(B)** CXCR4 fold change expression compared to untreated MDA-MB-231 cells and normalised to HPRT1. Data are representative of n=2.

4.2.2. Characterisation of MCF-10A cell line

MCF-10A is an immortalised normal-like breast epithelial cell line which expresses non-detectable levels of CXCR4 (Su et al., 2011) and moderate levels of FOXP3 in comparison to MDA-MB-231 cells (Shen et al., 2013, Liu et al., 2009b), making it an ideal model to assess *FOXP3* silencing effects. MCF-10A cells present a cuboidal or cobblestone morphology when confluent as observed in Figure 4-7, an appearance which is typical of epithelial cells.

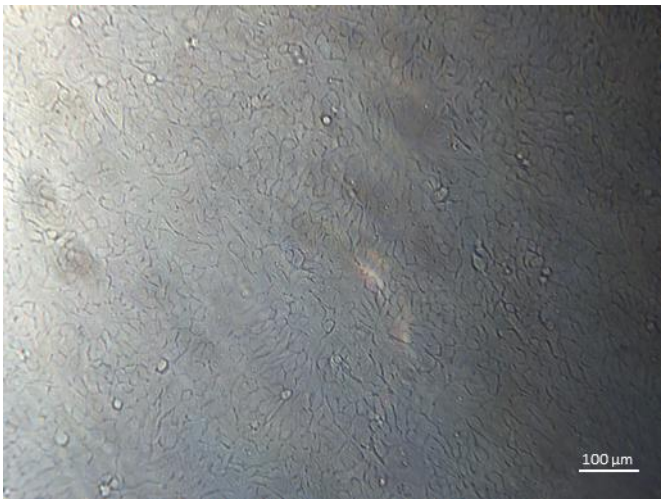

Figure 4-7. Morphology of MCF-10A cells.
MCF-10A cells were grown in a T-75 flask and imaged with a microscope at 10x magnification when they were at a 100% confluency.

In order to characterise the cell line and confirm the presence of epithelial markers, MCF-10A cells were stained for α-tubulin, Ki-67, E-cadherin and Integrin αV - the expression of CXCR4, phospho-CXCR4 and CXCR7 was also assessed. As shown in Figure 4-8, cells expressed high levels of α-tubulin and E-cadherin, low levels of integrin αV, no expression of CXCR4, CXCR7 or phospho-CXCR4 and very few cells were Ki-67 positive.

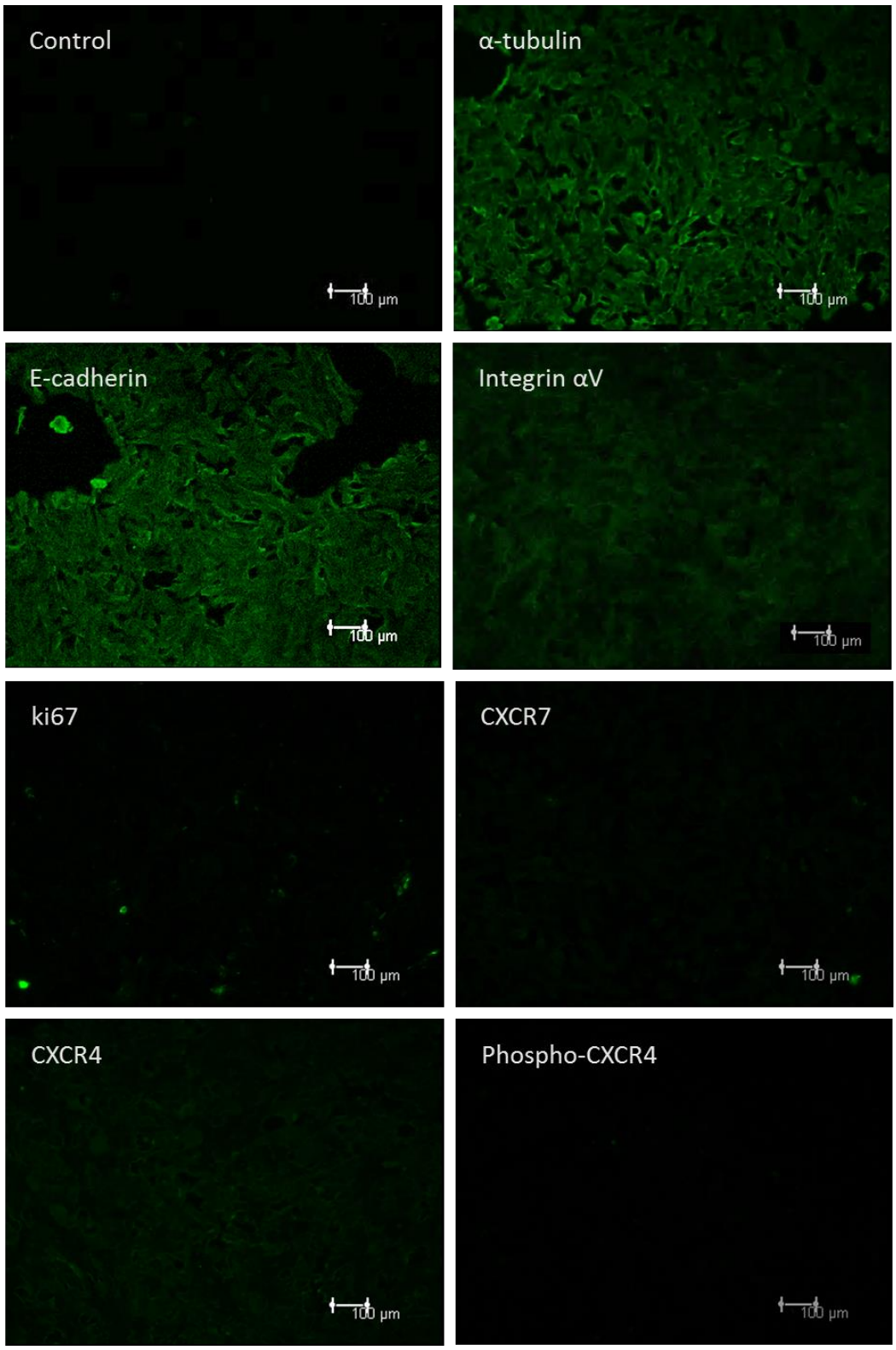

Figure 4-8. Immunofluorescence staining of several markers in MCF-10A cells.
MCF-10A cells were seeded in a 8-well chamber and grown until confluent. Cells were then fixed with 4-paraformaldehyde and permeabilised with Triton X-100 before being incubated overnight with antibodies for α-tubulin, CXCR4, phospho-CXCR4, CXCR7, Ki-67, E-cadherin and Integrin αV. The next day cells were incubated with a FITC-conjugated secondary antibody and counterstained with DAPI before visualization. No primary antibody (NPA) was included as a control.

qPCR was also carried out to assess the level of mRNA expression of FOXP3 and CXCR4. In contrast to MDA-MB-231 cells, CXCR4 was barely detectable whilst FOXP3 levels were moderate-low, with averages Cts of 34.9421 and 29.231, respectively – their ΔCt values normalised to GAPDH can be seen in figure 4-9.

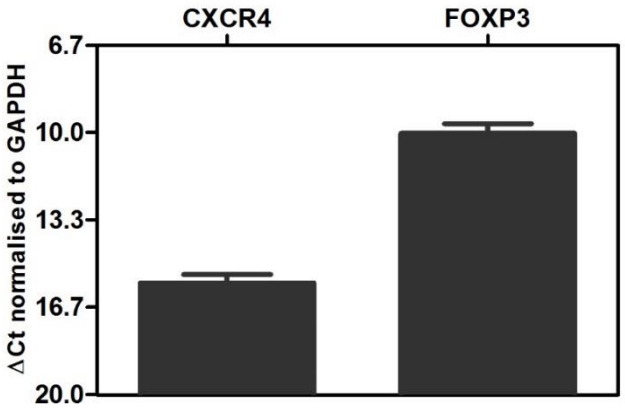

Figure 4-9. Gene expression of CXCR4 and FOXP3 in MCF-10A cells.
RNA of MCF-10A cells was isolated and retrotranscribed to cDNA in order to assess the expression levels of CXCR4 and FOXP3 using Taqman probes. ΔCt of CXCR4 and FOXP3 relative to the housekeeping gene GAPDH was carried out, where a higher ΔCt corresponds with lesser gene abundance. Error bars (SEM) show the fold change in the expression of the genes.

4.2.3. Optimisation of FOXP3 silencing in MCF-10A

In order to optimise the silencing protocol, the cell lines MDA-MB-231 and MCF-10A were transfected with GAPDH-Cy^3 siRNA (Ambion) and Silencer® Select Negative Control No. 1 siRNA using siPORT™NeoFX™ (Invitrogen) in OptiMEM. Transfection efficiency was determined at 24 and 48h by examination of the cells with a Leica fluorescent microscope, and fluorescence intensity was quantified using ImageJ software (National Institute of Health). As shown in Figure 4-10, Cy3-labelled GAPDH siRNA successfully transfected MDA-MB-231 and MCF-10A cells, as marked by the red fluorescence inside the cells. A higher transfection could be observed at 48h compared to 24h in both cell lines, which was confirmed when the fluorescence intensity was analysed. However, overall transfection was almost three times higher in MDA-MB-231 cells as compared to MCF-10A.

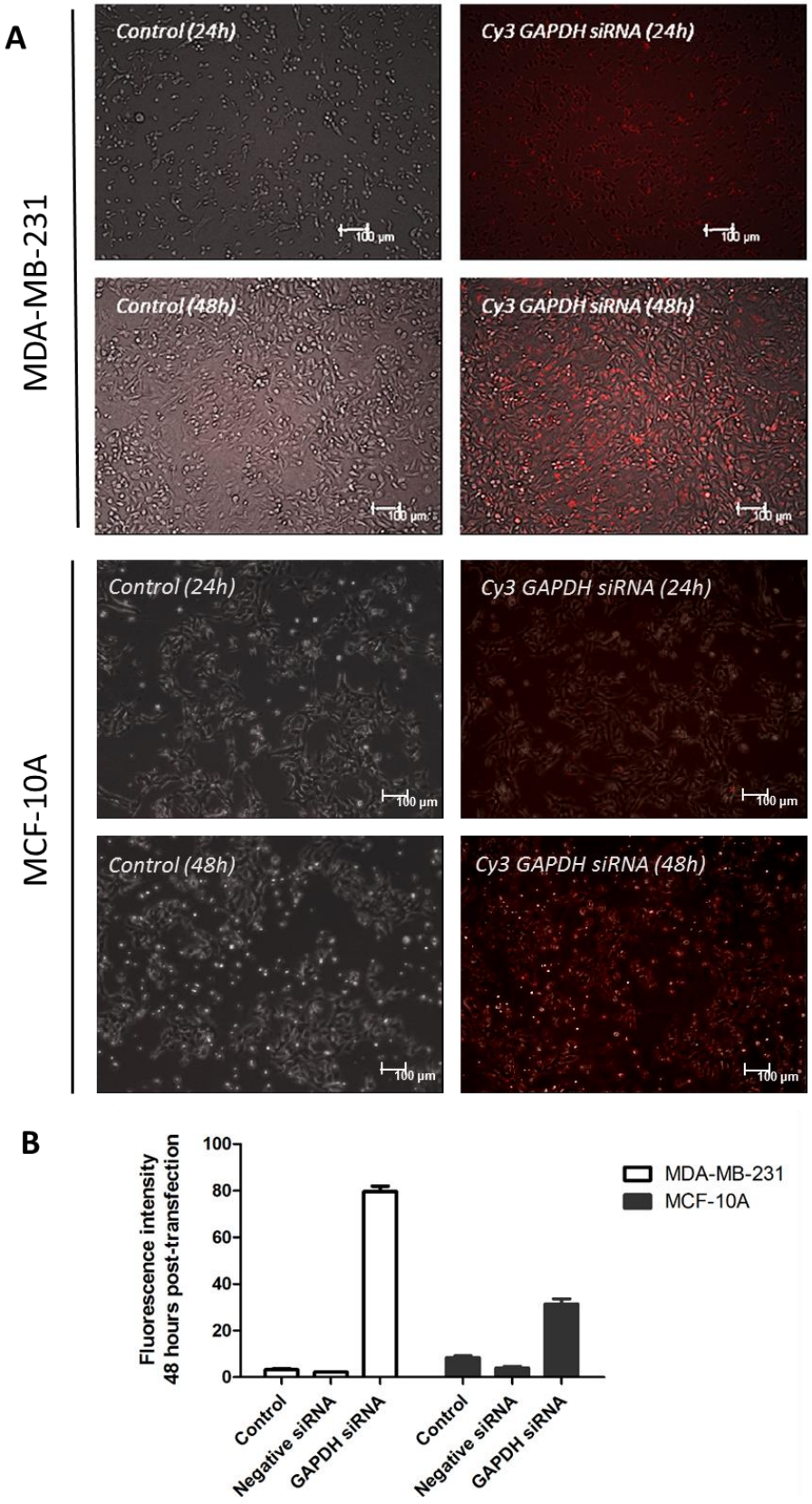

Figure 4-10. Transfection of MDA-MB-231 and MCF-10A cells with Cy3 GAPDH siRNA using siPORT™NeoFX™. **(A)** Cells were grown in six well plates and transfected with 30 nM of Cy3-GAPDH siRNA using NeoFX siPORT, a lipid based transfection reagent. Transfection was assessed 24 and 48 hours post-transfection by visualizing the cells using an inverted fluorescence microscope (Leica). **(B)** Fluorescence intensity 48 hours post transfection for both MDA-MB-231 (white) and MCF-10A (black) was measured using ImageJ. Data are representative of two independent experiments, for which three images per field were analysed per treatment.

Next, MCF-10A cells were transfected with 5nM of Silencer® Select FOXP3 s27192 siRNA and Silencer® Select Negative Control No. 1 siRNA (Ambion). Previous studies in the group had already trialled three FOXP3 Silencer Select siRNA and two Silencer Select Negative Control and similar results were observed among the siRNA used, thus the slightly optimal ones were chosen (Douglass et al., 2014). At 24 and 48 hours, RNA was isolated using the RNeasy® Plus Mini kit and reverse transcribed into cDNA. Relative transcript expression was determined by real-time PCR using FOXP3 and CXCR4 Taqman probes (Life technologies) in order to assess the effects of the knockdown. As shown in Figure 4-11, 24 hours post-transfection FOXP3 expression had been reduced by half, whilst after 48 hours the cell line showed a 10 fold reduction in FOXP3 expression. Conversely, CXCR4 expression increased by almost three-fold 24 hours post-transfection, but only by half at 48 hours.

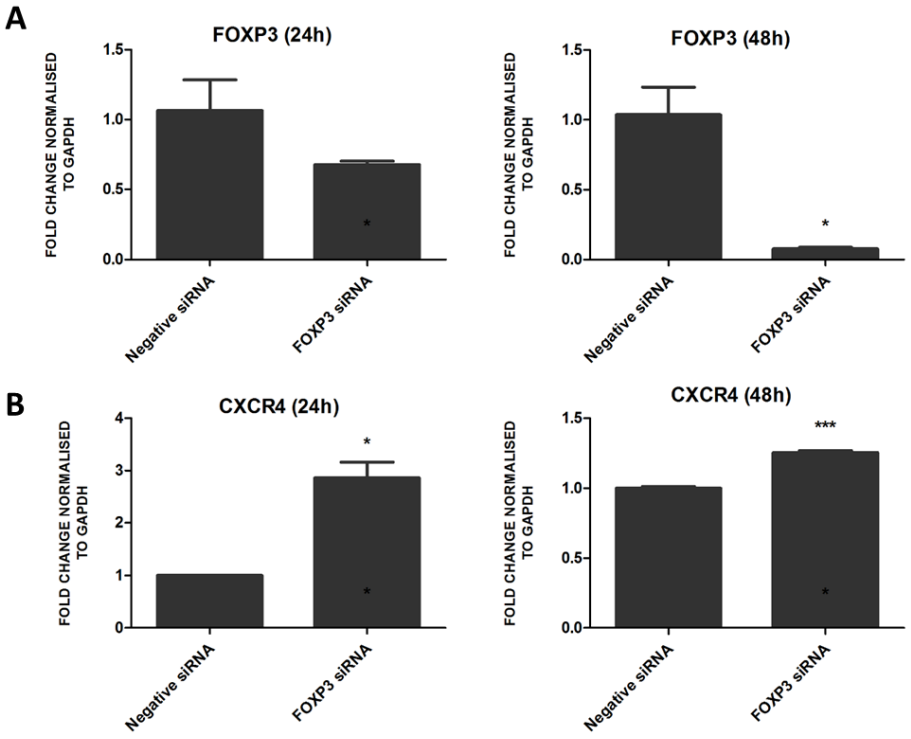

Figure 4-11. Transfection of FOXP3 siRNA was optimised using MCF-10A cells.
MCF-10A cells were seeded in 6-well plates and transfected with 5nM of *Silencer* Select Negative Control no 1 or FOXP3 *Silencer* Select s27192 using NeoFX siPORT. After 24h or 48h RNA was isolated and retrotranscribed to cDNA and CXCR4 and FOXP3 expression was analysed using Taqman qPCR. **(A)** Decreased expression of FOXP3 was observed at both 24 and 48 hours **(B)** correlating with an increase in CXCR4 expression. Data represent the mean ± SEM of three independent experiments and statistical significance was calculated using a Student's *t* test (* $p<0.05$, *** $p<0.001$).

4.2.4. Effects of FOXP3 knockdown in CXCR4 expression in pHMEC

To investigate whether FOXP3 can modulate CXCR4 expression not only indirectly through HER2, but also by directly binding the *CXCR4* gene, silencing of *FOXP3* in pHMEC was carried out using the protocol optimised with MCF-10A cells. GAPDH was selected as housekeeping gene due to more reproducible results.

In pHMEC, FOXP3 and CXCR4 expression was determined at 30 min, 2h, 4h and 8h post silencing to assess FOXP3 downregulation and CXCR4 response. As shown in figure 4-12, compared to the negative control a small but non-significant decrease in FOXP3 expression could be seen at 4 and 8 hours. Inversely, CXCR4 expression showed an upward trend at 4h, reaching a significant increase at 8h. As the FOXP3 protein has a short life of 21 minutes (Lee et al., 2008), we can assume that the drop in FOXP3 levels is due to the silencing, however this decrease does not become significant until 48 h later.

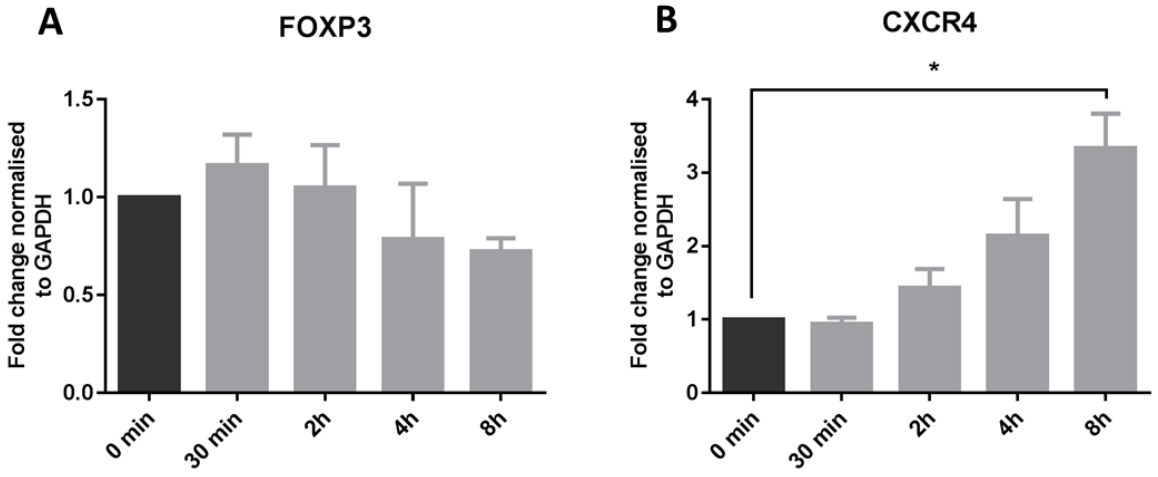

Figure 4-12. FOXP3 decrease in expression correlates with increase in CXCR4 expression in primary human mammary epithelial cells (pHMEC).
pHMEC cells were seeded in 6-well plates and transfected with 5nM of *Silencer* Select Negative Control no 1 or FOXP3 *Silencer* Select s27192 using NeoFX siPORT. Expression levels of FOXP3 **(A)** and CXCR4 **(B)** were assessed at 30 min, 2h, 4h and 8h post transfection using Taqman probes. Data represent the mean ± SEM of three independent experiments and statistical significance was calculated using a one way ANOVA (* $p<0.05$).

4.3. DISCUSSION

MDA-MB-231 are one of the most commonly used breast cancer cell lines in literature, and have been extensively used as models for metastasis, especially *in vivo* (Price et al., 1990, Jenkins et al., 2005). Not surprisingly, MDA-MB-231 cells have also been widely reported to express high levels of CXCR4, a key chemokine receptor in the metastatic process. However, in our hands CXCR4 staining in immunofluorescence was found to be weak, and mRNA expression low. Interestingly, reports of high CXCR4 expression in MDA-MB-231 cells are usually shown using western blot (Liang et al., 2005, Sun et al., 2014, Jin et al., 2012, Manu et al., 2011, Zhan et al., 2015), whilst only one example of high CXCR4 expression using immunofluorescence was found (Liang et al., 2005). Furthermore, in the latter study a custom biotinylated CXCR4 antagonist, and not a commercial antibody, was used (Liang et al., 2004), hinting that the available CXCR4 antibodies may not correctly pick up the receptor in fixed cells.

Further to this, albeit present, CXCR4 expression in MDA-MB-231 cells was shown to be 6 times lower than in primary breast cancer tumour (Müller et al., 2001), highlighting that CXCR4 levels in MDA-MB-231 cells are lower than what we observe *in vivo* in patient samples. Indeed, it is interesting to note that often more aggressive sub-lines are needed for a successful metastasis in murine models. For instance, a study showed that parental MDA-MB-231 showed little metastasis 5 weeks post-transfection, but this increased after selection of metastatic subpopulations (Minn et al., 2005). Indeed, in another study CXCR4 was one of the 52 genes overexpressed when weakly metastatic MDA-MB-231 subpopulations were compared to highly metastatic sublines (Kang et al., 2003). MDA-MB-231 were also negative for CXCR7, as has been described in literature (Hattermann et al., 2010). This suggests that albeit CXCR4 is present in MDA-MB-231 cells, it may not be as high as literature portrays.

To determine that the cell line used in this study had not been transformed or contaminated, cell morphology and marker staining was carried out. Indeed, it was found that these corresponded to what had been described in the literature, with MDA-MB-231 showing the typical spindle-shaped morphology and not expressing the epithelial marker E-cadherin. E-cadherin, or epithelial cadherin, is a cell-to-cell adhesion glycoprotein which is vital for adherent junctions between cells (Van Roy and Berx, 2008). Indeed, loss of E-cadherin has been linked to higher motility and thus higher invasion and metastasis (Onder et al., 2008). It is thus not surprising that MDA-MB-231 cells have been widely

reported to have undergone EMT and therefore express no E-cadherin (Lombaerts et al., 2006, Wong and Gumbiner, 2003). Immunostaining also revealed that MDA-MB-231 cells expressed cytokeratin-19 (CK19), an epithelial cytoskeleton marker. CK19 has been reported to be overexpressed in many tumours including breast cancer and can even be found in circulating tumour cells (Kahn et al., 2000). However, expression in MDA-MB-231 cells differs between studies. One paper reported CK19 mRNA expression (Zhang et al., 2010) and three others showed protein expression (Taylor et al., 2010, Leccia et al., 2012, Sellappan et al., 2004), whilst a fifth study did not find CK19 expression in MDA-MB-231 cells using western blot (Keyvani et al., 2016). Given the body of evidence, the lack of CK19 in this last study could be due to different passages of the cells or even contamination with agents such as mycoplasma. Finally, the cells also expressed high levels of S100A4, a calcium binding protein which modulates the action of many proteins such as actin and myosin (thus playing a role in cell motility) and MMPs (promoting invasion and angiogenesis) (Boye and Mælandsmo, 2010). As expected, MDA-MB-231 has been reported to express S100A4 (Wang et al., 2012b, Grottke et al., 2016, Tsuna et al., 2009, Radestock et al., 2008), which is consistent with our findings.

Fingerprinting of MDA-MB-231 cells also corroborated that the cells were not contaminated with a different cell line. To further ensure that the low levels of CXCR4 were not due to a poor detection from the antibody or the Taqman probes, MDA-MB-231 cells were treated with cobalt chloride, a well reported hypoxia inducer. Indeed, 24 hours after treatment the expression of CXCR4 by MDA-MB-231 cells had increased 5-fold, indicating that the probes were binding correctly.

The disparity in CXCR4 expression between the current and previous studies could be due to different reasons. As mentioned previously, one possibility is that levels that seem low in qPCR or immunofluorescence might correlate with strongly positive bands in Western Blot. Indeed, the cell fixation process in immunofluorescence may affect vital CXCR4 epitopes as this problem is not observed in flow cytometry (Lee et al., 2004, Wendel et al., 2012, Liang et al., 2004, Akekawatchai et al., 2005). Another option is that later passages are needed for high CXCR4 expression. Our cell line was used at passages 20-30, but as seen in other studies CXCR4-high subpopulations can be obtained through culturing passages. Indeed, MDA-MB-231 from other groups from Newcastle University which were at similarly low passages also showed low CXCR4 levels.

MCF-10A cells have often been used in literature as a "normal" breast cell line. As with MDA-MB-231 cells, to ensure that the cell line had not transformed or was not contaminated, cell morphology and marker staining was carried out. MCF-10A showed the typical cobblestone morphology of epithelial cells (Li and Mattingly, 2008) and expressed high levels of the epithelial marker E-cadherin as is widely reported in literature (Qu et al., 2015, Li and Mattingly, 2008, Chen et al., 2014, Yuki et al., 2014). MCF-10A also expressed low levels of integrin αV, a transmembrane receptor which plays a key role in cell-to-cell and cell-to-ECM adhesion. Indeed, integrin αV expression has been correlated with a high migratory phenotype and stem cell-like profile (van den Hoogen et al., 2011). Interestingly, despite being an endothelial cell marker integrin αV has also been detected at low levels in MCF-10A cells in other studies (Li et al., 2015, Mori et al., 2015), which can be further induced through TGF-β. However, this expression is much lower than that observed in aggressive breast cancer cell lines and thus is most likely due to their basal-like phenotype (Li et al., 2015). Our staining also showed that very few MCF-10A cells were Ki-67 positive, which is not surprising as it is a cell marker for proliferation and has been used as a prognostic marker in breast cancer to determine aggressiveness (Inwald et al., 2013). Indeed, similar results were found in literature (Imbalzano et al., 2009, Subik et al., 2010, Machowska et al., 2014), with the highest positive percentage being 30%. Furthermore, MCF-10A cells did not express CXCR4 (or phospho-CXCR4), which correlates with most (Ablett et al., 2014, Guo et al., 2014a, Salazar et al., 2014) but not all (Holland et al., 2006) studies. Once again, this disparity could be due to passage number, as CXCR4 expression has been shown to vary through time (Nelson et al., 2014). Furthermore, this CXCR4 expression in MCF-10A does not correlate with invasion as cells are unresponsive to CXCL12 (Nelson et al., 2014). Finally, our MCF-10A cells did not express CXCR7 either, which correlates with studies that show low CXCR7 levels similar to MDA-MB-231 cells (Salazar et al., 2014). MCF-10A cells also expressed abundant levels of α-tubulin, a vital component of the microtubules that mediates correct cell mitosis. This was included as a positive control to ensure that the staining had worked properly (Dow et al., 2007).

Given all these confirmatory studies, we pursued silencing of *FOXP3* in MCF-10A cells. MCF-10A have been used in the past as model systems for silencing (Caixeiro et al., 2013) and thus are a good model to optimise the transfection procedure. First, both MDA-MB-231 and MCF-10A were transfected with cy3-GAPDH siRNA to assess an overall timeline

for silencing, with transfection being detectable at 24 hours but maximal at 48 hours - this timeline is in correspondence to the manufacturer's instructions. Unfortunately, transfection efficiency couldn't be assessed at mRNA level as GAPDH silencing also affected the levels of the housekeeping genes β-tubulin and HPRT1. Similarly, *FOXP3* silencing in MCF-10A could be observed at 24 hours, but was not significant until 48 hours – however, CXCR4's consequent increase was significant as early as 24 hours.

Although MCF-10A are one of the most extensively used "normal" breast epithelial cell line, they do show some features of EMT, such as vimentin and N-cadherin expression (Sarrió et al., 2008, Qu et al., 2015). Thus, for our short-term silencing study, primary human mammary epithelial cells were used and silencing was determined at 30 minutes, 2 hours, 4 hours and 8 hours post-transfection. Similarly to what was observed at 24 hours with MCF-10A, FOXP3 showed a non-significant decreased expression at 8 hours, indicating that longer times may be needed for a significant knock down. On the other hand, CXCR4 expression started to increase as early as 2 hours and similarly to what was observed with MCF-10A at 24 and 48 hours, reached significance at 8 hours. As FOXP3 was not significantly knocked down at 8 hours, we cannot confirm that this CXCR4 increase was a direct consequence. However, other studies do strongly suggest that FOXP3 can directly bind the *CXCR4* gene and downregulate CXCR4 expression. This study complements what was shown by Douglass and colleagues (Douglass et al., 2014), where FOXP3-overexpressing MDA-MB-231 cells showed a decreased CXCR4 expression. Supporting this, another study also reported a four-fold decrease in CXCR4 after FOXP3 was induced in MCF-7 cells, and showed the co-precipitation of *CXCR4* and FOXP3 in a ChIP assay, indicating their direct interaction (Katoh et al., 2011).

Overall, this chapter highlights the importance of choosing and validating the correct models for your study. Data in this chapter also demonstrate that FOXP3-mediated regulation of CXCR4 occurs very early on, strongly supporting that FOXP3 can directly bind and regulate CXCR4.

5. CO-EXPRESSION OF CXCR7 CAN MODIFY CXCR4'S RESPONSE TO CXCL12 IN BREAST CANCER

5.1. INTRODUCTION

Although CXCR4's role in cancer has been well explored, it was only recently that CXCR7 overexpression was discovered in breast cancer (Miao et al., 2007, Burns et al., 2006). The receptor quickly gained interest partly due to the discovery that CXCR4's antagonist AMD3100 was also a CXCR7 agonist (Kalatskaya et al., 2009), questioning whether the effects of the recently FDA-approved drug could be, to a certain degree, due to the activation of this new receptor. Indeed, several reports suggest both CXCR4 and CXCR7 are implicated in breast cancer progression, with worse patient prognosis correlating with higher expression of the receptors in primary breast cancer tissue (Müller et al., 2001, Miao et al., 2007). This highlights the importance of gaining a better understanding of both their individual involvement and on how they modulate each other's activity - indeed, further to the discovery of CXCR7's new roles, new complexities arose when it was discovered that CXCR4 and CXCR7 could form heterodimers (Sierro et al., 2007, Luker et al., 2009b) that could signal differently to their homodimer counterparts.

Although it was originally believed that CXCR7 was only a scavenging receptor due to its lack of interaction with G-proteins, more recent studies showed that it can signal through non-canonical pathways, in particular via β-arrestin. Multiple studies have examined CXCR7's kinase phosphorylation through β-arrestin, but few have compared the difference in signalling between homodimers and CXCR4 heterodimers, and particularly whether there is a kinetic or spatial difference. Indeed, the few studies that have explored this activation through time produced different results (Kumar et al., 2012, Chen et al., 2015a, Sierro et al., 2007). Whilst receptor desensitisation has been assessed for CXCR4 or CXCR7 homodimers, heterodimers and the possibility to cross-desensitise CXCR4 through CXCR7 has not been explored extensively (Luker et al., 2009b). Cross-desensitisation is a common phenomenon in GPCRs and has been widely reported in chemokine receptors, opening a potential to prevent CXCR4-mediated migration through indirect targeting (O'Boyle et al., 2009). As for its functional consequences, heterodimerisation has been reported to have both a positive and a negative effect in chemotaxis (Décaillot et al., 2011, Mühlethaler-Mottet et al., 2015, Hartmann et al., 2008),

but this has not always been correlated with the activation of calcium flux, one of its main hallmarks (Sierro et al., 2007). With this in mind, this chapter aims to investigate the consequences of CXCR4 and CXCR7 activation (both when forming homodimers and heterodimers) and how signalling, receptor internalisation and migration correlate to each other using a transfected cell model.

5.1.1. Specific aims

- To assess ERK and Akt phosphorylation in CXCR4 and CXCR7 homodimers and heterodimers using Western Blot and cell-based ELISA
- To study receptor internalisation in CXCR4 and CXCR7 homodimers and heterodimers using flow cytometry and determine whether they undergo recycling or degradation after stimulation.
- To investigate whether CXCR4 can be desensitised using a CXCR7 agonist in CXCR4 and CXCR7 heterodimers using flow cytometry.
- To determine CXCL12's chemotactic effect in CXCR4 and CXCR7 homodimers and heterodimers using wound healing assays and assess using flow cytometry whether that corresponds with their calcium flux responses.

5.2. RESULTS

5.2.1. Expression of CXCR4 and CXCR7 in breast cancer cell lines

Previous studies have shown that both CXCR4 and CXCR7 are overexpressed in breast cancer tumours, but co-expression of these two receptors in breast cancer cell lines has been poorly defined. In order to investigate this, CXCR4 and CXCR7 expression was assessed in the cell lines MCF-7, MDA-MB-231, SKBR3 and T47D at both protein and mRNA levels using flow cytometry and qPCR, respectively. As seen in Figure 5-1A, no protein expression for the receptors was observed in any cell line except MCF-7, which expressed CXCR7 at high levels, and T47D, which expressed CXCR7 at low levels - the monocytic THP1 cell line was used as a positive control for CXCR4. Staining was carried out with two PE-conjugated anti-CXCR4 antibodies with similar results (clones 2B11 and 12G5, with only the latter being depicted).

To assess if protein levels extrapolated to transcriptional activity, receptor mRNA values were compared to the breast epithelial cell line MCF-10A as baseline expression. Similarly to what was observed in flow cytometry, there was no receptor expression in neither cell line except MCF-7, which showed high CXCR7 expression – this is depicted in Figure 5-1B. Although expression seems higher in the control cell line MCF-10A than in the breast cancer cell lines, this is due to expression being "undetermined" in many of them, whilst MCF-10A had very low expression (Ct~35). Overall, from the cell lines available none expressed both receptors abundantly and only MCF-7 expressed CXCR7 at sufficient levels.

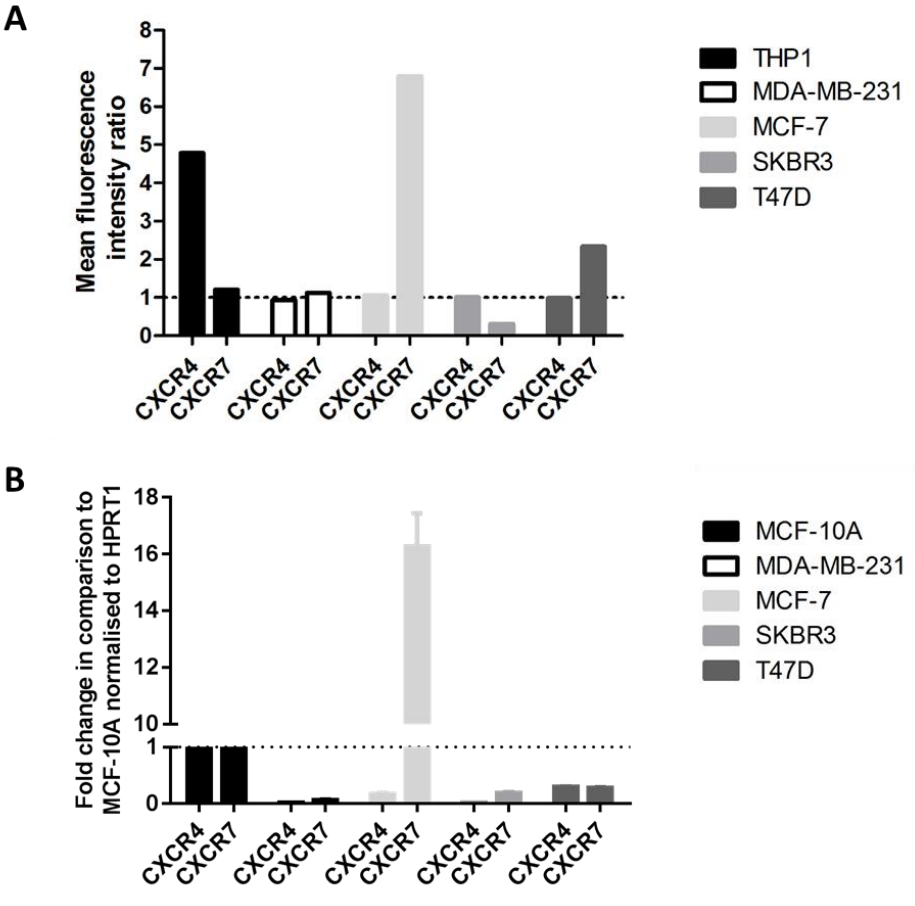

Figure 5-1. CXCR4 and CXCR7 expression of several breast cancer cell lines was assessed using flow cytometry and RT-PCR.
(A) $2x10^5$ cells were double stained with CXCR4-PE antibody (Clone 12G5, R&D) and CXCR7-APC antibody (Clone 11G8, R&D) and analysed in a FACS canto II flow cytometer (Becton Dickinson). Mean fluorescence intensity of the markers was determined using FlowJo software. **(B)** CXCR4 and CXCR7 expression was assessed at RNA level using qPCR and normalised to HPRT1. Expression level was compared to MCF-10A, an immortalised breast epithelial cell line. Error bars represent the fold change of one independent experiment.

5.2.2. Bacterial transformation

Given these results, CHO-CXCR7 and CHO-CXCR7-CXCR7 transfectants were created in order to assess the effect of the receptors in metastasis. The CHO-CXCR4 cell line had previously been generated in the department by Dr. James Harvey and selected using its zeocin resistance (Harvey et al., 2007).

In order to create a CHO-CXCR7 stable cell line, pcDNA3 was chosen as the destination vector as it possessed Neo/Kan resistance, allowing selection in mammary cells using G418. *E.coli* containing CXCR7 cloned into a pCMV-XL5 vector were grown and the plasmid extracted and cut using NotI to confirm its correct size. The uncut plasmid was sent for sequencing (Source bioscience) using the v1.5 forward and XL39 reverse primers flanking the insert. Sequencing results confirmed the correct sequence of CXCR7 (see Figure 5-2A) and revealed an EcoRI restriction site shortly after the NotI

site (see Figure 5-2B). The presence of this restriction site allowed directional cloning using the EcoRI and NotI restriction sites, which would not have been possible with the two NotI sites from the MCS. It was also confirmed that there were no other EcoRI nor NotI restriction targets in the CXCR7 sequence, and thus the insert was cut and extracted as seen in Figure 5-3. Furthermore, the presence of a start codon (ATG, aminoacid 215), an upstream Kozak sequence and a stop codon were confirmed in the sequencing.

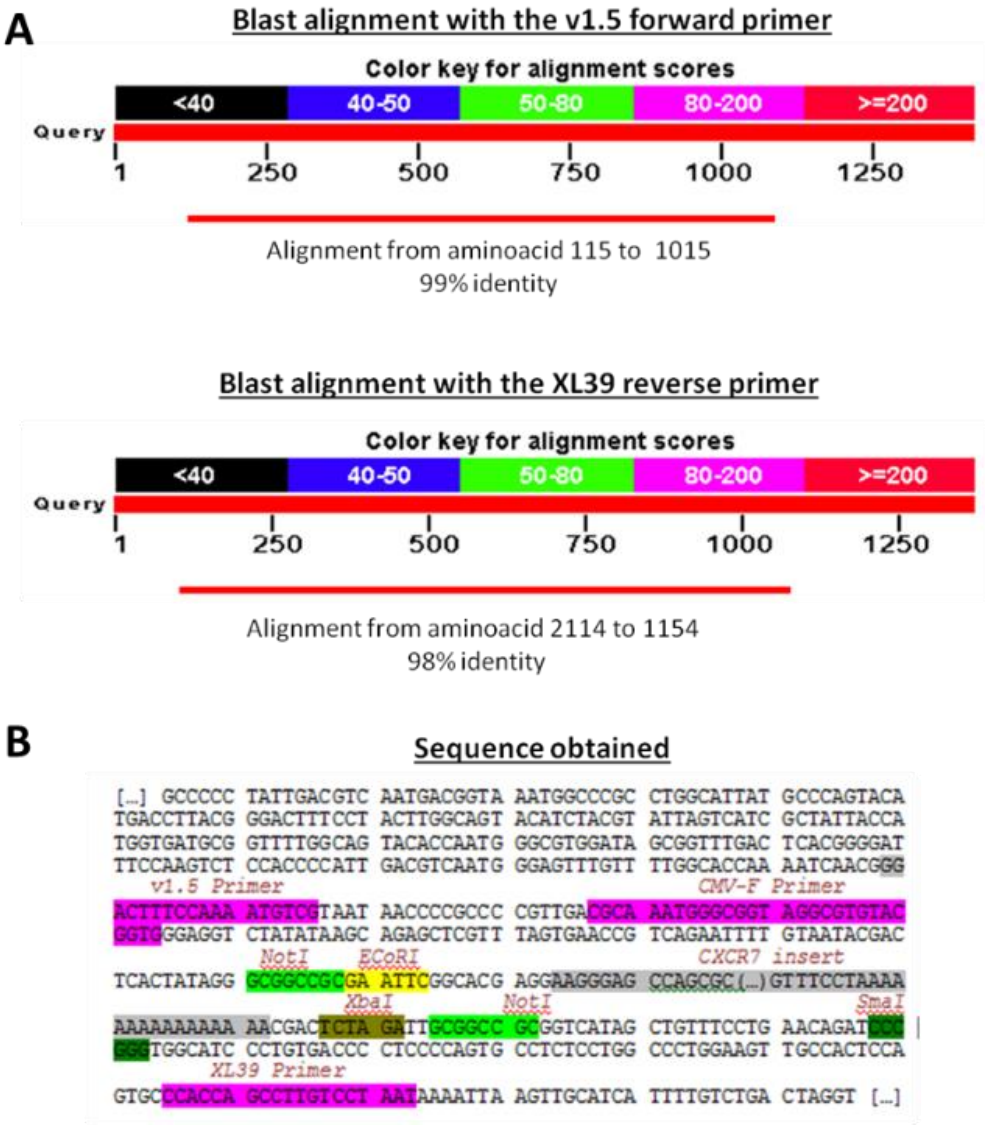

Figure 5-2. The pCMV6-XL5 + CXCR7 plasmid was sequenced to confirm the correct insert sequence and determine which restriction sites were compatible with the pcDNA3's MCS.
(A) BLAST alignment was carried out for the insert's sequence against the CXCR7 mRNA (accession number NM_020311.2), confirming the inserts' homology to CXCR7 when sequenced with both the v1.5 forward primer and the XL39 reverse primer. **(B)** According to the manufacturer's datasheet, the CXCR7 insert had been cloned into the pCMV6-XL5 vector using two NotI sites and thus restriction sites in between were believed to be lost. However, sequencing revealed an EcoRI restriction site was still present after the NotI site. All restriction and primer sites, together with the CXCR7 insert position, have been highlighted.

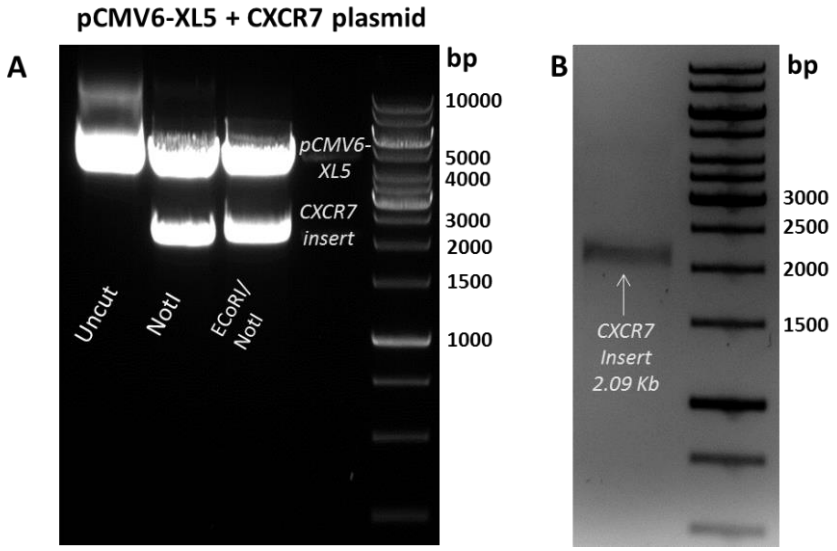

Figure 5-3. Assessing the extraction and restriction of the CXCR7-containing pCMV6-XL5 vector.
(A) Following plasmid extraction from *E.coli* using a QIAgen mini-prep kit (Qiagen), digestion was carried out with both NotI, and EcoRI and NotI restriction enzymes in order to test integrity of the restriction sites. Unrestricted and restricted plasmids were run on a 1% agarose gel together with a 1Kb DNA ladder. The 2.09 Kb band corresponds to the insert, whilst the 4.5 Kb band corresponds to the plasmid. **(B)** The CXCR7 insert restricted with EcoRI/Not I was excised from the gel using a sterile blade and eluted. 3 µl of the isolated insert was run in another agarose gel to confirm its correct extraction.

A similar approach was taken with the pcDNA3 vector – *E.coli* pre-transformed with the plasmid were cultured, and the vector extracted and sequentially restricted using the EcoRI/NotI sites as seen in figure 5-4. Before ligation, 3 µl of the eluted bands were run on an agarose gel to confirm the vector and insert's quality and approximate the relative quantity of the vector in relation to the insert.

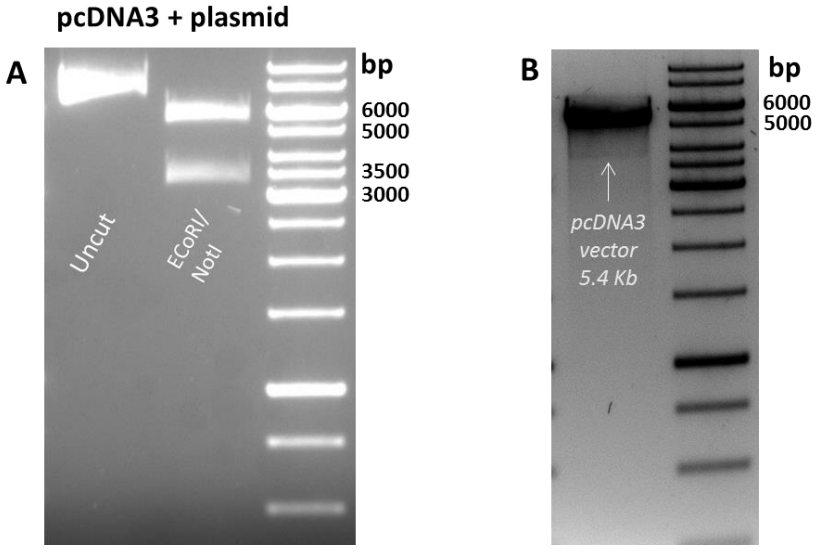

Figure 5-4. Assessing the extraction and restriction of the pcDNA3 vector.
(A) Following plasmid extraction from *E.coli* using a QIAgen mini-prep kit (Qiagen), digestion was carried out with EcoRI and NotI restriction enzymes in order to confirm the presence of the restriction sites and the size of the vector. Restricted plasmids were run on a 1% agarose gel together with a 1Kb DNA ladder. The 5.4 Kb band corresponds to the pcDNA3 vector, whilst the 3.2 Kb band corresponds to an already-present insert. **(B)** The pcDNA3 vector restricted with EcoRI/Not I was excised from the gel using a sterile blade and eluted. 3 µl of the isolated insert was run in another agarose gel to confirm its correct extraction.

Next, CXCR7 insert and pcDNA3 vector were ligated in proportions 1:1, 1:3 and 1:9 for four hours before cloning the plasmid into chemically competent *E.coli*. The next day, two positive colonies had grown in the 1:3 proportion agar plate. Colonies were grown in LB broth overnight and the following day plasmid was isolated and run in an agarose gel as seen in Figure 5-5A. The plasmid from colony 1 was then linearized, revealing a 5.4 Kb band corresponding to the vector and a 2.1 Kb band corresponding with the insert (see Figure 5-5B).

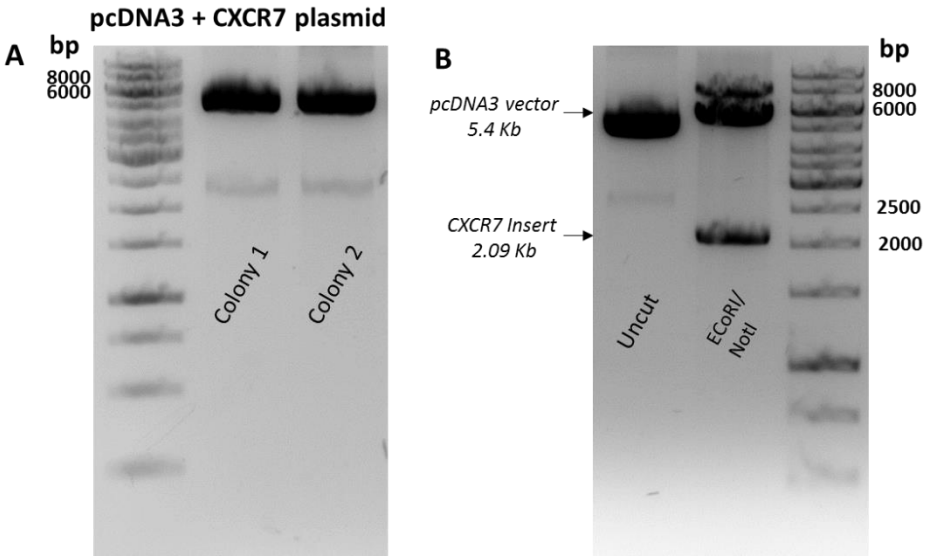

Figure 5-5. Transformation of E.coli with ligated CXCR7-pcDNA3 vector.
(A) Vector and insert were ligated in a proportion 1:3 at 4°C overnight and transformed into chemically competent DH5α E.coli. Briefly, competent E.coli were incubated with 5 µl of the ligation product for 30 minutes on ice and heat shocked for 30 seconds before placing back on ice. Cells were then grown in 1ml of LB for 1 hour at 37°C before spreading 200 µl onto LB agar plates containing ampicillin. After incubating overnight at 37°C, two colonies could be observed. These were grown in 10 ml LB overnight and plasmid was extracted the next day using a QIAgen mini-prep kit and run on a 1% agarose gel. A band of around 7-8 Kb could be observed in both colonies. **(B)** Plasmid from colony 1 was restricted using EcoRI and NotI and run on a 1% agarose gel together with a 1 Kb DNA ladder in order to confirm the size of the vector and insert. A 5.4 Kb and a 2.1 kb bands could be observed, corresponding to the vector and the insert respectively.

To confirm correct cloning, colony 1's plasmid was sent for sequencing (Source bioscience) using the T7F forward and SP6 reverse primers from the pcDNA3 vector. As seen in Figure 5-6, a BLAST revealed the insert had a 99% homology with CXCR7's sequence, with the mismatches being due to the computer not knowing the base pair during sequencing – this is shown as a "N" in the amino acid sequence, representing any nucleotide.

Figure 5-6. Sequencing of the pcDNA3-CXCR7 plasmid to confirm the correct insert sequence.
BLAST alignment was carried out for the insert's sequence against the CXCR7 mRNA (accession number NM_020311.2), confirming the insert's homology to CXCR7 when sequenced with both the T7F forward primer and the SP6 reverse primer from the pcDNA3 vector.

5.2.3. Creation of stable CHO-CXCR4 and CHO-CXCR7 transfectants

Previous to CHO cells' transfection, antibiotic resistance of the wild type CHO was assessed using a killing curve titration. As seen in Figure 5-7, cell death was achieved at all concentrations of zeocin and G418, with quicker results at higher concentrations. Thus, 150 µg/ml of Zeocin and 800 µg/ml of G418 were chosen as the lowest concentration that still achieved quick killing of the untransfected cells.

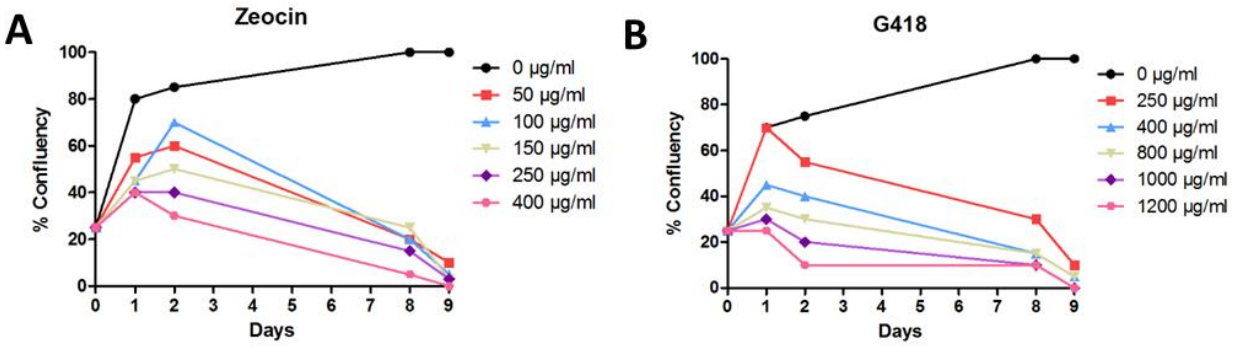

Figure 5-7. Zeocin and G418 killing curve on WT K1-CHO cells.
$4x10^4$ K1-CHO cells were seeded into two 6-well plates and incubated at 37°C overnight until ~30% confluent. The next day, **(A)** zeocin was added in 5 different concentrations ranging from 50µg/ml to 400µg/ml in one plate and **(B)** G418 was added in concentrations ranging from 250µg/ml to 1200µg/ml in the other. Confluency was assessed during 9 days. Results are plotted as mean confluency from one experiment performed in triplicate.

After successful cloning of the pcDNA3-CXCR7 plasmid in *E.coli* and acquisition of high numbers of copies, the plasmid was then transfected into WT CHO cells using Effectene (Qiagen). 31 CHO-CXCR7 colonies were isolated and their CXCR7 levels assessed using flow cytometry by staining the cells with an APC-conjugated anti-CXCR7 antibody, after which 5 colonies were shortlisted given their higher CXCR7 levels: colonies 23, 30, 35, 36 and 38 (see Figure 5-8A). CXCR7 expression in these 5 colonies was also assessed using qPCR and compared to two low-expressing colonies (8 and 9) and MCF-7 cells as seen in Figure 5-8B, with levels that mirrored what had been observed in flow cytometry. Eventually, colonies 23 and 30 were selected given their ability to sustain high CXCR7 expression throughout a 3 month period. Expression was also confirmed using Western Blot and antibody specificity was assessed by using a CXCR7 blocking peptide (ab38088, Abcam) (see Figure 5-8C).

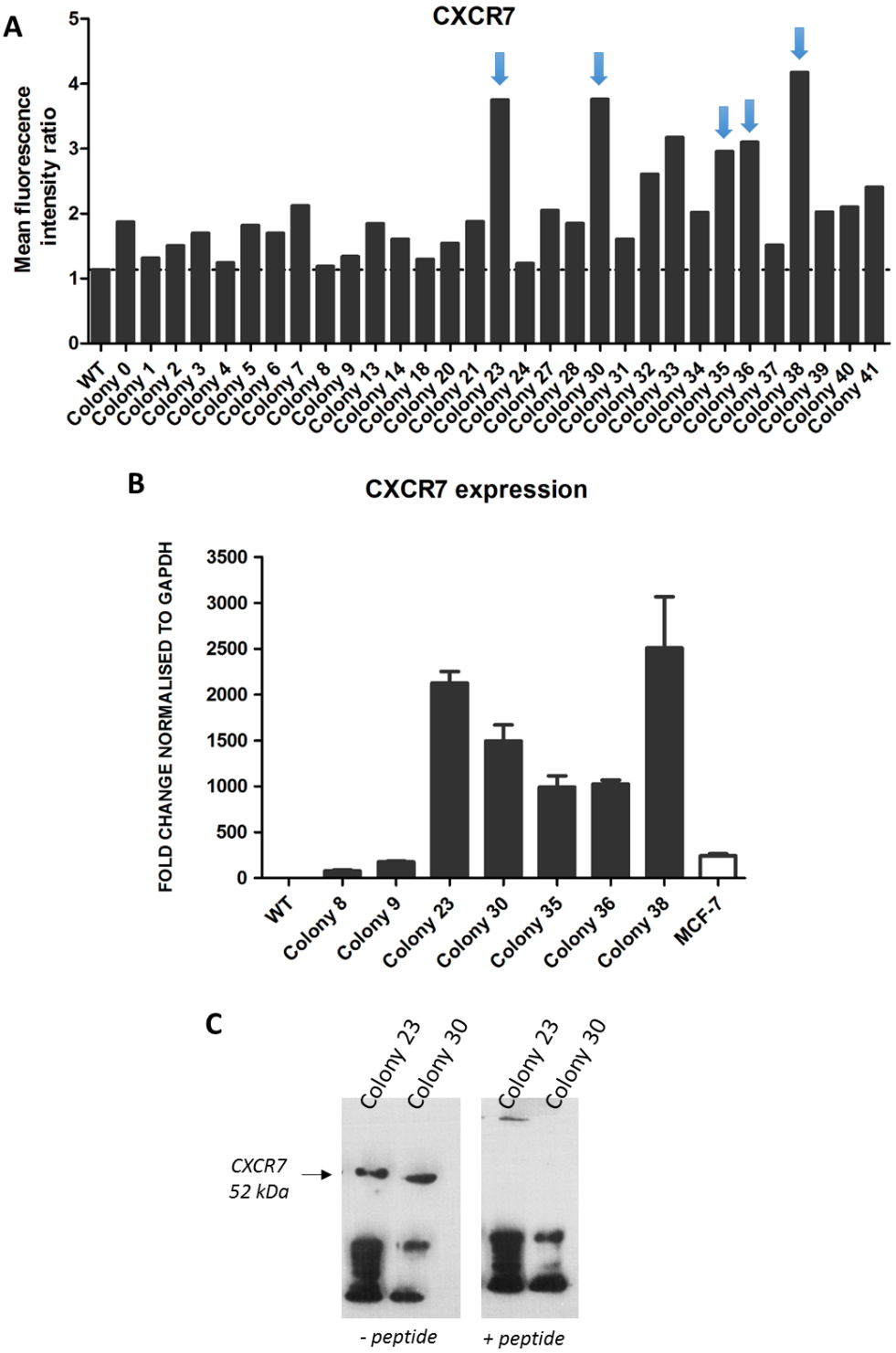

Figure 5-8. Selection of CHO-CXCR7 colonies.
Wild type CHO cells were seeded in 6-well plates and transfected with 2 µg of pcDNA3-CXCR7 using Effectene (Qiagen). The next day, media was replaced with DMEM-F12 containing 800 µg/ml G418 and changed every three days for up to three weeks. Surviving colonies were isolated using cloning rings and expanded. **(A)** Colonies were then stained with CXCR7-APC antibody and analysed in a FACS canto II flow cytometer. Mean fluorescence intensity of the markers was analysed using FlowJo software and higher expressing colonies were selected (n=1). **(B)** CXCR7 expression of five high and two low expressing colonies was assessed at RNA level using qPCR and normalised to GAPDH. Expression level was compared to CHO WT, and MCF-7 were also run for comparison. Data represent the fold change of one independent experiment. **(C)** CXCR7 expression of the two selected colonies was confirmed using Western Blot – a 52 kDa band can be seen in both colonies (left), which disappears when the blocking peptide for the anti-CXCR7 antibody is added (right)

Co-expression of CXCR7 can modify CXCR4's response to CXCL12 in breast cancer

The CHO-CXCR4 cell line created by Dr. James Harvey was recovered from liquid nitrogen and cultured in DMEM media with 150μg/ml of zeocin as described in previous studies (Harvey et al., 2007). In order to assess if the cells maintained CXCR4 expression through time, flow cytometry was carried out by staining the cells with a PE-conjugated anti-CXCR4 antibody. It was then observed that the CHO-CXCR4 cells presented two peaks of CXCR4 expression, indicating the presence of two distinct populations. Furthermore, flow cytometry analysis revealed two populations developing over time in the CHO-CXCR7 colonies, as observed by a bump in the histogram peak (see Figure 5-9A).

In order to remedy this, single cell dilution of the three colonies were carried out and 6 sub-colonies from CHO-CXCR4 and CHO-CXCR7-23 and 8 sub-colonies from CHO-CXCR7-30 were isolated. As seen in Figure 5-9B, receptor expression was assessed using flow cytometry and colonies CHO-CXCR4.2, CHO-CXCR7-23.7 and CHO-CXCR7-30.7 were selected (see histograms in Figure 5-9C).

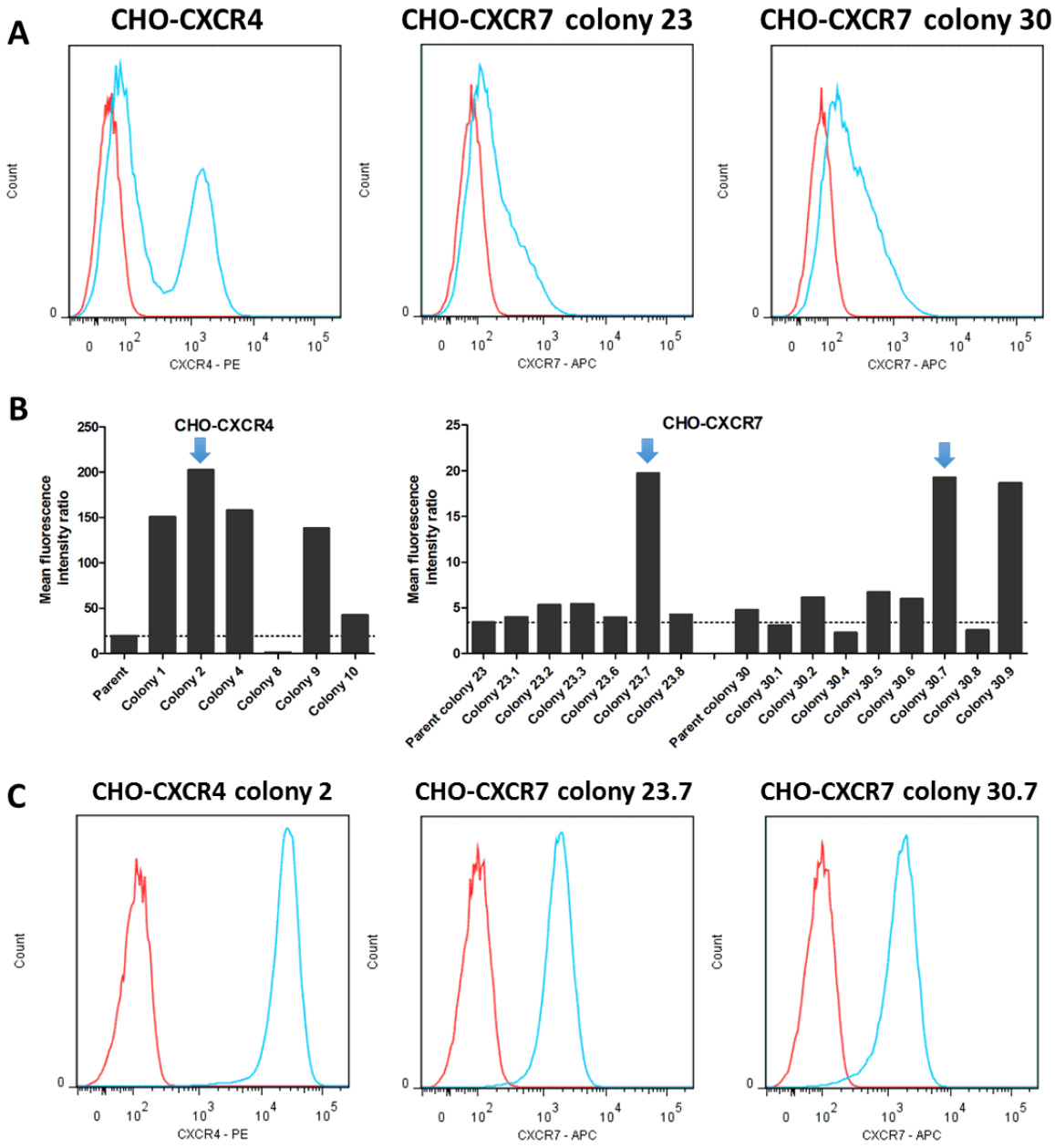

Figure 5-9. Single cell dilution to eliminate multiple populations within CHO-CXCR4 and CHO-CXCR7 colonies. **(A)** Selected CHO-CXCR4 and CHO-CXCR7 colonies presented two populations as seen in flow cytometry histograms. In all graphs the red line represents the isotype control and blue represents the antigen-specific antibody. **(B)** Selected colonies were seeded in a 96 well plate and a serial dilution performed until a single cell was present per well. Cells were allowed to grow and wells with single colonies were expanded. Colonies were then stained with CXCR7-APC or CXCR4-PE antibody and ran in a FACS canto II flow cytometer. Mean fluorescence intensity of the markers was analysed using FlowJo software, and highest expressing colonies were selected (n=1). **(C)** Histograms showing CXCR4 or CXCR7 expression in the final selected colonies.

5.2.4. Creation of transient CHO-CXCR4-CXCR7 transfectants

Simultaneously to the creation of the CHO-CXCR7 transfectants, the pcDNA3-CXCR7 plasmid was also transfected into CHO-CXCR4 cells using Effectene (Qiagen) to create double transfected cells. From the CHO-CXCR4-CXCR7 transfectants, 12 colonies were initially isolated and four colonies were selected given their receptor levels as assessed by flow cytometry (see Figure 5-10A) and qPCR (see Figure 5-10B): colonies 1, 5, 6 and 10. Unfortunately, despite strong G418-resistance selection, CXCR7 expression steadily decreased until it was too low to assess in experiments.

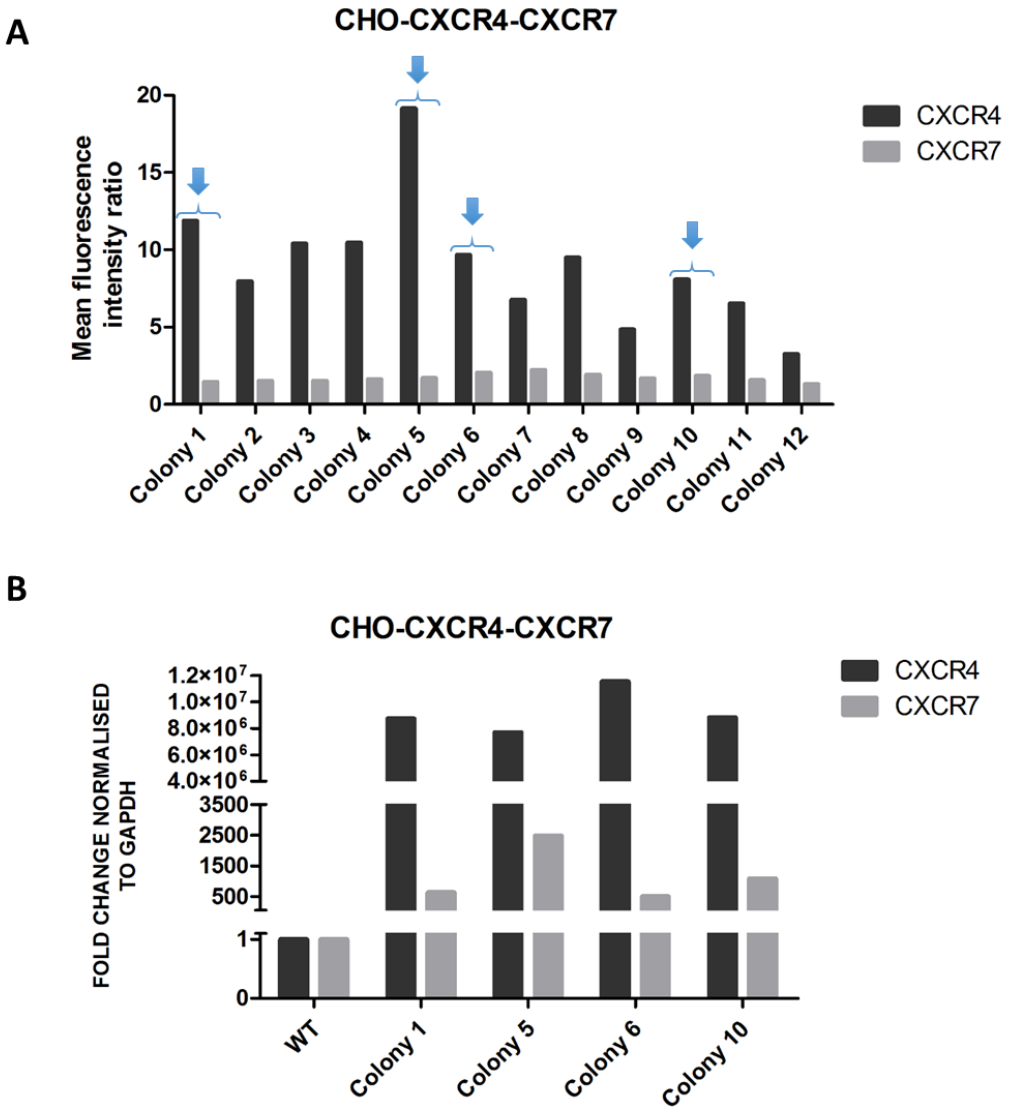

Figure 5-10. Selection of CHO-CXCR4-CXCR7 colonies.
CHO-CXCR4 cells were seeded in 6-well plates and transfected with 2 µg of pcDNA3-CXCR7 using Effectene (Qiagen). Next day, media was replaced with DMEM-F12 containing 800 µg/ml G418 and 150µg/ml Zeocin and changed every three days for up to three weeks. Surviving colonies were isolated using cloning rings and expanded. **(A)** Colonies were then stained with CXCR7-APC and CXCR4-PE antibodies and analysed using a FACS canto II flow cytometer. The mean fluorescence intensity of the markers was analysed using FlowJo software and highest expressing colonies were selected (n=1). **(B)** CXCR4 and CXCR7 expression of the four highest expressing colonies was assessed at RNA level using qPCR and normalised to GAPDH. The level of gene expression was compared to CHO WT cells (n=1).

To overcome this, a transient transfection protocol was optimised using nine different combinations of DNA and Effectene concentrations as determined in Table 2-2. Receptor expression was assessed 24 hours post transfection, which had been previously determined to be the optimal time-point, and treatments G and H were deemed best – those correspond with 2 µg plasmid, 16 µl enhancer and 5 or 12.5 µl of Effectene respectively. As seen in Figure 5-11A, further trials were carried out and treatment G was selected - an example of a successful transfection can be seen in Figure 5-11B.

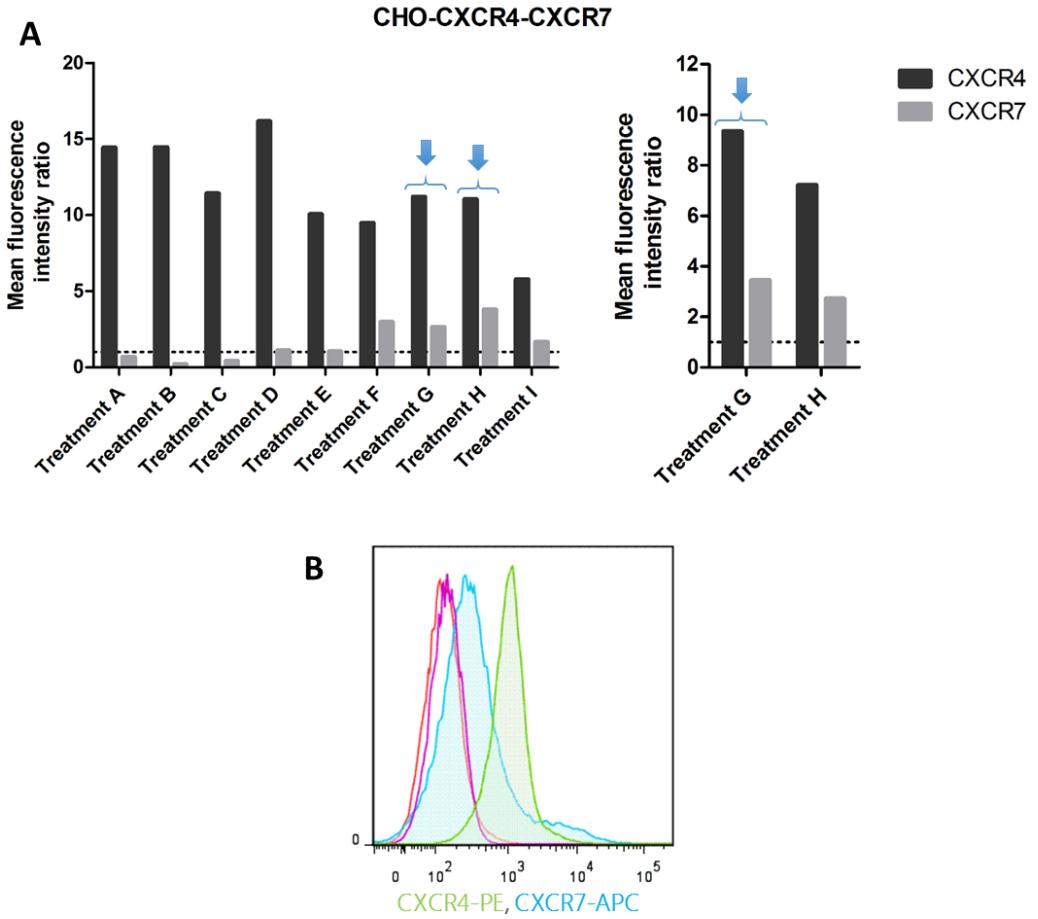

Figure 5-11. Optimisation of transient transfection of CHO-CXCR4 cells with CXCR7.
After CHO-CXCR4-CXCR7 stable transfectants failed to maintain expression throughout passages, CHO-CXCR4 cells were seeded in 6-cm petri dishes and transfection was optimised using different DNA quantities and ratios of DNA to Effectene reagent (see table 5-1). 24 hours later cells were stained with CXCR7-APC and CXCR4-PE antibodies and analysed in a FACS canto II flow cytometer. **(A)** Mean fluorescence intensity of the markers was analysed using FlowJo software and treatments that yielded higher transfection rates were selected (left). Further trial of treatments G and H was carried out to select the best approach (right) (n=1). **(B)** Histograms showing results of a successful transfection of CXCR7 in CHO-CXCR4 cells following treatment G. In the graph the red line indicates the isotype control, the purple line indicates the unstained control, the green line indicates the CXCR4-specific antibody and the blue line indicates the CXCR7-specific antibody.

Thus, CHO-CXCR4.2, CHO-CXCR7-23.7, CHO-CXCR7-30.7 and transient CHO-CXCR4-CXCR7 cells were chosen to carry out the experiments. Expression levels of the new transfectants were compared to the previously assessed breast cancer cell lines using flow cytometry as seen in Figure 5-12.

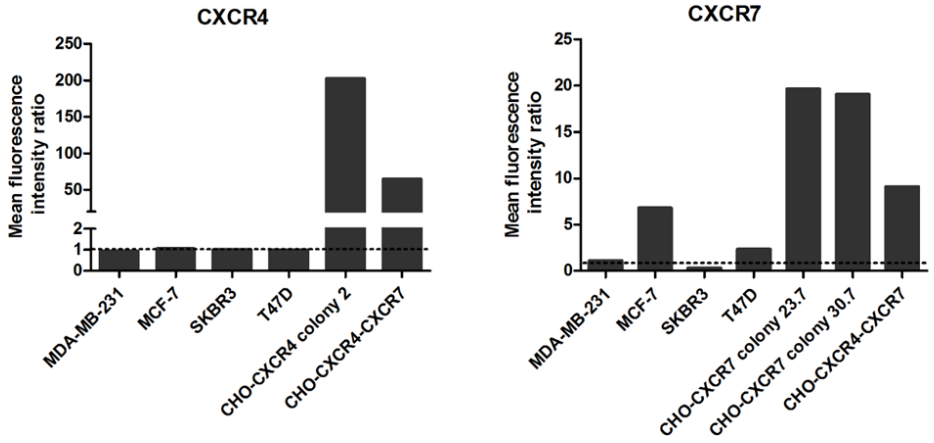

Figure 5-12. CXCR4 and CXCR7 expression in breast cancer cell lines compared to the transfected CHO cells. $2x10^5$ cells were double stained with CXCR4-PE and CXCR7-APC antibodies and analysed in a FACS canto II flow cytometer. Mean fluorescence intensity of the markers was determined using FlowJo software (n=1).

5.2.5. Characterisation of transfectant MDA-MB-231 cells

In order to corroborate the results observed with our transfectant CHO cells, MDA-MB-231 cells expressing CXCR4 and/or CXCR7 were obtained from Dr. Luker. The single transfectant cells had been transfected with a β-arrestin/mCherry vector and a CXCR4 or CXCR7/mTagBFP vector using lentiviral approaches and then selected through fluorescence. As seen in figure 5-13A, mCherry's red fluorescence could be observed in cultured live cells, but fluorescence absorption by the T-75 flask meant blue fluorescence could only be observed after fixing cells in a slide. It is important to note that in the construct used, receptor and fluorescent marker are not bound together, and thus the presence of the fluorescent marker indicates the receptor has been translated but does not pinpoint its location. To further confirm receptor expression, surface staining of CXCR4 or CXCR7 was carried out using flow cytometry, but little expression was observed.

MDA-MB-231 cells expressing both receptors were also gifted by Dr. Luker. These cells have no fluorescent markers, so receptor expression was solely assessed using flow cytometry. Unfortunately, as seen in figure 5-13B, no surface staining for either receptor could be observed. Culture with selection antibiotics improved staining for MDA-CXCR4 and MDA-CXCR7 enough to carry out internalisation assays, but expression in the MDA-CXCR4-CXCR7 cell line remained low.

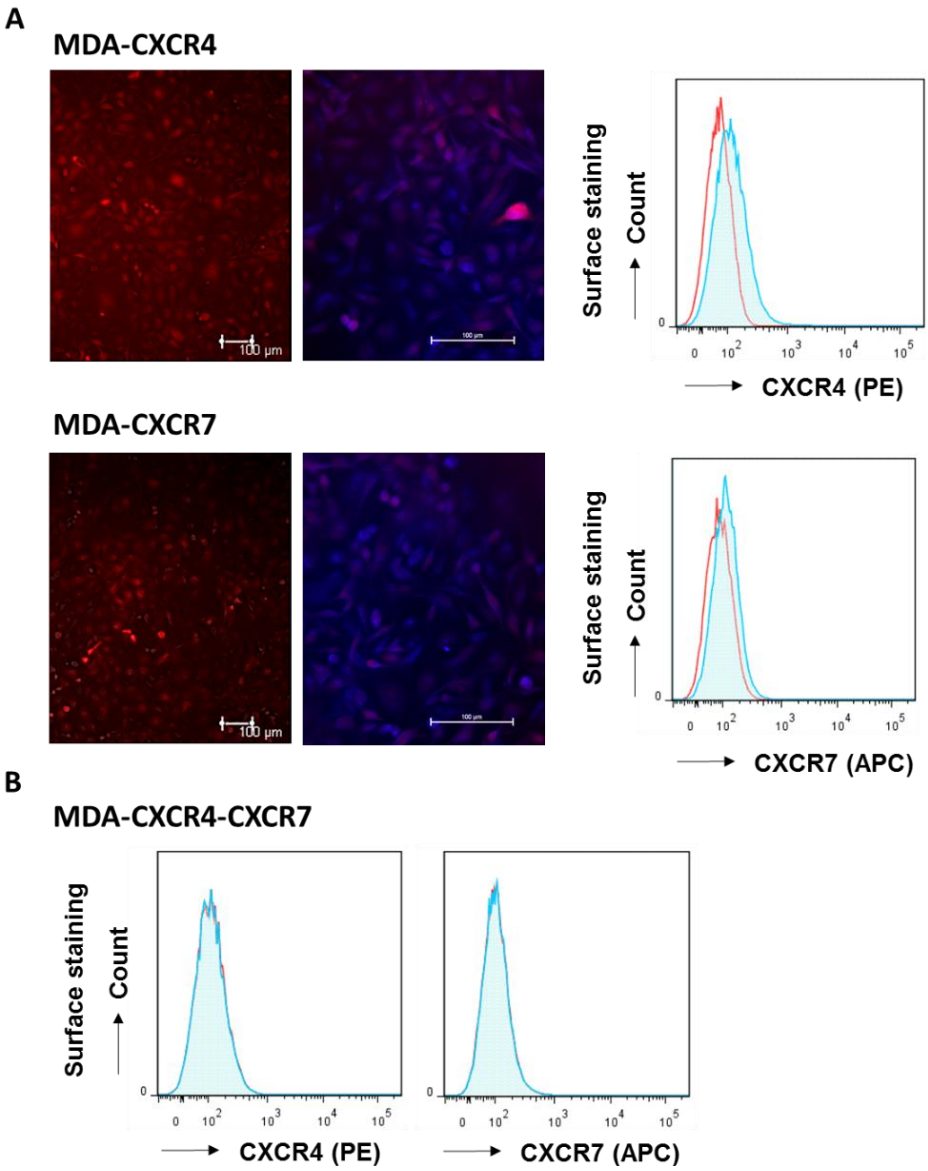

Figure 5-13. Assessment of CXCR4 and/or CXCR7 expression in transfected MDA-MB-231 cells.
(A) MDA-CXCR4 and MDA-CXCR7 cells were transfected by Dr. Luker using Clontech's lentiviral vector pLVX Ef1α IRES containing CXCR7 or CXCR4 and mTagBFP as transduction marker and pLVX Ef1α IRES containing β-arrestin and mCherry as transduction marker. (Left) Observation using a Leica fluorescent microscope allowed the visualisation of the mCherry marker, but not mTagBFP, in cells cultured in a T-75 flask. (Middle) Visualisation of 4% PFA-fixed cells in 8-well chamber slides using a Nikon fluorescent microscope allowed for the visualisation of both the mCherry and the mTagBFP markers. (Right) Receptor expression was also assessed by labelling cells with CXCR4-PE or CXCR7-APC antibodies and analysing using a FACS canto II flow cytometer. **(B)** The double transfectant MDA-MB-231 cell line was cloned using the lentiviral vector FUW, which does not express any fluorescent markers. Receptor expression was assessed by labelling cells with CXCR4-PE and CXCR7-APC antibodies and analysing using a FACS canto II flow cytometer, but no expression was seen. Red histograms represent the isotype control and blue histograms represent the antigen specific antibody.

In order to assess whether cells were expressing only low levels of the receptor or whether it was internalised, cells were fixed and permeabilised before being stained and analysed in a flow cytometer. As seen in Figure 5-14, MDA-CXCR4 and MDA-CXCR7 indeed expressed high levels of the receptor, whilst MDA-CXCR4-CXCR7 cells expressed small, but present, levels of both receptors.

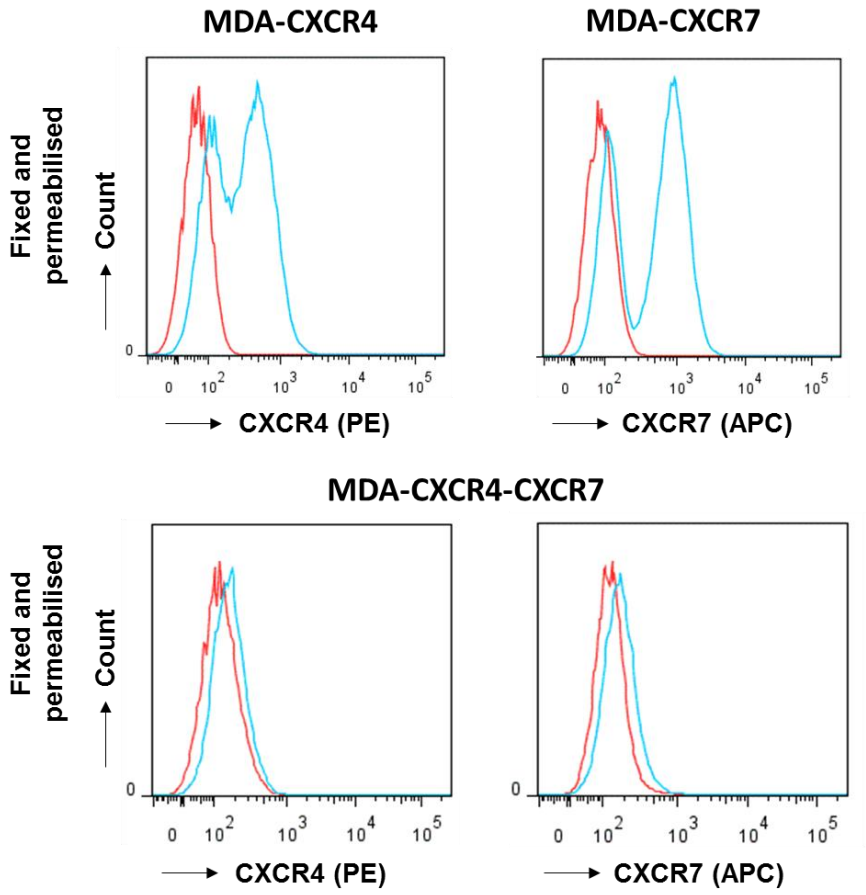

Figure 5-14. Assessment of total CXCR4 and/or CXCR7 expression in transfected MDA-MB-231 cells. 300,000 cells were fixed with 4% PFA and permeabilised with permeabilisation buffer before staining with CXCR4-PE and CXCR7-APC antibodies. Receptor expression was measured by flow cytometry. Red histograms show isotype control staining and blue histograms show staining with the antigen-specific antibody.

To further corroborate this, CXCR4 and CXCR7 mRNA levels were assessed using qPCR. As shown in Figure 5-15, in comparison to the MDA-MB-231 WT the corresponding receptors were upregulated almost 30-fold in the single transfectants and 10 to 20-fold in the double transfectants, indicating that CXCR4 and CXCR7 were being transcribed.

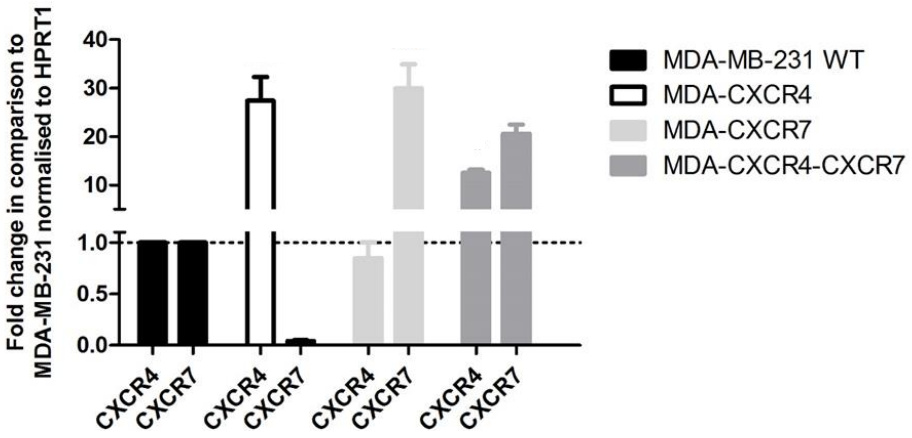

Figure 5-15. CXCR4 and CXCR7 RNA expression in MDA-MB-231 transfectant cells was assessed using qPCR. CXCR4 and CXCR7 expression in trasnsfected versus untransfected MDA-MB-231 cells was assessed at RNA level using Taqman probes. Expression level was normalised to HPRT1, and data represent the fold change of one independent experiment.

After confirming the presence of the receptor at protein and RNA level, attempts to bring it back to the surface were carried out by serum starving the cells for different time periods and assessing receptor presence using flow cytometry. As seen in Figure 5-16, serum starvation made no difference in the receptor expression of either MDA-CXCR4 or MDA-CXCR7 cells at any time point. Given these results, and the lack of a double transfect expressing both receptors at high levels to compare to, tranfectant CHO cells were chosen to carry out the bulk of the experiments.

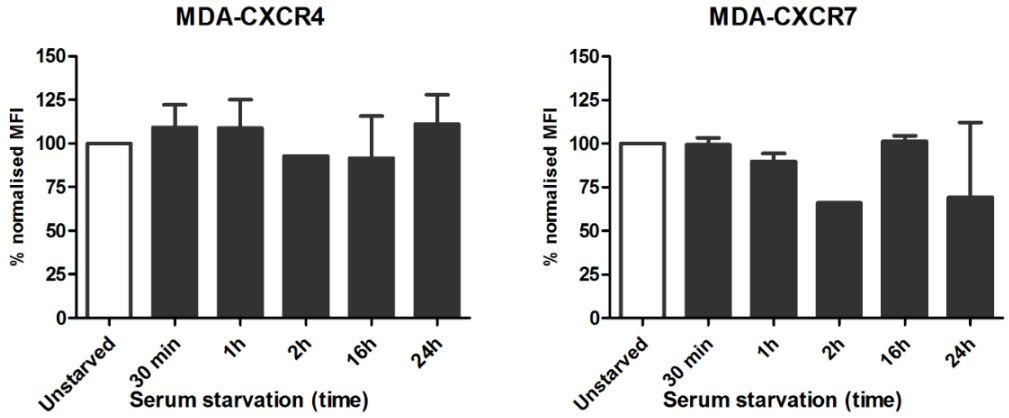

Figure 5-16. Serum starvation does not significantly affect surface receptor expression in transfected MDA-MB-231 cells.
MDA-CXCR4 and MDA-CXCR7 cells were serum starved for a spectrum of times ranging from 30 minutes to 24 hours before staining with CXCR4-PE and CXCR7-APC antibodies. Receptor expression was then measured using flow cytometry. Data represent the mean fluorescence intensity ± SEM of two independent experiments.

5.2.6. Optimisation of flow cytometry staining

Due to lack of positive control cell line for CXCR7, optimisation of antibody staining was carried out after the creation of the CHO-CXCR7 transfectants.

5.2.6.1. *Staining time*

Staining was first carried out for 30 minutes at room temperature as per manufacturer's instructions, but had to be changed to 4°C to prevent receptor internalisation. This considerably reduced the antibodies' staining as seen in Figure 5-17, and thus staining time was increased to 1.5h on ice.

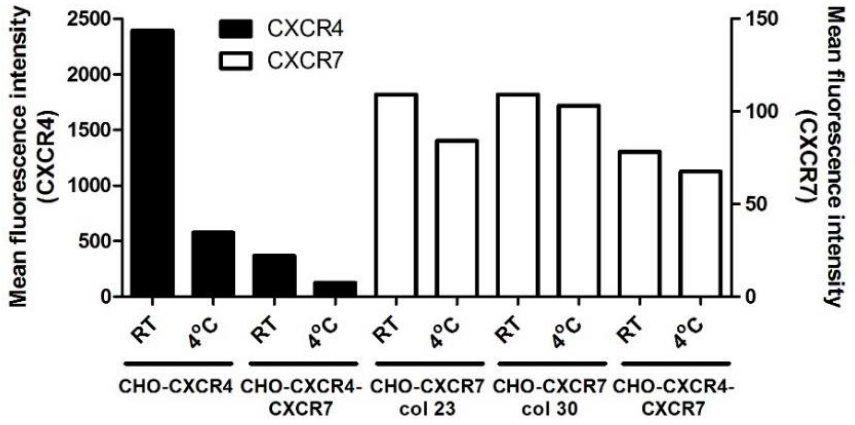

Figure 5-17. CXCR4 and CXCR7's mean fluorescence intensity after staining for 30 minutes at room temperature (RT) or on ice (4°C). Values of the four transfectant cell lines are shown (n=1).

5.2.6.2. *Antibody concentration*

In order to determine optimal antibody concentration, $2x10^5$ cells were resuspended in 50 µl of FACS buffer and a saturation curve was plotted. As seen in Figure 5-18, 5 µl of CXCR4 and 7.5 µl of CXCR7 antibodies were chosen to carry out the staining.

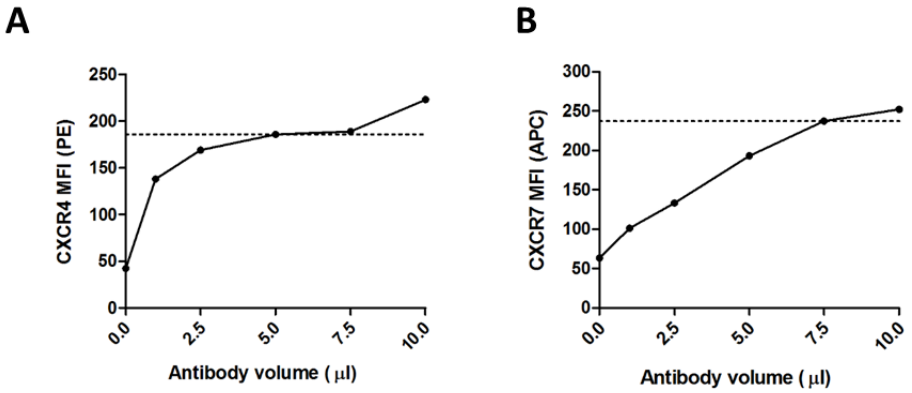

Figure 5-18. Antibody saturation curves for flow cytometry.
$2x10^5$ cells were stained in 50 µl of FACS buffer in order to optimise antibody concentration. Saturating antibody volume was defined as a volume at which subsequent increases of antibody caused less than 10% increase in the mean fluorescence intensity (MFI). This is represented in the graph as a dotted line. CXCR4 PE **(A)** and CXCR7 APC **(B)** antibody saturating curves are shown (n=1).

5.2.6.3. *Gating strategy*

Accurately gating the desired cell populations is a key step in the correct analysis of the data acquired using a flow cytometer. First, dead cells and debris need to be excluded. Whilst acquiring data with the cytometer, these cells can be readily identified as they will cluster in the lower left corner of the FSC/SSC scatter plot, indicating small size and complexity. A tell-tale sign is that they will remain in that corner even if the voltages of the FSC and SSC are increased. These cells can then be eliminated by setting a threshold, usually at a FSC value of around 25,000-40,000. Dying cells, however, are sometimes more difficult to separate by FSC and SSC alone. In those cases, a viability dye such as DAPI can be added - cells with a non-intact membrane, such as dying cells, will take up the dye and be positive in the violet laser (405 450/50) as seen in Figure 5-19A. Negative cells can then be gated as "live cells".

Another common occurrence, especially with cells that form very tight cell to cell junctions or secrete collagen, is the presence of doublets or even bigger cell conglomerates. These cells present as a second population which has double the size scatter and granularity to the main one, but they are hard to gate from the FSC/SSC plot alone. However, doublets present double height (H) or width (W) as compared to a single cell, and thus can be gated out by using the FSC-H or the SSC-W as seen in Figure 5-19B. This step is key as doublets will have double the fluorescence as single cells, incorrectly skewing the data.

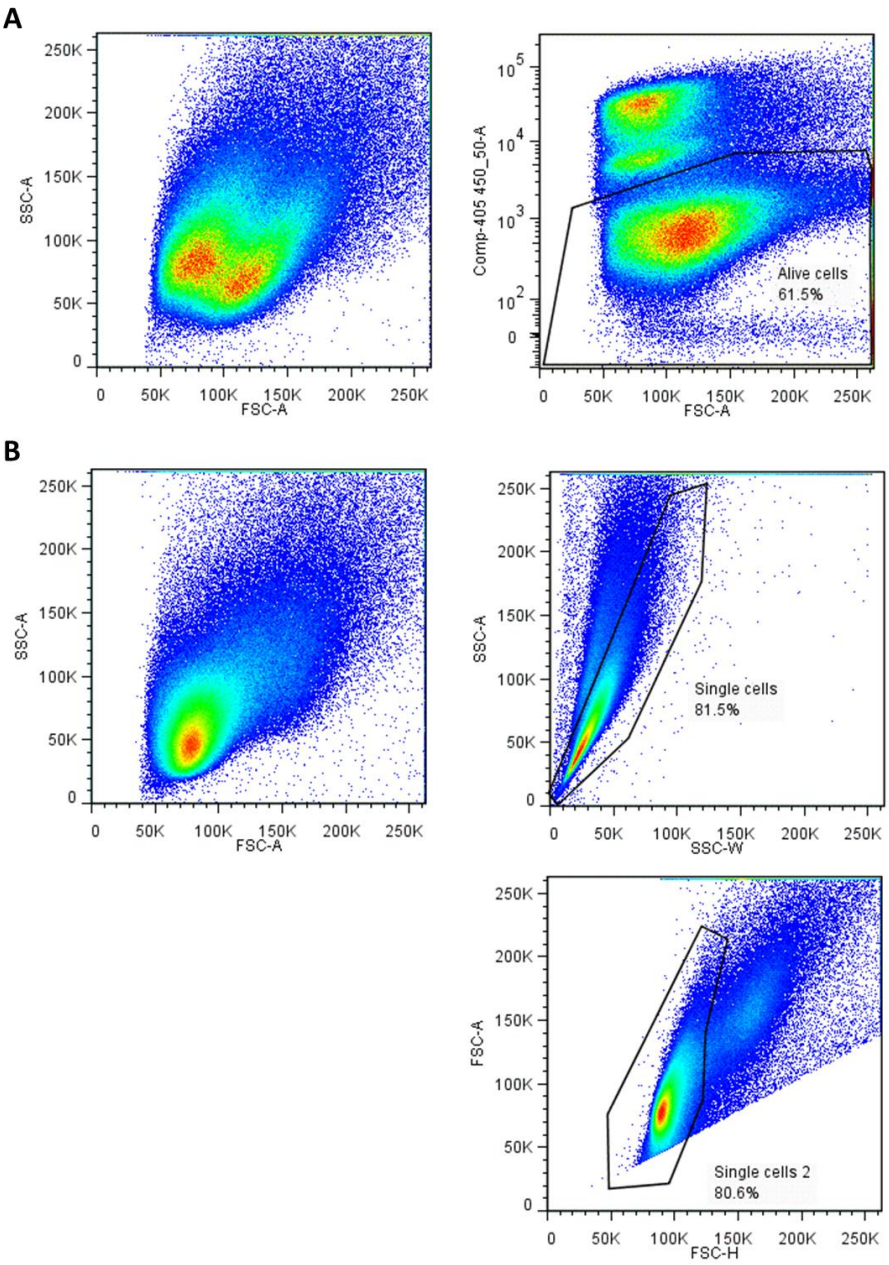

Figure 5-19. Gating strategy used in flow cytometry.
(A) Most dead cells and debris have a very small FSC and SSC signal and can be easily gated out by placing a threshold in the FSC at around 35,000 when collecting the samples. However sometimes dying but mostly intact cells create a second population that merges with alive cells as seen in the top left scatter plot. In order to gate the dying cells out, a life/dead stain such as DAPI can be added. Dying cells will absorb the dye through the pores on their membrane and appear positive in the violet laser (405 450/50) and thus can be easily gated out (top right). **(B)** Cell doublets should also be gated out as their double fluorescence intensity will give a false positive result. In a FSC/SSC scatter plot, this population appears diagonally on top of the main population, but gating can prove difficult (middle left). In order to do this, the SSC area (SSC-A) can be plotted against the SSC width (SSC-W) (middle right) and the FSC area (FSC-A) can be plotted against FSC height (FSC-H) (bottom right). Cells with the same area but double width or height can be gated out.

5.2.6.4. *Antigen binding capacity*

In order to compare the expression levels of CXCR4 and CXCR7, antigen binding capacity was assessed using beads. Briefly, fluorescence intensity depends on the number of bound antibodies, but is also influenced by the brightness of the fluorophore and the machine settings. In order to normalise these parameters, beads with a known number of binding sites are used to correlate a mean fluorescence value with a bound antibody number – a standard curve can then be plotted as seen in Figure 5-20A and B. CXCR4 and CXCR7 mean fluorescence can then be converted to Antigen Binding Capacity (ABC) and plotted in a comparable manner (see Figure 5-20C).

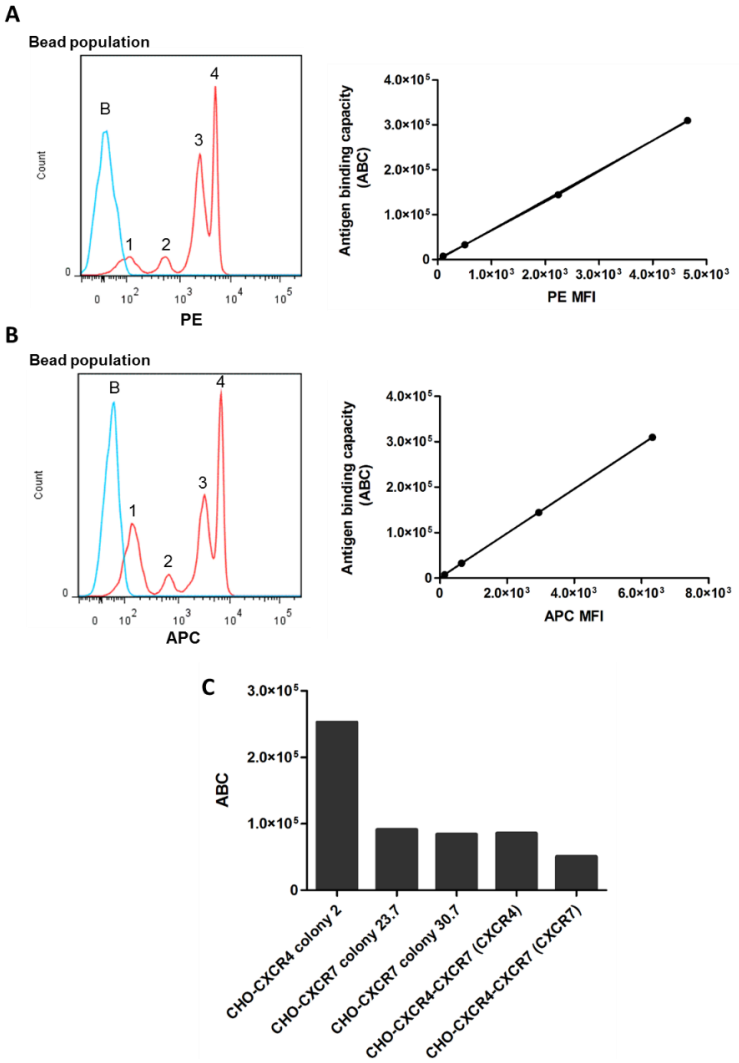

Figure 5-20. Determination of the Antigen Binding Capacity (ABC) using Quantum Simply Cellular (QSC) microspheres.
5 bead populations (1 blank and 4 with a known, increasing number of surface binding sites) were incubated with saturating concentrations of CXCR4 PE **(A)** or CXCR7 PE **(B)** antibodies and analysed using the same FACS II flow cytometer and instrument settings (e.g. PMT voltage) as the samples. MFI was analysed using FlowJo and using the template provided by Bangs Laboratories Inc, a linear regression was created. **(C)** This standard curve was used to convert the MFI of the samples to its ABC value, which should indicate the number of surface receptors present on the surface of the cell (n=1).

However, it is important to note that this assay will not account for how good the antibody is in binding the correct epitope in our cells, as it is the Fc region that binds the beads. Thus, comparisons between receptors must always bear this in mind.

5.2.7. Monitoring heterodimers using FRET

In order to assess whether CXCR4 and CXCR7 were forming heterodimers in the CHO-CXCR4-CXCR7 cells, FRET assays were carried out using a FACS Canto II. When FRET occurs, the fluorescence from the donor (PE) diminishes in the 488 585/42 channel and it transfers to the FRET channel (488 660/20) as seen in Figure 5-21A. To assess the change, electronic compensation was necessary to correct the spectral overlap between the PE and FRET channels (see Table 5-1). In order to assign a numerical value to this phenomena, FRET was assessed as the ratio between APC's mean fluorescence intensity (MFI) on its own and its lower MFI when FRET occurs (see Figure 5-21B). MHC class I was used as a negative FRET control as CXCR4 and MHC class I do not form dimers.

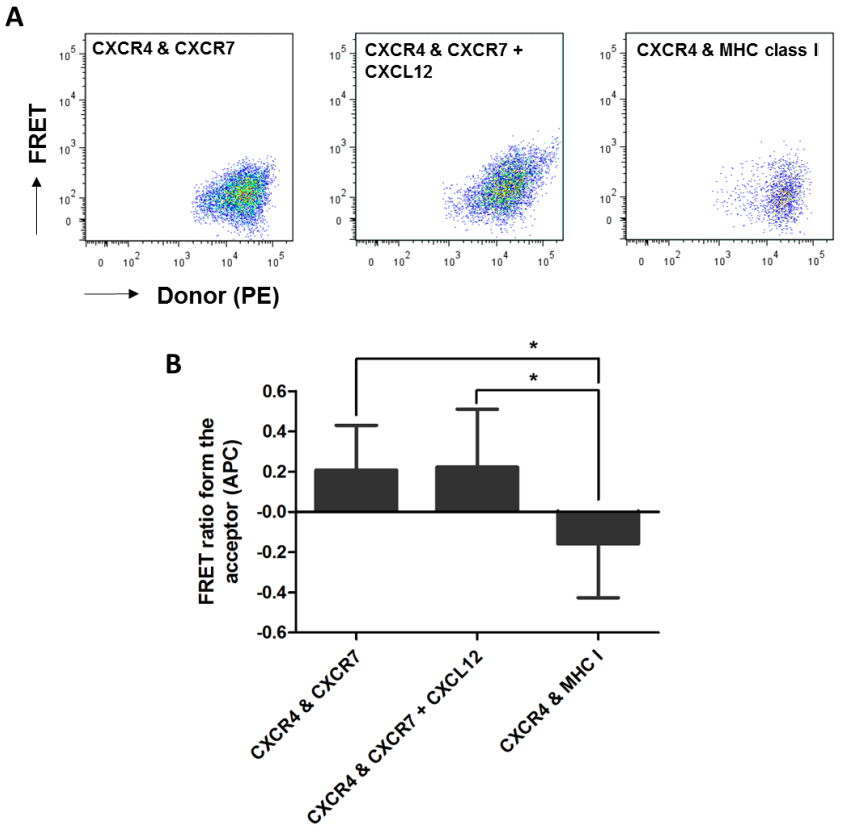

Figure 5-21. Determining heterodimer formation through fluorescence resonance energy transfer (FRET). 500,000 CHO-CXCR4-CXCR7 cells were stained with saturating concentration of CXCR4 and CXCR7 antibodies or with CXCR4 and MHC class I antibodies as a negative control. FRET was assessed with and without 10nM CXCL12 stimulation. **(A)** When FRET takes place, the MFI from PE (the donor fluorochrom) diminishes as the FRET MFI increases. In the negative control, no increase in the FRET MFI should occur. **(B)** This was quantified through the FRET ratio from APC (the acceptor fluorochrom). When FRET occurs, the APC ratio increases as the APC MFI increases. Data represent the mean ± SEM of three independent experiments and statistical significance was calculated using a one way ANOVA (*p<0.05).

	PE	***FRET***	***APC***	***DAPI***
PE	-	2.1%	0%	0%
FRET	0%	-	0%	0%
APC	0%	0%	-	
DAPI	0%	0%	0%	-

Table 5-1. Compensation matrix used in the FRET assay. Top row indicates the fluorochrome and left column indicates the detector.

5.2.8. p-ERK and p-Akt activation in CHO-CXCR4, CHO-CXCR7 and CHO-CXCR4-CXCR7 cells after CXCL12 stimulation

Since CXCR7 was linked to cancer malignancy, some studies have proposed it plays a role in metastasis and survival through the MAPK/Erk pathway (Wang et al., 2008b, Miao et al., 2007) - in particular, it has been suggested that the bound β-arrestin can become a scaffold for several kinases including ERK and Akt. Furthermore, when CXCR4 and CXCR7 form heterodimers conformational changes take place, which could affect the CXCR4/$G_{\alpha 1}$ interaction and thus the signalling response (Levoye et al., 2009). However, how the activation of these pathways may vary through time is still poorly understood.

Given this, we decided to investigate the effects that CXCL12 stimulation would have in the transfected CHO cells. $5x10^5$ cells were serum starved and treated with 10nM CXCL12 for several time points, and p-ERK and p-Akt activation was assessed using western blotting. The p-ERK results were then confirmed using a Phospho-ERK1 (T202/Y204)/ERK2 (T185/Y187) Cell-Based ELISA (R&D systems).

As seen in Figures 5-22 and 5-23, in both western blot and cell-based ELISA CHO-CXCR4 cells presented an early p-ERK activation that could be seen at 5 and 15 minutes but that had disappeared at 2 hours. A similar pattern could be seen in western blotting for p-Akt, with strong bands at 5 and 15 minutes that were greatly reduced at 120 minutes. Conversely, a continuous activation for both p-ERK and p-Akt could be observed for up to 2 hours in both CHO-CXCR7 colonies 23.7 and 30.7. These results were confirmed for p-ERK in the cell-based ELISA. Interestingly, similarly to CHO-CXCR4, CHO-CXCR4-CXCR7 cells presented an intense ERK phosphorylation at 5 minutes that had disappeared at 2 hours in both western blot and cell-based ELISA; but displayed a constant p-AKT activation throughout two hours mirroring CHO-CXCR7 cells' phosphorylation.

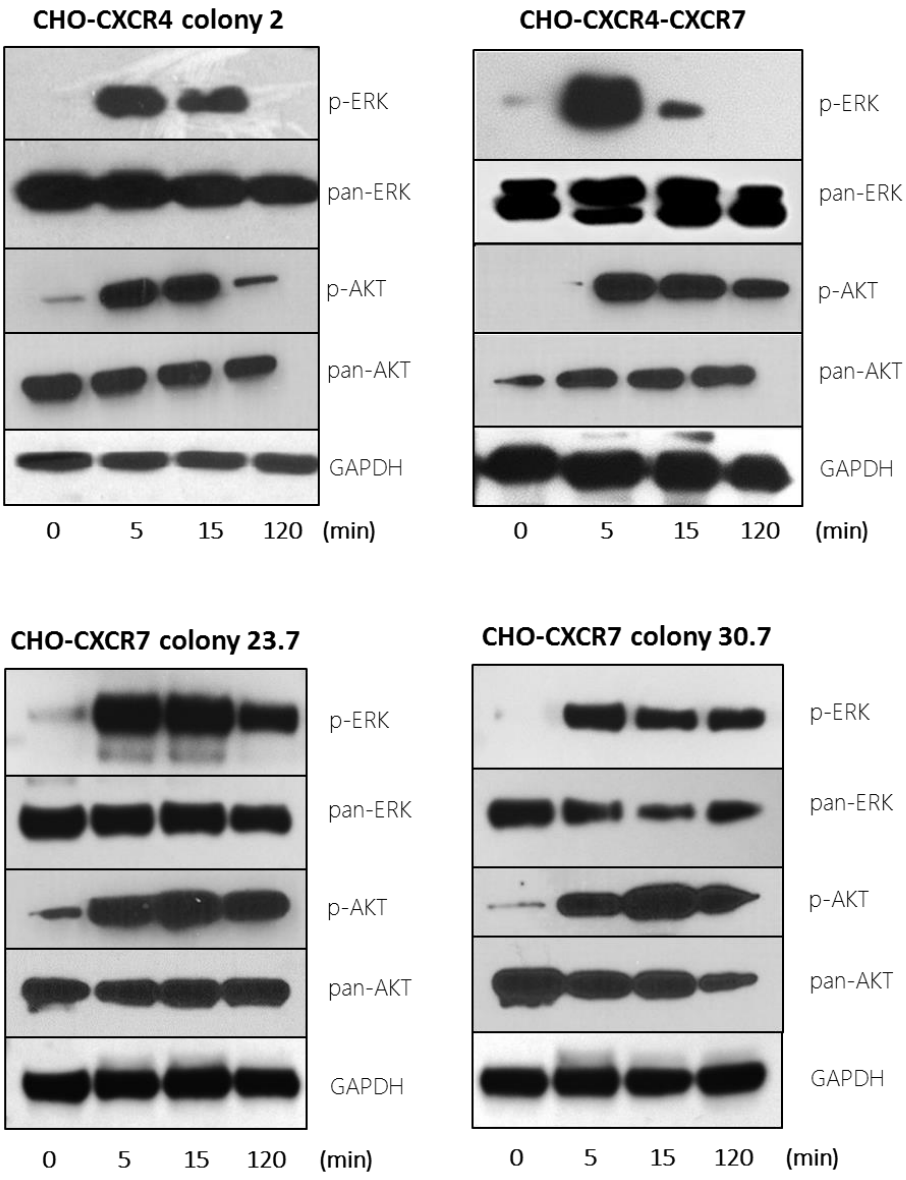

Figure 5-22. Western blot shows that CXCL12 treatment of transfected CHO cells differentially activates the ERK and Akt pathways.
Serum starved CHO-CXCR4, CHO-CXCR7 and CHO-CXCR4-CXCR7 cells were stimulated with 10 nM CXCL12 for 5, 15 and 120 minutes followed by cell lysis and western blotting using a p-ERK antibody or a p-AKT antibody (Cell Signalling). The membrane was then stripped and reprobed for pan-ERK or pan-AKT and GAPDH as a loading control. Images are representative of three independent experiments.

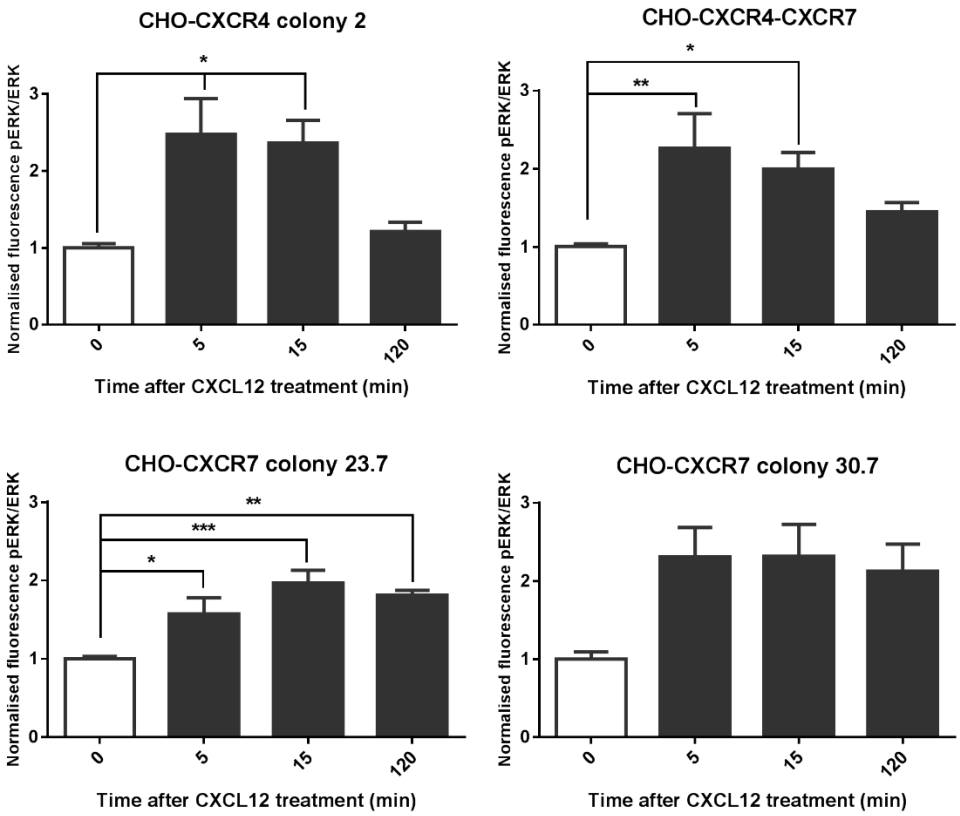

Figure 5-23. Cell-based ELISA shows CXCL12 treatment of transfected CHO cells differentially activates the ERK pathway.
Adherent transfected CHO cells were stimulated with 10 nM CXCL12 for 5, 15 and 120 minutes and then fixated with methanol. A cell-based ELISA was performed as per protocol using p-ERK and total-ERK antibodies and fluorescence intensity was read at 600 and 450 nm. Data represent the mean ± SEM of three independent experiments and statistical significance was calculated using a one way ANOVA (*p<0.05, **p<0.01, ***p<0.001).

5.2.9. Monitoring of receptor internalisation using ImageStream

To investigate whether this difference in signalling was due to receptor internalisation, cells were stained with CXCR4-PE or CXCR7-APC antibodies and analysed using the Amnis ImageStream^X Flow Cytometer. Unlike conventional flow cytometers, the staining's location in the single cell can be observed, making it ideal for assessing receptor internalisation after a 30 minute treatment with CXCL12. As cells were not fixed and permeabilised, CXCR4-PE staining will only monitor the internalisation of the receptor that was originally on the surface.

As observed in Figure 5-24, internalisation was observed in both CHO-CXCR7 colonies albeit at lower levels than those presented by CHO-CXCR4 (see Figure 5-25), correlating with the longer kinases' activation. We thus hypothesised that this lower internalisation level could be due to (A) diminished internalisation (for instance, if not all receptors internalise after CXCL12 binding; or if the ligand binds only some CXCR7 receptors) or (B) after internalisation, the receptor gets back to the surface within 30 minutes.

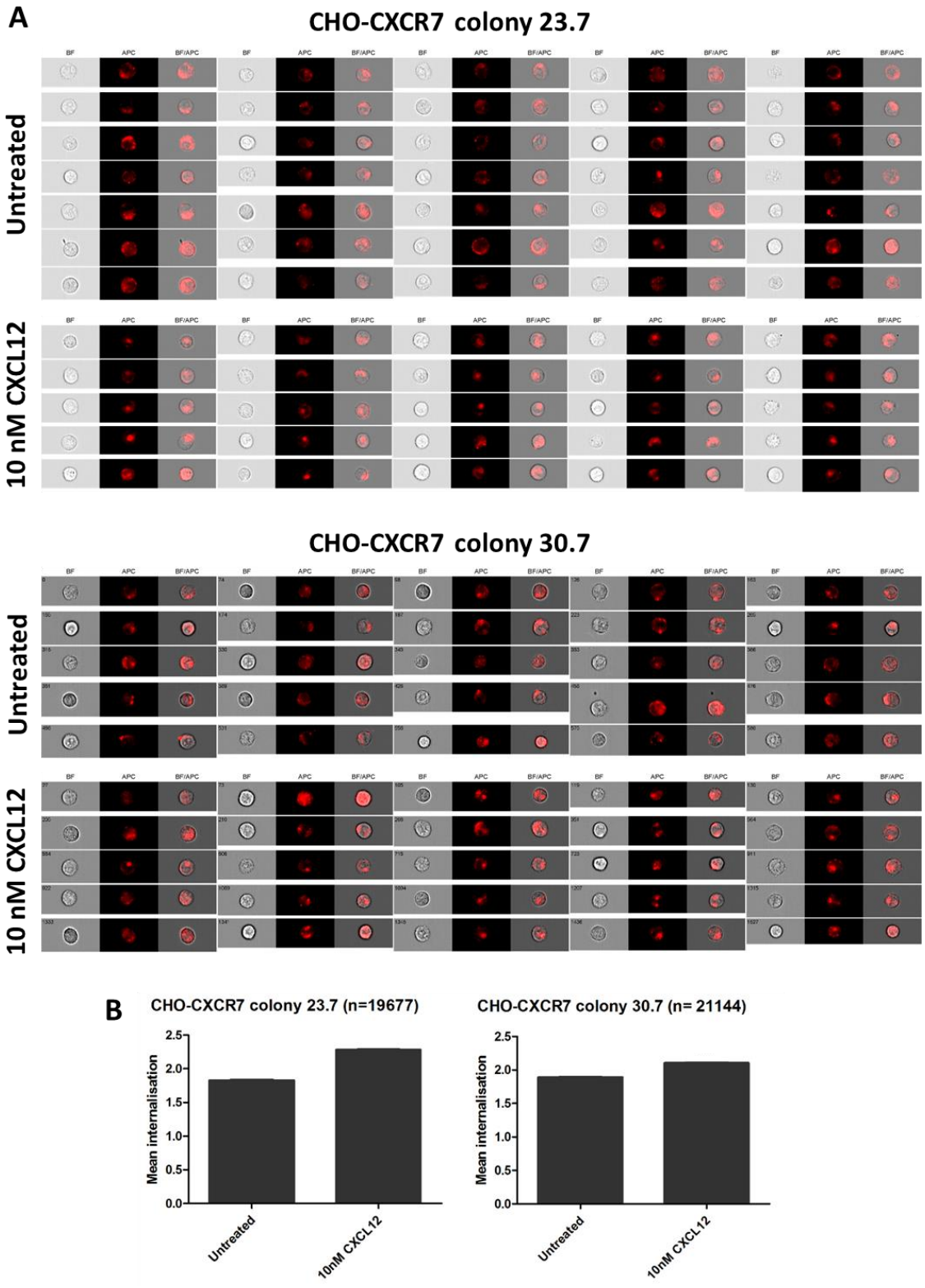

Figure 5-24 Quantification of receptor internalisation in CHO-CXCR7 colonies 23.7 and 30.7 using IMAGEstream.

2 million CHO-CXCR7 cells were treated with 10 nM CXCL12, stained with CXCR7-APC antibody in 60 µl FACS buffer and analysed using the Amnis ImageStreamX Flow Cytometer. **(A)** Representative images for both treated and untreated cells are depicted. The first column shows brightfield (BF) images, the second column shows CXCR7-APC fluorescence in red (APC) and the third column shows fluorescence merged with the brightfield images (BF/APC). **(B)** Mean internalisation was calculated by analysing 19,677 cells (for colony 23.7) and 21,144 cells (for colony 30.7) using the Amnis IDEAS software. Data are shown for one independent experiment and represented as mean internalisation ± SEM.

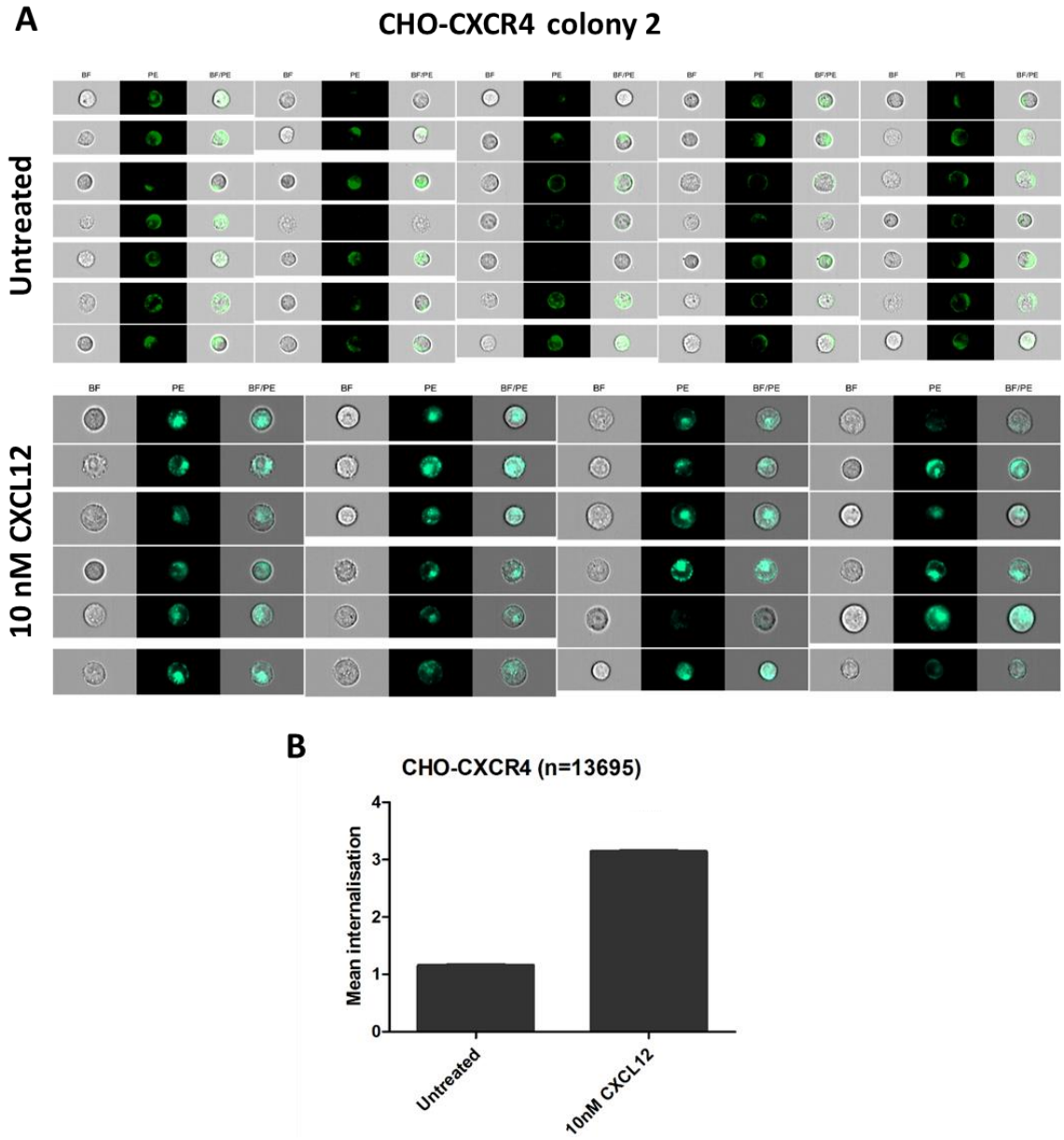

Figure 5-25. Quantification of receptor internalisation in CHO-CXCR4 colony 2 using IMAGEstream.
2 million CHO-CXCR4 cells were treated with 10 nM CXCL12, stained with CXCR4-PE antibody in 60 µl FACS buffer and analysed using the Amnis ImageStream^X Flow Cytometer. **(A)** Representative images for both treated and untreated cells are depicted. The first column shows brightfield (BF) images, the second column shows CXCR4-PE fluorescence in green (PE) and the third column shows fluorescence merged with the brightfield images (BF/PE). **(B)** Mean internalisation was calculated by analysing 13,695 cells using the Amnis IDEAS software. Data are shown for one independent experiment and represented as mean internalisation ± SEM.

The same experiments were carried out for the MDA-CXCR4 and MDA-CXCR7 cells, and the mCherry and tagBFP fluorescence was also assessed. As seen in Figure 5-26, internalisation was also greater in MDA-CXCR4 than in MDA-CXCR7 cells, suggesting that the same mechanism is occurring in both CHO and MDA-MB-231 cells. mCherry and tagBFP were also present in almost all cells, confirming what had been observed in immunofluorescence.

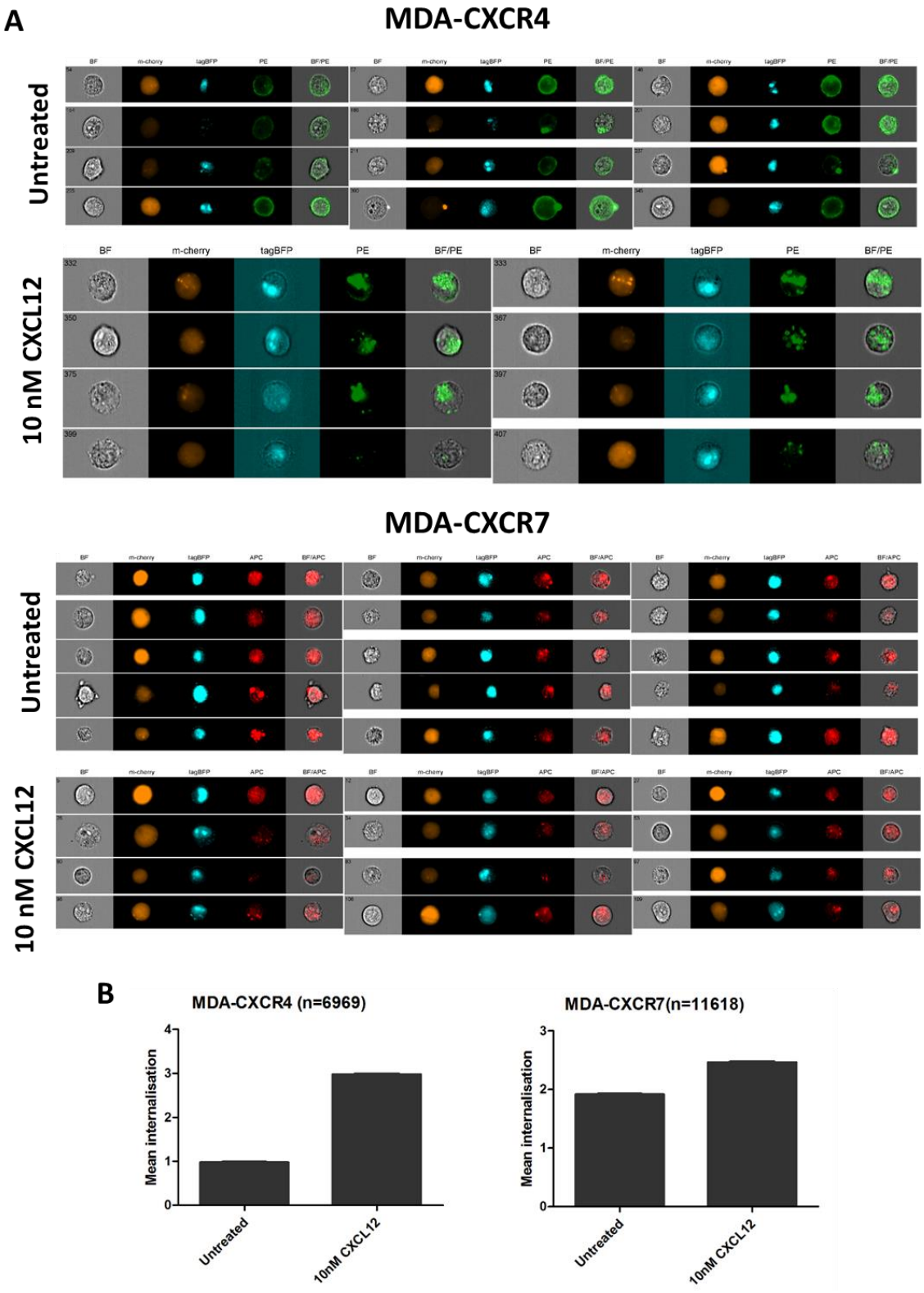

Figure 5-26 Quantification of receptor internalisation in MDA-CXCR4 and MDA-CXCR7 using IMAGEstream. 2 million transfected MDA-MB-231 cells were treated with 10 nM CXCL12, stained with CXCR7-APC or CXCR4-PE antibodies and analysed using the Amnis ImageStream^X Flow Cytometer. **(A)** Representative images for both treated and untreated cells are depicted after compensation was applied. The first column shows brightfield (BF) images, the second column shows m-cherry fluorescence in orange, the third column shows tagBFP fluorescence in blue, the fourth column shows the fluorescent marker (PE in green or APC in red) and the fifth column shows fluorescence merged with the brightfield images (BF/PE or BF/APC). **(B)** Mean internalisation was calculated by analysing 6,969 cells (for MDA-CXCR4) and 11,618 cells (for colony MDA-CXCR7) using the Amnis IDEAS software. Data are shown for one independent experiment and represented as mean internalisation ± SEM.

5.2.10. Optimisation of receptor internalisation assays

Before carrying out the recycling experiments, chemokine concentration and exposure times were first optimised in order to assess optimal receptor internalisation conditions. First, several CXCL12 concentrations were assessed in all cell lines as seen in Figure 5-27, and the lowest concentration that induced 50% internalisation or more was chosen. Thus, 10 nM was chosen for all cell lines except CHO-CXCR4-CXCR7 and MDA-CXCR7, where 50 nM was selected.

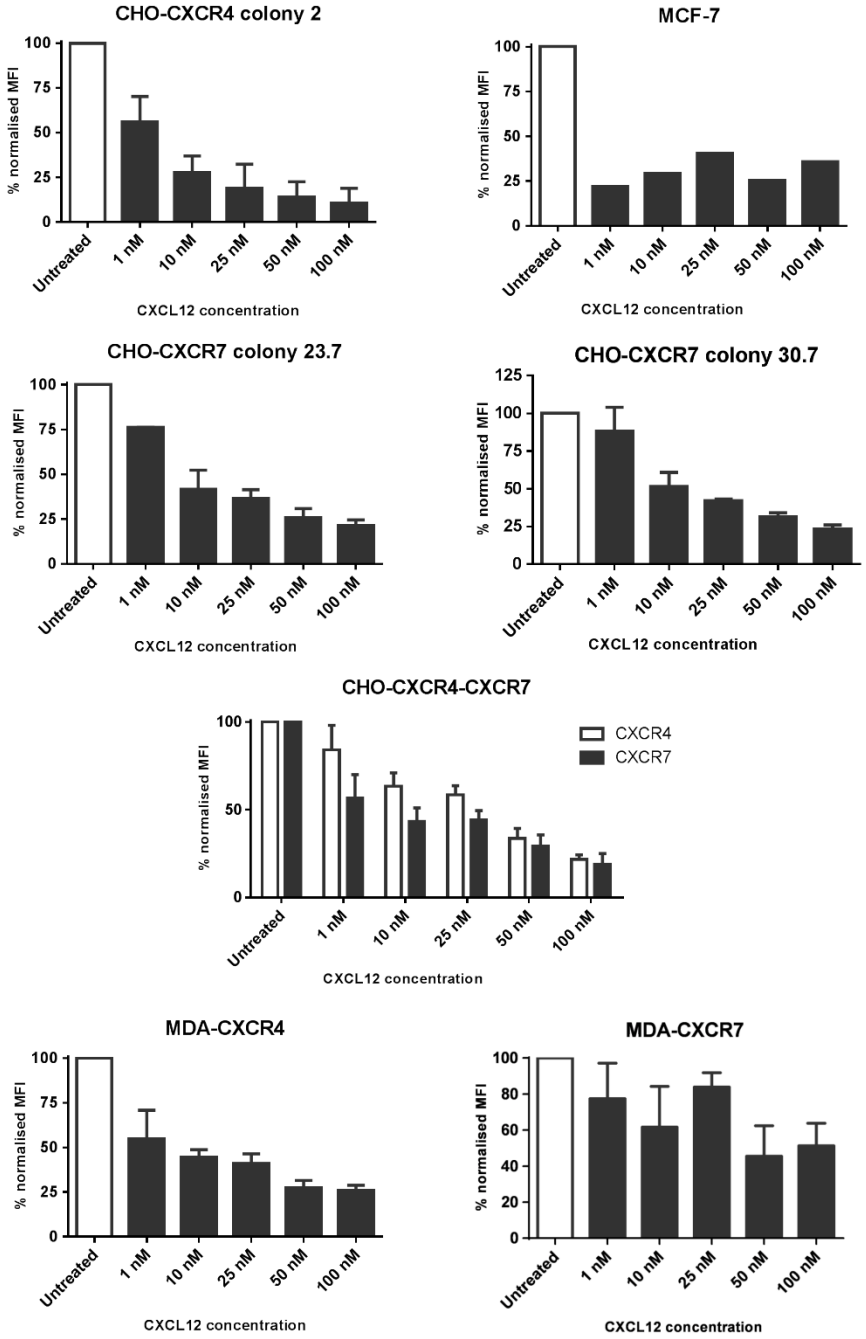

Figure 5-27. Optimisation of CXCL12 concentration necessary to induce receptor internalisation.
Cells were stimulated with a spectrum of CXCL12 concentrations ranging from 1 nM to 100 nM for 30 minutes, labelled with CXCR4-PE and/or CXCR7-APC antibodies and analysed using a FACS canto II flow cytometer. Data represent the mean fluorescence intensity ± SEM of two independent experiments (one for MCF-7 cells).

To ensure that the effects seen above were receptor-specific, cells were also treated with CXCL11, which is a ligand for CXCR7 but not CXCR4. As it can be seen in Figure 5-28, CXCL11 had no effect on CHO-CXCR4 cells at even 100 nM, whilst it was able to decrease CXCR7 expression by 50% in CHO-CXCR7 and MCF-7 cells. Overall, higher CXCL11 concentrations were necessary in order to see the same effect as CXCL12 - this is due to CXCR7 binding the latter with a 10 to 20 times higher affinity (Müller et al., 2001). A smaller effect could be seen in CHO-CXCR4-CXCR7 cells, indicating the formation of heterodimers affects CXCL11 binding. Further to this, the effect of CCL2's unspecific binding in CHO-CXCR4 cells was also assessed and although a slight non-concentration dependent internalisation could be observed, this was not significant. This 10% variation can be due to the natural receptor turnover or measurement differences.

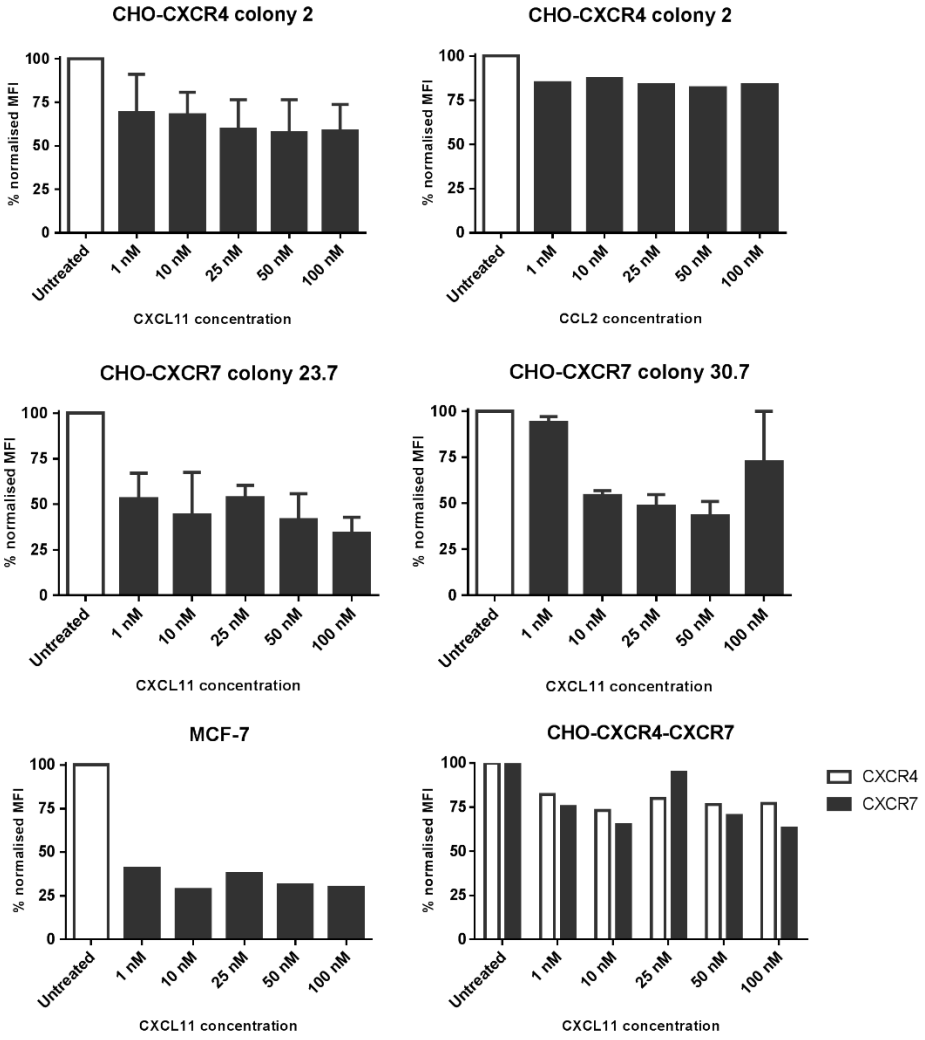

Figure 5-28. Determination of the specificity of chemokine internalisation with CXCL11 and CCL2.
Cells were stimulated with a spectrum of CXCL11 or CCL2 concentrations ranging from 1 nM to 100 nM for 30 minutes, labelled with CXCR4-PE and/or CXCR7-APC antibodies and analysed using a FACS canto II flow cytometer. Data represent the mean ± SEM of two (for CXCL11 with CHO-CXCR4 and CHO-CXCR7 cells) or one (for CCL2 with CHO-CXCR4 and CXCL11 with MCF-7 and CHO-CXCR4-CXCR7) independent experiments.

Next, the optimal amount of time to incubate the cells with the chemokine was optimised. As seen in figure 5-29, internalisation occurred very quickly and thus 15 minutes was chosen for CHO-CXCR7 cells and 30 minutes was used for CHO-CXCR4 and CHO-CXCR4-CXCR7 cells.

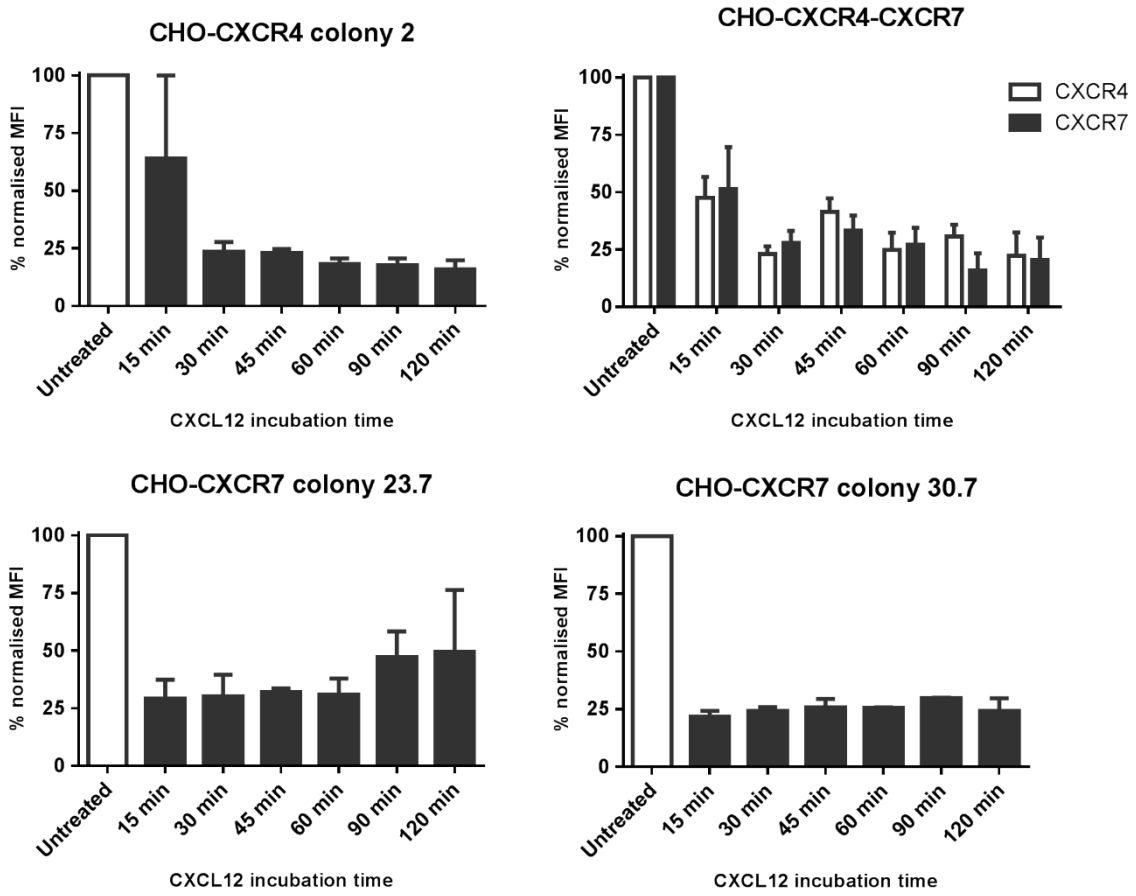

Figure 5-29. Optimisation of CXCL12 incubation time necessary to induce receptor internalisation.
Cells were stimulated with 10 nM (for CHO-CXCR4 and CHO-CXCR7) and 50 nM (for CHO-CXCR4-CXCR7) CXCL12 for a spectrum of times ranging from 15 to 120 minutes. Cells were then labelled with CXCR4-PE and/or CXCR7-APC antibodies and analysed using a FACS canto II flow cytometer. Data represent the mean ± SEM of two independent experiments and statistical significance was calculated using a one way ANOVA (*p<0.05, **p<0.01, ***p<0.001).

Finally, the optimal media to conduct the internalisation assay was determined. Initially, assays were carried out in basal media to serum-starve cells and obtain the most intense chemokine response. However, it was later observed that serum-free media also hindered the recycling of the receptor back to the surface after the removal of CXCL12 from the media. Thus, after the chemokine wash, serum-free, reduced-serum or complete-serum media were added and the difference in recycling levels was assessed. As seen in figure 5-30, complete media was found to enhance recycling the most.

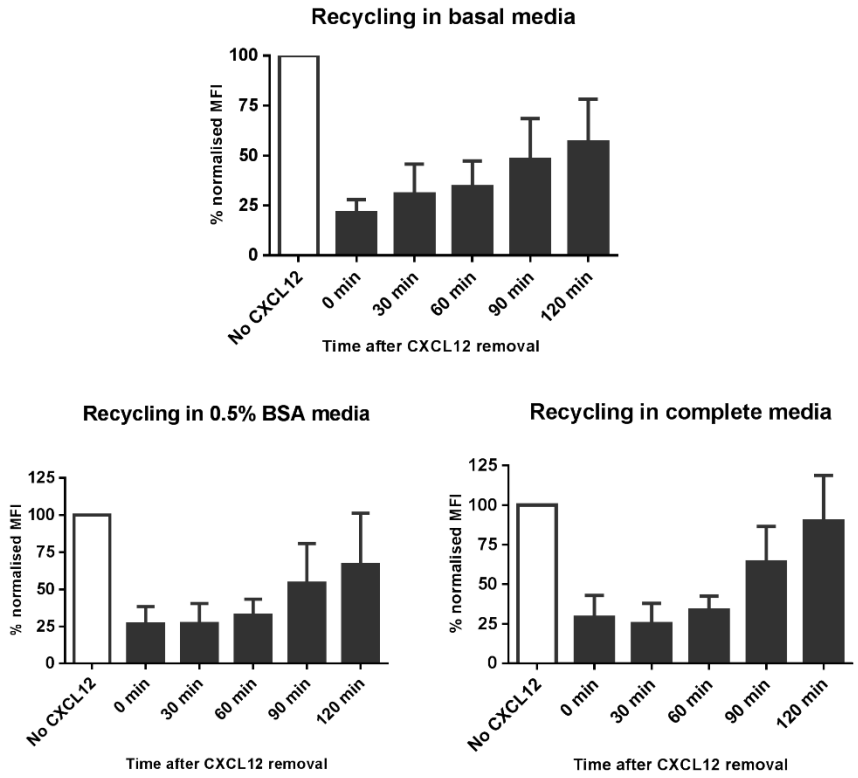

Figure 5-30. Optimisation of the best media to support receptor recycling.
CHO-CXCR7 colony 30.7 cells were stimulated with 10 nM CXCL12 for 15 minutes and then washed and incubated in basal media, 0.5% BSA media or complete (10% FBS) media for up to two hours. Cells were then labelled with CXCR7-APC antibody and analysed using a FACS canto II flow cytometer. Data represent the mean ± SEM of two independent experiments.

5.2.11. Receptor internalisation in transfected cells after CXCL12 stimulation

After stimulation with CXCL12 for the optimised concentration and time, media containing the ligand was replaced by fresh complete media and receptor levels were monitored using flow cytometry and compared to the untreated cells. As seen in Figure 5-31, in CHO-CXCR4 a 70% reduction of CXCR4 levels could be obtained after a 30 minute incubation with 10nM CXCL12. When replaced with fresh media, no recycling of the receptor to the surface could be seen after 2 hours – the same pattern was observed in MDA-CXCR4 cells.

Similarly, in both CHO-CXCR7 colonies a 70-80% receptor reduction could be seen after a 15-minute incubation with 10nM CXCL12. When media was replaced after stimulation, however, CXCR7 expression was recovered after 60-90 minutes, with receptor levels increasing over the initial ones. This phenomenon was also observed in MCF-7 but not MDA-CXCR7 cells.

In CHO-CXCR4-CXCR7, CXCR4 levels also remained at around 50% for up to two hours; conversely CXCR7 levels recycled back to the surface, albeit they did not reach the initial level after 2 hours.

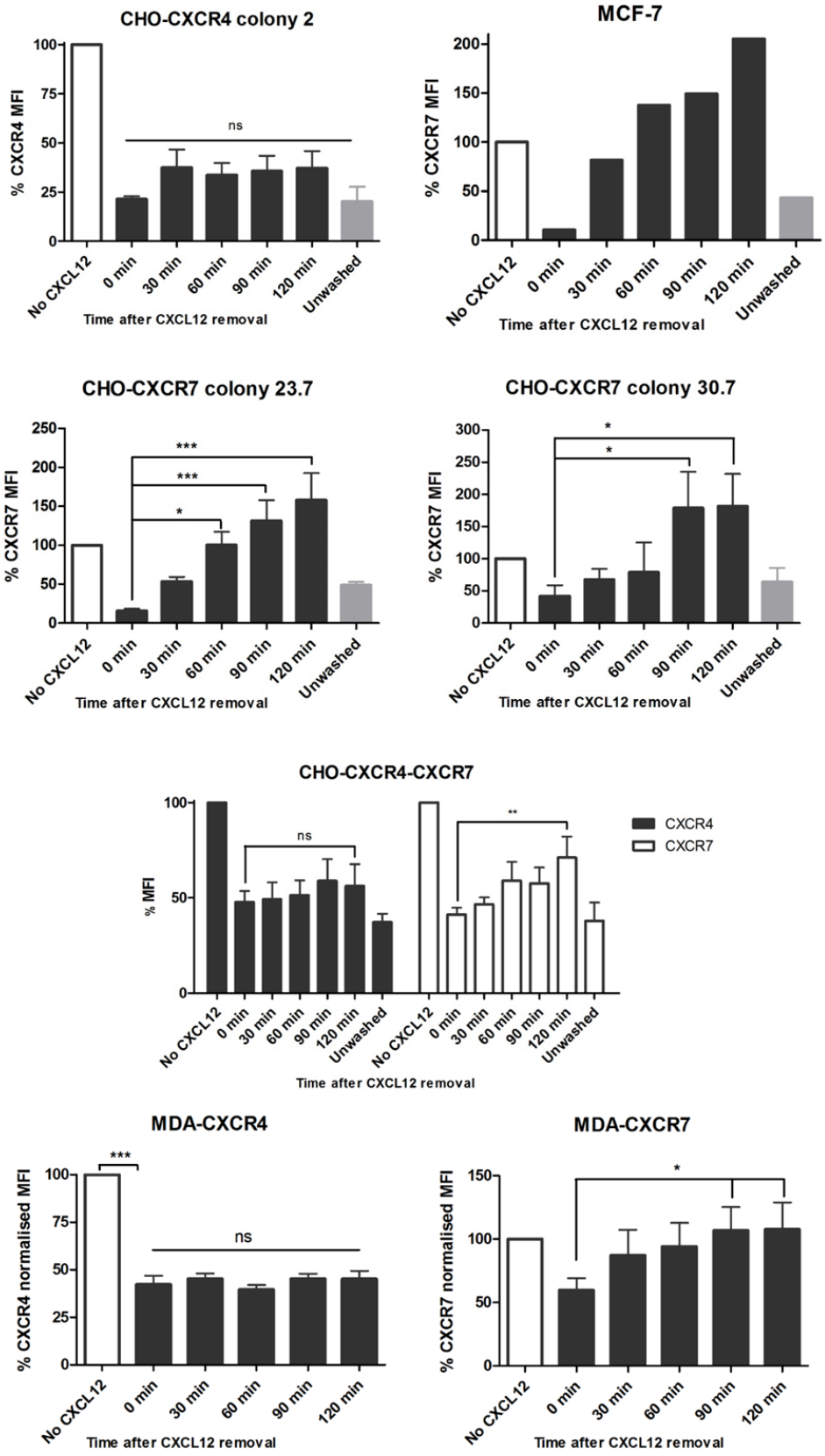

Figure 5-31. CXCR4 and CXCR7 follow different internalisation pathways after CXCL12 stimulation.
CHO-CXCR4 colony 2, MCF-7, CHO-CXCR7 colonies 23.7 and 30.7, CHO-CXCR4-CXCR7, MDA-CXCR4 and MDA-CXCR7 cells were treated with 10, 10, 10, 50, 10 and 50nM CXCL12 respectively for 30 minutes (15 minutes for CHO-CXCR7), then washed and incubated with chemokine-free media for up to 2 hours to assess receptor recycling. Cells were then labelled with CXCR4-PE and/or CXCR7-APC antibody and receptor expression was measured using flow cytometry. Data represent the mean ± SEM of three independent experiments and statistical significance was calculated using a one way ANOVA (*p<0.05, **p<0.01, ***p<0.001).

To confirm that CXCR4 was being degraded, cells were pre-treated with 10 μM lactacystin for 1 hour. Lactacystin is a potent and irreversible proteasome inhibitor first isolated from the bacteria *Streptomyces* (Omura et al., 1991) that inhibits cell cycle through its conversion to β-lactone, which then binds and modifies the proteasome's catalytic subunits, inactivating them (Fenteany et al., 1995, Dick et al., 1996). As seen in Figure 5-32, pre-treatment with lactacystin prevented the degradation of CXCR4 in CHO-CXCR4 cells after CXCL12 stimulation, with receptor levels returning to initial levels 2 hours after CXCL12 removal. Pre-treatment with lactacystin had no effect in CXCR7 recycling in both CHO-CXCR7 colonies, confirming that CXCR7 was not degraded after internalisation. Furthermore, a similar pattern could be observed in CHO-CXCR4-CXCR7 cells, with CXCR4 expression returning to higher levels when pre-treated with lactacystin, but having no effect in CXCR7 recycling.

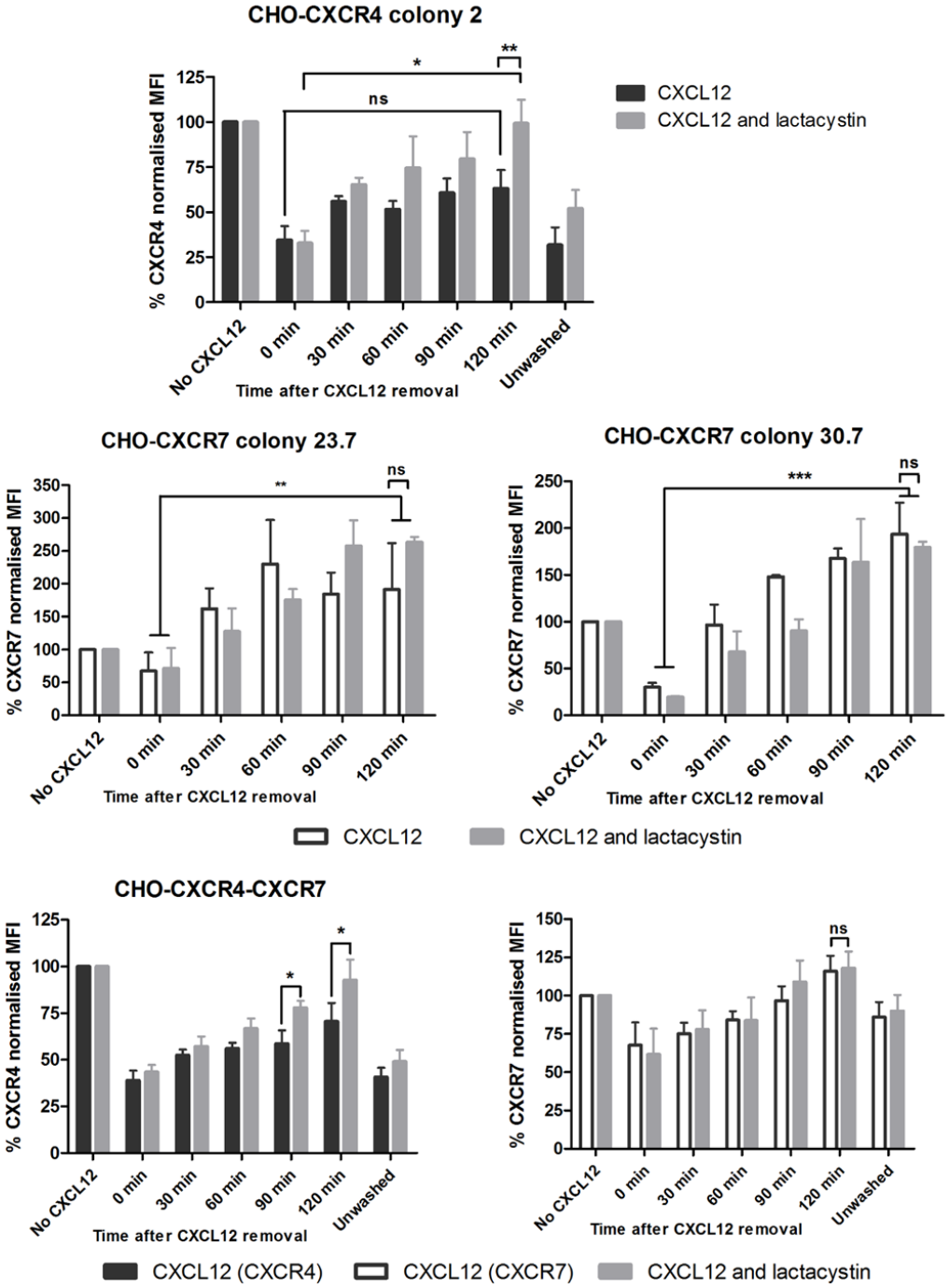

Figure 5-32. Preventing receptor degradation after CXCL12 stimulation using lactacystin, a proteasome inhibitor.
CHO-CXCR4, CHO-CXCR7 and CHO-CXCR4-CXCR7 cells were pre-treated for 1 hour with 10 μM lactacystin before incubating with 10, 10 and 50nM CXCL12 respectively for 30 minutes. Cells were then washed and incubated with chemokine-free media for up to 2 hours before being labelled with CXCR7-APC antibody and analysed using a FACS canto II flow cytometer. Data represent the mean ± SEM of three independent experiments and statistical significance was calculated using a one way ANOVA (*p<0.05, **p<0.01, ***p<0.001).

Furthermore, we investigated if different internalisation patterns occurred when cells were stimulated instead with the CXCR7 agonist VUF11207 (Tocris). First, optimal agonist concentration was assessed for CHO-CXCR7 and CHO-CXCR4-CXCR7 cells as seen in figure 5-33, and it was determined that the receptor's expression could be reduced by 80% with only 1nM VUF11207 after a 30-minute exposure.

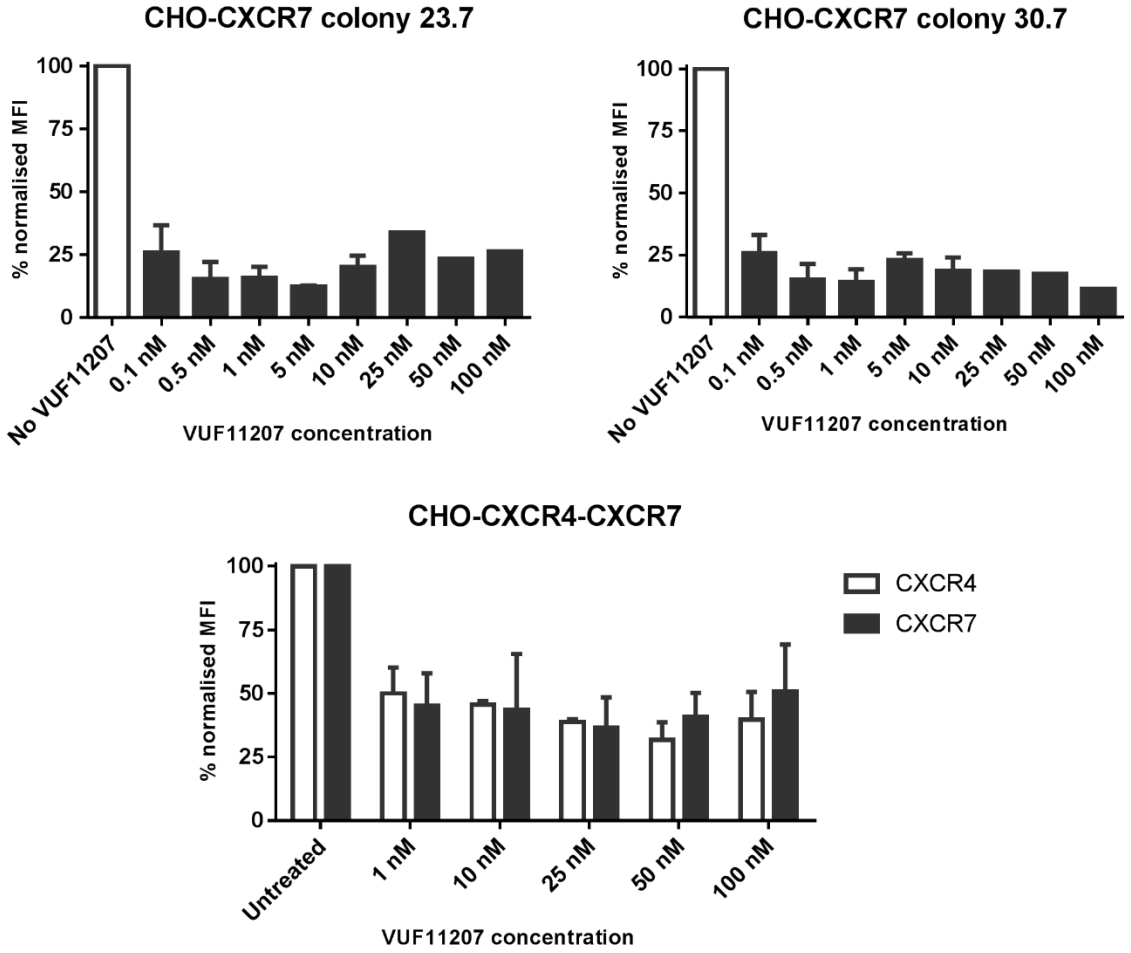

Figure 5-33. Optimisation of the necessary VUF11207 concentration, a CXCR7 agonist, to induce receptor internalisation.
Cells were stimulated with a spectrum of VUF11207 concentrations ranging from 1 nM to 100 nM for 30 minutes, labelled with CXCR4-PE and/or CXCR7-APC antibodies and analysed using a FACS canto II flow cytometer. Data represent the mean ± SEM of two independent experiments.

After stimulation with 1 nM VUF11207 for 30 minutes, media containing the ligand was replaced by fresh complete media and receptor levels were monitored using flow cytometry and compared to the initial levels. Similarly to what was observed with CXCL12, CXCR7 expression in CHO-CXCR7 increased after the wash; however expression after 2 hours it had only gone back to the original levels (see Figure 5-34). A similar trend was observed in the CXCR7-expressing MCF-7 cells; and no significant effect was seen in CHO-CXCR4 cells, confirming the specificity of the compound. In CHO-CXCR4-CXCR7, CXCR4 levels decreased around 25-30% reaching significance after 30 min, whilst a 40-50% receptor reduction could be seen for CXCR7. Unlike with CXCL12, CXCR7 did not recycle back to the surface after VUF11207 stimulation – this, together with the difference in CXCR7 recycling levels, seem to indicate that a different mechanism may be taking place after receptor activation with VUF11207.

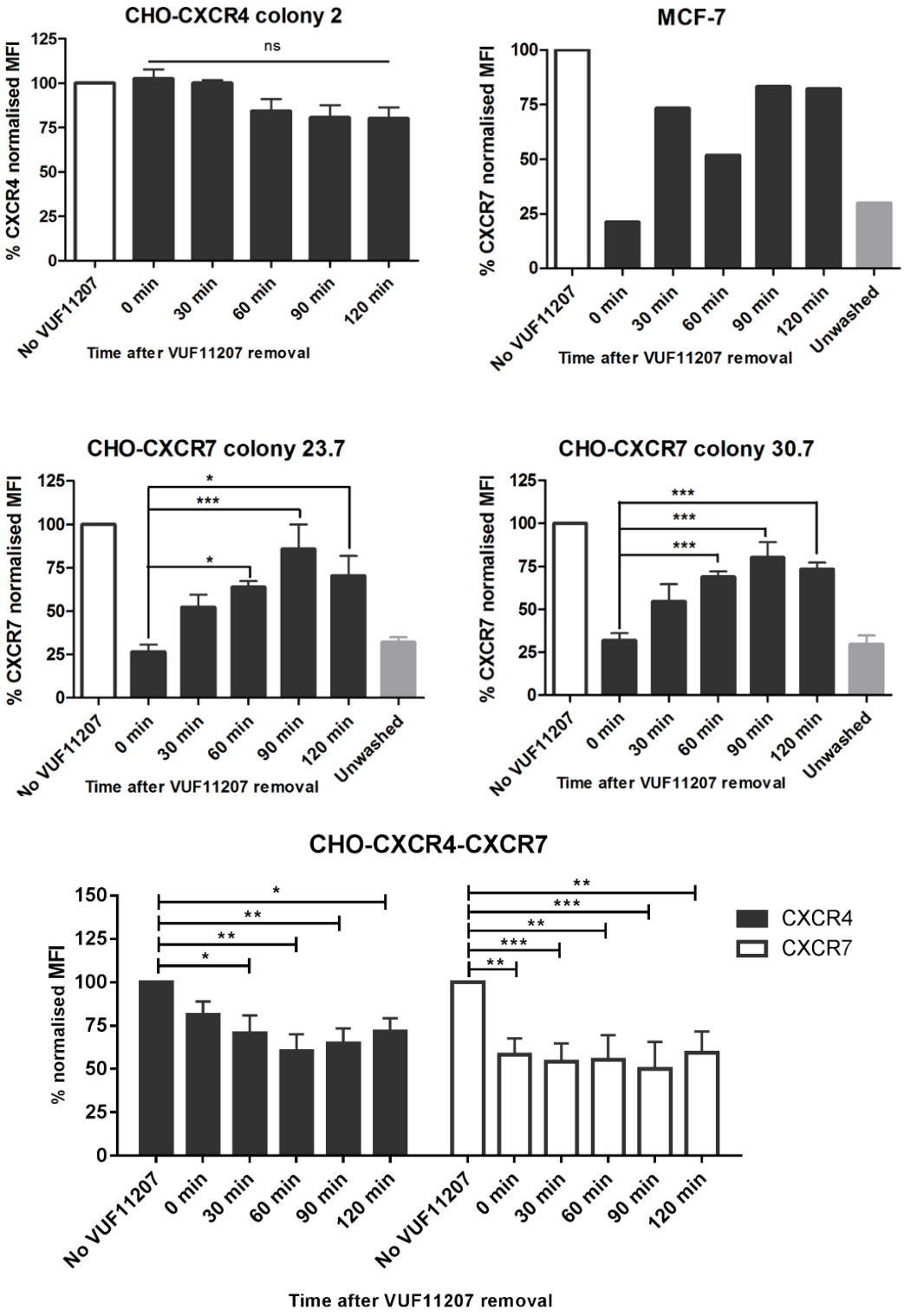

Figure 5-34 CXCR4 and CXCR7 follow different internalisation pathways after VUF11207 stimulation.
Cells were stimulated with 1nM VUF11207 for 30 minutes and then washed and incubated with agonist-free media for up to 2 hours to assess receptor recycling. Cells were then labelled with CXCR4-PE and/or CXCR7-APC antibody and receptor expression was measured using flow cytometry. Data represent the mean ± SEM of three independent experiments and statistical significance was calculated using a one way ANOVA (*p<0.05, **p<0.01, ***p<0.001).

Co-expression of CXCR7 can modify CXCR4's response to CXCL12 in breast cancer

In order to assess whether the increase in CXCR7 levels after CXC12-mediated recycling came from internal CXCR7 stored in vesicles or an increment in CXCR7 transcription, the receptor's RNA levels after stimulation with CXCL12 or VUF11207 were evaluated using qPCR. As seen in figure 5-35, a significant increase in CXCR7 expression could be observed at 60-90 minutes in the CXCL12-stimulated cells, whilst expression levels remained constant when cells had been treated with VUF11207. These results seem to suggest an upregulation triggered by the removal of CXCL12, with mRNA increase correlating with increased protein expression shortly thereafter.

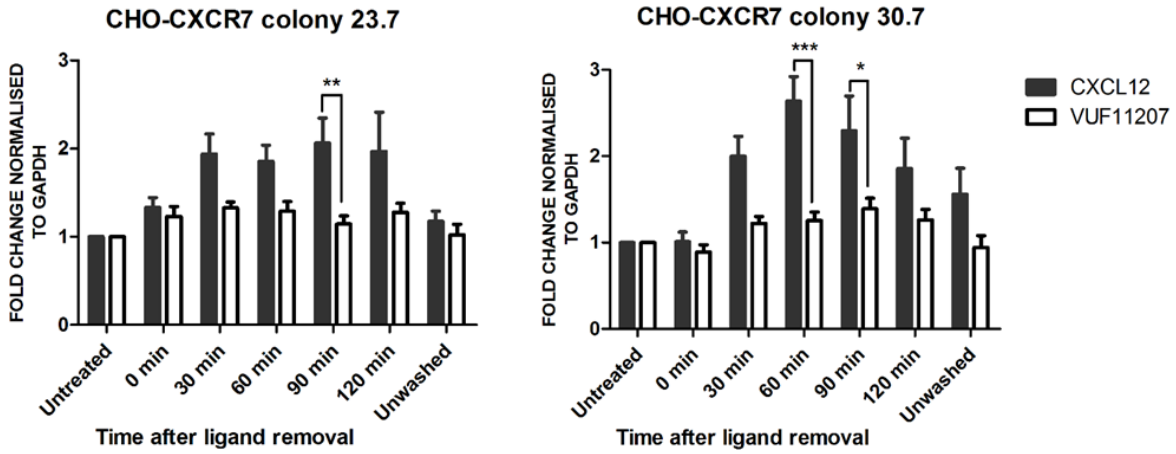

Figure 5-35. CXCL12 and VUF11207 have a different effect in CXCR7 transcription.
CHO-CXCR7 cells were stimulated with 1nM VUF11207 or 10nM CXCL12 for 30 minutes and then washed and incubated with agonist-free media for up to 2 hours. RNA was extracted at each time point and CXCR7 expression was assessed using Taqman probes and qPCR. Expression level was normalised to GAPDH. Data represent the mean ± SEM of three independent experiments and statistical significance was calculated using a one way ANOVA (*p<0.05, **p<0.01, ***p<0.001).

Next, we aimed to explore the effects of the CXCR4 antagonist and CXCR7 agonist AMD3100 (Merck Millipore). As seen in figure 5-36, no CXCR4 could be detected in CHO-CXCR4 cells after a 30 minute AMD3100 treatment at all concentrations, whilst a ~65% decrease in CXCR7 could be observed in both CHO-CXCR7 colonies for the whole concentration range. However, the complete lack of CXCR4 detection can be explained by AMD3100 blocking the binding of the anti-CXCR4 antibody 12G5 (Hatse et al., 2002). However, the other available CXCR4 antibody (clone 2B11) has been reported to cause the internalisation of the receptor (Ebioscience) and thus, it was decided not to pursue further the effect of AMD3100 in this study.

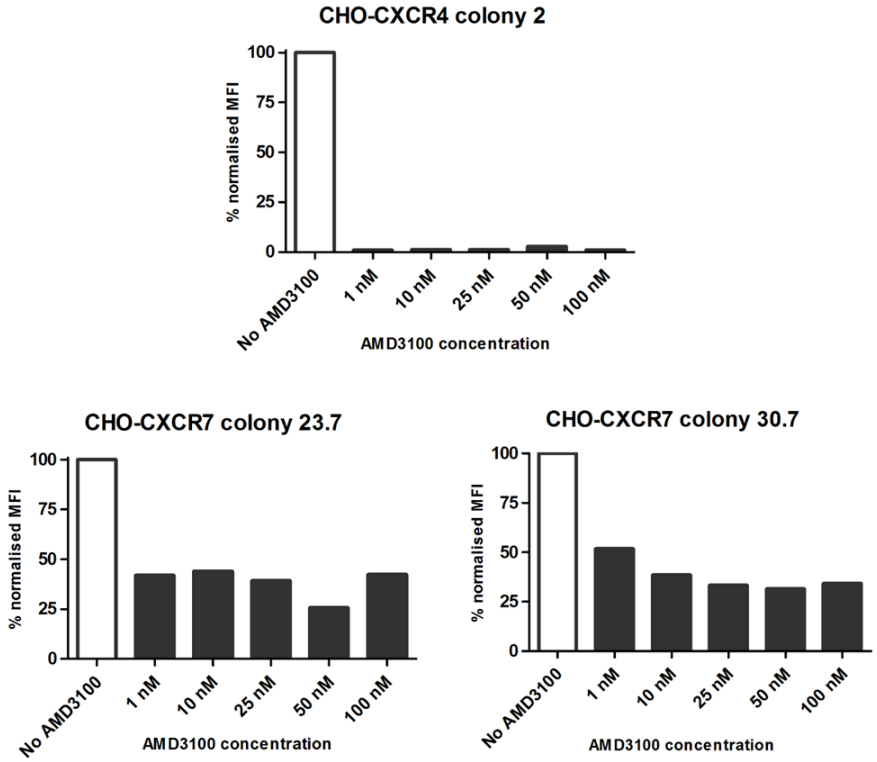

Figure 5-36. Preventing CXCL12 binding using AMD3100, a CXCR4 antagonist and CXCR7 agonist.
CHO-CXCR4 and CHO-CXCR7 cells were stimulated with a spectrum of AMD3100 concentrations ranging from 1 nM to 100 nM for 30 minutes, labelled with CXCR4-PE or CXCR7-APC antibodies and analysed using a FACS canto II flow cytometer (n=1).

Following this, we assessed whether CXCL12 effects could be prevented by pre-treating CHO-CXCR7 cells with the CXCR7 antagonist CCX771 (ChemoCentryx), which was a generous gift from Dr. Ashley McConnell. Briefly, cells were pre-treated with 1 μM CCX771 for 1h, overnight or 24 hours and then stimulated with 10 nM CXCL12 for 15 minutes. Interestingly, CXCL12 alone, CCX771 alone for 1h, and CCX771 for 1 hour with CXCL12 all caused a similar 50% reduction in CXCR7, indicating that either CCX771 caused CXCR7 internalisation or blocked the binding of the anti-CXCR7 antibody (see Figure 5-37). However, when cells were pre-treated with CCX771 for 18 or 24 hours, its presence did not affect CXCR7 levels, and prevented CXCR7 internalisation after CXCL12 addition.

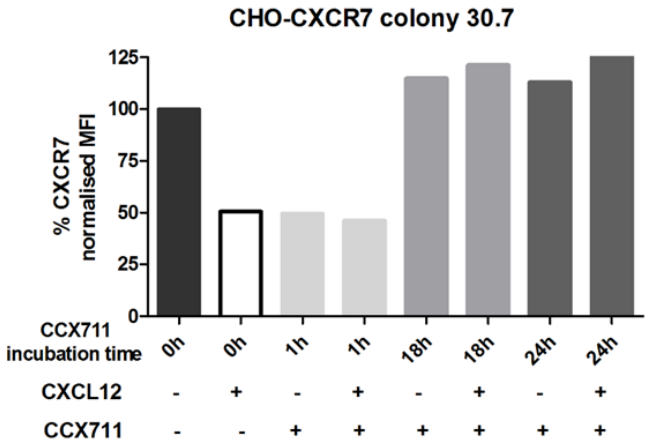

Figure 5-37. Preventing CXCL12 binding using CCX771, a CXCR7 antagonist.
CHO-CXCR7 colony 30.7 cells were incubated for 1h, 18h or 24 hours with CCX771 and then stimulated with 10 nM CXCL12 for 15 minutes. Cells were then labelled with CXCR7-APC antibody and receptor expression was measured using flow cytometry (n=1).

At last, we aimed to prevent CXCR7 internalisation in CHO-CXCR7 cells using sodium azide (NaN_3). Sodium azide is routinely used as a preservative in flow cytometry as it prevents capping and shedding of the antibody after it has bound its target antigen, and can prevent its internalisation (Mufson and Gesner, 1987). In our hands, no effect in internalisation could be seen with 0.1% NaN_3 (data not shown) but when pre-treating cells with 1% NaN_3 for 1 hour, up to 50% of CXCR7 internalisation could be prevented (see figure 5-38).

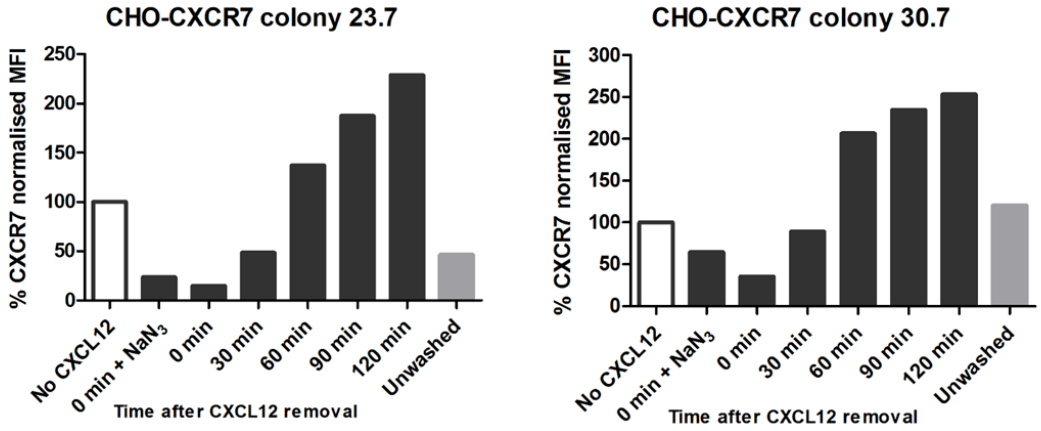

Figure 5-38. Preventing CXCR7 internalisation after CXCL12 stimulation using sodium azide (NaN_3).
CHO-CXCR7 cells were preteated for 30 minutes with 1% NaN_3 before incubating with 10 nM CXCL12 for 15 minutes. Cells were then washed and incubated with chemokine-free media for up to 2 hours before being labelled with CXCR7-APC antibody and analysed using a FACS canto II flow cytometer (n=1).

5.2.12. Effects of CXCR4 and CXCR7 expression in migration

Whilst CXCR4's role in migration has been well documented (Taichman et al., 2002, Helbig et al., 2003, Lee et al., 2004, Brand et al., 2005, Singh et al., 2004a), the role of CXCR7, in particular when in conjunction with CXCR4, is still a topic of debate.

In order to assess cell migration, transfilter chemotaxis was carried out as described in section 2.8.1. and CHO-CXCR4 migration was assessed in response to 50 nM CXCL12. However, despite high expressing colonies being re-selected, chemotactic index was lower than previously described (Harvey et al., 2007) due to high variability between filters and low overall migration (see figure 5-39).

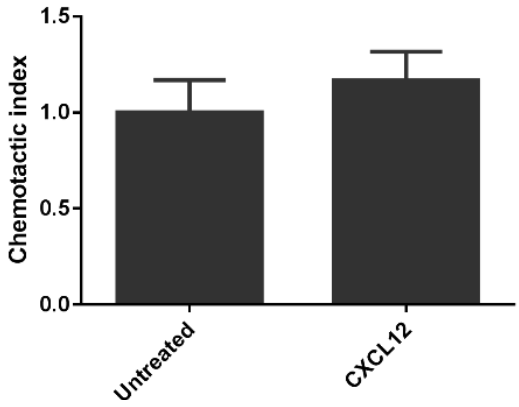

Figure 5-39. CXCL12 effect in CHO-CXCR4 cell migration using a chemotaxis assay.
CHO-CXCR4 cells were serum starved for an hour before being placed on top of a 8 μm filter above the 50 nM CXCL12-containing well. Cells were incubated at 37°C overnight and migrated cells counted. Graph represents the chemotactic index, or the ratio of migrated CHO-CXCR4 cells towards CXCL12 to cells migrated in the negative control. Data represent the mean ± SEM of six filters from two independent experiments, with five counted fields per filter.

To overcome this, a different assay was chosen to assess migration. Wound healing assays were selected, and gap closure was monitored every hour for 48 hours. Diminishing cell-free area was then calculated as a percentage of the original wound area as seen in figure 5-40A. CHO WT cells only closed approximately 40% of the gap, with the addition of chemokine making no overall difference. CHO-CXCR4 cells, on the other hand, managed to close the gap in 36 hours on average when chemokine was added, but only closed around 60% of the gap on their own. Both CXCR7 colonies showed slightly different wound closures, with colony 23 being approximately 20% faster; however, addition of CXCL12 in both colonies only increased the speed by 10% at most. At last, addition of CXCL12 in CHO-CXCR4-CXCR7 cells increased the wound healing speed from around 65% closed to almost completely closed. This difference in wound closure was plotted as cell front velocity and analysed in a quantitative manner as seen in figure 5-40B, with CXCL12 having a significant effect in wound healing closure in CHO-CXCR4 and CHO-CXCR4-CXCR7 cells only. Interestingly, CXCR7 expression appeared to increase spontaneous migration in CHO-CXCR7 colony 23 and in CHO-CXCR4-CXCR7 cells in comparison to CHO-WT, however this difference was not significant.

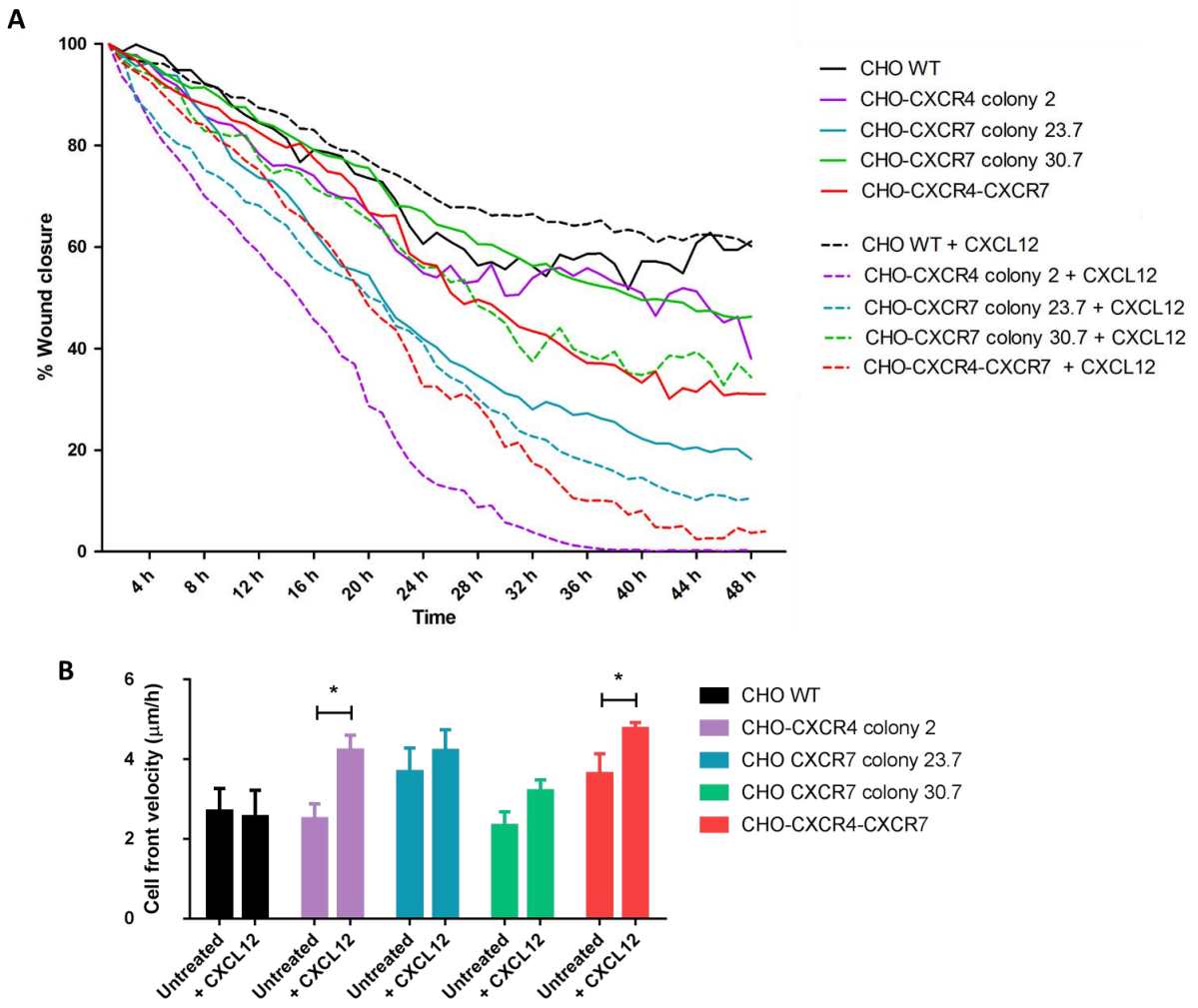

Figure 5-40. CXCR4, but not CXCR7, has an effect in wound healing after CXCL12 stimulation.
CHO WT, CHO-CXCR4, CHO-CXCR7 and CHO-CXCR4-CXCR7 cells were seeded into Ibidi inserts overnight. Inserts were then removed , creating a "wound" and wells were filled with 1% FBS media with or without 10 nM CXCL12. **(A)** Wound closure was monitored hourly for 48h using a Nikon Biostation. **(B)** Cell front velocity was then calculated from the wound area. Data represent the mean ± SEM of three independent experiments and statistical significance was calculated using a one way ANOVA (*p<0.05).

5.2.13. Effect of CXCR4 and CXCR7 in cell calcium signalling

Since the discovery of calcium flux's role in neutrophil's chemotaxis (Boucek and Snyderman, 1976), its role in many GPCR-mediated chemotaxis, including CXCR4, has been described (Foley, 2007). We thus aimed to investigate whether the observed increased migration was due to the ability of the receptor to transduce intracellular calcium signalling.

Calcium flux was then determined using flow cytometry for 10 nM CXCL12 and 4 μM ionomycin as a positive control to assess the maximum calcium release. As seen in figure 5-41, after CXCL12 stimulation calcium flux was achieved in CHO-CXCR4 cells and CHO-CXCR4-CXCR7 cells, but was almost absent in both CHO-CXCR7 colonies. Similarly to what was observed in the wound healing assay, CXCL12's effect in CHO-

CXCR4-CXCR7 was not significantly smaller than in CHO-CXCR4 cells. Jurkat cells were used as a positive control.

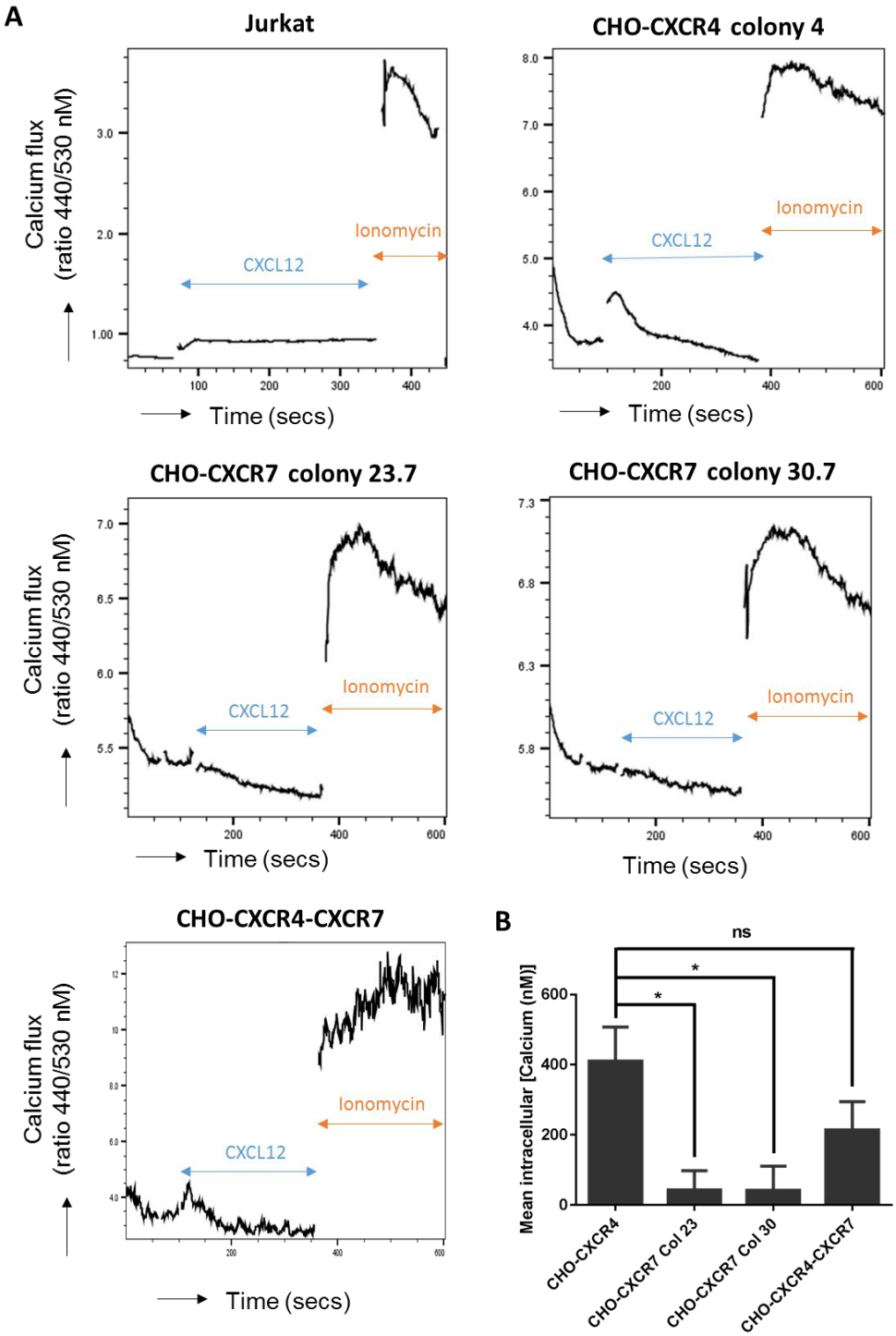

Figure 5-41. CXCR4-, but not CXCR7-expressing cells show calcium flux in response to CXCL12.
Cells were loaded with Indo-1am for 30 minutes at 37°C before being analysed using the BD LSRFortessa™ X-20 cell analyser for 1-2 minutes to stablish a baseline. Cells were then stimulated with 10 nM CXCL12 for 4 minutes and with 4 μM ionomycin for 4 minutes as a positive control. When intracellular calcium is released Indo-1 will bind it, changing its UV emission from 510 nm to 420 nm, and the ratio between these wavelengths will allow the determination of calcium concentration. **(A)** A representative plot of the intracellular calcium flux of the different CHO transfectants. Jurkat cells were used as a positive control. **(B)** Mean ± SEM of the intracellular calcium concentrations of the CHO transfectants. Data are representative of three independent experiments and statistical significance was calculated using a one way ANOVA (*p<0.05).

5.3. DISCUSSION

CXCR4 and CXCR7 expression and assessment

Since the discovery of CXCR7 as a CXCL12-binding receptor (Balabanian et al., 2005), its role in many diseases including cancer has been explored, but its effects are still the source of many conflicting reports. Indeed, CXCR7 is indubitably overexpressed in many cancers including breast (Luker et al., 2012), yet its role seems to differ between diseases. For instance, CXCR7 has been reported to increase cell survival and adhesion (Burns et al., 2006), being particularly key in transendothelial chemotaxis (Zabel et al., 2009); yet studies suggests it mediates (Balabanian et al., 2005, Kumar et al., 2012), enhances (Sánchez-Alcañiz et al., 2011, Décaillot et al., 2011) and decreases migration (Uto-Konomi et al., 2013), or has no effect in chemotaxis at all (Hartmann et al., 2008).

This disparity can be due to three different factors, which were assessed in this study. First, distinct cell types and chemokine concentrations may have a differential effect on CXCR7's downstream pathways. Second, not all studies considered the presence of CXCR4 in addition to CXCR7 – although its ten-fold lower CXCL12 affinity would minimise its binding, the possibility of heterodimers with unique signalling properties (Levoye et al., 2009) must be determined. And at last, interpretation of the available studies is further complicated by the use of suboptimal antibodies. For instance the anti-CXCR7 clone 358426 has been shown to underestimate CXCR7 expression (R&D systems, 2016), thus prompting the need to re-evaluate some of the existing studies (Berahovich et al., 2010b). Furthermore, clone 9C4 indicates CXCR7 expression in T lymphocytes (Balabanian et al., 2005), human umbilical vein endothelial cells (Naumann et al., 2010), B-cells (Humpert et al., 2014), monocytes, and mature dendritic cells (Infantino et al., 2006), but has had limited success in identifying the receptor in cancer cells (Liberman et al., 2012). Conversely, clone 11G8 suggests the opposite pattern, with no CXCR7 expression in non-transformed cells but positive staining in many tumour cells (Burns et al., 2006) including the neovasculature (Madden et al., 2004). Interestingly, both clones have been used as blocking antibodies to prevent CXCL12 binding (Torossian et al., 2014, Naumann et al., 2010), suggesting they may recognise a sequence near the residues D179 and D275 where CXCL12 binds CXCR7 (Benredjem et al., 2017). Unfortunately, although these residues are away from the N-ter, the target sequence of none of these CXCR7 clones is known and thus we cannot rule out that the GFP tag in the N-ter may prevent antibody binding in the MDA-CXCR7 cells.

Similarly, CXCR4 presents two available antibodies: clone 12G5, which targets the second extracellular loop and thus can be used as a blocking antibody (Endres et al., 1996); and clone 2B11, which binds the internal N-ter region and thus does not affect CXCL12 binding (Huskens et al., 2007, Förster et al., 1998). Furthermore, the latter has been targeted towards murine CXCR4, albeit it cross reacts with the human receptor (Schabath et al., 1999). This difference has been proven to be key in CXCR4 binding capacity, as clone 12G5 detects CXCR4 3 to 6 times brighter than 2B11 (van den Berg et al., 2011), although its location may cause some conformations to be undetected (Baribaud et al., 2001). This is particularly important for the transfectant MDA-CXCR4, which is tagged in its N-ter with GFP. Due to the relatively big size of this fluorescent protein (~27 kDa, (Hink et al., 2000)), it is likely that the 2B11 clone would not be able to bind due to steric hindrances.

Another approach to ensure that GFP is not preventing antibody binding in the MDA-CXCR4 and MDA-CXCR7 cells is to assess receptor expression using a CXCL12 binding assay. CXCL12 binding can be assessed by fusing the chemokine to a small luminescent probe (Luker et al., 2009a) or having it tagged with a fluorochrome (Hatse et al., 2005) or biotin (Le Brocq et al., 2014), and then monitoring the changes in signal using flow cytometry.

Given that the aim of our study was to assess receptor expression in breast cancer, we decided to use anti-CXCR7 clone 11G8 and anti-CXCR4 clone 12G5, and reassess receptor expression in the breast cancer cell lines we possessed. CXCR4 expression was undetectable in MDA-MB-231, MCF-7, SKBR3 and T47D cell lines, whilst CXCR7 expression was high in MCF-7 cells, low in T47D and undetectable in MDA-MB-231 and SKBR3. This is in correlation with literature, which describes no CXCR7 expression in MDA-MB-231 cell lines (Hattermann et al., 2010, Luker et al., 2009a, Salazar et al., 2014) – the absence of CXCR4 expression by MDA-MB-231 cells was discussed in Chapter 4. Lack of CXCR4 expression in MCF-7, T47D and SKBR3 is also supported by The Human Protein Atlas (The human protein atlas, 2016a), which also shows high CXCR7 expression in MCF-7 but no expression in SKBR3 and T47D (The human protein atlas, 2016b). Other literature reports low CXCR7 in SKBR3 (Rahimi et al., 2010), no CXCR7 protein in SKBR3 and T47D (Salazar et al., 2014) and high CXCR7 expression in MCF-7 (Luker et al., 2010, Salazar et al., 2014), corroborating the findings in the current study. However, literature regarding CXCR4 expression is contradictory, with some studies showing detectable levels in T47D and SKBR3 (Yang et al., 2014) and high levels in MCF-7 (Akekawatchai et

al., 2005); whilst others show no CXCR4 in T47D (Libura et al., 2002, Müller et al., 2001) and mostly low expression in MCF-7 (Sobolik et al., 2014, Sun et al., 2014, Pérez-Yépez et al., 2012, Müller et al., 2001). Once again, these variations could also be influenced by the method of CXCR4 assessment and to what independent scientists consider a moderate expression of the receptor.

Due to this lack of cells co-expressing both CXCR4 and CXCR7, we created single or double CHO transfectants in order to directly compare the functional consequences of expressing one or both receptors, which to the best of our knowledge has only been sparingly carried out and not with CHO cells. Furthermore, we confirmed the presence of CXCR4/CXCR7 heterodimers using FRET, which has been previously described in literature (Levoye et al., 2009, Luker et al., 2009b, Décaillot et al., 2011).

CXCL12-mediated pERK and pAkt activation

After CXCL12 stimulation, we observed a transient p-ERK and p-AKT peak activation at 5 and 15 minutes in CHO-CXCR4 cells; conversely, p-ERK and p-AKT activation remained constant for up to 2 hours in CHO-CXCR7 cells. This correlates with previous literature which suggests that CXCR7-mediated activation of these kinases is different from the canonical G-protein pathway in many ways. For instance, it has been reported that whilst G-protein-dependent ERK activation is quick and transient (Lagane et al., 2008), β-arrestin-mediated activation is slower but more sustained (Ahn et al., 2004, Ebisuya et al., 2005). It has been suggested that this is due to ERK being retained in the cytoplasm instead of being translocated to the nucleus (Ahn et al., 2004) due to its binding to β-arrestin (Rajagopal et al., 2010), and thus phosphorylating different substrates – for instance, p90RSK, cPLA2 and cytoskeletal proteins (Lefkowitz and Shenoy, 2005, Tohgo et al., 2003, Ebisuya et al., 2005). This activation causes actin reorganisation which could, in turn, enhance chemotaxis through the formation of a leading edge (Ge et al., 2003). Another theory for this prolonged activity is that the scaffold protects p-ERK from the activity of MAPK phosphatases (Ahn et al., 2004).

Other studies also report that CXCR7 can activate both the ERK and Akt pathways through the β-arrestin mechanism described above. In particular, one study reports ERK and Akt phosphorylation after CXCL12 stimulation in the glioma cell lines A764 and U343 (Ödemis et al., 2012); and another describes an increased phosphorylation when CXCR7 expression was induced in the human bladder cancer cell lines J82 and T24 (and

diminished phosphorylation when CXCR7 was silenced in the cell line RT4) (Hao et al., 2012). This phenomena has also been reported for ERK in the human hepatocellular carcinoma cell line HepG2 where overexpression of CXCR7 increased phosphorylation whilst knockdown reduced it (Lin et al., 2014a).

However kinetic reports vary, indicating that pathways may be activated differentially in time depending on the cell line. For instance, Liberman et al. (2012) reports the completely opposite effect in the transfected neuroblastoma cell line IGR-NB8, where a sustained pERK activation of up to 30 minutes was observed in NB8-CXCR4 cells whilst NB8-CXCR7 cells presented a transient expression at 5 and 10 minutes. Interestingly, they also did not observe Akt activation for any transfected cell despite it being widely reported in other studies. Another study reports that after blocking CXCR4 in Jurkat cells, CXCR7-mediated phosphorylation of ERK was present for up to 20 min with a peak at 10 min, whilst Akt peaked at 15 minutes and disappeared by 30 minutes (Kumar et al., 2012), in partial agreement with our finding. Furthermore, Ping et al. (2011) reported CXCR4-mediated activation of p-Akt and p-ERK from 15 to 60 minutes in U87 glioma stem cells with a maximum at 30 minutes, similar to what we observed but with a delayed timeline. This is similar to Sierro et al. (2007) who observed two responses, one with peak at 3 min and another at 30 min. Also in accordance with our findings, in the prostate cancer cell line C4-2B, cells that express less CXCR7 present less Akt phosphorylation, which is sustained for up to 45 minutes with a 5-10 minutes peak (Wang et al., 2008b).

Interestingly, p-ERK activation in CHO-CXCR4-CXCR7 showed a transient but intense peak at 5 minutes that disappeared with time, whilst Akt showed a sustained activation with no peaks. A possible explanation as to how this happens is that one kinase (e.g. Akt) activates an oncogene, such as c-Raf or KRAS, which in turn inhibits the phosphorylation of the other kinase (e.g. ERK) (Dhillon et al., 2007, Mendoza et al., 2011). Differences between the signalling patterns of homodimers and heterodimers are not surprising - indeed, it has been suggested that heterodimerisation modifies the interaction between CXCR4 and the Gα subunit by changing its conformation (Levoye et al., 2009). Similarly to our studies, Décaillot et al. (2011) proposed, using transfected HEK cells, that heterodimer formation caused a shift to β-arrestin signalling that promoted an ERK activation peak at 5 minutes – his study, however, reported a sustained p-ERK activation but only until 30 minutes. Sierro et al. (2007) also observed a delayed peak activation in p-ERK but was also only assessed until 30 min. A similar pattern was observed by Chen et

al. (2015a), who described that cancer stem cells, which expressed both CXCR4 and CXCR7, had a constant and sustained ERK activation of up to one hour, whilst pAkt peaked at 15 minutes before fading away. Conversely to these studies, and in agreement with our findings, Liberman et al. (2012) reported a similar pattern with the double transfected neuroblastoma cell line IGR-NB8 which showed a transient but intense ERK phosphorylation at 5 and 10 minutes. In addition to this, MCF-7 cells expressing both CXCR4 and CXCR7 also showed pERK activation at 15 minutes (Hattermann et al., 2014).

Once again, this is most likely due to the extreme variability in signalling pathways between cell lines, even within the same disease. Indeed, Heinrich et al. (2012) reported two different patterns in the pancreatic cell lines PANC-1 and miaPaCa2, both of which expressed CXCR7 and CXCR4. Whilst the first showed a late and sustained activation from 15 to 60 minutes, the second presented an early activation that peaked at 15 minutes and then faded away. As chemokine concentration was constant, this could be due to differences in receptor expression – indeed, higher CXCR7 expression could sequester all CXCL12, whilst lower expression would allow for CXCR4 homodimers to also intervene. Furthermore, differences between cell types are to be expected as these signalling pathways may have distinct kinetics and downstream effects, in particular between normal and cancer cell lines.

However, it is important to note that due to the lack of a negative control using CHO WT cells, we cannot confirm that the signalling observed is completely due to CXCL12. Our recombinant CXCL12 was purchased from R&D (Catalogue number 350-NS), which is synthesised in *E.coli* with >97% purity and thus could contain small traces of bacterial immunogens. This is unlikely as CHO-WT cells did not display calcium flux after CXCL12 stimulation, a mobilisation which is triggered by ERK phosphorylation; however the possibility cannot be ruled out.

CXCL12-mediated internalisation

We were interested to know whether these differences in ERK and Akt activation times could be correlated with the internalisation of the receptor, and whether it was then degraded or recycled back to the surface. Indeed, receptor internalisation in transfected CHO and MDA cells was observed using ImageSTREAM, a phenomenon that had been described previously (Balabanian et al., 2005, Boldajipour et al., 2008, Grymula et al., 2010, Minina et al., 2007), and it was also observed that CXCR7 internalisation occurred

in a dose and time dependent manner. It is important to note that there was a certain background internalisation for both CXCR4 and CXCR7, particularly the latter, observed in Imagestream. This could be due to three different reasons. First, studies have reported that CXCR7 is stored in internal reserves, and gets externalised upon CXCL12 activation (Chatterjee et al., 2014b). Other studies have also found CXCR7 expression in internal vesicles, confirming that it can occur in different cell types (Shimizu et al., 2011, Wang et al., 2011) – indeed, similar to what we observed these vesicles were in close proximity to the plasma membrane (Zhu et al., 2012). Second, constant trafficking of the receptors without chemokine stimulation. It has been reported that CXCR7 continuously recycles back to the surface even in the absence of CXCL12 (Luker et al., 2010), and CXCR4 can also recycle without ligand stimulation, albeit slowly (Signoret et al., 1997). Third, possible bivalent binding of the CXCR7 antibody – unlike the CXCR4 antibody, which we know recognises just one antigen, the binding of the CXCR7 antibody is unknown and thus could crosslink one antigen to another. Indeed, bivalent antibodies have been shown to promote receptor internalisation in other receptors (Greenall et al., 2012), given receptor crosslinking has been previously described to cause internalisation (Moody et al., 2015).

Furthermore, our studies discovered that after CXCL12 stimulation, CXCR4 expression in CHO-CXCR4 and MDA-CXCR4 cells diminished and did not recover for up to 2 hours, whilst CXCR7 levels in CHO-CXCR7, MCF-7 and MDA-CXCR7 had gone back to normal after 1 hour. A similar pattern was observed in the kidney epithelial cell line MDCK, where CXCR7 expression was only slightly reduced after incubation with CXCL12, whilst CXCR4 expression profoundly diminished after CXCL12 exposure (Naumann et al., 2010). This was followed up by Luker et al. (2010), who demonstrated that CXCR7 gets recycled after promoting CXCL12 degradation. Although one could argue that different times and concentrations could have an effect, it has been previously reported that chemokine concentration does not affect the fate of the receptor (Luker et al., 2010) although it can affect the kinetics (Neel et al., 2005). Indeed, other studies also optimise chemokine concentration and time before carrying out internalisation assays (Rose et al., 2004, Brandt et al., 2002).

A similar pattern was seen in CHO-CXCR4-CXCR7 cells, albeit CXCR7 levels did not recover as much. This is in accordance to Uto-Konomi et al. (2013), who reported in the bone osteosarcoma U2OS cell line that when both CXCR7 and CXCR4 were expressed, the stimulation with CXCL12 induced the degradation of CXCR4 but the recycling of CXCR7.

Co-internalisation of both CXCR4 and CXCR7 was also reported in MCF-7 cells, albeit further degradation or recycling was not studied (Hattermann et al., 2014). Furthermore, it was also reported in CXCR4- and CXCR7-expressing human platelets that after CXCL12 stimulation CXCR4 levels dropped, whilst CXCR7 levels rose, albeit they did not observe the initial drop (Chatterjee et al., 2014b). This could be due to only small amounts of the receptors being in the surface and these being quickly replaced by the intracellular CXCR7 present in the cytosolic compartments (Hartmann et al., 2008).

We also wanted to confirm that CXCR4 was being degraded through the proteasome pathway, and indeed we obtained higher CXCR4 levels when cells were pre-treated with the proteasome inhibitor lactacystin before CXCL12 stimulation. This is in accordance with other studies, which demonstrated that lactacystin could significantly increase CXCR4 levels after CXCL12-mediated internalisation in Jurkat cells (Fernandis et al., 2002) and increased CXCR4 expression in lymphocytes (Lapham et al., 2002).

VUF11207-mediated internalisation

Despite the correlation found between CXCR7 expression in cancer and worse prognosis, it has been proposed that the anti-cancer properties of some compounds (such as TC14012 or AMD3100) are not only due to their antagonistic CXCR4 activity, but also due to their CXCR7 activity. Indeed, CXCR7 antagonists have shown interesting results in inhibiting trans-endothelial migration (Zabel et al., 2009), but CXCR7 agonists have also shown promise (Uto-Konomi et al., 2013) proving CXCR7 is a potential therapeutic target. Furthermore, desensitisation through agonists has been shown to be a therapeutic avenue in anti-inflammatory diseases (Ali et al., 2007), and thanks to the formation of heterodimers, CXCR4 and CXCR7 are key candidates for cross-desensitisation.

To carry out this study we used VUF11207, a pure CXCR7 agonist derived from styrene-amide that binds CXCR7 with very high affinity (EC_{50} = 1.6 nM) (Wijtmans et al., 2012). This is a higher affinity for CXCR7 than CXCL12 (EC_{50} = 16 nM) (Levoye et al., 2009), and orders of magnitude above the dual agonist/antagonists TC14012 (EC_{50} = 350 nM) (Gravel et al., 2010) and AMD3100 (EC_{50} = 830 nM) (Xu et al., 2016) – indeed, it was observed that 1nM VUF11207 and 10 nM CXCL12 were needed to elicit the same response. For reference, EC_{50} indicates the *e*ffective *c*oncentration at which the drug induces half of the maximal response. In our study, it was observed that VUF11207 caused internalisation and recycling of CXCR7 in CHO-CXCR7 cells, albeit at lesser levels than

when stimulated by CXCL12 – qPCR results suggest that this difference in CXCR7 recovery levels could be partially explained by CXCL12 inducing CXCR7 transduction after stimulation (which was not observed with VUF11207), and not just by the induction of the internal CXCR7 reserves as other studies have found (Chatterjee et al., 2014b). However, it is important to note that whilst the RNA studies were carried out by stimulating the same batch of cells side by side, this was not the case in the internalisation studies. Thus, although care was taken so that conditions and receptor levels were the same between studies, temporal circumstances could impact the direct comparison between CXCL12 and VUF11207.

Interestingly, VUF11207 stimulation of CHO-CXCR4-CXCR7 caused a small significant reduction on CXCR4 levels but surprisingly CXCR7 did not recycle back to the surface after internalisation. One reason for this difference could be that VUF11207 binds in a different pocket than CXCL12 and causes changes in the recycling of the receptor – indeed, it has been observed that several CXCR7 ligands bind different residues to CXCL12 (Yoshikawa et al., 2013). For instance, it has been suggested that CXCL11 and CXCL12 do not interact with the exact same residues in CXCR7 and only have 22 in common (Costantini et al., 2013), albeit other studies report that there is no difference between the two in the recycling of CXCR7 (Luker et al., 2010). However, whilst different ligands do not usually affect the fate of the receptor (Signoret et al., 2005), they can affect its internalisation rate and desensitisation – for instance, CCR7 stimulation with CCL21 promotes less efficient internalisation than CCL19 and only CCL19, but not CCL21, can promote CCR7 desensitisation (Schaeuble et al., 2012, Otero et al., 2006). Indeed, different desensitisation levels have been observed with CCR5 and its several chemokine ligands, albeit they correlate with binding affinity (Oppermann et al., 1999). Second, the fate of VUF11207 and CXCL12 after recycling may be different, with the former being recycled with the receptor and the latter being degraded, which would cause the continuous internalisation of the receptor after reaching the surface. Indeed, other molecules such as AMD3100 have been reported to keep bound to CXCR4 for over 24 hours (Hatse et al., 2002). Third, due to their different molecular weight there may be changes in receptor dimerization after ligand binding - indeed, CXCL12 is approximately 8 kDa, whilst VUF11207 only has a molecular weight of 584 Da, which could result in different sterically hindrances that may cause an altered conformation. This is supported by Luker et al. (2009b), who reported that some specific inhibitors to CXCR4 or CXCR7 can cause

conformational changes in their homodimers, although consequences in receptor recycling were not assessed. These hypothesis, however, are difficult to determine given the challenge of modelling GPCR crystal structures, in particular the N-ter where most of the binding residues of their ligand are (McCusker et al., 2007, Michino et al., 2009, Ghosh et al., 2015), although some prediction models have been carried out (Yoshikawa et al., 2013, Wu et al., 2010a).

AMD3100 and CCX771 -mediated internalisation

Unfortunately, AMD3100 effects could not be assessed as it prevented the binding of our CXCR4 antibody - indeed previous studies report a 90% blocking of the monoclonal antibody (mAb) 12G5 in the first 24 hours and a 60% block at 48h (Huskens et al., 2007, Hatse et al., 2002, Gerlach et al., 2001, Labrosse et al., 1998). AMD3100 has been found to bind in the central hydrophobic core, with one study highlighting residues Phe^{189}, Tyr^{190}, Asp^{262}, and Glu^{288} (Trent et al., 2003) and the other $Asp^{171}$and Asp^{262} (Gerlach et al., 2001). Indeed, this overlaps with CXCL12, which has been known to interact with residues Asp^{171} and Glu^{288} of CXCR4 (Tamamis and Floudas, 2014), and mAb 12G5 which interacts with Asp^{182} and Tyr^{190} (Carnec et al., 2005). CXCR4 clone 2B11 could have been used as it does not interfere with AMD3100 binding (Schols and De Clercq, 2003), but as described before it may underestimate CXCR4 presence and can cause receptor internalisation, making it not comparable to the previous results obtained with clone 12G5. Furthermore, a similar problem also occurred with CXCR7 clone 11G8 as it also prevents CXCL12 binding (Ierano et al., 2014, Burns et al., 2006)

In contrast to VUF1120, CCX771 is a CXCR7-specific antagonist with very similar affinity for the receptor (IC_{50} = 4.1 nM, *i*nhibition *c*oncentration at which the drug reduces the response by half) (Zabel et al., 2009). However, in our hands it was only effective after incubating overnight or for 24 hours, in disagreement with other studies that incubated for 10 minutes at room temperature (Zabel et al., 2011, Ierano et al., 2014), 30 minutes (Steel et al., 2014) or 1 hour in the incubator (Wani et al., 2014) although concentrations of the molecule were the same (1 μM); given this disparity, and due to lack of time, we decided to not assess this further.

Wound healing

In order to assess cell migration, we carried out wound healing assays with and without the presence of CXCL12. CXCL12 significantly increased the wound healing speed in CHO-CXCR4 cells, a phenomena that has been reported in other wound healing assays with MDA-MB-231 cells (Guo et al., 2014b, Liang et al., 2007c), prostate cancer PC- 3 cells (Sakao et al., 2015) and human laryngeal cancer Hep-2 cells (Niu et al., 2015) and widely described in Boyden-chamber chemotaxis assays including breast cancer (Fernandis et al., 2004).

It was also found that CXCL12 only slightly increased wound healing speed in both CHO-CXCR7 colonies, however the baseline speed in colony 23 was greater than in CHO-WT and CHO colony 30. Hao et al. (2012) observed a similar effect, where two bladder cancer cell lines transfected with CXCR7 closed the wound faster than their WT counterparts, but with a 24-hour difference between themselves in would healing speed. Similarly, it has been reported that CXCR7 overexpression in the hepatocellular carcinoma cell line HepG2 increased wound healing speed, whilst knock down reduced it (Lin et al., 2014a). In support of our finding, Mazzinghi et al. (2008) reported that in renal multipotent progenitors CXCR4, but not CXCR7, was key in migration towards CXCL12. This was also corroborated in the A764 and U343 glioma cell lines (which express high levels of CXCR7 but no CXCR4), where the addition of CXC12 did not affect migration in a wound healing assay (Hattermann et al., 2010). Other studies using Boyden chambers to assess migration corroborate that CXCR7 has no involvement in CXCL12-mediated chemotaxis of T-cells (Hartmann et al., 2008), breast cancer cells (Burns et al., 2006) and mammary adenocarcinoma cells (Hernandez et al., 2011); whereas Balabanian et al. (2005) and Kumar et al. (2012) observed that CXCR7 is involved in the migration towards CXCL12 of T-cells and Jurkat cells, respectively. It is interesting to note, however, that CXCR7 staining in these studies was carried out after cells had been permeabilised (and thus included not only surface CXCR7, but internalised CXCR7), making it impossible to quantify the real involvement of membrane CXCR7 in the migration. Furthermore, another study defending the involvement of CXCR7 in migration has been retracted (Meijer et al., 2008).

At last, we observed that similarly to CHO-CXCR7 colony 23, CHO-CXCR4-CXCR7 had a higher migratory baseline; however CXCL12 caused a significant increase in wound healing speed. This is in correlation to what was by Décaillot et al. (2011), who reported that MDA-MB-231 and the primary glioblastoma cell line U87-CD4, which express both

receptors, can migrate towards CXCL12. Similarly, Ierano et al. (2014) reported significantly increased migration towards CXCL12 (as compared to control) in the human renal carcinoma cell lines A498 and SN12C. However, it is important to note that whilst A498 expresses high levels of both receptors, SN12C expresses low levels; however migration towards CXCL12 in a chemotaxis assay was significantly higher in the latter. A similar effect is seen in the wound healing assay, where low-expressing SN12C close the scratch twice as fast as A498 in response to CXCL12. Given these results, it is possible that there are some other factors apart from CXCR4 and CXCR7 expression that are modulating their migration, and thus conclusions should be taken with caution.

Interestingly, some invasion assays showed a similar pattern to our scratch assay, with CXCL12 having no effect in CXCR7 transfected cells in the rat mammary adenocarcinoma cell line MTLn3 JP (Hernandez et al., 2011) and the transfected human neuroblastoma cell line NB8 (Mühlethaler-Mottet et al., 2015). However, contrary to our study, CXCR4-CXCR7 transfected MTLn3 JP cells showed an increased chemotaxis as compared to CXCR4 alone (Hernandez et al., 2011), indicating CXCR7 is not implicated in migration but has the potential to enhance it. In opposition to this and our study, Hartmann et al. (2008) and Sierro et al. (2007) observed that expression of CXCR7 in conjunction to CXCR4 had no effect as compared to CXCR4 alone. These discrepancies in effect are most likely due to different expression levels of the receptor – our hypothesis is that high CXCR7 to CXCR4 expression is more likely to scavenge all CXCL12, impairing migration, whilst low CXCR7 (in particular if most of the expression detected was in fact intracellular) will most likely have no impact in migration. Furthermore, we have demonstrated that heterodimers form a complex with distinct signalling pathways, which may also affect cell migration in a unique manner.

Calcium flux

Calcium flux has been widely reported to mediate cell migration through actin polarisation, pseudopodia formation and adhesion to fibronectin (Maxfield, 1993) and thus we aimed to assess whether the differences observed in cell migration were due to an impaired intracellular calcium release. Indeed, we observed calcium flux induction in CHO-CXCR4 cells after the addition of CXCL12, a phenomena that has also been observed in U87 glioma stem cells (Ping et al., 2011) and the T-cell line CEM.NKR (Burns et al., 2006).

Furthermore, little or no calcium flux was observed in CHO-CXCR7 cells, similarly to what Burns et al. (2006) described for CXCR7-expressing MCF-7 cells. CXCR7 failing to trigger calcium mobilisation was also described in T-lymphocytes and $CD34^+$ progenitors (Hartmann et al., 2008), transfected HEK cells (Sierro et al., 2007) and rat vascular smooth muscle cells which express CXCR7 but low CXCR4 (Rajagopal et al., 2010). This further supports that CXCR7 does not interact with G-proteins due to having a DRYLSIT, instead of DRYLAIV, motif (Haraldsen and Rot, 2006).

In CHO-CXCR4-CXCR7, a significant calcium flux in response to CXCL12 was also observed. Indeed, in the Jurkat T-cell line, blocking CXCR7 had no impact in calcium release but blocking of CXCR4 abrogated calcium flux signalling (Kumar et al., 2012). This could be because blocking of the receptor did not reverse the heterodimer conformation, which is the one responsible for the recruitment of β-arrestin instead of G-proteins and thus impaired calcium release (Décaillot et al., 2011). However, Levoye et al. (2009) reported that CXCR4-CXCR7 heterodimers impair calcium flux in transfected HEK cells due to their inability to activate G-proteins, a trend that we observed but was not significant. Furthermore, conversely to our studies, Sierro et al. (2007) reported that heterodimer formation in transfected HEK cells increased calcium flux in comparison to HEK-CXCR4 cells – this, however, did not correlate with an increased chemotaxis. Once again, the expression ratio between the two receptors may be the reason for these differences in response.

Conclusion

Overall, this chapter highlights that CXCR4 and CXCR7 heterodimers create a distinct signalling entity with unique properties and answers the proposed aims. Growing evidence has suggested that while CXCR7 cannot interact with G proteins, it can signal through other mechanisms such as β-arrestin (Rajagopal et al., 2010) and can modify CXCR4's actions (Levoye et al., 2009).

- We have shown that CXCL12 treatment of transfected CHO cells induces the phosphorylation of ERK and Akt in a different kinetic and spatial sequence. In particular, CXCR4 causes a quick and transient activation, whilst CXCR7 induces a sustained phosphorylation and the combination of the two receptors cause an early ERK activation but a continuous Akt phosphorylation.
- The data presented in this chapter also shows that this difference can be partially explained by divergent internalisation pathways that CXCR4 and CXCR7 follow, which cause the degradation or recycling of the receptors.
- Furthermore, we have also shown that the CXCR7 agonist VUF11207 differentially desensitises CXCR7, which could contribute to a new line of therapy.
- Despite its over-expression in many cancer cell lines (Burns et al., 2006), the data presented in this chapter suggests that CXCR7 does not have a role in chemotaxis, but its presence can modulate CXCR4-mediated migration through the inhibition of calcium flux. However, CXCR7 may be involved in other pathways such as NF-κB-mediated survival, tumour growth and angiogenesis (Wang et al., 2008b, Burns et al., 2006, Miao et al., 2007) depending on the cell type it is expressed in.

6. CONTRIBUTION OF GLYCOSAMINOGLYCAN BINDING IN CCL21-MEDIATED MIGRATION OF BREAST CANCER CELLS.

6.1. INTRODUCTION

6.1.1. Mutated CCL21

Lymph node invasion is usually the first step in the metastatic process, where CCR7-expressing tumour cells are attracted to its ligand CCL21 which is abundantly expressed in the lymph nodes (Müller et al., 2001). This emulates the homing of naïve T-cells and dendritic cells to the T-cell zones of the lymph nodes (Gunn et al., 1999), where endothelial cells are presenting the chemokine via GAGs as described in section 1.4. of the introduction. Most chemokines, including CCL21, bind to GAGs such as heparan sulphate through their positively charged C-terminal region, which interacts with the negatively charged heparan sulphate (Proudfoot, 2006). Indeed, elimination of all heparan sulphate from the lymph node endothelium abrogated CCL21 presentation and lymphocyte homing in a murine model (Bao et al., 2010). With this in mind, previous studies in the group synthesised a truncated CCL21 chemokine that lacks residues 98-134 from the C-ter (see Figure 6-1) to assess the effect of GAG binding. This mutated CCL21 (mutCCL21) can still bind its receptor CCR7 but lacks the residues that mediate its binding to heparan sulphate, and thus its potential to compete with WT CCL21 and abrogate the metastasis of breast cancer cells to the lymph nodes was assessed.

```
        10         20         30         40         50
MAQSLALSLL ILVLAFGIPR TQGSDGGAQD CCLKYSQRKI PAKVVRSYRK
        60         70         80         90        100
QEPSLGCSIP AILFLPRKRS QAELCADPKE LWVQQLMQHL DKTPSPQKPA
       110        120        130    134
QGCRKDRGAS KTGKKGKGSK GCKRTERSQT PKGP
```

GAG binding residues

Figure 6-1. CCL21 chemokine amino acid sequence.
In order to create a non-HS binding CCL21, residues Δ98-134 (marked in red) were eliminated from the C-ter extension of CCL21 WT. This truncated chemokine used in this study will therefore be referred to as "mutated CCL21" or mutCCL21.

6.1.2. Specific aims

- To characterise the murine breast cancer cell line 4T1-Luc, including the detection of luminescence using different systems and their migratory potential in a trans-filter and trans-endothelial chemotaxis system.
- To create and optimise a murine model of breast cancer to assess metastasis to the lymph nodes from a primary tumour.
- To determine whether mutCCL21 can diminish metastasis to the lymph nodes *in vivo*.

6.1.3. Work leading up to this project

Initial *in vitro* work for this project was carried out by Dr. Imad Malki (Malki et al., 2013). First, the effect of the truncation on CCL21 activity was assessed in MDA-MB-231 cells, which express low levels of CCR7 as determined by PCR (see figure 6-2A). As seen in Figure 6-3A, calcium flux was reduced when using 10 nM of mutCCL21 in comparison to CCL21 WT, but reached comparable levels when using 50 nM of the chemokine, indicating binding and activation of CCR7 is impaired only at low chemokine concentrations.

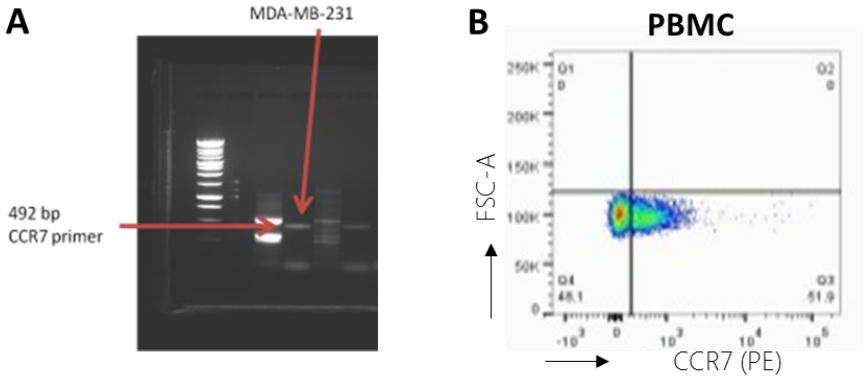

Figure 6-2. CCR7 expression by MDA-MB-231 and PBMCs.
(A) RNA was extracted from MDA-MB-231 and amplified using a CCR7 primer before being run on an agarose gel. **(B)** PBMC cells were stained with a CCR7-PE antibody and receptor expression was assessed using flow cytometry. Over 50% of the population demonstrates positive staining.

To confirm that this difference in calcium flux induction was due to impaired GAG binding, surface plasmon resonance (SPR) was carried out to assess the interaction between the ligand (GAG), which is bound to the sensor chip, and the analyte (CCL21), which is flown over the surface. If binding occurs, when polarised light hits the chip surface it will be reflected in a different angle depending on the proportion of the mass bound, and this can be recorded as resonance units (RU).

As seen in Figure 6-3B, mutCCL21 did not bind to heparin, as opposed to the WT form. When heparin density was increased on the chip surface (see Figure 6-3C), a higher RU could be seen for both forms but mutCCL21 binding remained very low. The same binding pattern could be seen when heparan sulphate was immobilised instead of heparin (see Figure 6-3D), which is the only GAG involved in CCL21 presentation in HEV *in vivo* (Tsuboi et al., 2013) and thus the most relevant physiologically. These results are in accordance with Hirose et al. (2002), who also observed reduced binding to GAGs using an ELISA.

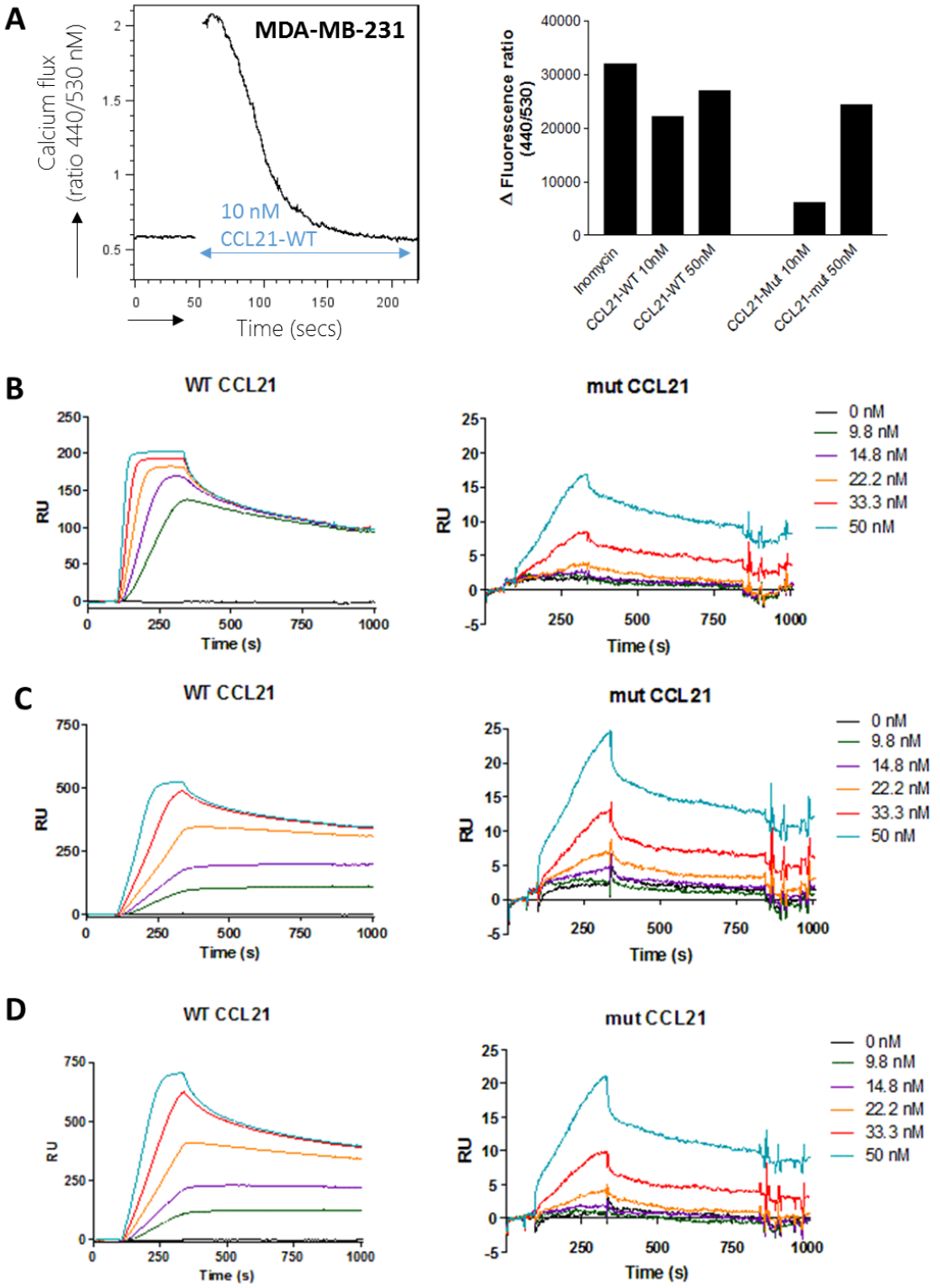

Figure 6-3. Biological activity of mutant and WT CCL21.
(A) Calcium flux. MDA-MB-231 cells were loaded with Indo-1am for 30 minutes at 37°C before being run in the BD LSRFortessa™ *X-20* cell analyser. Cells were then stimulated with different concentrations of wild type and mutated CCL21 and calcium flux was assessed. When the intracellular calcium is released, the Indo-1am binds it, changing its UV emission from 510 nm to 420 nm and thus increasing the ratio between these wavelengths (left). Fluorescence ratio was assessed, with ionomycin as positive control (right) (n=1). **Surface plasmon resonance (SPR) assay**. Gold-coated Biacore chips were used to assess the alteration in GAG binding of the mutCCL21 as compared to the control. **(B)** 0-50 nM chemokine was flowed over immobilised heparin (50RU bound) and the alteration in resonance units (RU) shown. **(C)** 0-50 nM chemokine was flowed over immobilised heparin (142RU bound) and the alteration in resonance units (RU) shown. **(D)** 0-50 nM chemokine was flowed over immobilised heparan sulphate (237RU bound) and the alteration in resonance units (RU) shown (n=1).

To assess the functional consequences of this impaired GAG binding, chemotactic migration was assessed in CCR7-expressing PBMCs (see figure 6-2B) and MDA-MB-231 cells. As seen in Figure 6-4A, 20 nM of both mutated and WT CCL21 were needed to reach significant migratory levels of PBMCs in a transfilter chemotaxis assay, with no statistical significance between the two chemokines. Similarly, significant migration of MDA-MB-231 was achieved at 20 nM, with migration towards mutCCL21 being slightly lower than WT CCL21. Finally, trans-endothelial migration (TEM) of PBMCs across a monolayer of HMEC-1 was carried out. As seen in Figure 6-4B, migration towards mutCCL21 was severely impaired at 30 nM and 50 nM in comparison to the WT, with levels comparable to the no-chemokine control.

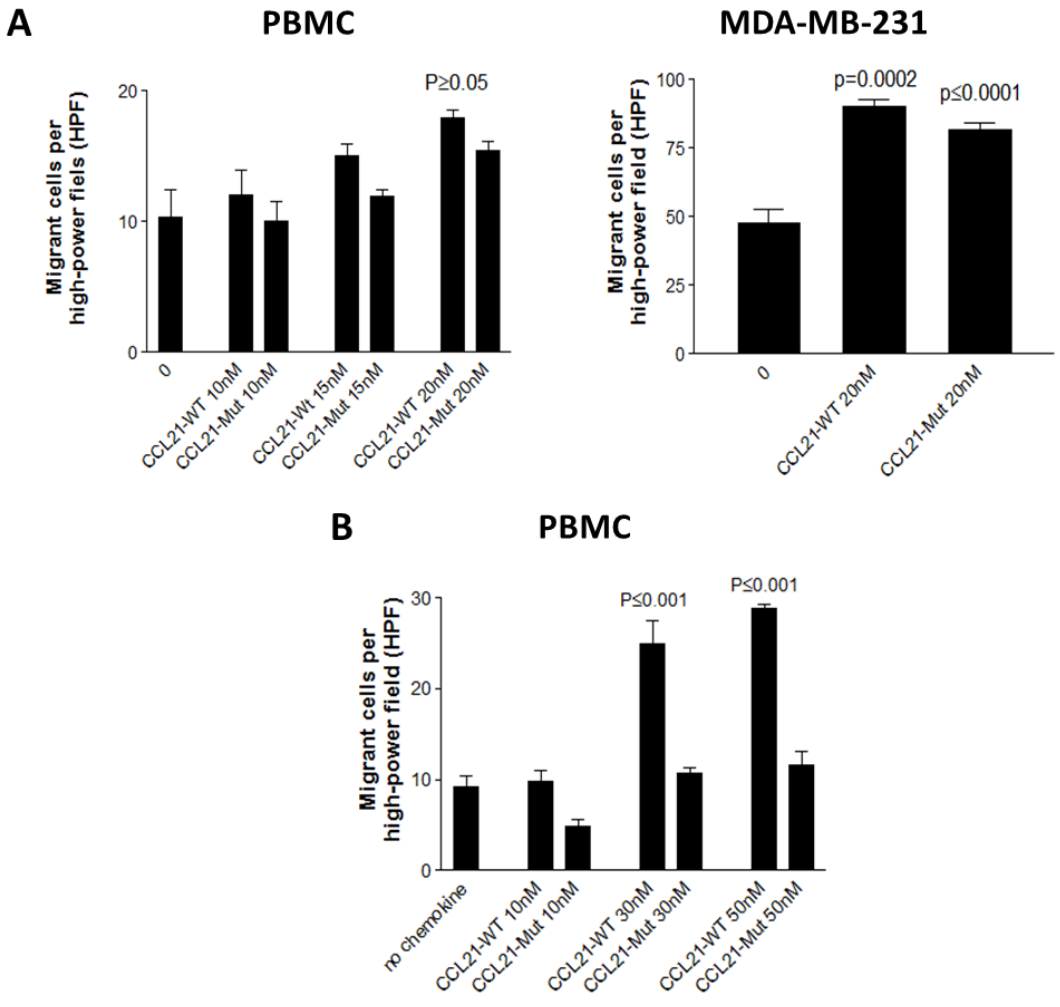

Figure 6-4. *In vitro* migration of MDA-MB-231 cells and PMBCs.
(A) Trans-filter chemotaxis. PBMC and MDA-MB-231 cells were serum starved for an hour before being placed on top of a 3µm or 8 µm filter above the well containing WT or mutated chemokine. Cells were incubated at 37°C for 2 hours or overnight and migrated cells counted. Graph shows the number of migrated cells to the bottom well (PBMC, left) or adhered to the filter (MDA-MB-231, right) per filter field. Data represent the mean ± SEM of three independent experiments and statistical significance was calculated using one way ANOVA. **(B) Trans-endothelial chemotaxis** Previous to the chemotaxis assay, 3µm filters were coated with HMEC-1 cells and let to grow until they formed a confluent monolayer. PBMC cells were then placed on top of the filter and above the well containing WT or mutated CCL21. Cells were incubated at 37°C for 2 hours and migrated cells counted. Data represent the mean ± SEM of three independent experiments and statistical significance was calculated using one way ANOVA.

These results suggest that deletion of residues 98 to 134 in CCL21 impairs its presentation by GAGs in the HMEC-1 cell surface, preventing PBMCs' adhesion and their migration through the endothelial monolayer. To confirm GAG's involvement in the impaired chemotaxis, 50 nM of WT or mutated CCL21 were incubated with increasing concentrations of several GAGs (heparin, heparan sulphate, chondroitin sulphate A and chondroitin sulphate B) before assessing PBMC transwell chemotaxis for 2 hours. As seen in Figure 6-5A, heparin and heparan sulphate bound WT CCL21 in a dose dependent manner and achieved maximal inhibition at 250 and 500 μg/ml. However, a minimal effect was seen when competing with the truncated CCL21, suggesting that the GAG-binding domain is key to abrogate chemotaxis using heparinoids. However, no effect was seen with either chondroitin sulphate A or B – this was expected from chondroitin sulphate A, as it does not bind CCL21 (Zhou et al., 2014), but chondroitin sulphate B (also known as dermatan sulphate) has been described to bind CCL21 in their C-ter and inhibit calcium flux (Hirose et al., 2001, Hirose et al., 2002). However, no studies have assessed chondroitin sulphate B's effects in chemotaxis and its affinity towards different chemokines is still not well studied either (Trowbridge and Gallo, 2002). Overall, this study shows that heparin and heparan sulphate having a stronger binding affinity for the receptor than chondroitin sulphate A or B.

Furthermore, to assess receptor internalisation PBMC cells were incubated with 20 nM CCL21 WT or mutCCL21 and receptor internalisation was assessed for up to 90 minutes. As seen in Figure 6-5B, longer and higher internalisation rates could be observed with mutCCL21, although after 1 hour CCR7 levels were back to original levels with both chemokines. This is not surprising as CCL21 has been documented to cause the recycling of the receptor after internalisation (Otero et al., 2006), although it is in conflict with other studies that suggest that this process is impaired with the truncated CCL21 (Hjortø et al., 2016).

Given these promising results in impairing transendothelial chemotaxis, we hypothesised that the truncation in mutCCL21 inhibited GAG binding whilst still maintaining its ability to bind CCR7, and designed a series of experiments to assess mutCCL21's potential in inhibiting *in vivo* migration to the lymph nodes in a murine model of breast cancer.

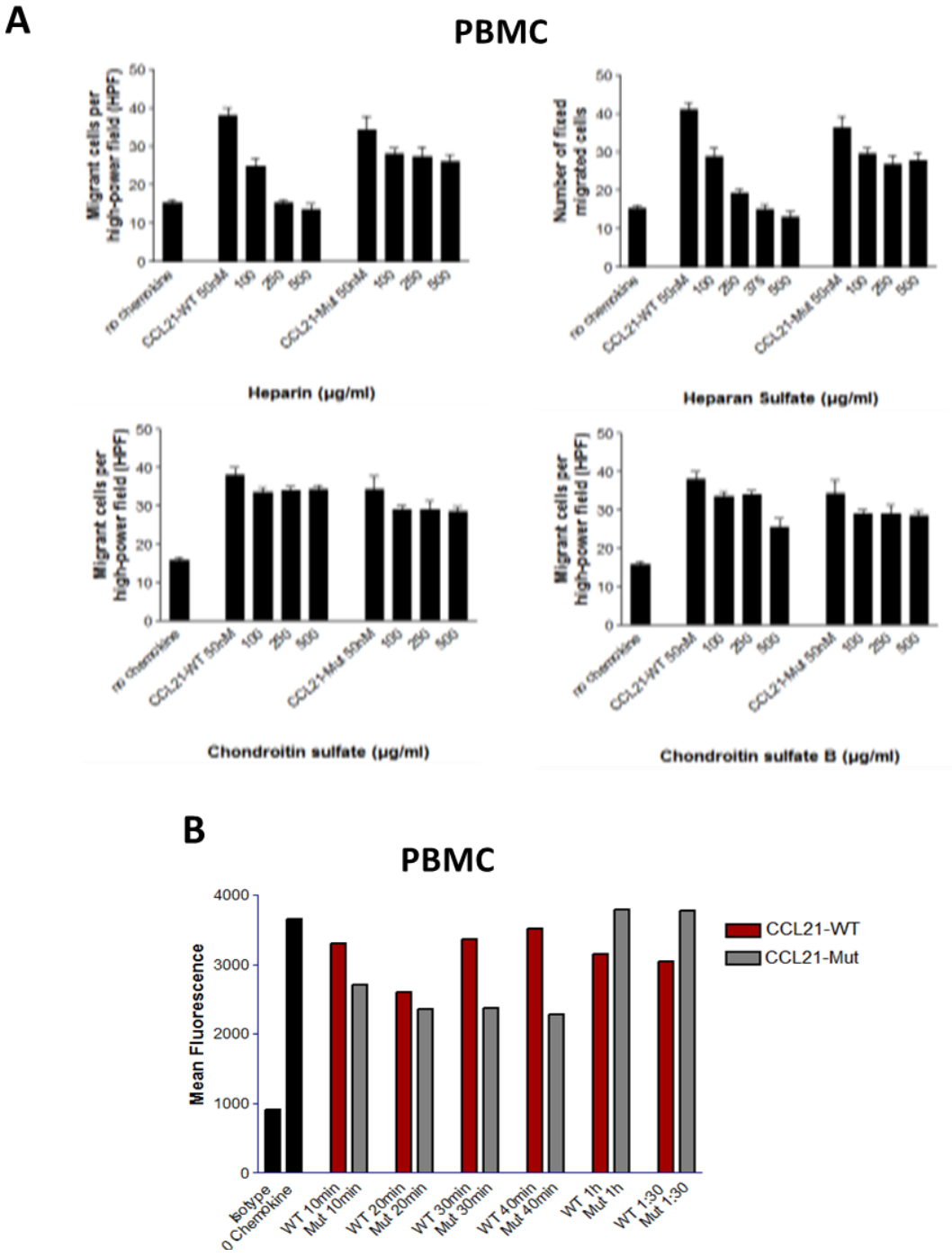

Figure 6-5. Inhibition of PBMC's chemotactic response toward heparin and receptor desensitisation.
(A) 50 nM WT or mutated chemokine were incubated with 100, 250 or 500 µg/ml of heparin (upper left), heparan sulphate (upper right), chondroitin sulphate A (lower left) or B (lower right) before assessing PBMC migration for 2 hours across a 3µm filter. Migrated cells to the bottom well were counted using counting beads and a flow cytometer. Data represent the mean ± SEM of three independent experiments and statistical significance was calculated using one-way ANOVA. **(B)** PBMC were incubated with 20 nM WT or mutated chemokine for up to 90 minutes and changes on surface receptor expression was assessed using flow cytometry.

6.2. SPECIFIC MATERIALS AND METHODS

6.2.1. Creation of an *in vivo* model of breast cancer metastasis

6.2.1.1. *Home Office Licence*

The experiments were carried out in full compliance of the Home Office Project License PPL 60/4497 titled "Investigation and modulation of cell migration", in particular under protocol number 19b4. The license was subsequently amended during the project to include further endpoints to minimise animal suffering, and animals were monitored daily and weighed weekly to ensure their health. All experiments were carried out with the support of Katie Cook and Dr. Ben Millar within the Comparative Biology Centre (CBC) of Newcastle University.

6.2.1.2. *Mice*

6 to 8-week-old female Balb/c mice (Charles River Laboratories) were used for all experiments. Balb/c are an albino, inbred strain of mice stablished in 1913 by Hasley Bagg (Potter, 1985) and commonly used for the study of cancer given their sensitivity to carcinogens (Heppner et al., 2000). This strain was chosen for two main reasons: (a) 4T1 cells were originally isolated from Balb/c mice, making them the perfect host, and (b) their white fur makes them ideal for luminescence observation as it does not absorb the light like C57BL/6's black fur.

Mice were housed in a ventilated cage with a maximum occupancy of 6 mice and given food and water *ad libitum.* Upon arrival, the mice were given one week to acclimatise to the facility before the start of the study.

6.2.1.3. *Creation of a mouse model of breast cancer*

In order to emulate the metastasis from the primary tumour to the draining lymph nodes, we decided to use a syngeneic transplantation model with murine cells in a mouse host. Unlike xenotransplantation models, they do not require an immunocompromised host (Heppner et al., 2000), allowing us to take into account the presence of natural chemokines and chemokines receptors in the recipient mouse. Furthermore, to allow for the assessment of cancer cell dissemination through the lymph vessels and to target cell intravasation, we chose to first generate a primary tumour in the mammary fat pad. Indeed, previous studies have reported that 4T1 injection into the fat pad results in metastasis to the lymph nodes, lungs, liver, bone and brain (Aslakson and Miller, 1992, Yang et al., 2004a). This model

allows for tumour growth simulation in an appropriate microenvironment and mimics the cell interactions that take place at the primary site. This model, known as "spontaneous metastasis", is in juxtaposition to the "experimental metastasis" assay where the cells are injected directly into the bloodstream as circulating cancer cells (Khanna and Hunter, 2005).

Given the lack of consensus in the literature on the number of 4T1 cells to be injected, several cell numbers were tried in order to establish a timeline for tumour growth and metastasis in our chosen model. When harvesting for injection, cells should be (a) 50-60% confluent, (b) of early passage and (c) had been in culture for less than two months (ideally one month). The cells were then passed through an insulin syringe, counted using the Tali Image-Based Cytometer, spun down, resuspended in 100 µl of basal media and kept on ice until injection.

Injections into the mammary fat pad were carried out by Chris G. Huggins in the CBC. Briefly, mice were anesthetised in a 2.5% isoflurane chamber (see Figure 6-6A) and pedal reflexes were tested by pinching the toe pads before placing them under a face mask to maintain anaesthesia during the procedure (see Figure 6-6B). The cells were then mixed to resuspend any settled cells and 100 µl were loaded in an insulin syringe, taking care to remove any air bubbles. The left fat pad was sterilised with 70% ethanol and pinched with tweezers to assist with injection (see Figure 6-6C). Cells were then carefully injected into the fat pad (see Figure 6-6D) and mice were given 1mg/kg buprenorphine as analgesic before placing them back in the cage and allow them to recover from anaesthesia. 3 further doses of buprenorphine were given every 12 hours to assist with pain relief.

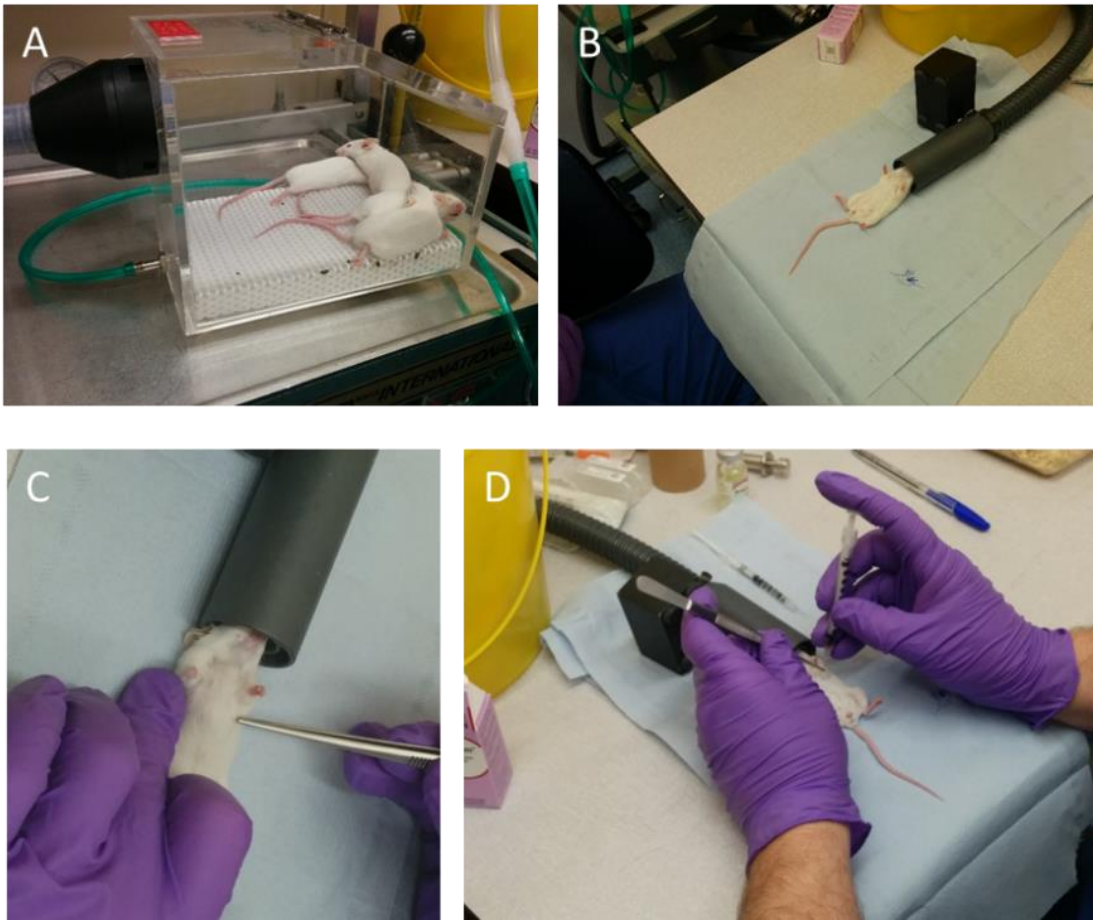

Figure 6-6. 4T1 cell injection into the mammary fat pad.
8-week female Balb/c mice were anesthetised in an isoflurane chamber **(A)** and maintained under anaesthesia using a facemask **(B).** The left fat pad was pinched using forceps in order to expose the nipple **(C)** and 50-100 µl of 4T1 cells were injected using an insulin syringe **(D)**. Mice were then returned to the cage and allowed to recover from anaesthesia.

Mice were weighted and visualised with the IVIS the next day (see section 6.2.5.6.) and weekly thereafter. Tumour growth was monitored daily and measured using callipers, and mice were terminated when the tumour (a) reached 1 cm in two directions, (b) reached 1.5 cm in one direction, (c) ulcerated with skin breakdown, causing a bloody or mucopurulent discharge, or (d) interfered with the mouse's normal locomotion. Tumour volume was then calculated using the following formula (Tomayko and Reynolds, 1989, Euhus et al., 1986):

$$Tumour\ volume = \frac{lenght\ x\ width\ x\ width}{2}$$

6.2.1.4. *Tissue processing*

Several culling methods were attempted, including CO_2 chamber, neck dislocation, cardiac puncture, and overdose of anaesthetic. For the final experiment the latter was chosen, and isofluorane-anesthetised mice were terminated by injecting 200 µl of Euthatal intraperitoneally (i.p.). Overall, it was concluded that CO_2 took too long for *ex vivo* luminescence to be assessed afterwards and *rigor mortis* complicated the organs' retrieval. Both neck dislocation and cardiac puncture complicated the retrieval of lymph nodes, as neck dislocation filled the neck cavity with blood, making the retrieval of superficial cervical lymph nodes impossible; whilst cardiac puncture made removal of the skin from the left side arduous and thus compromised the retrieval of lymph nodes from that side.

After death, the liver, lungs, spleen, fat pad and axillary lymph nodes were harvested and prepared for either paraffin embedding, snap freezing or placed in 100 µl of RNAlater. Briefly, organs for paraffin embedding were placed in an orange cassette and submerged in a 10% formalin pot overnight before being sent to the Histopathology Department of the Royal Victoria Infirmary, Newcastle. For snap freezing, organs were placed on a small piece of blotting paper to remove moisture before being dipped for 10 seconds into liquid nitrogen-cooled isopentane. Samples were then placed in small zip bags and submerged in liquid nitrogen until they could be placed in -80°C.

6.2.1.5. *Tumour visualisation using IVIS*

In order to monitor tumour growth, mice were imaged weekly using the Xenogen IVIS Spectrum In Vivo Imaging System with the assistance of Mr Saimir Luli. Briefly, mice were weighted and injected i.p. with 150 mg/kg of 15mg/ml luciferin (approximately 80-100 µl) before being anesthetised with 2.5% isoflurane and assessing their luminescence at 10 minutes using the IVIS. Luminescence was then quantified by defining a region of interest (or ROI) and determining its average radiance using the Living Image® software (Perkin Elme). The ROI was then applied to all the animals to compare the signals.

Furthermore, on the day of culling two different *ex vivo* imaging strategies were trialled. In the first approach, mice were imaged at 10 minutes and then terminated by cervical dislocation. Their chest cavity was then cracked open, exposing the

organs, and the main tumour removed before being imaged again to visualise any luminescence coming from the organs (Nham et al., 2012). In the second approach, after opening the mouse the desired organs were removed and placed on a plate before imaging with the IVIS. Due to the shorter time required, the first approach was chosen for the final experiment.

6.2.2. Assessment of mutCCL21 efficacy in preventing lymph node metastasis

For the final experiment, two treatment groups of 8 female BALB/c mice and one control group with 2 mice were selected. Given the pilot data, 8 mice accounts for the minimal number needed according to the power calculation with one extra mouse to account for any possible complications due to the rapid growth of the tumour (e.g. mucopurulent ulceration). Briefly, the power of an experiment indicates the probability it can successfully detect a significant difference (p= 0.05) between means, which we set to 80% (Charan and Kantharia, 2013).

On day 0, both treatment groups were injected with 50,000 4T1-Luc cells as described previously, whilst the control group was injected with media. When the tumour became visible (day 7), one treatment group was injected i.v. in the tail vein with 20 µg mutated CCL21 in 100 µl PBS, whilst the second group was injected with 100 µl PBS alone. Treatment was carried out daily for 7 days, and mice were imaged with the IVIS before and after the treatment. On day 18, all mice were imaged again and humanely terminated as tumour size surpassed the established guidelines. A summary of the timeline can be seen in Figure 6-7.

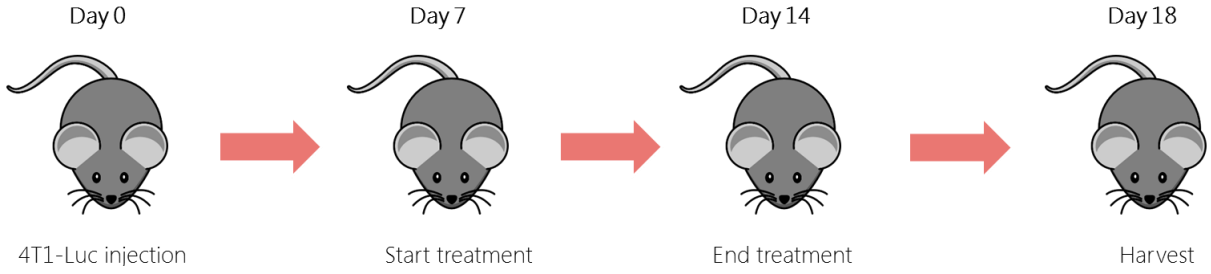

Figure 6-7. Schematic of the syngeneic breast cancer metastasis model.

After sacrifice, organs were imaged *ex vivo* and processed. One lung and half of the tumour was placed in formalin for paraffin embedding, and the other lung and half of the tumour was snap frozen in isopentane. In order to assess lymph node metastasis, it was determined that luciferase expression using qPCR was the most accurate methodology. Thus, 10 lymph nodes were also retrieved and placed in Eppendorf tubes

containing 100 µl of RNA*later*: 4 superficial cervical, 2 axillary, 2 branchial and 2 inguinal. The position of these lymph nodes can be found in Figure 6-8. Lymph nodes were left completely submerged overnight at 4°C before being transferred to -20°C for storage. To extract RNA, lymph nodes were transferred from RNAlater to an Eppendorf tube containing 350 µl of lysis buffer from the RNAeasy kit and homogenised with the Qiagen Tissue lyser II as described in section 2.3.1.2. of the General Materials and Methods.

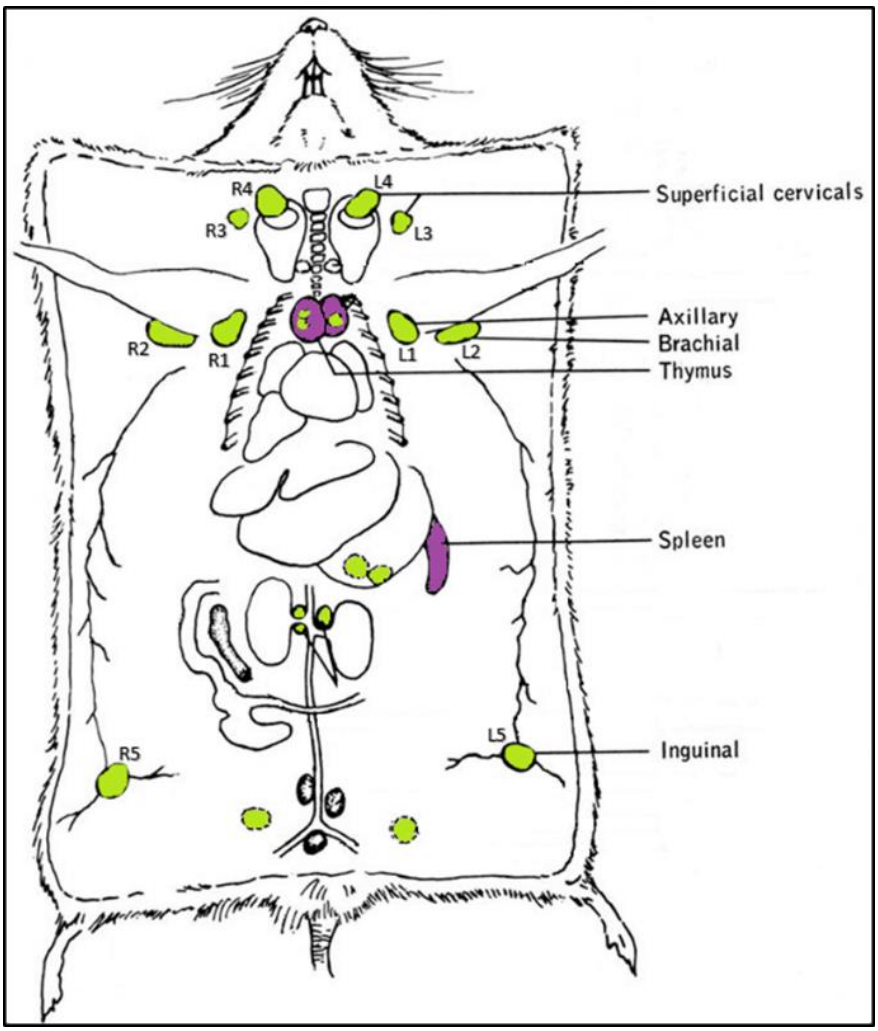

Figure 6-8. Diagram showing the location of the harvested lymph nodes.
Image adapted from Dunn (1954).

6.3. RESULTS

6.3.1. Expression of CCR7 in breast cancer cell lines

CCR7 expression has been widely linked to metastatic spread to the lymph nodes (Cabioglu et al., 2005b, Müller et al., 2001) but expression in breast cancer cell lines, in particular 4T1, has been poorly defined. Thus, CCR7 expression in the available cell lines was assessed at protein level using flow cytometry and at RNA level using qPCR. As can be seen in Figure 6-9, 4T1 was the only cell line that expressed moderate CCR7 levels in both flow cytometry and qPCR assays.

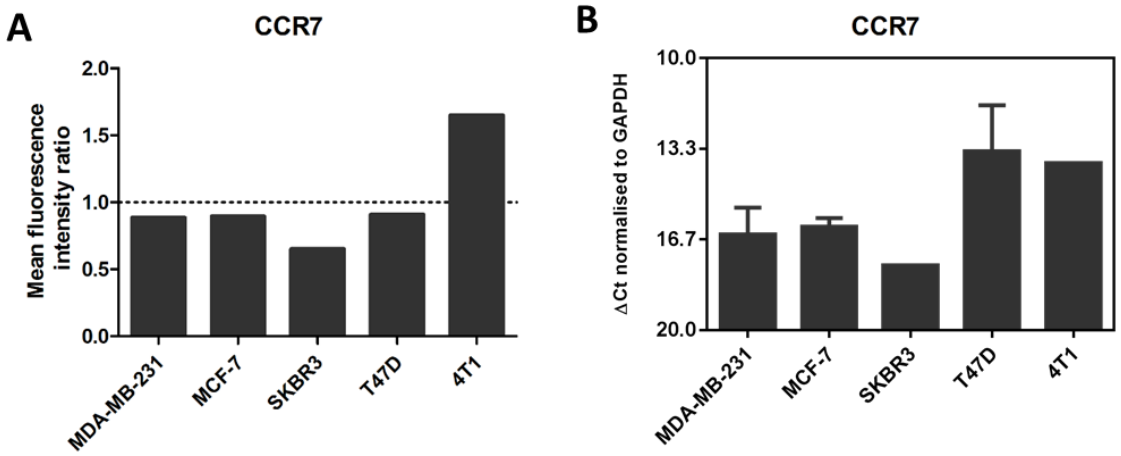

Figure 6-9. CCR7 expression in several breast cancer cell lines was assessed using flow cytometry and qPCR. **(A)** $2x10^5$ cells were stained with anti-human or anti-mouse CCR7-Phycoerythrin (PE) antibody, ran in a FACS canto II flow cytometer (Becton Dickinson) and analysed using FlowJo software. Data represent the ratio between the mean fluorescence intensity of CCR7 and the isotype control of one experiment. **(B)** CCR7 expression was assessed at RNA level using qPCR and normalised to GAPDH. Data represent the mean ΔCt ± SEM of two experiments performed in triplicate.

6.3.2. 4T1-Luc characterisation

In order to validate the cell line used, immunofluorescence of several markers was carried out. Although 4T1 cells have an epithelial origin, many cancers have undergone EMT and will also express mesenchymal markers, thus assessment for both was carried out. This experiment was conducted in collaboration with undergrad student Pan Ching Yeong.

As seen in Figure 6-10, staining for both epithelial makers E-cadherin and ZO-1 is strongly positive on the cell surface where the cell to cell junctions are present. Cells are also positive for the mesenchymal marker vimentin, which extends in the form of filaments in the cytoplasm, and murine but not human CCR7, indicating the antibody's binding site was human-specific. However, CCR7 expression was not restricted only to the cell surface but was also present in the cytoplasm, indicating that part of the

receptor is being internalised. Background fluorescence was assessed through no primary control.

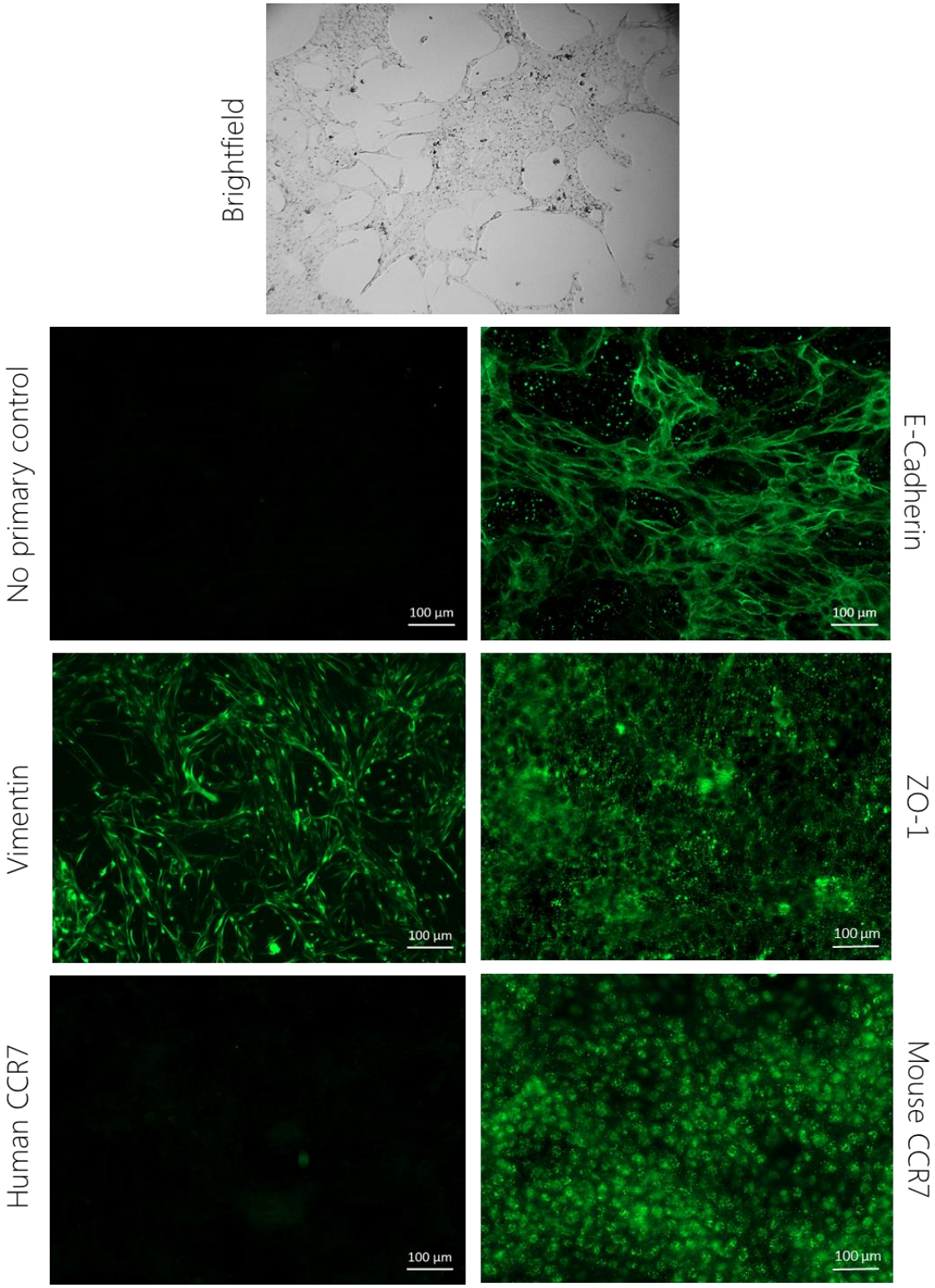

Figure 6-10. Immunofluorescence staining of several markers in 4T1-Luc cells.
4T1-Luc cells were seeded in an 8-well chamber and grown until confluent. Cells were then fixed with ice-cold methanol and permeabilised with triton X-100 before being incubated overnight with antibodies for e-cadherin, vimentin, ZO-1 and human and mouse CCR7. The next day cells were incubated with their correspondent fluorescent secondary antibody and counterstained with DAPI before visualization. No primary antibody (NPA) was included as a control.

Next, luciferase activity of the 4T1-Luc cells was assessed to confirm the presence of the *Luc* gene and the correct synthesis and function of the enzyme. Furthermore, correlation between luminescence intensity and cell number was also evaluated. These experiments were also conducted in collaboration with undergrad student Pan Ching Yeong. As seen in Figure 6-11A, an excellent correlation (R^2 = 0.9705) was observed when assessing firefly luciferase's activity against cell number using the luminometer and Dual-Luciferase® Reporter Assay System. Values for the negative control, the *Renilla* luciferase, were consistently well below 1. An also good but more variable correlation (R^2 = 0.8984) could be observed when cells were incubated with the substrate d-luciferin and its luminescence assessed in triplicate using a plate reader (see Figure 6-11B). As expected, this luminescence diminished with time (slope at 5 min = 0.0056, slope at 15 min = 0.0041). Finally, luminescence detection with the IVIS was also measured. Due to the delay in the addition of the substrate a good correlation could not be determined but we could estimate that cell numbers of up to 15,000 cells could be detected in the presence of cell clusters of 1,000,000 cells (see Figure 6-11C).

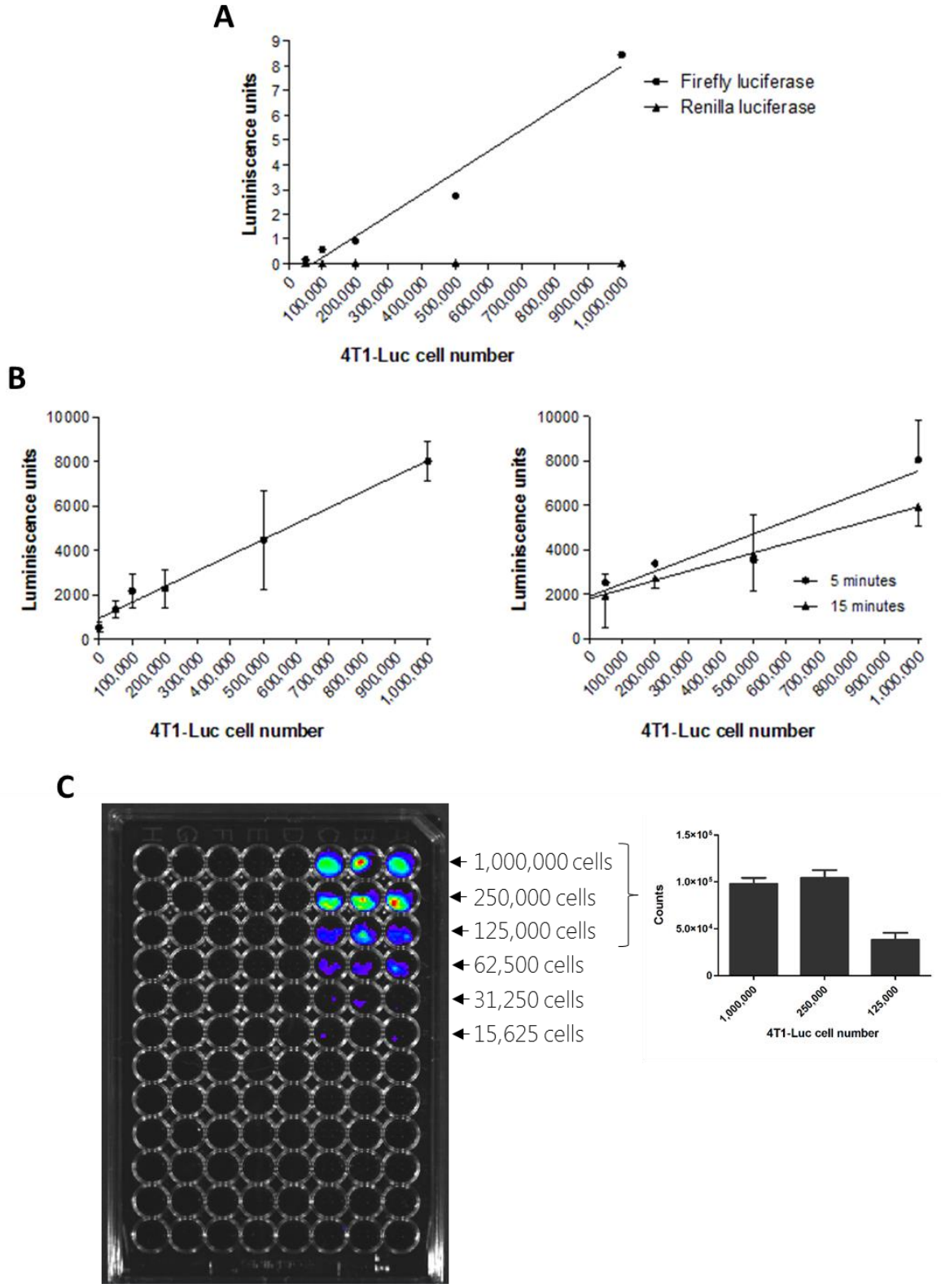

Figure 6-11. Luciferase activity in 4T1-Luc cells.
(A) A range of 4T1-Luc cell numbers were analysed using the Dual-Luciferase Reporter assay system and their luminescence was assessed. Firefly luciferase activity correlates with 4T1-Luc cell number, whilst the Renilla luciferase, which is not present, serves as a negative control (n=1). (**B)** A range of 4T1-Luc cell numbers were placed in triplicate in a 96-well plate and 1 µl D-luciferin was added. Luminescence was assessed using a plate reader 5 minutes later (left). This luminescence diminishes with time (right). Data represent mean luminescence ± SEM (n=1). **(C)** A range of 4T1-Luc cell numbers were placed in triplicate in a 96-well plate and 1 µl D-luciferin was added. Luminescence was assessed using an IVIS spectrum CT system and analysed using Living Image software (n=1).

6.3.3. Effects of mutCCL21 in *in vitro* chemotaxis

After CCR7 expression in 4T1-Luc cells was confirmed, the capacity of these cells to migrate towards CCL21 was determined. Indeed, this was key to ensure that after implantation in the fat pad, 4T1-Luc cells would migrate from the primary tumour towards the lymph nodes where CCL21 is present. Furthermore, it was also assessed that mutCCL21 was capable of significantly inhibiting the chemotaxis of 4T1-Luc cells at a similar level to that observed with MDA-MB-231 and PMBCs.

6.3.3.1. *Trans-filter chemotaxis*

This experiment was conducted in collaboration with undergrad student Pan Ching Yeong. To assess transfilter chemotaxis, cells were allowed to migrate overnight through an 8-µm pore size filter towards different concentrations of WT or mutated CCL21. As seen in Figure 6-12A, there was an increased migration at all chemokine concentrations, with a migration peak at 30 nM for both. However, 4T1-Luc migration was significantly reduced towards mutCCL21 as compared to the WT at both 30 nM and 50 nM concentrations as seen in Figure 6-12B. As reference, an example filter of the number of migrated cells observed with no chemokine, 30 nM mutCCL21 and 30 nM CCL21 WT can be seen in Figure 6-12D. Interestingly, both WT and mutant chemokines induced PBMCs migration at 30 and 50 nm at similar levels (see Figure 6-12C). Indeed, smaller migrations had been observed in previous experiments with PBMCs in comparison to breast cancer cell lines (refer to figure 6-2A).

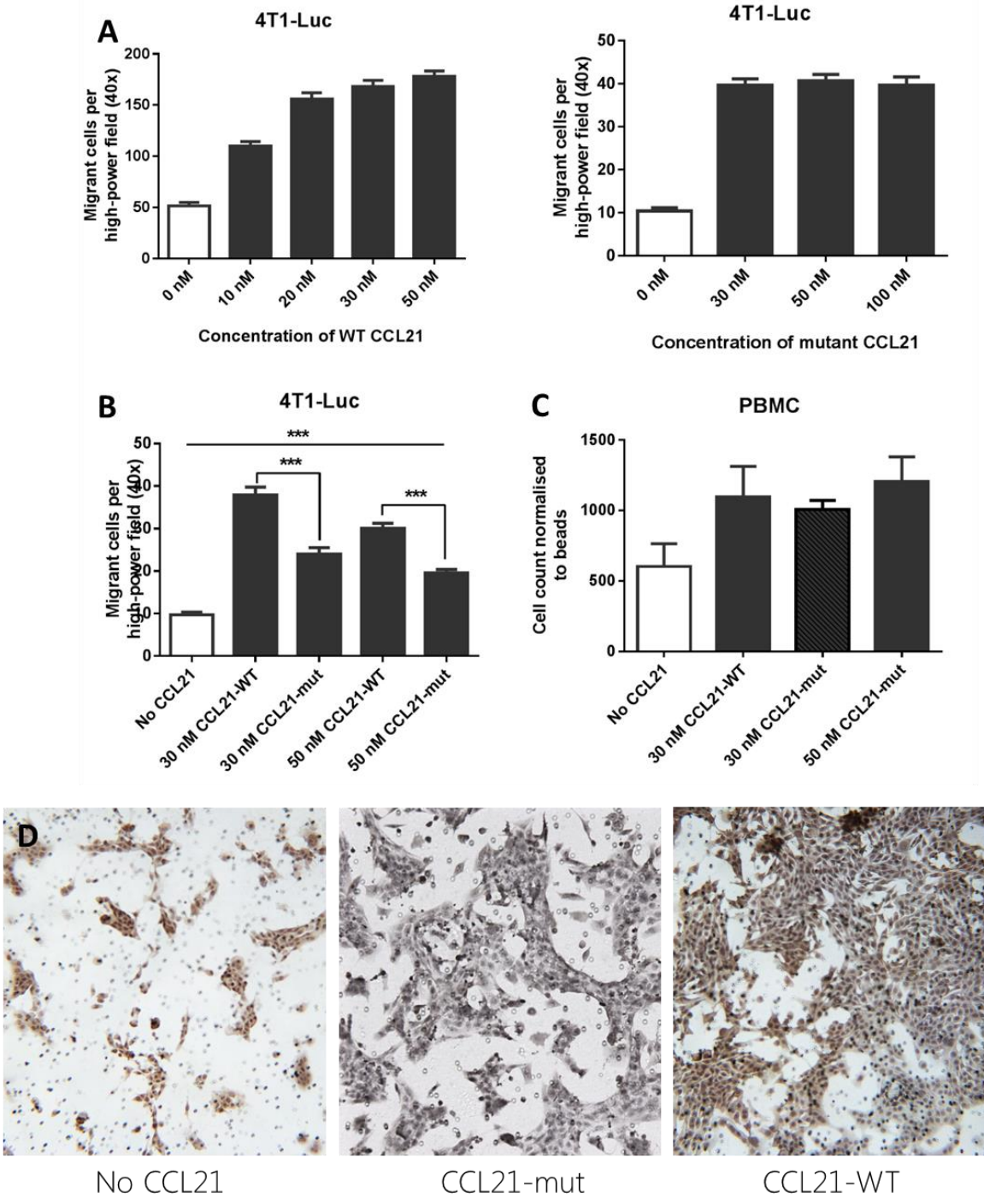

Figure 6-12. Trans-filter chemotactic migration of PBMC and 4T1 cells towards WT and mutated CCL21.
(A) 200,000 4T1-Luc cells were serum starved for an hour before being placed on top of a 8 µm filter above the well containing several concentrations of WT CCL21 (left) or mutated CCL21 (right). Cells were incubated at 37°C overnight and migrant cells counted using a microscope. Graph shows the number of migrated cells adhered to the filter per filter field. Data represent the mean ± SEM of two independent experiments and statistical significance was calculated using one way ANOVA (*p<0.05, ***p<0.001). **(B)** 200,000 4T1-Luc cells were serum starved for an hour before being placed on top of an 8 µm filter above the well containing 30 or 50 nM of WT or mutCCL21. Cells were incubated at 37°C overnight and migrant cells counted using a microscope. Graph shows the number of migrated cells adhered to the filter per filter field. Data represent the mean ± SEM of three independent experiments and statistical significance was calculated using one way ANOVA (***p<0.001). **(C)** 500,000 PBMC cells were placed on top of a 3 µm filter above the well containing WT or mutated CCL21 and left to migrate for two hours at 37°C. Migrant cells in the bottom well were then counted using counting beads and a flow cytometer. Data represent the mean ± SEM of one independent experiment and statistical significance was calculated using one way ANOVA. **(D)** Examples showing migrant 4T1-Luc cells on the filters.

6.3.3.2. *Trans-endothelial chemotaxis*

In order to assess TEM, migration of 4T1-Luc cells through an HMEC-1 monolayer overnight was assessed. Due to the similar morphology of the two cell lines, to distinguish between them the 4T1-Luc cells were labelled beforehand with the live dye orange CMRA and filters were visualised under a fluorescent microscope as seen in Figure 6-13A. However, despite care being taken, part of the monolayer was compromised when removing media and fixing of the filter. Furthermore, sometimes it was difficult to distinguish between fluorescent cells that had migrated through and fluorescent cells that were attached to the other side of the filter due to cells being in more than one plane. In order to assess the percentage of cells that appeared fluorescent but had not migrated, a trial was carried out where the HMEC-1 monolayer and the non-migrated 4T1-Luc cells were wiped off with a cotton q-tip in half of the filters. As seen in Figure 6-13B, fluorescence greatly diminished, indicating that a significant number of false positive cells were being counted. It was thus decided that a separate filter with only HMEC-1 would be used to assess the monolayer integrity and that in the remaining filters endothelial monolayer and non-migrant cells would be scraped off. As seen in Figure 6-13C, 4T1-Luc TEM was significantly impaired when migrating toward the mutated CCL21 in comparison to the WT CCL21, with levels remaining similar to the unstimulated cells.

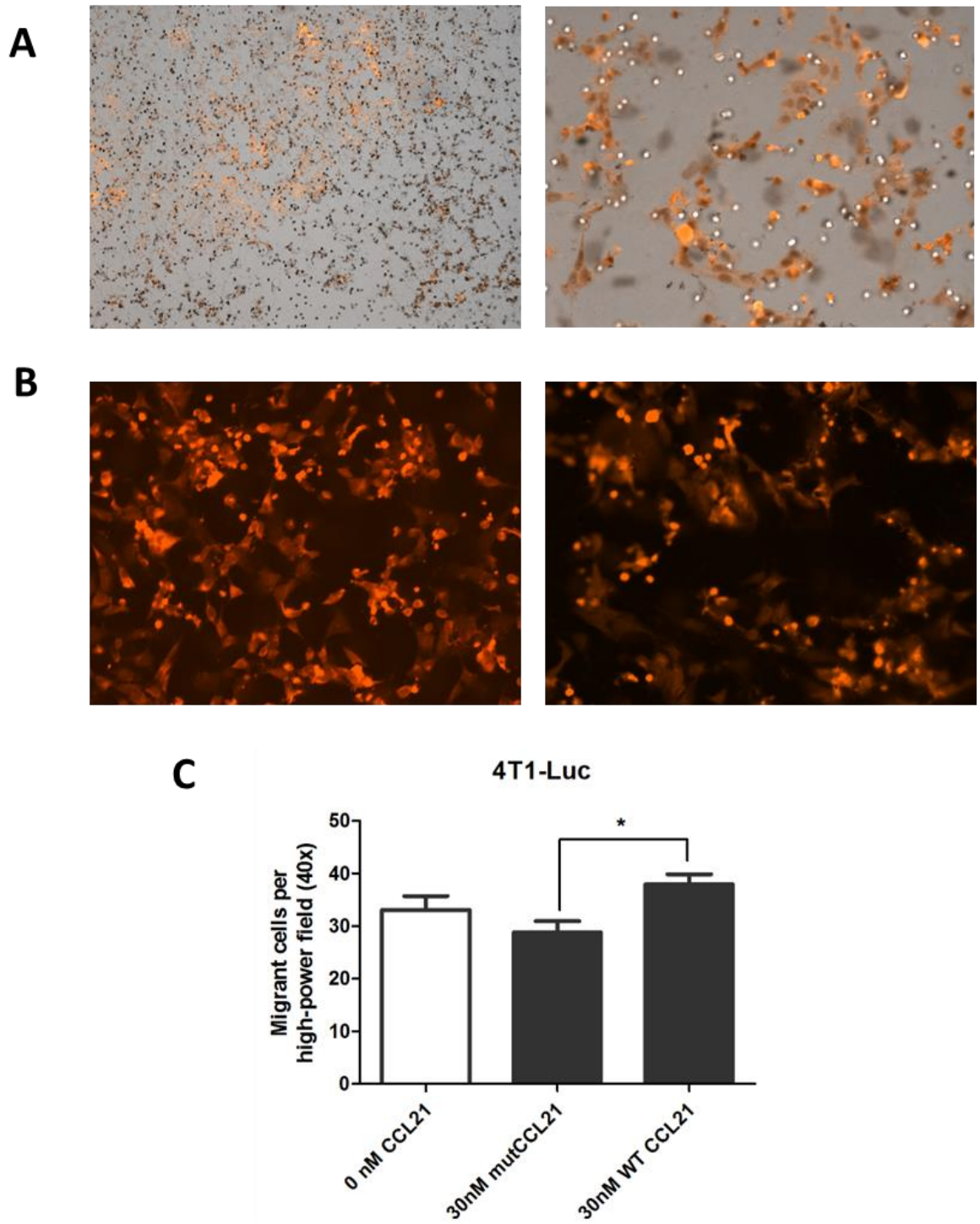

Figure 6-13. Trans-endothelial chemotactic migration of 4T1 cells towards WT and mutated CCL21.
(A) Previous to the chemotaxis assay, 8µm filters were coated with HMEC-1 cells and let to grow until they formed a confluent monolayer. 200,000 4T1-Luc cells were serum starved and stained with cell-tracker Orange CMRA before being placed on top of the coated filter above the well containing WT or mutated CCL21. Cells were incubated at 37°C overnight and filters were observed under a fluorescent microscope, which would allow the distinction of labelled-4T1 cells from the HMEC-1 monolayer. **(B)** In order to ensure that only migrated 4T1 cells were being counted, a trial was carried out where the top of the filter was wiped with a cotton bud, removing the HMEC-1 monolayer and non-migrated 4T1-cells (right). When compared to an intact filter (left), less fluorescence can be observed. **(C)** After TEM, the HMEC-1 monolayer was scraped off with a cotton bud and migrated 4T1 cells were counted using a microscope. Graph shows the number of migrated cells adhered to the filter per filter field. Data represent the mean ± SEM of three independent experiments and statistical significance was calculated using one way ANOVA (*$p<0.05$).

6.3.4. Creation of a murine model for lymph node metastasis: timeline

To investigate the potential of mutCCL21 to inhibit metastasis to the lymph nodes *in vivo,* a spontaneous metastasis, syngeneic murine model was created using female BALB/c mice. Due to the different 4T1 cell numbers used in literature reports, first the optimal cell number to be injected in the mammary fat pad was determined. In order to ensure that the 4T1 cells had time to metastasise to the lymph nodes, the model had to last a minimum of 14 days and a maximum of 28 days. Thus, two sets of experiments were carried out with 5 mice per group: the first one injecting 500,000, 1,000,000 or 2,000,000 cells and the second injecting 50,000 or 100,000 cells into the fat pad.

In order to assess tumour growth, mice were imaged weekly with the IVIS at day 1, day 7, day 14 and day 21 and luminescence was measured 10 minutes post luciferin injection by determining the number of radiating photons in the ROI. An example of the images analysed for the different 4T1-Luc numbers injected can be seen in Figure 6-14. As seen in Figure 6-15, luminescence between the three higher cell groups ($5x10^5$, $1x10^6$ and $2x10^6$) was very similar at day 1 post injection - however by day 7 two of the mice from the highest cohort had been killed due to tumour size, lowering the average luminescence. Overall, on day 7 luminescence increased in all groups in comparison to day 1 but not significantly, and there was no statistical difference among the groups. On day 15, luminescence levels had significantly increased in the 100,000 group as compared to day 1 (but not to day 7) and there was no statistical difference among the groups. On day 21, both lower cell groups' luminescence ($5x10^4$ and $1x10^5$ cells) had significantly increased from day 1 and there was no statistical difference among the groups.

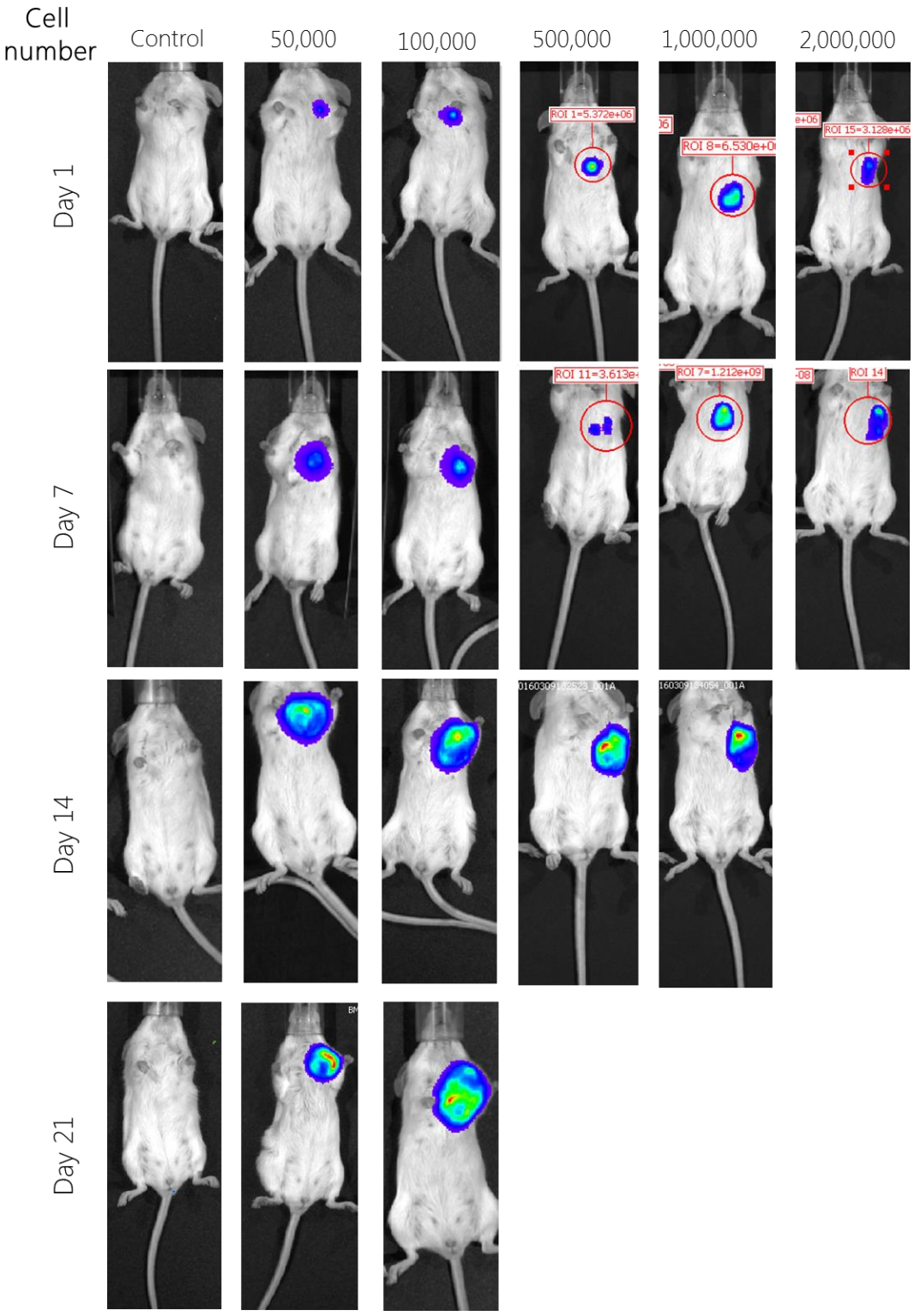

Figure 6-14. Monitoring of tumour growth's progression during three weeks using IVIS spectrum.
$5x10^4$, $1x10^5$, $5x10^5$, $1x10^6$ or $2x10^6$ 4T1-Luc cells were injected into the mammary fat pad of five 8-week female BALB/c mice per group and imaged weekly for three weeks. The animals were killed when the tumour was bigger than 1 cm in two directions or 1.5 cm in one direction. Images representative of one animal per group are shown.

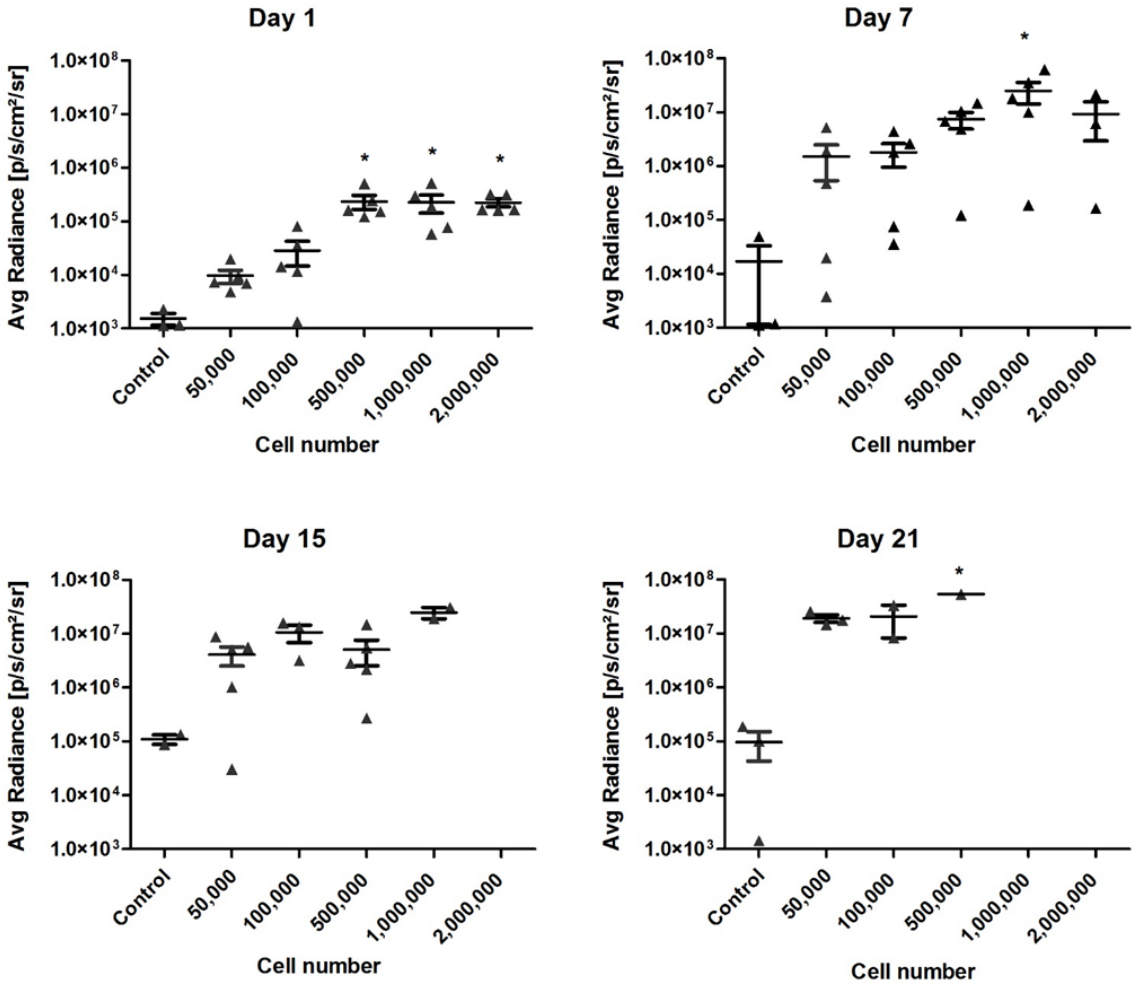

Figure 6-15. Quantification of the primary tumour's luciferase activity throughout three weeks.
After injection with 4T1-Luc cells, animals were monitored weekly to assess tumour growth. Briefly, mice were injected i.p. with 150mg/kg luciferin and then anesthetised with 2% isoflurane before imaging in the IVIS spectrum. Luciferase bioluminescence was measured 10 minutes after luciferin injection for the optimal exposure time and analysed using Living Image software. Each triangle represents the mean average radiance ± SEM of one mouse (experimental group size: n=5) and statistical significance was calculated using a Krustal-Wallis test (*p<0.05).

As described in section 6.2.5.3., mice were terminated when tumours reached a size of 1 cm in both directions or 1.5 cm in one direction. As seen in Figure 6-16A, the two million cells group all had to be killed by day 8, whilst the last mice of the one million cells group were culled on day 16. Most of the 500,000 cells group were terminated on day 15, although the last mouse was alive until day 23. Both the 50,000 and 100,000 groups had a 100% survival up to day 17 but two mice had to be terminated the following day, making day 18 the cut off point for the final experiment. The last mouse from the 50,000 cells group was culled on day 23, whilst the last from the 100,000 group was killed on day 29. Furthermore, as seen in Figure 6-16B there is a significant correlation between the tumour weight and the day of sacrifice, with heavier tumours occurring after day 17 of sacrifice.

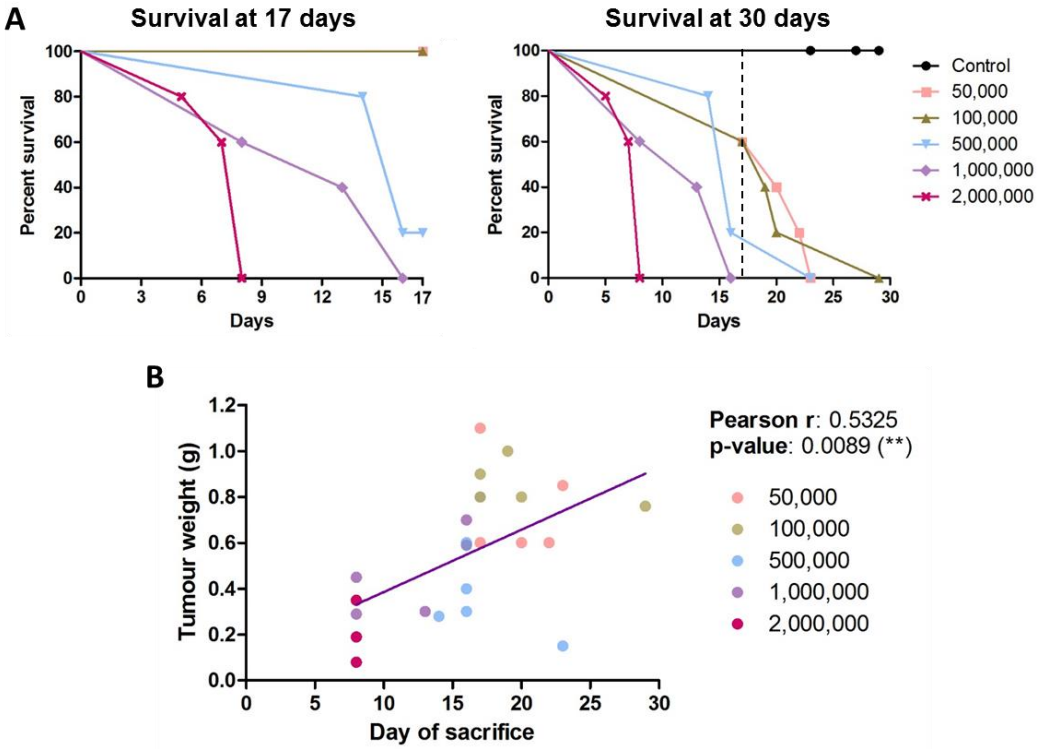

Figure 6-16. Kaplan-Meyer survival curve after injection with different 4T1-Luc cell numbers.
(A) $5x10^4$, $1x10^5$, $5x10^5$, $1x10^6$ or $2x10^6$ 4T1-Luc cells were injected into the mammary fat pad of five 8-week female BALB/c mice and terminated when the tumour was bigger than 1 cm in two directions or 1.5 cm in one direction. A survival curve was drawn for up to 17 (left) and 30 days (right). **(B)** Graph showing the correlation between the tumour weight and the day of sacrifice (p=0.0089, Spearman's rank correlation coefficient (r) =0.5325). Each group is coloured separately (n=24).

The differences in organ weight after sacrifice between groups was also assessed. As seen in Figure 6-17, albeit there was a small downward trend there was no statistical difference in liver or lung weight between the six groups; however spleen weight was raised in most groups, although only significantly in the 50,000 group. Interestingly, tumour weight was significantly increased in groups with 50,000, 100,000 and 1,000,000 cells, particularly the former two, indicating that longer disease time correlates with bigger tumours despite the smaller starting cell number. Furthermore, there was no statistical significance between the 50,000 and 100,000 cells groups or between the 500,000, 1,000,000 and 2,000,000 cells groups.

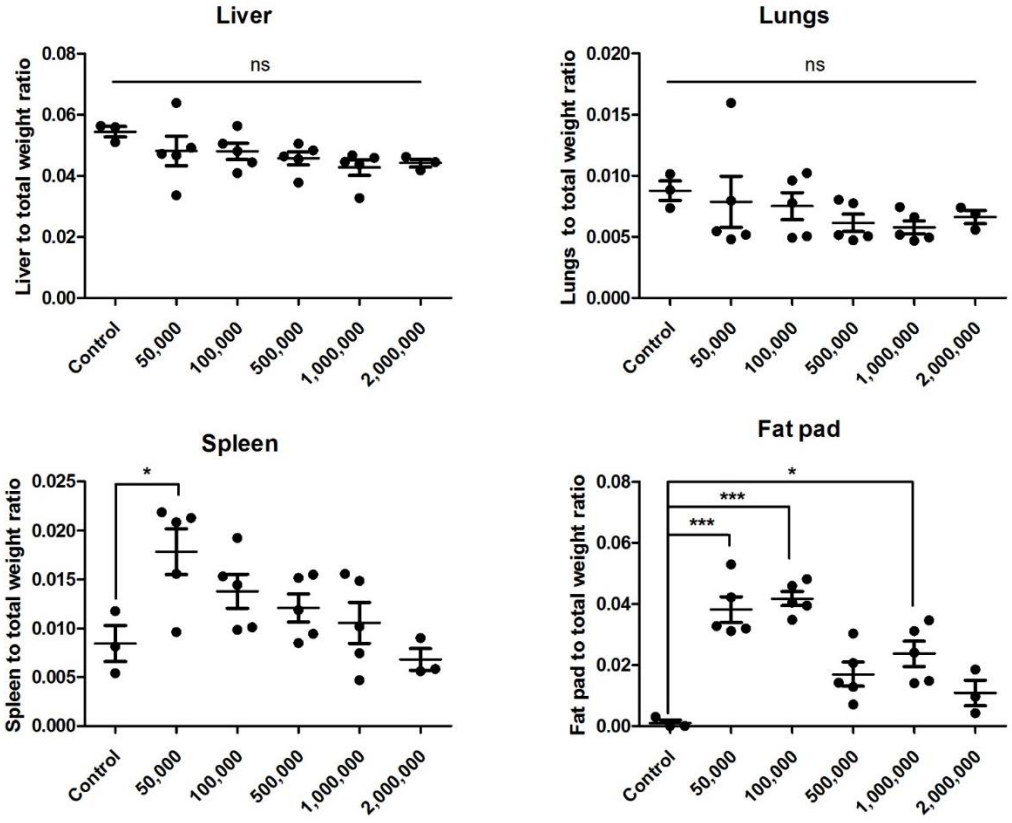

Figure 6-17. Variation on organ weight after sacrifice.
Mice were killed when the tumour was bigger than 1 cm in two directions or 1.5 cm in one direction, and their organs surgically removed and weighted. Organ weight was divided by the mouse total weight in order to normalise their mass. The scatter dot plot shows the individual mice together with the group mean and SEM (experimental group size: n=5); statistical significance was calculated using one way ANOVA (*p<0.05, ***p<0.001).

Overall weight was also assessed to ensure that mice did not lose more than 10% of their weight throughout the experiment. As seen in Figure 6-18, in the lower cell number groups, animals maintained or gained weight whilst in the higher cell number groups, mice lost more weight. In particular, the 50,000 cells group maintained weight the day after cell injection and significantly increased weight on day 16, but lost it by day 21. The same trend could be seen for the 100,000 cells group, with a significant weight gain on day 7 and 16 which was lost by day 21. There was no statistical weight change for the 500,000, 1,000,000 and 2,000,000 cells groups, however they all followed the same trend: small weight loss on day 1 post injection, weight gain by day 7 and progressive weight loss until the final day.

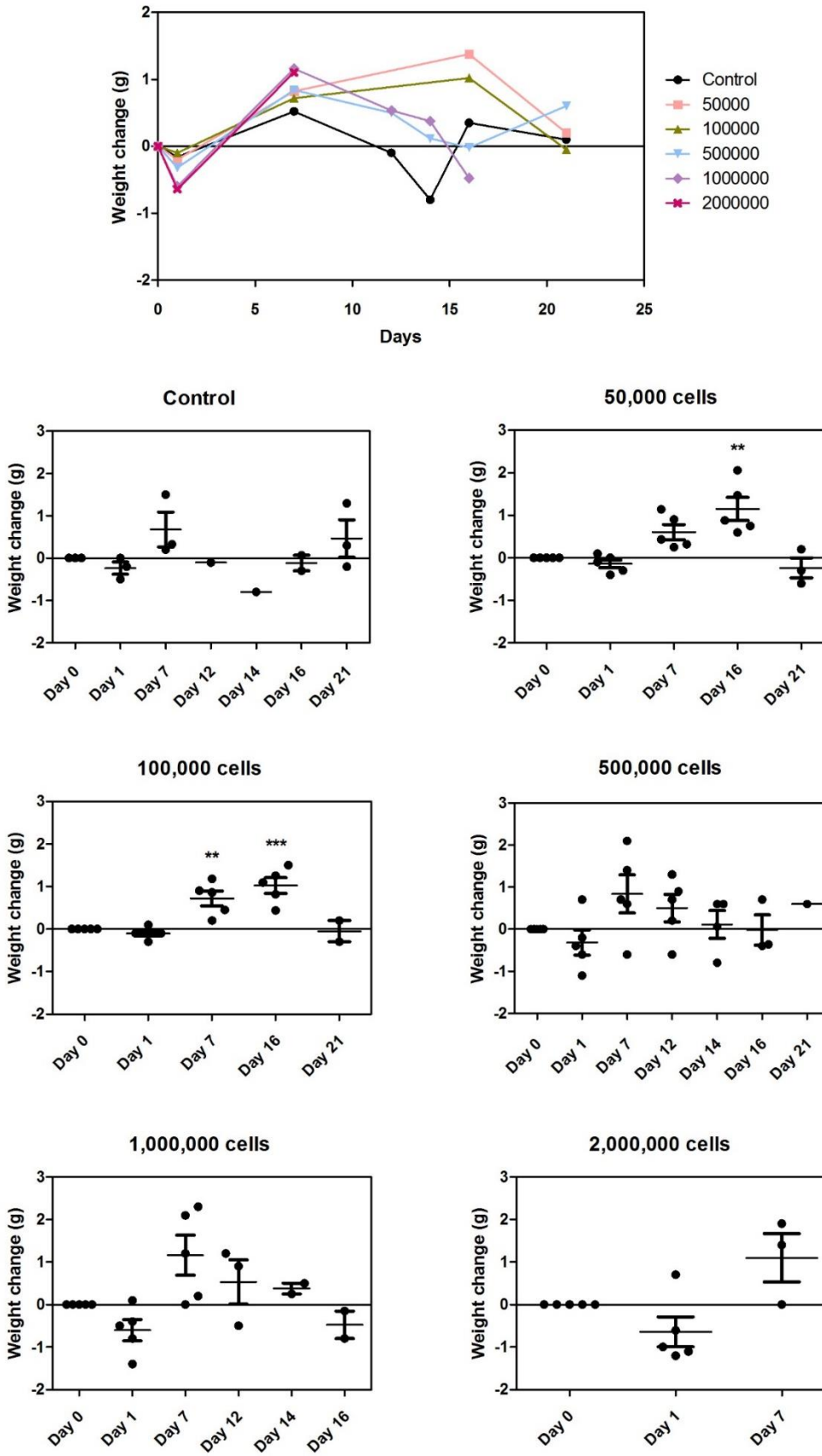

Figure 6-18. Variation on mouse weight throughout three weeks.
Mice were weighted weekly before IVIS imaging and their mass change from week to week was calculated. The scatter dot plot shows the individual mice together with the group mean and SEM (experimental group size: n=5); statistical significance was calculated using one way ANOVA (**p<0.01, ***p<0.001).

6.3.5. Creation of a murine model for lymph node metastasis: luciferase determination

6.3.5.1. *Ex vivo imaging*

During the pilot study, the best methodology to quantify luciferase expression was also determined. First, we assessed the best procedure to assess *ex vivo* luminescence. For the first approach, immediately after culling the mice, the organs were retrieved and imaged using the IVIS at approximately 20 min post-luciferin injection. As seen in Figure 6-19, two small metastases could be observed in the lungs, together with some luminescence in the axillary and mandibular lymph nodes 1, 2 and 4.

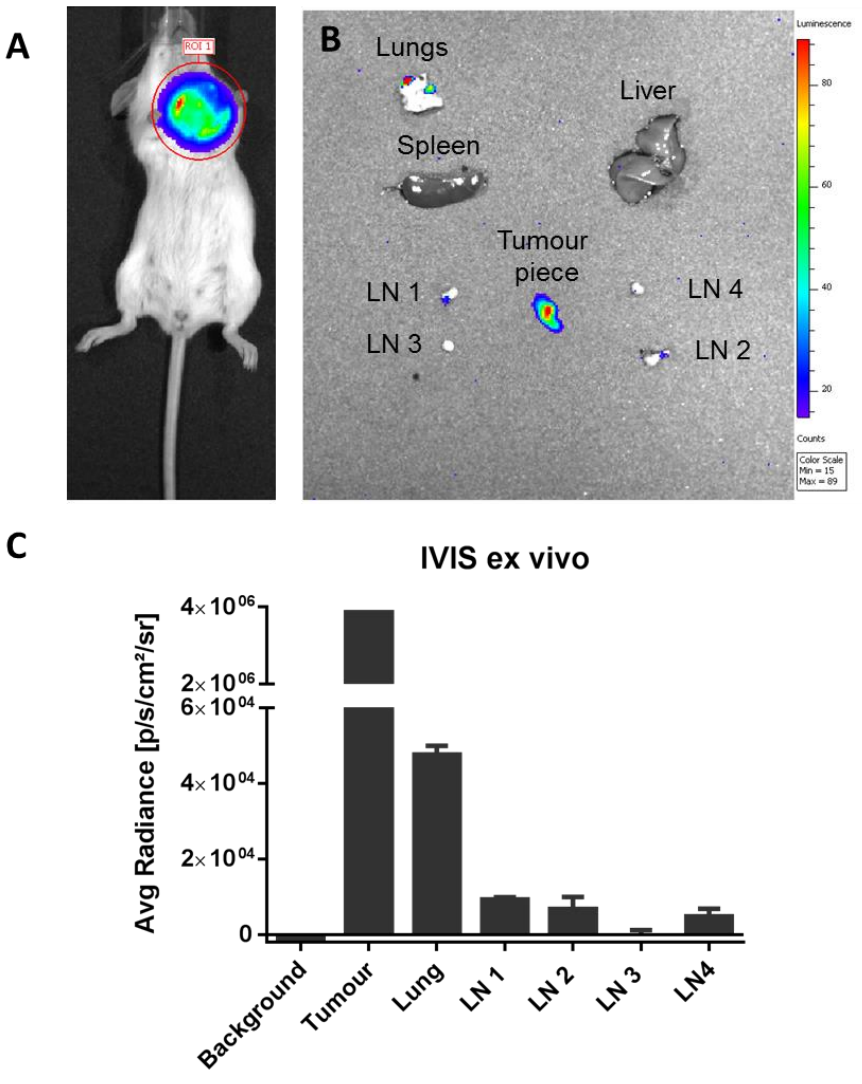

Figure 6-19. Identification of metastasis by ex vivo bioluminescence imaging.
(A) IVIS imaging of mouse injected with 50,000 4T1 cells. Due to the size and high luminescence of the primary tumour, *in vivo* observation of metastasis was difficult**. (B)** On day 23 post-4T1-Luc cell injection, luciferin was injected i.p. and the mouse was terminated 8 minutes later by neck dislocation. Liver, lungs, spleen and axillary and mandibular lymph nodes were surgically removed and visualised 20 minutes post-injection. A small piece of tumour was also imaged as reference. **(C)** Bioluminiscence of several images was analysed using Living Image software. Data represent the mean ± SEM of one experiment (mouse: n=1).

For the second approach, immediately after culling the mouse its chest was opened, exposing the organs, and the tumour was removed in order to observe smaller sources of luminescence. The mouse was then imaged using the IVIS at approximately 15 min post-luciferin injection. As seen in Figure 6-20, small metastases could be observed in the axillary lymph nodes 1 and 2 and the pyloric lymph nodes 3 and 4, in addition to the remaining tumour's luminescence. This approach yielded slightly higher luminescence values due to the shorter visualisation time after injection.

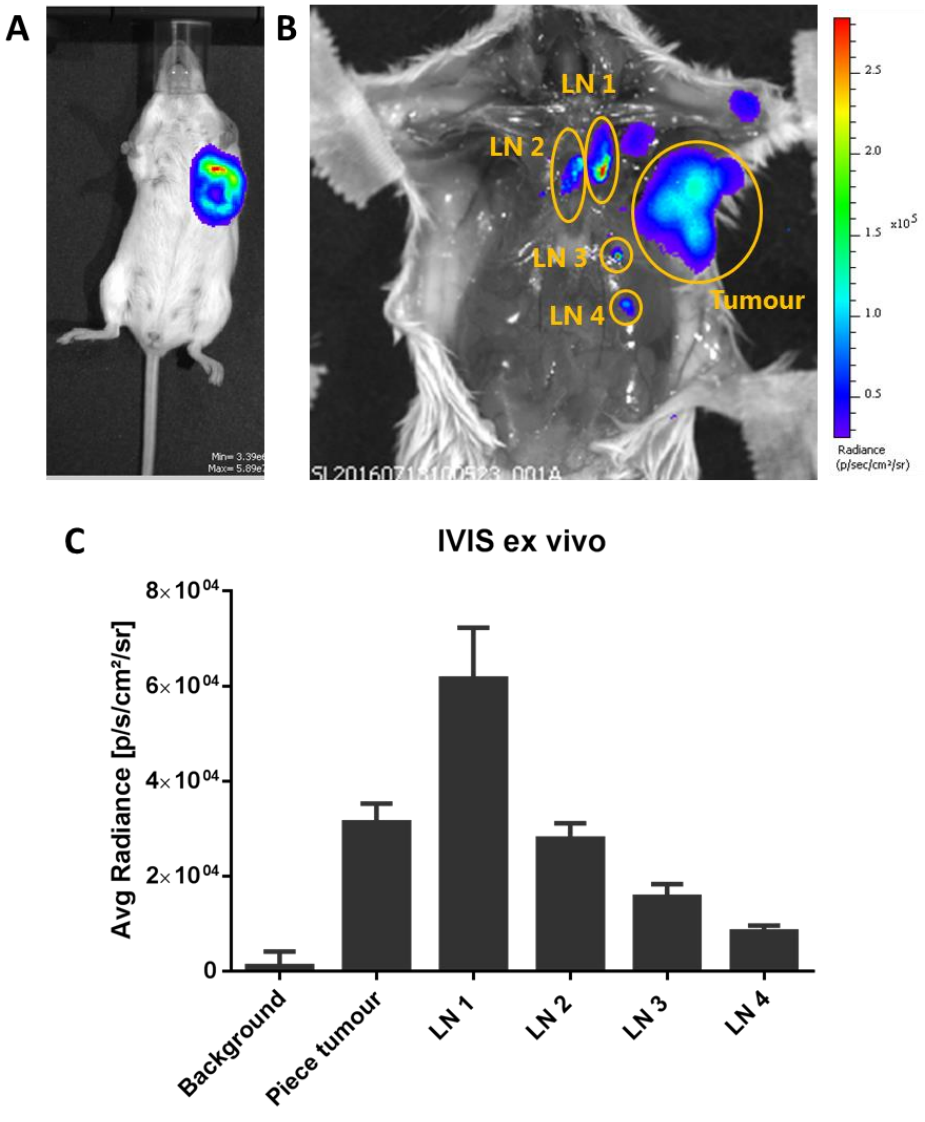

Figure 6-20. Identification of metastasis by ex vivo bioluminescence imaging.
(A) IVIS imaging of mouse injected with 100,000 4T1 cells. Due to the size and high luminescence of the primary tumour, *in vivo* observation of metastasis was difficult. **(B)** On day 29 post-4T1-Luc cell injection, luciferin was intraperitoneally injected and the mouse terminated 8 minutes later by neck dislocation. Skin was pulled away in order to reveal the internal organs and the tumour was surgically removed. The "open mouse" was visualised 15 minutes post-injection. A small piece of tumour was also imaged as reference. **(C)** Bioluminiscence of several images was analysed using Living Image software. Data represent the mean ± SEM of one experiment (mouse; n=1).

6.3.5.2. *Ex vivo luciferase activity*

We also wanted to assess whether luminescence could be detected from tissue that had already been frozen. Previous studies had reported that luciferase activity is stable at -80°C but will start to decay with increased temperature, achieving a half-life of 2 hours on ice (Millar et al., 1992). Indeed, previous studies have successfully measured luciferase activity from frozen murine organs including the lymph nodes (Zhang et al., 2013). We thus cut a small (0.2x0.2 mm aprox.) piece from the tumour, homogenised with pestle and mortar, and assessed luciferase activity using the Dual-Luciferase® Reporter Assay System (Promega). Initially, luminescence was too great to be measured with the luminometer, so a 1:4 dilution was carried out before attempting the assay again. The results can be seen in Figure 6-21 in addition to two negative controls (lysate without substrate; and lysis buffer with substrate but no tissue), demonstrating that luciferase can easily and strongly be detected from frozen tissue. The downside to this method is that comparability is compromised as sample measurement at the precise same time between samples is very arduous, and luciferase is known to have a very variable activity with time.

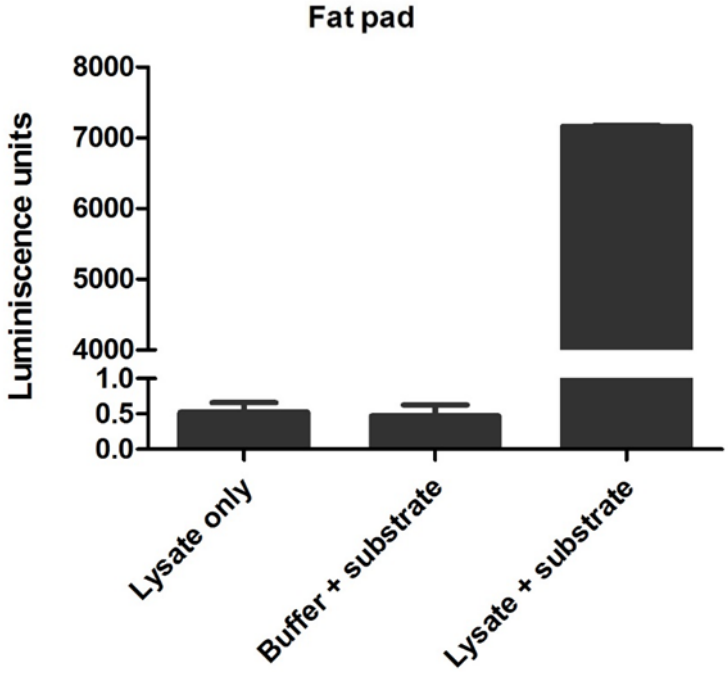

Figure 6-21. Luciferase activity from frozen mouse tumours.
A piece of frozen tumour (~0.2x0.2 cm) from a mouse injected with 50,000 4T1-Luc cells was homogenised using a pestle, mortar and liquid nitrogen. 250 µl of 1xPassive lysis buffer (1xPLB) from the Dual-Luciferase Reporter assay system was added and further homogenised. Lysate was placed into an Eppendorf tube and centrifuged at 12,000g for 2 min at 4°C. 5 µl of supernatant was mixed with 50 µl Luciferase Assay Reporter II (LARII) and bioluminescence measured three times with a luminometer. Lysate supernatant only and PLB with LARII was also measured as reference background (n=1).

6.3.5.3. *Immunohistochemistry of murine tissue*

Detection of luciferase's expression using immunohistochemistry was attempted in the murine lymph nodes. First, staining was optimised in the murine tumour. As seen in Figure 6-22, two different concentrations of antibody (1:50 and 1:80) and three different antigen retrieval pre-treatments (Citrate buffer, EDTA buffer or Trypsin) were tried, but staining was very patchy for all combinations. Nevertheless, citrate buffer was chosen to optimise further.

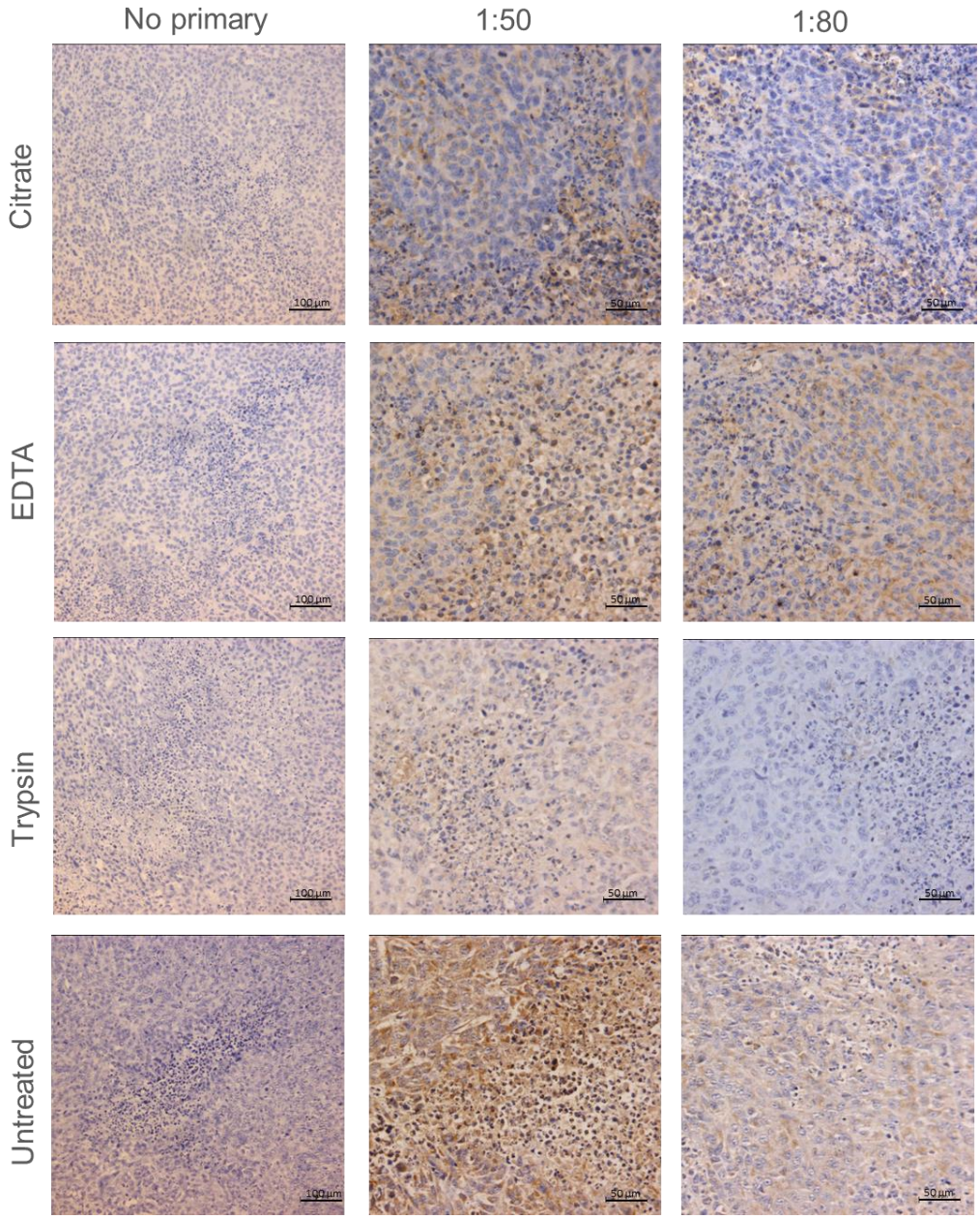

Figure 6-22. Optimisation of luciferase staining using IHC in paraffin-embedded murine breast cancer.
4µm sections from murine tumours were stained for luciferase using immunohistochemistry following three different antigen retrieval pre-treatments (Citrate buffer, EDTA buffer or Trypsin) or no pre-treatment. Two different antibody concentrations, 1:50 and 1:80, were used for two hours at room temperature. Briefly, the protocol from the VECTASTAIN ABC HRP kit was followed and signal was developed using DAB (brown stain) and counterstained with haematoxylin (blue). No primary antibody was used as a control.

Next, staining was carried out at 1:50 and 1:80 for one hour instead of two at room temperature, and at 1:80 overnight at 4°C. However, as seen in Figure 6-23, staining was less intense in all conditions and thus a 1:50 dilution for 2h at room temperature after antigen retrieval with citrate buffer was used in the lymph nodes (see Figure 6-24).

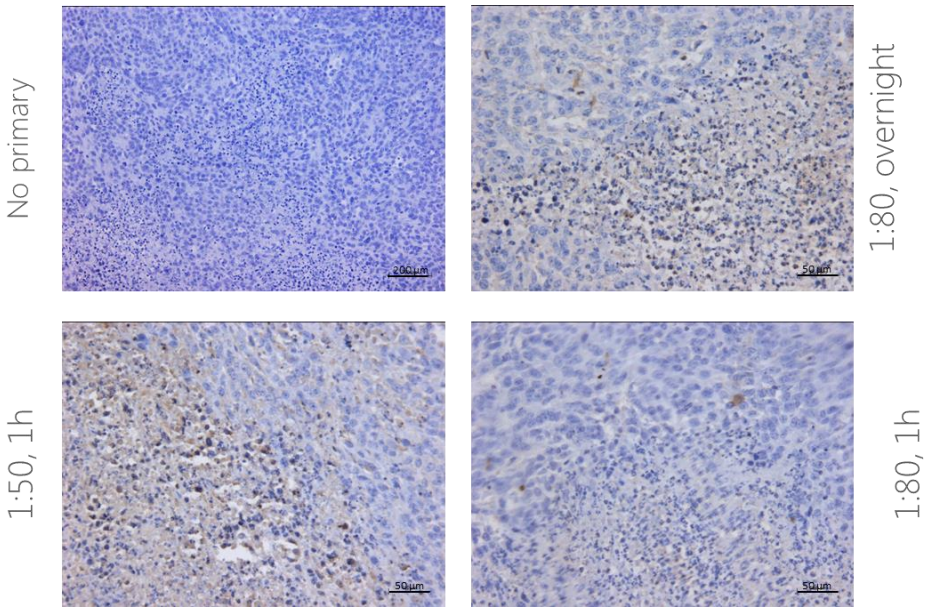

Figure 6-23. Further optimisation of luciferase staining using IHC in paraffin-embedded murine breast cancer. 4µm sections from murine tumours were stained for luciferase using immunohistochemistry following citrate buffer antigen retrieval. Two different antibody concentrations, 1:50 and 1:80, were used for one hour at room temperature or overnight at 4°C. Briefly, the protocol from the VECTASTAIN ABC HRP kit was followed and signal was developed using DAB (brown stain) and counterstained with haematoxylin (blue). No primary antibody was used as a control.

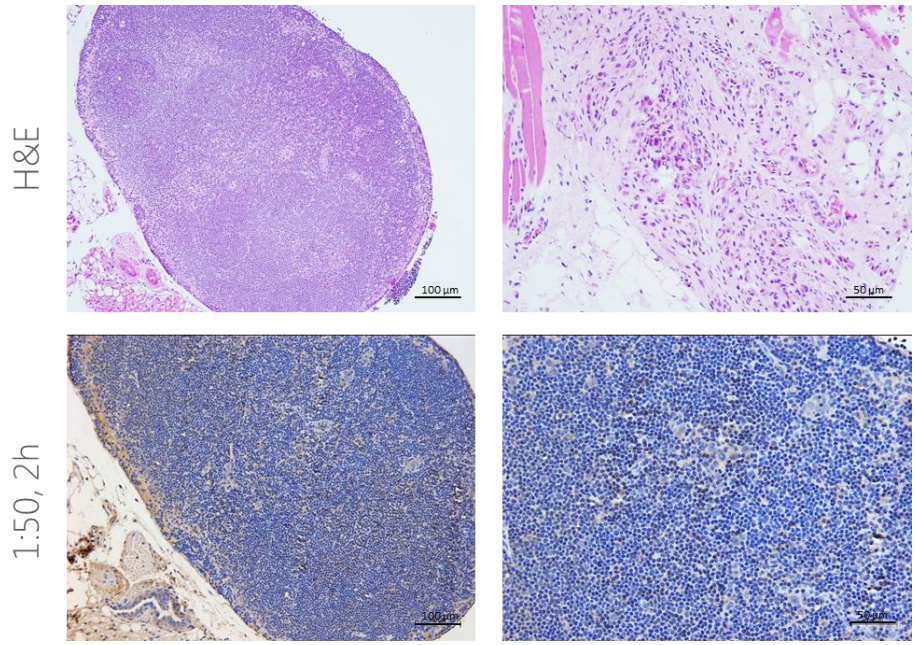

Figure 6-24. Luciferase staining using IHC in paraffin-embedded murine lymph nodes.
4µm sections from murine lymph nodes were stained for luciferase using immunohistochemistry following citrate buffer antigen retrieval at 1:50 for two hours at room temperature. Briefly, protocol from the VECTASTAIN ABC HRP kit was followed. Signal was developed using DAB (brown stain) and counterstained with haematoxylin (blue). H&E images are included for reference.

Although present, luciferase staining was even less clear in the lymph node as compared to the breast tumour. In order to determine whether it was a suboptimal antibody or whether paraffin embedding was not compatible with the antibody, 4T1-Luc cells were grown in a chamber slide and fixed with ice-cold methanol before staining with the luciferase antibody at 1:50 and 1:80 dilutions. As seen in Figure 6-25, staining was much clearer, indicating that the antibody was better suited to use with fresh tissue. Thus, to detect luciferase it was decided to stain frozen tissue embedded in OCT with 1:50 antibody dilution.

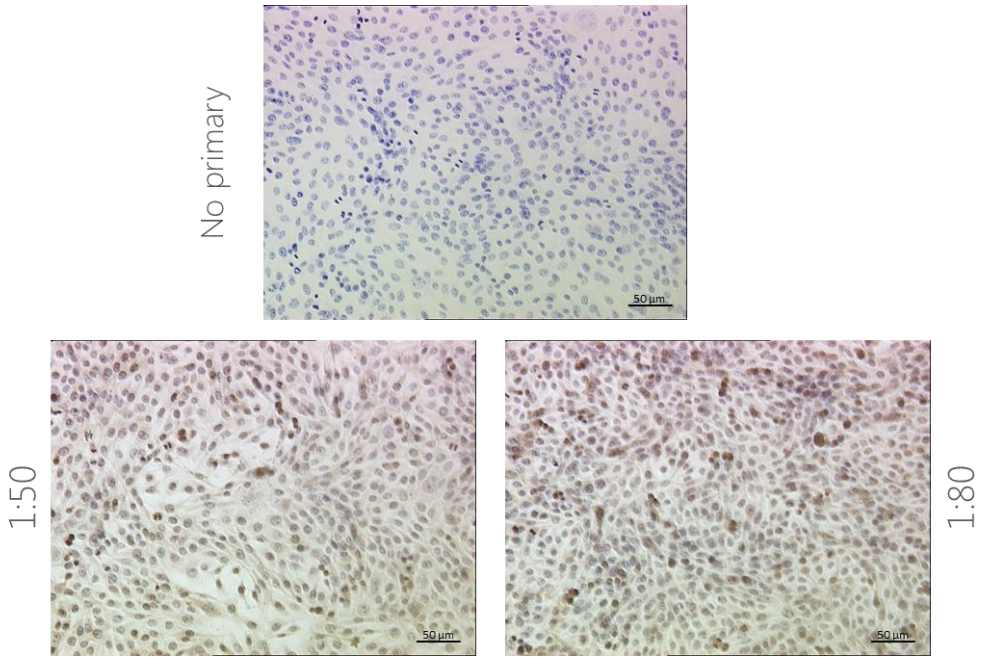

Figure 6-25. Luciferase staining using IHC in fixed 4T1-cells.
4T1-cells were grown in 8-well chamber slides until confluent and then fixed with ice-cold methanol. Two different antibody concentrations, 1:50 and 1:80, were used for two hours at room temperature. Briefly, protocol from the VECTASTAIN ABC HRP kit was followed, signal was developed using DAB (brown stain) and counterstained with haematoxylin (blue). No primary antibody was used as a control.

As seen in Figure 6-26, staining of frozen, OCT-embedded murine breast cancer tissue was much clearer than in paraffin embedded samples, however unfortunately all tissue morphology was lost.

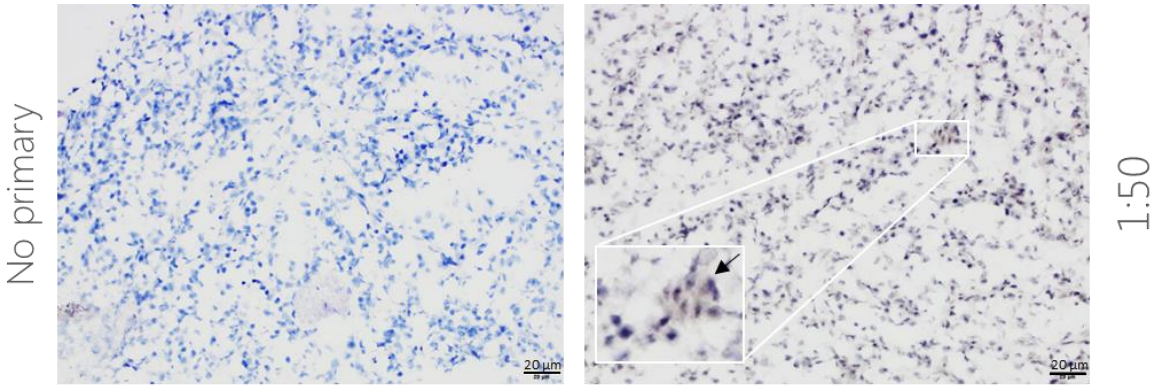

Figure 6-26. Luciferase staining using IHC in frozen murine breast cancer.
7µm sections from OCT-embedded murine tumours were stained for luciferase (1:50) for 1h at room temperature. Briefly, protocol from the VECTASTAIN ABC HRP kit was followed, signal was developed using DAB (brown stain) and counterstained with haematoxylin (blue). An amplified image of luciferase-positive cells can be seen in the bottom left corner and marked with an arrow. No primary antibody was used as a control.

6.3.5.4. *qPCR of murine tissue*

In the final series of experiments, assessment of luciferase expression using qPCR was attempted in the 50,000 and 100,000 cells mice groups. RNA was extracted from small (0.1x0.1 cm) pieces of frozen tumours using the TissueLyser II and the RNeasy extraction kit and Ct levels from four different murine housekeeping genes were assessed. One mouse tumour from the 50,000 cells group could not be processed as it had been embedded in OCT to cut frozen sections from, and thus 9 individual mouse tumours were used for these experiments. As seen in Figure 6-27A (left), HPRT1 was not detected whilst TPT1 and RPI13A presented Cts over 30, indicating low expression, and GAPDH presented in abundant levels with a Ct of 20. Furthermore, an early plateau was observed in HPRT1, TPT1 and RPI13A compared to GAPDH (right), most likely due to the VIC dye not being properly mixed. Thus, GAPDH was chosen to be the housekeeping control. Next, luciferase expression was determined in one murine breast tumour and compared to 4T1-Luc as a positive control, and to the breast cancer cell lines MDA-MB-231, T47D, SKBR3 and MCF-7 as a negative control. As can be seen in Figure 6-27B, the luciferase expression in the tumour is slightly higher than in 1 µg RNA of 4T1-Luc cells, and several cycles lower than all the breast cancer cell lines. Next, we aimed to assess the luciferase expression in the tumours of mice from the 100,000 and 50,000 cells groups. Given

the nature of the untransformed fat pad, very little yield could be obtained from the control mouse and thus its GAPDH came approximately 10 Cts later than the other mice, making normalisation difficult (Figure 6-27C). Nevertheless, luciferase expression was markedly upregulated in all tumours except number 6, most likely due to having extracted RNA from the tumour margins instead of the tumour. At last, we confirmed that there was no relationship between the normalised luciferase ΔCt and how long the tumour had to develop ("day of killing") or the tumour weight (see Figure 6-27D), indicating that there probably is a maximum number of 4T1-Luc cells that can survive in the tumour before there are not enough nutrients or space.

Overall, from the three methods of luciferase detection, qPCR was considered to be the most quantitative and robust for the analysis of a high number of lymph nodes.

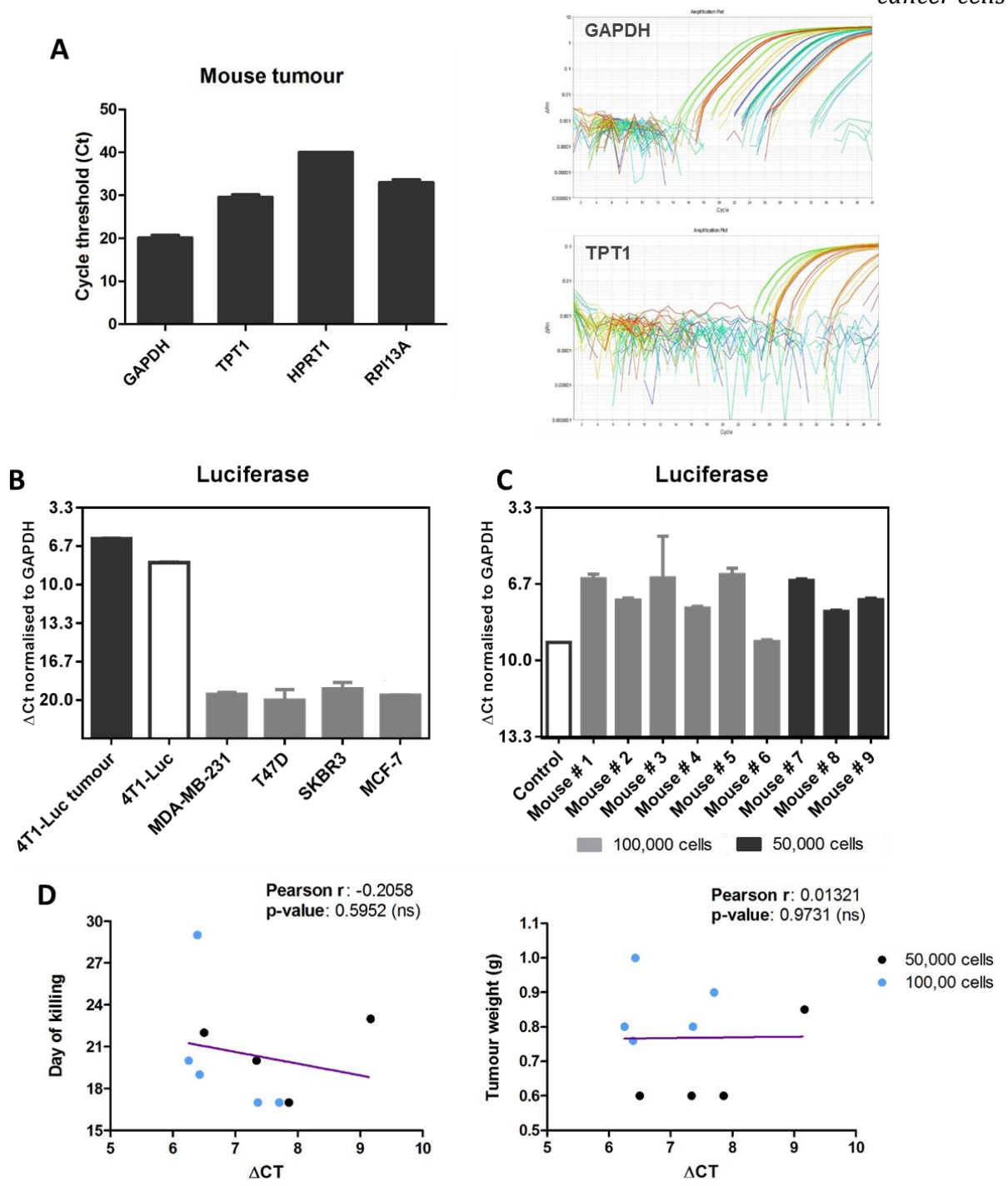

Figure 6-27. Luciferase expression in frozen tumours from mice injected with 50,000 and 100,000 4T1 cells using RT-PCR.

RNA was extracted from frozen murine tumour using the TisueLyser II and Rneasy mini kit (Qiagen) and qPCR was performed. **(A)** Four housekeeping genes (GAPDH, TPT1, HPRT1 and RPI13A) were analysed in order to determine the most suitable one (n=9 mice). Left: Housekeeping's Ct values, right: example of the amplification plots for GAPDH and TPT1. **(B)** Luciferase expression was first assessed in a piece of frozen murine tumour and compared to 4T1-Luc as a positive control and to several breast cancer cell lines (MDA-MB-231, T47D, SKBR3 and MCF-7) as a negative control. Data was normalised to GAPDH and error bars (SEM) show the difference between technical replicates (n=1). **(C)** Luciferase expression in murine tumours. Due to the nature of the fat pad, very little yield was obtained from the control mice, skewing the ΔCt values. Error bars (SEM) show the difference between technical replicates (n=1). **(D)** Graphs showing there is no correlation between luciferase ΔCt and day of killing or tumour weight for the 50,000 and 100,000 cells groups. Statistical significance was calculated using Spearman's rank correlation coefficient (r). Each group is coloured separately (experimental group size: n=9).

Next, luciferase expression from frozen lymph nodes was assessed. RNA concentrations and quality were very variable between the lymph nodes, indicating that snap freezing did not completely preserve the RNA. However, normalised luciferase ΔCt showed that positive lymph nodes were present in both cell groups (see Figure 6-28A), indicating that the killing time was sufficient to see lymph node metastases. As seen in Figure 6-28B, there was a trend between higher luciferase expression and longer cancer growth, but there was no significant correlation between the two.

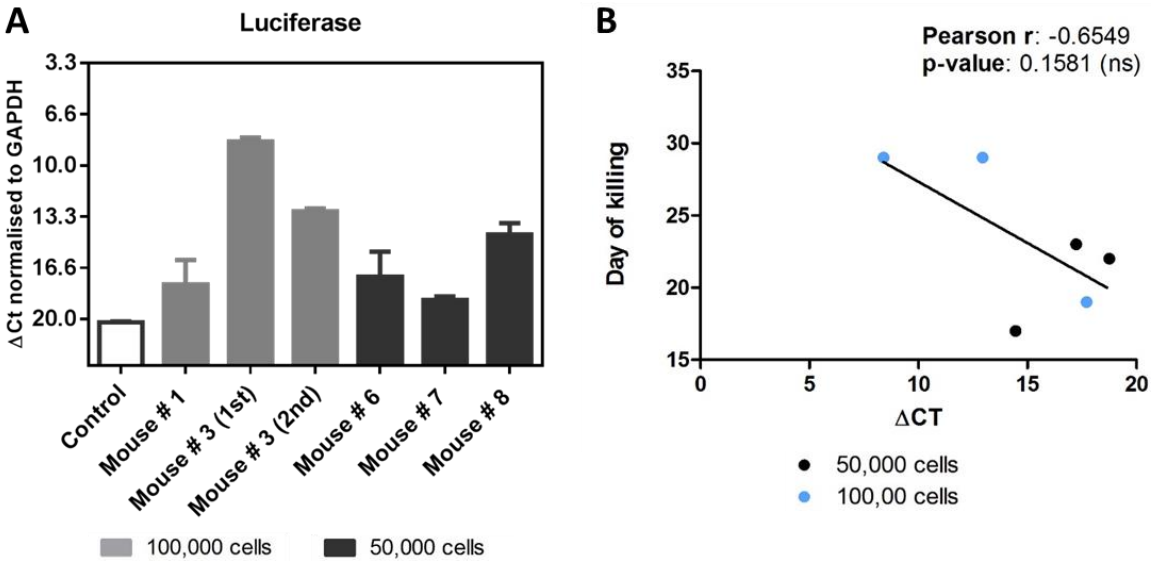

Figure 6-28. Luciferase expression in frozen lymph nodes from mice injected with 50,000 and 100,000 4T1 cells using RT-PCR.
RNA was extracted from frozen murine lymph nodes using the TisueLyser II and Rneasy mini kit (Qiagen) and RTPCR was performed. **(A)** Luciferase expression was assessed in lymph nodes of 6 mice. A great variability in the GAPDH Cts was observed, making the ΔΔCt an unreliable indicator and thus ΔCt was plotted. Error bars (SEM) show the difference between technical replicates (n=1). **(B)** Graphs showing there is no correlation between luciferase ΔCt and day of killing for the 50,000 and 100,000 cells groups. Statistical significance was calculated using Spearman's rank correlation coefficient (r). Each group is coloured separately (experimental group size: n=6).

Thus, for the final breast cancer murine model, it was decided to inject 50,000 4T1-Luc cells in the mammary fat pad, sacrifice the mice at day 18, and then assess the metastasis to the lymph nodes using qPCR for a more quantitative and robust analysis. It was also decided to place the lymph nodes in RNAlater instead of snap freezing them to better preserve the RNA.

6.3.6. Effects of mutCCL21 in in vivo metastasis

The final part of the project involved the treatment of the murine model with mutCCL21 or PBS (8 mice per group) in order to assess the potential of mutCCL21 to prevent the metastasis of 4T1-Luc cells to the lymph nodes of BALB/c mice. Treatment started when tumour became visible (day 7) and chemokine or PBS was injected i.v.

daily for one week. Tumours were monitored non-invasively using the IVIS and measured daily using callipers.

As seen in Figure 6-29A, luminescence for all mice significantly increased from day 1 to day 7 as the tumour grew. Interestingly, no statistical difference could be seen between day 7, day 14 and day 18 for any group, indicating that despite the tumour growing in size, cell death was also taking place – indeed, a couple of mice presented with a grade three dry ulceration with a central cavity, which occurs when cells in the centre of the tumour die due to the lack of oxygen and nutrients. It is also interesting to note that during treatment, tumour luminescence diminished in the mutCCL21 group. In particular, five tumours decreased in size versus two in the PBS group; one remained the same, versus three in the PBS group, and two increased in size, versus three in the PBS group. A more detailed view of this can be seen in Figure 6-29B for both the overall change in luminescence (left) or the individual luminescence before and after the treatment.

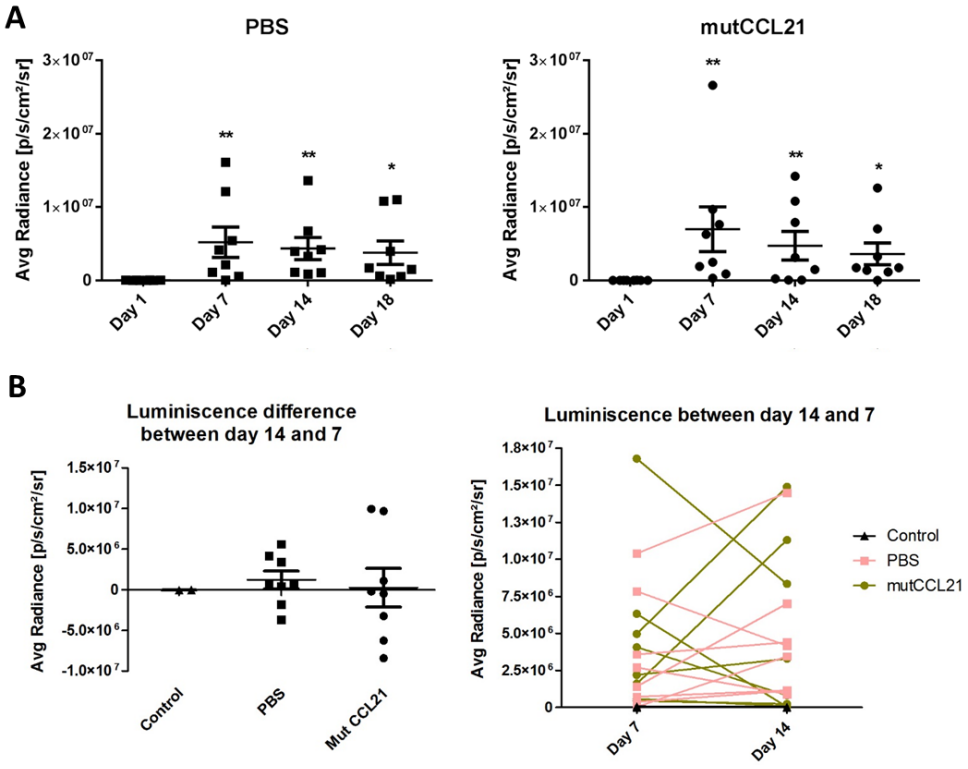

Figure 6-29. Quantification of the primary tumour's luciferase activity throughout 18 days.
After injection with 4T1-Luc cells, animals were monitored weekly to assess tumour growth. Briefly, mice were injected intraperitoneally with 150mg/kg luciferin and then anesthetised with 2% isoflurane before imaging in the IVIS spectrum. Luciferase bioluminescence was measured 10 minutes after luciferin injection for the optimal exposure time and analysed using Living Image software (experimental group size: n=8). **(A)** Overall luminescence on days 1, 7, 14 and 18 post cell injection. Statistical significance was calculated using a Krustal-Wallis test (*p<0.05, **p<0.01). **(B)** Comparison of individual mice luminescence between day 14 (day after end of treatment) and day 7 (first day of treatment). This is plotted as a luminescence difference (left), where negative values indicate tumour luminescence diminished after treatment and positive values indicate the tumour luminescence increased; and as individual mice luminescence (right).

After killing the mice, tumour weight and volume was calculated and compared between the treatment and PBS groups. As seen in Figure 6-30A, the two groups were virtually identical in tumour volume growth, with tumours only increasing slightly until day 12 and then starting an exponential growth. Furthermore, when tumours were harvested and weighted no statistical difference was found between the two groups (see Figure 6-30B). However, it is important to note that in the PBS group one of the tumours had grown inside the chest cavity, making tumour retrieval more difficult and possibly losing part of it. Furthermore, two tumours ulcerated in the PBS group whilst none did in the treatment group, which would also cause a smaller tumour weight.

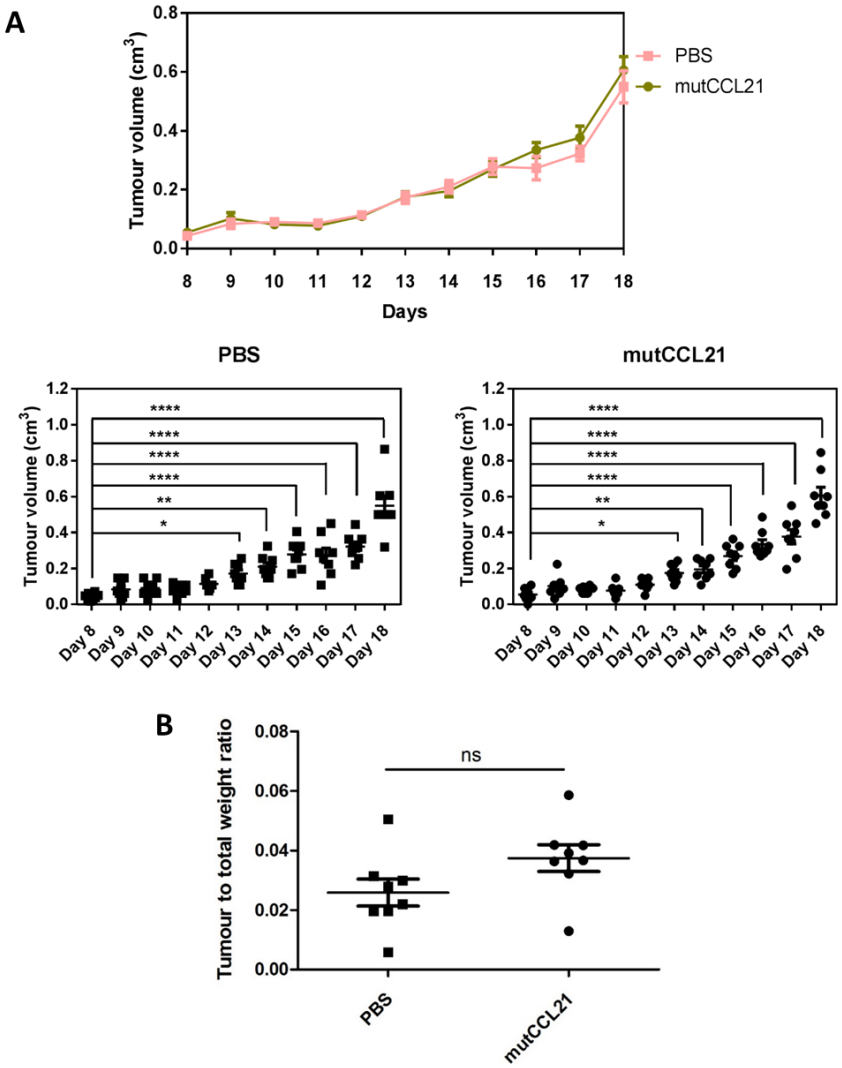

Figure 6-30. Assessment of mice's tumour size.
(A) Tumour length and width was measured daily after tumour became visible and mice were killed when the tumour was bigger than 1 cm in two directions or 1.5 cm in one direction (experimental group size: n=8). Volume was then calculated and plotted as an average (top) or individually (bottom); statistical significance was calculated using one way ANOVA (*p<0.05, **p<0.01, ****p<0.0001). **(B)** Tumour was then surgically removed and the tumour weight was divided by the mouse total weight in order to normalise their mass. The scatter dot plot shows the individual mice together with the group mean and SEM (experimental group size: n=8); statistical significance was calculated using an unpaired t-test.

Next, mouse weight was assessed throughout the experiment. As seen in Figure 6-31, both groups lost a small amount of weight the day after the injection, but that was offset by a significant weight gain by day 7 (start of the treatment). Weight remained the same during the second day of the treatment, but by the end (day 14) only the PBS group had lost a significant amount of weight, whilst the mutCCL21 weight remained stable. By the day of the culling (day 18), weight had stabilised in the PBS group and dropped a little in the mutCCL21 group. No statistical difference was seen in the control group. Overall, mice were slightly healthier in the mutCCL21group.

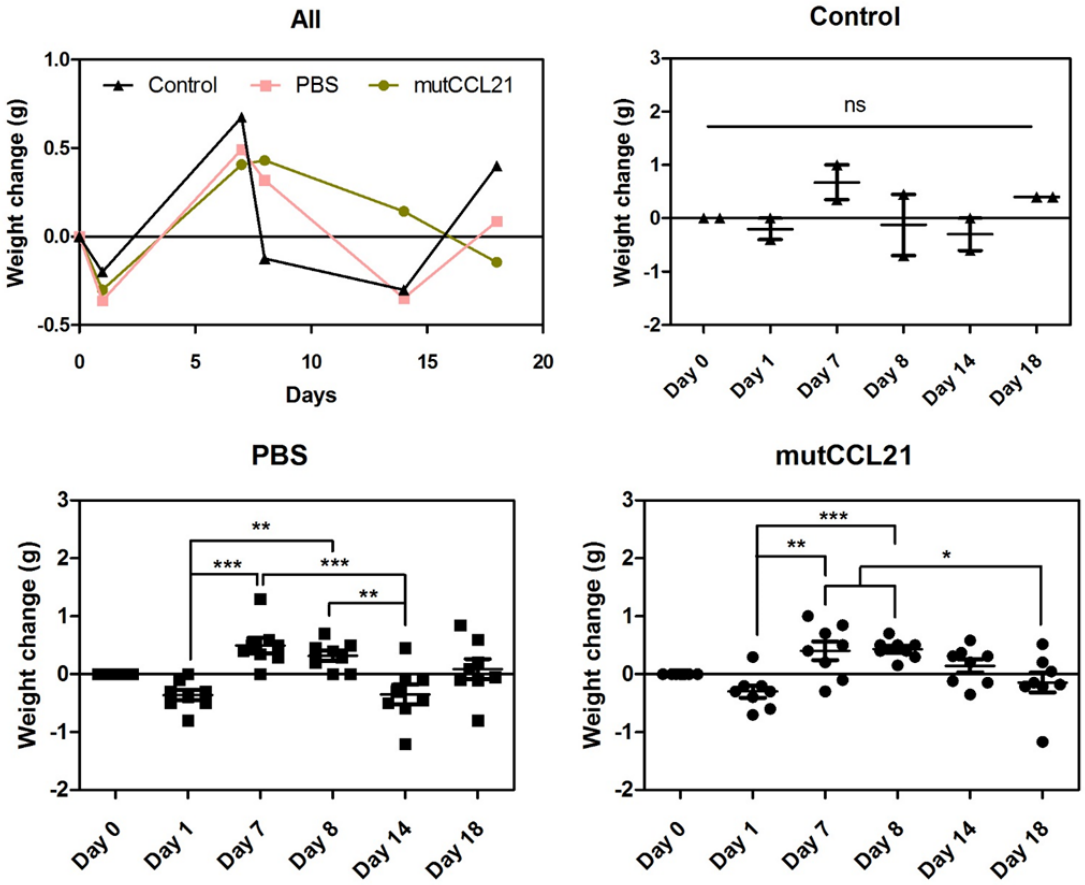

Figure 6-31. Variation on mouse weight throughout 18 days.
Mice were weighted weekly before IVIS imaging and their mass change from week to week was calculated. Mean weight (top left) and individual weights (top right and bottom) are plotted. The scatter dot plot shows the individual mice together with the group mean and SEM (n= 8 mice per group, 2 in control); statistical significance was calculated using a one way ANOVA (*p<0.05 **p<0.01, ***p<0.001).

Finally, lymph node positivity was assessed through *ex vivo* luminescence and luciferase expression using qPCR. As seen in Figure 6-32A, lymph nodes were identified and average radiance calculated; however the difference in luminescence between the mutCCL21 and the PBS groups was not significant. Next, RNA from the axillary and branchial lymph nodes was extracted, and luciferase expression was assessed and normalised to GAPDH. Similarly to what was observed with the luciferase luminescence, luciferase expression change was not significant when all lymph nodes were analysed separately ($p=0.909$, see Figure 6-32B left), however when luciferase expression was grouped and averaged per mouse there was a significant decrease ($p= 0.0205$, see Figure 6-32C left). The remaining superficial cervical and inguinal lymph nodes were mostly negative for both groups, which increased the p-value when analysed separately ($p=0.3202$, see Figure 6-32B right) but decreased it when values where averaged per mouse ($p=0.0148$, see Figure 6-32B right).

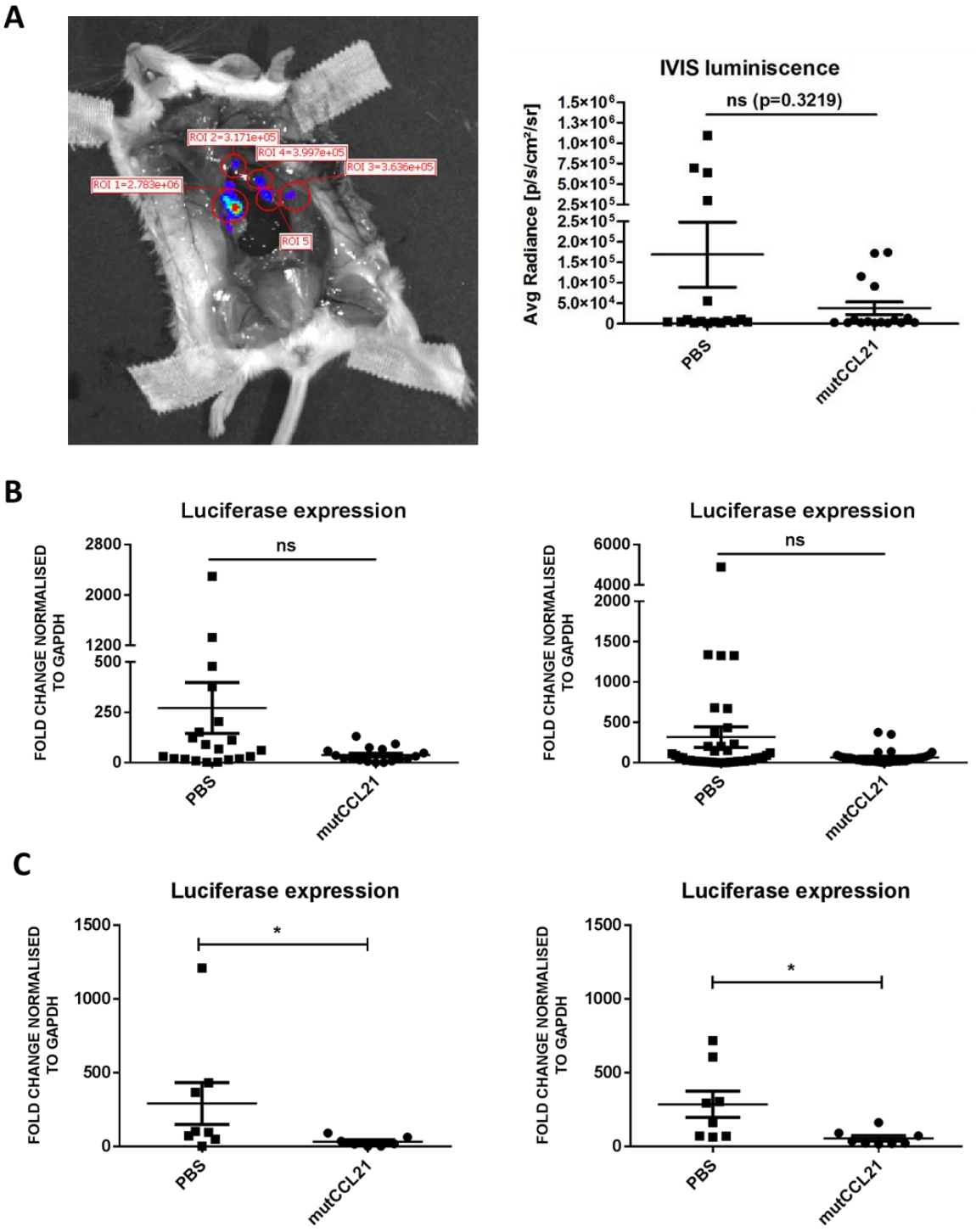

Figure 6-32 Identification of metastasis by ex vivo bioluminescence imaging and RTPCR.
(A) On day 18 post-4T1-Luc cell injection, luciferin was intraperitoneally injected and the mouse terminated 8 minutes later by overdose of anaesthetic. Skin was pulled away in order to reveal the internal organs and the tumour was surgically removed. The "open mouse" was visualised 15 minutes post-injection (left) and positive lymph nodes bioluminiscence was measured and then analysed using Living Image software (right). Data represent the mean ± SEM of 33 lymph nodes and statistical significance was calculated using a Krustal-Wallis test.
Excised lymph nodes were put in RNAlater and RNA was afterwards extracted using the Qiagen Tissue lyser II and RNeasy mini kit (Qiagen). DNase treatment (Promega) was carried out before synthesising cDNA and measuring luciferase expression using qPCR. **(B)** Data represent the mean ± SEM of 37 axillary and branchial lymph nodes (left) or 75 cervical, inguinal, axillary and branchial lymph nodes (right). Statistical significance was calculated using a Krustal-Wallis test (experimental group size: n=8). **(C)** Luciferase expression values of axillary and branchial lymph npdes (left) or all lymph nodes (right) were averaged per mouse and statistical significance was calculated using a Krustal-Wallis test (experimental group size: n=8).

6.4. DISCUSSION

CCR7 was first linked to breast cancer metastasis in 2001, when Müller et al. (2001) reported that the receptor CCR7 was present in both normal and malignant mammary cells but was markedly upregulated in the latter at mRNA level. Since then, CCR7 has been suggested as a biomarker for lymph node metastasis (Cabioglu et al., 2005b) but, unlike CXCR4, few potential therapies have been developed (Pan et al., 2008, Somovilla-Crespo et al., 2013, Schlereth et al., 2012). The potential of a non-GAG binding, truncated CCL21, to prevent metastasis was thus hypothesised: first, the *in vivo* anti-inflammatory potential for non-GAG binding chemokines has been demonstrated by previous studies in the group (O'Boyle et al., 2009, Ali et al., 2010); and second, a CCL19 with a truncated N-ter was successfully used in *in vivo* studies as an antagonist to prevent chemotaxis (Boyle et al., 2016, Pilkington et al., 2004).

CCR7 expression in breast cancer cell lines

When we assessed CCR7 expression by the breast cancer cell lines MDA-MB-231, MCF-7, SKBR3, T47D and 4T1, we found low levels of mRNA in all the cell lines, but only 4T1 expressed detectable CCR7 protein. This is consistent with other studies that report low CCR7 mRNA levels in T47D, MDA-MB-231 and MCF-7 (Müller et al., 2001), low but inducible levels in SKBR3, MDA-MB-231 and MCF-7 (Wilson et al., 2006), and no mRNA expression in MDA-MB-231 (Tamamura et al., 2003). Pan et al. (2008) also described low expression in MCF-7 cells, but conversely to our studies and other literature, reported high expression in MDA-MB-231 cells. In our hands, MDA-MB-231 expressed functional CCR7 as demonstrated by calcium mobilisation after CCL21 stimulation, but expression is low as shown in the PCR studies. This discrepancy could be explained by a difference in the amount of RNA added to the different PCRs, as higher amounts of template would give a stronger signal after amplification.

4T1 characterisation

As discussed previously, 4T1 has an epithelial origin but also expresses mesenchymal markers. Interestingly, studies highlighting the importance of both markers in breast cancer metastasis have been described – on one hand, acquisition of mesenchymal markers such as vimentin causes a higher motility (Xue et al., 2003), which has been linked to increased invasion (Thompson et al., 1994). On the other hand, it has also been suggested that the presence of epithelial markers such as E-cadherin enhances metastatic

potential, particularly during colonisation – indeed, 4T1 cells form more metastasis than other murine cancer cell lines which do not express E-cadherin (Dykxhoorn et al., 2009, Lou et al., 2008). This suggests that although loss of E-cadherin has been linked to metastasis (Onder et al., 2008), expression of both E-cadherin and vimentin could also offer unique advantages in the establishment of new tumours.

With this in mind, we assessed the expression of the epithelial markers E-cadherin and zonula occludens (ZO-1) and the mesenchymal marker vimentin in addition to human and murine CCR7. In common with other studies we found high expression of E-cadherin and vimentin. Indeed, high protein expression of E-cadherin and moderate amounts of vimentin were described in other studies through both Western blotting (Lou et al., 2008, Dykxhoorn et al., 2009, Campbell et al., 2011) and immunofluorescence (Hanai et al., 2005, Lou et al., 2008). We only assessed the expression in 4T1-Luc cells, but other studies reported no difference between luciferase-transfected and parental 4T1 cells (Lou et al., 2008). Robust expression of ZO-1 on the cell to cell junctions was also reported through immunofluorescence (Lou et al., 2008).

4T1 cells also expressed murine CCR7, however the receptor was largely confined to the cytoplasm. This was also reported by Cabioglu et al. (2005b) and (2007) in tumours from breast cancer patients, where over 50% of the tumours expressed cytoplasmic CCR7, a phenomena also observed by Liu et al. (2010) and Andre et al. (2006). This cytoplasmic expression suggests receptor internalisation after ligand binding, and thus is a potential sign of receptor activation. Furthermore, CCR7 expression by 4T1 cells was also corroborated by Leung et al. (2015) and Su et al. (2014) at the protein level.

4T1 migration *in vitro*

Compared to the WT CCL21, trans-filter chemotaxis of 4T1 cells towards the mutCCL21 was impaired, although cells still significantly migrated when compared to the no-chemokine control. This was similar to what was observed in previous studies in the group with PBMC and MDA-MB-231 cells (Malki et al., 2013). This lesser migration towards mutCCL21 could be due to a less potent activation of the G-protein and lack of puncta formation, as discussed by Hjortø et al. (2016). However, conversely to our results, this study also showed that chemotaxis of CCR7-expressing dendritic cells towards 10 nM mutCCL21was increased as compared to the WT, albeit this difference was lost at 100 nM (Hjortø et al., 2016). Nonetheless, it is interesting to note that the chemotaxis index for

both the mutated and WT CCL21 was below 0.5, indicating that migration was smaller than the no-chemokine control. Furthermore, the study was carried out with dendritic and not cancer cells, and chemotaxis was assessed using an Ibidi 3D migration assay instead of a Boyden chamber, which are factors that could also explain the divergent results. Furthermore, other studies reported different results – on one hand, according to Hirose et al. (2002) both chemokines elicit similar calcium flux levels, which should correspond to a similar chemotactic response (Hong et al., 2016). On the other hand, Christopherson et al. (2002) described that heparin can greatly inhibit trans-filter chemotaxis by binding to the GAG-region of CCL21, a similar strategy to our mutCCL21. Indeed, previous studies in our group were also successful in inhibiting CXCL12-mediated trans-filter chemotaxis with heparinoids (Mellor et al., 2007) or heparin (Harvey et al., 2007). Our results, thus, correlate more with the latter reports.

TEM studies show that migration towards mutCCL21 was the same as the baseline control, but was significantly lower than towards WT CCL21. Indeed, it has been reported that CCL21 presentation by GAGs is key for leukocyte rolling and diapedesis (Bao et al., 2010, Weber et al., 2013), the same process involved in lymph node extravasation during metastasis (Lazennec and Richmond, 2010). These results are supported by previous studies, which were also successful in inhibiting CXCL12-mediated (O'Boyle et al., 2009) and CCL7-mediated (Ali et al., 2010) TEM using a similar mutCXCL12 or mutCCL7 which could not bind GAGs.

Mouse model

As described in section 6.2.5.3., a syngeneic mouse model was used in order to best emulate the human disease and different cell numbers were injected. In our hands, 4T1 cells grew very quickly once the tumour reached a certain size, with a lesser number of cells increasing the lifespan just by a couple of days. Injecting $5x10^4$ cells gave palpable tumours within one week and allowed us to monitor tumours for up to 18 days, a quicker rate than most of the studies cited where tumours were just palpable at that stage (Sai et al., 2016). Indeed, there was a wide variation between studies in the number of 4T1 cells injected into the mammary fat pad and the tumour growth rate, although it has been described that as few as 500 cells can initiate a tumour (Miller et al., 1981). A summary of these studies can be found in table 6-1.

Study	***Cell number***	***Length study***	***Palpable tumour***
Lou et al. (2008)	$1x10^6$ cells	56 days	N/A
Su et al. (2014)	$5x10^5$ cells	10 days	N/A
Sai et al. (2016)	$5x10^4$ cells	42 days	Week 2
Tao et al. (2008)	$1x10^7$ cells	6 weeks	N/A
Miller et al. (1981)	$5x10^5$ cells	N/A	Day 8
	$5x10^4$ cells	N/A	Day 21
Yang et al. (2012)	$5x10^5$ cells	21 days	1 week
Redelman and Hunter (2007)	$1x10^4$ cells	29 days	N/A
Pulaski and Ostrand-Rosenberg (2001)	$7x10^3$ cells	6 to 8 weeks	2 to 3 weeks
	$1x10^6$ cells	N/A	4 to 7 days
Bove et al. (2002)	$1x10^4$ cells	23 days	N/A

Table 6-1. Summary of studies injecting 4T1-Luc cells into the mammary fat pad in mice.
Table indicates study, cell number injected, length of the study, and when the tumour became palpable.

The difference between the studies above and ours could be due to cells having been cultured for too long, a variable which other studies did not mention unlike confluency or passage number. Surprisingly, despite having similar dimensions, tumours that had been allowed to develop longer weighted more, indicating they had become more compact. Indeed, cell death in the centre of the tumour was observed for some mice, indicating that the rapid growth could not be supported by the available nutrients. Surprisingly, no other study has reported this despite being a well-known effect (Pulaski and Ostrand-Rosenberg, 2001).

Lymph node metastasis were observed as early as day 14, and were present in most axillary lymph nodes by day 18. In correlation to our studies, 4T1 metastasis were described as early as 8 days (Redelman and Hunter, 2007, Pulaski and Ostrand-Rosenberg, 2001), but overall the average seemed to be two weeks for lymph nodes (Aslakson and Miller, 1992, Pulaski and Ostrand-Rosenberg, 2001, Pulaski and Ostrand-Rosenberg, 1998), three weeks for lungs and up to 6 weeks for the rest of organs (Tao et al., 2008).

Evaluation of mutCCL21 *in vivo*

When establishing a murine model, mimicking the human disease and expected treatment course is key to simulate the cancer timeline in humans. Depending on the characteristics of the drug, including but not limited to half-life, absorption rate, and method of administration of the drug (Checkley et al., 2015), the starting point and frequency of the treatment may vary. For instance, injection of attenuated bacteria is only carried out once (Rosenberg et al., 2002), viruses are injected 3-4 times in total every other day (Kulu et al., 2009, Kasuya et al., 2005) and antibodies are administered biweekly for four weeks (Müller et al., 2001). Furthermore, different treatment schedules for the same drug have also been reported, for instance AMD3100 has been injected subcutaneously every other day for 10 days (Zhang et al., 2013), administered continuously with osmotic pumps (Rubin et al., 2003) or injected just once (Nervi et al., 2009).

For our study, we decided on a 7-day course of treatment from the moment the tumour was palpable, as that has been described as the moment when metastases start (Pulaski and Ostrand-Rosenberg, 1998). Given the very short half-life of chemokines *in vivo* (Lambeir et al., 2001, Zhou et al., 2010) and that CCL21 does not desensitise CCR7 (Otero et al., 2006), constant treatment would have been needed. However, truncated chemokines have been reported to have longer half-lives than their wild type counterparts – for instance, WT CXCL12 was cleared from the circulation 1 hour post injection, whilst mutCXCL12 could still be detected 24 hours later (O'Boyle et al., 2009). Thus, it was decided that daily injections would be sufficient to maintain a therapeutic level of mutCCL21 in blood. However, the number of injections was limited due to (a) the amount of mutCCL21 we possessed and (b) the number of IV injections in the tail vein that could be carried out before fibrosis of the tail made it impossible. After careful consideration, we decided that daily injections for 7 days would keep a constant source of treatment yet cover most of the mice's lifespan.

When analysed separately, the mutCCL21 effect was not significant due to the high number of negative lymph nodes; however, when the fold change was averaged per mice, a significant decrease could be observed. In particular, no mice had particularly positive lymph nodes overall in the mutCCL21 group, whilst three (when considering only axillary and branchial LN) or four (when considering superficial cervical, axillary, branchial and inguinal LN) mice were particularly positive in the PBS group.

In particular, 15 lymph nodes were positive in the PBS cohort (36.6%), whilst only 5 were positive in the mutCCL21 cohort (14.7%), an almost 60% decrease. Furthermore, when looking at very positive lymph nodes (over a 300-fold increase), this was reduced to 8 lymph nodes (19.5%) and 2 lymph nodes (5.9%), an almost 70% decrease. This is consistent with other studies that report a similar reduction (50-30%) in lymphocyte homing to the peripheral lymph nodes in mice that lacked HS in their HEV, thus abrogating the presentation of CCL21 *in vivo* (Tsuboi et al., 2013) and causing an increase in leukocyte rolling (Bao et al., 2010). This suggests that lack of chemokine presentation by HS can hamper but not completely abrogate TEM. Interestingly, *in vitro* studies with HUVEC that lacked HS expression showed impairment of CCL2-mediated TEM in neutrophils but not T-cells (Stoler-Barak et al., 2014), indicating that this process may be dependent on cell type and chemokine being presented. Another point to consider is that targeting the chemokine pathway alone has not always given significant efficacy (Duda et al., 2011, Kozin et al., 2010) but has been very effective when in combination with other therapies such as the chemotherapeutic compound BCNU (Redjal et al., 2006), cyclophosphamide (Murakami et al., 2009a, Lee et al., 2006) or an anti-CTLA antibody (Lee et al., 2006); and should be investigated further with our mutCCL21.

Finally, no effect was observed in the final size of the primary tumour. This is not unexpected as unlike CXCL12, CCL21's homeostatic role is exclusively in homing and inflammatory migration and not in development (Förster et al., 2008, Epstein, 2004). However, other studies have reported that whenever CCL21 is overexpressed by the tumour, the effect is reversed – instead of the tumour cells migrating towards the lymph nodes, T-cells, dendritic cells and NK cells are attracted towards the site of the tumour, infiltrating it and decreasing its growth rate (Nomura et al., 2001, Vicari et al., 2000, Sharma et al., 2000, Yousefieh et al., 2009). This highlights the importance of the site of injection when therapy is administered – indeed, there are studies investigating fine-tuning chemokine delivery with polymers (Lin et al., 2014b) and nanocapsules (Kar et al., 2011) to target the relevant tissues. This effect seems to be dependent on the amount of CCL21 being released (Novak et al., 2007), and thus could be correlated with the modest effect our mutCCL21 had on tumour growth during the therapy.

Another aspect to consider is whether the ulceration of the tumour in two mice of the PBS group had an effect on the subsequent metastasis. Tissue necrosis is not uncommon, and can occur when tumours develop subcutaneously if the injection site was close to the

derma of the host (Wallace, 2000). On one hand, cell death diminishes the chances of cancer cells to migrate, but on the other hand, the hypoxic environment confers the cell a higher metastatic potential through the HIF-1 pathway (Wilson et al., 2006). Nevertheless, these ulcerations occurred after the end of the treatment, and it is unlikely that they impacted the results of the study. Similarly, in one mouse of the PBS group the tumour had grown inside the chest cavity, most likely due to the site of injection being a bit further in – this, however, should not impact metastasis to the lymph nodes although it could impact invasion to the lungs.

To confirm that the effect that we are seeing is CCR7-mediated, we could assess if cell recruitment is impaired when CCR7 is knocked down in the 4T1-Luc cells. Indeed, it has been reported that CCR7 ablation results in smaller tumours that are palpable later on (Boyle et al., 2016).

Conclusions

Overall, this study highlights the importance of CCL21, and in particular its presentation by GAGs, in the metastasis of breast cancer cells to the lymph nodes. The data presented showed that:

- 4T1-Luc cells are an excellent cell line to monitor cell number through luminescence and assess CCL21-mediated chemotaxis. Indeed, we showed that a non-GAG binding truncated CCL21 can decrease 4T1 trans-filter chemotaxis and significantly impair trans-endothelial chemotaxis *in vitro.*
- We created a murine model to assess the potential of mutCCL21 in preventing metastasis to the lymph node *in vivo*. Injection of $5x10^4$ cells into the mammary fat pad gave palpable tumours within one week and allowed us to monitor tumours for up to 18 days, when metastasis to the axillary lymph nodes had occurred in most mice.
- MutCCL21 significantly decreased lymph node positivity as compared to PBS control after daily i.v. injections for 7 days.

This depicts the potential for mutCCL21 to be used in therapy, particularly in combination – indeed, administration of WT CCL21 is currently being considered in clinical trials as a possible immunotherapy for lung cancer (Sharma et al., 2013), highlighting the importance this chemokine has in cancer.

7. General discussion

Chemokine-mediated metastasis in breast cancer is a well-documented process, with CXCR4 being the main regulator of metastasis to bone, brain and lung, and CCR7 mediating metastasis to the lymph node (Müller et al., 2001, Cabioglu et al., 2005b). In health, chemokines are key regulators of cell migration, both for homeostatic processes and to recruit immune cells during inflammation and, not surprisingly, they have become a target of interest in drug development, in particular for inflammatory diseases and transplantation. Unfortunately, chemokine pathways are as complex as the systems they regulate, often displaying redundancy or controlling more than one process. This characteristic has meant that very few drugs targeting chemokine receptors have proceeded past phase II clinical trials. Indeed, only Maraviroc, a CCR5 antagonist against HIV, and AMD3100, a CXCR4 antagonist for hematopoietic stem cell mobilisation, have been approved by the FDA so far, despite many anti-CXCR4 targeted therapies showing success in preventing breast cancer metastasis *in vivo* (Liang et al., 2004, Veldkamp et al., 2010, Ramsey and McAlpine, 2013). Often, studies that show promise in mouse models fail due to lack of efficacy or unspecific side effects, most likely as a result of not all human chemokines existing in mouse, one chemokine having two counterparts in the other species, chemokines being dissimilar between the two species (Zlotnik et al., 2006), or the use of immunocompromised mice where immunological context is lost (Kelland, 2004). The current study was designed to study the function of the chemokine receptors CXCR4, CXCR7 and CCR7 and to propose therapeutic avenues not yet explored for their regulation, such as GAG targeting and receptor cross-desensitisation.

7.1. The role of FOXP3 in regulation of CXCR4 expression

The first aim of this project was to investigate the role of FOXP3 in modulating CXCR4 expression. FOXP3 was believed to only be expressed by Tregs, where its function is to supress auto-reactive T-cells. However, FOXP3 has recently been observed on epithelial cells from several organs, including breast (Zuo et al., 2007b, Zuo et al., 2007a, Merlo et al., 2009). In malignant cells, however, FOXP3 ceases to be expressed or is translocated from the nucleus to the cytoplasm, where it cannot mediate its function as a tumour suppressor. Indeed, FOXP3 has been described to regulate several oncogenes including HER-2 (Zuo et al., 2007b), SKP2 (Zuo et al., 2007a), c-Myc (Wang et al., 2009), p21 (Liu et

al., 2009b) and LATS2 (Li et al., 2011c). Furthermore, CXCR4 is upregulated in tissues where there is a diminished expression of FOXP3 (Overbeck-Zubrzycka, 2012). Thus, FOXP3 could regulate CXCR4 in two ways – directly by binding to *CXCR4* (Katoh et al., 2011) or through HER2, which can increase CXCR4 protein synthesis and prevent its degradation (Madden et al., 2004).

In order to assess this, *FOXP3* was silenced in primary human mammary epithelial cells and expression of FOXP3 and CXCR4's was assessed at 30 minutes, 2 hours, 4 hours and 8 hours. FOXP3 expression was reduced after 4 hours, with CXCR4 showing a concomitant increase. This supports Katoh et al. (2011) observations of FOXP3 directly regulating CXCR4, and raises the potential for FOXP3-targeted therapies.

7.1.1. Implications of this work for therapy

One potential approach to increasing FOXP3 is, theoretically, reactivation of the *FOXP3* gene. As FOXP3 is present in the X-chromosome, there is only one active copy of the gene. In females, due to dose-compensation, the second X-chromosome is condensed into the Barr body in the early stages of development, where it cannot be transcribed (Chadwick and Willard, 2003). This makes FOXP3 susceptible to inactivation after a single-hit somatic mutation event (Wang et al., 2009, Spatz et al., 2004). Heterozygous deletion of *FOXP3* has been described in breast cancer (Zuo et al., 2007b), indicating that the wild type allele remains silenced in the cell and can potentially be induced to mediate its tumour suppressor effect. One study used anisomycin, an antibiotic which inhibits protein synthesis at high doses, to induce FOXP3 expression through the ATF-2 and JNK pathways. Briefly, both ATF-2 and c-Jun can interact with an enhancer in *FOXP3´*s intron 1 and induce its synthesis from the WT allele, greatly reducing tumour growth in mice (Liu et al., 2009c). A similarly elegant approach was used by Jung et al. (2010), who induced FOXP3 expression by the chemotherapeutic agent doxorubicin through the p53 pathway. Although the exact mechanism is still unknown, this study suggested that FOXP3 is induced by p53 binding to the distal region of the *FOXP3* promoter. These approaches, however, rely on the activation of specific genes in the X-chromosome in order to avoid dangerous unspecific effects.

A different approach is the use of protein replacement therapy to deliver FOXP3 into the cell. Heinze et al. (2009) created a fusion protein containing the nuclei-penetrating Fv single chain fragment of the huntingtin monoclonal antibody 3E10 and FOXP3

cDNA. This construct was able to transport FOXP3 into the cell nucleus and induce cell apoptosis, thus reducing tumour burden in a murine model of breast cancer.

Recently, gene therapy has also become a popular option, albeit implementation in patients is still in the early stages. Nonetheless, FOXP3 has been stably transferred into $CD4^+$ T-cells using lentivirus in both *in vitro* and *in vivo* studies of immune dysregulation polyendocrinopathy enteropathy X-linked (IPEX) syndrome, successfully acquiring a functional Treg phenotype (Passerini et al., 2013). This same strategy could be used for graft-versus-host disease in transplantation (Trzonkowski et al., 2009) and cancer, nevertheless achieving sufficient levels remains a challenge.

7.2. THE ROLE OF CXCR7 ON CXCR4 EXPRESSION

The second aim of this project was to assess CXCR7's effect in metastasis, and how its presence might regulate CXCR4's activity. Co-expression of both receptors was observed in breast cancer tumour samples following immunohistochemical staining or qPCR; this result is consistent with previous reports (Wu et al., 2015). It has also been proposed that CXCR4 and CXCR7 can form heterodimers (Levoye et al., 2009) and that this co-expression can affect CXCR4's downstream signalling pathways (Décaillot et al., 2011).

To investigate the effects of receptor co-expression, CHO cells were chosen for transfection. Like other model cell lines such as HEK-293 or COS-1, CHO cells express moderate levels of β-arrestin (Santini et al., 2000) which would allow for the normal internalisation, desensitisation and signalling of the receptors. Breast cancer cell lines were not chosen given their difficulty to transfect using electroporation or lipid based reagents, and the lack of access to lentiviral-transfection facilities. However, it is important to note that cell lines MDA-MB-231 (Hoshino et al., 1999) and SKBR3 (Efferson et al., 2006, Sioud, 2007) constitutively activate the ERK pathway and thus would not have been good models for this study – this phenomena, however, is not observed in MCF-7 (Hoshino et al., 1999).

In our hands, CXCR7 co-expression with CXCR4 did not affect ligand induced ERK phosphorylation, which remained transient at 5-15 minutes (Lagane et al., 2008). However, co-expression of these receptors shifted Akt activation to a sustained response for up to 2 hours, which is similar to that observed for CXCR7 alone (Ebisuya et al., 2005, Ahn et al., 2004). This correlated with differential receptor internalisation, a well-reported phenomenon where CXCR4 is degraded and CXCR7 is recycled back to the

surface (Balabanian et al., 2005, Boldajipour et al., 2008, Grymula et al., 2010, Naumann et al., 2010, Luker et al., 2010). A similar but attenuated pattern was seen when both receptors were expressed. The current study also identified CXCR4, but not CXCR7, as the main driver of cell migration as assessed by wound healing assays, with co-expressed CXCR7 reducing migration. This could be at least partially explained by a diminished induction of calcium flux after the addition of CXCL12 whenever both CXCR4 and CXCR7 were expressed. Based on the data from the current study and the available literature, a model representing the pathways by which CXCR7 can modify CXCR4's signalling can be found in Figure 7-1 below.

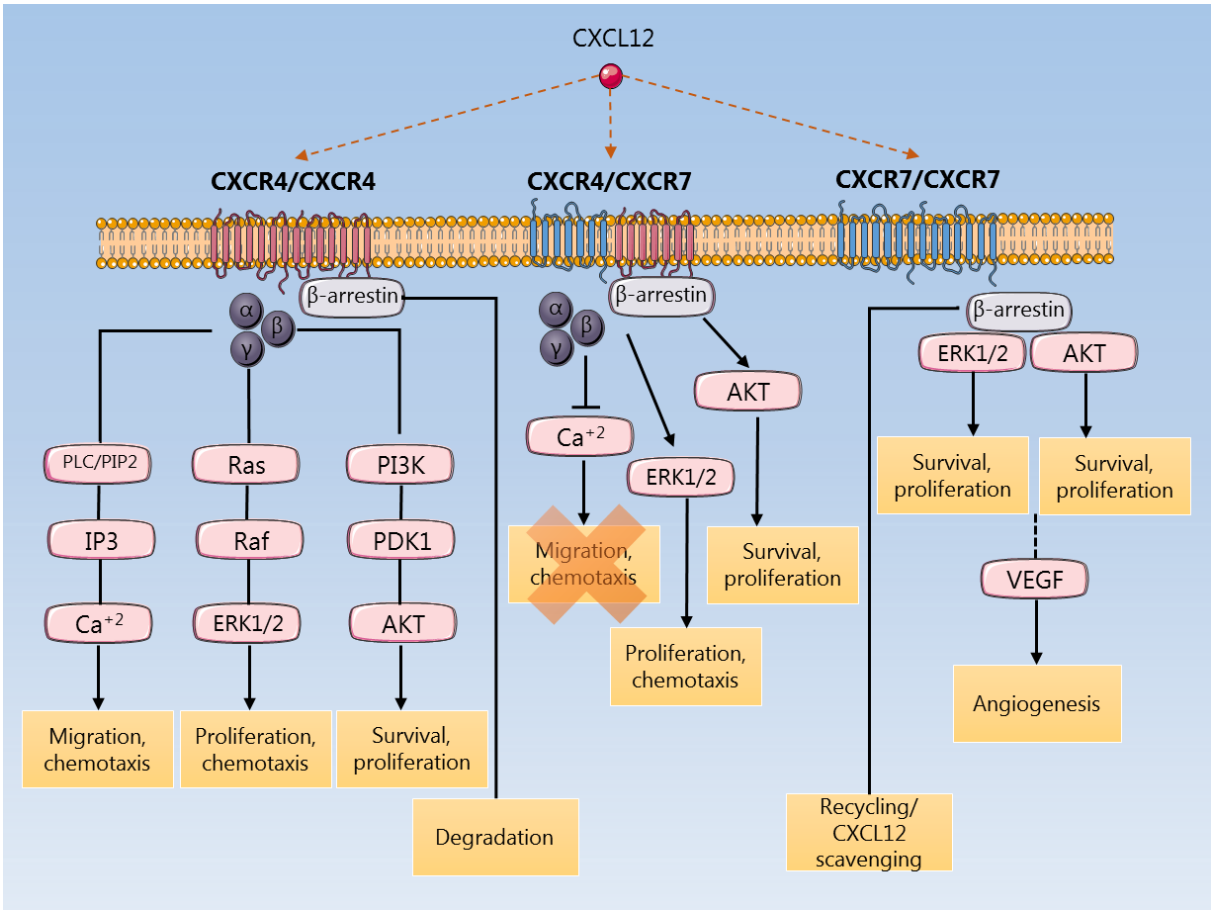

Figure 7-1. Schematic diagram of proposed CXCR4-CXCR7 downstream pathways.
CXCL12 can bind (1) CXCR4 homodimers, which will trigger G-protein signalling pathways such as IP3, Ras and PI3K; (2) CXCR7 homodimers, which will trigger β-arrestin mediated kinase pathways but not calcium flux; or (3) CXCR4/CXCR7 heterodimers, which will cause a conformational change between CXCR4 and the G-proteins, abrogating their signalling and fomenting β-arrestin mediated signalling.

7.2.1. Implications of this work for therapy

After differential receptor desensitisation pathways were observed, cross-desensitisation of CXCR4 through CXCR7 was attempted using the specific CXCR7 agonist VUF11207. Although no link was observed between CXCR7 and metastasis, many other studies have reported that CXCR7 may play a role in tumour growth (Miao

et al., 2007, Meijer et al., 2008, Singh and Lokeshwar, 2011, Zheng et al., 2010), survival (Wang et al., 2008b, Hattermann et al., 2010, Burns et al., 2006), invasion (Wang et al., 2008b, Zheng et al., 2010, Burns et al., 2006) and angiogenesis (Miao et al., 2007, Kollmar et al., 2010, Zheng et al., 2010) instead. Indeed, we observed strong CXCR7 staining in the blood vessels. This is consistent with reports showing CXCR7 upregulation on the tumour endothelium, which might be mediated by VEGF (Zheng et al., 2010). Thus, targeting of both CXCR4 and CXCR7 is still an interesting therapeutic option that has not been extensively explored.

It was observed that when heterodimers were formed, VUF11207 did not stimulate CXCR7 recycling but reduced both CXCR4 and CXCR7 expression, making it a possible candidate to target both receptors' degradation at the same time. Indeed, cross-desensitisation, or heterologous desensitisation, has been used to prevent CXCR3, CXCR4 and CCR5-mediated leukocyte migration through a CXCR3 agonist (O'Boyle et al., 2012). Desensitisation has also been proved as a viable therapeutic option in multiple sclerosis, where the sphingosine 1-phosphate receptor (S1PR) agonist Fingolimod (Gilenya®) mediates its immunosupressive effect through receptor internalisation (Adachi and Chiba, 2007); this drug gained FDA approval as an immunoregulator in 2010 (Food and Drug Administration, 2012). Chemokine antagonists, on the other hand, have been extensively used *in vitro* and *in vivo* but have had limited success in clinical trials so far, with only AMD3100 having been approved (Hainsworth et al., 2016). A detailed view of the drugs available can be found in section 1.7 of the Introduction.

7.3. THE ROLE OF GAGS ON CCR7 BINDING

In vitro, most chemokines (including CXCL12 and CCL21) bind to GAGs such as heparan sulphate (Lortat-Jacob et al., 2002); indeed it has been seen that the presentation of chemokines by endothelial GAGs is an important requirement for extravasation of leukocytes *in vivo* (Middleton et al., 2002, Johnson et al., 2005). The hypothesis tested in the current study was based on the premise that cancer cells use the same mechanism as leukocytes to extravasate blood and lymph vessels, using CCL21's presentation by GAGs to metastasise to the lymph nodes (Bao et al., 2010, Weber et al., 2013). In order to compete with WT CCL21, a mutant form of CCL21 with a truncated GAG-binding domain was created. This mutant chemokine was initially shown to impair trans-endothelial

migration of cancer cells and PBMCs *in vitro,* and further experiments were carried out to assess its potential in a murine model.

Results *in vivo* were found to mirror *in vitro*, where mice that had been treated with mutCCL21 presented a 59% decrease in the number of positive lymph nodes and a 69% decrease in the number of very positive lymph nodes in comparison to the PBS control, indicating that a 20 μg dose was sufficient to mediate a significant reduction in metastatic spread with no side effects. Indeed, mice undergoing mutCCL21 treatment were able to maintain or increase their weight during treatment whilst the PBS group lost weight. A limitation of this study is that the treatment started when the tumour had been established, but no metastatic spread to the lymph nodes had been observed. Thus, mutCCL21 was only assessed for its potential to prevent lymph node metastasis but not for its curative effect once the metastases have been established.

No survival benefit was observed, most likely due rapid primary tumour growth. Thus, a possible improvement to this model would be to resect the primary tumour once the metastatic disease has been established, but ideally when the tumour is still under 6 mm of diameter to avoid invasion through the peritoneal lining, which would complicate surgery (Pulaski and Ostrand-Rosenberg, 2001). In this model, it would be better to inject the 4T1 cells in the inguinal fourth mammary fat pad, which would eliminate the risk of the tumour penetrating the chest cavity. Furthermore, it has been reported that removal of the tumour causes the release of tumour cells into the vasculature and surrounding tissue, a phenomena also observed in mice (Exadaktylos et al., 2006, Shapiro et al., 1981), and thus treatment should start as soon as mice have recovered from the procedure.

Although no side effects were observed in immunocompetent mice, it is important to note that CCL21 is crucial to the homing of naive T-cells to lymph nodes through the high endothelial venules (Förster et al., 1999). Chronic disruption of this process could cause a reduced response towards inflammation, including the attack of the primary tumour itself. Whether alternative pathways can compensate for any reduced response towards CCL21 is still unknown, although it has been seen that mice lacking CCL21 still show a T-cell immune response, albeit one that is delayed (Mori et al., 2001). Another way to circumvent this would be to directly target this treatment towards epithelial cells. Direct targeting of epithelial cells in the ileum (Haneda et al., 2007), renal proximal tubule (Lin et al., 2013) and human airway (Allon et al., 2012) among others has been achieved, however currently this delivery has been limited to the nucleus whilst we would require

the mutCCL21 to bind a cell surface receptor. A possible strategy could be to encapsulate mutCCL21 in sterically stabilized immunoliposomes, which are guided by antibodies that bind specifically to antigens on the tumour cell surface (Hussain et al., 2007, Atobe et al., 2007, Roth et al., 2007). However, the target antigen must be chosen with care as chemokine internalisation is not desirable. Indeed, one of the main hurdles with nanoparticles for chemokine delivery is that they are designed to effectively penetrate the cell surface (Singh and Lillard, 2009).

Overall, evidence from this study suggests that mutCCL21 shows decreased binding to the GAGs present in the endothelial cells, and thus fails to create the chemotaxis gradient necessary for trans-endothelial migration and extravasation (Proudfoot et al., 2003). However, mutCCL21 can still bind and activate CCR7 as demonstrated by calcium flux, confirming that GAGs are not necessary for the binding and activation of the chemokine receptors *in vitro*. This impaired extravasation was also observed *in vivo*, where mutCCL21 could reduce the number of metastatic lymph nodes in a breast cancer murine model. This is summarised in Figure 7-2 below.

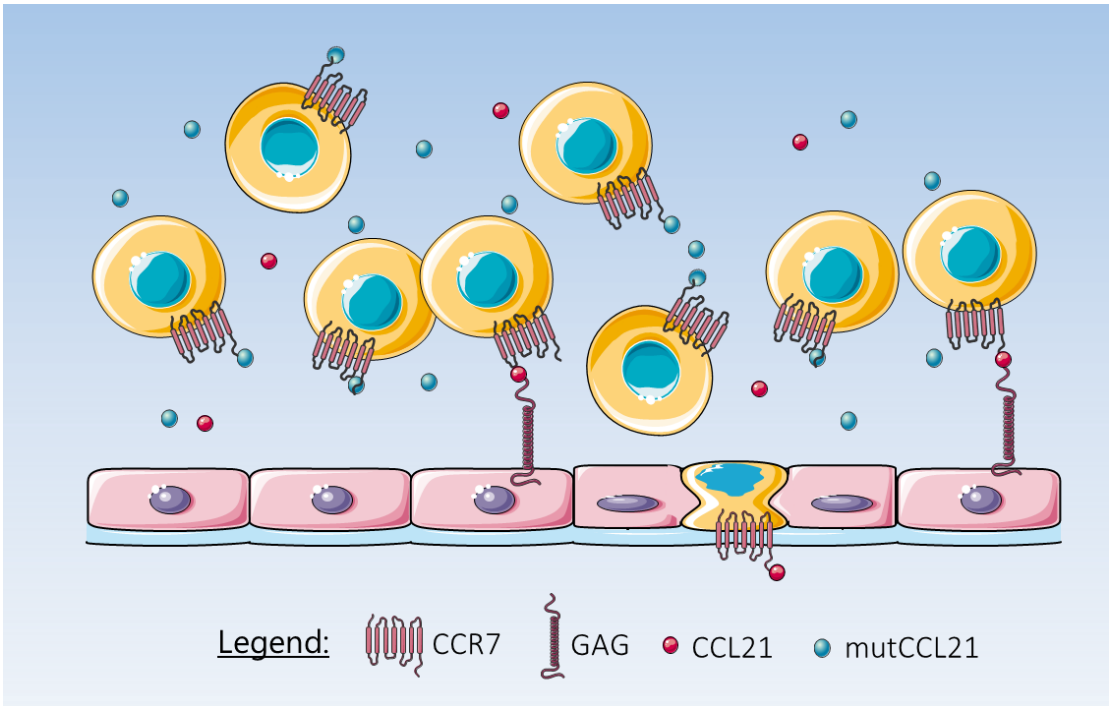

Figure 7-2. Schematic diagram of mutCCL21 proposed action.
Both mutCCL21 and WT CCL21 can bind and activate CCR7, but only the latter can tether the binding to glycosaminoglycans present in the endothelial monolayer, allowing extravasation into the lymph or blood vessel.

7.3.1. Implications of this work for therapy

Recent studies have explored the use of WT CCL21 in cancer immunotherapy as a chemoattractant for dendritic and T-cells (Warnock et al., 2000, Willimann et al., 1998) into the tumour (Kirk et al., 2001). This has been assessed for immunocompetent mice either by direct injection of CCL21 into the tumour (Sharma et al., 2000, Baratelli et al., 2008) or using a more advanced delivery system, in which CCL21 is encoded in a recombinant adeno-associated virus in order to allow its transduction after the intratumoural injection (Liang et al., 2007a). Both of these systems resulted in reduced tumour growth, with the second requiring less frequent administration. Another option is to inject DCs or fibroblasts that overexpress CCL21 into the tumour (Yang et al., 2006, Yang et al., 2004b); this treatment has also been shown to eradicate cancer cells. Furthermore, it has been reported that melanoma cells (Novak et al., 2007) and prostate cells (Yousefieh et al., 2009) engineered to express CCL21 are cleared by the system in a murine model.

Indeed, immunotherapy using DCs has been approved by the FDA for the treatment of metastatic asymptomatic, hormone refractory, prostate cancer (Hovden and Appel, 2010), proving that DC vaccines are a feasible option to treat cancer. Based on the aforementioned studies, a phase I clinical trial with DC cells expressing CCL21 was started in 2013 for late stage non-small cell lung cancer patients (Lee et al., 2014), a cancer type where circulating mature DCs are greatly decreased. These naive DC-CCL21 were injected intratumorally so they would mature *in vivo* upon presentation of tumour antigens in the site – the DC would then present the antigens to T-cells which would recognise and attack the cancer. The vaccine was deemed safe and showed a promising anti-tumour response (Lee et al., 2014), but the definitive trial is still ongoing.

7.4. LIMITATIONS AND FUTURE WORK

7.4.1. Limitations

Specific limitations for the different parts of the study were discussed in appropriate chapters. The main overall limitation of this study was the difficulty to find a cell line that accurately modelled the disease in patients. Both CXCR4 and CXCR7 were overexpressed in primary tumours, but none of our breast cancer cell lines expressed both receptors at high levels. To circumvent this we would optimally use primary cells

derived from patients, but this was beyond the scope of the present study given the difficulties to obtain and grow these cells. Furthermore, some of the most widely used cell lines such as MDA-MB-231 have permanently activated pathways such as ERK which precludes them from being an appropriate model to investigate cell effects mediated by this kinase. Indeed, although the use of cell lines is necessary to clearly see the effect of chemokines and agonists in the cells, they also do not take into consideration the patient variability observed *in vivo*, where the same stimulus can elicit a different response, or the modulation by the microenvironment.

The CXCR4/CXCR7 study is also limited by the chosen time-points and ligand concentrations, as a smaller scope was necessary in order to limit the length of the study. Although these were carefully chosen after optimisation, missing an effect at a later time or with a higher dose cannot be discarded. Indeed, it has been suggested that CXCL12's effect on CXCR7 could be different depending on the chemokine abundance (Luker et al., 2010, Levoye et al., 2009) and thus the results found can only be applied for the concentrations used. Another limitation is the accurate comparison between CXCR4 and CXCR7's expression levels– indeed, although ABC assays were carried out to compare the two, some antibodies may underestimate the presence of the receptor, a phenomena which has been reported with other CXCR7 clones.

In addition to this, although β-arrestin has been reported in CHO cells (Santini et al., 2000), expression of β-arrestin and its interaction with chemokine receptors was not assessed in this study. Thus, it cannot be confirmed that the results seen were due to differential β-arrestin recruitment and not, for instance, due to different G-proteins being recruited (e.g. $G\alpha_{q/11}$ instead of $G\alpha_i$) (Rubin, 2009), which has been also shown to alter desensitisation and prolong the cell signalling (Mellado et al., 2001c).

A further limitation of the CXCR4/CXCR7 study is that it is based on *in vitro* assays. However, further *in vitro* studies with the agonist VUF11207 would have been necessary before introducing mouse models and assessing the effect of the agonist *in vivo*. Lastly, due to lack of material or bad condition of the frozen patient tumours, the number of samples assessed was small, which meant that no significant conclusions could be derived from CXCR4, CXCR7 and CCR7 staining or their RNA expression, and clinical variables such as tumour grade or lymph node involvement. Furthermore, in both immunohistochemistry and qPCR there was a great variability in expression between tumours of the same clinical status.

7.4.2. Future work

This study investigated the role of CXCR4 and CXCR7 homodimers and heterodimers, with a specific focus on the effects mediated by G-coupled proteins and β-arrestin. It was observed that CXCR7's role in migration was limited, and thus the question of which other effects it may modulate still remains. To address this, the following further studies could be carried out:

- A sustained activation of Akt was observed, which can regulate the mTOR signalling pathway (Edros et al., 2014). Indeed, it has been reported that both CXCR4 and CXCR7 can regulate the mTOR pathway through P70S6K and 4EBP1 in metastatic renal cell carcinoma (Ierano et al., 2014). A similar pattern could be seen in neuroendocrine tumours (Circelli et al., 2016), and thus it would be interesting to see if the same pathway is also activated in our cell lines using western blot.
- A suggested mechanism for CXCR7 is the regulation of apoptosis – in particular, it has been shown to inhibit apoptosis in glioma (Hattermann et al., 2010) , prostate (Wang et al., 2008b) and colorectal cancer (Chatterjee et al., 2014a), a process that could be mediated by Akt signalling (Chatterjee et al., 2014a). This could be determined in our cell lines by staining cells with annexin-V to assess loss of cellular membrane integrity in flow cytometry.
- High CXCR7 expression around the blood vessels was observed in primary breast tumours, suggesting that CXCR7 expression may be linked to the VEGF pathway. Indeed, VEGF has been shown to upregulate CXCR7 expression in hepatocellular carcinoma (Zheng et al., 2010). This could be a potential feedback loop, as CXCR7 has been shown to produce VEGF after CXCL12 stimulation in prostate cancer (Wang et al., 2008b). Hence, the production of VEGF could be assessed in our cell lines using an ELISA.

Lastly, due to time constraints the effect of VUF11207 could only be assessed in the context of receptor internalisation. Future studies could determine the effect that the agonist has in receptor activation, including ERK and Akt phosphorylation, calcium flux and wound healing assays.

The work contained in this thesis also assessed the potential for mutCCL21 as a possible therapy to prevent metastasis *in vivo*. However, before taking this further into

the clinic additional analysis should be carried out to determine the mutCCL21 concentration in blood at 1 hour, 6 hours and 24 hours post-i.v. chemokine injection to approximate its half-life. Due to its reduced binding to GAGs in the vascular endothelium, we expect the mutCCL21 to circulate in blood for longer times than its WT counterpart. However it will still be susceptible to binding to circulating cells and to protease degradations (Van Damme et al., 2004, Sadir et al., 2004), which will diminish its concentration in plasma.

7.4.2.1. *New avenues*

Other interesting new projects could stem from the results of these thesis, as CXCR7 is not the only receptor CXCR4 forms heterodimers with. Literature has reported that CXCR4 heterodimerises with TCR (Dinkel et al., 2016, Kremer et al., 2011), CCR2, CCR5 (Steel et al., 2014, Contento et al., 2008), Cannabinoid Receptor 2 (CBR2) (Coke et al., 2016) and δ opioid receptors (Pello et al., 2008, Burbassi et al., 2010) among others, which can alter their signalling. Meanwhile, anaesthesia has also been linked to metastasis and cancer recurrence (Divatia and Ambulkar, 2014) – in fact, breast cancer patients undergoing mastectomy and axillary clearance had almost 4 times better survival when they had received regional instead of general anaesthesia (Exadaktylos et al., 2006). This could be due to a longer immunosuppression period when general anaesthesia is given, during which cancer cells have a window of opportunity to establish new niches (Coffey et al., 2003), whilst local anaesthesia reduces the amount of volatile anaesthetics and opioids administered (Votta-Velis et al., 2013) and thus has a shorter effect on the immune system.

However, these higher metastatic rates could also be due to the longer activation of the opioid receptors in the cancer cells themselves. Indeed, it has been observed that opioid receptors are expressed on various cancer cell lines, including MCF-7 cells which express all three opioid receptor types, μ, δ and κ (Gach et al., 2009). These receptors can then in turn activate VEGF receptors, increasing vascular permeability and transendothelial migration (Singleton et al., 2006), a phenomena that was seen in a non-small-cell lung cancer model (Lennon et al., 2012). Thus, it would be interesting to see if opioid receptors can also enhance migration on breast cancer cells, and whether their expression can modulate CXCR4's role in metastasis. Indeed, previous studies show that the κ-opioid receptor, but not μ and δ-opioid receptors,

can cross-desensitize CXCR4 (Finley et al., 2008, Szabo et al., 2003), and that CXCR4 activation by CXCL12 can cross-desensitize μ and δ-opioid receptors (Chen et al., 2007, Heinisch et al., 2011); but whether this also occurs in breast cancer has not been assessed. Thus, it would be interesting to investigate whether chemokine receptors and opioid receptors are co-expressed in breast cancer and whether they heterodimerise, enhancing the migration of tumour cells whenever anaesthetics such as fentanyl are used during surgery.

REFERENCES

ABLETT, M. P., O'BRIEN, C. S., SIMS, A. H., FARNIE, G. & CLARKE, R. B. 2014. A differential role for CXCR4 in the regulation of normal versus malignant breast stem cell activity. *Oncotarget,* 5**,** 599-612.

ADACHI, K. & CHIBA, K. 2007. FTY720 story. Its discovery and the following accelerated development of sphingosine 1-phosphate receptor agonists as immunomodulators based on reverse pharmacology. *Perspectives in medicinal chemistry,* 1**,** 11.

ADAMS, S., DIAMOND, J., HAMILTON, E., POHLMANN, P., TOLANEY, S., MOLINERO, L., ZOU, W., LIU, B., WATERKAMP, D. & FUNKE, R. Safety and clinical activity of atezolizumab (anti-PDL1) in combination with nab-paclitaxel in patients with metastatic triple-negative breast cancer. Proceedings of the Thirty-Eighth Annual CTRC-AACR San Antonio Breast Cancer Symposium, 2015. 6-10.

ADES, E. W., CANDAL, F. J., SWERLICK, R. A., GEORGE, V. G., SUMMERS, S., BOSSE, D. C. & LAWLEY, T. J. 1992. HMEC-1: establishment of an immortalized human microvascular endothelial cell line. *Journal of Investigative Dermatology,* 99**,** 683-690.

AGUIRRE-GHISO, J. A. 2007. Models, mechanisms and clinical evidence for cancer dormancy. *Nature Reviews Cancer,* 7**,** 834-846.

AHN, S., SHENOY, S. K., WEI, H. & LEFKOWITZ, R. J. 2004. Differential kinetic and spatial patterns of β-arrestin and G protein-mediated ERK activation by the angiotensin II receptor. *Journal of Biological Chemistry,* 279**,** 35518-35525.

AKEKAWATCHAI, C., HOLLAND, J. D., KOCHETKOVA, M., WALLACE, J. C. & MCCOLL, S. R. 2005. Transactivation of CXCR4 by the insulin-like growth factor-1 receptor (IGF-1R) in human MDA-MB-231 breast cancer epithelial cells. *Journal of Biological Chemistry,* 280**,** 39701-39708.

ALANEN, K., DENG, D. X. & CHAKRABARTI, S. 2000. Augmented expression of endothelin-1, endothelin-3 and the endothelin-B receptor in breast carcinoma. *Histopathology,* 36**,** 161-167.

ALCAMI, A. 2003. Viral mimicry of cytokines, chemokines and their receptors. *Nature Reviews Immunology,* 3**,** 36-50.

ALI, S., FRITCHLEY, S. J., CHAFFEY, B. T. & KIRBY, J. A. 2002. Contribution of the putative heparan sulfate–binding motif BBXB of RANTES to transendothelial migration. *Glycobiology,* 12**,** 535-543.

ALI, S., O'BOYLE, G., HEPPLEWHITE, P., TYLER, J., ROBERTSON, H. & KIRBY, J. 2010. Therapy with Nonglycosaminoglycan-Binding Mutant CCL7: A Novel Strategy to Limit Allograft Inflammation. *American Journal of Transplantation,* 10**,** 47-58.

ALI, S., O'BOYLE, G., MELLOR, P. & KIRBY, J. A. 2007. An apparent paradox: chemokine receptor agonists can be used for anti-inflammatory therapy. *Molecular immunology,* 44**,** 1477-1482.

ALLAN, S. E., PASSERINI, L., BACCHETTA, R., CRELLIN, N., DAI, M., ORBAN, P. C., ZIEGLER, S. F., RONCAROLO, M. G. & LEVINGS, M. K. 2005. The role of 2 FOXP3 isoforms in the generation of human CD4+ Tregs. *Journal of Clinical Investigation,* 115**,** 3276-3284.

ALLEGRETTI, M., BERTINI, R., CESTA, M. C., BIZZARRI, C., DI BITONDO, R., DI CIOCCIO, V., GALLIERA, E., BERDINI, V., TOPAI, A. & ZAMPELLA, G. 2005. 2-Arylpropionic CXC chemokine receptor 1 (CXCR1) ligands as novel noncompetitive CXCL8 inhibitors. *Journal of medicinal chemistry,* 48**,** 4312-4331.

ALLEN, S. J., CROWN, S. E. & HANDEL, T. M. 2007. Chemokine: receptor structure, interactions, and antagonism. *Annu. Rev. Immunol.,* 25**,** 787-820.

ALLINEN, M., BEROUKHIM, R., CAI, L., BRENNAN, C., LAHTI-DOMENICI, J., HUANG, H., PORTER, D., HU, M., CHIN, L. & RICHARDSON, A. 2004. Molecular characterization of the tumor microenvironment in breast cancer. *Cancer cell,* 6**,** 17-32.

ALLON, N., SAXENA, A., CHAMBERS, C. & DOCTOR, B. P. 2012. A new liposome-based gene delivery system targeting lung epithelial cells using endothelin antagonist. *Journal of controlled release,* 160**,** 217-224.

ALTENBURG, J. D. 2008. *Structure-function Analysis of the CXCL12 Chemokine*, ProQuest Dissertations Publishing.

AMERICAN CANCER SOCIETY. 2013. *Breast cancer survival rates by stage* [Online]. Available: http://www.cancer.org/cancer/breastcancer/detailedguide/breast-cancer-survival-by-stage [Accessed November 2013].

AMIT, I., CITRI, A., SHAY, T., LU, Y., KATZ, M., ZHANG, F., TARCIC, G., SIWAK, D., LAHAD, J. & JACOB-HIRSCH, J. 2007. A module of negative feedback regulators defines growth factor signaling. *Nature genetics,* 39**,** 503-512.

ANDRE, F., CABIOGLU, N., ASSI, H., SABOURIN, J. C., DELALOGE, S., SAHIN, A., BROGLIO, K., SPANO, J. P., COMBADIERE, C. & BUCANA, C. 2006. Expression of chemokine receptors predicts the site of metastatic relapse in patients with axillary node positive primary breast cancer. *Annals of oncology,* 17**,** 945-951.

ANGERS, S., SALAHPOUR, A., JOLY, E., HILAIRET, S., CHELSKY, D., DENNIS, M. & BOUVIER, M. 2000. Detection of β2-adrenergic receptor dimerization in living cells using bioluminescence resonance energy transfer (BRET). *Proceedings of the National Academy of Sciences,* 97**,** 3684-3689.

ANTONIOU, A., PHAROAH, P. D. P., NAROD, S., RISCH, H. A., EYFJORD, J. E., HOPPER, J. L., LOMAN, N., OLSSON, H., JOHANNSSON, O. & BORG, Å. 2003. Average risks of breast and ovarian cancer associated with BRCA1 or BRCA2 mutations detected in case series unselected for family history: a combined analysis of 22 studies. *The American Journal of Human Genetics,* 72**,** 1117-1130.

AO, M., FRANCO, O. E., PARK, D., RAMAN, D., WILLIAMS, K. & HAYWARD, S. W. 2007. Cross-talk between paracrine-acting cytokine and chemokine pathways promotes malignancy in benign human prostatic epithelium. *Cancer research,* 67**,** 4244-4253.

AONUMA, M., SAEKI, Y., AKIMOTO, T., NAKAYAMA, Y., HATTORI, C., YOSHITAKE, Y., NISHIKAWA, K., SHIBUYA, M. & TANAKA, N. G. 1999. Vascular endothelial growth factor overproduced by tumour cells acts predominantly as a potent angiogenic factor contributing to malignant progression. *International journal of experimental pathology,* 80**,** 271.

ARAVINDAN, B. K., PRABHAKAR, J., SOMANATHAN, T. & SUBHADRA, L. 2015. The role of chemokine receptor 4 and its ligand stromal cell derived factor 1 in breast cancer. *Annals of translational medicine,* 3.

ARIGAMI, T., NATSUGOE, S., UENOSONO, Y., YANAGITA, S., ARIMA, H., HIRATA, M., ISHIGAMI, S. & AIKOU, T. 2009. CCR7 and CXCR4 expression predicts lymph node status including micrometastasis in gastric cancer. *International journal of oncology,* 35**,** 19.

ARTANDI, S. E. & DEPINHO, R. A. 2000. Mice without telomerase: what can they teach us about human cancer? *Nature medicine,* 6.

ASLAKSON, C. J. & MILLER, F. R. 1992. Selective events in the metastatic process defined by analysis of the sequential dissemination of subpopulations of a mouse mammary tumor. *Cancer research,* 52**,** 1399-1405.

ATOBE, K., ISHIDA, T., ISHIDA, E., HASHIMOTO, K., KOBAYASHI, H., YASUDA, J., AOKI, T., OBATA, K.-I., KIKUCHI, H. & AKITA, H. 2007. In vitro efficacy of a sterically stabilized immunoliposomes targeted to membrane type 1 matrix metalloproteinase (MT1-MMP). *Biological and Pharmaceutical Bulletin,* 30**,** 972-978.

AUTELITANO, D. J. 1998. Cardiac expression of genes encoding putative adrenomedullin/calcitonin gene-related peptide receptors. *Biochemical and biophysical research communications,* 250**,** 689-693.

AUWERX, J. 1991. The human leukemia cell line, THP-1: a multifacetted model for the study of monocyte-macrophage differentiation. *Experientia,* 47**,** 22-31.

AYOUB, M. A., COUTURIER, C., LUCAS-MEUNIER, E., ANGERS, S., FOSSIER, P., BOUVIER, M. & JOCKERS, R. 2002. Monitoring of ligand-independent dimerization and ligand-induced conformational changes of melatonin receptors in living cells by bioluminescence resonance energy transfer. *Journal of Biological Chemistry,* 277**,** 21522-21528.

AZIM, H. A., DE AZAMBUJA, E., COLOZZA, M., BINES, J. & PICCART, M. J. 2011. Long-term toxic effects of adjuvant chemotherapy in breast cancer. *Annals of oncology,* 22**,** 1939-1947.

AZZI, M., CHAREST, P. G., ANGERS, S., ROUSSEAU, G., KOHOUT, T., BOUVIER, M. & PIÑEYRO, G. 2003. β-Arrestin-mediated activation of MAPK by inverse agonists reveals distinct active conformations for G protein-coupled receptors. *Proceedings of the National Academy of Sciences,* 100**,** 11406-11411.

BABA, M., NISHIMURA, O., KANZAKI, N., OKAMOTO, M., SAWADA, H., IIZAWA, Y., SHIRAISHI, M., ARAMAKI, Y., OKONOGI, K. & OGAWA, Y. 1999. A small-molecule, nonpeptide CCR5 antagonist with highly potent and selective anti-HIV-1 activity. *Proceedings of the National Academy of Sciences,* 96**,** 5698-5703.

BABCOCK, G. J., FARZAN, M. & SODROSKI, J. 2003. Ligand-independent dimerization of CXCR4, a principal HIV-1 coreceptor. *Journal of Biological Chemistry,* 278**,** 3378-3385.

BACHELDER, R. E., WENDT, M. A. & MERCURIO, A. M. 2002. Vascular endothelial growth factor promotes breast carcinoma invasion in an autocrine manner by regulating the chemokine receptor CXCR4. *Cancer research,* 62**,** 7203-7206.

BACHELERIE, F., GRAHAM, G. J., LOCATI, M., MANTOVANI, A., MURPHY, P. M., NIBBS, R., ROT, A., SOZZANI, S. & THELEN, M. 2014. New nomenclature for atypical chemokine receptors. *Nature immunology,* 15**,** 207-208.

BACON, K., BAGGIOLINI, M., BROXMEYER, H., HORUK, R., LINDLEY, I., MANTOVANI, A., MATSUSHIMA, K., MURPHY, P., NOMIYAMA, H. & OPPENHEIM, J. 2003. Chemokine/chemokine receptor nomenclature. *Cytokine,* 21**,** 48-49.

BAGGIOLINI, M. 1998. Chemokines and leukocyte traffic. *Nature,* 392**,** 565-568.

BAGGIOLINI, M., DEWALD, B. & MOSER, B. 1997. Human chemokines: an update. *Annual review of immunology,* 15**,** 675-705.

BAJÉNOFF, M., EGEN, J. G., KOO, L. Y., LAUGIER, J. P., BRAU, F., GLAICHENHAUS, N. & GERMAIN, R. N. 2006. Stromal cell networks regulate lymphocyte entry, migration, and territoriality in lymph nodes. *Immunity,* 25**,** 989-1001.

BALABANIAN, K., LAGANE, B., INFANTINO, S., CHOW, K. Y., HARRIAGUE, J., MOEPPS, B., ARENZANA-SEISDEDOS, F., THELEN, M. & BACHELERIE, F. 2005. The chemokine SDF-1/CXCL12 binds to and signals through the orphan receptor RDC1 in T lymphocytes. *Journal of Biological Chemistry,* 280**,** 35760-35766.

BALKWILL, F. The significance of cancer cell expression of the chemokine receptor CXCR4. Seminars in cancer biology, 2004. Elsevier, 171-179.

BANCHEREAU, J. & STEINMAN, R. M. 1998. Dendritic cells and the control of immunity. *Nature,* 392**,** 245-252.

BANSAL, C., SINGH, U. S., MISRA, S., SHARMA, K. L., TIWARI, V. & SRIVASTAVA, A. N. 2012. Comparative evaluation of the modified Scarff-Bloom-Richardson grading system on breast carcinoma aspirates and histopathology. *Cytojournal,* 9**,** 4.

BAO, X., MOSEMAN, E. A., SAITO, H., PETRYANIK, B., THIRIOT, A., HATAKEYAMA, S., ITO, Y., KAWASHIMA, H., YAMAGUCHI, Y. & LOWE, J. B. 2010. Endothelial heparan sulfate controls chemokine presentation in recruitment of lymphocytes and dendritic cells to lymph nodes. *Immunity,* 33**,** 817-829.

BARATELLI, F., TAKEDATSU, H., HAZRA, S., PEEBLES, K., LUO, J., KURIMOTO, P. S., ZENG, G., BATRA, R. K., SHARMA, S. & DUBINETT, S. M. 2008. Pre-clinical characterization of GMP grade CCL21-gene modified dendritic cells for application in a phase I trial in non-small cell lung cancer. *Journal of translational medicine,* 6**,** 38.

BARBERO, S., BONAVIA, R., BAJETTO, A., PORCILE, C., PIRANI, P., RAVETTI, J. L., ZONA, G. L., SPAZIANTE, R., FLORIO, T. & SCHETTINI, G. 2003. Stromal cell-derived factor 1α stimulates human glioblastoma cell growth through the activation of both extracellular signal-regulated kinases 1/2 and Akt. *Cancer research,* 63**,** 1969-1974.

BARDI, G., LIPP, M., BAGGIOLINI, M. & LOETSCHER, P. 2001. The T cell chemokine receptor CCR7 is internalized on stimulation with ELC, but not with SLC. *European journal of immunology,* 31**,** 3291-3297.

BARIBAUD, F., EDWARDS, T. G., SHARRON, M., BRELOT, A., HEVEKER, N., PRICE, K., MORTARI, F., ALIZON, M., TSANG, M. & DOMS, R. W. 2001. Antigenically distinct conformations of CXCR4. *Journal of virology,* 75**,** 8957-8967.

BARNARD, M. E., BOEKE, C. E. & TAMIMI, R. M. 2015. Established breast cancer risk factors and risk of intrinsic tumor subtypes. *Biochimica et Biophysica Acta (BBA)-Reviews on Cancer,* 1856**,** 73-85.

BARYSHNIKOVA, O. K. & SYKES, B. D. 2006. Backbone dynamics of SDF-1α determined by NMR: Interpretation in the presence of monomer–dimer equilibrium. *Protein science,* 15**,** 2568-2578.

BASHKIN, P., DOCTROW, S., KLAGSBRUN, M., SVAHN, C. M., FOLKMAN, J. & VLODAVSKY, I. 1989. Basic fibroblast growth factor binds to subendothelial extracellular matrix and is released by heparitinase and heparin-like molecules. *Biochemistry,* 28**,** 1737-1743.

BASSANI, J., BASSANI, R. A. & BERS, D. M. 1995. Calibration of indo-1 and resting intracellular [Ca] i in intact rabbit cardiac myocytes. *Biophysical Journal,* 68**,** 1453.

BAZAN, J. F., BACON, K. B., HARDIMAN, G., WANG, W., SOO, K., ROSSI, D., GREAVES, D. R., ZLOTNIK, A. & SCHALL, T. J. 1997. A new class of membrane-bound chemokine with a CX3C motif. *Nature* 385**,** 640.

BD BIOSCIENCE. 2017. *Indo-1 AM* [Online]. Available: http://www.bdbiosciences.com/us/reagents/research/antibodies-buffers/cell-biology-reagents/cell-biology-buffers-and-ancillary-reagents/indo-1-am/p/565879 [Accessed May 2017.

BEATSON, G. T. 1901. The Treatment of Cancer of the Breast by Oöphorectomy and Thyroid Extract. *The British Medical Journal***,** 1145-1148.

BELL, D., CHOMARAT, P., BROYLES, D., NETTO, G., HARB, G. M., LEBECQUE, S., VALLADEAU, J., DAVOUST, J., PALUCKA, K. A. & BANCHEREAU, J. 1999. In breast carcinoma tissue, immature dendritic cells reside within the tumor, whereas mature dendritic cells are located in peritumoral areas. *The Journal of experimental medicine,* 190**,** 1417-1426.

BELPERIO, J. A., KEANE, M. P., ARENBERG, D. A., ADDISON, C. L., EHLERT, J. E., BURDICK, M. D. & STRIETER, R. M. 2000. CXC chemokines in angiogenesis. *Journal of Leukocyte Biology,* 68**,** 1-8.

BENREDJEM, B., GIRARD, M., RHAINDS, D., ONGE, G. S.-. & HEVEKER, N. 2017. Mutational Analysis of Atypical Chemokine Receptor 3 (ACKR3/CXCR7) Interaction with Its Chemokine Ligands CXCL11 and CXCL12. *Journal of Biological Chemistry,* 292**,** 31-42.

BERAHOVICH, R. D., PENFOLD, M. E. T. & SCHALL, T. J. 2010a. Nonspecific CXCR7 antibodies. *Immunology letters,* 133**,** 112-114.

BERAHOVICH, R. D., ZABEL, B. A., LEWÉN, S., WALTERS, M. J., EBSWORTH, K., WANG, Y., JAEN, J. C. & SCHALL, T. J. 2014. Endothelial expression of CXCR7 and the regulation of systemic CXCL12 levels. *Immunology,* 141**,** 111-122.

BERAHOVICH, R. D., ZABEL, B. A., PENFOLD, M. E., LEWÉN, S., WANG, Y., MIAO, Z., GAN, L., PEREDA, J., DIAS, J. & SLUKVIN, I. I. 2010b. CXCR7 protein is not expressed on human or mouse leukocytes. *The Journal of Immunology,* 185**,** 5130-5139.

BHOWMICK, N. A., NEILSON, E. G. & MOSES, H. L. 2004. Stromal fibroblasts in cancer initiation and progression. *Nature,* 432**,** 332-337.

BISHOP, J. R., SCHUKSZ, M. & ESKO, J. D. 2007. Heparan sulphate proteoglycans fine-tune mammalian physiology. *Nature,* 446**,** 1030-1037.

BLACKHALL, F. H., MERRY, C. L. R., MALCOLM, L., JAYSON, G. C., FOLKMAN, J., JAVAHERIAN, K. & GALLAGHER, J. T. 2003. Binding of endostatin to endothelial heparan sulphate shows a differential requirement for specific sulphates. *Biochemical Journal,* 375**,** 131-139.

BLAMEY, R. W., ELLIS, I. O., PINDER, S. E., LEE, A. H. S., MACMILLAN, R. D., MORGAN, D. A. L., ROBERTSON, J. F. R., MITCHELL, M. J., BALL, G. R. & HAYBITTLE, J. L. 2007. Survival of invasive breast cancer according to the Nottingham Prognostic Index in cases diagnosed in 1990–1999. *European journal of cancer,* 43**,** 1548-1555.

BLOOM, H. J. G. & RICHARDSON, W. W. 1957. Histological grading and prognosis in breast cancer: a study of 1409 cases of which 359 have been followed for 15 years. *British journal of cancer,* 11**,** 359.

BLOT, E., COUTEULX, S. L. L., JAMALI, H., CORNIC, M., GUILLEMET, C., DUVAL, C., HELLOT, M. F., PILLE, J. Y., PICQUENOT, J. M. & VEYRET, C. 2008. CxCR4 Membrane Expression in Node-Negative Breast Cancer. *The breast journal,* 14**,** 268-274.

BOLDAJIPOUR, B., MAHABALESHWAR, H., KARDASH, E., REICHMAN-FRIED, M., BLASER, H., MININA, S., WILSON, D., XU, Q. & RAZ, E. 2008. Control of chemokine-guided cell migration by ligand sequestration. *Cell,* 132**,** 463-473.

BONNOMET, A., BRYSSE, A., TACHSIDIS, A., WALTHAM, M., THOMPSON, E. W., POLETTE, M. & GILLES, C. 2010. Epithelial-to-mesenchymal transitions and circulating tumor cells. *Journal of mammary gland biology and neoplasia,* 15**,** 261-273.

BORST, M. J. & INGOLD, J. A. 1993. Metastatic patterns of invasive lobular versus invasive ductal carcinoma of the breast. *Surgery,* 114**,** 637-41.

BOUCEK, M. M. & SNYDERMAN, R. 1976. Calcium influx requirement for human neutrophil chemotaxis: inhibition by lanthanum chloride. *Science,* 193**,** 905-907.

BOUDOT, A., KERDIVEL, G., HABAUZIT, D., EECKHOUTE, J., LE DILY, F., FLOURIOT, G., SAMSON, M. & PAKDEL, F. 2011. Differential estrogen-regulation of CXCL12 chemokine receptors, CXCR4 and CXCR7, contributes to the growth effect of estrogens in breast cancer cells. *PloS one,* 6**,** e20898.

BOVE, K., LINCOLN, D. W. & TSAN, M.-F. 2002. Effect of resveratrol on growth of 4T1 breast cancer cells in vitro and in vivo. *Biochemical and biophysical research communications,* 291**,** 1001-1005.

BOYDEN, S. 1962. The chemotactic effect of mixtures of antibody and antigen on polymorphonuclear leucocytes. *The Journal of experimental medicine,* 115**,** 453-466.

BOYE, K. & MÆLANDSMO, G. M. 2010. S100A4 and metastasis: a small actor playing many roles. *The American journal of pathology,* 176**,** 528-535.

BOYLE, S., INGMAN, W., POLTAVETS, V., FAULKNER, J., WHITFIELD, R., MCCOLL, S. & KOCHETKOVA, M. 2016. The chemokine receptor CCR7 promotes mammary tumorigenesis through amplification of stem-like cells. *Oncogene,* 35**,** 105-115.

BRAND, S., DAMBACHER, J., BEIGEL, F., OLSZAK, T., DIEBOLD, J., OTTE, J.-M., GÖKE, B. & EICHHORST, S. T. 2005. CXCR4 and CXCL12 are inversely expressed in colorectal cancer cells and modulate cancer cell migration, invasion and MMP-9 activation. *Experimental cell research,* 310**,** 117-130.

BRANDT, S. M., MARIANI, R., HOLLAND, A. U., HOPE, T. J. & LANDAU, N. R. 2002. Association of chemokine-mediated block to HIV entry with coreceptor internalization. *Journal of Biological Chemistry,* 277**,** 17291-17299.

BRAUN, S. E., CHEN, K., FOSTER, R. G., KIM, C. H., HROMAS, R., KAPLAN, M. H., BROXMEYER, H. E. & CORNETTA, K. 2000. The CC chemokine CKβ-11/MIP-3β/ELC/Exodus 3 mediates tumor rejection of murine breast cancer cells through NK cells. *The Journal of Immunology,* 164**,** 4025-4031.

BREASTED, J. H. 1930. *The Edwin Smith Surgical Papyrus: published in facsimile and hieroglyphic transliteration with translation and commentary in two volumes,* Oriental Institute Publications, Chicago: The University of Chicago Press.

BRITSCHGI, M. R., FAVRE, S. & LUTHER, S. A. 2010. CCL21 is sufficient to mediate DC migration, maturation and function in the absence of CCL19. *European journal of immunology,* 40**,** 1266-1271.

BUCHWALOW, I., SAMOILOVA, V., BOECKER, W. & TIEMANN, M. 2011. Non-specific binding of antibodies in immunohistochemistry: fallacies and facts. *Scientific reports,* 1**,** 28.

BURBASSI, S., SENGUPTA, R. & MEUCCI, O. 2010. Alterations of CXCR4 function in μ-opioid receptor-deficient glia. *European Journal of Neuroscience,* 32**,** 1278-1288.

BURGER, J. A., BURGER, M. & KIPPS, T. J. 1999. Chronic lymphocytic leukemia B cells express functional CXCR4 chemokine receptors that mediate spontaneous migration beneath bone marrow stromal cells. *Blood,* 94**,** 3658-3667.

BURGER, J. A. & KIPPS, T. J. 2002. Chemokine receptors and stromal cells in the homing and homeostasis of chronic lymphocytic leukemia B cells. *Leukemia & lymphoma,* 43**,** 461-466.

BURGER, J. A. & KIPPS, T. J. 2006. CXCR4: a key receptor in the crosstalk between tumor cells and their microenvironment. *Blood,* 107**,** 1761-1767.

BURGER, J. A. & PELED, A. 2009. CXCR4 antagonists: targeting the microenvironment in leukemia and other cancers. *Leukemia,* 23**,** 43-52.

BURKHART, D. L. & SAGE, J. 2008. Cellular mechanisms of tumour suppression by the retinoblastoma gene. *Nature Reviews Cancer,* 8**,** 671-682.

BURNS, J. M., SUMMERS, B. C., WANG, Y., MELIKIAN, A., BERAHOVICH, R., MIAO, Z., PENFOLD, M. E. T., SUNSHINE, M. J., LITTMAN, D. R. & KUO, C. J. 2006. A novel chemokine receptor for SDF-1 and I-TAC involved in cell survival, cell adhesion, and tumor development. *The Journal of experimental medicine,* 203**,** 2201-2213.

BUSILLO, J. M. & BENOVIC, J. L. 2007. Regulation of CXCR4 signaling. *Biochimica et Biophysica Acta (BBA)-Biomembranes,* 1768**,** 952-963.

CABIOGLU, N., GONG, Y., ISLAM, R., BROGLIO, K. R., SNEIGE, N., SAHIN, A., GONZALEZ-ANGULO, A. M., MORANDI, P., BUCANA, C. & HORTOBAGYI, G. N. 2007. Expression of growth factor and chemokine receptors: new insights in the biology of inflammatory breast cancer. *Annals of oncology,* 18**,** 1021-1029.

CABIOGLU, N., SAHIN, A., MORANDI, P., MERIC-BERNSTAM, F., ISLAM, R., LIN, H., BUCANA, C., GONZALEZ-ANGULO, A., HORTOBAGYI, G. & CRISTOFANILLI, M. 2009. Chemokine receptors in advanced breast cancer: differential expression in metastatic disease sites with diagnostic and therapeutic implications. *Annals of oncology,* 20**,** 1013-1019.

CABIOGLU, N., SUMMY, J., MILLER, C., PARIKH, N. U., SAHIN, A. A., TUZLALI, S., PUMIGLIA, K., GALLICK, G. E. & PRICE, J. E. 2005a. CXCL-12/stromal cell–derived factor-1α transactivates HER2-neu in breast cancer cells by a novel pathway involving Src kinase activation. *Cancer research,* 65**,** 6493-6497.

CABIOGLU, N., YAZICI, M. S., ARUN, B., BROGLIO, K. R., HORTOBAGYI, G. N., PRICE, J. E. & SAHIN, A. 2005b. CCR7 and CXCR4 as novel biomarkers predicting axillary lymph node metastasis in T1 breast cancer. *Clinical Cancer Research,* 11**,** 5686-5693.

CAILLEAU, R., YOUNG, R., OLIVE, M. & REEVES, W. J. 1974. Breast tumor cell lines from pleural effusions. *Journal of the National Cancer Institute,* 53**,** 661-674.

CAIXEIRO, N. J., MARTIN, J. L. & SCOTT, C. D. 2013. Silencing the mannose 6-phosphate/IGF-II receptor differentially affects tumorigenic properties of normal breast epithelial cells. *International Journal of Cancer,* 133**,** 2542-2550.

CAMPBELL, C. I., THOMPSON, D. E., SIWICKY, M. D. & MOOREHEAD, R. A. 2011. Murine mammary tumor cells with a claudin-low genotype. *Cancer cell international,* 11**,** 28.

CAMPBELL, J. J., MURPHY, K. E., KUNKEL, E. J., BRIGHTLING, C. E., SOLER, D., SHEN, Z., BOISVERT, J., GREENBERG, H. B., VIERRA, M. A. & GOODMAN, S. B. 2001. CCR7 expression and memory T cell diversity in humans. *The Journal of Immunology,* 166**,** 877-884.

CANALS, M., MARCELLINO, D., FANELLI, F., CIRUELA, F., DE BENEDETTI, P., GOLDBERG, S. R., NEVE, K., FUXE, K., AGNATI, L. F. & WOODS, A. S. 2003. Adenosine A2A-dopamine D2 receptor-receptor heteromerization qualitative and quantitative assessment by fluorescence and bioluminescence energy transfer. *Journal of Biological Chemistry,* 278**,** 46741-46749.

CANCER RESEARCH UK. 2010. *Breast cancer statistics* [Online]. Available: http://www.cancerresearchuk.org/cancer-info/cancerstats/types/breast/ [Accessed November 2013].

CAO, J. X., GERSHON, P. D. & BLACK, D. N. 1995. Sequence analysis of HindIII Q2 fragment of capripoxvirus reveals a putative gene encoding a G-protein-coupled chemokine receptor homologue. *Virology,* 209**,** 207-212.

CAPILA, I. & LINHARDT, R. J. 2002. Heparin–protein interactions. *Angewandte Chemie International Edition,* 41**,** 390-412.

CARDONES, A. R., MURAKAMI, T. & HWANG, S. T. 2003. CXCR4 enhances adhesion of B16 tumor cells to endothelial cells in vitro and in vivo via β1 integrin. *Cancer research,* 63**,** 6751-6757.

CARLSEN, H. S., BAEKKEVOLD, E. S., MORTON, H. C., HARALDSEN, G. & BRANDTZAEG, P. 2004. Monocyte-like and mature macrophages produce CXCL13 (B cell–attracting chemokine 1) in inflammatory lesions with lymphoid neogenesis. *Blood,* 104**,** 3021-3027.

CARNEC, X., QUAN, L., OLSON, W. C., HAZAN, U. & DRAGIC, T. 2005. Anti-CXCR4 monoclonal antibodies recognizing overlapping epitopes differ significantly in their ability to inhibit entry of human immunodeficiency virus type 1. *Journal of virology,* 79**,** 1930-1933.

CARTER, N. M., ALI, S. & KIRBY, J. A. 2003. Endothelial inflammation: the role of differential expression of N-deacetylase/N-sulphotransferase enzymes in alteration of the immunological properties of heparan sulphate. *Journal of cell science,* 116**,** 3591-3600.

CASSIER, P. A., TREILLEUX, I., BACHELOT, T., RAY-COQUARD, I., BENDRISS-VERMARE, N., MÉNÉTRIER-CAUX, C., TRÉDAN, O., GODDARD-LÉON, S., PIN, J.-J. & MIGNOTTE, H. 2011. Prognostic value of the expression of C-Chemokine Receptor 6 and 7 and their ligands in non-metastatic breast cancer. *BMC cancer,* 11**,** 213.

CAVALLARO, U. & CHRISTOFORI, G. 2004. Cell adhesion and signalling by cadherins and Ig-CAMs in cancer. *Nature Reviews Cancer,* 4**,** 118-132.

CERADINI, D. J., KULKARNI, A. R., CALLAGHAN, M. J., TEPPER, O. M., BASTIDAS, N., KLEINMAN, M. E., CAPLA, J. M., GALIANO, R. D., LEVINE, J. P. & GURTNER, G. C. 2004. Progenitor cell trafficking is regulated by hypoxic gradients through HIF-1 induction of SDF-1. *Nature medicine,* 10**,** 858-864.

CHADWICK, B. P. & WILLARD, H. F. 2003. Chromatin of the Barr body: histone and non-histone proteins associated with or excluded from the inactive X chromosome. *Human molecular genetics,* 12**,** 2167-2178.

CHANG, T. L.-Y., GORDON, C. J., ROSCIC-MRKIC, B., POWER, C., PROUDFOOT, A. E. I., MOORE, J. P. & TRKOLA, A. 2002. Interaction of the CC-chemokine RANTES with glycosaminoglycans activates a p44/p42 mitogen-activated protein kinase-dependent signaling pathway and enhances human immunodeficiency virus type 1 infectivity. *Journal of virology,* 76**,** 2245-2254.

CHARAN, J. & KANTHARIA, N. D. 2013. How to calculate sample size in animal studies? *Journal of Pharmacology and Pharmacotherapeutics,* 4**,** 303.

CHATTERJEE, M., BORST, O., WALKER, B., FOTINOS, A., VOGEL, S., SEIZER, P., MACK, A. F., ALAMPOUR-RAJABI, S., RATH, D. & GEISLER, T. 2014a. Macrophage migration inhibitory factor (MIF) limits activation-induced apoptosis of platelets via CXCR7-dependent Akt signaling. *Circulation research,* 115**,** 939-949.

CHATTERJEE, M., SEIZER, P., BORST, O., SCHÖNBERGER, T., MACK, A., GEISLER, T., LANGER, H. F., MAY, A. E., VOGEL, S. & LANG, F. 2014b. SDF-1α induces differential trafficking of CXCR4-CXCR7 involving cyclophilin A, CXCR7 ubiquitination and promotes platelet survival. *The FASEB Journal,* 28**,** 2864-2878.

CHECKLEY, S., MACCALLUM, L., YATES, J., JASPER, P., LUO, H., TOLSMA, J. & BENDTSEN, C. 2015. Bridging the gap between in vitro and in vivo: Dose and schedule predictions for the ATR inhibitor AZD6738. *Scientific reports,* 5**,** 13545.

CHEN, A., BEETHAM, H., BLACK, M. A., PRIYA, R., TELFORD, B. J., GUEST, J., WIGGINS, G. A. R., GODWIN, T. D. & GUILFORD, P. J. 2014. E-cadherin loss alters cytoskeletal organization and adhesion in non-malignant breast cells but is insufficient to induce an epithelial-mesenchymal transition. *BMC cancer,* 14**,** 552.

CHEN, D., XIA, Y., ZUO, K., WANG, Y., ZHANG, S., KUANG, D., DUAN, Y., ZHAO, X. & WANG, G. 2015a. Crosstalk between SDF-1/CXCR4 and SDF-1/CXCR7 in cardiac stem cell migration. *Scientific reports,* 5**,** 16813.

CHEN, X., GELLER, E. B., ROGERS, T. J. & ADLER, M. W. 2007. Rapid heterologous desensitization of antinociceptive activity between mu or delta opioid receptors and chemokine receptors in rats. *Drug and alcohol dependence,* 88**,** 36-41.

CHEN, Y., RAMJIAWAN, R. R., REIBERGER, T., NG, M. R., HATO, T., HUANG, Y., OCHIAI, H., KITAHARA, S., UNAN, E. C. & REDDY, T. P. 2015b. CXCR4 inhibition in tumor microenvironment facilitates anti-programmed death receptor-1 immunotherapy in sorafenib-treated hepatocellular carcinoma in mice. *Hepatology,* 61**,** 1591-1602.

CHENG, N., CHYTIL, A., SHYR, Y., JOLY, A. & MOSES, H. L. 2008. Transforming growth factor-β signaling–deficient fibroblasts enhance hepatocyte growth factor signaling in mammary carcinoma cells to promote scattering and invasion. *Molecular Cancer Research,* 6**,** 1521-1533.

CHIDIAC, P., GREEN, M. A., PAWAGI, A. B. & WELLS, J. W. 1997. Cardiac muscarinic receptors. Cooperativity as the basis for multiple states of affinity. *Biochemistry,* 36**,** 7361-7379.

CHOI, Y. H., BURDICK, M. D., STRIETER, B. A., MEHRAD, B. & STRIETER, R. M. 2014. CXCR4, but not CXCR7, discriminates metastatic behavior in non–small cell lung cancer cells. *Molecular Cancer Research,* 12**,** 38-47.

CHRISTOPHERSON, K. W., CAMPBELL, J. J., TRAVERS, J. B. & HROMAS, R. A. 2002. Low-molecular-weight heparins inhibit CCL21-induced T cell adhesion and migration. *Journal of Pharmacology and Experimental Therapeutics,* 302**,** 290-295.

CIRCELLI, L., SCIAMMARELLA, C., GUADAGNO, E., TAFUTO, S., DE CARO, M. D. B., BOTTI, G., PEZZULLO, L., ARIA, M., RAMUNDO, V. & TATANGELO, F. 2016. CXCR4/CXCL12/CXCR7 axis is functional in neuroendocrine tumors and signals on mTOR. *Oncotarget,* 7**,** 18865.

CITRI, A. & YARDEN, Y. 2006. EGF–ERBB signalling: towards the systems level. *Nature reviews Molecular cell biology,* 7**,** 505-516.

CLATWORTHY, M. R., ARONIN, C. E. P., MATHEWS, R. J., MORGAN, N. Y., SMITH, K. G. C. & GERMAIN, R. N. 2014. Immune complexes stimulate CCR7-dependent dendritic cell migration to lymph nodes. *Nature medicine,* 20**,** 1458-1463.

COFFEY, J. C., WANG, J. H., SMITH, M. J. F., BOUCHIER-HAYES, D., COTTER, T. G. & REDMOND, H. P. 2003. Excisional surgery for cancer cure: therapy at a cost. *The lancet oncology,* 4**,** 760-768.

COKE, C. J., SCARLETT, K. A., CHETRAM, M. A., JONES, K. J., SANDIFER, B. J., DAVIS, A. S., MARCUS, A. I. & HINTON, C. V. 2016. Simultaneous Activation of Induced Heterodimerization between CXCR4 Chemokine Receptor and Cannabinoid Receptor 2 (CB2) Reveals a Mechanism for Regulation of Tumor Progression. *Journal of Biological Chemistry,* 291**,** 9991-10005.

COLDITZ, G. A., HANKINSON, S. E., HUNTER, D. J., WILLETT, W. C., MANSON, J. E., STAMPFER, M. J., HENNEKENS, C., ROSNER, B. & SPEIZER, F. E. 1995. The use of estrogens and progestins and the risk of breast cancer in postmenopausal women. *New England Journal of Medicine,* 332**,** 1589-1593.

COLLABORATIVE GROUP ON HORMONAL FACTORS IN BREAST CANCER 1996. Breast cancer and hormonal contraceptives: collaborative reanalysis of individual data on 53 297 women with breast cancer and 100 239 women without breast cancer from 54 epidemiological studies. *The Lancet,* 347**,** 1713-1727.

COLLABORATIVE GROUP ON HORMONAL FACTORS IN BREAST CANCER 1997. Breast cancer and hormone replacement therapy: collaborative reanalysis of data from 51 epidemiological studies of 52 705 women with breast cancer and 108 411 women without breast cancer. *The Lancet,* 350**,** 1047-1059.

COLLABORATIVE GROUP ON HORMONAL FACTORS IN BREAST CANCER 2012. Menarche, menopause, and breast cancer risk: individual participant meta-analysis, including 118 964 women with breast cancer from 117 epidemiological studies. *The lancet oncology,* 13**,** 1141-1151.

COLOTTA, F., ALLAVENA, P., SICA, A., GARLANDA, C. & MANTOVANI, A. 2009. Cancer-related inflammation, the seventh hallmark of cancer: links to genetic instability. *Carcinogenesis,* 30**,** 1073-1081.

COMERFORD, I., MILASTA, S., MORROW, V., MILLIGAN, G. & NIBBS, R. 2006. The chemokine receptor CCX-CKR mediates effective scavenging of CCL19 in vitro. *European journal of immunology,* 36**,** 1904-1916.

CONRAD, H. E. 1997. *Heparin-binding proteins*, Academic Press.

CONSALES, C., PORTELLA, L., NAPOLITANO, M., PENFOLD, M. E. T., POLIMENO, M. N., CIOFFI, M., D'ALTERIO, C., CALEMMA, R., CASTELLO, G. & SCALA, S. 2010. CXCR7 is a functional receptor in renal cancer cell lines. *Cancer Research,* 70**,** 5211-5211.

CONTENTO, R. L., MOLON, B., BOULARAN, C., POZZAN, T., MANES, S., MARULLO, S. & VIOLA, A. 2008. CXCR4–CCR5: a couple modulating T cell functions. *Proceedings of the National Academy of Sciences,* 105**,** 10101-10106.

COOK, J. S., WOLSING, D. H., LAMEH, J., OLSON, C. A., CORREA, P. E., SADEE, W., BLUMENTHAL, E. M. & ROSENBAUM, J. S. 1992. Characterization of the RDC1 gene which encodes the canine omolog of a proposed human VIP receptor Expression does not correlate with an increase in VIP binding sites. *FEBS letters,* 300**,** 149-152.

CORCIONE, A., ARDUINO, N., FERRETTI, E., PISTORIO, A., SPINELLI, M., OTTONELLO, L., DALLEGRI, F., BASSO, G. & PISTOIA, V. 2006. Chemokine receptor expression and function in childhood acute lymphoblastic leukemia of B-lineage. *Leukemia research,* 30**,** 365-372.

COSTANTINI, S., RAUCCI, R., DE VERO, T., CASTELLO, G. & COLONNA, G. 2013. Common structural interactions between the receptors CXCR3, CXCR4 and CXCR7 complexed with their natural ligands, CXCL11 and CXCL12, by a modeling approach. *Cytokine,* 64**,** 316-321.

COUSSENS, L. M. & WERB, Z. 2002. Inflammation and cancer. *Nature,* 420**,** 860-867.

CRONIN, P. A., WANG, J. H. & REDMOND, H. P. 2010. Hypoxia increases the metastatic ability of breast cancer cells via upregulation of CXCR4. *BMC cancer,* 10**,** 225.

CVEJIC, S. & DEVI, L. A. 1997. Dimerization of the δ opioid receptor: implication for a role in receptor internalization. *Journal of Biological Chemistry,* 272**,** 26959-26964.

D'ALTERIO, C., AVALLONE, A., TATANGELO, F., DELRIO, P., PECORI, B., CELLA, L., PELELLA, A., D'ARMIENTO, F. P., CARLOMAGNO, C. & BIANCO, F. 2014. A prognostic model comprising pT stage, N status, and the chemokine receptors CXCR4 and CXCR7 powerfully predicts outcome in neoadjuvant resistant rectal cancer patients. *International journal of cancer,* 135**,** 379-390.

D'ALTERIO, C., CONSALES, C., POLIMENO, M., FRANCO, R., CINDOLO, L., PORTELLA, L., CIOFFI, M., CALEMMA, R., MARRA, L. & CLAUDIO, L. 2010. Concomitant CXCR4 and CXCR7 expression predicts poor prognosis in renal cancer. *Current cancer drug targets,* 10**,** 772-781.

DAMBLY-CHAUDIÈRE, C., CUBEDO, N. & GHYSEN, A. 2007. Control of cell migration in the development of the posterior lateral line: antagonistic interactions between the chemokine receptors CXCR4 and CXCR7/RDC1. *BMC developmental biology,* 7**,** 23.

DAMERON, K. M., VOLPERT, O. V., TAINSKY, M. A. & BOUCK, N. 1994. Control of angiogenesis in fibroblasts by p53 regulation of thrombospondin-1. *Science,* 265**,** 1582-1584.

DAMUS, P. S., HICKS, M. & ROSENBERG, R. D. 1973. Anticoagulant action of heparin. *Nature,* 246**,** 355-357.

DARASH-YAHANA, M., PIKARSKY, E., ABRAMOVITCH, R., ZEIRA, E., PAL, B., KARPLUS, R., BEIDER, K., AVNIEL, S., KASEM, S. & GALUN, E. 2004. Role of high expression levels of CXCR4 in tumor growth, vascularization, and metastasis. *The FASEB Journal,* 18**,** 1240-1242.

DAVIES, M. A. & SAMUELS, Y. 2010. Analysis of the genome to personalize therapy for melanoma. *Oncogene,* 29**,** 5545-5555.

DE WET, J. R., WOOD, K., DELUCA, M., HELINSKI, D. R. & SUBRAMANI, S. 1987. Firefly luciferase gene: structure and expression in mammalian cells. *Molecular and cellular biology,* 7**,** 725-737.

DÉCAILLOT, F. M., KAZMI, M. A., LIN, Y., RAY-SAHA, S., SAKMAR, T. P. & SACHDEV, P. 2011. CXCR7/CXCR4 heterodimer constitutively recruits β-arrestin to enhance cell migration. *Journal of Biological Chemistry,* 286**,** 32188-32197.

DEMICHELI, R., RETSKY, M. W., HRUSHESKY, W. J. M., BAUM, M. & GUKAS, I. D. 2008. The effects of surgery on tumor growth: a century of investigations. *Annals of Oncology,* 19**,** 1821-1828.

DEVALARAJA, M. N. & RICHMOND, A. 1999. Multiple chemotactic factors: fine control or redundancy? *Trends in pharmacological sciences,* 20**,** 151-156.

DEWS, M., HOMAYOUNI, A., YU, D., MURPHY, D., SEVIGNANI, C., WENTZEL, E., FURTH, E. E., LEE, W. M., ENDERS, G. H. & MENDELL, J. T. 2006. Augmentation of tumor angiogenesis by a Myc-activated microRNA cluster. *Nature genetics,* 38**,** 1060-1065.

DEXTER, D. L., KOWALSKI, H. M., BLAZAR, B. A., FLIGIEL, Z., VOGEL, R. & HEPPNER, G. H. 1978. Heterogeneity of tumor cells from a single mouse mammary tumor. *Cancer research,* 38**,** 3174-3181.

DHILLON, A. S., HAGAN, S., RATH, O. & KOLCH, W. 2007. MAP kinase signalling pathways in cancer. *Oncogene,* 26**,** 3279-3290.

DICK, L. R., CRUIKSHANK, A. A., GRENIER, L., MELANDRI, F. D., NUNES, S. L. & STEIN, R. L. 1996. Mechanistic Studies on the Inactivation of the Proteasome by Lactacystin A CENTRAL ROLE FOR clasto-LACTACYSTIN β-LACTONE. *Journal of Biological Chemistry,* 271**,** 7273-7276.

DIEU, M.-C., VANBERVLIET, B., VICARI, A., BRIDON, J.-M., OLDHAM, E., AÏT-YAHIA, S., BRIÈRE, F., ZLOTNIK, A., LEBECQUE, S. & CAUX, C. 1998. Selective recruitment of immature and mature dendritic cells by distinct chemokines expressed in different anatomic sites. *The Journal of experimental medicine,* 188**,** 373-386.

DING, Y., SHIMADA, Y., MAEDA, M., KAWABE, A., KAGANOI, J., KOMOTO, I., HASHIMOTO, Y., MIYAKE, M., HASHIDA, H. & IMAMURA, M. 2003. Association of CC chemokine receptor 7 with lymph node metastasis of esophageal squamous cell carcinoma. *Clinical Cancer Research,* 9**,** 3406-3412.

DINGER, M. C., BADER, J. E., KÓBOR, A. D., KRETZSCHMAR, A. K. & BECK-SICKINGER, A. G. 2003. Homodimerization of neuropeptide y receptors investigated by fluorescence resonance energy transfer in living cells. *Journal of Biological Chemistry,* 278**,** 10562-10571.

DINKEL, B. A., KREMER, K., OSBORNE, D. G., REED, B. K., SCHRUM, A. G. & HEDIN, K. E. 2016. Molecular mechanisms required for TCR-mediated formation of TCR-CXCR4 heterodimers. *The Journal of Immunology,* 196**,** 128.6.

DIVATIA, J. V. & AMBULKAR, R. 2014. Anesthesia and cancer recurrence: What is the evidence? *Journal of anaesthesiology, clinical pharmacology,* 30**,** 147.

DOITSIDOU, M., REICHMAN-FRIED, M., STEBLER, J., KÖPRUNNER, M., DÖRRIES, J., MEYER, D., ESGUERRA, C. V., LEUNG, T. & RAZ, E. 2002. Guidance of primordial germ cell migration by the chemokine SDF-1. *Cell,* 111**,** 647-659.

DONZELLA, G. A., SCHOLS, D., LIN, S. W., ESTÉ, J. A., NAGASHIMA, K. A., MADDON, P. J., ALLAWAY, G. P., SAKMAR, T. P., HENSON, G. & DECLERCQ, E. 1998. AMD3100, a small molecule inhibitor of HIV-1 entry via the CXCR4 co-receptor. *Nature medicine,* 4**,** 72-77.

DORSAM, R. T. & GUTKIND, J. S. 2007. G-protein-coupled receptors and cancer. *Nature reviews cancer,* 7**,** 79-94.

DOUGLASS, S., ALI, S., MEESON, A. P., BROWELL, D. & KIRBY, J. A. 2012. The role of FOXP3 in the development and metastatic spread of breast cancer. *Cancer and Metastasis Reviews,* 31**,** 843-854.

DOUGLASS, S., MEESON, A. P., OVERBECK-ZUBRZYCKA, D., BRAIN, J. G., BENNETT, M. R., LAMB, C. A., LENNARD, T. W. J., BROWELL, D., ALI, S. & KIRBY, J. A. 2014. Breast cancer metastasis: demonstration that FOXP3 regulates CXCR4 expression and the response to CXCL12. *The Journal of pathology,* 234**,** 74-85.

DOUGLASS, S. M. 2014. *The roles of FOXP3 and CXCR4 in breast cancer.* PhD, Newcastle University.

DOW, L. E., KAUFFMAN, J. S., CADDY, J., PETERSON, A. S., JANE, S. M., RUSSELL, S. M. & HUMBERT, P. O. 2007. The tumour-suppressor Scribble dictates cell polarity during directed epithelial migration: regulation of Rho GTPase recruitment to the leading edge. *Oncogene,* 26**,** 2272-2282.

DRURY, L. J., ZIAREK, J. J., GRAVEL, S., VELDKAMP, C. T., TAKEKOSHI, T., HWANG, S. T., HEVEKER, N., VOLKMAN, B. F. & DWINELL, M. B. 2011. Monomeric and dimeric CXCL12 inhibit metastasis

through distinct CXCR4 interactions and signaling pathways. *Proceedings of the National Academy of Sciences,* 108**,** 17655-17660.

DUDA, D. G., KOZIN, S. V., KIRKPATRICK, N. D., XU, L., FUKUMURA, D. & JAIN, R. K. 2011. CXCL12 (SDF1α)-CXCR4/CXCR7 pathway inhibition: an emerging sensitizer for anticancer therapies? *Clinical Cancer Research,* 17**,** 2074-2080.

DUNN, T. B. 1954. Normal and pathologic anatomy of the reticular tissue in laboratory mice, with a classification and discussion of neoplasms. *Journal of the National Cancer Institute,* 14**,** 1281-1433.

DUVIC, M., EVANS, M. & WANG, C. 2016. Mogamulizumab for the treatment of cutaneous T-cell lymphoma: recent advances and clinical potential. *Therapeutic advances in hematology,* 7**,** 171-174.

DWYER, M. P., YU, Y., CHAO, J., AKI, C., CHAO, J., BIJU, P., GIRIJAVALLABHAN, V., RINDGEN, D., BOND, R. & MAYER-EZEL, R. 2006. Discovery of 2-hydroxy-N, N-dimethyl-3-{2-[[(R)-1-(5-methylfuran-2-yl) propyl] amino]-3, 4-dioxocyclobut-1-enylamino} benzamide (SCH 527123): a potent, orally bioavailable CXCR2/CXCR1 receptor antagonist. *Journal of medicinal chemistry,* 49**,** 7603-7606.

DYKXHOORN, D. M., WU, Y., XIE, H., YU, F., LAL, A., PETROCCA, F., MARTINVALET, D., SONG, E., LIM, B. & LIEBERMAN, J. 2009. miR-200 enhances mouse breast cancer cell colonization to form distant metastases. *PloS one,* 4**,** e7181.

EARLY BREAST CANCER TRIALISTS' COLLABORATIVE GROUP 2006. Effects of radiotherapy and of differences in the extent of surgery for early breast cancer on local recurrence and 15-year survival: an overview of the randomised trials. *The Lancet,* 366**,** 2087-2106.

EARLY BREAST CANCER TRIALISTS' COLLABORATIVE GROUP 2011. Relevance of breast cancer hormone receptors and other factors to the efficacy of adjuvant tamoxifen: patient-level meta-analysis of randomised trials. *The lancet,* 378**,** 771-784.

EARLY BREAST CANCER TRIALISTS' COLLABORATIVE GROUP 2015. Aromatase inhibitors versus tamoxifen in early breast cancer: patient-level meta-analysis of the randomised trials. *The Lancet,* 386**,** 1341-1352.

EBIOSCIENCE. *Anti-Mouse CD184 (CXCR4) PE clone 2B11* [Online]. Available: https://www.thermofisher.com/antibody/product/CD184-CXCR4-Antibody-clone-2B11-Monoclonal/12-9991-81#/legacy=ebioscience.com?c=Belarus.

EBISUYA, M., KONDOH, K. & NISHIDA, E. 2005. The duration, magnitude and compartmentalization of ERK MAP kinase activity: mechanisms for providing signaling specificity. *Journal of cell science,* 118**,** 2997-3002.

EDROS, R., MCDONNELL, S. & AL-RUBEAI, M. 2014. The relationship between mTOR signalling pathway and recombinant antibody productivity in CHO cell lines. *BMC biotechnology,* 14**,** 15.

EFFERSON, C. L., TSUDA, N., KAWANO, K., NISTAL-VILLÁN, E., SELLAPPAN, S., YU, D., MURRAY, J. L., GARCÍA-SASTRE, A. & IOANNIDES, C. G. 2006. Prostate tumor cells infected with a recombinant influenza virus expressing a truncated NS1 protein activate cytolytic CD8+ cells to recognize noninfected tumor cells. *Journal of virology,* 80**,** 383-394.

EGAN, K. M., TRICHOPOULOS, D., STAMPFER, M. J., WILLETT, W. C., NEWCOMB, P. A., TRENTHAM-DIETZ, A., LONGNECKER, M. P. & BARON, J. A. 1996. Jewish religion and risk of breast cancer. *The Lancet,* 347**,** 1645-1646.

EISENHARDT, A., FREY, U., TACK, M., ROSSKOPF, D., LÜMMEN, G., RÜBBEN, H. & SIFFERT, W. 2005. Expression analysis and potential functional role of the CXCR4 chemokine receptor in bladder cancer. *European urology,* 47**,** 111-117.

ELKIN, M., COHEN, I., ZCHARIA, E., ORGEL, A., GUATTA-RANGINI, Z., PERETZ, T., VLODAVSKY, I. & KLEINMAN, H. K. 2003. Regulation of heparanase gene expression by estrogen in breast cancer. *Cancer research,* 63**,** 8821-8826.

ELLIS, I. O., GALEA, M., BROUGHTON, N., LOCKER, A., BLAMEY, R. W. & ELSTON, C. W. 1992. Pathological prognostic factors in breast cancer. II. Histological type. Relationship with survival in a large study with long-term follow-up. *Histopathology,* 20**,** 479-489.

ELSTON, C. W. & ELLIS, I. O. 1991. Pathological prognostic factors in breast cancer. I. The value of histological grade in breast cancer: experience from a large study with long-term follow-up. *Histopathology,* 19**,** 403-410.

EMENS, L. A., BRAITEH, F. S., CASSIER, P., DELORD, J.-P., EDER, J. P., FASSO, M., XIAO, Y., WANG, Y., MOLINERO, L. & CHEN, D. S. 2015. Inhibition of PD-L1 by MPDL3280A leads to clinical activity in patients with metastatic triple-negative breast cancer (TNBC). *Cancer Research,* 75**,** 2859-2859.

ENDRES, M. J., CLAPHAM, P. R., MARSH, M., AHUJA, M., TURNER, J. D., MCKNIGHT, A., THOMAS, J. F., STOEBENAU-HAGGARTY, B., CHOE, S. & VANCE, P. J. 1996. CD4-independent infection by HIV-2 is mediated by fusin/CXCR4. *Cell,* 87**,** 745-756.

EPSTEIN, R. J. 2004. The CXCL12–CXCR4 chemotactic pathway as a target of adjuvant breast cancer therapies. *Nature Reviews Cancer,* 4**,** 901-909.

ERTAULT-DANESHPOUY, M., DESCHAUMES, C., LEBOEUF, C., BRUS-RAMER, M., AMIRA, F., LEGRES, L. & JANIN, P. A. 2009. Histochemical and immunohistochemical protocols for routine biopsies embedded in Lowicryl resin. *Biotechnic & histochemistry,* 78**,** 35-42.

EUHUS, D. M., HUDD, C., LAREGINA, M. C. & JOHNSON, F. E. 1986. Tumor measurement in the nude mouse. *Journal of surgical oncology,* 31**,** 229-234.

EWERTZ, M., DUFFY, S. W., ADAMI, H. O., KVÅLE, G., LUND, E., MEIRIK, O., MELLEMGAARD, A., SOINI, I. & TULINIUS, H. 1990. Age at first birth, parity and risk of breast cancer: A meta-analysis of 8 studies from the nordic countries. *International journal of cancer,* 46**,** 597-603.

EXADAKTYLOS, A. K., BUGGY, D. J., MORIARTY, D. C., MASCHA, E. & SESSLER, D. I. 2006. Can anesthetic technique for primary breast cancer surgery affect recurrence or metastasis? *The Journal of the American Society of Anesthesiologists,* 105**,** 660-664.

FASCHING, P. A., HEUSINGER, K., HAEBERLE, L., NIKLOS, M., HEIN, A., BAYER, C. M., RAUH, C., SCHULZ-WENDTLAND, R., BANI, M. R. & SCHRAUDER, M. 2011. Ki67, chemotherapy response, and prognosis in breast cancer patients receiving neoadjuvant treatment. *BMC cancer,* 11**,** 486

FEIG, C., JONES, J. O., KRAMAN, M., WELLS, R. J., DEONARINE, A., CHAN, D. S., CONNELL, C. M., ROBERTS, E. W., ZHAO, Q. & CABALLERO, O. L. 2013. Targeting CXCL12 from FAP-expressing carcinoma-associated fibroblasts synergizes with anti–PD-L1 immunotherapy in pancreatic cancer. *Proceedings of the National Academy of Sciences,* 110**,** 20212-20217.

FEIL, C. & AUGUSTIN, H. G. 1998. Endothelial cells differentially express functional CXC-chemokine receptor-4 (CXCR-4/fusin) under the control of autocrine activity and exogenous cytokines. *Biochemical and biophysical research communications,* 247**,** 38-45.

FELDING-HABERMANN, B., O'TOOLE, T. E., SMITH, J. W., FRANSVEA, E., RUGGERI, Z. M., GINSBERG, M. H., HUGHES, P. E., PAMPORI, N., SHATTIL, S. J. & SAVEN, A. 2001. Integrin activation controls metastasis in human breast cancer. *Proceedings of the National Academy of Sciences,* 98**,** 1853-1858.

FENTEANY, G., STANDAERT, R. F., LANE, W. S. & CHOI, S. 1995. Inhibition of proteasome activities and subunit-specific amino-terminal threonine modification by lactacystin. *Science,* 268**,** 726.

FERNANDEZ, E. J. & LOLIS, E. 2002. Structure, function, and inhibition of chemokines. *Annual review of pharmacology and toxicology,* 42**,** 469-499.

FERNANDIS, A. Z., CHERLA, R. P., CHERNOCK, R. D. & GANJU, R. K. 2002. CXCR4/CCR5 down-modulation and chemotaxis are regulated by the proteasome pathway. *Journal of Biological Chemistry,* 277**,** 18111-18117.

FERNANDIS, A. Z., PRASAD, A., BAND, H., KLÖSEL, R. & GANJU, R. K. 2004. Regulation of CXCR4-mediated chemotaxis and chemoinvasion of breast cancer cells. *Oncogene,* 23**,** 157-167.

FIDLER, I. J. 2002. The organ microenvironment and cancer metastasis. *Differentiation,* 70**,** 498-505.

FIDLER, I. J. 2003. The pathogenesis of cancer metastasis: the'seed and soil'hypothesis revisited. *Nature Reviews Cancer,* 3**,** 453-458.

FIFE, B. T. & BLUESTONE, J. A. 2008. Control of peripheral T-cell tolerance and autoimmunity via the CTLA-4 and PD-1 pathways. *Immunological reviews,* 224**,** 166-182.

FINLEY, M. J., CHEN, X., BARDI, G., DAVEY, P., GELLER, E. B., ZHANG, L., ADLER, M. W. & ROGERS, T. J. 2008. Bi-directional heterologous desensitization between the major HIV-1 co-receptor CXCR4 and the κ-opioid receptor. *Journal of neuroimmunology,* 197**,** 114-123.

FISHER, B., ANDERSON, S., REDMOND, C. K., WOLMARK, N., WICKERHAM, D. L. & CRONIN, W. M. 1995. Reanalysis and results after 12 years of follow-up in a randomized clinical trial comparing total mastectomy with lumpectomy with or without irradiation in the treatment of breast cancer. *New England Journal of Medicine,* 333**,** 1456-1461.

FISHER, E. R., GREGORIO, R. M., REDMOND, C., KIM, W. S. & FISHER, B. 1976. Pathologic findings from the National Surgical Adjuvant Breast Project (Protocol No. 4): III. The significance of extranodal extension of axillary metastases. *American journal of clinical pathology,* 65**,** 439-444.

FLOYD, D. H., GEVA, A., BRUINSMA, S. P., OVERTON, M. C., BLUMER, K. J. & BARANSKI, T. J. 2003. C5a receptor oligomerization II. Fluorescence resonance energy transfer studies of a human G protein-coupled receptor expressed in yeast. *Journal of Biological Chemistry,* 278**,** 35354-35361.

FOGH, J., FOGH, J. M. & ORFEO, T. 1977. One hundred and twenty-seven cultured human tumor cell lines producing tumors in nude mice. *Journal of the National Cancer Institute,* 59**,** 221-226.

FOLEY, J. F. 2007. Calcium and Chemotaxis. *Science Signaling,* 2007**,** tw293.

FOLKMAN, J. 1986. How is blood vessel growth regulated in normal and neoplastic tissue?—GHA Clowes Memorial Award Lecture. *Cancer research,* 46**,** 467-473.

FONG, A. M., PREMONT, R. T., RICHARDSON, R. M., YEN-REI, A. Y., LEFKOWITZ, R. J. & PATEL, D. D. 2002. Defective lymphocyte chemotaxis in β-arrestin2-and GRK6-deficient mice. *Proceedings of the National Academy of Sciences,* 99**,** 7478-7483.

FONG, Y. F., EVANS, J., BROOKES, D. & THOMAS, K. G. 2012. The Nottingham Prognostic Index: 5-year and 10-year survival data for all-cause survival within a screened population. *Breast Cancer Research,* 14**,** 1-14.

FOOD AND DRUG ADMINISTRATION. 2012. *FDA drug safety communication: revised recommendations for cardiovascular monitoring and use of multiple sclerosis drug Gilenya (fingolimod)* [Online]. Available: http://www.fda.gov/Drugs/DrugSafety/ucm303192.htm

[Accessed May 2017.

FÖRSTER, R., DAVALOS-MISSLITZ, A. C. & ROT, A. 2008. CCR7 and its ligands: balancing immunity and tolerance. *Nature Reviews Immunology,* 8**,** 362-371.

FÖRSTER, R., KREMMER, E., SCHUBEL, A., BREITFELD, D., KLEINSCHMIDT, A., NERL, C., BERNHARDT, G. & LIPP, M. 1998. Intracellular and surface expression of the HIV-1 coreceptor CXCR4/fusin on various leukocyte subsets: rapid internalization and recycling upon activation. *The Journal of Immunology,* 160**,** 1522-1531.

FÖRSTER, R., SCHUBEL, A., BREITFELD, D., KREMMER, E., RENNER-MÜLLER, I., WOLF, E. & LIPP, M. 1999. CCR7 coordinates the primary immune response by establishing functional microenvironments in secondary lymphoid organs. *Cell,* 99**,** 23-33.

FÖRSTER, T. 1965. *Delocalized excitation and excitation transfer,* Modern Quantum Chemistry, Florida State University.

FRANCISCO, L. M., SAGE, P. T. & SHARPE, A. H. 2010. The PD-1 pathway in tolerance and autoimmunity. *Immunological reviews,* 236**,** 219-242.

FRICKER, S. P., ANASTASSOV, V., COX, J., DARKES, M. C., GRUJIC, O., IDZAN, S. R., LABRECQUE, J., LAU, G., MOSI, R. M. & NELSON, K. L. 2006. Characterization of the molecular pharmacology of AMD3100: a specific antagonist of the G-protein coupled chemokine receptor, CXCR4. *Biochemical pharmacology,* 72**,** 588-596.

FRIEDL, P., BORGMANN, S. & BRÖCKER, E.-B. 2001. Amoeboid leukocyte crawling through extracellular matrix: lessons from the Dictyostelium paradigm of cell movement. *Journal of leukocyte biology,* 70**,** 491-509.

FULLER, M. S., LEE, C. I. & ELMORE, J. G. 2015. Breast cancer screening: an evidence-based update. *Medical Clinics of North America,* 99**,** 451-468.

GACH, K., PIESTRZENIEWICZ, M., FICHNA, J., SZEMRAJ, J. & JANECKA, A. 2009. Opioid antagonist-induced regulation of the mu-opioid receptor expression in MCF-7 breast cancer cell line. *Endocrine regulations,* 43**,** 23-28.

GALEA, M. H., BLAMEY, R. W., ELSTON, C. E. & ELLIS, I. O. 1992. The Nottingham Prognostic Index in primary breast cancer. *Breast cancer research and treatment,* 22**,** 207-219.

GANDHI, N. S. & MANCERA, R. L. 2008. The structure of glycosaminoglycans and their interactions with proteins. *Chemical biology & drug design,* 72**,** 455-482.

GAO, H., SUN, Y., WU, Y., LUAN, B., WANG, Y., QU, B. & PEI, G. 2004. Identification of β-arrestin2 as a G protein-coupled receptor-stimulated regulator of NF-κB pathways. *Molecular cell,* 14**,** 303-317.

GEBAUER, F., TACHEZY, M., EFFENBERGER, K., VON LOGA, K., ZANDER, H., MARX, A., KAIFI, J. T., SAUTER, G., IZBICKI, J. R. & BOCKHORN, M. 2011. Prognostic impact of CXCR4 and CXCR7 expression in pancreatic adenocarcinoma. *Journal of surgical oncology,* 104**,** 140-145.

GEISSMANN, F., JUNG, S. & LITTMAN, D. R. 2003. Blood monocytes consist of two principal subsets with distinct migratory properties. *Immunity,* 19**,** 71-82.

GEORGE, S. R., O'DOWD, B. F. & LEE, S. P. 2002. G-protein-coupled receptor oligomerization and its potential for drug discovery. *Nature Reviews Drug Discovery,* 1**,** 808-820.

GERLACH, L. O., SKERLJ, R. T., BRIDGER, G. J. & SCHWARTZ, T. W. 2001. Molecular interactions of cyclam and bicyclam non-peptide antagonists with the CXCR4 chemokine receptor. *Journal of Biological Chemistry,* 276**,** 14153-14160.

GERRITS, H., VAN INGEN SCHENAU, D. S., BAKKER, N. E. C., VAN DISSELDORP, A. J. M., STRIK, A., HERMENS, L. S., KOENEN, T. B., KRAJNC-FRANKEN, M. A. M. & GOSSEN, J. A. 2008. Early postnatal lethality and cardiovascular defects in CXCR7-deficient mice. *Genesis,* 46**,** 235-245.

GHEBEH, H., BARHOUSH, E., TULBAH, A., ELKUM, N., AL-TWEIGERI, T. & DERMIME, S. 2008. FOXP3+ T regs and B7-H1+/PD-1+ T lymphocytes co-infiltrate the tumor tissues of high-risk breast cancer patients: Implication for immunotherapy. *BMC cancer,* 8**,** 57.

GHEBRANIOUS, N. & DONEHOWER, L. A. 1998. Mouse models in tumor suppression. *Oncogene,* 17**,** 3385-400.

GHOSH, E., KUMARI, P., JAIMAN, D. & SHUKLA, A. K. 2015. Methodological advances: the unsung heroes of the GPCR structural revolution. *Nature Reviews Molecular Cell Biology,* 16**,** 69-81.

GOCKEL, I., SCHIMANSKI, C. C., HEINRICH, C., WEHLER, T., FRERICHS, K., DRESCHER, D., VON LANGSDORFF, C., DOMEYER, M., BIESTERFELD, S. & GALLE, P. R. 2006. Expression of chemokine receptor CXCR4 in esophageal squamous cell and adenocarcinoma. *BMC cancer,* 6**,** 290.

GODLEE, F., SMITH, R. & GOLDMANN, D. 1999. Antithrombotic therapy in cancer. *BMJ,* 318**,** 1571-2.

GOGUET-SURMENIAN, E., RICHARD-FIARDO, P., GUILLEMOT, E., BENCHETRIT, M., GOMEZ-BROUCHET, A., BUZZO, P., KARIMDJEE-SOILIHI, B., ALEMANNO, P., MICHIELS, J. F. & SCHMID-ALLIANA, A. 2013. CXCR7-mediated progression of osteosarcoma in the lungs. *British journal of cancer,* 109**,** 1579-1585.

GOLDMANN, T., DRÖMANN, D., RADTKE, J., MARWITZ, S., LANG, D. S., SCHULTZ, H. & VOLLMER, E. 2008. CXCR7 transcription in human non-small cell lung cancer and tumor-free lung tissues; possible regulation upon chemotherapy. *Virchows Archiv,* 452**,** 347-348.

GOMES, I., JORDAN, B. A., GUPTA, A., RIOS, C., TRAPAIDZE, N. & DEVI, L. A. 2001. G protein coupled receptor dimerization: implications in modulating receptor function. *Journal of molecular medicine,* 79**,** 226-242.

GONSIOREK, W., FAN, X., HESK, D., FOSSETTA, J., QIU, H., JAKWAY, J., BILLAH, M., DWYER, M., CHAO, J. & DENO, G. 2007. Pharmacological characterization of Sch527123, a potent allosteric CXCR1/CXCR2 antagonist. *Journal of Pharmacology and Experimental Therapeutics,* 322**,** 477-485.

GONZÁLEZ-MARTÍN, A., GÓMEZ, L., LUSTGARTEN, J., MIRA, E. & MAÑES, S. 2011. Maximal T cell–mediated antitumor responses rely upon CCR5 expression in both CD4+ and CD8+ T cells. *Cancer research,* 71**,** 5455-5466.

GORDON, S. & TAYLOR, P. R. 2005. Monocyte and macrophage heterogeneity. *Nature Reviews Immunology,* 5**,** 953-964.

GOSLING, J., DAIRAGHI, D. J., WANG, Y., HANLEY, M., TALBOT, D., MIAO, Z. & SCHALL, T. J. 2000. Cutting edge: identification of a novel chemokine receptor that binds dendritic cell-and T cell-active chemokines including ELC, SLC, and TECK. *The Journal of Immunology,* 164**,** 2851-2856.

GOTO, M., YOSHIDA, T., YAMAMOTO, Y., FURUKITA, Y., INOUE, S., FUJIWARA, S., KAWAKITA, N., NISHINO, T., MINATO, T. & YUASA, Y. 2015. CXCR4 Expression is Associated with Poor Prognosis in Patients with Esophageal Squamous Cell Carcinoma. *Annals of surgical oncology,* 24**,** 832-840.

GRANT, S. W., KYSHTOOBAYEVA, A. S., KUROSAKI, T., JAKOWATZ, J. & FRUEHAUF, J. P. 1997. Mutant p53 correlates with reduced expression of thrombospondin-1, increased angiogenesis, and metastatic progression in melanoma. *Cancer detection and prevention,* 22**,** 185-194.

GRAVEL, S., MALOUF, C., BOULAIS, P. E., BERCHICHE, Y. A., OISHI, S., FUJII, N., LEDUC, R., SINNETT, D. & HEVEKER, N. 2010. The peptidomimetic CXCR4 antagonist TC14012 recruits β-arrestin to CXCR7 roles of receptor domains. *Journal of Biological Chemistry,* 285**,** 37939-37943.

GREENALL, S. A., GHERARDI, E., LIU, Z., DONOGHUE, J. F., VITALI, A. A., LI, Q., MURPHY, R., IAMELE, L., SCOTT, A. M. & JOHNS, T. G. 2012. Non-agonistic bivalent antibodies that promote c-MET degradation and inhibit tumor growth and others specific for tumor related c-MET. *PloS one,* 7**,** e34658.

GRIFFITH, J. W., SOKOL, C. L. & LUSTER, A. D. 2014. Chemokines and chemokine receptors: positioning cells for host defense and immunity. *Annual review of immunology,* 32**,** 659-702.

GRIVENNIKOV, S. I., GRETEN, F. R. & KARIN, M. 2010. Immunity, inflammation, and cancer. *Cell,* 140**,** 883-899.

GROOM, J. R., RICHMOND, J., MUROOKA, T. T., SORENSEN, E. W., SUNG, J. H., BANKERT, K., VON ANDRIAN, U. H., MOON, J. J., MEMPEL, T. R. & LUSTER, A. D. 2012. CXCR3 chemokine receptor-ligand interactions in the lymph node optimize CD4+ T helper 1 cell differentiation. *Immunity,* 37**,** 1091-1103.

GROTTKE, A., EWALD, F., LANGE, T., NÖRZ, D., HERZBERGER, C., BACH, J., GRABINSKI, N., GRÄSER, L., HÖPPNER, F. & NASHAN, B. 2016. Downregulation of AKT3 Increases Migration and Metastasis in Triple Negative Breast Cancer Cells by Upregulating S100A4. *PloS one,* 11**,** e0146370.

GRYMULA, K., TARNOWSKI, M., WYSOCZYNSKI, M., DRUKALA, J., BARR, F. G., RATAJCZAK, J., KUCIA, M. & RATAJCZAK, M. Z. 2010. Overlapping and distinct role of CXCR7-SDF-1/ITAC and CXCR4-SDF-1 axes in regulating metastatic behavior of human rhabdomyosarcomas. *International journal of cancer,* 127**,** 2554-2568.

GUILLEMOT, E., KARIMDJEE-SOILIHI, B., PRADELLI, E., BENCHETRIT, M., GOGUET-SURMENIAN, E., MILLET, M. A., LARBRET, F., MICHIELS, J. F., BIRNBAUM, D. & ALEMANNO, P. 2012. CXCR7 receptors facilitate the progression of colon carcinoma within lung not within liver. *British journal of cancer,* 107**,** 1944-1949.

GUNN, M. D., KYUWA, S., TAM, C., KAKIUCHI, T., MATSUZAWA, A., WILLIAMS, L. T. & NAKANO, H. 1999. Mice lacking expression of secondary lymphoid organ chemokine have defects in lymphocyte homing and dendritic cell localization. *The Journal of experimental medicine,* 189**,** 451-460.

GÜNTHER, K., LEIER, J., HENNING, G., DIMMLER, A., WEIßBACH, R., HOHENBERGER, W. & FÖRSTER, R. 2005. Prediction of lymph node metastasis in colorectal carcinoma by expressionof chemokine receptor CCR7. *International journal of cancer,* 116**,** 726-733.

GUO, J., LOU, W., JI, Y. & ZHANG, S. 2013. Effect of CCR7, CXCR4 and VEGF‐C on the lymph node metastasis of human pancreatic ductal adenocarcinoma. *Oncology letters,* 5**,** 1572-1578.

GUO, J. C., LI, J., ZHOU, L., YANG, J. Y., ZHANG, Z. G., LIANG, Z. Y., ZHOU, W. X., YOU, L., ZHANG, T. P. & ZHAO, Y. P. 2016. CXCL12-CXCR7 axis contributes to the invasive phenotype of pancreatic cancer. *Oncotarget,* 7**,** 62006-62018.

GUO, P., YOU, J.-O., YANG, J., JIA, D., MOSES, M. A. & AUGUSTE, D. T. 2014a. Inhibiting metastatic breast cancer cell migration via the synergy of targeted, pH-triggered siRNA delivery and chemokine axis blockade. *Molecular pharmaceutics,* 11**,** 755-765.

GUO, S., XIAO, D., LIU, H., ZHENG, X., LIU, L. & LIU, S. 2014b. Interfering with CXCR4 expression inhibits proliferation, adhesion and migration of breast cancer MDA‐MB‐231 cells. *Oncology letters,* 8**,** 1557-1562.

GUREVICH, V. V. & GUREVICH, E. V. 2004. The molecular acrobatics of arrestin activation. *Trends in pharmacological sciences,* 25**,** 105-111.

HAINSWORTH, J. D., REEVES, J. A., MACE, J. R., CRANE, E. J., HAMID, O., STILLE, J. R., FLYNT, A., ROBERSON, S., POLZER, J. & ARROWSMITH, E. R. 2016. A Randomized, Open-Label Phase 2 Study of the CXCR4 Inhibitor LY2510924 in Combination with Sunitinib Versus Sunitinib Alone in Patients with Metastatic Renal Cell Carcinoma (RCC). *Targeted oncology,* 11**,** 643-653.

HANAHAN, D. & FOLKMAN, J. 1996. Patterns and emerging mechanisms of the angiogenic switch during tumorigenesis. *cell,* 86**,** 353-364.

HANAHAN, D. & WEINBERG, R. A. 2000. The hallmarks of cancer. *cell,* 100**,** 57-70.

HANAHAN, D. & WEINBERG, R. A. 2011. Hallmarks of cancer: the next generation. *cell,* 144**,** 646-674.

HANAI, J.-I., MAMMOTO, T., SETH, P., MORI, K., KARUMANCHI, S. A., BARASCH, J. & SUKHATME, V. P. 2005. Lipocalin 2 diminishes invasiveness and metastasis of Ras-transformed cells. *Journal of Biological Chemistry,* 280**,** 13641-13647.

HANEDA, S., FUKUSHIMA, K., FUNAYAMA, Y., SHIBATA, C., TAKAHASHI, K.-I., TABATA, Y. & SASAKI, I. 2007. A new drug delivery system targeting ileal epithelial cells induced electrogenic sodium absorption: possible promotion of intestinal adaptation. *Journal of Gastrointestinal Surgery,* 11**,** 568-577.

HANSELL, C. A. H., SIMPSON, C. V. & NIBBS, R. J. B. 2006. Chemokine sequestration by atypical chemokine receptors. *Biochemical Society Transactions,* 34**,** 1009-13.

HAO, L., ZHANG, C., QIU, Y., WANG, L., LUO, Y., JIN, M., ZHANG, Y., GUO, T. B., MATSUSHIMA, K. & ZHANG, Y. 2007. Recombination of CXCR4, VEGF, and MMP-9 predicting lymph node metastasis in human breast cancer. *Cancer letters,* 253**,** 34-42.

HAO, M., ZHENG, J., HOU, K., WANG, J., CHEN, X., LU, X., BO, J., XU, C., SHEN, K. & WANG, J. 2012. Role of chemokine receptor CXCR7 in bladder cancer progression. *Biochemical pharmacology,* 84**,** 204-214.

HARALDSEN, G. & ROT, A. 2006. Coy decoy with a new ploy: interceptor controls the levels of homeostatic chemokines. *European journal of immunology,* 36**,** 1659-1661.

HARBECK, N., BECKMANN, M. W., RODY, A., SCHNEEWEISS, A., MÜLLER, V., FEHM, T., MARSCHNER, N., GLUZ, O., SCHRADER, I. & HEINRICH, G. 2013. HER2 dimerization inhibitor pertuzumab-mode of action and clinical data in breast cancer. *Breast Care,* 8**,** 49-55.

HARTMANN, T. N., GRABOVSKY, V., PASVOLSKY, R., SHULMAN, Z., BUSS, E. C., SPIEGEL, A., NAGLER, A., LAPIDOT, T., THELEN, M. & ALON, R. 2008. A crosstalk between intracellular CXCR7 and CXCR4 involved in rapid CXCL12-triggered integrin activation but not in chemokine-triggered motility of human T lymphocytes and CD34+ cells. *Journal of leukocyte biology,* 84**,** 1130-1140.

HARVEY, J. R., MELLOR, P., ELDALY, H., LENNARD, T. W. J., KIRBY, J. A. & ALI, S. 2007. Inhibition of CXCR4-mediated breast cancer metastasis: a potential role for heparinoids? *Clinical Cancer Research,* 13**,** 1562-1570.

HASEGAWA, H., NOMURA, T., KOHNO, M., TATEISHI, N., SUZUKI, Y., MAEDA, N., FUJISAWA, R., YOSHIE, O. & FUJITA, S. 2000. Increased chemokine receptor CCR7/EBI1 expression enhances the infiltration of lymphoid organs by adult T-cell leukemia cells. *Blood,* 95**,** 30-38.

HATSE, S., PRINCEN, K., BRIDGER, G., DE CLERCQ, E. & SCHOLS, D. 2002. Chemokine receptor inhibition by AMD3100 is strictly confined to CXCR4. *FEBS letters,* 527**,** 255-262.

HATSE, S., PRINCEN, K., DE CLERCQ, E., ROSENKILDE, M. M., SCHWARTZ, T. W., HERNANDEZ-ABAD, P. E., SKERLJ, R. T., BRIDGER, G. J. & SCHOLS, D. 2005. AMD3465, a monomacrocyclic CXCR4 antagonist and potent HIV entry inhibitor. *Biochemical pharmacology,* 70**,** 752-761.

HATSE, S., PRINCEN, K., GERLACH, L.-O., BRIDGER, G., HENSON, G., DE CLERCQ, E., SCHWARTZ, T. W. & SCHOLS, D. 2001. Mutation of Asp171 and Asp262 of the chemokine receptor CXCR4 impairs its coreceptor function for human immunodeficiency virus-1 entry and abrogates the antagonistic activity of AMD3100. *Molecular pharmacology,* 60**,** 164-173.

HATTERMANN, K., HELD-FEINDT, J., LUCIUS, R., MÜERKÖSTER, S. S., PENFOLD, M. E., SCHALL, T. J. & MENTLEIN, R. 2010. The chemokine receptor CXCR7 is highly expressed in human glioma cells and mediates antiapoptotic effects. *Cancer research,* 70**,** 3299-3308.

HATTERMANN, K., HOLZENBURG, E., HANS, F., LUCIUS, R., HELD-FEINDT, J. & MENTLEIN, R. 2014. Effects of the chemokine CXCL12 and combined internalization of its receptors CXCR4 and CXCR7 in human MCF-7 breast cancer cells. *Cell and tissue research,* 357**,** 253-266.

HATTEVILLE, L., MAHE, C. & HILL, C. 2002. Prediction of the long-term survival in breast cancer patients according to the present oncological status. *Statistics in medicine,* 21**,** 2345-2354.

HATTORI, K., HEISSIG, B., TASHIRO, K., HONJO, T., TATENO, M., SHIEH, J.-H., HACKETT, N. R., QUITORIANO, M. S., CRYSTAL, R. G. & RAFII, S. 2001. Plasma elevation of stromal cell–derived factor-1 induces mobilization of mature and immature hematopoietic progenitor and stem cells. *Blood,* 97**,** 3354-3360.

HAYBITTLE, J. L., BLAMEY, R. W., ELSTON, C. W., JOHNSON, J., DOYLE, P. J., CAMPBELL, F. C., NICHOLSON, R. I. & GRIFFITHS, K. 1982. A prognostic index in primary breast cancer. *British journal of cancer,* 45**,** 361.

HE, Y., RAJANTIE, I., PAJUSOLA, K., JELTSCH, M., HOLOPAINEN, T., YLA-HERTTUALA, S., HARDING, T., JOOSS, K., TAKAHASHI, T. & ALITALO, K. 2005. Vascular endothelial cell growth factor receptor 3–mediated activation of lymphatic endothelium is crucial for tumor cell entry and spread via lymphatic vessels. *Cancer research,* 65**,** 4739-4746.

HECHT, I., CAHALON, L., HERSHKOVIZ, R., LAHAT, A., FRANITZA, S. & LIDER, O. 2003. Heterologous desensitization of T cell functions by CCR5 and CXCR4 ligands: inhibition of cellular signaling, adhesion and chemotaxis. *International immunology,* 15**,** 29-38.

HECHT, I., HERSHKOVIZ, R., SHIVTIEL, S., LAPIDOT, T., COHEN, I. R., LIDER, O. & CAHALON, L. 2004. Heparin-disaccharide affects T cells: inhibition of NF-κB activation, cell migration, and modulation of intracellular signaling. *Journal of leukocyte biology,* 75**,** 1139-1146.

HEDRICK, J. A. & ZLOTNIK, A. 1997. Identification and characterization of a novel beta chemokine containing six conserved cysteines. *The Journal of Immunology,* 159**,** 1589-1593.

HEESEN, M., BERMAN, M. A., CHAREST, A., HOUSMAN, D., GERARD, C. & DORF, M. E. 1998. Cloning and chromosomal mapping of an orphan chemokine receptor: mouse RDC1. *Immunogenetics,* 47**,** 364-370.

HEINISCH, S., PALMA, J. & KIRBY, L. G. 2011. Interactions between chemokine and mu-opioid receptors: anatomical findings and electrophysiological studies in the rat periaqueductal grey. *Brain, behavior, and immunity,* 25**,** 360-372.

HEINRICH, E. L., LEE, W., LU, J., LOWY, A. M. & KIM, J. 2012. Chemokine CXCL12 activates dual CXCR4 and CXCR7-mediated signaling pathways in pancreatic cancer cells. *Journal of translational medicine,* 10**,** 68.

HEINZE, E., BALDWIN, S., CHAN, G., HANSEN, J., SONG, J., CLEMENTS, D., ARAGON, R., NISHIMURA, R., REEVES, M. & WEISBART, R. 2009. Antibody-mediated FOXP3 protein therapy induces apoptosis in cancer cells in vitro and inhibits metastasis in vivo. *International journal of oncology,* 35**,** 167.

HELBIG, G., CHRISTOPHERSON, K. W., BHAT-NAKSHATRI, P., KUMAR, S., KISHIMOTO, H., MILLER, K. D., BROXMEYER, H. E. & NAKSHATRI, H. 2003. NF-κ B promotes breast cancer cell migration and metastasis by inducing the expression of the chemokine receptor CXCR4. *Journal of Biological Chemistry,* 278**,** 21631-21638.

HENDRIX, C. W., COLLIER, A. C., LEDERMAN, M. M., SCHOLS, D., POLLARD, R. B., BROWN, S., JACKSON, J. B., COOMBS, R. W., GLESBY, M. J. & FLEXNER, C. W. 2004. Safety, pharmacokinetics, and antiviral activity of AMD3100, a selective CXCR4 receptor inhibitor, in HIV-1 infection. *JAIDS Journal of Acquired Immune Deficiency Syndromes,* 37**,** 1253-1262.

HENDRIX, C. W., FLEXNER, C., MACFARLAND, R. T., GIANDOMENICO, C., FUCHS, E. J., REDPATH, E., BRIDGER, G. & HENSON, G. W. 2000. Pharmacokinetics and safety of AMD-3100, a novel antagonist of the CXCR-4 chemokine receptor, in human volunteers. *Antimicrobial agents and chemotherapy,* 44**,** 1667-1673.

HENSBERGEN, P. J., WIJNANDS, P. G. J. T. B., SCHREURS, M. W. J., SCHEPER, R. J., WILLEMZE, R. & TENSEN, C. P. 2005. The CXCR3 targeting chemokine CXCL11 has potent antitumor activity in vivo involving attraction of CD8+ T lymphocytes but not inhibition of angiogenesis. *Journal of Immunotherapy,* 28**,** 343-351.

HEPPNER, G. H., MILLER, F. R. & SHEKHAR, P. M. 2000. Nontransgenic models of breast cancer. *Breast Cancer Research,* 2**,** 331–334.

HERESI, G. A., WANG, J., TAICHMAN, R., CHIRINOS, J. A., REGALADO, J. J., LICHTSTEIN, D. M. & ROSENBLATT, J. D. 2005. Expression of the chemokine receptor CCR7 in prostate cancer presenting with generalized lymphadenopathy: report of a case, review of the literature, and analysis of chemokine receptor expression. *Urologic Oncology,* 23**,** 261-267.

HERNANDEZ, L., MAGALHAES, M. A. O., CONIGLIO, S. J., CONDEELIS, J. S. & SEGALL, J. E. 2011. Opposing roles of CXCR4 and CXCR7 in breast cancer metastasis. *Breast Cancer Research,* 13**,** R128.

HERNANDEZ, P. A., GORLIN, R. J., LUKENS, J. N., TANIUCHI, S., BOHINJEC, J., FRANCOIS, F., KLOTMAN, M. E. & DIAZ, G. A. 2003. Mutations in the chemokine receptor gene CXCR4 are associated with WHIM syndrome, a combined immunodeficiency disease. *Nature genetics,* 34**,** 70-74.

HERRICK-DAVIS, K., WEAVER, B. A., GRINDE, E. & MAZURKIEWICZ, J. E. 2006. Serotonin 5-HT2C Receptor Homodimer Biogenesis in the Endoplasmic Reticulum REAL-TIME VISUALIZATION WITH CONFOCAL FLUORESCENCE RESONANCE ENERGY TRANSFER. *Journal of Biological Chemistry,* 281**,** 27109-27116.

HESSELGESSER, J., NG, H. P., LIANG, M., ZHENG, W., MAY, K., BAUMAN, J. G., MONAHAN, S., ISLAM, I., WEI, G. P. & GHANNAM, A. 1998. Identification and characterization of small molecule functional antagonists of the CCR1 chemokine receptor. *Journal of Biological Chemistry,* 273**,** 15687-15692.

HEYDTMANN, M. & ADAMS, D. 2002. Understanding selective trafficking of lymphocyte subsets. *Gut,* 50**,** 150-152.

HINK, M. A., GRIEP, R. A., BORST, J. W., VAN HOEK, A., EPPINK, M. H., SCHOTS, A. & VISSER, A. J. 2000. Structural dynamics of green fluorescent protein alone and fused with a single chain Fv protein. *Journal of Biological Chemistry,* 275**,** 17556-17560.

HIROSE, J., KAWASHIMA, H., WILLIS, M. S., SPRINGER, T. A., HASEGAWA, H., YOSHIE, O. & MIYASAKA, M. 2002. Chondroitin sulfate B exerts its inhibitory effect on secondary lymphoid tissue chemokine (SLC) by binding to the C-terminus of SLC. *Biochimica et Biophysica Acta (BBA)-General Subjects,* 1571**,** 219-224.

HIROSE, J., KAWASHIMA, H., YOSHIE, O., TASHIRO, K. & MIYASAKA, M. 2001. Versican interacts with chemokines and modulates cellular responses. *Journal of Biological Chemistry,* 276**,** 5228-5234.

HJORTØ, G. M., LARSEN, O., STEEN, A., DAUGVILAITE, V., BERG, C., FARES, S., HANSEN, M., ALI, S. & ROSENKILDE, M. M. 2016. Differential CCR7 targeting in dendritic cells by three naturally occurring CC-chemokines. *Frontiers in Immunology,* 7**,** 568.

HOLLAND, J. D., KOCHETKOVA, M., AKEKAWATCHAI, C., DOTTORE, M., LOPEZ, A. & MCCOLL, S. R. 2006. Differential functional activation of chemokine receptor CXCR4 is mediated by G proteins in breast cancer cells. *Cancer research,* 66**,** 4117-4124.

HOLLIDAY, D. L. & SPEIRS, V. 2011. Choosing the right cell line for breast cancer research. *Breast Cancer Research,* 13**,** 215.

HOLM, N. T., BYRNES, K., LI, B. D. L., TURNAGE, R. H., ABREO, F., MATHIS, J. M. & CHU, Q. D. 2007. Elevated levels of chemokine receptor CXCR4 in HER-2 negative breast cancer specimens predict recurrence. *Journal of Surgical Research,* 141**,** 53-59.

HONCZARENKO, M., LE, Y., GLODEK, A. M., MAJKA, M., CAMPBELL, J. J., RATAJCZAK, M. Z. & SILBERSTEIN, L. E. 2002. CCR5-binding chemokines modulate CXCL12 (SDF-1)–induced responses of progenitor B cells in human bone marrow through heterologous desensitization of the CXCR4 chemokine receptor. *Blood,* 100**,** 2321-2329.

HONG, C. Y., LEE, H.-J., CHOI, N.-R., JUNG, S.-H., VO, M.-C., HOANG, M. D., KIM, H.-J. & LEE, J.-J. 2016. Sarcoplasmic reticulum Ca2+ ATPase 2 (SERCA2) reduces the migratory capacity of CCL21-treated monocyte-derived dendritic cells. *Experimental & Molecular Medicine,* 48**,** e253.

HOOGEWERF, A. J., KUSCHERT, G. S. V., PROUDFOOT, A. E. I., BORLAT, F., CLARK-LEWIS, I., POWER, C. A. & WELLS, T. N. C. 1997. Glycosaminoglycans mediate cell surface oligomerization of chemokines. *Biochemistry,* 36**,** 13570-13578.

HORUK, R. 2009. Chemokine receptor antagonists: overcoming developmental hurdles. *Nature reviews Drug discovery,* 8**,** 23-33.

HOSHINO, R., CHATANI, Y., YAMORI, T., TSURUO, T., OKA, H., YOSHIDA, O., SHIMADA, Y., ARI-I, S., WADA, H. & FUJIMOTO, J. 1999. Constitutive activation of the 41-/43-kDa mitogen-activated protein kinase signaling pathway in human tumors. *Oncogene,* 18**,** 813-822.

HOVDEN, A. O. & APPEL, S. 2010. The First Dendritic Cell-Based Therapeutic Cancer Vaccine is Approved by the FDA. *Scandinavian journal of immunology,* 72**,** 554-554.

HOWARD, A. D., MCALLISTER, G., FEIGHNER, S. D., LIU, Q., NARGUND, R. P., VAN DER PLOEG, L. H. T. & PATCHETT, A. A. 2001. Orphan G-protein-coupled receptors and natural ligand discovery. *Trends in pharmacological sciences,* 22**,** 132-140.

HSU, P. P. & SABATINI, D. M. 2008. Cancer cell metabolism: Warburg and beyond. *Cell,* 134**,** 703-707.

HUANG, E. H., SINGH, B., CRISTOFANILLI, M., GELOVANI, J., WEI, C., VINCENT, L., COOK, K. R. & LUCCI, A. 2009. A CXCR4 antagonist CTCE-9908 inhibits primary tumor growth and metastasis of breast cancer. *Journal of Surgical Research,* 155**,** 231-236.

HUANG, S., OUYANG, N., LIN, L., CHEN, L., WU, W., SU, F., YAO, Y. & YAO, H. 2012. HGF-induced PKCζ activation increases functional CXCR4 expression in human breast cancer cells. *PLoS One,* 7**,** e29124.

HUANG, X., SHEN, J., CUI, M., SHEN, L., LUO, X., LING, K., PEI, G., JIANG, H. & CHEN, K. 2003. Molecular Dynamics Simulations on SDF-1α: Binding with CXCR4 Receptor. *Biophysical journal,* 84**,** 171-184.

HUGGINS, C. & YANG, N. C. 1962. Induction and extinction of mammary cancer. *Science,* 137**,** 257-62.

HUMPERT, M. L., PINTO, D., JARROSSAY, D. & THELEN, M. 2014. CXCR7 influences the migration of B cells during maturation. *European journal of immunology,* 44**,** 694-705.

HUNTER, D. J., COLDITZ, G. A., HANKINSON, S. E., MALSPEIS, S., SPIEGELMAN, D., CHEN, W., STAMPFER, M. J. & WILLETT, W. C. 2010. Oral contraceptive use and breast cancer: a prospective study of young women. *Cancer Epidemiology and Prevention Biomarkers,* 19**,** 2496-502.

HUNTER, T. M., MCNAE, I. W., LIANG, X., BELLA, J., PARSONS, S., WALKINSHAW, M. D. & SADLER, P. J. 2005. Protein recognition of macrocycles: Binding of anti-HIV metallocyclams to lysozyme. *Proceedings of the National Academy of Sciences of the United States of America,* 102**,** 2288-2292.

HUSKENS, D., PRINCEN, K., SCHREIBER, M. & SCHOLS, D. 2007. The role of N-glycosylation sites on the CXCR4 receptor for CXCL-12 binding and signaling and X4 HIV-1 viral infectivity. *Virology,* 363**,** 280-287.

HUSSAIN, S., PLÜCKTHUN, A., ALLEN, T. M. & ZANGEMEISTER-WITTKE, U. 2007. Antitumor activity of an epithelial cell adhesion molecule–targeted nanovesicular drug delivery system. *Molecular Cancer Therapeutics,* 6**,** 3019-3027.

IERANO, C., SANTAGATA, S., NAPOLITANO, M., GUARDIA, F., GRIMALDI, A., ANTIGNANI, E., BOTTI, G., CONSALES, C., RICCIO, A. & NANAYAKKARA, M. 2014. CXCR4 and CXCR7 transduce through mTOR in human renal cancer cells. *Cell death & disease,* 5**,** e1310.

IKEDA, Y., KUMAGAI, H., SKACH, A., SATO, M. & YANAGISAWA, M. 2013. Modulation of circadian glucocorticoid oscillation via adrenal opioid-CXCR7 signaling alters emotional behavior. *Cell,* 155**,** 1323-1336.

IMBALZANO, K. M., TATARKOVA, I., IMBALZANO, A. N. & NICKERSON, J. A. 2009. Increasingly transformed MCF-10A cells have a progressively tumor-like phenotype in three-dimensional basement membrane culture. *Cancer cell international,* 9**,** 7.

INFANTINO, S., MOEPPS, B. & THELEN, M. 2006. Expression and regulation of the orphan receptor RDC1 and its putative ligand in human dendritic and B cells. *The Journal of Immunology,* 176**,** 2197-2207.

INWALD, E. C., KLINKHAMMER-SCHALKE, M., HOFSTÄDTER, F., ZEMAN, F., KOLLER, M., GERSTENHAUER, M. & ORTMANN, O. 2013. Ki-67 is a prognostic parameter in breast cancer patients: results of a large population-based cohort of a cancer registry. *Breast cancer research and treatment,* 139**,** 539-552.

IOZZO, R. V. & SAN ANTONIO, J. D. 2001. Heparan sulfate proteoglycans: heavy hitters in the angiogenesis arena. *The Journal of clinical investigation,* 108**,** 349-355.

ISHIDA, T., INAGAKI, H., UTSUNOMIYA, A., TAKATSUKA, Y., KOMATSU, H., IIDA, S., TAKEUCHI, G., EIMOTO, T., NAKAMURA, S. & UEDA, R. 2004. CXC chemokine receptor 3 and CC chemokine receptor 4 expression in T-cell and NK-cell lymphomas with special reference to clinicopathological significance for peripheral T-cell lymphoma, unspecified. *Clinical Cancer Research,* 10**,** 5494-5500.

ISHIGAMI, S., NATSUGOE, S., NAKAJO, A., TOKUDA, K., UENOSONO, Y., ARIGAMI, T., MATSUMOTO, M., OKUMURA, H., HOKITA, S. & AIKOU, T. 2007. Prognostic value of CCR7 expression in gastric cancer. *Hepato-gastroenterology,* 54**,** 1025-1028.

ISHII, M., HAYAKAWA, S., SUZUKI, M. K., CHISHIMA, F., NAGAISHI, M., SATOH, K., YOSHINO, N., HONDA, M. & NISHINARITA, S. 2000. Expression of functional chemokine receptors of human placental cells. *American Journal of Reproductive Immunology,* 44**,** 365-373.

ISSAFRAS, H., ANGERS, S., BULENGER, S., BLANPAIN, C., PARMENTIER, M., LABBÉ-JULLIÉ, C., BOUVIER, M. & MARULLO, S. 2002. Constitutive agonist-independent CCR5 oligomerization and antibody-mediated clustering occurring at physiological levels of receptors. *Journal of Biological Chemistry,* 277**,** 34666-34673.

IWAKIRI, S., MINO, N., TAKAHASHI, T., SONOBE, M., NAGAI, S., OKUBO, K., WADA, H. & MIYAHARA, R. 2009. Higher expression of chemokine receptor CXCR7 is linked to early and metastatic recurrence in pathological stage I nonsmall cell lung cancer. *Cancer,* 115**,** 2580-2593.

JABERIPOUR, M., HABIBAGAHI, M., HOSSEINI, A., HABIBABAD, S. R., TALEI, A. & GHADERI, A. 2010. Increased CTLA-4 and FOXP3 transcripts in peripheral blood mononuclear cells of patients with breast cancer. *Pathology & Oncology Research,* 16**,** 547-551.

JAHNKE, K., COUPLAND, S. E., NA, I.-K., LODDENKEMPER, C., KEILHOLZ, U., KORFEL, A., STEIN, H., THIEL, E. & SCHEIBENBOGEN, C. 2005. Expression of the chemokine receptors CXCR4, CXCR5, and CCR7 in primary central nervous system lymphoma. *Blood,* 106**,** 384-385.

JANOWSKI, M. 2009. Functional diversity of SDF-1 splicing variants. *Cell adhesion & migration,* 3**,** 243-249.

JENKINS, D. E., HORNIG, Y. S., OEI, Y., DUSICH, J. & PURCHIO, T. 2005. Bioluminescent human breast cancer cell lines that permit rapid and sensitive in vivo detection of mammary tumors and multiple metastases in immune deficient mice. *Breast Cancer Research,* 7**,** R444-54.

JENKINSON, S., THOMSON, M., MCCOY, D., EDELSTEIN, M., DANEHOWER, S., LAWRENCE, W., WHEELAN, P., SPALTENSTEIN, A. & GUDMUNDSSON, K. 2010. Blockade of X4-tropic HIV-1 cellular entry by GSK812397, a potent noncompetitive CXCR4 receptor antagonist. *Antimicrobial agents and chemotherapy,* 54**,** 817-824.

JIN, F., BROCKMEIER, U., OTTERBACH, F. & METZEN, E. 2012. New insight into the SDF-1/CXCR4 axis in a breast carcinoma model: hypoxia-induced endothelial SDF-1 and tumor cell CXCR4 are required for tumor cell intravasation. *Molecular Cancer Research,* 10**,** 1021-1031.

JOHNSON-HOLIDAY, C., SINGH, R., JOHNSON, E., SINGH, S., STOCKARD, C. R., GRIZZLE, W. E. & LILLARD JR, J. W. 2011. CCL25 mediates migration, invasion and matrix metalloproteinase expression by breast cancer cells in a CCR9-dependent fashion. *International journal of oncology,* 38**,** 1279.

JOHNSON, Z., PROUDFOOT, A. E. & HANDEL, T. M. 2005. Interaction of chemokines and glycosaminoglycans: a new twist in the regulation of chemokine function with opportunities for therapeutic intervention. *Cytokine & growth factor reviews,* 16**,** 625-636.

JONES, R. G. & THOMPSON, C. B. 2009. Tumor suppressors and cell metabolism: a recipe for cancer growth. *Genes & development,* 23**,** 537-548.

JORDAN, B. A. & DEVI, L. A. 1999. G-protein-coupled receptor heterodimerization modulates receptor function. *Nature,* 399**,** 697-700.

JUNG, D.-J., JIN, D.-H., HONG, S.-W., KIM, J.-E., SHIN, J.-S., KIM, D., CHO, B.-J., HWANG, Y.-I., KANG, J.-S. & LEE, W.-J. 2010. Foxp3 expression in p53-dependent DNA damage responses. *Journal of Biological Chemistry,* 285**,** 7995-8002.

KAHN, H. J., YANG, L.-Y., BLONDAL, J., LICKLEY, L., HOLLOWAY, C., HANNA, W., NAROD, S., MCCREADY, D. R., SETH, A. & MARKS, A. 2000. RT-PCR amplification of CK19 mRNA in the blood of breast cancer patients: correlation with established prognostic parameters. *Breast cancer research and treatment,* 60**,** 143-151.

KAIFI, J. T., YEKEBAS, E. F., SCHURR, P., OBONYO, D., WACHOWIAK, R., BUSCH, P., HEINECKE, A., PANTEL, K. & IZBICKI, J. R. 2005. Tumor-cell homing to lymph nodes and bone marrow and CXCR4 expression in esophageal cancer. *Journal of the National Cancer Institute,* 97**,** 1840-1847.

KALATSKAYA, I., BERCHICHE, Y. A., GRAVEL, S., LIMBERG, B. J., ROSENBAUM, J. S. & HEVEKER, N. 2009. AMD3100 is a CXCR7 ligand with allosteric agonist properties. *Molecular pharmacology,* 75**,** 1240-1247.

KANG, H., MANSEL, R. E. & JIANG, W. G. 2005. Genetic manipulation of stromal cell-derived factor-1 attests the pivotal role of the autocrine SDF-1-CXCR4 pathway in the aggressiveness of breast cancer cells. *International journal of oncology,* 26**,** 1429.

KANG, Y., SIEGEL, P. M., SHU, W., DROBNJAK, M., KAKONEN, S. M., CORDÓN-CARDO, C., GUISE, T. A. & MASSAGUÉ, J. 2003. A multigenic program mediating breast cancer metastasis to bone. *Cancer cell,* 3**,** 537-549.

KAPLAN, R. N., RIBA, R. D., ZACHAROULIS, S., BRAMLEY, A. H., VINCENT, L., COSTA, C., MACDONALD, D. D., JIN, D. K., SHIDO, K. & KERNS, S. A. 2005. VEGFR1-positive haematopoietic bone marrow progenitors initiate the pre-metastatic niche. *Nature,* 438**,** 820-827.

KAR, U. K., SRIVASTAVA, M. K., ANDERSSON, Å., BARATELLI, F., HUANG, M., KICKHOEFER, V. A., DUBINETT, S. M., ROME, L. H. & SHARMA, S. 2011. Novel CCL21-vault nanocapsule intratumoral delivery inhibits lung cancer growth. *PLoS One,* 6**,** e18758.

KASHYAP, M. K., KUMAR, D., JONES, H., AMAYA-CHANAGA, C. I., CHOI, M. Y., MELO-CARDENAS, J., ALE-ALI, A., KUHNE, M. R., SABBATINI, P. & COHEN, L. J. 2016. Ulocuplumab (BMS-936564/MDX1338): a fully human anti-CXCR4 antibody induces cell death in chronic lymphocytic leukemia mediated through a reactive oxygen species-dependent pathway. *Oncotarget,* 7**,** 2809.

KASUYA, H., KURUPPU, D. K., DONAHUE, J. M., CHOI, E. W., KAWASAKI, H. & TANABE, K. K. 2005. Mouse models of subcutaneous spleen reservoir for multiple portal venous injections to treat liver malignancies. *Cancer research,* 65**,** 3823-3827.

KATAYAMA, A., OGINO, T., BANDOH, N., NONAKA, S. & HARABUCHI, Y. 2005. Expression of CXCR4 and its down-regulation by IFN-γ in head and neck squamous cell carcinoma. *Clinical cancer research,* 11**,** 2937-2946.

KATO, M., KITAYAMA, J., KAZAMA, S. & NAGAWA, H. 2003. Expression pattern of CXC chemokine receptor-4 is correlated with lymph node metastasis in human invasive ductal carcinoma. *Breast Cancer Research,* 5**,** 5.

KATOH, H., QIN, Z. S., LIU, R., WANG, L., LI, W., LI, X., WU, L., DU, Z., LYONS, R. & LIU, C.-G. 2011. FOXP3 orchestrates H4K16 acetylation and H3K4 trimethylation for activation of multiple genes by recruiting MOF and causing displacement of PLU-1. *Molecular cell,* 44**,** 770-784.

KAWADA, K., HOSOGI, H., SONOSHITA, M., SAKASHITA, H., MANABE, T., SHIMAHARA, Y., SAKAI, Y., TAKABAYASHI, A., OSHIMA, M. & TAKETO, M. M. 2007. Chemokine receptor CXCR3 promotes colon cancer metastasis to lymph nodes. *Oncogene,* 26**,** 4679-4688.

KAWADA, K., SONOSHITA, M., SAKASHITA, H., TAKABAYASHI, A., YAMAOKA, Y., MANABE, T., INABA, K., MINATO, N., OSHIMA, M. & TAKETO, M. M. 2004. Pivotal role of CXCR3 in melanoma cell metastasis to lymph nodes. *Cancer Research,* 64**,** 4010-4017.

KELLAND, L. R. 2004. "Of mice and men": values and liabilities of the athymic nude mouse model in anticancer drug development. *European Journal of Cancer,* 40**,** 827-836.

KELLY, E., BAILEY, C. P. & HENDERSON, G. 2008. Agonist-selective mechanisms of GPCR desensitization. *British journal of pharmacology,* 153**,** S379-S388.

KELLY, T., MIAO, H.-Q., YANG, Y., NAVARRO, E., KUSSIE, P., HUANG, Y., MACLEOD, V., CASCIANO, J., JOSEPH, L. & ZHAN, F. 2003. High heparanase activity in multiple myeloma is associated with elevated microvessel density. *Cancer research,* 63**,** 8749-8756.

KELLY, T., SUVA, L. J., HUANG, Y., MACLEOD, V., MIAO, H.-Q., WALKER, R. C. & SANDERSON, R. D. 2005. Expression of heparanase by primary breast tumors promotes bone resorption in the absence of detectable bone metastases. *Cancer research,* 65**,** 5778-5784.

KELSEY, J. L. 1993. Breast cancer epidemiology: summary and future directions. *Epidemiologic Reviews,* 15**,** 256-63.

KEY, T. J., VERKASALO, P. K. & BANKS, E. 2001. Epidemiology of breast cancer. *The lancet oncology,* 2**,** 133-140.

KEYDAR, I., CHEN, L., KARBY, S., WEISS, F. R., DELAREA, J., RADU, M., CHAITCIK, S. & BRENNER, H. J. 1979. Establishment and characterization of a cell line of human breast carcinoma origin. *European Journal of Cancer (1965),* 15**,** 659-670.

KEYVANI, S., KARIMI, N., ORAFA, Z., BOUZARI, S. & OLOOMI, M. 2016. Assessment of Cytokeratin-19 Gene Expression in Peripheral Blood of Breast Cancer Patients and Breast Cancer Cell Lines. *Biomarkers in cancer,* 8**,** 57.

KHANNA, C. & HUNTER, K. 2005. Modeling metastasis in vivo. *Carcinogenesis,* 26**,** 513-523.

KIJIMA, T., MAULIK, G., MA, P. C., TIBALDI, E. V., TURNER, R. E., ROLLINS, B., SATTLER, M., JOHNSON, B. E. & SALGIA, R. 2002. Regulation of cellular proliferation, cytoskeletal function, and signal transduction through CXCR4 and c-Kit in small cell lung cancer cells. *Cancer Research,* 62**,** 6304-6311.

KIJOWSKI, J., BAJ-KRZYWORZEKA, M., MAJKA, M., RECA, R., MARQUEZ, L. A., CHRISTOFIDOU-SOLOMIDOU, M., JANOWSKA-WIECZOREK, A. & RATAJCZAK, M. Z. 2001. The SDF-1-CXCR4 axis stimulates VEGF secretion and activates integrins but does not affect proliferation and survival in lymphohematopoietic cells. *Stem Cells,* 19**,** 453-466.

KIM, C. H., PELUS, L. M., APPELBAUM, E., JOHANSON, K., ANZAI, N. & BROXMEYER, H. E. 1999. CCR7 ligands, SLC/6Ckine/Exodus2/TCA4 and CKβ-11/MIP-3β/ELC, are chemoattractants for CD56+ CD16− NK cells and late stage lymphoid progenitors. *Cellular immunology,* 193**,** 226-235.

KIM, H. Y., CHOI, J. H., KANG, Y. J., PARK, S. Y., CHOI, H. C. & KIM, H. S. 2011. Reparixin, an inhibitor of CXCR1 and CXCR2 receptor activation, attenuates blood pressure and hypertension-related mediators expression in spontaneously hypertensive rats. *Biological and Pharmaceutical Bulletin,* 34**,** 120-127.

KIM, J., TAKEUCHI, H., LAM, S. T., TURNER, R. R., WANG, H.-J., KUO, C., FOSHAG, L., BILCHIK, A. J. & HOON, D. S. B. 2005. Chemokine receptor CXCR4 expression in colorectal cancer patients increases the risk for recurrence and for poor survival. *Journal of Clinical Oncology,* 23**,** 2744-2753.

KIM, M.-Y., OSKARSSON, T., ACHARYYA, S., NGUYEN, D. X., ZHANG, X. H. F., NORTON, L. & MASSAGUÉ, J. 2009. Tumor self-seeding by circulating cancer cells. *Cell,* 139**,** 1315-1326.

KIM, N. W., PIATYSZEK, M. A., PROWSE, K. R. & HARLEY, C. B. 1994. Specific association of human telomerase activity with immortal cells and cancer. *Science,* 266**,** 2011-5.

KIM, R., EMI, M. & TANABE, K. 2007. Cancer immunoediting from immune surveillance to immune escape. *Immunology,* 121**,** 1-14.

KIM, S. Y., LEE, C. H., MIDURA, B. V., YEUNG, C., MENDOZA, A., HONG, S. H., REN, L., WONG, D., KORZ, W. & MERZOUK, A. 2008. Inhibition of the CXCR4/CXCL12 chemokine pathway reduces the

development of murine pulmonary metastases. *Clinical & experimental metastasis,* 25**,** 201-211.

KIRK, C. J., HARTIGAN-O'CONNOR, D. & MULÉ, J. J. 2001. The Dynamics of the T-Cell Antitumor Response. *Cancer research,* 61**,** 8794-8802.

KLEDAL, T. N., ROSENKILDE, M. M., COULIN, F., SIMMONS, G., JOHNSEN, A. H., ALOUANI, S., POWER, C. A., LÜTTICHAU, H. R., GERSTOFT, J. & CLAPHAM, P. R. 1997. A broad-spectrum chemokine antagonist encoded by Kaposi's sarcoma-associated herpesvirus. *Science,* 277**,** 1656-1659.

KLEIN, C. A. 2009. Parallel progression of primary tumours and metastases. *Nature Reviews Cancer,* 9**,** 302-312.

KLEIN, K. R., KARPINICH, N. O., ESPENSCHIED, S. T., WILLCOCKSON, H. H., DUNWORTH, W. P., HOOPES, S. L., KUSHNER, E. J., BAUTCH, V. L. & CARON, K. M. 2014. Decoy receptor CXCR7 modulates adrenomedullin-mediated cardiac and lymphatic vascular development. *Developmental cell,* 30**,** 528-540.

KODAMA, J., KUSUMOTO, T., SEKI, N., MATSUO, T., OJIMA, Y., NAKAMURA, K., HONGO, A. & HIRAMATSU, Y. 2007. Association of CXCR4 and CCR7 chemokine receptor expression and lymph node metastasis in human cervical cancer. *Annals of Oncology,* 18**,** 70-76.

KODAMA, J., SEKI, N., KUSUMOTO, T. & HIRAMATSU, Y. 2006. Expression of the CXCR4 and CCR7 chemokine receptors in human endometrial cancer. *European journal of gynaecological oncology,* 28**,** 370-375.

KOHOUT, T. A. & LEFKOWITZ, R. J. 2003. Regulation of G protein-coupled receptor kinases and arrestins during receptor desensitization. *Molecular pharmacology,* 63**,** 9-18.

KOHOUT, T. A., NICHOLAS, S. L., PERRY, S. J., REINHART, G., JUNGER, S. & STRUTHERS, R. S. 2004. Differential desensitization, receptor phosphorylation, β-arrestin recruitment, and ERK1/2 activation by the two endogenous ligands for the CC chemokine receptor 7. *Journal of Biological Chemistry,* 279**,** 23214-23222.

KOIZUMI, K., KOZAWA, Y., OHASHI, Y., NAKAMURA, E. S., AOZUKA, Y., SAKURAI, H., ICHIKI, K., DOKI, Y., MISAKI, T. & SAIKI, I. 2007. CCL21 promotes the migration and adhesion of highly lymph node metastatic human non-small cell lung cancer Lu-99 in vitro. *Oncology reports,* 17**,** 1511-1516.

KOLLIAS, J., MURPHY, C. A., ELSTON, C. W., ELLIS, I. O., ROBERTSON, J. F. R. & BLAMEY, R. W. 1999. The prognosis of small primary breast cancers. *European Journal of Cancer,* 35**,** 908-912.

KOLLMAR, O., RUPERTUS, K., SCHEUER, C., NICKELS, R. M., HABERL, G. C. Y., TILTON, B., MENGER, M. D. & SCHILLING, M. K. 2010. CXCR4 and CXCR7 regulate angiogenesis and CT26. WT tumor growth independent from SDF-1. *International journal of cancer,* 126**,** 1302-1315.

KOSHIBA, T., HOSOTANI, R., MIYAMOTO, Y., IDA, J., TSUJI, S., NAKAJIMA, S., KAWAGUCHI, M., KOBAYASHI, H., DOI, R. & HORI, T. 2000. Expression of stromal cell-derived factor 1 and CXCR4 ligand receptor system in pancreatic cancer: a possible role for tumor progression. *Clinical cancer research,* 6**,** 3530-3535.

KOZIN, S. V., KAMOUN, W. S., HUANG, Y., DAWSON, M. R., JAIN, R. K. & DUDA, D. G. 2010. Recruitment of myeloid but not endothelial precursor cells facilitates tumor regrowth after local irradiation. *Cancer research,* 70**,** 5679-5685.

KRAG, D. N., WEAVER, D. L., ALEX, J. C., FAIRBANK, J. T. & ET AL. 1993. Surgical resection and radiolocalization of the sentinel lymph node in breast cancer using a gamma probe. *Surgical oncology,* 2**,** 335-340.

KRATHWOHL, M. D., HROMAS, R., BROWN, D. R., BROXMEYER, H. E. & FIFE, K. H. 1997. Functional characterization of the C—C chemokine-like molecules encoded by molluscum contagiosum virus types 1 and 2. *Proceedings of the National Academy of Sciences,* 94**,** 9875-9880.

KREMER, K. N., CLIFT, I. C., MIAMEN, A. G., BAMIDELE, A. O., QIAN, N.-X., HUMPHREYS, T. D. & HEDIN, K. E. 2011. Stromal cell-derived factor-1 signaling via the CXCR4-TCR heterodimer requires phospholipase C-β3 and phospholipase C-γ1 for distinct cellular responses. *The Journal of Immunology,* 187**,** 1440-1447.

KROEGER, K. M., HANYALOGLU, A. C., SEEBER, R. M., MILES, L. E. C. & EIDNE, K. A. 2001. Constitutive and agonist-dependent homo-oligomerization of the thyrotropin-releasing hormone receptor

detection in living cells using bioluminescence resonance energy transfer. *Journal of Biological Chemistry,* 276**,** 12736-12743.

KUFAREVA, I., SALANGA, C. L. & HANDEL, T. M. 2015. Chemokine and chemokine receptor structure and interactions: implications for therapeutic strategies. *Immunology and cell biology,* 93**,** 372-383.

KUHNE, M. R., MULVEY, T., BELANGER, B., CHEN, S., PAN, C., CHONG, C., CAO, F., NIEKRO, W., KEMPE, T. & HENNING, K. A. 2013. BMS-936564/MDX-1338: a fully human anti-CXCR4 antibody induces apoptosis in vitro and shows antitumor activity in vivo in hematologic malignancies. *Clinical Cancer Research,* 19**,** 357-366.

KULU, Y., DORFMAN, J. D., KURUPPU, D., FUCHS, B. C., GOODWIN, J. M., FUJII, T., KURODA, T., LANUTI, M. & TANABE, K. K. 2009. Comparison of intravenous versus intraperitoneal administration of oncolytic herpes simplex virus 1 for peritoneal carcinomatosis in mice. *Cancer gene therapy,* 16**,** 291-297.

KUMAR, A., KREMER, K. N., SIMS, O. L. & HEDIN, K. E. 2009. Measuring the Proximity of T-Lymphocyte CXCR4 and TCR by Fluorescence Resonance Energy Transfer (FRET). *Methods in enzymology,* 460**,** 379-397.

KUMAR, A., KUMAR, S., DINDA, A. & LUTHRA, K. 2004. Differential expression of CXCR4 receptor in early and term human placenta. *Placenta,* 25**,** 347-351.

KUMAR, R., TRIPATHI, V., AHMAD, M., NATH, N., MIR, R. A., CHAUHAN, S. S. & LUTHRA, K. 2012. CXCR7 mediated Giα independent activation of ERK and Akt promotes cell survival and chemotaxis in T cells. *Cellular immunology,* 272**,** 230-241.

KUSCHERT, G. S. V., COULIN, F., POWER, C. A., PROUDFOOT, A. E. I., HUBBARD, R. E., HOOGEWERF, A. J. & WELLS, T. N. C. 1999. Glycosaminoglycans interact selectively with chemokines and modulate receptor binding and cellular responses. *Biochemistry,* 38**,** 12959-12968.

LABROSSE, B., BRELOT, A., HEVEKER, N., SOL, N., SCHOLS, D., DE CLERCQ, E. & ALIZON, M. 1998. Determinants for sensitivity of human immunodeficiency virus coreceptor CXCR4 to the bicyclam AMD3100. *Journal of virology,* 72**,** 6381-6388.

LADOIRE, S., ARNOULD, L., MIGNOT, G., COUDERT, B., RÉBÉ, C., CHALMIN, F., VINCENT, J., BRUCHARD, M., CHAUFFERT, B. & MARTIN, F. 2011. Presence of Foxp3 expression in tumor cells predicts better survival in HER2-overexpressing breast cancer patients treated with neoadjuvant chemotherapy. *Breast cancer research and treatment,* 125**,** 65-72.

LAGANE, B., CHOW, K. Y., BALABANIAN, K., LEVOYE, A., HARRIAGUE, J., PLANCHENAULT, T., BALEUX, F., GUNERA-SAAD, N., ARENZANA-SEISDEDOS, F. & BACHELERIE, F. 2008. CXCR4 dimerization and β-arrestin–mediated signaling account for the enhanced chemotaxis to CXCL12 in WHIM syndrome. *Blood,* 112**,** 34-44.

LAMBEIR, A.-M., PROOST, P., DURINX, C., BAL, G., SENTEN, K., AUGUSTYNS, K., SCHARPÉ, S., VAN DAMME, J. & DE MEESTER, I. 2001. Kinetic investigation of chemokine truncation by CD26/dipeptidyl peptidase IV reveals a striking selectivity within the chemokine family. *Journal of Biological Chemistry,* 276**,** 29839-29845.

LÄMMERMANN, T., BADER, B. L., MONKLEY, S. J., WORBS, T., WEDLICH-SÖLDNER, R., HIRSCH, K., KELLER, M., FÖRSTER, R., CRITCHLEY, D. R. & FÄSSLER, R. 2008. Rapid leukocyte migration by integrin-independent flowing and squeezing. *Nature,* 453**,** 51-55.

LANGLEY, R. R. & FIDLER, I. J. 2011. The seed and soil hypothesis revisited—The role of tumor-stroma interactions in metastasis to different organs. *International Journal of Cancer,* 128**,** 2527-2535.

LAPHAM, C. K., ROMANTSEVA, T., PETRICOIN, E., KING, L. R., MANISCHEWITZ, J., ZAITSEVA, M. B. & GOLDING, H. 2002. CXCR4 heterogeneity in primary cells: possible role of ubiquitination. *Journal of leukocyte biology,* 72**,** 1206-1214.

LAPHAM, C. K., ZAITSEVA, M. B., LEE, S., ROMANSTSEVA, T. & GOLDING, H. 1999. Fusion of monocytes and macrophages with HIV-1 correlates with biochemical properties of CXCR4 and CCR5. *Nature medicine,* 5**,** 303-308.

LAPTEVA, N., YANG, A.-G., SANDERS, D. E., STRUBE, R. W. & CHEN, S.-Y. 2005. CXCR4 knockdown by small interfering RNA abrogates breast tumor growth in vivo. *Cancer gene therapy,* 12**,** 84-89.

LAU, E. K., PAAVOLA, C. D., JOHNSON, Z., GAUDRY, J.-P., GERETTI, E., BORLAT, F., KUNGL, A. J., PROUDFOOT, A. E. & HANDEL, T. M. 2004. Identification of the glycosaminoglycan binding site of the CC chemokine, MCP-1 implications for structure and function in vivo. *Journal of Biological Chemistry,* 279**,** 22294-22305.

LAVERDIERE, C., HOANG, B. H., YANG, R., SOWERS, R., QIN, J., MEYERS, P. A., HUVOS, A. G., HEALEY, J. H. & GORLICK, R. 2005. Messenger RNA expression levels of CXCR4 correlate with metastatic behavior and outcome in patients with osteosarcoma. *Clinical Cancer Research,* 11**,** 2561-2567.

LÁZÁR-MOLNÁR, E., HEGYESI, H., TÓTH, S. & FALUS, A. 2000. Autocrine and paracrine regulation by cytokines and growth factors in melanoma. *Cytokine,* 12**,** 547-554.

LAZENNEC, G. & RICHMOND, A. 2010. Chemokines and chemokine receptors: new insights into cancer-related inflammation. *Trends in molecular medicine,* 16**,** 133-144.

LE BROCQ, M. L., FRASER, A. R., COTTON, G., WOZNICA, K., MCCULLOCH, C. V., HEWIT, K. D., MCKIMMIE, C. S., NIBBS, R. J., CAMPBELL, J. D. & GRAHAM, G. J. 2014. Chemokines as novel and versatile reagents for flow cytometry and cell sorting. *The Journal of Immunology,* 192**,** 6120-6130.

LE DRAN, H.-F. 1768. *The operations in surgery*, London : Printed for J. Dodsley and B. Law.

LECCIA, F., NARDONE, A., CORVIGNO, S., VECCHIO, L. D., DE PLACIDO, S., SALVATORE, F. & VENEZIANI, B. M. 2012. Cytometric and biochemical characterization of human breast cancer cells reveals heterogeneous myoepithelial phenotypes. *Cytometry Part A,* 81**,** 960-972.

LEE, B.-C., LEE, T.-H., AVRAHAM, S. & AVRAHAM, H. K. 2004. Involvement of the chemokine receptor CXCR4 and its ligand stromal cell-derived factor 1alpha in breast cancer cell migration through human brain microvascular endothelial cells. *Molecular Cancer Research,* 2**,** 327-338.

LEE, B., SHARRON, M., MONTANER, L. J., WEISSMAN, D. & DOMS, R. W. 1999. Quantification of CD4, CCR5, and CXCR4 levels on lymphocyte subsets, dendritic cells, and differentially conditioned monocyte-derived macrophages. *Proceedings of the National Academy of Sciences,* 96**,** 5215-5220.

LEE, C.-H., KAKINUMA, T., WANG, J., ZHANG, H., PALMER, D. C., RESTIFO, N. P. & HWANG, S. T. 2006. Sensitization of B16 tumor cells with a CXCR4 antagonist increases the efficacy of immunotherapy for established lung metastases. *Molecular cancer therapeutics,* 5**,** 2592-2599.

LEE, J. M., GARON, E. B., LEE, M., BARATELLI, F., WANG, G., ABTIN, F., SUH, R., WALLACE, W. D., ZENG, G. & SHARMA, S. 2014. Phase I trial of trans-thoracic injection of CCL21 gene modified dendritic cells in human non-small cell lung carcinoma. *Journal of Surgical Research,* 186**,** 558.

LEE, K. K. & WORKMAN, J. L. 2007. Histone acetyltransferase complexes: one size doesn't fit all. *Nature reviews Molecular cell biology,* 8**,** 284-295.

LEE, S.-M., GAO, B. & FANG, D. 2008. FoxP3 maintains Treg unresponsiveness by selectively inhibiting the promoter DNA-binding activity of AP-1. *Blood,* 111**,** 3599-3606.

LEE, S. P., O'DOWD, B. F., NG, G. Y. K., VARGHESE, G., AKIL, H., MANSOUR, A., NGUYEN, T. & GEORGE, S. R. 2000. Inhibition of cell surface expression by mutant receptors demonstrates that D2 dopamine receptors exist as oligomers in the cell. *Molecular Pharmacology,* 58**,** 120-128.

LEFKOWITZ, R. J. & SHENOY, S. K. 2005. Transduction of receptor signals by ß-arrestins. *Science,* 308**,** 512-517.

LELEKAKIS, M., MOSELEY, J. M., MARTIN, T. J., HARDS, D., WILLIAMS, E., HO, P., LOWEN, D., JAVNI, J., MILLER, F. R. & SLAVIN, J. 1999. A novel orthotopic model of breast cancer metastasis to bone. *Clinical & experimental metastasis,* 17**,** 163-170.

LEMMON, M. A., FLANAGAN, J. M., HUNT, J. F., ADAIR, B. D., BORMANN, B. J., DEMPSEY, C. E. & ENGELMAN, D. M. 1992. Glycophorin A dimerization is driven by specific interactions between transmembrane alpha-helices. *Journal of Biological Chemistry,* 267**,** 7683-7689.

LENNON, F. E., MIRZAPOIAZOVA, T., MAMBETSARIEV, B., SALGIA, R., MOSS, J. & SINGLETON, P. A. 2012. Overexpression of the μ-opioid receptor in human non-small cell lung cancer promotes Akt and mTOR activation, tumor growth, and metastasis. *The Journal of the American Society of Anesthesiologists,* 116**,** 857-867.

LETSCH, A., KEILHOLZ, U., SCHADENDORF, D., ASSFALG, G., ASEMISSEN, A. M., THIEL, E. & SCHEIBENBOGEN, C. 2003. Functional CCR9 expression is associated with small intestinal metastasis. *Journal of Investigative Dermatology,* 122**,** 685-690.

LEUNG, H.-W., ZHAO, S.-M., YUE, G. G.-L., LEE, J. K.-M., FUNG, K.-P., LEUNG, P.-C., TAN, N.-H. & BIK-SAN LAU, C. 2015. RA-XII inhibits tumour growth and metastasis in breast tumour-bearing mice via reducing cell adhesion and invasion and promoting matrix degradation. *Scientific reports,* 5**,** 16985

LEVOYE, A., BALABANIAN, K., BALEUX, F., BACHELERIE, F. & LAGANE, B. 2009. CXCR7 heterodimerizes with CXCR4 and regulates CXCL12-mediated G protein signaling. *Blood,* 113**,** 6085-6093.

LEWISON, E. F. 1953. The surgical treatment of breast cancer: an historical and collective review. *Surgery,* 34**,** 904.

LEY, K., LAUDANNA, C., CYBULSKY, M. I. & NOURSHARGH, S. 2007. Getting to the site of inflammation: the leukocyte adhesion cascade updated. *Nature Reviews Immunology,* 7**,** 678-689.

LI, J., SUN, R., TAO, K. & WANG, G. 2011a. The CCL21/CCR7 pathway plays a key role in human colon cancer metastasis through regulation of matrix metalloproteinase-9. *Digestive and Liver Disease,* 43**,** 40-47.

LI, M., WANG, I. X., LI, Y., BRUZEL, A., RICHARDS, A. L., TOUNG, J. M. & CHEUNG, V. G. 2011b. Widespread RNA and DNA sequence differences in the human transcriptome. *science,* 333**,** 53-58.

LI, Q. & MATTINGLY, R. R. 2008. Restoration of E-cadherin cell-cell junctions requires both expression of E-cadherin and suppression of ERK MAP kinase activation in Ras-transformed breast epithelial cells. *Neoplasia,* 10**,** 1444-1458.

LI, Q., PARK, P. W., WILSON, C. L. & PARKS, W. C. 2002. Matrilysin shedding of syndecan-1 regulates chemokine mobilization and transepithelial efflux of neutrophils in acute lung injury. *Cell,* 111**,** 635-646.

LI, S.-D., CHONO, S. & HUANG, L. 2008. Efficient oncogene silencing and metastasis inhibition via systemic delivery of siRNA. *Molecular Therapy,* 16**,** 942-946.

LI, W., WANG, L., KATOH, H., LIU, R., ZHENG, P. & LIU, Y. 2011c. Identification of a tumor suppressor relay between the FOXP3 and the Hippo pathways in breast and prostate cancers. *Cancer research,* 71**,** 2162-2171.

LI, Y., DRABSCH, Y., PUJUGUET, P., REN, J., VAN LAAR, T., ZHANG, L., VAN DAM, H., CLÉMENT-LACROIX, P. & TEN DIJKE, P. 2015. Genetic depletion and pharmacological targeting of αv integrin in breast cancer cells impairs metastasis in zebrafish and mouse xenograft models. *Breast Cancer Research,* 17**,** 28.

LI, Y. M., PAN, Y., WEI, Y., CHENG, X., ZHOU, B. P., TAN, M., ZHOU, X., XIA, W., HORTOBAGYI, G. N. & YU, D. 2004. Upregulation of CXCR4 is essential for HER2-mediated tumor metastasis. *Cancer cell,* 6**,** 459-469.

LIANG, C.-M., ZHONG, C.-P., SUN, R.-X., LIU, B.-B., HUANG, C., QIN, J., ZHOU, S., SHAN, J., LIU, Y.-K. & YE, S.-L. 2007a. Local expression of secondary lymphoid tissue chemokine delivered by adeno-associated virus within the tumor bed stimulates strong anti-liver tumor immunity. *Journal of virology,* 81**,** 9502-9511.

LIANG, M., MALLARI, C., ROSSER, M., NG, H. P., MAY, K., MONAHAN, S., BAUMAN, J. G., ISLAM, I., GHANNAM, A. & BUCKMAN, B. 2000. Identification and characterization of a potent, selective, and orally active antagonist of the CC chemokine receptor-1. *Journal of Biological Chemistry,* 275**,** 19000-19008.

LIANG, Z., BROOKS, J., WILLARD, M., LIANG, K., YOON, Y., KANG, S. & SHIM, H. 2007b. CXCR4/CXCL12 axis promotes VEGF-mediated tumor angiogenesis through Akt signaling pathway. *Biochemical and biophysical research communications,* 359**,** 716-722.

LIANG, Z., WU, H., REDDY, S., ZHU, A., WANG, S., BLEVINS, D., YOON, Y., ZHANG, Y. & SHIM, H. 2007c. Blockade of invasion and metastasis of breast cancer cells via targeting CXCR4 with an artificial microRNA. *Biochemical and biophysical research communications,* 363**,** 542-546.

LIANG, Z., WU, T., LOU, H., YU, X., TAICHMAN, R. S., LAU, S. K., NIE, S., UMBREIT, J. & SHIM, H. 2004. Inhibition of breast cancer metastasis by selective synthetic polypeptide against CXCR4. *Cancer research,* 64**,** 4302-4308.

LIANG, Z., YOON, Y., VOTAW, J., GOODMAN, M. M., WILLIAMS, L. & SHIM, H. 2005. Silencing of CXCR4 blocks breast cancer metastasis. *Cancer research,* 65**,** 967-971.

LIANG, Z., ZHAN, W., ZHU, A., YOON, Y., LIN, S., SASAKI, M., KLAPPROTH, J.-M. A., YANG, H., GROSSNIKLAUS, H. E. & XU, J. 2012. Development of a unique small molecule modulator of CXCR4. *PLoS One,* 7**,** e34038.

LIBERMAN, J., SARTELET, H., FLAHAUT, M., MÜHLETHALER-MOTTET, A., COULON, A., NYALENDO, C., VASSAL, G., JOSEPH, J.-M. & GROSS, N. 2012. Involvement of the CXCR7/CXCR4/CXCL12 axis in the malignant progression of human neuroblastoma. *PloS one,* 7**,** e43665.

LIBERT, F., PASSAGE, E., PARMENTIER, M., SIMONS, M.-J., VASSART, G. & MATTEI, M.-G. 1991. Chromosomal mapping of A1 and A2 adenosine receptors, VIP receptor, and a new subtype of serotonin receptor. *Genomics,* 11**,** 225-227.

LIBURA, J., DRUKALA, J., MAJKA, M., TOMESCU, O., NAVENOT, J. M., KUCIA, M., MARQUEZ, L., PEIPER, S. C., BARR, F. G. & JANOWSKA-WIECZOREK, A. 2002. CXCR4–SDF-1 signaling is active in rhabdomyosarcoma cells and regulates locomotion, chemotaxis, and adhesion. *Blood,* 100**,** 2597-2606.

LIEKENS, S., SCHOLS, D. & HATSE, S. 2010. CXCL12-CXCR4 axis in angiogenesis, metastasis and stem cell mobilization. *Current pharmaceutical design,* 16**,** 3903-3920.

LILES, W. C., BROXMEYER, H. E., RODGER, E., WOOD, B., HÜBEL, K., COOPER, S., HANGOC, G., BRIDGER, G. J., HENSON, G. W. & CALANDRA, G. 2003. Mobilization of hematopoietic progenitor cells in healthy volunteers by AMD3100, a CXCR4 antagonist. *Blood,* 102**,** 2728-2730.

LIN, L., HAN, M., WANG, F., XU, L., YU, H. & YANG, P. 2014a. CXCR7 stimulates MAPK signaling to regulate hepatocellular carcinoma progression. *Cell death & disease,* 5**,** e1488.

LIN, Y., LI, Y., WANG, X., GONG, T., ZHANG, L. & SUN, X. 2013. Targeted drug delivery to renal proximal tubule epithelial cells mediated by 2-glucosamine. *Journal of Controlled Release,* 167**,** 148-156.

LIN, Y., LUO, J., ZHU, W. E., SRIVASTAVA, M., SCHAUE, D., ELASHOFF, D. A., DUBINETT, S. M., SHARMA, S., WU, B. & JOHN, M. A. S. 2014b. A cytokine-delivering polymer is effective in reducing tumor burden in a head and neck squamous cell carcinoma murine model. *Otolaryngology--Head and Neck Surgery,* 151**,** 447-53.

LISTON, A. & MCCOLL, S. 2003. Subversion of the chemokine world by microbial pathogens. *Bioessays,* 25**,** 478-488.

LIU, C. & HERMANN, T. E. 1978. Characterization of ionomycin as a calcium ionophore. *Journal of Biological Chemistry,* 253**,** 5892-5894.

LIU, C., PHAM, K., LUO, D., REYNOLDS, B. A., HOTHI, P., FOLTZ, G. & HARRISON, J. K. 2013. Expression and functional heterogeneity of chemokine receptors CXCR4 and CXCR7 in primary patient-derived glioblastoma cells. *PLoS One,* 8**,** e59750.

LIU, D., SHRIVER, Z., VENKATARAMAN, G., EL SHABRAWI, Y. & SASISEKHARAN, R. 2002. Tumor cell surface heparan sulfate as cryptic promoters or inhibitors of tumor growth and metastasis. *Proceedings of the National Academy of Sciences,* 99**,** 568-573.

LIU, F., LANG, R., WEI, J., FAN, Y., CUI, L., GU, F., GUO, X., PRINGLE, G. A., ZHANG, X. & FU, L. 2009a. Increased expression of SDF-1/CXCR4 is associated with lymph node metastasis of invasive micropapillary carcinoma of the breast. *Histopathology,* 54**,** 741-750.

LIU, L., CAO, Y., CHEN, C., ZHANG, X., MCNABOLA, A., WILKIE, D., WILHELM, S., LYNCH, M. & CARTER, C. 2006. Sorafenib blocks the RAF/MEK/ERK pathway, inhibits tumor angiogenesis, and induces tumor cell apoptosis in hepatocellular carcinoma model PLC/PRF/5. *Cancer research,* 66**,** 11851-11858.

LIU, R., WANG, L., CHEN, G., KATOH, H., CHEN, C., LIU, Y. & ZHENG, P. 2009b. FOXP3 up-regulates p21 expression by site-specific inhibition of histone deacetylase 2/histone deacetylase 4 association to the locus. *Cancer research,* 69**,** 2252-2259.

LIU, Y., JI, R., LI, J., GU, Q., ZHAO, X., SUN, T., WANG, J., LI, J., DU, Q. & SUN, B. 2010. Correlation effect of EGFR and CXCR4 and CCR7 chemokine receptors in predicting breast cancer metastasis and prognosis. *Journal of Experimental & Clinical Cancer Research,* 29**,** 16.

LIU, Y., WANG, Y., LI, W., ZHENG, P. & LIU, Y. 2009c. Activating Transcription Factor 2 and c-Jun–Mediated Induction of FoxP3 for Experimental Therapy of Mammary Tumor in the Mouse. *Cancer research,* 69**,** 5954-5960.

LOMBAERTS, M., VAN WEZEL, T., PHILIPPO, K., DIERSSEN, J. W. F., ZIMMERMAN, R. M. E., OOSTING, J., VAN EIJK, R., EILERS, P. H., VAN DE WATER, B. & CORNELISSE, C. J. 2006. E-cadherin transcriptional downregulation by promoter methylation but not mutation is related to epithelial-to-mesenchymal transition in breast cancer cell lines. *British journal of cancer,* 94**,** 661-671.

LOPES, J. E., TORGERSON, T. R., SCHUBERT, L. A., ANOVER, S. D., OCHELTREE, E. L., OCHS, H. D. & ZIEGLER, S. F. 2006. Analysis of FOXP3 reveals multiple domains required for its function as a transcriptional repressor. *The Journal of Immunology,* 177**,** 3133-3142.

LORTAT-JACOB, H., GROSDIDIER, A. & IMBERTY, A. 2002. Structural diversity of heparan sulfate binding domains in chemokines. *Proceedings of the National Academy of Sciences,* 99**,** 1229-1234.

LOU, Y., PREOBRAZHENSKA, O., SUTCLIFFE, M., BARCLAY, L., MCDONALD, P. C., ROSKELLEY, C., OVERALL, C. M. & DEDHAR, S. 2008. Epithelial–mesenchymal transition (EMT) is not sufficient for spontaneous murine breast cancer metastasis. *Developmental Dynamics,* 237**,** 2755-2768.

LUKER, K. E., GUPTA, M. & LUKER, G. D. 2009a. Bioluminescent CXCL12 fusion protein for cellular studies of CXCR4 and CXCR7. *Biotechniques,* 47**,** 625.

LUKER, K. E., GUPTA, M. & LUKER, G. D. 2009b. Imaging chemokine receptor dimerization with firefly luciferase complementation. *The FASEB Journal,* 23**,** 823-834.

LUKER, K. E., LEWIN, S. A., MIHALKO, L. A., SCHMIDT, B. T., WINKLER, J. S., COGGINS, N. L., THOMAS, D. G. & LUKER, G. D. 2012. Scavenging of CXCL12 by CXCR7 promotes tumor growth and metastasis of CXCR4-positive breast cancer cells. *Oncogene,* 31**,** 4750-4758.

LUKER, K. E. & LUKER, G. D. 2006. Functions of CXCL12 and CXCR4 in breast cancer. *Cancer letters,* 238**,** 30-41.

LUKER, K. E., STEELE, J. M., MIHALKO, L. A., RAY, P. & LUKER, G. D. 2010. Constitutive and chemokine-dependent internalization and recycling of CXCR7 in breast cancer cells to degrade chemokine ligands. *Oncogene,* 29**,** 4599-4610.

LUTTRELL, L. M., ROUDABUSH, F. L., CHOY, E. W., MILLER, W. E., FIELD, M. E., PIERCE, K. L. & LEFKOWITZ, R. J. 2001. Activation and targeting of extracellular signal-regulated kinases by β-arrestin scaffolds. *Proceedings of the National Academy of Sciences,* 98**,** 2449-2454.

MA, Q., JONES, D., BORGHESANI, P. R., SEGAL, R. A., NAGASAWA, T., KISHIMOTO, T., BRONSON, R. T. & SPRINGER, T. A. 1998. Impaired B-lymphopoiesis, myelopoiesis, and derailed cerebellar neuron migration in CXCR4-and SDF-1-deficient mice. *Proceedings of the National Academy of Sciences,* 95**,** 9448-9453.

MA, X., NORSWORTHY, K., KUNDU, N., RODGERS, W. H., GIMOTTY, P. A., GOLOUBEVA, O., LIPSKY, M., LI, Y., HOLT, D. & FULTON, A. 2009. CXCR3 expression is associated with poor survival in breast cancer and promotes metastasis in a murine model. *Molecular cancer therapeutics,* 8**,** 490-498.

MACHOWSKA, M., WACHOWICZ, K., SOPEL, M. & RZEPECKI, R. 2014. Nuclear location of tumor suppressor protein maspin inhibits proliferation of breast cancer cells without affecting proliferation of normal epithelial cells. *BMC cancer,* 14**,** 142.

MACK, M., PFIRSTINGER, J., WEBER, C., WEBER, K. S. C., NELSON, P. J., RUPP, T., MALETZ, K., BRÜHL, H. & SCHLÖNDORFF, D. 2002. Chondroitin sulfate A released from platelets blocks RANTES presentation on cell surfaces and RANTES-dependent firm adhesion of leukocytes. *European journal of immunology,* 32**,** 1012-1020.

MADDEN, S. L., COOK, B. P., NACHT, M., WEBER, W. D., CALLAHAN, M. R., JIANG, Y., DUFAULT, M. R., ZHANG, X., ZHANG, W. & WALTER-YOHRLING, J. 2004. Vascular gene expression in nonneoplastic and malignant brain. *The American journal of pathology,* 165**,** 601-608.

MAHALINGAM, S. & KARUPIAH, G. 1999. Chemokines and chemokine receptors in infectious diseases. *Immunology and cell biology,* 77**,** 469-475.

MAHMOUD, S. M. A., PAISH, E. C., POWE, D. G., MACMILLAN, R. D., GRAINGE, M. J., LEE, A. H. S., ELLIS, I. O. & GREEN, A. R. 2011. Tumor-infiltrating CD8+ lymphocytes predict clinical outcome in breast cancer. *Journal of Clinical Oncology,* 29**,** 1949-1955.

MALKI, M. I., COBB, S., POHL, E., KIRBY, J. & ALI, S. 2013. Contribution of heparan sulphate binding domain of chemokine Ccl21 to trans-endothelial migration of breast cancer cells. *Immunology,* 140**,** 68.

MANDRIOTA, S. J., JUSSILA, L., JELTSCH, M., COMPAGNI, A., BAETENS, D., PREVO, R., BANERJI, S., HUARTE, J., MONTESANO, R. & JACKSON, D. G. 2001. Vascular endothelial growth factor-C-mediated lymphangiogenesis promotes tumour metastasis. *The EMBO journal,* 20**,** 672-682.

MANU, K. A., SHANMUGAM, M. K., RAJENDRAN, P., LI, F., RAMACHANDRAN, L., HAY, H. S., KANNAIYAN, R., SWAMY, S. N., VALI, S. & KAPOOR, S. 2011. Plumbagin inhibits invasion and migration of breast and gastric cancer cells by downregulating the expression of chemokine receptor CXCR4. *Molecular cancer,* 10**,** 107.

MARCHBANKS, P. A., MCDONALD, J. A., WILSON, H. G., FOLGER, S. G., MANDEL, M. G., DALING, J. R., BERNSTEIN, L., MALONE, K. E., URSIN, G. & STROM, B. L. 2002. Oral contraceptives and the risk of breast cancer. *New England Journal of Medicine,* 346**,** 2025-2032.

MARCHESE, A., RAIBORG, C., SANTINI, F., KEEN, J. H., STENMARK, H. & BENOVIC, J. L. 2003. The E3 ubiquitin ligase AIP4 mediates ubiquitination and sorting of the G protein-coupled receptor CXCR4. *Developmental cell,* 5**,** 709-722.

MARCHESI, F., MONTI, P., LEONE, B. E., ZERBI, A., VECCHI, A., PIEMONTI, L., MANTOVANI, A. & ALLAVENA, P. 2004. Increased survival, proliferation, and migration in metastatic human pancreatic tumor cells expressing functional CXCR4. *Cancer research,* 64**,** 8420-8427.

MARECHAL, R., DEMETTER, P., NAGY, N., BERTON, A., DECAESTECKER, C., POLUS, M., CLOSSET, J., DEVIÈRE, J., SALMON, I. & VAN LAETHEM, J.-L. 2009. High expression of CXCR4 may predict poor survival in resected pancreatic adenocarcinoma. *British journal of cancer,* 100**,** 1444-1451.

MARINISSEN, M. J. & GUTKIND, J. S. 2001. G-protein-coupled receptors and signaling networks: emerging paradigms. *Trends in pharmacological sciences,* 22**,** 368-376.

MARSHALL, L. J., RAMDIN, L. S. P., BROOKS, T. & SHUTE, J. K. 2003. Plasminogen activator inhibitor-1 supports IL-8-mediated neutrophil transendothelial migration by inhibition of the constitutive shedding of endothelial IL-8/heparan sulfate/syndecan-1 complexes. *The Journal of Immunology,* 171**,** 2057-2065.

MARSLAND, B. J., BÄTTIG, P., BAUER, M., RUEDL, C., LÄSSING, U., BEERLI, R. R., DIETMEIER, K., IVANOVA, L., PFISTER, T. & VOGT, L. 2005. CCL19 and CCL21 induce a potent proinflammatory differentiation program in licensed dendritic cells. *Immunity,* 22**,** 493-505.

MARTIN, F., LADOIRE, S., MIGNOT, G., APETOH, L. & GHIRINGHELLI, F. 2010. Human FOXP3 and cancer. *Oncogene,* 29**,** 4121-4129.

MASHINO, K., SADANAGA, N., YAMAGUCHI, H., TANAKA, F., OHTA, M., SHIBUTA, K., INOUE, H. & MORI, M. 2002. Expression of chemokine receptor CCR7 is associated with lymph node metastasis of gastric carcinoma. *Cancer research,* 62**,** 2937-2941.

MASON, W. T. 1999. *Fluorescent and luminescent probes for biological activity: a practical guide to technology for quantitative real-time analysis*, Academic Press.

MATSUSUE, R., KUBO, H., HISAMORI, S., OKOSHI, K., TAKAGI, H., HIDA, K., NAKANO, K., ITAMI, A., KAWADA, K. & NAGAYAMA, S. 2009. Hepatic stellate cells promote liver metastasis of colon cancer cells by the action of SDF-1/CXCR4 axis. *Annals of surgical oncology,* 16**,** 2645-2653.

MAXFIELD, F. R. 1993. Regulation of leukocyte locomotion by Ca 2+. *Trends in cell biology,* 3**,** 386-391.

MAZZINGHI, B., RONCONI, E., LAZZERI, E., SAGRINATI, C., BALLERINI, L., ANGELOTTI, M. L., PARENTE, E., MANCINA, R., NETTI, G. S. & BECHERUCCI, F. 2008. Essential but differential role for CXCR4 and CXCR7 in the therapeutic homingof human renal progenitor cells. *The Journal of experimental medicine,* 205**,** 479-490.

MCCONNELL, A. T., ELLIS, R., PATHY, B., PLUMMER, R., LOVAT, P. E. & O'BOYLE, G. 2016. The prognostic significance and impact of the CXCR4/CXCR7/CXCL12 axis in primary cutaneous melanoma. *British Journal of Dermatology,* 175**,** 1210-1220.

MCCUSKER, E. C., BANE, S. E., O'MALLEY, M. A. & ROBINSON, A. S. 2007. Heterologous GPCR expression: a bottleneck to obtaining crystal structures. *Biotechnology progress,* 23**,** 540-547.

MCDONALD, P. H., CHOW, C.-W., MILLER, W. E., LAPORTE, S. A., FIELD, M. E., LIN, F.-T., DAVIS, R. J. & LEFKOWITZ, R. J. 2000. β-Arrestin 2: a receptor-regulated MAPK scaffold for the activation of JNK3. *Science,* 290**,** 1574-1577.

MEIJER, J., OGINK, J. & ROOS, E. 2008. Effect of the chemokine receptor CXCR7 on proliferation of carcinoma cells in vitro and in vivo. *British journal of cancer,* 99**,** 1493-1501.

MELLADO, M., RODRÍGUEZ-FRADE, J. M., MAÑES, S. & MARTÍNEZ-A, C. 2001a. Chemokine signaling and functional responses: the role of receptor dimerization and TK pathway activation. *Annual review of immunology,* 19**,** 397-421.

MELLADO, M., RODRÍGUEZ-FRADE, J. M., VILA-CORO, A. J., FERNÁNDEZ, S., DE ANA, A. M., JONES, D. R., TORÁN, J. L. & MARTÍNEZ-A, C. 2001b. Chemokine receptor homo-or heterodimerization activates distinct signaling pathways. *The EMBO Journal,* 20**,** 2497-2507.

MELLADO, M., RODRÍGUEZ-FRADE, J. M., VILA-CORO, A. J., FERNÁNDEZ, S., DE ANA, A. M., JONES, D. R., TORÁN, J. L. & MARTÍNEZ, C. 2001c. Chemokine receptor homo-or heterodimerization activates distinct signaling pathways. *The EMBO Journal,* 20**,** 2497-2507.

MELLOR, P., HARVEY, J. R., MURPHY, K. J., PYE, D., O'BOYLE, G., LENNARD, T. W. J., KIRBY, J. A. & ALI, S. 2007. Modulatory effects of heparin and short-length oligosaccharides of heparin on the metastasis and growth of LMD MDA-MB 231 breast cancer cells in vivo. *British journal of cancer,* 97**,** 761-768.

MELO, R. D. C. C., LONGHINI, A. L., BIGARELLA, C. L., BARATTI, M. O., TRAINA, F., FAVARO, P., DE MELO CAMPOS, P. & SAAD, S. T. O. 2014. CXCR7 is highly expressed in acute lymphoblastic leukemia and potentiates CXCR4 response to CXCL12. *PloS one,* 9**,** e85926.

MENDOZA, M. C., ER, E. E. & BLENIS, J. 2011. The Ras-ERK and PI3K-mTOR pathways: cross-talk and compensation. *Trends in biochemical sciences,* 36**,** 320-328.

MENTEN, P., SACCANI, A., DILLEN, C., WUYTS, A., STRUYF, S., PROOST, P., MANTOVANI, A., WANG, J. M. & VAN DAMME, J. 2002. Role of the autocrine chemokines MIP-1α and MIP-1β in the metastatic behavior of murine T cell lymphoma. *Journal of leukocyte biology,* 72**,** 780-789.

MERLO, A., CASALINI, P., CARCANGIU, M. L., MALVENTANO, C., TRIULZI, T., MÈNARD, S., TAGLIABUE, E. & BALSARI, A. 2009. FOXP3 expression and overall survival in breast cancer. *Journal of clinical oncology,* 27**,** 1746-1752.

MIAO, Z., LUKER, K. E., SUMMERS, B. C., BERAHOVICH, R., BHOJANI, M. S., REHEMTULLA, A., KLEER, C. G., ESSNER, J. J., NASEVICIUS, A. & LUKER, G. D. 2007. CXCR7 (RDC1) promotes breast and lung tumor growth in vivo and is expressed on tumor-associated vasculature. *Proceedings of the National Academy of Sciences,* 104**,** 15735-15740.

MICHINO, M., ABOLA, E., DOCK, G., BROOKS, C. L., DIXON, J. S., MOULT, J. & STEVENS, R. C. 2009. Community-wide assessment of GPCR structure modelling and ligand docking: GPCR Dock 2008. *Nature Reviews Drug Discovery,* 8**,** 455-463.

MICKE, P. & ÖSTMAN, A. 2005. Exploring the tumour environment: cancer-associated fibroblasts as targets in cancer therapy. *Expert Opinion on Therapeutic Targets,* 9**,** 1217-33.

MIDDLETON, J., PATTERSON, A. M., GARDNER, L., SCHMUTZ, C. & ASHTON, B. A. 2002. Leukocyte extravasation: chemokine transport and presentation by the endothelium. *Blood,* 100**,** 3853-3860.

MILLAR, A. J., SHORT, S. R., HIRATSUKA, K., CHUA, N.-H. & KAY, S. A. 1992. Firefly luciferase as a reporter of regulated gene expression in higher plants. *Plant Molecular Biology Reporter,* 10**,** 324-337.

MILLER, F. R., MEDINA, D. & HEPPNER, G. H. 1981. Preferential growth of mammary tumors in intact mammary fatpads. *Cancer research,* 41**,** 3863-3867.

MILLIKEN, D., SCOTTON, C., RAJU, S., BALKWILL, F. & WILSON, J. 2002. Analysis of chemokines and chemokine receptor expression in ovarian cancer ascites. *Clinical Cancer Research,* 8**,** 1108-1114.

MILLION WOMEN STUDY COLLABORATORS 2003. Breast cancer and hormone-replacement therapy in the Million Women Study. *The Lancet,* 362**,** 419-427.

MILNE, R. S., MATTICK, C., NICHOLSON, L., DEVARAJ, P., ALCAMI, A. & GOMPELS, U. A. 2000. RANTES binding and down-regulation by a novel human herpesvirus-6 β chemokine receptor. *The Journal of Immunology,* 164**,** 2396-2404.

MININA, S., REICHMAN-FRIED, M. & RAZ, E. 2007. Control of receptor internalization, signaling level, and precise arrival at the target in guided cell migration. *Current biology,* 17**,** 1164-1172.

MINN, A. J., GUPTA, G. P., SIEGEL, P. M., BOS, P. D., SHU, W., GIRI, D. D., VIALE, A., OLSHEN, A. B., GERALD, W. L. & MASSAGUÉ, J. 2005. Genes that mediate breast cancer metastasis to lung. *Nature,* 436**,** 518-524.

MIRISOLA, V., ZUCCARINO, A., BACHMEIER, B. E., SORMANI, M. P., FALTER, J., NERLICH, A. & PFEFFER, U. 2009. CXCL12/SDF1 expression by breast cancers is an independent prognostic marker of disease-free and overall survival. *European Journal of Cancer,* 45**,** 2579-2587.

MISSLITZ, A., PABST, O., HINTZEN, G., OHL, L., KREMMER, E., PETRIE, H. T. & FÖRSTER, R. 2004. Thymic T cell development and progenitor localization depend on CCR7. *The Journal of experimental medicine,* 200**,** 481-491.

MITRI, Z., CONSTANTINE, T. & O'REGAN, R. 2012. The HER2 receptor in breast cancer: pathophysiology, clinical use, and new advances in therapy. *Chemotherapy research and practice,* 2012**,** 743193.

MO, M., ZHOU, M., WANG, L., QI, L., ZHOU, K., LIU, L.-F., CHEN, Z. & ZU, X.-B. 2015. CCL21/CCR7 Enhances the Proliferation, Migration, and Invasion of Human Bladder Cancer T24 Cells. *PloS one,* 10**,** e0119506.

MONNIER, J., BOISSAN, M., L'HELGOUALC'H, A., LACOMBE, M.-L., TURLIN, B., ZUCMAN-ROSSI, J., THÉRET, N., PIQUET-PELLORCE, C. & SAMSON, M. 2012. CXCR7 is up-regulated in human and murine hepatocellular carcinoma and is specifically expressed by endothelial cells. *European journal of cancer,* 48**,** 138-148.

MOODY, P. R., SAYERS, E. J., MAGNUSSON, J. P., ALEXANDER, C., BORRI, P., WATSON, P. & JONES, A. T. 2015. Receptor crosslinking: a general method to trigger internalization and lysosomal targeting of therapeutic receptor: ligand complexes. *Molecular Therapy,* 23**,** 1888-98.

MOORE, G. E., GERNER, R. E. & FRANKLIN, H. A. 1967. Culture of normal human leukocytes. *Jama,* 199**,** 519-524.

MORGAN, A. J. & JACOB, R. 1994. Ionomycin enhances Ca2+ influx by stimulating store-regulated cation entry and not by a direct action at the plasma membrane. *Biochemical Journal,* 300**,** 665-672.

MORI, S., KODAIRA, M., ITO, A., OKAZAKI, M., KAWAGUCHI, N., HAMADA, Y., TAKADA, Y. & MATSUURA, N. 2015. Enhanced Expression of Integrin αvβ3 Induced by TGF-β Is Required for the Enhancing Effect of Fibroblast Growth Factor 1 (FGF1) in TGF-β-Induced Epithelial-Mesenchymal Transition (EMT) in Mammary Epithelial Cells. *PloS one,* 10**,** e0137486.

MORI, S., NAKANO, H., ARITOMI, K., WANG, C.-R., GUNN, M. D. & KAKIUCHI, T. 2001. Mice lacking expression of the chemokines CCL21-ser and CCL19 (plt mice) demonstrate delayed but enhanced T cell immune responses. *Journal of Experimental Medicine,* 193**,** 207-218.

MORI, T., KIM, J., YAMANO, T., TAKEUCHI, H., HUANG, S., UMETANI, N., KOYANAGI, K. & HOON, D. S. B. 2005. Epigenetic up-regulation of CC chemokine receptor 7 and CXC chemokine receptor 4 expression in melanoma cells. *Cancer research,* 65**,** 1800-1807.

MORIMOTO, M., MATSUO, Y., KOIDE, S., TSUBOI, K., SHAMOTO, T., SATO, T., SAITO, K., TAKAHASHI, H. & TAKEYAMA, H. 2016. Enhancement of the CXCL12/CXCR4 axis due to acquisition of gemcitabine resistance in pancreatic cancer: effect of CXCR4 antagonists. *BMC cancer,* 16**,** 305.

MORRIS, V. L., MACDONALD, I. C., KOOP, S., SCHMIDT, E. E., CHAMBERS, A. F. & GROOM, A. C. 1993. Early interactions of cancer cells with the microvasculature in mouse liver and muscle during

hematogenous metastasis: videomicroscopic analysis. *Clinical & experimental metastasis,* 11**,** 377-390.

MORTON, D. L., WEN, D.-R., WONG, J. H., ECONOMOU, J. S., CAGLE, L. A., STORM, F. K., FOSHAG, L. J. & COCHRAN, A. J. 1992. Technical details of intraoperative lymphatic mapping for early stage melanoma. *Archives of surgery,* 127**,** 392-399.

MOSI, R. M., ANASTASSOVA, V., COX, J., DARKES, M. C., IDZAN, S. R., LABRECQUE, J., LAU, G., NELSON, K. L., PATEL, K. & SANTUCCI, Z. 2012. The molecular pharmacology of AMD11070: an orally bioavailable CXCR4 HIV entry inhibitor. *Biochemical pharmacology,* 83**,** 472-479.

MOYLE, G., DEJESUS, E., BOFFITO, M., WONG, R. S., GIBNEY, C., BADEL, K., MACFARLAND, R., CALANDRA, G., BRIDGER, G. & BECKER, S. 2009. Proof of activity with AMD11070, an orally bioavailable inhibitor of CXCR4-tropic HIV type 1. *Clinical Infectious Diseases,* 48**,** 798-805.

MUFSON, R. & GESNER, T. 1987. Binding and internalization of recombinant human erythropoietin in murine erythroid precursor cells. *Blood,* 69**,** 1485-1490.

MÜHLETHALER-MOTTET, A., LIBERMAN, J., ASCENÇÃO, K., FLAHAUT, M., BOURLOUD, K. B., YAN, P., JAUQUIER, N., GROSS, N. & JOSEPH, J.-M. 2015. The CXCR4/CXCR7/CXCL12 axis is involved in a secondary but complex control of neuroblastoma metastatic cell homing. *PloS one,* 10**,** e0125616.

MÜLLER, A., HOMEY, B., SOTO, H., GE, N., CATRON, D., BUCHANAN, M. E., MCCLANAHAN, T., MURPHY, E., YUAN, W. & WAGNER, S. N. 2001. Involvement of chemokine receptors in breast cancer metastasis. *Nature,* 410**,** 50-56.

MULLER, A., SONKOLY, E., EULERT, C., GERBER, P. A., KUBITZA, R., SCHIRLAU, K., FRANKEN-KUNKEL, P., POREMBA, C., SNYDERMAN, C. & KLOTZ, L. O. 2006. Chemokine receptors in head and neck cancer: association with metastatic spread and regulation during chemotherapy. *International journal of cancer,* 118**,** 2147-2157.

MURAKAMI, J., LI, T. S., UEDA, K., TANAKA, T. & HAMANO, K. 2009a. Inhibition of accelerated tumor growth by blocking the recruitment of mobilized endothelial progenitor cells after chemotherapy. *International journal of cancer,* 124**,** 1685-1692.

MURAKAMI, T., KUMAKURA, S., YAMAZAKI, T., TANAKA, R., HAMATAKE, M., OKUMA, K., HUANG, W., TOMA, J., KOMANO, J. & YANAKA, M. 2009b. The novel CXCR4 antagonist KRH-3955 is an orally bioavailable and extremely potent inhibitor of human immunodeficiency virus type 1 infection: comparative studies with AMD3100. *Antimicrobial agents and chemotherapy,* 53**,** 2940-2948.

MURAKAMI, T., MAKI, W., CARDONES, A. R., FANG, H., KYI, A. T., NESTLE, F. O. & HWANG, S. T. 2002. Expression of CXC chemokine receptor-4 enhances the pulmonary metastatic potential of murine B16 melanoma cells. *Cancer research,* 62**,** 7328-7334.

MURAKAMI, T., NAKAJIMA, T., KOYANAGI, Y., TACHIBANA, K., FUJII, N., TAMAMURA, H., YOSHIDA, N., WAKI, M., MATSUMOTO, A. & YOSHIE, O. 1997. A small molecule CXCR4 inhibitor that blocks T cell line–tropic HIV-1 infection. *The Journal of experimental medicine,* 186**,** 1389-1393.

MURPHY, P. M. 1994. The molecular biology of leukocyte chemoattractant receptors. *Annual review of immunology,* 12**,** 593-633.

MURPHY, P. M., BAGGIOLINI, M., CHARO, I. F., HÉBERT, C. A., HORUK, R., MATSUSHIMA, K., MILLER, L. H., OPPENHEIM, J. J. & POWER, C. A. 2000. International union of pharmacology. XXII. Nomenclature for chemokine receptors. *Pharmacological reviews,* 52**,** 145-176.

MUSTACCHI, P. 1961. Ramazzini and Rigoni-Stern on Parity and Breast Cancer: Clinical Impression and Statistical Corroboration. *Archives of internal medicine,* 108**,** 639-642.

MUYLDERMANS, S., BARAL, T. N., RETAMOZZO, V. C., DE BAETSELIER, P., DE GENST, E., KINNE, J., LEONHARDT, H., MAGEZ, S., NGUYEN, V. K. & REVETS, H. 2009. Camelid immunoglobulins and nanobody technology. *Veterinary immunology and immunopathology,* 128**,** 178-183.

NAGIRA, M., IMAI, T., HIESHIMA, K., KUSUDA, J., RIDANPÄÄ, M., TAKAGI, S., NISHIMURA, M., KAKIZAKI, M., NOMIYAMA, H. & YOSHIE, O. 1997. Molecular cloning of a novel human CC chemokine secondary lymphoid-tissue chemokine that is a potent chemoattractant for lymphocytes and mapped to chromosome 9p13. *Journal of Biological Chemistry,* 272**,** 19518-19524.

NANDA, R., CHOW, L. Q., DEES, E. C., BERGER, R., GUPTA, S., GEVA, R., PUSZTAI, L., DOLLED-FILHART, M., EMANCIPATOR, K. & GONZALEZ, E. J. 2015. Abstract S1-09: a phase Ib study of pembrolizumab (MK-3475) in patients with advanced triple-negative breast cancer. *Cancer Research,* 75**,** S1-09-S1-09.

NATCHUS, M., ARRENDALE, R. & DONALD, L. 2008. MSX-122, an orally available small molecule CXCR4 antagonist, promotes leukocytosis in monkeys at doses that were well tolerated in a 28 day toxicology study. *Cancer Research,* 68**,** 1189-1189.

NATHANSON, S. D. 2003. Insights into the mechanisms of lymph node metastasis. *Cancer,* 98**,** 413-423.

NAUMANN, U., CAMERONI, E., PRUENSTER, M., MAHABALESHWAR, H., RAZ, E., ZERWES, H.-G., ROT, A. & THELEN, M. 2010. CXCR7 functions as a scavenger for CXCL12 and CXCL11. *PloS one,* 5**,** e9175.

NAUMOV, G. N., FOLKMAN, J., STRAUME, O. & AKSLEN, L. A. 2008. Tumor-vascular interactions and tumor dormancy. *Apmis,* 116**,** 569-585.

NAYA, A., KOBAYASHI, K., ISHIKAWA, M., OHWAKI, K., SAEKI, T., NOGUCHI, K. & OHTAKE, N. 2003. Structure-activity relationships of 2-(benzothiazolylthio) acetamide class of CCR3 selective antagonist. *Chemical and pharmaceutical bulletin,* 51**,** 697-701.

NEEL, N. F., SCHUTYSER, E., SAI, J., FAN, G.-H. & RICHMOND, A. 2005. Chemokine receptor internalization and intracellular trafficking. *Cytokine & growth factor reviews,* 16**,** 637-658.

NEGRINI, S., GORGOULIS, V. G. & HALAZONETIS, T. D. 2010. Genomic instability—an evolving hallmark of cancer. *Nature reviews Molecular cell biology,* 11**,** 220-228.

NELSON, M. T., SHORT, A., COLE, S. L., GROSS, A. C., WINTER, J., EUBANK, T. D. & LANNUTTI, J. J. 2014. Preferential, enhanced breast cancer cell migration on biomimetic electrospun nanofiber 'cell highways'. *BMC cancer,* 14**,** 825.

NERVI, B., RAMIREZ, P., RETTIG, M. P., UY, G. L., HOLT, M. S., RITCHEY, J. K., PRIOR, J. L., PIWNICA-WORMS, D., BRIDGER, G. & LEY, T. J. 2009. Chemosensitization of acute myeloid leukemia (AML) following mobilization by the CXCR4 antagonist AMD3100. *Blood,* 113**,** 6206-6214.

NEVES, S. R., RAM, P. T. & IYENGAR, R. 2002. G protein pathways. *Science,* 296**,** 1636-1639.

NHAM, T., FILALI, S., DANNE, C., DERBISE, A. & CARNIEL, E. 2012. Imaging of bubonic plague dynamics by in vivo tracking of bioluminescent Yersinia pestis. *PloS one,* 7**,** e34714.

NIBBS, R. J. B. & GRAHAM, G. J. 2013. Immune regulation by atypical chemokine receptors. *Nature Reviews Immunology,* 13**,** 815-829.

NILLESEN, S. T. M., GEUTJES, P. J., WISMANS, R., SCHALKWIJK, J., DAAMEN, W. F. & VAN KUPPEVELT, T. H. 2007. Increased angiogenesis and blood vessel maturation in acellular collagen–heparin scaffolds containing both FGF2 and VEGF. *Biomaterials,* 28**,** 1123-1131.

NIMCHINSKY, E. A., HOF, P. R., JANSSEN, W. G. M., MORRISON, J. H. & SCHMAUSS, C. 1997. Expression of dopamine D3 receptor dimers and tetramers in brain and in transfected cells. *Journal of Biological Chemistry,* 272**,** 29229-29237.

NIU, J., HUANG, Y. & ZHANG, L. 2015. CXCR4 silencing inhibits invasion and migration of human laryngeal cancer Hep-2 cells. *International journal of clinical and experimental pathology,* 8**,** 6255.

NOMURA, T., HASEGAWA, H., KOHNO, M., SASAKI, M. & FUJITA, S. 2001. Enhancement of anti-tumor immunity by tumor cells transfected with the secondary lymphoid tissue chemokine EBI-1-ligand chemokine and stromal cell–derived factor-1αchemokine genes. *International journal of cancer,* 91**,** 597-606.

NOVAK, L., IGOUCHEVA, O., CHO, S. & ALEXEEV, V. 2007. Characterization of the CCL21-mediated melanoma-specific immune responses and in situ melanoma eradication. *Molecular cancer therapeutics,* 6**,** 1755-1764.

O'BOYLE, G. 2012. The yin and yang of chemokine receptor activation. *British journal of pharmacology,* 166**,** 895-897.

O'BOYLE, G., FOX, C. R. J., WALDEN, H. R., WILLET, J. D. P., MAVIN, E. R., HINE, D. W., PALMER, J. M., BARKER, C. E., LAMB, C. A. & ALI, S. 2012. Chemokine receptor CXCR3 agonist prevents human

T-cell migration in a humanized model of arthritic inflammation. *Proceedings of the National Academy of Sciences,* 109**,** 4598-4603.

O'BOYLE, G., MELLOR, P., KIRBY, J. A. & ALI, S. 2009. Anti-inflammatory therapy by intravenous delivery of non-heparan sulfate-binding CXCL12. *The FASEB Journal,* 23**,** 3906-3916.

O'BOYLE, G., SWIDENBANK, I., MARSHALL, H., BARKER, C. E., ARMSTRONG, J., WHITE, S. A., FRICKER, S. P., PLUMMER, R., WRIGHT, M. & LOVAT, P. E. 2013. Inhibition of CXCR4–CXCL12 chemotaxis in melanoma by AMD11070. *British journal of cancer,* 108**,** 1634-1640.

O'BRIEN, S. J., MENOTTI-RAYMOND, M., MURPHY, W. J., NASH, W. G., WIENBERG, J., STANYON, R., COPELAND, N. G., JENKINS, N. A., WOMACK, J. E. & GRAVES, J. A. M. 1999. The promise of comparative genomics in mammals. *Science,* 286**,** 458-481.

O'DONOVAN, N., GALVIN, M. & MORGAN, J. G. 1999. Physical mapping of the CXC chemokine locus on human chromosome 4. *Cytogenetic and Genome Research,* 84**,** 39-42.

ÖDEMIS, V., LIPFERT, J., KRAFT, R., HAJEK, P., ABRAHAM, G., HATTERMANN, K., MENTLEIN, R. & ENGELE, J. 2012. The presumed atypical chemokine receptor CXCR7 signals through Gi/o proteins in primary rodent astrocytes and human glioma cells. *Glia,* 60**,** 372-381.

OH, Y. S., KIM, H. Y., SONG, I.-C., YUN, H.-J., JO, D.-Y., KIM, S. & LEE, H. J. 2012. Hypoxia induces CXCR4 expression and biological activity in gastric cancer cells through activation of hypoxia-inducible factor-1α. *Oncology reports,* 28**,** 2239-2246.

OHL, L., MOHAUPT, M., CZELOTH, N., HINTZEN, G., KIAFARD, Z., ZWIRNER, J., BLANKENSTEIN, T., HENNING, G. & FÖRSTER, R. 2004. CCR7 governs skin dendritic cell migration under inflammatory and steady-state conditions. *Immunity,* 21**,** 279-288.

OMURA, S., FUJIMOTO, T., OTOGURO, K., MATSUZAKI, K., MORIGUCHI, R., TANAKA, H. & SASAKI, Y. 1991. Lactacystin, a novel microbial metabolite, induces neuritogenesis of neuroblastoma cells. *The Journal of antibiotics,* 44**,** 113-116.

ONDER, T. T., GUPTA, P. B., MANI, S. A., YANG, J., LANDER, E. S. & WEINBERG, R. A. 2008. Loss of E-cadherin promotes metastasis via multiple downstream transcriptional pathways. *Cancer research,* 68**,** 3645-3654.

OPPERMANN, M., MACK, M., PROUDFOOT, A. E. & OLBRICH, H. 1999. Differential effects of CC chemokines on CC chemokine receptor 5 (CCR5) phosphorylation and identification of phosphorylation sites on the CCR5 carboxyl terminus. *Journal of Biological Chemistry,* 274**,** 8875-8885.

ORIMO, A., GUPTA, P. B., SGROI, D. C., ARENZANA-SEISDEDOS, F., DELAUNAY, T., NAEEM, R., CAREY, V. J., RICHARDSON, A. L. & WEINBERG, R. A. 2005. Stromal fibroblasts present in invasive human breast carcinomas promote tumor growth and angiogenesis through elevated SDF-1/CXCL12 secretion. *Cell,* 121**,** 335-348.

ORSINI, M. J., PARENT, J.-L., MUNDELL, S. J. & BENOVIC, J. L. 1999. Trafficking of the HIV coreceptor CXCR4. Role of arrestins and identification of residues in the c-terminal tail that mediate receptor internalization. *Journal of Biological Chemistry,* 274**,** 31076-31086.

OSBORNE, M. P. 2000. *Breast anatomy and development*, Philadelphia: Lippincott Williams & Wilkins.

OTERO, C., GROETTRUP, M. & LEGLER, D. F. 2006. Opposite fate of endocytosed CCR7 and its ligands: recycling versus degradation. *The Journal of Immunology,* 177**,** 2314-2323.

OVERBECK-ZUBRZYCKA, D. 2012. *FOXP3 regulates metastatic spread of breast cancer via control of expression of CXCR4 chemokine receptor.* MD, Newcastle University.

PAN, J., MESTAS, J., BURDICK, M. D., PHILLIPS, R. J., THOMAS, G. V., RECKAMP, K., BELPERIO, J. A. & STRIETER, R. M. 2006. Stromal derived factor-1 (SDF-1/CXCL12) and CXCR4 in renal cell carcinoma metastasis. *Molecular cancer,* 5**,** 56.

PAN, M.-R., HOU, M.-F., CHANG, H.-C. & HUNG, W.-C. 2008. Cyclooxygenase-2 up-regulates CCR7 via EP2/EP4 receptor signaling pathways to enhance lymphatic invasion of breast cancer cells. *Journal of Biological Chemistry,* 283**,** 11155-11163.

PAPATHEODOROU, H., PAPANASTASIOU, A. D., SIRINIAN, C., SCOPA, C., KALOFONOS, H. P., LEOTSINIDIS, M. & PAPADAKI, H. 2014. Expression patterns of SDF1/CXCR4 in human invasive

breast carcinoma and adjacent normal stroma: Correlation with tumor clinicopathological parameters and patient survival. *Pathology-Research and Practice,* 210**,** 662-667.

PAPAVRAMIDOU, N., PAPAVRAMIDIS, T. & DEMETRIOU, T. 2010. Ancient Greek and Greco–Roman methods in modern surgical treatment of cancer. *Annals of surgical oncology,* 17**,** 665-667.

PARAMESWARAN, R., YU, M., LIM, M., GROFFEN, J. & HEISTERKAMP, N. 2011. Combination of drug therapy in acute lymphoblastic leukemia with a CXCR4 antagonist. *Leukemia,* 25**,** 1314-1323.

PARISH, C. R., FREEMAN, C., BROWN, K. J., FRANCIS, D. J. & COWDEN, W. B. 1999. Identification of sulfated oligosaccharide-based inhibitors of tumor growth and metastasis using novel in vitro assays for angiogenesis and heparanase activity. *Cancer research,* 59**,** 3433-3441.

PARK, C., SEID, P., MORITA, E., IWANAGA, K., WEINBERG, V., QUIVEY, J., HWANG, E. S., ESSERMAN, L. J. & LEONG, S. P. 2005. Internal mammary sentinel lymph node mapping for invasive breast cancer: implications for staging and treatment. *The breast journal,* 11**,** 29-33.

PARKIN, D. M. 2011. 10. Cancers attributable to exposure to hormones in the UK in 2010. *British journal of cancer,* 105**,** S42-S48.

PASSERINI, L., MEL, E. R., SARTIRANA, C., FOUSTERI, G., BONDANZA, A., NALDINI, L., RONCAROLO, M. G. & BACCHETTA, R. 2013. CD4+ T cells from IPEX patients convert into functional and stable regulatory T cells by FOXP3 gene transfer. *Science translational medicine,* 5**,** 215ra174.

PATEL, R. C., KUMAR, U., LAMB, D. C., EID, J. S., ROCHEVILLE, M., GRANT, M., RANI, A., HAZLETT, T., PATEL, S. C. & GRATTON, E. 2002. Ligand binding to somatostatin receptors induces receptor-specific oligomer formation in live cells. *Proceedings of the National Academy of Sciences,* 99**,** 3294-3299.

PELLO, O. M., MARTÍNEZ-MUÑOZ, L., PARRILLAS, V., SERRANO, A., RODRÍGUEZ-FRADE, J. M., TORO, M. J., LUCAS, P., MONTERRUBIO, M., MARTÍNEZ-A, C. & MELLADO, M. 2008. Ligand stabilization of CXCR4/δ-opioid receptor heterodimers reveals a mechanism for immune response regulation. *European journal of immunology,* 38**,** 537-549.

PELUS, L. M., BIAN, H., FUKUDA, S., WONG, D., MERZOUK, A. & SALARI, H. 2005. The CXCR4 agonist peptide, CTCE-0021, rapidly mobilizes polymorphonuclear neutrophils and hematopoietic progenitor cells into peripheral blood and synergizes with granulocyte colony-stimulating factor. *Experimental hematology,* 33**,** 295-307.

PEPPER, M. S. 2001. Lymphangiogenesis and tumor metastasis. *Clinical Cancer Research,* 7**,** 462-468.

PERCHERANCIER, Y., BERCHICHE, Y. A., SLIGHT, I., VOLKMER-ENGERT, R., TAMAMURA, H., FUJII, N., BOUVIER, M. & HEVEKER, N. 2005. Bioluminescence resonance energy transfer reveals ligand-induced conformational changes in CXCR4 homo-and heterodimers. *Journal of Biological Chemistry,* 280**,** 9895-9903.

PÉREZ-YÉPEZ, E. A., AYALA-SUMUANO, J.-T., REVELES-ESPINOZA, A. M. & MEZA, I. 2012. Selection of a MCF-7 breast cancer cell subpopulation with high sensitivity to IL-1β: characterization of and correlation between morphological and molecular changes leading to increased invasiveness. *International journal of breast cancer,* 2012**,** 609148.

PEREZ, L. E., ALPDOGAN, O., SHIEH, J.-H., WONG, D., MERZOUK, A., SALARI, H., O'REILLY, R. J., VAN DEN BRINK, M. R. M. & MOORE, M. A. S. 2004. Increased plasma levels of stromal-derived factor-1 (SDF-1/CXCL12) enhance human thrombopoiesis and mobilize human colony-forming cells (CFC) in NOD/SCID mice. *Experimental hematology,* 32**,** 300-307.

PERONA, R. 2006. Cell signalling: growth factors and tyrosine kinase receptors. *Clinical and Translational Oncology,* 8**,** 77-82.

PETIT, I., JIN, D. & RAFII, S. 2007. The SDF-1–CXCR4 signaling pathway: a molecular hub modulating neo-angiogenesis. *Trends in immunology,* 28**,** 299-307.

PHILLIPS, R. J., BURDICK, M. D., LUTZ, M., BELPERIO, J. A., KEANE, M. P. & STRIETER, R. M. 2003. The stromal derived factor–1/CXCL12–CXC chemokine receptor 4 biological axis in non–small cell lung cancer metastases. *American journal of respiratory and critical care medicine,* 167**,** 1676-1686.

PIERCE, K. L. & LEFKOWITZ, R. J. 2001. Classical and new roles of β-arrestins in the regulation of G-protein-coupled receptors. *Nature reviews neuroscience,* 2**,** 727-733.

PILKINGTON, K. R., CLARK-LEWIS, I. & MCCOLL, S. R. 2004. Inhibition of generation of cytotoxic T lymphocyte activity by a CCL19/macrophage inflammatory protein (MIP)-3β antagonist. *Journal of Biological Chemistry,* 279**,** 40276-40282.

PINDER, S. E. 2010. Ductal carcinoma in situ (DCIS): pathological features, differential diagnosis, prognostic factors and specimen evaluation. *Modern Pathology,* 23**,** S8-S13.

PING, Y. F., YAO, X. H., JIANG, J. Y., ZHAO, L. T., YU, S. C., JIANG, T., LIN, M., CHEN, J. H., WANG, B. & ZHANG, R. 2011. The chemokine CXCL12 and its receptor CXCR4 promote glioma stem cell-mediated VEGF production and tumour angiogenesis via PI3K/AKT signalling. *The Journal of pathology,* 224**,** 344-354.

PORVASNIK, S., SAKAMOTO, N., KUSMARTSEV, S., ERUSLANOV, E., KIM, W. J., CAO, W., URBANEK, C., WONG, D., GOODISON, S. & ROSSER, C. J. 2009. Effects of CXCR4 antagonist CTCE-9908 on prostate tumor growth. *The Prostate,* 69**,** 1460-1469.

POSTOW, M. A. Managing immune checkpoint-blocking antibody side effects. 2015. American Society of Clinical Oncology, 76-83.

POTTER, M. 1985. History of the BALB/c family. *The BALB/c Mouse.* Springer.

POWER, C. A. 2003. Knock out models to dissect chemokine receptor function in vivo. *Journal of immunological methods,* 273**,** 73-82.

PRICE, J. E., POLYZOS, A., ZHANG, R. D. & DANIELS, L. M. 1990. Tumorigenicity and metastasis of human breast carcinoma cell lines in nude mice. *Cancer research,* 50**,** 717-721.

PROUDFOOT, A. E. 2006. The biological relevance of chemokine–proteoglycan interactions. *Biochemical Society Transactions,* 34**,** 422-426.

PROUDFOOT, A. E. I., HANDEL, T. M., JOHNSON, Z., LAU, E. K., LIWANG, P., CLARK-LEWIS, I., BORLAT, F., WELLS, T. N. C. & KOSCO-VILBOIS, M. H. 2003. Glycosaminoglycan binding and oligomerization are essential for the in vivo activity of certain chemokines. *Proceedings of the National Academy of Sciences,* 100**,** 1885-1890.

PULASKI, B. A. & OSTRAND-ROSENBERG, S. 1998. Reduction of established spontaneous mammary carcinoma metastases following immunotherapy with major histocompatibility complex class II and B7. 1 cell-based tumor vaccines. *Cancer research,* 58**,** 1486-1493.

PULASKI, B. A. & OSTRAND-ROSENBERG, S. 2001. Mouse 4T1 breast tumor model. *Current protocols in immunology***,** 20.2. 1-20.2. 16.

PUSIC, I. & DIPERSIO, J. F. 2010. Update on clinical experience with AMD3100, an SDF-1/CXCL12–CXCR4 inhibitor, in mobilization of hematopoietic stem and progenitor cells. *Current opinion in hematology,* 17**,** 319-326.

QI, X. W., XIA, S. H., YIN, Y., JIN, L. F., PU, Y., HUA, D. & WU, H. R. 2014. Expression features of CXCR5 and its ligand, CXCL13 associated with poor prognosis of advanced colorectal cancer. *Eur Rev Med Pharmacol Sci,* 18**,** 1916-1924.

QIAN, B.-Z. & POLLARD, J. W. 2010. Macrophage diversity enhances tumor progression and metastasis. *Cell,* 141**,** 39-51.

QIAN, F., HANAHAN, D. & WEISSMAN, I. L. 2001. L-selectin can facilitate metastasis to lymph nodes in a transgenic mouse model of carcinogenesis. *Proceedings of the National Academy of Sciences,* 98**,** 3976-3981.

QU, Y., HAN, B., YU, Y., YAO, W., BOSE, S., KARLAN, B. Y., GIULIANO, A. E. & CUI, X. 2015. Evaluation of MCF10A as a Reliable Model for Normal Human Mammary Epithelial Cells. *PloS one,* 10**,** e0131285.

QUOYER, J., JANZ, J. M., LUO, J., REN, Y., ARMANDO, S., LUKASHOVA, V., BENOVIC, J. L., CARLSON, K. E., HUNT, S. W. & BOUVIER, M. 2013. Pepducin targeting the CXC chemokine receptor type 4 acts as a biased agonist favoring activation of the inhibitory G protein. *Proceedings of the National Academy of Sciences,* 110**,** 5088-5097.

R&D SYSTEMS. 2016. *Human CXCR7/RDC-1 APC-conjugated Antibody* [Online]. Available: https://www.rndsystems.com/products/human-cxcr7-rdc-1-apc-conjugated-antibody-358426_fab42271a [Accessed May 2017.

RADESTOCK, Y., HOANG-VU, C. & HOMBACH-KLONISCH, S. 2008. Relaxin reduces xenograft tumour growth of human MDA-MB-231 breast cancer cells. *Breast Cancer Research,* 10**,** R71.

RAEDLER, L. A. 2015a. Keytruda (Pembrolizumab): first PD-1 inhibitor approved for previously treated unresectable or metastatic melanoma. *American health & drug benefits,* 8**,** 96.

RAEDLER, L. A. 2015b. Opdivo (nivolumab): Second PD-1 inhibitor receives FDA approval for unresectable or metastatic melanoma. *American health & drug benefits,* 8**,** 180.

RAHIMI, M., GEORGE, J. & TANG, C. 2010. EGFR variant-mediated invasion by enhanced CXCR4 expression through transcriptional and post-translational mechanisms. *International journal of cancer,* 126**,** 1850-1860.

RAJAGOPAL, S., KIM, J., AHN, S., CRAIG, S., LAM, C. M., GERARD, N. P., GERARD, C. & LEFKOWITZ, R. J. 2010. β-arrestin-but not G protein-mediated signaling by the "decoy" receptor CXCR7. *Proceedings of the National Academy of Sciences,* 107**,** 628-632.

RAKHA, E. A., REIS-FILHO, J. S., BAEHNER, F., DABBS, D. J., DECKER, T., EUSEBI, V., FOX, S. B., ICHIHARA, S., JACQUEMIER, J. & LAKHANI, S. R. 2010. Breast cancer prognostic classification in the molecular era: the role of histological grade. *Breast Cancer Research,* 12**,** 207.

RAMSEY, D. M. & MCALPINE, S. R. 2013. Halting metastasis through CXCR4 inhibition. *Bioorganic & medicinal chemistry letters,* 23**,** 20-25.

RANDOLPH, G. J. Dendritic cell migration to lymph nodes: cytokines, chemokines, and lipid mediators. Seminars in immunology, 2001. Elsevier, 267-274.

RAO, S., SENGUPTA, R., CHOE, E. J., WOERNER, B. M., JACKSON, E., SUN, T., LEONARD, J., PIWNICA-WORMS, D. & RUBIN, J. B. 2012. CXCL12 mediates trophic interactions between endothelial and tumor cells in glioblastoma. *PloS one,* 7**,** e33005.

REDELMAN, D. & HUNTER, K. W. 2007. The mouse mammary carcinoma 4T1: characterization of the cellular landscape of primary tumours and metastatic tumour foci. *International journal of experimental pathology,* 88**,** 351-360.

REDJAL, N., CHAN, J. A., SEGAL, R. A. & KUNG, A. L. 2006. CXCR4 inhibition synergizes with cytotoxic chemotherapy in gliomas. *Clinical Cancer Research,* 12**,** 6765-6771.

REDONDO-MUÑOZ, J., TEROL, M. J., GARCÍA-MARCO, J. A. & GARCÍA-PARDO, A. 2008. Matrix metalloproteinase-9 is up-regulated by CCL21/CCR7 interaction via extracellular signal-regulated kinase-1/2 signaling and is involved in CCL21-driven B-cell chronic lymphocytic leukemia cell invasion and migration. *Blood,* 111**,** 383-386.

REID, Y., STORTS, D., RISS, T. & MINOR, L. 2013. *Authentication of human cell lines by STR DNA profiling analysis*, Bethesda (MD): Eli Lilly & Company and the National Center for Advancing Translational Sciences.

REIF, K., EKLAND, E. H., OHL, L., NAKANO, H., LIPP, M., FÖRSTER, R. & CYSTER, J. G. 2002. Balanced responsiveness to chemoattractants from adjacent zones determines B-cell position. *Nature,* 416**,** 94-99.

REMMEL, E., TERRACCIANO, L., NOPPEN, C., ZAJAC, P., HEBERER, M., SPAGNOLI, G. C. & PADOVAN, E. 2001. Modulation of dendritic cell phenotype and mobility by tumor cells in vitro. *Human immunology,* 62**,** 39-49.

RICHARDSON, R. M., TOKUNAGA, K., MARJORAM, R., SATA, T. & SNYDERMAN, R. 2003. Interleukin-8-mediated Heterologous Receptor Internalization Provides Resistance to HIV-1 Infectivity ROLE OF SIGNAL STRENGTH AND RECEPTOR DESENSITIZATION. *Journal of Biological Chemistry,* 278**,** 15867-15873.

RICHERT, M. M., VAIDYA, K. S., MILLS, C. N., WONG, D., KORZ, W., HURST, D. R. & WELCH, D. R. 2009. Inhibition of CXCR4 by CTCE-9908 inhibits breast cancer metastasis to lung and bone. *Oncology reports,* 21**,** 761.

ROCHEVILLE, M., LANGE, D. C., KUMAR, U., PATEL, S. C., PATEL, R. C. & PATEL, Y. C. 2000. Receptors for dopamine and somatostatin: formation of hetero-oligomers with enhanced functional activity. *Science,* 288**,** 154-157.

RODRíGUEZ-FRADE, J. M., MELLADO, M. & MARTíNEZ-A, C. 2001. Chemokine receptor dimerization: two are better than one. *Trends in immunology,* 22**,** 612-617.

RODRÍGUEZ-FRADE, J. M., VILA-CORO, A. J., DE ANA, A. M., ALBAR, J. P., MARTÍNEZ-A, C. & MELLADO, M. 1999. The chemokine monocyte chemoattractant protein-1 induces functional responses through dimerization of its receptor CCR2. *Proceedings of the National Academy of Sciences,* 96**,** 3628-3633.

ROSCIC-MRKIC, B., FISCHER, M., LEEMANN, C., MANRIQUE, A., GORDON, C. J., MOORE, J. P., PROUDFOOT, A. E. I. & TRKOLA, A. 2003. RANTES (CCL5) uses the proteoglycan CD44 as an auxiliary receptor to mediate cellular activation signals and HIV-1 enhancement. *Blood,* 102**,** 1169-1177.

ROSE, J. J., FOLEY, J. F., MURPHY, P. M. & VENKATESAN, S. 2004. On the mechanism and significance of ligand-induced internalization of human neutrophil chemokine receptors CXCR1 and CXCR2. *Journal of Biological Chemistry,* 279**,** 24372-24386.

ROSENBERG, S. A., SPIESS, P. J. & KLEINER, D. E. 2002. Antitumor effects in mice of the intravenous injection of attenuated Salmonella typhimurium. *Journal of immunotherapy,* 25**,** 218.

ROSENKILDE, M. M., GERLACH, L.-O., JAKOBSEN, J. S., SKERLJ, R. T., BRIDGER, G. J. & SCHWARTZ, T. W. 2004. Molecular mechanism of AMD3100 antagonism in the CXCR4 receptor Transfer of binding site to the CXCR3 receptor. *Journal of Biological Chemistry,* 279**,** 3033-3041.

ROSNER, B., COLDITZ, G. A. & WILLETT, W. C. 1994. Reproductive risk factors in a prospective study of breast cancer: the Nurses' Health Study. *American journal of epidemiology,* 139**,** 819-835.

ROSTAND, K. S. & ESKO, J. D. 1997. Microbial adherence to and invasion through proteoglycans. *Infection and immunity,* 65**,** 1-8.

ROT, A. & VON ANDRIAN, U. H. 2004. Chemokines in innate and adaptive host defense: basic chemokinese grammar for immune cells. *Annu. Rev. Immunol.,* 22**,** 891-928.

ROTH, A., DRUMMOND, D. C., CONRAD, F., HAYES, M. E., KIRPOTIN, D. B., BENZ, C. C., MARKS, J. D. & LIU, B. 2007. Anti-CD166 single chain antibody-mediated intracellular delivery of liposomal drugs to prostate cancer cells. *Molecular Cancer Therapeutics,* 6**,** 2737-2746.

ROZENFELD, R. & DEVI, L. A. 2007. Receptor heterodimerization leads to a switch in signaling: β-arrestin2-mediated ERK activation by μ-δ opioid receptor heterodimers. *The FASEB Journal,* 21**,** 2455-2465.

RUBIN, J. B. 2009. Chemokine signaling in cancer: one hump or two? *Seminars in cancer biology,* 19**,** 116-122.

RUBIN, J. B., KUNG, A. L., KLEIN, R. S., CHAN, J. A., SUN, Y., SCHMIDT, K., KIERAN, M. W., LUSTER, A. D. & SEGAL, R. A. 2003. A small-molecule antagonist of CXCR4 inhibits intracranial growth of primary brain tumors. *Proceedings of the National Academy of Sciences,* 100**,** 13513-13518.

RUSSELL, H. V., HICKS, J., OKCU, M. F. & NUCHTERN, J. G. 2004. CXCR4 expression in neuroblastoma primary tumors is associated with clinical presentation of bone and bone marrow metastases. *Journal of pediatric surgery,* 39**,** 1506-1511.

SABROE, I., PECK, M. J., VAN KEULEN, B. J., JORRITSMA, A., SIMMONS, G., CLAPHAM, P. R., WILLIAMS, T. J. & PEASE, J. E. 2000. A small molecule antagonist of chemokine receptors CCR1 and CCR3 potent inhibition of eosinophil function and CCR3-mediated HIV-1 entry. *Journal of Biological Chemistry,* 275**,** 25985-25992.

SADIR, R., IMBERTY, A., BALEUX, F. & LORTAT-JACOB, H. 2004. Heparan sulfate/heparin oligosaccharides protect stromal cell-derived factor-1 (SDF-1)/CXCL12 against proteolysis induced by CD26/dipeptidyl peptidase IV. *Journal of Biological Chemistry,* 279**,** 43854-43860.

SAEKI, H., MOORE, A. M., BROWN, M. J. & HWANG, S. T. 1999. Cutting edge: secondary lymphoid-tissue chemokine (SLC) and CC chemokine receptor 7 (CCR7) participate in the emigration pathway of mature dendritic cells from the skin to regional lymph nodes. *The Journal of Immunology,* 162**,** 2472-2475.

SAI, J., OWENS, P., NOVITISKIY, S. V., HAWKINS, O. E., VILGELM, A. E., YANG, J., SOBOLIK-DELMAIRE, T., LAVENDER, N., JOHNSON, A. C. & MCCLAIN, C. 2016. PI3K Inhibition Reduces Mammary Tumor Growth and Facilitates Anti-tumor Immunity and Anti-PD1 Responses. *Clinical Cancer Research***,** CCR-16-2142.

SAKAO, K., VYAS, A. R., CHINNI, S. R., AMJAD, A. I., PARIKH, R. & SINGH, S. V. 2015. CXCR4 is a novel target of cancer chemopreventative isothiocyanates in prostate cancer cells. *Cancer Prevention Research,* 8**,** 365-374.

SALAZAR, N., MUÑOZ, D., KALLIFATIDIS, G., SINGH, R. K., JORDÀ, M. & LOKESHWAR, B. L. 2014. The chemokine receptor CXCR7 interacts with EGFR to promote breast cancer cell proliferation. *Molecular cancer,* 13**,** 198.

SALLUSTO, F., LENIG, D., FÖRSTER, R., LIPP, M. & LANZAVECCHIA, A. 1999. Two subsets of memory T lymphocytes with distinct homing potentials and effector functions. *Nature,* 401**,** 708-712.

SALMAGGI, A., MADERNA, E., CALATOZZOLO, C., GAVIANI, P., CANAZZA, A., MILANESI, I., SILVANI, A., DI MECO, F., CARBONE, A. & POLLO, B. 2009. CXCL12, CXCR4 and CXCR7 expression in brain metastases. *Cancer biology & therapy,* 8**,** 1608-1614.

SALVUCCI, O., BOUCHARD, A., BACCARELLI, A., DESCHENES, J., SAUTER, G., SIMON, R., BIANCHI, R. & BASIK, M. 2006. The role of CXCR4 receptor expression in breast cancer: a large tissue microarray study. *Breast cancer research and treatment,* 97**,** 275-283.

SÁNCHEZ-ALCAÑIZ, J. A., HAEGE, S., MUELLER, W., PLA, R., MACKAY, F., SCHULZ, S., LÓPEZ-BENDITO, G., STUMM, R. & MARÍN, O. 2011. Cxcr7 controls neuronal migration by regulating chemokine responsiveness. *Neuron,* 69**,** 77-90.

SANCHO, M., VIEIRA, J. M., CASALOU, C., MESQUITA, M., PEREIRA, T., CAVACO, B. M., DIAS, S. & LEITE, V. 2006. Expression and function of the chemokine receptor CCR7 in thyroid carcinomas. *Journal of Endocrinology,* 191**,** 229-238.

SANDERSON, R. D. 2001. Heparan sulfate proteoglycans in invasion and metastasis. *Seminars in cell & developmental biology,* 12**,** 89-98.

SANDERSON, R. D., YANG, Y., KELLY, T., MACLEOD, V., DAI, Y. & THEUS, A. 2005. Enzymatic remodeling of heparan sulfate proteoglycans within the tumor microenvironment: growth regulation and the prospect of new cancer therapies. *Journal of cellular biochemistry,* 96**,** 897-905.

SANTINI, F., PENN, R. B., GAGNON, A. W., BENOVIC, J. L. & KEEN, J. H. 2000. Selective recruitment of arrestin-3 to clathrin coated pits upon stimulation of G protein-coupled receptors. *J Cell Sci,* 113**,** 2463-2470.

SAPPEY, M. P. C. 1874. *Anatomie, physiologie, pathologie des vaisseaux lymphatiques: considérés chez l'homme et les vertébrés*, Paris, Delahaye.

SARRIÓ, D., RODRIGUEZ-PINILLA, S. M., HARDISSON, D., CANO, A., MORENO-BUENO, G. & PALACIOS, J. 2008. Epithelial-mesenchymal transition in breast cancer relates to the basal-like phenotype. *Cancer research,* 68**,** 989-997.

SASISEKHARAN, R., SHRIVER, Z., VENKATARAMAN, G. & NARAYANASAMI, U. 2002. Roles of heparan-sulphate glycosaminoglycans in cancer. *Nature Reviews Cancer,* 2**,** 521-528.

SAUR, D., SEIDLER, B., SCHNEIDER, G., ALGÜL, H., BECK, R., SENEKOWITSCH–SCHMIDTKE, R., SCHWAIGER, M. & SCHMID, R. M. 2005. CXCR4 expression increases liver and lung metastasis in a mouse model of pancreatic cancer. *Gastroenterology,* 129**,** 1237-1250.

SCALA, S., OTTAIANO, A., ASCIERTO, P. A., CAVALLI, M., SIMEONE, E., GIULIANO, P., NAPOLITANO, M., FRANCO, R., BOTTI, G. & CASTELLO, G. 2005. Expression of CXCR4 predicts poor prognosis in patients with malignant melanoma. *Clinical Cancer Research,* 11**,** 1835-1841.

SCALTRITI, M., VERMA, C., GUZMAN, M., JIMENEZ, J., PARRA, J. L., PEDERSEN, K., SMITH, D. J., LANDOLFI, S., Y CAJAL, S. R. & ARRIBAS, J. 2009. Lapatinib, a HER2 tyrosine kinase inhibitor, induces stabilization and accumulation of HER2 and potentiates trastuzumab-dependent cell cytotoxicity. *Oncogene,* 28**,** 803-814.

SCARFF, R. W. & TORLONI, H. 1968. *Histological Typing of Breast Tumours: By RW Scarff and H. Torloni, in Collaboration with Twelve Pathologists in Ten Countries*, World Health Organization.

SCHABATH, R., MÜLLER, G., SCHUBEL, A., KREMMER, E., LIPP, M. & FÖRSTER, R. 1999. The murine chemokine receptor CXCR4 is tightly regulated during T cell development and activation. *Journal of Leukocyte Biology,* 66**,** 996-1004.

SCHAEUBLE, K., HAUSER, M. A., RIPPL, A. V., BRUDERER, R., OTERO, C., GROETTRUP, M. & LEGLER, D. F. 2012. Ubiquitylation of the chemokine receptor CCR7 enables efficient receptor recycling and cell migration. *J Cell Sci,* 125**,** 4463-4474.

SCHALL, T. J. & BACON, K. B. 1994. Chemokines, leukocyte trafficking, and inflammation. *Current opinion in immunology,* 6**,** 865-873.

SCHIMANSKI, C. C., BAHRE, R., GOCKEL, I., JUNGINGER, T., SIMIANTONAKI, N., BIESTERFELD, S., ACHENBACH, T., WEHLER, T., GALLE, P. R. & MOEHLER, M. 2006. Chemokine receptor CCR7 enhances intrahepatic and lymphatic dissemination of human hepatocellular cancer. *Oncology reports,* 16**,** 109-114.

SCHIMANSKI, C. C., SCHWALD, S., SIMIANTONAKI, N., JAYASINGHE, C., GÖNNER, U., WILSBERG, V., JUNGINGER, T., BERGER, M. R., GALLE, P. R. & MOEHLER, M. 2005. Effect of chemokine receptors CXCR4 and CCR7 on the metastatic behavior of human colorectal cancer. *Clinical Cancer Research,* 11**,** 1743-1750.

SCHIOPPA, T., URANCHIMEG, B., SACCANI, A., BISWAS, S. K., DONI, A., RAPISARDA, A., BERNASCONI, S., SACCANI, S., NEBULONI, M. & VAGO, L. 2003. Regulation of the chemokine receptor CXCR4 by hypoxia. *The Journal of experimental medicine,* 198**,** 1391-1402.

SCHLERETH, S., LEE, H. S., KHANDELWAL, P. & SABAN, D. R. 2012. Blocking CCR7 at the ocular surface impairs the pathogenic contribution of dendritic cells in allergic conjunctivitis. *The American journal of pathology,* 180**,** 2351-2360.

SCHMID, B. C., RUDAS, M., REZNICZEK, G. A., LEODOLTER, S. & ZEILLINGER, R. 2004. CXCR4 is expressed in ductal carcinoma in situ of the breast and in atypical ductal hyperplasia. *Breast cancer research and treatment,* 84**,** 247-250.

SCHMITTGEN, T. D. & ZAKRAJSEK, B. A. 2000. Effect of experimental treatment on housekeeping gene expression: validation by real-time, quantitative RT-PCR. *Journal of biochemical and biophysical methods,* 46**,** 69-81.

SCHOLS, D., CLAES, S., HATSE, S., PRINCEN, K., VERMEIRE, K., DE CLERCQ, E., SKERLJ, R., BRIDGER, G. & CALANDRA, G. Anti-HIV activity profile of AMD070, an orally bioavailable CXCR4 antagonist. 10th Conference on Retroviruses and Opportunistic Infections, 2003 Boston, MA. Abstract 563.

SCHOLS, D. & DE CLERCQ, E. 2003. *Cellular receptors as targets for anti-human immunodeficiency virus agents,* Antiretroviral Therapy, ASM Press, Washington, D.C.

SCHRADER, A. J., LECHNER, O., TEMPLIN, M., DITTMAR, K. E. J., MACHTENS, S., MENGEL, M., PROBST-KEPPER, M., FRANZKE, A., WOLLENSAK, T. & GATZLAFF, P. 2002. CXCR4/CXCL12 expression and signalling in kidney cancer. *British journal of cancer,* 86**,** 1250-1256.

SCHREVEL, M., KARIM, R., TER HAAR, N. T., VAN DER BURG, S. H., TRIMBOS, J., FLEUREN, G. J., GORTER, A. & JORDANOVA, E. S. 2012. CXCR7 expression is associated with disease-free and disease-specific survival in cervical cancer patients. *British journal of cancer,* 106**,** 1520-1525.

SCHUMANN, K., LÄMMERMANN, T., BRUCKNER, M., LEGLER, D. F., POLLEUX, J., SPATZ, J. P., SCHULER, G., FÖRSTER, R., LUTZ, M. B., SOROKIN, L. & SIXT, M. 2010. Immobilized chemokine fields and soluble chemokine gradients cooperatively shape migration patterns of dendritic cells. *Immunity,* 32**,** 703-713.

SCHUTYSER, E., SU, Y., YU, Y., GOUWY, M., ZAJA-MILATOVIC, S., VAN DAMME, J. & RICHMOND, A. 2007. Hypoxia enhances CXCR4 expression in human microvascular endothelial cells and human melanoma cells. *European cytokine network,* 18**,** 59-70.

SCHWANHÄUSSER, B., BUSSE, D., LI, N., DITTMAR, G., SCHUCHHARDT, J., WOLF, J., CHEN, W. & SELBACH, M. 2011. Global quantification of mammalian gene expression control. *Nature,* 473**,** 337-342.

SCOTTON, C. J., WILSON, J. L., SCOTT, K., STAMP, G., WILBANKS, G. D., FRICKER, S., BRIDGER, G. & BALKWILL, F. R. 2002. Multiple actions of the chemokine CXCL12 on epithelial tumor cells in human ovarian cancer. *Cancer Research,* 62**,** 5930-5938.

SEGAL, N. H., ANTONIA, S. J., BRAHMER, J. R., MAIO, M., BLAKE-HASKINS, A., LI, X., VASSELLI, J., IBRAHIM, R. A., LUTZKY, J. & KHLEIF, S. Preliminary data from a multi-arm expansion study of

MEDI4736, an anti-PD-L1 antibody. 50th Annual Meeting of the American Society of Clinical Oncology (ASCO), May 30–June 03, 2014 2014 Chicago, IL, USA. Abstract 3002.

SELLAPPAN, S., GRIJALVA, R., ZHOU, X., YANG, W., ELI, M. B., MILLS, G. B. & YU, D. 2004. Lineage Infidelity of MDA-MB-435 Cells Expression of Melanocyte Proteins in a Breast Cancer Cell Line. *Cancer Research,* 64**,** 3479-3485.

SEMENZA, G. L. 2001. Hypoxia-inducible factor 1: oxygen homeostasis and disease pathophysiology. *Trends in molecular medicine,* 7**,** 345-350.

SEMENZA, G. L. 2010. HIF-1: upstream and downstream of cancer metabolism. *Current opinion in genetics & development,* 20**,** 51-56.

SENGUPTA, S., SCHIFF, R. & KATZENELLENBOGEN, B. S. 2009. Post-transcriptional regulation of chemokine receptor CXCR4 by estrogen in HER2 overexpressing, estrogen receptor-positive breast cancer cells. *Breast cancer research and treatment,* 117**,** 243-251.

SETHI, T., RINTOUL, R. C., MOORE, S. M., MACKINNON, A. C., SALTER, D., CHOO, C., CHILVERS, E. R., DRANSFIELD, I., DONNELLY, S. C. & STRIETER, R. 1999. Extracellular matrix proteins protect small cell lung cancer cells against apoptosis: a mechanism for small cell lung cancer growth and drug resistance in vivo. *Nature medicine,* 5**,** 662-668.

SHAH, D. R., TSENG, W. H. & MARTINEZ, S. R. 2012. Treatment options for metaplastic breast cancer. *ISRN oncology,* 2012**,** 706162.

SHAMRI, R., GRABOVSKY, V., GAUGUET, J.-M., FEIGELSON, S., MANEVICH, E., KOLANUS, W., ROBINSON, M. K., STAUNTON, D. E., VON ANDRIAN, U. H. & ALON, R. 2005. Lymphocyte arrest requires instantaneous induction of an extended LFA-1 conformation mediated by endothelium-bound chemokines. *Nature immunology,* 6**,** 497-506.

SHANG, Z. J., LIU, K. & SHAO, Z. 2009. Expression of chemokine receptor CCR7 is associated with cervical lymph node metastasis of oral squamous cell carcinoma. *Oral oncology,* 45**,** 480-485.

SHAPIRO, J., JERSKY, J., KATZAV, S., FELDMAN, M. & SEGAL, S. 1981. Anesthetic drugs accelerate the progression of postoperative metastases of mouse tumors. *Journal of Clinical Investigation,* 68**,** 678.

SHARMA, S., STOLINA, M., LUO, J., STRIETER, R. M., BURDICK, M., ZHU, L. X., BATRA, R. K. & DUBINETT, S. M. 2000. Secondary lymphoid tissue chemokine mediates T cell-dependent antitumor responses in vivo. *The Journal of Immunology,* 164**,** 4558-4563.

SHARMA, S., ZHU, L., SRIVASTAVA, M. K., HARRIS-WHITE, M., HUANG, M., LEE, J. M., ROSEN, F., LEE, G., WANG, G. & KICKHOEFER, V. 2013. CCL21 chemokine therapy for lung cancer. *International trends in immunity,* 1**,** 10.

SHAYAN, R., ACHEN, M. G. & STACKER, S. A. 2006. Lymphatic vessels in cancer metastasis: bridging the gaps. *Carcinogenesis,* 27**,** 1729-1738.

SHEN, Z., CHEN, L., YANG, X., ZHAO, Y., PIER, E., ZHANG, X., YANG, X. & XIONG, Y. 2013. Downregulation of Ezh2 methyltransferase by FOXP3: new insight of FOXP3 into chromatin remodeling? *Biochimica et Biophysica Acta (BBA)-Molecular Cell Research,* 1833**,** 2190-2200.

SHERR, C. J. & MCCORMICK, F. 2002. The RB and p53 pathways in cancer. *Cancer cell,* 2**,** 103-112.

SHIBUTA, K., MORI, M., SHIMODA, K., INOUE, H., MITRA, P. & BARNARD, G. F. 2002. Regional Expression of CXCL12/CXCR4 in Liver and Hepatocellular Carcinoma and Cell-cycle Variation during in vitro Differentiation. *Japanese journal of cancer research,* 93**,** 789-797.

SHIELDS, J. D., EMMETT, M. S., DUNN, D. B. A., JOORY, K. D., SAGE, L. M., RIGBY, H., MORTIMER, P. S., ORLANDO, A., LEVICK, J. R. & BATES, D. O. 2007a. Chemokine-mediated migration of melanoma cells towards lymphatics–a mechanism contributing to metastasis. *Oncogene,* 26**,** 2997-3005.

SHIELDS, J. D., FLEURY, M. E., YONG, C., TOMEI, A. A., RANDOLPH, G. J. & SWARTZ, M. A. 2007b. Autologous chemotaxis as a mechanism of tumor cell homing to lymphatics via interstitial flow and autocrine CCR7 signaling. *Cancer cell,* 11**,** 526-538.

SHIELDS, J. D., KOURTIS, I. C., TOMEI, A. A., ROBERTS, J. M. & SWARTZ, M. A. 2010. Induction of lymphoidlike stroma and immune escape by tumors that express the chemokine CCL21. *Science,* 328**,** 749-752.

SHIMIZU, N., SODA, Y., KANBE, K., LIU, H.-Y., MUKAI, R., KITAMURA, T. & HOSHINO, H. 2000. A putative G protein-coupled receptor, RDC1, is a novel coreceptor for human and simian immunodeficiency viruses. *Journal of virology,* 74**,** 619-626.

SHIMIZU, S., BROWN, M., SENGUPTA, R., PENFOLD, M. E. & MEUCCI, O. 2011. CXCR7 protein expression in human adult brain and differentiated neurons. *PloS one,* 6**,** e20680.

SHUKLA, D., LIU, J., BLAIKLOCK, P., SHWORAK, N. W., BAI, X., ESKO, J. D., COHEN, G. H., EISENBERG, R. J., ROSENBERG, R. D. & SPEAR, P. G. 1999. A novel role for 3-O-sulfated heparan sulfate in herpes simplex virus 1 entry. *Cell,* 99**,** 13-22.

SIERRO, F., BIBEN, C., MARTÍNEZ-MUÑOZ, L., MELLADO, M., RANSOHOFF, R. M., LI, M., WOEHL, B., LEUNG, H., GROOM, J. & BATTEN, M. 2007. Disrupted cardiac development but normal hematopoiesis in mice deficient in the second CXCL12/SDF-1 receptor, CXCR7. *Proceedings of the National Academy of Sciences,* 104**,** 14759-14764.

SIGMA-ALDRICH. 2017. *Calcium in Cell Culture* [Online]. Available: http://www.sigmaaldrich.com/life-science/cell-culture/learning-center/media-expert/calcium.html [Accessed May 2017.

SIGNORET, N., HEWLETT, L., WAVRE, S., PELCHEN-MATTHEWS, A., OPPERMANN, M. & MARSH, M. 2005. Agonist-induced endocytosis of CC chemokine receptor 5 is clathrin dependent. *Molecular biology of the cell,* 16**,** 902-917.

SIGNORET, N., OLDRIDGE, J., PELCHEN-MATTHEWS, A., KLASSE, P. J., TRAN, T., BRASS, L. F., ROSENKILDE, M. M., SCHWARTZ, T. W., HOLMES, W. & DALLAS, W. 1997. Phorbol esters and SDF-1 induce rapid endocytosis and down modulation of the chemokine receptor CXCR4. *The Journal of cell biology,* 139**,** 651-664.

SINGH, R. & LILLARD, J. W. 2009. Nanoparticle-based targeted drug delivery. *Experimental and molecular pathology,* 86**,** 215-223.

SINGH, R., STOCKARD, C. R., GRIZZLE, W. E., LILLARD JR, J. W. & SINGH, S. 2011. Expression and histopathological correlation of CCR9 and CCL25 in ovarian cancer. *International journal of oncology,* 39**,** 373.

SINGH, R. K. & LOKESHWAR, B. L. 2011. The IL-8–Regulated Chemokine Receptor CXCR7 stimulates EGFR signaling to promote prostate cancer growth. *Cancer research,* 71**,** 3268-3277.

SINGH, S., SINGH, R., SINGH, U. P., RAI, S. N., NOVAKOVIC, K. R., CHUNG, L. W. K., DIDIER, P. J., GRIZZLE, W. E. & LILLARD, J. W. 2009. Clinical and biological significance of CXCR5 expressed by prostate cancer specimens and cell lines. *International Journal of Cancer,* 125**,** 2288-2295.

SINGH, S., SINGH, U. P., GRIZZLE, W. E. & LILLARD, J. W. 2004a. CXCL12–CXCR4 interactions modulate prostate cancer cell migration, metalloproteinase expression and invasion. *Laboratory investigation,* 84**,** 1666-1676.

SINGH, S., SINGH, U. P., STILES, J. K., GRIZZLE, W. E. & LILLARD, J. W. 2004b. Expression and functional role of CCR9 in prostate cancer cell migration and invasion. *Clinical Cancer Research,* 10**,** 8743-8750.

SINGLETON, P. A., LINGEN, M. W., FEKETE, M. J., GARCIA, J. G. N. & MOSS, J. 2006. Methylnaltrexone inhibits opiate and VEGF-induced angiogenesis: role of receptor transactivation. *Microvascular research,* 72**,** 3-11.

SINN, H.-P., SCHNEEWEISS, A., KELLER, M., SCHLOMBS, K., LAIBLE, M., SEITZ, J., LAKIS, S., VELTRUP, E., ALTEVOGT, P. & EIDT, S. 2017. Comparison of immunohistochemistry with PCR for assessment of ER, PR, and Ki-67 and prediction of pathological complete response in breast cancer. *BMC cancer,* 17**,** 124.

SIOUD, M. 2007. *Target Discovery and Validation: Reviews and Protocols*, Springer Science & Business Media.

SKOBE, M., HAWIGHORST, T., JACKSON, D. G., PREVO, R., JANES, L., VELASCO, P., RICCARDI, L., ALITALO, K., CLAFFEY, K. & DETMAR, M. 2001. Induction of tumor lymphangiogenesis by VEGF-C promotes breast cancer metastasis. *Nature medicine,* 7**,** 192-198.

SMORENBURG, S. M. & VAN NOORDEN, C. J. F. 2001. The complex effects of heparins on cancer progression and metastasis in experimental studies. *Pharmacological reviews,* 53**,** 93-106.

SOBOLIK, T., SU, Y.-J., WELLS, S., AYERS, G. D., COOK, R. S. & RICHMOND, A. 2014. CXCR4 drives the metastatic phenotype in breast cancer through induction of CXCR2 and activation of MEK and PI3K pathways. *Molecular biology of the cell,* 25**,** 566-582.

SOMOVILLA-CRESPO, B., ALFONSO-PÉREZ, M., CUESTA-MATEOS, C., CARBALLO-DE DIOS, C., BELTRÁN, A. E., TERRÓN, F., PÉREZ-VILLAR, J. J., GAMALLO-AMAT, C., PÉREZ-CHACÓN, G. & FERNÁNDEZ-RUIZ, E. 2013. Anti-CCR7 therapy exerts a potent anti-tumor activity in a xenograft model of human mantle cell lymphoma. *Journal of hematology & oncology,* 6**,** 89.

SONDAK, V. K., SMALLEY, K. S. M., KUDCHADKAR, R., GRIPPON, S. & KIRKPATRICK, P. 2011. Ipilimumab. *Nature reviews Drug discovery,* 10**,** 411-412.

SOULE, H. D., MALONEY, T. M., WOLMAN, S. R., PETERSON, W. D., BRENZ, R., MCGRATH, C. M., RUSSO, J., PAULEY, R. J., JONES, R. F. & BROOKS, S. C. 1990. Isolation and characterization of a spontaneously immortalized human breast epithelial cell line, MCF-10. *Cancer research,* 50**,** 6075-6086.

SOULE, H. D., VAZQUEZ, J., LONG, A., ALBERT, S. & BRENNAN, M. 1973. A human cell line from a pleural effusion derived from a breast carcinoma. *Journal of the National Cancer Institute,* 51**,** 1409-1416.

SOZZANI, S., ALLAVENA, P., D'AMICO, G., LUINI, W., BIANCHI, G., KATAURA, M., IMAI, T., YOSHIE, O., BONECCHI, R. & MANTOVANI, A. 1998. Cutting edge: differential regulation of chemokine receptors during dendritic cell maturation: a model for their trafficking properties. *The Journal of Immunology,* 161**,** 1083-1086.

SPANO, J. P., ANDRE, F., MORAT, L., SABATIER, L., BESSE, B., COMBADIERE, C., DETERRE, P., MARTIN, A., AZORIN, J. & VALEYRE, D. 2004. Chemokine receptor CXCR4 and early-stage non-small cell lung cancer: pattern of expression and correlation with outcome. *Annals of Oncology,* 15**,** 613-617.

SPATZ, A., BORG, C. & FEUNTEUN, J. 2004. X-chromosome genetics and human cancer. *Nature Reviews Cancer,* 4**,** 617-629.

STACER, A. C., FENNER, J., CAVNAR, S. P., XIAO, A., ZHAO, S., CHANG, S. L., SALOMONNSON, A., LUKER, K. E. & LUKER, G. D. 2015. Endothelial CXCR7 regulates breast cancer metastasis. *Oncogene,* 35**,** 1716–1724.

STALLER, P., SULITKOVA, J., LISZTWAN, J., MOCH, H., OAKELEY, E. J. & KREK, W. 2003. Chemokine receptor CXCR4 downregulated by von Hippel–Lindau tumour suppressor pVHL. *Nature,* 425**,** 307-311.

STANLEY, P. E. & KRICKA, L. J. Bioluminescence and chemiluminescence. Current status. Proceedings of the VIth International symposium of bioluminescence and chemiluminescence, 1991 Cambridge. Luminescence, 75.

STEEL, E., MURRAY, V. L. & LIU, A. P. 2014. Multiplex detection of homo-and heterodimerization of G protein-coupled receptors by proximity biotinylation. *PloS one,* 9**,** e93646.

STEIN, J. V., ROT, A., LUO, Y., NARASIMHASWAMY, M., NAKANO, H., GUNN, M. D., MATSUZAWA, A., QUACKENBUSH, E. J., DORF, M. E. & VON ANDRIAN, U. H. 2000. The CC chemokine thymus-derived chemotactic agent 4 (TCA-4, secondary lymphoid tissue chemokine, 6Ckine, exodus-2) triggers lymphocyte function–associated antigen 1–mediated arrest of rolling T lymphocytes in peripheral lymph node high endothelial venules. *Journal of Experimental Medicine,* 191**,** 61-76.

STETLER-STEVENSON, W. G. 1999. Matrix metalloproteinases in angiogenesis: a moving target for therapeutic intervention. *Journal of Clinical Investigation,* 103**,** 1237-1241.

STOLER-BARAK, L., BARZILAI, S., ZAUBERMAN, A. & ALON, R. 2014. Transendothelial migration of effector T cells across inflamed endothelial barriers does not require heparan sulfate proteoglycans. *International immunology,* 26**,** 315-24.

STRIETER, R. M., POLVERINI, P. J., KUNKEL, S. L., ARENBERG, D. A., BURDICK, M. D., KASPER, J., DZUIBA, J., VAN DAMME, J., WALZ, A. & MARRIOTT, D. 1995. The functional role of the ELR motif in CXC chemokine-mediated angiogenesis. *Journal of Biological Chemistry,* 270**,** 27348-27357.

SU, H., NAJUL, E. J. S., TOTH, T. A., NG, C. M., LELIEVRE, S. A., FRED, M. & TANG, C. K. 2011. Chemokine receptor CXCR4-mediated transformation of mammary epithelial cells by enhancing multiple RTKs expression and deregulation of the p53/MDM2 axis. *Cancer letters,* 307**,** 132-140.

SU, M.-L., CHANG, T.-M., CHIANG, C.-H., CHANG, H.-C., HOU, M.-F., LI, W.-S. & HUNG, W.-C. 2014. Inhibition of chemokine (CC motif) receptor 7 sialylation suppresses CCL19-stimulated proliferation, invasion and anti-anoikis. *PloS one,* 9**,** e98823.

SU, Y. C., WU, M. T., HUANG, C. J., HOU, M. F., YANG, S. F. & CHAI, C. Y. 2006. Expression of CXCR4 is associated with axillary lymph node status in patients with early breast cancer. *The Breast,* 15**,** 533-539.

SUBIK, K., LEE, J.-F., BAXTER, L., STRZEPEK, T., COSTELLO, D., CROWLEY, P., XING, L., HUNG, M.-C., BONFIGLIO, T. & HICKS, D. G. 2010. The expression patterns of ER, PR, HER2, CK5/6, EGFR, Ki-67 and AR by immunohistochemical analysis in breast cancer cell lines. *Breast cancer: basic and clinical research,* 4**,** 35.

SUBRAMANIAM, J. M., WHITESIDE, G., MCKEAGE, K. & CROXTALL, J. C. 2012. Mogamulizumab. *Drugs,* 72**,** 1293-1298.

SUN, Y., CHENG, Z., MA, L. & PEI, G. 2002. β-arrestin2 is critically involved in CXCR4-mediated chemotaxis, and this is mediated by its enhancement of p38 MAPK activation. *Journal of Biological Chemistry,* 277**,** 49212-49219.

SUN, Y., LI, Y., LUO, D. & LIAO, D. J. 2012. Pseudogenes as weaknesses of ACTB (Actb) and GAPDH (Gapdh) used as reference genes in reverse transcription and polymerase chain reactions. *PloS one,* 7**,** e41659.

SUN, Y., MAO, X., FAN, C., LIU, C., GUO, A., GUAN, S., JIN, Q., LI, B., YAO, F. & JIN, F. 2014. CXCL12-CXCR4 axis promotes the natural selection of breast cancer cell metastasis. *Tumor Biology,* 35**,** 7765-7773.

SUN, Y. X., SCHNEIDER, A., JUNG, Y., WANG, J., DAI, J., WANG, J., COOK, K., OSMAN, N. I., KOH-PAIGE, A. J. & SHIM, H. 2005. Skeletal localization and neutralization of the SDF-1 (CXCL12)/CXCR4 axis blocks prostate cancer metastasis and growth in osseous sites in vivo. *Journal of Bone and Mineral Research,* 20**,** 318-329.

SUZUKI, Y., RAHMAN, M. & MITSUYA, H. 2001. Diverse transcriptional response of CD4+ T cells to stromal cell-derived factor (SDF)-1: cell survival promotion and priming effects of SDF-1 on CD4+ T cells. *The Journal of Immunology,* 167**,** 3064-3073.

SZABO, I., CHEN, X.-H., XIN, L., ADLER, M. W., HOWARD, O. M. Z., OPPENHEIM, J. J. & ROGERS, T. J. 2002. Heterologous desensitization of opioid receptors by chemokines inhibits chemotaxis and enhances the perception of pain. *Proceedings of the National Academy of Sciences,* 99**,** 10276-10281.

SZABO, I., WETZEL, M. A., ZHANG, N., STEELE, A. D., KAMINSKY, D. E., CHEN, C., LIU-CHEN, L.-Y., BEDNAR, F., HENDERSON, E. E. & HOWARD, O. M. Z. 2003. Selective inactivation of CCR5 and decreased infectivity of R5 HIV-1 strains mediated by opioid-induced heterologous desensitization. *Journal of leukocyte biology,* 74**,** 1074-1082.

SZANYA, V., ERMANN, J., TAYLOR, C., HOLNESS, C. & FATHMAN, C. G. 2002. The subpopulation of CD4+ CD25+ splenocytes that delays adoptive transfer of diabetes expresses L-selectin and high levels of CCR7. *The Journal of Immunology,* 169**,** 2461-2465.

TACHEZY, M., ZANDER, H., GEBAUER, F., VON LOGA, K., PANTEL, K., IZBICKI, J. R. & BOCKHORN, M. 2013. CXCR7 expression in esophageal cancer. *Journal of translational medicine,* 11**,** 238.

TACHIBANA, K., HIROTA, S., IIZASA, H., YOSHIDA, H., KAWABATA, K., KATAOKA, Y., KITAMURA, Y., MATSUSHIMA, K., YOSHIDA, N. & NISHIKAWA, S.-I. 1998. The chemokine receptor CXCR4 is essential for vascularization of the gastrointestinal tract. *Nature,* 393**,** 591-594.

TAICHMAN, R. S., COOPER, C., KELLER, E. T., PIENTA, K. J., TAICHMAN, N. S. & MCCAULEY, L. K. 2002. Use of the stromal cell-derived factor-1/CXCR4 pathway in prostate cancer metastasis to bone. *Cancer research,* 62**,** 1832-1837.

TAK, P. P. 2006. Chemokine inhibition in inflammatory arthritis. *Best Practice & Research Clinical Rheumatology,* 20**,** 929-939.

TAKANAMI, I. 2003. Overexpression of CCR7 mRNA in nonsmall cell lung cancer: correlation with lymph node metastasis. *International journal of cancer,* 105**,** 186-189.

TAKEKOSHI, T., ZIAREK, J. J., VOLKMAN, B. F. & HWANG, S. T. 2012. A locked, dimeric CXCL12 variant effectively inhibits pulmonary metastasis of CXCR4-expressing melanoma cells due to enhanced serum stability. *Molecular cancer therapeutics,* 11**,** 2516-2525.

TAKEUCHI, H., FUJIMOTO, A., TANAKA, M., YAMANO, T., HSUEH, E. & HOON, D. S. B. 2004. CCL21 chemokine regulates chemokine receptor CCR7 bearing malignant melanoma cells. *Clinical Cancer Research,* 10**,** 2351-2358.

TAMAMIS, P. & FLOUDAS, C. A. 2014. Elucidating a key component of cancer metastasis: CXCL12 (SDF-1α) binding to CXCR4. *Journal of chemical information and modeling,* 54**,** 1174-1188.

TAMAMURA, H., HORI, A., KANZAKI, N., HIRAMATSU, K., MIZUMOTO, M., NAKASHIMA, H., YAMAMOTO, N., OTAKA, A. & FUJII, N. 2003. T140 analogs as CXCR4 antagonists identified as anti-metastatic agents in the treatment of breast cancer. *FEBS letters,* 550**,** 79-83.

TANIGUCHI, Y., CHOI, P. J., LI, G.-W., CHEN, H., BABU, M., HEARN, J., EMILI, A. & XIE, X. S. 2010. Quantifying E. coli proteome and transcriptome with single-molecule sensitivity in single cells. *science,* 329**,** 533-538.

TAO, K., FANG, M., ALROY, J. & SAHAGIAN, G. G. 2008. Imagable 4T1 model for the study of late stage breast cancer. *BMC cancer,* 8**,** 228.

TARAPCHAK, P. 2016. Tecentriq Approved for Targeted Treatment of Bladder Cancer. *Oncology Times*.

TAYLOR, A. P., LEON, E. & GOLDENBERG, D. M. 2010. Placental growth factor (PlGF) enhances breast cancer cell motility by mobilising ERK1/2 phosphorylation and cytoskeletal rearrangement. *British journal of cancer,* 103**,** 82-89.

TCHERNYCHEV, B., REN, Y., SACHDEV, P., JANZ, J. M., HAGGIS, L., O'SHEA, A., MCBRIDE, E., LOOBY, R., DENG, Q. & MCMURRY, T. 2010. Discovery of a CXCR4 agonist pepducin that mobilizes bone marrow hematopoietic cells. *Proceedings of the National Academy of Sciences,* 107**,** 22255-22259.

TEICHER, B. A. & FRICKER, S. P. 2010. CXCL12 (SDF-1)/CXCR4 pathway in cancer. *Clinical Cancer Research,* 16**,** 2927-2931.

TERRILLON, S., BARBERIS, C. & BOUVIER, M. 2004. Heterodimerization of V1a and V2 vasopressin receptors determines the interaction with β-arrestin and their trafficking patterns. *Proceedings of the National Academy of Sciences of the United States of America,* 101**,** 1548-1553.

TERRILLON, S., DURROUX, T., MOUILLAC, B., BREIT, A., AYOUB, M. A., TAULAN, M., JOCKERS, R., BARBERIS, C. & BOUVIER, M. 2003. Oxytocin and vasopressin V1a and V2 receptors form constitutive homo-and heterodimers during biosynthesis. *Molecular endocrinology,* 17**,** 677-691.

THE HUMAN PROTEIN ATLAS. 2016a. *CXCR4* [Online]. Available: http://www.proteinatlas.org/ENSG00000121966-CXCR4/cell [Accessed May 2017.

THE HUMAN PROTEIN ATLAS. 2016b. *CXCR7* [Online]. Available: http://www.proteinatlas.org/ENSG00000144476-ACKR3/cell [Accessed May 2017.

THE HUMAN PROTEIN ATLAS. 2017. *CCR7* [Online]. Available: http://www.proteinatlas.org/ENSG00000126353-CCR7/tissue/tonsil [Accessed May 2017.

THELEN, M. & THELEN, S. 2008. CXCR7, CXCR4 and CXCL12: an eccentric trio? *Journal of neuroimmunology,* 198**,** 9-13.

THOMPSON, E. W., TORRI, J., SABOL, M., SOMMERS, C. L., BYERS, S., VALVERIUS, E. M., MARTIN, G. R., LIPPMAN, M. E., STAMPFER, M. R. & DICKSON, R. B. 1994. Oncogene-induced basement membrane invasiveness in human mammary epithelial cells. *Clinical & experimental metastasis,* 12**,** 181-194.

TILL, K. J., LIN, K., ZUZEL, M. & CAWLEY, J. C. 2002. The chemokine receptor CCR7 and α4 integrin are important for migration of chronic lymphocytic leukemia cells into lymph nodes. *Blood,* 99**,** 2977-2984.

TJIO, J. H. & PUCK, T. T. 1958. Genetics of somatic mammalian cells: II. Chromosomal constitution of cells in tissue culture. *The Journal of experimental medicine,* 108**,** 259.

TOHGO, A., PIERCE, K. L., CHOY, E. W., LEFKOWITZ, R. J. & LUTTRELL, L. M. 2002. β-Arrestin scaffolding of the ERK cascade enhances cytosolic ERK activity but inhibits ERK-mediated transcription following angiotensin AT1a receptor stimulation. *Journal of Biological Chemistry,* 277**,** 9429-9436.

TOMAYKO, M. M. & REYNOLDS, C. P. 1989. Determination of subcutaneous tumor size in athymic (nude) mice. *Cancer chemotherapy and pharmacology,* 24**,** 148-154.

TOOLE, B. P. Hyaluronan in morphogenesis. Seminars in cell & developmental biology, 2001. Elsevier, 79-87.

TORISAWA, Y.-S., MOSADEGH, B., BERSANO-BEGEY, T., STEELE, J. M., LUKER, K. E., LUKER, G. D. & TAKAYAMA, S. 2010. Microfluidic platform for chemotaxis in gradients formed by CXCL12 source-sink cells. *Integrative Biology,* 2**,** 680-686.

TOROSSIAN, F., ANGINOT, A., CHABANON, A., CLAY, D., GUERTON, B., DESTERKE, C., BOUTIN, L., MARULLO, S., SCOTT, M. G. & LATAILLADE, J.-J. 2014. CXCR7 participates in CXCL12-induced CD34+ cell cycling through β-arrestin–dependent Akt activation. *Blood,* 123**,** 191-202.

TOTH, P. T., REN, D. & MILLER, R. J. 2004. Regulation of CXCR4 receptor dimerization by the chemokine SDF-1α and the HIV-1 coat protein gp120: a fluorescence resonance energy transfer (FRET) study. *Journal of Pharmacology and Experimental Therapeutics,* 310**,** 8-17.

TRASTOY, M. O., DEFAIS, M. & LARMINAT, F. 2005. Resistance to the antibiotic Zeocin by stable expression of the Sh ble gene does not fully suppress Zeocin-induced DNA cleavage in human cells. *Mutagenesis,* 20**,** 111-114.

TREMPE, G. L. 1976. Human breast cancer in culture. *Recent results in cancer research,* 57**,** 33-41.

TRENT, J. O., WANG, Z.-X., MURRAY, J. L., SHAO, W., TAMAMURA, H., FUJII, N. & PEIPER, S. C. 2003. Lipid bilayer simulations of CXCR4 with inverse agonists and weak partial agonists. *Journal of Biological Chemistry,* 278**,** 47136-47144.

TRENTIN, L., CABRELLE, A., FACCO, M., CAROLLO, D., MIORIN, M., TOSONI, A., PIZZO, P., BINOTTO, G., NICOLARDI, L. & ZAMBELLO, R. 2004. Homeostatic chemokines drive migration of malignant B cells in patients with non-Hodgkin lymphomas. *Blood,* 104**,** 502-508.

TRETTEL, F., DI BARTOLOMEO, S., LAURO, C., CATALANO, M., CIOTTI, M. T. & LIMATOLA, C. 2003. Ligand-independent CXCR2 dimerization. *Journal of Biological Chemistry,* 278**,** 40980-40988.

TRIOZZI, P. L., KHURRAM, R., ALDRICH, W. A., WALKER, M. J., KIM, J. A. & JAYNES, S. 2000. Intratumoral injection of dendritic cells derived in vitro in patients with metastatic cancer. *Cancer,* 89**,** 2646-2654.

TROWBRIDGE, J. M. & GALLO, R. L. 2002. Dermatan sulfate: new functions from an old glycosaminoglycan. *Glycobiology,* 12**,** 117R-125R.

TRZONKOWSKI, P., BIENIASZEWSKA, M., JUŚCIŃSKA, J., DOBYSZUK, A., KRZYSTYNIAK, A., MAREK, N., MYŚLIWSKA, J. & HELLMANN, A. 2009. First-in-man clinical results of the treatment of patients with graft versus host disease with human ex vivo expanded CD4+ CD25+ CD127− T regulatory cells. *Clinical immunology,* 133**,** 22-26.

TSOLI, E., TSANTOULIS, P. K., PAPALAMBROS, A., PERUNOVIC, B., ENGLAND, D., RAWLANDS, D. A., REYNOLDS, G. M., VLACHODIMITROPOULOS, D., MORGAN, S. L. & SPILIOPOULOU, C. A. 2007. Simultaneous evaluation of maspin and CXCR4 in patients with breast cancer. *Journal of clinical pathology,* 60**,** 261-266.

TSUBOI, K., HIRAKAWA, J., SEKI, E., IMAI, Y., YAMAGUCHI, Y., FUKUDA, M. & KAWASHIMA, H. 2013. Role of High Endothelial Venule–Expressed Heparan Sulfate in Chemokine Presentation and Lymphocyte Homing. *The Journal of Immunology,* 191**,** 448-455.

TSUNA, M., KAGEYAMA, S.-I., FUKUOKA, J., KITANO, H., DOKI, Y., TEZUKA, H. & YASUDA, H. 2009. Significance of S100A4 as a prognostic marker of lung squamous cell carcinoma. *Anticancer research,* 29**,** 2547-2554.

TSUZUKI, H., TAKAHASHI, N., KOJIMA, A., NARITA, N., SUNAGA, H., TAKABAYASHI, T. & FUJIEDA, S. 2006. Oral and oropharyngeal squamous cell carcinomas expressing CCR7 have poor prognoses. *Auris Nasus Larynx,* 33**,** 37-42.

TUTUNEA-FATAN, E., MAJUMDER, M., XIN, X. & LALA, P. K. 2015. The role of CCL21/CCR7 chemokine axis in breast cancer-induced lymphangiogenesis. *Molecular cancer,* 14**,** 35.

UCHIDA, D., ONOUE, T., KURIBAYASHI, N., TOMIZUKA, Y., TAMATANI, T., NAGAI, H. & MIYAMOTO, Y. 2011. Blockade of CXCR4 in oral squamous cell carcinoma inhibits lymph node metastases. *European Journal of Cancer,* 47**,** 452-459.

UCHIDA, D., ONOUE, T., TOMIZUKA, Y., BEGUM, N. M., MIWA, Y., YOSHIDA, H. & SATO, M. 2007. Involvement of an Autocrine Stromal Cell–Derived Factor-1/CXCR4 System on the Distant Metastasis of Human Oral Squamous Cell Carcinoma. *Molecular cancer research,* 5**,** 685-694.

ULVMAR, M. H., HUB, E. & ROT, A. 2011. Atypical chemokine receptors. *Experimental cell research,* 317**,** 556-568.

UTO-KONOMI, A., MCKIBBEN, B., WIRTZ, J., SATO, Y., TAKANO, A., NANKI, T. & SUZUKI, S. 2013. CXCR7 agonists inhibit the function of CXCL12 by down-regulation of CXCR4. *Biochemical and biophysical research communications,* 431**,** 772-776.

VAIDYA, J. S., TOBIAS, J. S., BAUM, M., KESHTGAR, M., JOSEPH, D., WENZ, F., HOUGHTON, J., SAUNDERS, C., CORICA, T. & D'SOUZA, D. 2004. Intraoperative radiotherapy for breast cancer. *The lancet oncology,* 5**,** 165-173.

VAJDIC, C. M. & VAN LEEUWEN, M. T. 2009. Cancer incidence and risk factors after solid organ transplantation. *International journal of cancer,* 125**,** 1747-1754.

VAN DAMME, J., STRUYF, S. & OPDENAKKER, G. 2004. Chemokine–protease interactions in cancer. *Seminars in cancer biology,* 14**,** 201-208.

VAN DEN BERG, N. S., BUCKLE, T., KUIL, J., WESSELING, J. & VAN LEEUWEN, F. W. 2011. Immunohistochemical detection of the CXCR4 expression in tumor tissue using the fluorescent peptide antagonist Ac-TZ14011-FITC. *Translational oncology,* 4**,** 234–240.

VAN DEN BOSCH, T., KOOPMANS, A. E., VAARWATER, J., VAN DEN BERG, M., DE KLEIN, A. & VERDIJK, R. M. 2013. Chemokine Receptor CCR7 Expression Predicts Poor Outcome in Uveal Melanoma and Relates to Liver Metastasis Whereas Expression of CXCR4 Is Not of Clinical Relevance. *Investigative ophthalmology & visual science,* 54**,** 7354-7361.

VAN DEN HOOGEN, C., VAN DER HORST, G., CHEUNG, H., BUIJS, J. T., PELGER, R. C. M. & VAN DER PLUIJM, G. 2011. Integrin αv expression is required for the acquisition of a metastatic stem/progenitor cell phenotype in human prostate cancer. *The American journal of pathology,* 179**,** 2559-2568.

VAN ROY, F. & BERX, G. 2008. The cell-cell adhesion molecule E-cadherin. *Cellular and molecular life sciences,* 65**,** 3756-3788.

VANDER HEIDEN, M. G., CANTLEY, L. C. & THOMPSON, C. B. 2009. Understanding the Warburg effect: the metabolic requirements of cell proliferation. *science,* 324**,** 1029-1033.

VARKI, N. M. & VARKI, A. 2002. Heparin inhibition of selectin-mediated interactions during the hematogenous phase of carcinoma metastasis: rationale for clinical studies in humans. *Seminars in thrombosis and hemostasis,* 28**,** 53-66.

VAUPEL, P., SCHLENGER, K., KNOOP, C. & HÖCKEL, M. 1991. Oxygenation of human tumors: evaluation of tissue oxygen distribution in breast cancers by computerized O2 tension measurements. *Cancer research,* 51**,** 3316-3322.

VELDKAMP, C. T., ZIAREK, J. J., PETERSON, F. C., CHEN, Y. & VOLKMAN, B. F. 2010. Targeting SDF-1/CXCL12 with a ligand that prevents activation of CXCR4 through structure-based drug design. *Journal of the American Chemical Society,* 132**,** 7242-7243.

VERONESI, U., PAGANELLI, G., GALIMBERTI, V., VIALE, G., ZURRIDA, S., BEDONI, M., COSTA, A., DE CICCO, C., GERAGHTY, J. G. & LUINI, A. 1997. Sentinel-node biopsy to avoid axillary dissection in breast cancer with clinically negative lymph-nodes. *The Lancet,* 349**,** 1864-1867.

VICARI, A. P., AIT-YAHIA, S., CHEMIN, K., MUELLER, A., ZLOTNIK, A. & CAUX, C. 2000. Antitumor effects of the mouse chemokine 6Ckine/SLC through angiostatic and immunological mechanisms. *The Journal of Immunology,* 165**,** 1992-2000.

VILA-CORO, A. J., RODRÍGUEZ-FRADE, J. M., DE ANA, A. N. A. M., MORENO-ORTÍZ, M. C., MARTÍNEZ-A, C. & MELLADO, M. 1999. The chemokine SDF-1α triggers CXCR4 receptor dimerization and activates the JAK/STAT pathway. *The FASEB Journal,* 13**,** 1699-1710.

VILLALOBOS, V., NAIK, S., BRUINSMA, M., DOTHAGER, R. S., PAN, M.-H., SAMRAKANDI, M., MOSS, B., ELHAMMALI, A. & PIWNICA-WORMS, D. 2010. Dual-color click beetle luciferase heteroprotein fragment complementation assays. *Chemistry & biology,* 17**,** 1018-1029.

VLODAVSKY, I., GOLDSHMIDT, O., ZCHARIA, E., ATZMON, R., RANGINI-GUATTA, Z., ELKIN, M., PERETZ, T. & FRIEDMANN, Y. Mammalian heparanase: involvement in cancer metastasis, angiogenesis and normal development. Seminars in cancer biology, 2002. Elsevier, 121-129.

VOGEL, C. & MARCOTTE, E. M. 2012. Insights into the regulation of protein abundance from proteomic and transcriptomic analyses. *Nature Reviews Genetics,* 13**,** 227-232.

VOLIN, M. V., JOSEPH, L., SHOCKLEY, M. S. & DAVIES, P. F. 1998. Chemokine receptor CXCR4 expression in endothelium. *Biochemical and biophysical research communications,* 242**,** 46-53.

VOTTA-VELIS, E. G., PIEGELER, T., MINSHALL, R. D., AGUIRRE, J., BECK-SCHIMMER, B., SCHWARTZ, D. E. & BORGEAT, A. 2013. Regional anaesthesia and cancer metastases: the implication of local anaesthetics. *Acta Anaesthesiologica Scandinavica,* 57**,** 1211-1229.

WALENTOWICZ-SADLECKA, M., SADLECKI, P., BODNAR, M., MARSZALEK, A., WALENTOWICZ, P., SOKUP, A., WILIŃSKA-JANKOWSKA, A. & GRABIEC, M. 2014. Stromal derived factor-1 (SDF-1) and its receptors CXCR4 and CXCR7 in endometrial cancer patients. *PloS one,* 9**,** e84629.

WALLACE, J. 2000. Humane endpoints and cancer research. *ILAR journal,* 41**,** 87-93.

WANG, J., HE, L., COMBS, C. A., RODERIQUEZ, G. & NORCROSS, M. A. 2006. Dimerization of CXCR4 in living malignant cells: control of cell migration by a synthetic peptide that reduces homologous CXCR4 interactions. *Molecular cancer therapeutics,* 5**,** 2474-2483.

WANG, J., SEETHALA, R. R., ZHANG, Q., GOODING, W., VAN WAES, C., HASEGAWA, H. & FERRIS, R. L. 2008a. Autocrine and paracrine chemokine receptor 7 activation in head and neck cancer: implications for therapy. *Journal of the National Cancer Institute,* 100**,** 502-512.

WANG, J., SHIOZAWA, Y., WANG, J., WANG, Y., JUNG, Y., PIENTA, K. J., MEHRA, R., LOBERG, R. & TAICHMAN, R. S. 2008b. The role of CXCR7/RDC1 as a chemokine receptor for CXCL12/SDF-1 in prostate cancer. *Journal of Biological Chemistry,* 283**,** 4283-4294.

WANG, L., CHEN, W., GAO, L., YANG, Q., LIU, B., WU, Z., WANG, Y. & SUN, Y. 2012a. High expression of CXCR4, CXCR7 and SDF-1 predicts poor survival in renal cell carcinoma. *World journal of surgical oncology,* 10**,** 212.

WANG, L., LIU, R., LI, W., CHEN, C., KATOH, H., CHEN, G.-Y., MCNALLY, B., LIN, L., ZHOU, P. & ZUO, T. 2009. Somatic single hits inactivate the X-linked tumor suppressor FOXP3 in the prostate. *Cancer cell,* 16**,** 336-346.

WANG, L., WANG, X., LIANG, Y., DIAO, X. & CHEN, Q. 2012b. S100A4 promotes invasion and angiogenesis in breast cancer MDA-MB-231 cells by upregulating matrix metalloproteinase-13. *Acta Biochim Pol,* 59**,** 593-598.

WANG, N., WU, Q.-L., FANG, Y., MAI, H.-Q., ZENG, M.-S., SHEN, G.-P., HOU, J.-H. & ZENG, Y.-X. 2005. Expression of chemokine receptor CXCR4 in nasopharyngeal carcinoma: pattern of expression and correlation with clinical outcome. *Journal of translational medicine,* 3**,** 26.

WANG, P., GAO, H., NI, Y., WANG, B., WU, Y., JI, L., QIN, L., MA, L. & PEI, G. 2003. β-Arrestin 2 functions as a G-protein-coupled receptor-activated regulator of oncoprotein Mdm2. *Journal of Biological Chemistry,* 278**,** 6363-6370.

WANG, Y., LI, G., STANCO, A., LONG, J. E., CRAWFORD, D., POTTER, G. B., PLEASURE, S. J., BEHRENS, T. & RUBENSTEIN, J. L. 2011. CXCR4 and CXCR7 have distinct functions in regulating interneuron migration. *Neuron,* 69**,** 61-76.

WANG, Y. & ZHOU, B. P. 2011. Epithelial-mesenchymal transition in breast cancer progression and metastasis. *Chinese journal of cancer,* 30**,** 603.

WANI, N. A., NASSER, M. W., AHIRWAR, D. K., ZHAO, H., MIAO, Z., SHILO, K. & GANJU, R. K. 2014. CXC motif chemokine 12/CXC chemokine receptor type 7 signaling regulates breast cancer growth and metastasis by modulating the tumor microenvironment. *Breast Cancer Research,* 16**,** 26.

WARNOCK, R. A., CAMPBELL, J. J., DORF, M. E., MATSUZAWA, A., MCEVOY, L. M. & BUTCHER, E. C. 2000. The role of chemokines in the microenvironmental control of T versus B cell arrest in Peyer's patch high endothelial venules. *Journal of Experimental Medicine,* 191**,** 77-88.

WEBER, M., BLAIR, E., SIMPSON, C. V., O'HARA, M., BLACKBURN, P. E., ROT, A., GRAHAM, G. J. & NIBBS, R. J. B. 2004. The chemokine receptor D6 constitutively traffics to and from the cell surface to internalize and degrade chemokines. *Molecular biology of the cell,* 15**,** 2492-2508.

WEBER, M., HAUSCHILD, R., SCHWARZ, J., MOUSSION, C., DE VRIES, I., LEGLER, D. F., LUTHER, S. A., BOLLENBACH, T. & SIXT, M. 2013. Interstitial dendritic cell guidance by haptotactic chemokine gradients. *Science,* 339**,** 328-332.

WELLS, T. N., POWER, C. A., LUSTI-NARASIMHAN, M., HOOGEWERF, A. J., COOKE, R. M., CHUNG, C. W., PEITSCH, M. C. & PROUDFOOT, A. E. 1996. Selectivity and antagonism of chemokine receptors. *Journal of Leukocyte Biology,* 59**,** 53-60.

WENDEL, C., HEMPING-BOVENKERK, A., KRASNYANSKA, J., MEES, S. T., KOCHETKOVA, M., STOEPPELER, S. & HAIER, J. 2012. CXCR4/CXCL12 participate in extravasation of metastasizing breast cancer cells within the liver in a rat model. *PLoS One,* 7**,** e30046.

WENDEL, M., GALANI, I. E., SURI-PAYER, E. & CERWENKA, A. 2008. Natural killer cell accumulation in tumors is dependent on IFN-γ and CXCR3 ligands. *Cancer research,* 68**,** 8437-8445.

WENDT, M. K., TAYLOR, M. A., SCHIEMANN, B. J. & SCHIEMANN, W. P. 2011. Down-regulation of epithelial cadherin is required to initiate metastatic outgrowth of breast cancer. *Molecular biology of the cell,* 22**,** 2423-2435.

WHITELOCK, J. M. & IOZZO, R. V. 2005. Heparan sulfate: a complex polymer charged with biological activity. *Chemical reviews,* 105**,** 2745-2764.

WIJTMANS, M., MAUSSANG, D., SIRCI, F., SCHOLTEN, D. J., CANALS, M., MUJIĆ-DELIĆ, A., CHONG, M., CHATALIC, K. L., CUSTERS, H. & JANSSEN, E. 2012. Synthesis, modeling and functional activity of substituted styrene-amides as small-molecule CXCR7 agonists. *European journal of medicinal chemistry,* 51**,** 184-192.

WILLIMANN, K., LEGLER, D. F., LOETSCHER, M., ROOS, R. S., DELGADO, M. B., CLARK-LEWIS, I., BAGGIOLINI, M. & MOSER, B. 1998. The chemokine SLC is expressed in T cell areas of lymph nodes and mucosal lymphoid tissues and attracts activated T cells via CCR7. *European journal of immunology,* 28**,** 2025-2034.

WILSON, J. L., BURCHELL, J. & GRIMSHAW, M. J. 2006. Endothelins induce CCR7 expression by breast tumor cells via endothelin receptor A and hypoxia-inducible factor-1. *Cancer Research,* 66**,** 11802-11807.

WITHEROW, D. S., GARRISON, T. R., MILLER, W. E. & LEFKOWITZ, R. J. 2004. β-Arrestin inhibits NF-κB activity by means of its interaction with the NF-κB inhibitor IκBα. *Proceedings of the National Academy of Sciences of the United States of America,* 101**,** 8603-8607.

WITSCH, E., SELA, M. & YARDEN, Y. 2010. Roles for growth factors in cancer progression. *Physiology,* 25**,** 85-101.

WITT, D. P. & LANDER, A. D. 1994. Differential binding of chemokines to glycosaminoglycan subpopulations. *Current Biology,* 4**,** 394-400.

WOERNER, B. M., WARRINGTON, N. M., KUNG, A. L., PERRY, A. & RUBIN, J. B. 2005. Widespread CXCR4 activation in astrocytomas revealed by phospho-CXCR4-specific antibodies. *Cancer Research,* 65**,** 11392-11399.

WONG, A. S. T. & GUMBINER, B. M. 2003. Adhesion-independent mechanism for suppression of tumor cell invasion by E-cadherin. *The Journal of cell biology,* 161**,** 1191-1203.

WONG, D., KANDAGATLA, P., KORZ, W. & CHINNI, S. R. 2014. Targeting CXCR4 with CTCE-9908 inhibits prostate tumor metastasis. *BMC urology,* 14**,** 12.

WOO, S. U., BAE, J. W., KIM, C. H., LEE, J. B. & KOO, B. W. 2008. A significant correlation between nuclear CXCR4 expression and axillary lymph node metastasis in hormonal receptor negative breast cancer. *Annals of Surgical Oncology,* 15**,** 281-285.

WORBS, T., MEMPEL, T. R., BÖLTER, J., VON ANDRIAN, U. H. & FÖRSTER, R. 2007. CCR7 ligands stimulate the intranodal motility of T lymphocytes in vivo. *Journal of Experimental Medicine,* 204**,** 489-495.

WU, B., CHIEN, E. Y., MOL, C. D., FENALTI, G., LIU, W., KATRITCH, V., ABAGYAN, R., BROOUN, A., WELLS, P. & BI, F. C. 2010a. Structures of the CXCR4 chemokine GPCR with small-molecule and cyclic peptide antagonists. *Science,* 330**,** 1066-1071.

WU, W., QIAN, L., CHEN, X. & DING, B. 2015. Prognostic significance of CXCL12, CXCR4, and CXCR7 in patients with breast cancer. *International journal of clinical and experimental pathology,* 8**,** 13217.

WU, X., LI, D.-J., YUAN, M.-M., ZHU, Y. & WANG, M.-Y. 2004. The Expression of CXCR4/CXCL12 in First-Trimester Human Trophoblast Cells 1. *Biology of reproduction,* 70**,** 1877-1885.

WU, Y., JIN, M., XU, H., SHIMIN, Z., HE, S., WANG, L. & ZHANG, Y. 2010b. Clinicopathologic Significance of HIF-1 *Clinical and developmental immunology,* 2010**,** 537531.

WURCH, T., MATSUMOTO, A. & PAUWELS, P. J. 2001. Agonist-independent and-dependent oligomerization of dopamine D2 receptors by fusion to fluorescent proteins. *FEBS letters,* 507**,** 109-113.

WYCKOFF, J. B., JONES, J. G., CONDEELIS, J. S. & SEGALL, J. E. 2000. A critical step in metastasis: in vivo analysis of intravasation at the primary tumor. *Cancer research,* 60**,** 2504-2511.

XU, D., LI, R., WU, J., JIANG, L. & A ZHONG, H. 2016. Drug Design targeting the CXCR4/CXCR7/CXCL12 pathway. *Current Topics in Medicinal Chemistry,* 16**,** 1441-1451.

XU, H., WU, Q., DANG, S., JIN, M., XU, J., CHENG, Y., PAN, M., WU, Y., ZHANG, C. & ZHANG, Y. 2011a. Alteration of CXCR7 expression mediated by TLR4 promotes tumor cell proliferation and migration in human colorectal carcinoma. *PloS one,* 6**,** e27399.

XU, Y., LIU, L., QIU, X., JIANG, L., HUANG, B., LI, H., LI, Z., LUO, W. & WANG, E. 2011b. CCL21/CCR7 Promotes G 2/M Phase Progression via the ERK Pathway in Human Non-Small Cell Lung Cancer Cells. *PLoS One,* 6**,** e21119.

XU, Y., LIU, L., QIU, X., LIU, Z., LI, H., LI, Z., LUO, W. & WANG, E. 2012. CCL21/CCR7 prevents apoptosis via the ERK pathway in human non-small cell lung cancer cells. *PLoS One,* 7**,** e33262.

XU, Y., SWERLICK, R. A., SEPP, N., BOSSE, D., ADES, E. W. & LAWLEY, T. J. 1994. Characterization of expression and modulation of cell adhesion molecules on an immortalized human dermal microvascular endothelial cell line (HMEC-1). *Journal of Investigative Dermatology,* 102**,** 833-837.

XUE, C., PLIETH, D., VENKOV, C., XU, C. & NEILSON, E. G. 2003. The gatekeeper effect of epithelial-mesenchymal transition regulates the frequency of breast cancer metastasis. *Cancer research,* 63**,** 3386-3394.

YANAGIHARA, S., KOMURA, E., NAGAFUNE, J., WATARAI, H. & YAMAGUCHI, Y. 1998. EBI1/CCR7 is a new member of dendritic cell chemokine receptor that is up-regulated upon maturation. *The Journal of Immunology,* 161**,** 3096-3102.

YANG, J., MANI, S. A., DONAHER, J. L., RAMASWAMY, S., ITZYKSON, R. A., COME, C., SAVAGNER, P., GITELMAN, I., RICHARDSON, A. & WEINBERG, R. A. 2004a. Twist, a master regulator of morphogenesis, plays an essential role in tumor metastasis. *Cell,* 117**,** 927-939.

YANG, Q., ZHANG, F., DING, Y., HUANG, J., CHEN, S., WU, Q., WANG, Z. & CHEN, C. 2014. Antitumour activity of the recombination polypeptide GST-NT21MP is mediated by inhibition of CXCR4 pathway in breast cancer. *British journal of cancer,* 110**,** 1288**–**1297.

YANG, S.-C., BATRA, R. K., HILLINGER, S., RECKAMP, K. L., STRIETER, R. M., DUBINETT, S. M. & SHARMA, S. 2006. Intrapulmonary administration of CCL21 gene-modified dendritic cells reduces tumor burden in spontaneous murine bronchoalveolar cell carcinoma. *Cancer research,* 66**,** 3205-3213.

YANG, S.-C., HILLINGER, S., RIEDL, K., ZHANG, L., ZHU, L., HUANG, M., ATIANZAR, K., KUO, B. Y., GARDNER, B. & BATRA, R. K. 2004b. Intratumoral administration of dendritic cells overexpressing CCL21 generates systemic antitumor responses and confers tumor immunity. *Clinical Cancer Research,* 10**,** 2891-2901.

YANG, S., ZHANG, J. J. & HUANG, X.-Y. 2012. Mouse models for tumor metastasis. *Rational Drug Design: Methods and Protocols***,** 221-228.

YANG, Y., MACLEOD, V., BENDRE, M., HUANG, Y., THEUS, A. M., MIAO, H.-Q., KUSSIE, P., YACCOBY, S., EPSTEIN, J. & SUVA, L. J. 2005. Heparanase promotes the spontaneous metastasis of myeloma cells to bone. *Blood,* 105**,** 1303-1309.

YAO, X., ZHOU, L., HAN, S. & CHEN, Y. 2011. High expression of CXCR4 and CXCR7 predicts poor survival in gallbladder cancer. *Journal of International Medical Research,* 39**,** 1253-1264.

YASUOKA, H., TSUJIMOTO, M., YOSHIDOME, K., NAKAHARA, M., KODAMA, R., SANKE, T. & NAKAMURA, Y. 2008. Cytoplasmic CXCR4 expression in breast cancer: induction by nitric oxide and correlation with lymph node metastasis and poor prognosis. *BMC cancer,* 8**,** 340.

YENOFSKY, R. L., FINE, M. & PELLOW, J. W. 1990. A mutant neomycin phosphotransferase II gene reduces the resistance of transformants to antibiotic selection pressure. *Proceedings of the National Academy of Sciences,* 87**,** 3435-3439.

YOON, Y., LIANG, Z., ZHANG, X., CHOE, M., ZHU, A., CHO, H. T., SHIN, D. M., GOODMAN, M. M. & SHIM, H. 2007. CXC chemokine receptor-4 antagonist blocks both growth of primary tumor and metastasis of head and neck cancer in xenograft mouse models. *Cancer research,* 67**,** 7518-7524.

YOSHIDA, R., NAGIRA, M., KITAURA, M., IMAGAWA, N., IMAI, T. & YOSHIE, O. 1998. Secondary lymphoid-tissue chemokine is a functional ligand for the CC chemokine receptor CCR7. *Journal of Biological Chemistry,* 273**,** 7118-7122.

YOSHIKAWA, Y., OISHI, S., KUBO, T., TANAHARA, N., FUJII, N. & FURUYA, T. 2013. Optimized method of G-protein-coupled receptor homology modeling: its application to the discovery of novel CXCR7 ligands. *Journal of medicinal chemistry,* 56**,** 4236-4251.

YOUSEFIEH, N., HAHTO, S. M., STEPHENS, A. L. & CIAVARRA, R. P. 2009. Regulated expression of CCL21 in the prostate tumor microenvironment inhibits tumor growth and metastasis in an orthotopic model of prostate cancer. *Cancer Microenvironment,* 2**,** 59-67.

YU, Y., LI, H., XUE, B., JIANG, X., HUANG, K., GE, J., ZHANG, H. & CHEN, B. 2014. SDF-1/CXCR7 axis enhances ovarian cancer cell invasion by MMP-9 expression through p38 MAPK pathway. *DNA and cell biology,* 33**,** 543-549.

YUAN, T. L. & CANTLEY, L. C. 2008. PI3K pathway alterations in cancer: variations on a theme. *Oncogene,* 27**,** 5497-5510.

YUKI, K., YOSHIDA, Y., INAGAKI, R., HIAI, H. & NODA, M. 2014. E-cadherin-downregulation and RECK-upregulation are coupled in the non-malignant epithelial cell line MCF10A but not in multiple carcinoma-derived cell lines. *Scientific reports,* 4**,** 4568.

ZABEL, B. A., LEWÉN, S., BERAHOVICH, R. D., JAÉN, J. C. & SCHALL, T. J. 2011. The novel chemokine receptor CXCR7 regulates trans-endothelial migration of cancer cells. *Molecular cancer,* 10**,** 73.

ZABEL, B. A., WANG, Y., LEWÉN, S., BERAHOVICH, R. D., PENFOLD, M. E. T., ZHANG, P., POWERS, J., SUMMERS, B. C., MIAO, Z. & ZHAO, B. 2009. Elucidation of CXCR7-mediated signaling events and inhibition of CXCR4-mediated tumor cell transendothelial migration by CXCR7 ligands. *The Journal of Immunology,* 183**,** 3204-3211.

ZACHARSKI, L. R., ORNSTEIN, D. L. & MAMOURIAN, A. C. 2000. *Low-molecular-weight heparin and cancer*, Thieme Medical Publishers, Inc.

ZAGZAG, D., KRISHNAMACHARY, B., YEE, H., OKUYAMA, H., CHIRIBOGA, L., ALI, M. A., MELAMED, J. & SEMENZA, G. L. 2005. Stromal cell–derived factor-1α and CXCR4 expression in hemangioblastoma and clear cell-renal cell carcinoma: von Hippel-Lindau loss-of-function induces expression of a ligand and its receptor. *Cancer research,* 65**,** 6178-6188.

ZENG, F.-Y. & WESS, J. 1999. Identification and molecular characterization of m3 muscarinic receptor dimers. *Journal of Biological Chemistry,* 274**,** 19487-19497.

ZHAN, Y., ZHANG, H., LI, J., ZHANG, Y., ZHANG, J. & HE, L. 2015. A novel biphenyl urea derivate inhibits the invasion of breast cancer through the modulation of CXCR4. *Journal of cellular and molecular medicine,* 19**,** 1614-1623.

ZHANG, L., YEGER, H., DAS, B., IRWIN, M. S. & BARUCHEL, S. 2007. Tissue microenvironment modulates CXCR4 expression and tumor metastasis in neuroblastoma. *Neoplasia,* 9**,** 36-46.

ZHANG, Q., FAN, H., SHEN, J., HOFFMAN, R. M. & XING, H. R. 2010. Human breast cancer cell lines co-express neuronal, epithelial, and melanocytic differentiation markers in vitro and in vivo. *PloS one,* 5**,** e9712.

ZHANG, Y., LIANG, Z., WU, H., ZHU, A., YOON, Y., WANG, S. & SHIM, H. 2008. MSX-122, an orally available small molecule targeting CXCR4, inhibits primary tumor growth in an orthotopic mouse model of lung cancer and improves the effect of paclitaxel. *Cancer Research,* 68**,** 1190-1190.

ZHANG, Y., YANG, P., SUN, T., LI, D., XU, X., RUI, Y., LI, C., CHONG, M., IBRAHIM, T. & MERCATALI, L. 2013. miR-126 and miR-126* repress recruitment of mesenchymal stem cells and inflammatory monocytes to inhibit breast cancer metastasis. *Nature cell biology,* 15**,** 284-294.

ZHANG, Z., NI, C., CHEN, W., WU, P., WANG, Z., YIN, J., HUANG, J. & QIU, F. 2014. Expression of CXCR4 and breast cancer prognosis: a systematic review and meta-analysis. *BMC cancer,* 14**,** 49.

ZHAO, B., CUI, K., WANG, C. L., WANG, A. L., ZHANG, B., ZHOU, W. Y., ZHAO, W. H. & LI, S. 2011. The chemotactic interaction between CCL21 and its receptor, CCR7, facilitates the progression of pancreatic cancer via induction of angiogenesis and lymphangiogenesis. *Journal of hepato-biliary-pancreatic sciences,* 18**,** 821-828.

ZHAO, X.-P., HUANG, Y.-Y., HUANG, Y., LEI, P., PENG, J.-L., WU, S., WANG, M., LI, W.-H., ZHU, H.-F. & SHEN, G.-X. 2010. Transforming growth factor-β1 upregulates the expression of CXC chemokine receptor 4 (CXCR4) in human breast cancer MCF-7 cells. *Acta Pharmacologica Sinica,* 31**,** 347-354.

ZHENG, K., LI, H.-Y., SU, X.-L., WANG, X.-Y., TIAN, T., LI, F. & REN, G.-S. 2010. Chemokine receptor CXCR7 regulates the invasion, angiogenesis and tumor growth of human hepatocellular carcinoma cells. *Journal of Experimental & Clinical Cancer Research,* 29**,** 31.

ZHOU, N., LUO, Z., LUO, J., FAN, X., CAYABYAB, M., HIRAOKA, M., LIU, D., HAN, X., PESAVENTO, J. & DONG, C.-Z. 2002a. Exploring the stereochemistry of CXCR4-peptide recognition and inhibiting HIV-1 entry with D-peptides derived from chemokines. *Journal of Biological Chemistry,* 277**,** 17476-17485.

ZHOU, X., FRAGALA, M. S., MCELHANEY, J. E. & KUCHEL, G. A. 2010. Conceptual and methodological issues relevant to cytokine and inflammatory marker measurements in clinical research. *Current opinion in clinical nutrition and metabolic care,* 13**,** 541.

ZHOU, Y., LARSEN, P. H., HAO, C. & YONG, V. W. 2002b. CXCR4 is a major chemokine receptor on glioma cells and mediates their survival. *Journal of Biological Chemistry,* 277**,** 49481-49487.

ZHOU, Z.-H., KARNAUKHOVA, E., RAJABI, M., REEDER, K., CHEN, T., DHAWAN, S. & KOZLOWSKI, S. 2014. Oversulfated chondroitin sulfate binds to chemokines and inhibits stromal cell-derived factor-1 mediated signaling in activated T cells. *PloS one,* 9**,** e94402.

ZHU, B., XU, D., DENG, X., CHEN, Q., HUANG, Y., PENG, H., LI, Y., JIA, B., THORESON, W. B. & DING, W. 2012. CXCL12 Enhances Human Neural Progenitor Cell Survival Through a CXCR7-and CXCR4-Mediated Endocytotic Signaling Pathway. *Stem Cells,* 30**,** 2571-2583.

ZHU, C.-C., COOK, L. B. & HINKLE, P. M. 2002. Dimerization and phosphorylation of thyrotropin-releasing hormone receptors are modulated by agonist stimulation. *Journal of Biological Chemistry,* 277**,** 28228-28237.

ZLOTNIK, A. 2006. Chemokines and cancer. *International journal of cancer,* 119**,** 2026-2029.

ZLOTNIK, A., BURKHARDT, A. M. & HOMEY, B. 2011. Homeostatic chemokine receptors and organ-specific metastasis. *Nature reviews Immunology,* 11**,** 597-606.

ZLOTNIK, A. & YOSHIE, O. 2000. Chemokines: a new classification system and their role in immunity. *Immunity,* 12**,** 121-127.

ZLOTNIK, A., YOSHIE, O. & NOMIYAMA, H. 2006. The chemokine and chemokine receptor superfamilies and their molecular evolution. *Genome biology,* 7**,** 243.

ZOU, Y.-R., KOTTMANN, A. H., KURODA, M., TANIUCHI, I. & LITTMAN, D. R. 1998. Function of the chemokine receptor CXCR4 in haematopoiesis and in cerebellar development. *Nature,* 393**,** 595-599.

ZUMSTEG, A. & CHRISTOFORI, G. 2009. Corrupt policemen: inflammatory cells promote tumor angiogenesis. *Current opinion in oncology,* 21**,** 60-70.

ZUO, T., LIU, R., ZHANG, H., CHANG, X., LIU, Y., WANG, L., ZHENG, P. & LIU, Y. 2007a. FOXP3 is a novel transcriptional repressor for the breast cancer oncogene SKP2. *The Journal of clinical investigation,* 117**,** 3765-3773.

ZUO, T., WANG, L., MORRISON, C., CHANG, X., ZHANG, H., LI, W., LIU, Y., WANG, Y., LIU, X. & CHAN, M. W. Y. 2007b. FOXP3 is an X-linked breast cancer suppressor gene and an important repressor of the HER-2/ErbB2 oncogene. *Cell,* 129**,** 1275-1286.

APPENDIX 1

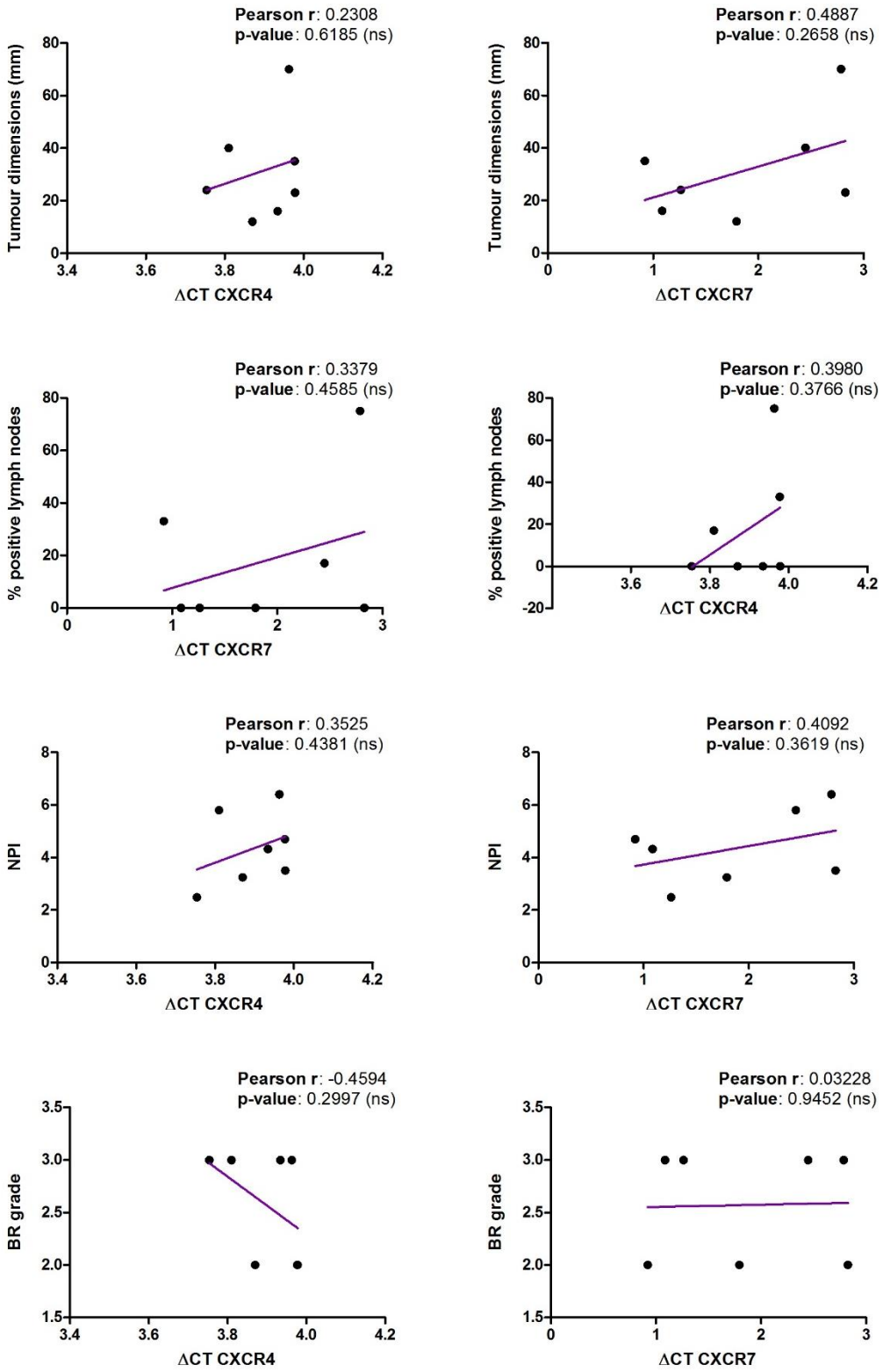

Figure 0-1. Correlation between CXCR4 and CXCR7 ΔCt in the tumour and the tumour dimensions, the percentage of positive lymph nodes, the Nottingham prognostic index (NPI) or the Bloom and Richardson's grade.

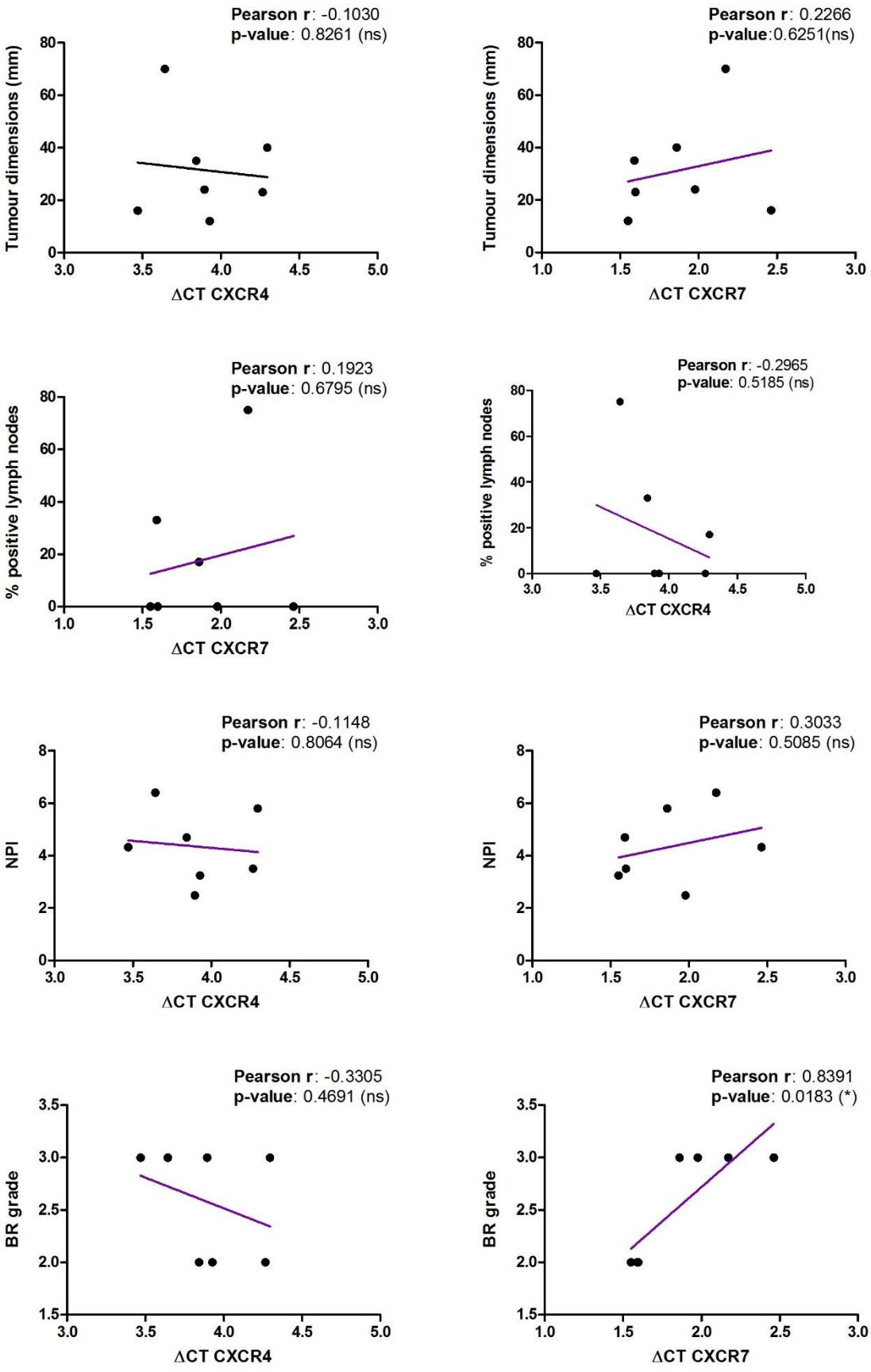

Figure 0-2. Correlation between CXCR4 and CXCR7 ΔCt in the microenvironment and the tumour dimensions, the percentage of positive lymph nodes, the Nottingham prognostic index (NPI) or the Bloom and Richardson's grade.

APPENDIX 2

Conferences

International

- Gordon Research Seminar "Chemotactic Chemokines", Girona (Spain): 28-29th May 2016, **poster presentation.**
- AACR Annual meeting 2016, New Orleans (USA): 16-20th April 2016, **poster presentation.**

National

- North East Postgraduate Conference (NEPG), Newcastle upon Tyne (UK): 24-25th November 2016, **oral presentation.**
- ICM Director's Research day, Newcastle upon Tyne (UK): 17th June 2016, **oral presentation.**
- Women's cancer detection society (WCDS) annual committee meeting: 12th April 2016, **oral presentation.**
- Postgraduate Cancer Conference Day, Newcastle upon Tyne (UK): 4th March 2016, **oral presentation**.
- ICM Seminar Program, Newcastle University (UK): 10th February 2016, **oral presentation**.
- Scientific Facilities conference, Newcastle upon Tyne (UK): 9th November 2015, **poster presentation.**
- British association for cancer research conference (Breast Cancer: Bridging gaps in our knowledge to improve patient outcome), Gateshead (UK): 7th-9th October 2015, **poster presentation.**
- ICM Seminar Program, Newcastle University (UK): 28th May 2014, **oral presentation**.

Publications

- **del Barrio, I. D. M.**, Kirby, J., & Ali, S. (2016). Chapter Fifteen-T he Role of Chemokine and Glycosaminoglycan Interaction in Chemokine-Mediated Migration In Vitro and In Vivo. Methods in enzymology, 570, 309-333.
- **del Barrio, I. D. M**., Ali, S., Kirby, J., & Meeson, A. (2016). CXCR4 and CXCR7 homodimers and heterodimers play differential roles in breast cancer. Cancer Research, 76(14 Supplement), 1453-1453.
- *(Manuscript in progress, pending submission)* **del Barrio, I. D. M**., Meeson, A., Ali & S., Kirby, J. Coexpression of CXCR7 can modify CXCR4's response to CXCL12 in breast cancer.
- *(Manuscript in progress, pending submission)* **del Barrio, I. D. M.***, Malki, I.*, Millar, B., Cooke, K., Barker, C., Meeson, A., Ali & S., Kirby, J. Contribution of heparan

sulphate binding to chemokine CCL21 in the migration of breast cancer cells. *co-first authors

Awards and grants

- Winner of the ULTSEC Innovation fund award (2015/2016), Newcastle University (UK).
- Travel grant awarded by Newcastle University graduate school - £650 (2016)
- Amnis Travel Stipend Program - $500 (2016)
- EFIS societies fund – $320 (2016)
- NHS Trust stipend award - £7,650 (2016).

Professional memberships

- Student member of the British society for immunology (BSI), UK.
- Associate Member of the American Association for Cancer Research (AACR), USA.